Regulation of mitochondrial fusion by the Ubiquitin Proteasome System and physical contacts between mitochondria and peroxisomes in yeast Saccharomyces cerevisiae

Cynthia Alsayyah

PSL UNIVERSITÉ PARIS

THÈSE DE DOCTORAT
DE L'UNIVERSITÉ PSL

Préparée à l'Institut de Biologie Physico-Chimique

Régulation de la fusion mitochondriale par le Système Ubiquitine Protéasome et les contacts physiques mitochondrie-peroxysomes chez la levure *Saccharomyces cerevisiae*.

Soutenue par
Cynthia ALSAYYAH
Le 14 Septembre 2021

Ecole doctorale n° 515
Complexité du vivant

Spécialité
Biologie cellulaire et développement

Composition du jury :

Sébastien, LEON DR CNRS, IJM	*Président*
Fanny, PILOT-STORCK PR, IMRB ENVA /UPEC	*Rapporteur*
Irina, LASSOT CR CNRS, IGMM	*Rapporteur*
Thomas, RIVAL MCU, IBDM	*Examinateur*
Cédric, DELEVOYE DR INSERM, Institut Curie	*Examinateur*
Mickael, COHEN DR CNRS, IBPC	*Directeur de thèse*

IBPC

Remerciements

Tout d'abord, j'aimerai remercier les membres du jury. Merci à Fanny Pilot-Storck et Irina Lassot qui ont donné beaucoup de leur temps pour lire et évaluer cette thèse. Je remercie aussi Sébastien Léon, Cédric Delevoye et Thomas Rival qui ont accepté d'être examinateurs.
Vous avez tous accepté immédiatement et avec grand enthousiasme de participer à cette dernière étape de ma thèse et je vous en remercie énormément. Je suis certaine que les remarques que vous ferez et les discussions que nous aurons seront d'une très grande qualité scientifique.

J'aimerai aussi remercier mon directeur de thèse, Mickael pour son soutien tout au long de ces cinq dernières années. Je te remercie de m'avoir accompagné dans ce cheminement scientifique, reboosté dans les moments difficiles et enfin merci de m'avoir formé pour être la chercheuse que je suis aujourd'hui.

Merci à Naima qui était toujours à l'écoute dans les bons et les mauvais moments de ce long chemin. Ton humour, ton ouverture d'esprit et ta gentillesse sont incomparables, une maman que tout le monde rêverait avoir !
Je voudrais aussi remercier Laetitia qui as toujours été là pour m'aider, discuter et m'apprendre ! Et pas que la biomol et les clonages mais aussi la couture et le tricot.
Je remercie Manish pour sa gentillesse et sa galanterie et Mohammad d'être toujours à l'écoute, pour ses conseils et les bons moments partagés à la libanaise.

Justin et Héloïse… à nos trains de massage, les frites, les bières, Titus, les gaufres dunkerquoises, les soirées chez Oliver, New York, nos conneries et encore les bières. Malgré la distance qui nous sépare je ne vous (ai pas oublié) oublierais jamais.

Oznur ! Merci pour ta joie, pour ta bienveillance, ton aide sans conditions ni limites, ton organisation incomparable et pour tous les O'tacos qu'on a partagé. Pensée à toi qui penses toujours aux autres avant de penser à toi-même, j'avais beaucoup de chance de pouvoir partager ce chemin avec toi.

Bechara, pas besoin d'une longue description toi-même tu sais. A nos soirées, la marche des fiertés, de Cité U à Chromatica, c'était un super voyage.

Merci à Cyrielle, Félix, Prisca, Jeanne, Théo, Nicolas, Margaux, Aurélia, Pascale, Erin, Pierre, Oliver, Marion, Dhenesh, Nathalie, Maxence, Suzanne et tous les autres membres de l'unité et de l'IBPC avec qui j'ai pu passer des super moments qui ont fait que j'ai autant aimé faire cette thèse.

En outre, je n'oublierai jamais la fidélité dont mes amis ont fait preuve. Même si je n'étais pas souvent là à cause de mon travail, ils ont toujours été au rendez-vous pour me faire oublier les problèmes de la thèse et me soutenir. Pascale, Jad, Catherine, Jihane, Charlotte et Melyssa merci à vous.
Je remercie Jade qui a réussi à supporter la vie avec moi, mes horaires, mon manque d'organisation et tous les weekends au travail. Merci pour ta compréhension, ton aide et ton soutien infaillible.

Enfin, mes remerciements vont surtout à mes parents, ainsi que l'ensemble de ma famille qui même en étant loin ont cru en moi, surtout mes oncles Albert et Ibrahim. Vous m'avez donné la possibilité de poursuivre mes études en France et vous m'avez soutenu dans cette aventure. J'espère ne jamais vous décevoir.

Table of contents

Part 1: Introduction

Part 2: Results

Part 3: Discussion and Perspectives

Part 4: Materials and Methods

Part 5: Bibliography

Annexes

Resumés

Part 1: Introduction

I- General Introduction

During the last decade, we shifted from the old-fashioned and untrue picture of "bean-shaped" isolated mitochondria to a far more accurate vision. Mitochondria and all the other organelles share a common apartment called the cell. Just like your typical roommates they exchange and communicate on a daily basis not only to maintain their own independent functions but also to achieve a higher common goal: upkeeping cellular homeostasis. This communication can be indirect, through vesicular trafficking for example or direct by transient physical contacts with each other. But when it comes to physical inter-organelle contacts, mitochondria rank at the top of the class thanks to their dynamic nature. Indeed, mitochondria are very dynamic organelles whose morphology is governed by fusion and fission events of their outer and inner mitochondrial membranes (Westermann, 2010). The process of mitochondrial membrane fusion in particular is not a simple task as an intricate balance between two key systems is at play (Cavellini et al., 2017). The first one is the Ubiquitin Proteasome System which is famously known for its crucial role in protein and organelle turnover, trafficking, DNA repair, endocytosis, signaling pathways, and cell cycle progression and the list goes on (Foot et al., 2017). The second is the Ole pathway which is essential for *de novo* biosynthesis of unsaturated fatty acids (UFAs) that constitute lipid building blocks for cellular membranes (Ernst et al., 2016). The crosstalk between these 2 systems is essential for successful mitochondrial outer membrane fusion to take place (Cavellini et al., 2017). Thanks to these dynamics, mitochondrial networks quickly adapt to the energy needs of the cell (Schrepfer and Scorrano, 2016), maintain the cell's redox potential (Willems et al., 2015) and interact with most if not all cellular organelles (Lackner, 2019). Perhaps the oldest and most famous mitochondrial partner identified is the Endoplasmic reticulum, as their functional relationship was established back in the 90's (Vance, 1990). Since then the field has been booming thanks to different technologies allowing us to characterize organelle contacts and the proteins that participate in these interactions. From systems-level spectral imaging (Valm et al., 2017) to split fluorophores proximity detection (Shai et al., 2018), the sky is the limit. Recently, a new study shed the light on Peroxisome-Mitochondria contacts, which were quite elusive until now. Using split Venus complementation assays they identified two novel tethers between Peroxisomes and Mitochondria: the peroxisomal membrane protein Pex34 and the yeast mitofusin Fzo1 (Shai et al., 2018). This study particularly sparked our interest as Fzo1 has never

been suggested (or yet proven) to be located on membranes other than mitochondria where it serves its primary purpose of tethering and driving mitochondrial outer membrane homotypic fusion. The mitofusin is now placed at the heart of Peroxisome-Mitochondria contacts but this discovery is still riddled with question marks which I tried to find answers to during my thesis. By characterizing Fzo1-mediated Peroxisome-Mitochondria contacts and deciphering the mechanisms behind their regulation, we ultimately aimed to uncover their physiological function in the cell.

II- 3 letters 1 system: U-P-S

1) The Ubiquitin Machinery

Ubiquitin is a small polypeptide of 76 amino acids that covalently links to other polypeptides or to itself to form chains that can get disassembled, like “Lego” pieces. This process of ubiquitination involves a multistep enzymatic cascade (Hershko and Ciechanover, 1998) where, at least, 3 distinct enzymes participate in attaching one or more ubiquitin subunits to lysine residues of a target protein (Komander and Rape, 2012; Clague et al., 2015). The three types of enzymes driving this reaction include a single ubiquitin activating enzyme E1, several ubiquitin-conjugating enzymes E2s and even more ubiquitin ligase E3s which contribute to the broad substrate specificity of ubiquitination (**Fig1**). Once ubiquitin gets activated by the E1, it is next transferred to the cysteine residue of an E2 through a thioester bond (Stewart et al., 2016). The E3 then facilitates the transfer of the ubiquitin from the E2 to the lysine residue of the target substrate through an iso-peptide linkage (**Fig1**). This transfer occurs directly from the E2 to the substrate with RING (Really Interesting New Gene)-domain E3s which constitute the largest family of E3s (approx. 600 in the human genome). With HECT (Homologous to the E6-AP Carboxyl Terminus) or RBR (Ring Between Ring)-domain E3s, ubiquitin is first conjugated to the catalytic cysteine of the E3 through a thio-ester linkage before conjugation to the lysine of the target substrate (Zheng and Shabek, 2017). Ubiquitination is a complex yet reversible reaction, many deubiquitinating enzymes (DUBs) are present in the cell (approx. 100 in the human genome).

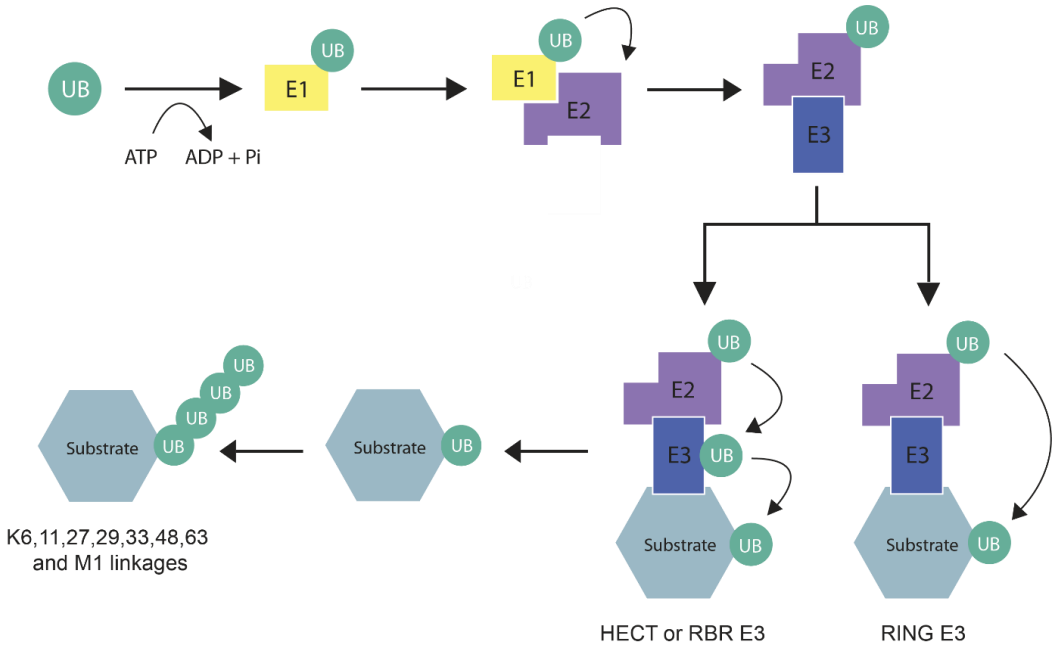

Fig1: The Ubiquitination cascade. An ubiquitin activating enzyme E1, promotes a thioester bond between the C-terminus of ubiquitin and the catalytic cysteine of a conjugating enzyme E2. The ubiquitin ligase then links the loaded E2 to a specific substrate. The direct (RING E3s) or sequential (HECT or RBR E3s) transfer of ubiquitin from the E2 to the substrate then induces the formation of an isopeptide bond between the C-terminus of ubiquitin and a target lysine of the substrate. With its seven lysines or its N-terminal methionine, ubiquitin can itself be the target of the ubiquitination cascade. This results in the formation of chains with diverse ubiquitin linkages that can trigger very distinct functions. Adapted from:(Alsayyah et al., 2020).

Substrates can be modified in a variety of ways such as mono-ubiquitination or poly-ubiquitination at one or different lysine residues (Fig 1). Ubiquitin chains can be homotypic or heterotypic as Ubiquitin itself contains 7 lysine residues (K6, 11, 27, 29, 33, 48, 63) and an amino terminus which allows the formation of polymeric ubiquitin chains (Yau and Rape, 2016). Discoveries that ubiquitin can also be phosphorylated, acetylated or SUMOylated widened the field of possibilities (Swatek and Komander, 2016; Stewart et al., 2016; Kwon and Ciechanover, 2017; Ohtake and Tsuchiya, 2017; Liu et al., 2015). The ubiquitin bible once known as “The Ubiquitin code” (Komander and Rape, 2012) is now “The expanded Ubiquitin code” (Swatek and Komander, 2016). A myriad of combinations of ubiquitin linkages are possible many of which leading to distinct outcomes (Kwon and Ciechanover, 2017; Ohtake and Tsuchiya, 2017). Nonetheless, two types of chains are predominant: K48-linked chains which account for more than 50% of all linkages in the cell and K63-linked chains (Swatek and Komander, 2016). K63-linked poly-ubiquitin chains can regulate the subcellular localization of target molecules, their affinity to partner proteins and/or their activity (Liu et al., 2015; Kwon and Ciechanover, 2017; Spence et al., 1995). In contrast, K48-linked ubiquitination leads to the degradation of target substrates by the 26S proteasome, a 2.5mDa multi-subunit enzyme complex that breaks down peptide bonds in its proteolytic core (Bard et al., 2018).The proteasome itself is made up of 2 subcomplexes: A 20S catalytic core protease (CP) associated with one or two 19S terminal regulatory particles (RP) (Groll et al., 1999, 1997). Binding of one or two 19S to the barrel-shaped 20S core form an enzymatically active proteasome (**Fig 2**). The RP’s recognize ubiquitinated targets, remove the ubiquitin chains and probably play a role in the unfolding and translocation to the interior of the CP for destruction by peptidases (Marshall and Vierstra, 2019). Proteasomes are notoriously efficient due to their dynamic behavior: by dissociating into free RP and CP sub-particles that shuttle between the cytoplasm and nucleus re-locating in response to different growth, development or environmental

challenges (Marshall et al., 2016; Russell et al., 1999; Marshall and Vierstra, 2019). For that, it is no surprise that most proteins are degraded by the Ubiquitin Proteasome System (UPS), making it the primary cytosolic "predator" of misfolded and damaged proteins.

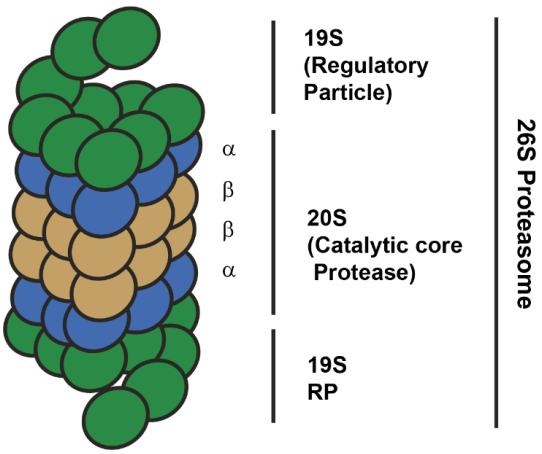

Fig2: Schematic representation of the 26S Proteasome. The 26S proteasome consists of: the 20S catalytic core particle (CP) which is composed of 2 outer α-rings (in blue) and two inner β-rings (in beige) and the 19S Regulatory Particle (RP or PA700). The RP lid is in green.

2) Roles of the UPS in the cell

Through protein degradation and quality control, the UPS plays an important role in many cellular processes such as signal transduction, cell cycle progression, cell death, immune responses, development, membrane homeostasis and protein quality control at specific organelles in which proteasomes degrade short-lived or structurally aberrant proteins.

2.1) ER-associated Degradation (ERAD)

Newly synthesized proteins enter the ER in an unfolded state through the translocon (Rapoport, 2007). As these proteins need to arrive at their site of action in a functional state, the ER machinery has to fold them before releasing them to their final destination along the secretory pathway (or outside the cell). However, a significant fraction of newly synthesized polypeptides fails to acquire a native conformation (Hartl and Hayer-Hartl, 2009). The accumulation of such misfolded proteins in the lumen and membrane of the ER causes ER stress, a condition common to several diseases (Walter and Ron, 2011a) that may even lead to cell death (Yagishita et al., 2005; Eura et al., 2012; Francisco et al., 2010).

Thanks to pioneering work from different labs, we now know that aberrant proteins found in the lumen and the membrane of the ER are extracted and degraded in the cytoplasm by the

ubiquitin–proteasome pathway via a process termed ER-associated degradation (ERAD) (Hiller et al., 1996; Lippincott-Schwartz et al., 1988; Ward et al., 1995; Jensen et al., 1995; Sommer and Jentsch, 1993; Wiertz et al., 1996). Almost 10 years later, many different ERAD clients were identified and in turn multiple branches for of ERAD were discovered each with a distinct specificity for different classes of misfolded proteins (Vashist and Ng, 2004; Carvalho et al., 2006; Christianson et al., 2012; Taxis et al., 2003). Nonetheless, the general components of this system are highly conserved across eukaryotic evolution and regardless of the branch, the same sequence of events awaits all ERAD substrates. The first step of the process is the recognition of a substrate in the crowded ER environment. The second step is retro-translocation in which the substrate is transported from the ER back to the cytoplasm. Finally, the substrate will be ubiquitinated by a membrane-associated ubiquitin ligase (**Fig3**). This will target the extraction of the ubiquitinated substrate in an ATP-dependent manner and it's degradation by the proteasome in the cytoplasm. The E3's involved in ERAD are best characterized in yeast (**Table 1**) such as the Doa10 (Swanson et al., 2001) and Hrd1 (Bordallo et al., 1998; Bays et al., 2001) which assemble into complexes, each responsible for the degradation of a class of ERAD substrates (Carvalho et al., 2006). In mammalian cells the best-studied E3 ligases are Hrd1 and Gp78 (**Table 1**) and they are both homologous to yeast Hrd1 (Nadav et al., 2003; Kikkert et al., 2004). As the E3 ligase complex specificity appears to be determined by the location of the misfolded region in a substrate relatively to the ER membrane, we can distinguish 3 different types of ERAD-substrates: ERAD-C, ERAD-L, and ERAD-M (**Fig 3**). ERAD-C substrates are degraded via the Doa10 complex while ERAD-L and ERAD-M are degraded via the Hrd1 complex (Taxis et al., 2003; Carvalho et al., 2006; Vashist and Ng, 2004).

Complex	Component	Function	Mammalian homolog
Hrd1 complex	Hrd1	E3 ligase activity/retro-translocation	HRD1, gp78
	Hrd3	Substrate recognition, Hrd1 stability	SEL1
	Yos9	Substrate recognition	OS9, XTP3-B
	Kar2	Chaperone activity, substrate recognition	Bip
	Usa1	Hrd1 and Der1 oligomerization	HERP
	Der1	Recognition/transfer of substrate to Hrd1/retro-translocation	Derlin-1, -2, -3
Doa10 complex	Doa10	E3 ligase activity	TEB4
	Ubc6	E2 ubiquitin-conjugating activity	Ubc6, Ubc6e
Common to Hrd1 and Doa10 complexes	Ubc7	E2 ubiquitin-conjugating activity	UBE2G1, UBE2G2
	Cue1	Recruitment and activation of Ubc7	
	Ubx2	Membrane-recruiting factor for Cdc48	UBXD8
	Cdc48	Substrate retro-translocation and membrane extraction	p97/VCP
	Npl4	Cdc48 cofactor	NPL4
	Ufd1	Cdc48 cofactor	UFD1

Table 1: Components of the yeast E3 ligase complexes and their mammalian counterparts. Adapted from (Ruggiano et al., 2014).

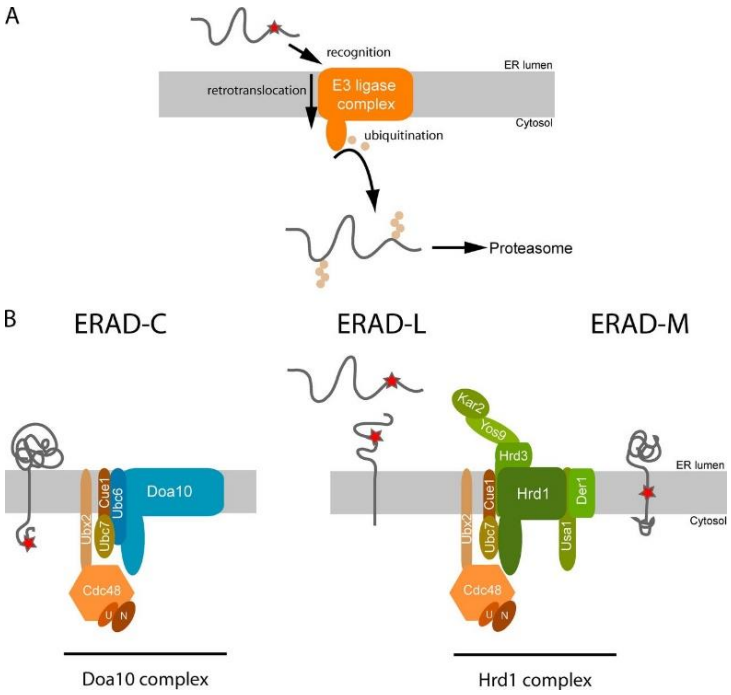

Fig 3: The different types of ERAD substrates. **(A)** ERAD events of a generic misfolded substrate in the ER lumen. The embedded E3 ligase complex coordinates substrate recognition,

retro-translocation, and ubiquitination. **(B)** *S. cerevisiae* E3 ligase complexes involved in ERAD and their possible types of substrates. ER proteins with a misfolded domain in the cytoplasm (ERAD-C substrates) are degraded by the Doa10 complex. Proteins with luminal (ERAD-L) or intramembrane (ERAD-M) misfolded domains are degraded via the Hrd1 complex. Misfolded domains of the proteins are indicated by a red star. Ubiquitin is represented by small beige circles. The Cdc48 cofactors Npl4 and Ufd1 are represented by N and U respectively. Adapted from: (Ruggiano et al., 2014).

Some late components such as the Cdc48/p97 ATPase complex which act at the end of ERAD, are common to all E3 ligase complexes thus to all ERAD branches. Furthermore, these "promiscuous" factors are not exclusively active at ER membranes they are also involved in similar processes at neighboring organelles such as mitochondria.

2.2) Mitochondria-associated degradation (MAD)

Mitochondrial Associated Degradation (MAD) is a similar quality control system that takes place at the mitochondrial outer membrane (MOM) (Braun and Westermann, 2017). MAD is thought to employ the same machinery as ERAD to extract proteins from the outer membrane and trigger their degradation by the UPS (Ye et al., 2001). This machinery relies on the AAA-ATPase Cdc48/p97, one of the most abundant cellular proteins which is highly conserved in all eukaryotes. Cdc48 works in concert with several identified co-factors including Ufd1, Npl4, Ubx2 and Doa1 in both ERAD and MAD (Ye et al., 2001; Neuber et al., 2005; Bruderer et al., 2004; Wu et al., 2016; Meyer et al., 2000) to recognize poly-ubiquitinated substrates, dissociate them from their protein complexes or respective membranes and allow their turnover by the proteasome (Xia et al., 2016; Bodnar and Rapoport, 2017).
Mitochondrial proteins are synthetized as precursors on cytosolic ribosomes before entering mitochondria through the TOM (Translocase of Outer Membrane) and TIM (Translocase of inner membrane) complexes (Neupert, 2015). Consequently, these imported proteins are under heavy surveillance at different levels to avoid any mitochondrial dysfunction.

The correct folding and escort of proteins on their way to mitochondria is usually ensured by chaperones (such as HSP70 and HSP90) (**Figure 4, Panel I**). During import, the proteins that clog the TOM import channel are recognized and ubiquitinated by a mitochondrial pool of Ubx2 before being extracted by the Cdc48-Ufd1-Npl4 complex and degraded by the proteasome in the mitoTAD pathway (**Figure 4, Panel I**) (Mårtensson et al., 2019). At the level of cytosolic ribosomes, the translation products remain under surveillance by an elaborate Ribosomal

Quality Control (RQC) system in order to maintain mitochondrial homeostasis (**Figure 4, Panel II**) (Izawa et al., 2017; Brandman and Hegde, 2016). Upon stress or when mitochondrial protein import is defective, several mitoprotein-induced stress responses such as mPOS, UPRam and mitoCPR are triggered (**Figure 4, Panel III**). The AAA-ATPase Msp1 is an AAA-ATPase which seems to play a key role in both mitoCPR pathway and MAD-TA (Mitochondrial Associated Degradation of Tail Anchored proteins) where it extracts tail-anchored proteins from mitochondrial membranes and transfers them to the ER where they are treated as ERAD substrates (**Figure 4, Panel IV**).

All of these processes are detailed in our review on the regulation of mitochondrial homeostasis by the ubiquitin proteasome system (Alsayyah et al., 2020).

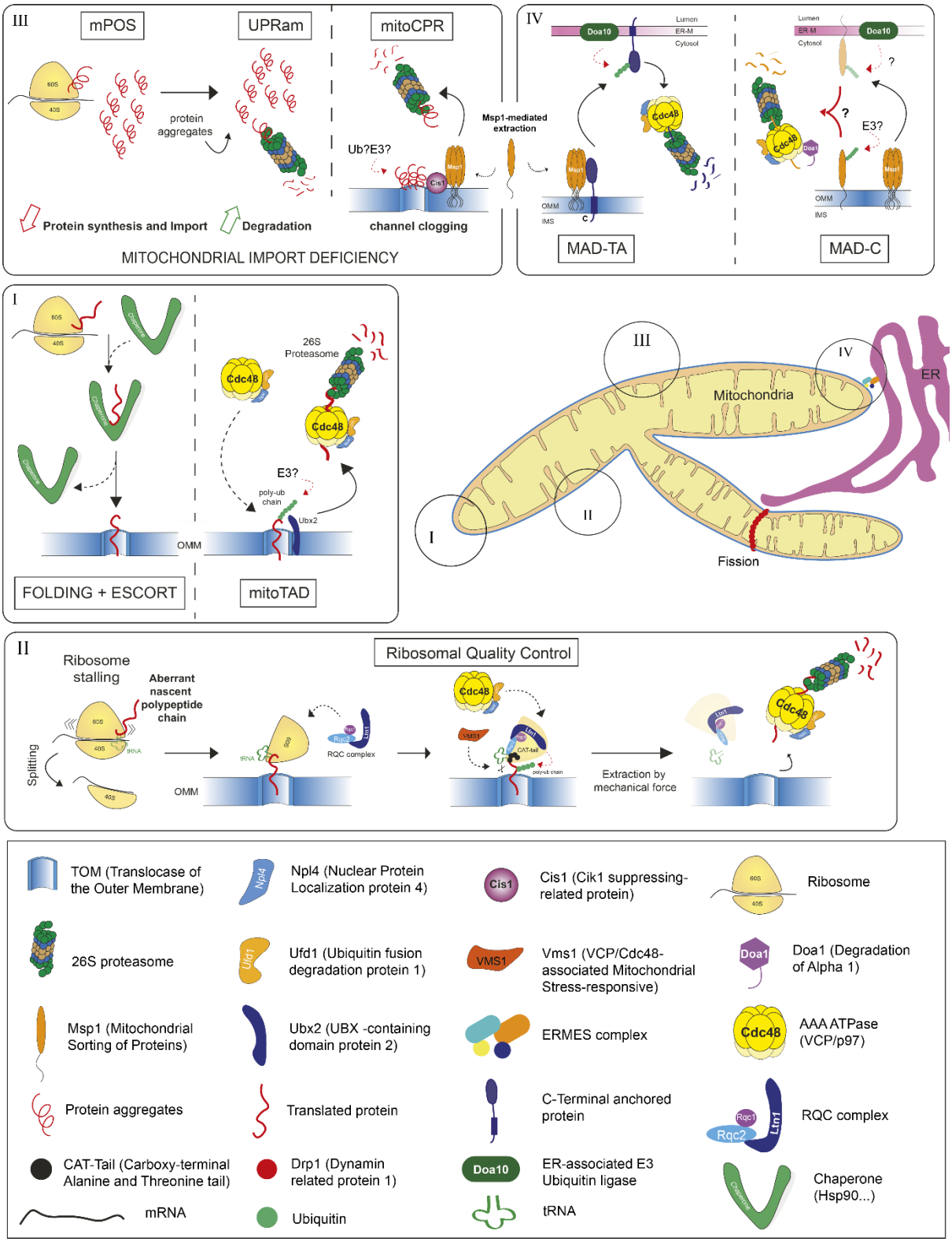

Fig4: UPS-mediated degradation at the mitochondrial outer membrane. Mitochondrial morphology is maintained by ongoing events of fusion and fission and intimate contacts with the ER. The UPS, through E3s that are known (Ltn1, Doa10, Mdm30) or yet to be identified, safeguards the transport of proteins inside the organelle but also specific proteins embedded in outer membranes. (I) In the absence of cellular stress, proteins encoded by the nuclear genome

are synthesized, folded and escorted to mitochondria. Import through the TOM complex is continuously monitored by the TOM Associated Degradation (mitoTAD) pathway. (II) Upon ribosomal stalling, the Ribosomal Quality Control (RQC) pathway is activated which also prevents clogging of the TOM channel. (III) When the level of stress increases and the mitochondrial import is inhibited, the mitochondrial Precursor Over-accumulation Stress (mPOS) initiates the Unfolded Protein Response Activated by the mis-targeting of proteins (UPRam) which allows clearance of protein aggregates. If clogging of the TOM channel persists, the Mitochondrial Compromised Protein import Response (mitoCPR) is activated. (IV) Two Mitochondrial Associated Degradation (MAD) pathways that may share some common features also target mis-targeted Tail Anchored proteins (MAD-TA) and C-terminally anchored outer membranes proteins (MAD-C). Adapted from: (Alsayyah et al., 2020).

2.3) Quality control at the Plasma membrane and the Endo-Lysosome system

The endo-lysosomal protein quality control system includes both cytosolic and membrane-bound quality control machineries working hand in hand to facilitate the downregulation of targets in response to substrate-induced trafficking cues and environmental stresses (Zhao et al., 2013b; Babst, 2014). This response also provides a mean to take the heat off from the ERAD system as target proteins are eventually sorted into the lumen of the lysosome for degradation instead of joining the ER secretory pathway. The dynamic nature of the endocytic pathway also allows sampling of the same protein at multiple locations along the endocytic pathway through a variety E3 ubiquitin ligases and their adaptor proteins (Léon and Haguenauer-Tsapis, 2009; Sardana et al., 2018; Puca and Brou, 2014; Hovsepian et al., 2018) (**Table 2**).

The remodeling of plasma membrane (PM) proteins is the first quick adaptation response to environmental changes. The yeast master ligase Rsp5, plays a central role in the ubiquitin-dependent endocytosis of most cell surface proteins (Hein et al., 1995; Wang et al., 1999; Belgareh-Touzé et al., 2008). This soluble HECT E3 is recruited to the target PM protein in response to specific cues or via an adaptor protein which interacts with the target (Léon and Haguenauer-Tsapis, 2009). In addition, Rsp5 and its adaptors are key regulators not only at the PM but also at post-endocytic ubiquitination steps (in the TGN, endosomes, and the vacuole) (Sardana et al., 2018; Léon et al., 2008; Hovsepian et al., 2017).

System	Mammals	Yeast	Component
Plasma Membrane	Nedd4, Nedd4-2, Itch WWP1, WWP2, Smurf1, Smurf2, CHIP, Cbl, RFFL, MARCH1/2/3/8	Rsp5	E3 ligases
	ARRDC1,2,3,4 TXNIP	Art1-10, Bul1, Bul2, Rcr1	Adaptors
Golgi and Endosomes	Nedd4, Nedd4-2, Itch WWP1, WWP2, Smurf1, Smurf2, CHIP, Cbl, RFFL, MARCH1/2/3/4/8/9/11, ZNRF1, ZNRF2, RNF152, RNF167	Rsp5, Pib1, Tul1	E3 ligases
	NDFIP1, NDFIP2, ARRDC3, ARRDC4	Bsd2, Ear1, Tre1, Tre2, Sna3, Sna4, Art3/4/6/9	Adaptors
Lysosome/ Vacuole	Nedd4, CHIP, MARCH1/2/3/4/8/9/11, ZNRF1, ZNRF2, RNF152, RNF167	Rsp5, Pib1, Tul1	E3 ligases
	NDFIP1, NDFIP2, ARRDC3, ARRDC4	Ssh4, Sna3, Sna4, Rcr2	Adaptors

Table 2: E3 ligases and adaptors active along the Endo-Lysosomal system in Yeast and Mammals. Adapted from (Sardana and Emr, 2021).

The mammalian counterparts that mediate PM target protein ubiquitination include the Nedd4 (Neural precursor cell expressed developmentally downregulated 4) family of HECT ubiquitin ligases (such as WWP1/2, Nedd4-2, Itch, Smurf1/2) all of which contribute to the downregulation of multiple ion channels and transporters (Piper et al., 2014; Wang et al., 2020). Rsp5 (yeast) and Nedd4 (human) are closely related and they recognize the PPxY (proline rich) motifs in their target or adaptor proteins, interacting with it via their own WW domains (Léon and Haguenauer-Tsapis, 2009). Other types of E3s also participate in ubiquitinating PM proteins such as the U-Box E3 CHIP and the RING E3 RFFL among others (Tang et al., 2019; Okiyoneda et al., 2018; MacGurn, 2014) (**Table 2**).

Adaptor proteins of E3 ligases are extremely important in the regulation of PM targets as they can play the role of signaling scaffolds as it is the case for mammalian α -arrestins (or ARRDCs) (Puca and Brou, 2014; Shenoy and Lefkowitz, 2011) (**Table 2).**

As mentioned in the beginning of this section, quality control at the PM also intertwines with the machineries that recognize damaged cytoplasmic proteins. This is especially true in mammalian cells where the chaperones Hsp70 and Hsp90 and the ubiquitin ligase CHIP were found to be important for PM quality control (Apaja et al., 2010; Okiyoneda et al., 2011). These chaperones recognize unfolded cytoplasmic regions of the cell surface proteins and recruit CHIP to ubiquitinate the target which will be degraded via the MVB pathway.

2.4) Protein sorting and endocytosis

The degradation of cell surface proteins is mediated by the MVB pathway after the ubiquitinated targets are recognized by a conserved family of endocytic adaptors called the Epsins. These adaptor proteins like Ede1/End3 in yeast (EPS15 and EPS15R in mammals) trigger clathrin-mediated endocytosis which delivers the ubiquitinated protein to an early endosome (Haglund and Dikic, 2012) (**Fig 5-1**). This is often the canonical method by which a cell removes membrane proteins including cell surface receptors. Once at the endosome, these proteins that were just sorted through the endosomal system are now called "cargo" and have two possible fates: recycling to the cell surface either directly or indirectly via the trans-Golgi network (TGN) or continuing to the vacuole for degradation (**Fig 5-2, 5**). It is thought that competing de-ubiquitination and re-ubiquitination reactions at the endosome are key to deciding the fate of the cargoes (Piper et al., 2014). If ubiquitin wins, the cargo will be recognized and captured by the ESCRT (endosomal sorting complex required for transport) machinery. This group of evolutionary conserved complexes (ESCRT-0, I, II, III, and Vps4 AAA-ATPase) sorts ubiquitin-tagged transmembrane proteins into vesicles that bud into the lumen of the endosome generating intralumenal vesicles (ILVs) (Hurley, 2010) (**Fig 5-4**). The ESCRTs are also in charge of the formation of ILVs by a membrane deformation event opposed from all other vesicle formation events of the cell. The presence of ILVs is indicates that we have late endosomes, which are also called multivesicular bodies (MVBs). After the MVB is fully matured (all the protein sorting is done), the limiting membrane of the MVB fuses with the vacuolar membrane and releases the ILVs into the lumen of the vacuole (**Fig 5-7**). The lumen of the vacuole contains many hydrolases and lipases that degrade the lipids and proteins contained within the vesicles (**Fig 5-7**). Protein sorting at the TGN also feeds into the MVB pathway.

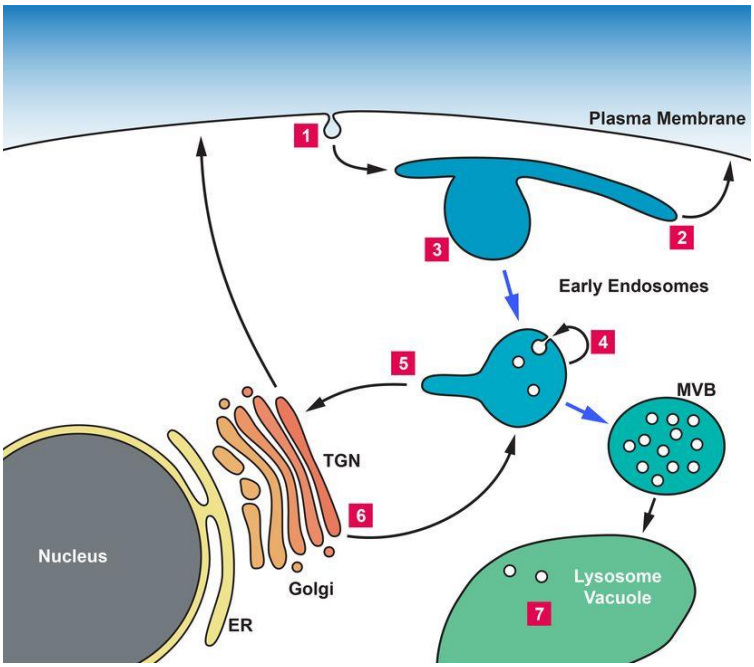

Fig5: Clathrin mediated endocytosis in Eukaryotic cells. **Step 1:** clathrin-mediated endocytosis delivers the ubiquitinated protein to an early endosome following recognition of ubiquitinated substrate. **Step 2 and 5:** Once at the endosome, the cargo has two options: either recycling to the cell surface (directly in 2) or via the trans-Golgi (indirectly in 5) or continuing to the vacuole for degradation. **Step 3:** Proteins are "re-checked" at the endosome in order to avoid degrading cell surface proteins that temporarily appear unfolded but are just temporarily "flexing". **Step 4:** the ubiquitinated cargo is captured by the ESCRT machinery and we can observe the presence of MVBs. **Step 5:** The MVB pathway is in turn fed by the proteins in the endosome as well as newly synthesized transmembrane proteins that passed the ER QC with the help of the retromer protein complex. **Step 6:** Unfolded proteins are recognized by the TGN QC system and tags them with ubiquitin. Ubiquitinated proteins are then bound by sorting receptors such as the GGA proteins that concentrate the ubiquitinated cargoes into vesicles destined for the endosome. **Step 7:** When all the protein sorting has occurred, the limiting membrane of the MVB fuses with the vacuolar membrane and releases cargo into the lumen of the vacuole which is full of hydrolases and proteases consequently destroying the delivered cargo. Adapted from: (Babst, 2014).

To conclude, endosomes, MVBs and lysosomes regulate signaling, secretion, and the degradation of receptors and other cellular components. Alternatively to degradation, MVBs can also fuse with the plasma membrane and release their ILVs into the extracellular environment as exosomes which are a hallmark of cell-to-cell communication (Simons and Raposo, 2009). Vesicles are also involved in inter-organelle communication as it is the case

between mitochondria and the endo-lysosomal system for example (Soubannier et al., 2012). Indeed, mitochondria were shown to form specific vesicles (MDVs) targeted to the MVB where they finally fuse with lysosome for degradation. This form of vesicle formation may be a rapid response to stress in order to preserve the integrity of the organelle (McLelland et al., 2014; Sugiura et al., 2014). MDV formation is a faster and less drastic process to handle damage and could be considered as a first response to mitochondrial stress (McLelland et al., 2014; Sugiura et al., 2014). However, when the damage is too important the cell relies on another process to remove entire parts of damaged mitochondria.

2.5) Ubiquitination and Mitophagy

Mitophagy is a selective form of autophagy that leads to the clearance of unnecessary or damaged mitochondria by the lysosomal/vacuolar compartment. The mitochondria destined to be cleared are recognized by the autophagic machinery and subsequently enveloped by a double membrane structure called the autophagosome. The autophagosome then fuses with the lysosome so its mitochondrial content gets degraded by lysosomal proteases (Palikaras et al., 2018). The autophagic machinery relies on 2 factors: Atg8 (LC3 and GABARAP in mammals) and Atg32 for Autophagy related protein 32. Atg8 is an ubiquitin like protein that has the exceptional ability to conjugate itself to lipids (Wen and Klionsky, 2016). This allows Atg8/LC3 to be lipidated to the membrane of the autophagosome where it is exposed. After induction of mitophagy, Atg32 is phosphorylated and interacts with the soluble protein adaptor Atg11 (Aoki et al., 2011). Atg11 targets the complex to the pre-autophagosomal assembly site where Atg32 can interact with lipidated Atg8 that is anchored to the membrane of the autophagosome (Okamoto et al., 2009). Mitophagy mediated by such receptors occurs in all eukaryotes including yeast. Even though receptor-mediated mitophagy is distinct from ubiquitin-dependent mitophagy, its regulation still relies on ubiquitin.

In ubiquitin-dependent mitophagy the modifier (ubiquitin) is itself modified by phosphorylation (Kane et al., 2014; Kazlauskaite et al., 2014; Koyano et al., 2014). This phospho-ubiquitination process involves the RBR-type ubiquitin ligase PARKIN and it's activating kinase the mitochondrial targeted protein kinase PINK1 (Phosphatase and Tensin homolog (PTEN)-Induced putative Kinase 1) (**Figure 6A**). When the $\Delta\Psi m$ drops down, PINK1 is trapped on the outer membrane of depolarized mitochondria where it forms a dimer in association with the TOM complex (**Figure 6A)**. At this stage, PINK1 activates and induces its autophosphorylation (Okatsu et al., 2012, 2013, 2015). A cascade of PINK1-dependent phosphorylation then targets

the conserved Serine 65 residue of the ubiquitin ligase PARKIN on its Ubl (Ubiquitin like) domain (Koyano et al., 2014; Kane et al., 2014). PARKIN, is a RING/HECT hybrid E3 of the RBR family of ubiquitin ligases (**Figure 6B**). Located in the cytoplasm in a tightly packed autoinhibited state (**Figure 6B, Inactive form**), PARKIN begins its activation after binding to phospho-ubiquitin (**Figure 6B, active form**) (Spratt et al., 2013; Trempe et al., 2013; Wauer and Komander, 2013). This induces the transfer of PARKIN from the cytosol to depolarized mitochondria in a feed-forward amplification process (Ordureau et al., 2014) where the two enzymes trigger the phospho-ubiquitination of numerous proteins from the mitochondrial outer membrane such as the voltage anion channels VDAC(1, 2, 3), the GTPases MIRO1 and 2, TOM70 and mitofusins (MFN1 and 2) (Gegg et al., 2010; Narendra et al., 2008; Tanaka et al., 2010a; Matsuda et al., 2010; Chan et al., 2011; Chen and Dorn, 2013; Sarraf et al., 2013; Rose et al., 2016). The phospho-ubiquitin tag is then recognized and bound by ubiquitin binding receptors such as p62, OPTN (optineurin) or NDP52 (nuclear domain 10 protein 52) (Nguyen et al., 2016). These adaptor proteins contain an ubiquitin interacting motif and an AIM/LIR motif that connect ubiquitinated proteins from the outer membrane to Atg8-like proteins on the auto-phagosomal membrane. Damaged mitochondria are then associated to autophagosomes (engulfment) before fusion and degradation by the lysosome (**Figure 6A**).

MFN1 and 2 were shown to be ubiquitinated by PARKIN and degraded by the proteasome in a p97 dependent manner leading to reduced mitochondrial fusion followed by segregation of defective mitochondria, a characteristic of mitophagy (Tanaka et al., 2010b) (**Figure 6C**).
On the other hand, the role of ubiquitin in yeast mitophagy remained elusive with no E3 ligase or ubiquitination substrates identified until Rsp5 was shown to ubiquitinate Mdm12 and Mdm34, two mitochondrial outer membrane proteins (bridging the ER to mitochondria) in order for mitophagy to be efficient (Belgareh-Touzé et al., 2017).
At this point it is clear that Rsp5 does not vainly hold the title of the yeast master ligase as it crucial to the maintenance of cellular and homeostasis. But in reality, the dominance of Rsp5 goes way beyond the organellar scale into the organization and composition of the biological membranes that constitute them.

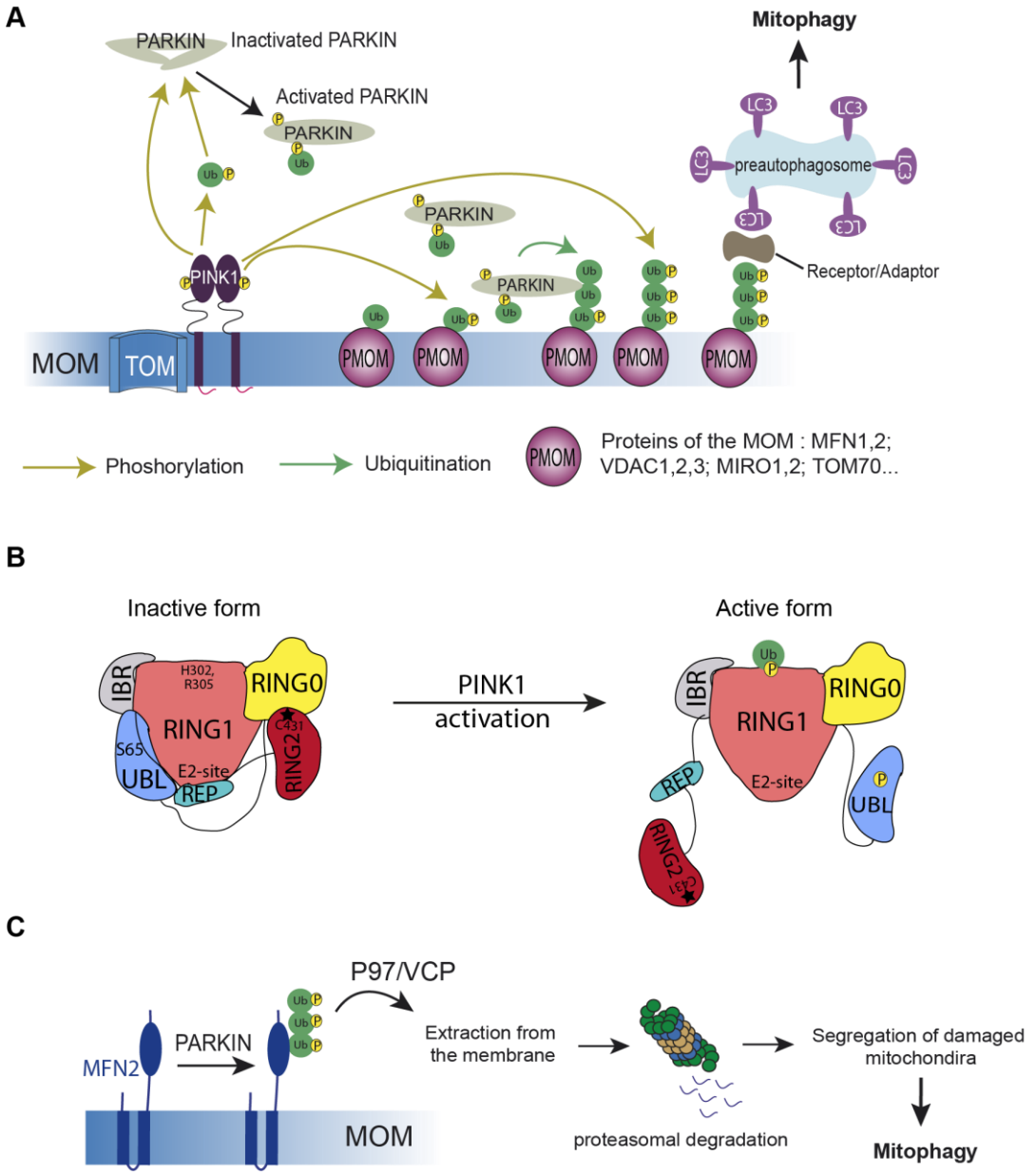

Fig6: Ubiquitin-dependent mitophagy in metazoans. **(A)** In damaged mitochondria that have lost their membrane potential, the import of PINK1 is blocked which induces its accumulation on the mitochondrial outer membrane (MOM). Autophosphorylation, dimerization and association with the TOM complex activate PINK1 which phosphorylates ubiquitin either free or already conjugated to substrates. Parkin activation leads to its recruitment to the mitochondria where it associates with phospho-ubiquitinated substrates and induces massive ubiquitination of proteins from the outer membrane. Phospho-ubiquitinated substrates associate with ubiquitin binding adaptors that themselves bind to LC3 on pre-autophagosomal membranes. After full engulfment in the autophagosome that fuses with the lysosome, mitochondria are degraded and their components recycled. **(B)** Transition of PARKIN from the

inactive to active state initiates with the binding of phospho-ubiquitin to His302 and Arg305 of RING1. This shifts the Ubl which is phosphorylated by PINK1 on Ser65, giving robust access to the E2 binding site on RING1. Since RBR ligases function like HECT E3s, ubiquitin from the loaded E2 can be transferred to the catalytic Cys431 of RING2 that became accessible after its dissociation from RING0. **(C)** Ubiquitination and degradation process of MFN1 and MFN2 by PARKIN leading to mitophagy. Adapted from: (Alsayyah et al., 2020).

III- Lipids and Membrane Homeostasis

Biological membranes are a complex mix of proteins and lipids forming the boundary between the cell and it's environment and compartmentalizing biochemical processes in their respective organelles (van Meer et al., 2008; Bigay and Antonny, 2012). They are much more than simple passive solvents for protein-mediated activity, in fact membranes contribute to cellular functionality at all relevant scales: individual membrane lipids act as substrates for enzymes and signaling molecules (Moravcevic et al., 2012), lipid assemblies regulate protein recruitment and interactions (Sezgin et al., 2017), and bulk membrane properties determine protein structure and function (Marsh, 2008). Thus, it is no surprise that the cell must monitor the chemical composition as well as the physicochemical membrane properties such as fluidity, permeability, phase behavior, and surface charge density in order to maintain organelle identity and to sustain cellular fitness (Bigay and Antonny, 2012; Ernst et al., 2018; Harayama and Riezman, 2018). The lipidome of a eukaryotic cell comprises hundreds, if not thousands, of lipid species and it can be remodeled upon dietary perturbation, by the growth phase, and in response to external cues such as temperature or nutrient availability (Shevchenko and Simons, 2010; Casanovas et al., 2015; Levental et al., 2020). Thanks to this diversity, biological membranes are highly plastic and adaptive.

1) The lipid repertoire

Hundreds to thousands of lipid molecules are synthetized by Eukaryotic cells. They differ from each other in their molecular structures, physicochemical properties, and molar abundances. This stunning diversity derives from the combinatorial complexity of the lipid "building blocks" (van Meer et al., 2008) (**Fig 7**). Although combinatorial permutations of these lipid building blocks could theoretically generate tens of thousands of lipid species (Shevchenko and Simons, 2010), in real life membranes typically use "only" up to 1000 different species.

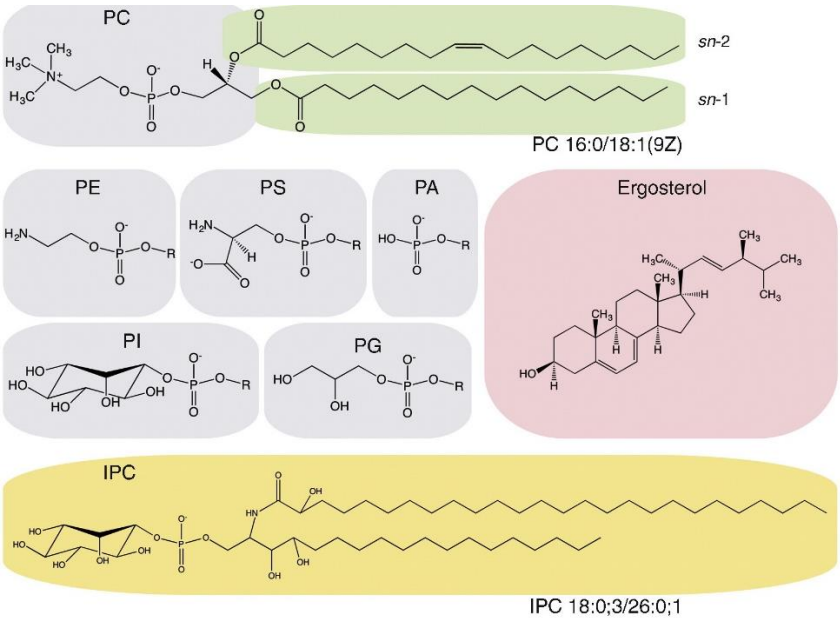

Fig7: The three major categories of membrane lipids: glycerophospholipids (GPL) (in green and gray), sterols (in pink), and sphingolipids (SL) (in yellow). Classes of glycerophospholipids are defined by the headgroups (in gray) attached to the acyl chain backbone. The acyl chains (green) of the glycerophospholipids contribute to the species diversity within lipid classes. Sphingolipids also constitute a large category of lipids with diverse headgroups and acyl chains. Sterols (in pink) have a four-ring core structure also called steroid nucleus. Adapted from: (Ernst et al., 2016).

The cell's different lipid species can be categorized into 3 main classes: glycerophospholipids, sphingolipids, and sterols.

Glycerophospholipids and sphingolipids have a modular design featuring two apolar hydrocarbon chains (or acyl chains) and a hydrophilic headgroup. The acyl chains are fatty acids (FAs), fatty alcohols, or long-chain bases differing in length and the number and positions of double bonds and hydroxylation.

Glycerophospholipids (GPL) are the major structural lipids in eukaryotic membranes.

The head group of a glycerophospholipid can be modified by the addition of various chemical moieties such as choline, ethanolamine, serine or inositol in the phospholipid itself. Therefore, GPL branch from phosphatidic acid (PA) and are classified upon the structure of the PL head group leading to a number of different phosphatidyl lipids, such as phosphatidylcholine (PC), -ethanolamine (PE), -serine (PS), -glycerol (PG), -inositol (PI), or the unmodified phosphatidic acid (PA). Each of these phospholipid classes is defined by a shared structure but then includes

a battery of molecular species upon the length and degree of saturation in their acyl chains (double bonds). PC accounts for more than 50% of all phospholipids in most eukaryotes and usually contains one *cis*-unsaturated acyl chain, such as oleic acid (C18:1). The rigid kink of the *cis*-double bond lowers the packing density of the acyl chains, which increases membrane fluidity (Koynova and Caffrey, 1998).

Sphingolipids (SL) are the second most abundant structural lipid. Sphingolipids, unlike glycerophospholipids, are based on a lipid backbone, specifically sphingosine, which is amide-bonded to a fatty acid to form Ceramide its simplest representative.

Sterols are monohydroxy alcohols with a four-ring core structure or steroid nucleus showing a hydroxyl group (A-ring) and a small branched hydrophobic tail (D-ring). Cholesterol (Chol) is the most abundant sterol in animal tissues. In membranes, the rigid steroid backbone of cholesterol favors its interaction with SL. Chol-SL platforms are the basic element of lipid rafts. Sterols rigidify fluid membranes by reducing the flexibility of neighboring unsaturated acyl chains, thereby increasing membrane thickness and impermeability to solutes (the so-called condensing effect of sterols) (Brown and London, 1998).

The headgroups define the lipid class and are chemically diverse structures spanning from simple structures such as choline to complex oligosaccharide structures.

These different lipid species come together in biological membranes determining the physicochemical properties of these membranes.

2) Membrane Physicochemical properties

Three of the main membrane physicochemical properties are:

- **Membrane electrostatics** which depend on the fraction of negatively charged lipids (such as phosphatidylserine (PS) and phosphoinositides). As rudimentary as it may seem, electrostatics stringently controls the localization of peripheral proteins. In the cell, electrostatics seem to define two territories: membranes of the early secretory pathway whose cytosolic leaflet is weakly charged (ER, *cis*-Golgi), and membranes of the late secretory pathway whose cytosolic leaflet is highly charged (endosomes, PM) (Fairn et al., 2011; Bigay and Antonny, 2012; Levental et al., 2016; Holthuis and Menon, 2014).

- **Membrane viscosity** which depend on lipid packing. Biological membranes are not perfect, the geometrical arrangements of lipids depend on two factors:

a) The size of polar heads: phosphatidylethanolamine (PE) and diacylglycerol are defined as conical since their polar heads are smaller than that of phosphatidyl-choline (PC) which has a cylindrical shape (van den Brink-van der Laan et al., 2004; Janmey and Kinnunen, 2006)
b) The shape of the Acyl chains**:** An oleyl chain (C18:1) occupies a larger volume because the double bond induces a "kink" in the middle of the chain compared to a palmitoyl chain (C16:0) thus taking up more space.

Similarly to electrostatics, lipid-packing territories are defined: the early secretory pathway seems to combine loose lipid packing and low electrostatic, whereas membranes of the late secretory pathway seem to combine tight lipid packing and high electrostatics (Brügger et al., 2000; Holthuis and Levine, 2005; Klemm et al., 2009)

- **Membrane curvature** which is affected by the lipid composition in the membrane and the size of headgroups. Lipids that have a small head group and relatively large hydrophobic tail form concave structures whereas lipids that have a large head group and relatively small hydrophobic tail form convex structures (Ashery et al., 2014).

Those 3 parameters are pillars in lipid membrane biology, they are tuned in such a way that they contribute to the identity of cellular organelles. Interestingly, lipids are not distributed homogeneously throughout the main organelles of mammals and yeast. Within eukaryotic cells, the synthesis of structural lipids is actually geographically restricted. This localized lipid metabolism is the first determinant of the unique compositions of organelles.

3) Lipid biosynthesis and Regulation

Lipids have a pivotal role in membrane remodeling processes and their biosynthesis and turnover are tightly regulated. Membrane lipid biosynthesis in eukaryotic cells is orchestrated by four major metabolic modules: Fatty acid Metabolism, *de novo* glycerol-phospholipid synthesis and acyl chain remodeling, sphingolipid biosynthesis and sterol biosynthesis. The details of all these metabolic pathways will not be discussed in this thesis for simplification reasons but it is worth mentioning that the palette of Fatty Acids (FA) is a key determinant of the complexity of lipid compositions in biological systems.

The pool of available FAs is determined by *de novo* synthesis, FA uptake, activation, desaturation, elongation, and turnover. Following activation, FA-CoA esters can be subjected to further chemical modifications, including hydrocarbon chain extension and insertion of double bonds by desaturases to produce unsaturated FAs (UFAs). Through

combinations, the different pathways of FA biosynthesis can produce a wide repertoire of FAs serving as building blocks for making glycerol-phospholipids and sphingolipids. This available palette of FAs is a key determinant of the lipid compositional complexity in biological systems.

The rate by which lipids are synthesized and turned over can be regulated by a wide range of mechanisms. The first important determinant is the law of mass action, a mechanism which is commonly at play when a lipid metabolic precursor becomes exhausted or is not delivered to the subcellular location harboring the lipid enzyme. The second crucial determinant of lipid metabolic flux is enzyme abundance and activity, which is governed by an array of molecular mechanisms that span transcriptional and translational control (Goldstein et al., 2006; Henry et al., 2012), enzyme stability and controlled degradation (Foresti et al., 2013), post-translational (Breslow et al., 2010), protein–protein interactions, and protein–lipid interactions (Goldstein et al., 2006). The third crucial determinant of lipid metabolic flux is subcellular compartmentalization.

3.1) The ER: the main site of lipid synthesis

The endoplasmic reticulum (ER) is the cell's main lipid factory: the bulk of phospholipids, sterols and substantial amounts of storage lipids such as triacylglycerol are produced by this organelle (**Fig 8**). In addition, the ER synthesizes ceramide, the precursor of all sphingolipids. Although the ER is the main site of cholesterol synthesis, this lipid is rapidly transported to other organelles, mainly the Plasma membrane. Indeed, the ER - which resides at the beginning of the secretory pathway - displays only low concentrations of sterols and complex sphingolipids. The resulting loose packing of ER membrane lipids is consistent with the function of the organelle in the insertion and transport of newly synthesized lipids and proteins. Furthermore, the ER is the main supplier for a large percentage of membrane lipids in the Golgi and PM, which are distal secretory organelles having little to no capacity to produce their own lipids (Holthuis and Menon, 2014).

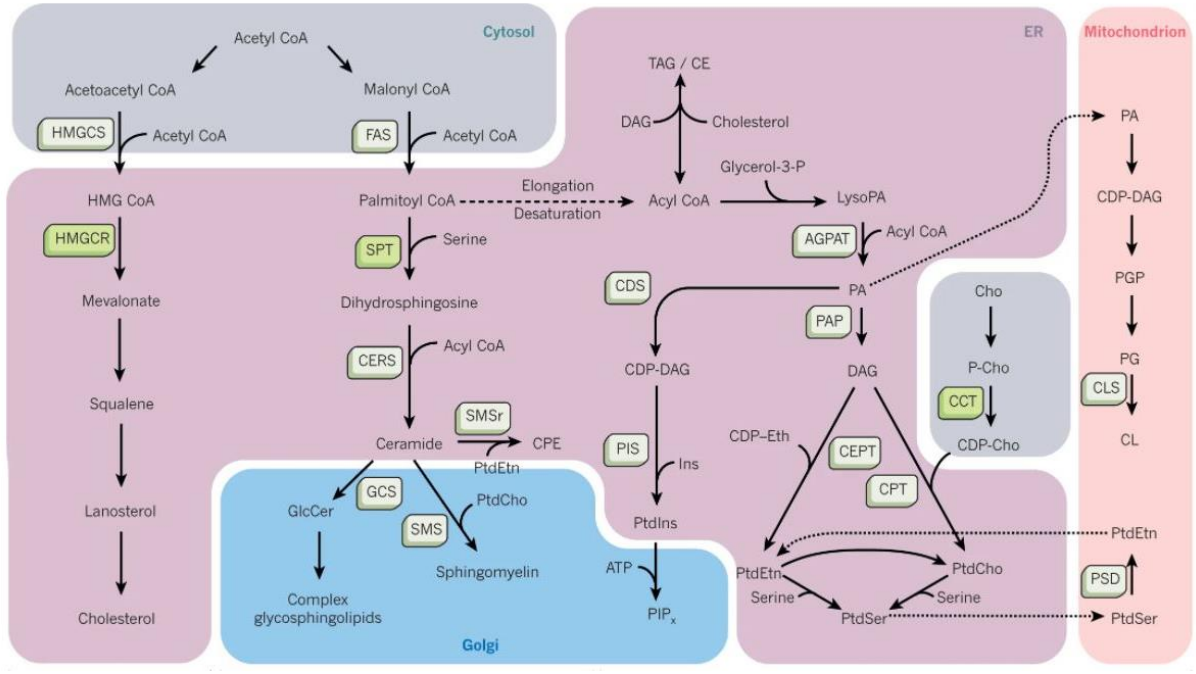

Fig8: Principal pathways for the production of sterols, sphingolipids and phospholipids in mammals. The bulk of phospholipids, sterols and substantial amounts of storage lipids such as triacylglycerol are produced by the ER (in light purple). The ER is the main supplier for a large percentage of membrane lipids in the Golgi and PM (in blue). Cardiolipin (CL) is exclusively produced by mitochondria (in pink) but depends on PA which is synthetized by the ER. Enzymes are indicated in green and light green. Adapted from: (Holthuis and Menon, 2014).

3.2) Golgi and the Plasma membrane

Golgi resembles a lipid-based sorting station where significant levels of lipid synthesis occur. The mammalian Golgi specializes in sphingolipid synthesis, which are primarily destined for the PM. In contrast, the PM cannot autonomously synthetize its structural lipids, however numerous reactions for either synthesizing or degrading lipids that are involved in signaling cascades have been described at the PM (Di Paolo and De Camilli, 2006). The Eukaryotic plasma membrane has 2 leaflets, and each one has a specific lipid composition. The outer leaflet contains mostly PC and SLs while the inner leaflet involves PE, PS, and PI (Kobayashi and Menon, 2018). Plasma membranes are enriched in sphingolipids and sterols which are packed at a higher density than glycerol-lipids and resist mechanical stress. Thus, the *trans*-Golgi defines a border line between two broad membrane territories with distinct physical and functional features (Sharpe et al., 2010; Bigay and Antonny, 2012) , from the thin and loosely packed membrane of the ER to the thick and rigid bilayer of the PM.

3.3) Mitochondria

Mitochondria also have two membranes: The MOM forms a smooth lipid rich envelope with high membrane fluidity. In contrast, the inner membrane is highly folded and exhibits an elevated protein level and lower lipid content compared to the outer membrane. Despite the fact that mitochondria synthesize several lipids on their own, they pretty much rely on the transfer of lipids mostly produced in the ER (Tatsuta et al., 2014). Mitochondria synthesize PA and phosphatidylglycerol (PG), which is used for the synthesis of Cardiolipin (a lipid that is unique to the mitochondria) as well as PE. PC and PE are the major mitochondrial phospholipid classes in all cell types. The presence of PG and up to 25 mole percent of CL in the IMM in addition to its high PE/PC ratio, are reminiscent of the bacterial origin of this membrane and are probably required for oxidative phosphorylation (Daum, 1985).

Other mitochondrial membrane lipids such as PC, PS, PI, sterols and SL have to be imported, thus a continuous supply and exchange of lipids is required to maintain mitochondrial membrane integrity and its functions.

Interestingly, the ER and it's specific subfraction: the mitochondria associated membranes (MAMs) are particularly enriched in specific lipid biosynthetic enzymes in both mammals and yeast (Pichler et al., 2001; Rusiñol et al., 1994). Several mechanisms have been discussed for the import of lipids from their site of synthesis into mitochondria including vesicular transport, protein-mediated translocation, direct transfer *via* membrane contact sites and involvement of membrane tethering complexes.

4) Membrane contact sites: built-in platforms for lipid transfer

As discussed previously, the plasma membrane, endosomes and lysosomes depend completely on lipid transport from other organelles mainly the ER.

Lipid transport can occur by several mechanisms. The first one is through the budding and fusion of membrane vesicles. This is the major membrane transport pathway between cellular organelles in the secretory and endocytic pathways. Particularly remarkable is the transport of Cholesterol between ER and the PM. The PM concentrates 80% of total cellular cholesterol but lacks sterol regulatory element-binding proteins (SREBPs). In contrast, the ER membrane, with less than 1% of total cellular cholesterol, contains both SREBPs and the sensors controlling SREBP activation (Lange and Steck, 2016). Careful coordination of the lipid transport between PM and ER enables ER cholesterol sensors to continuously follow PM cholesterol content (Infante and Radhakrishnan, 2017).

Lipids can also laterally diffuse through membrane continuities, such as those that exist between the ER and the outer and the inner nuclear membranes which are thought to receive lipids from the ER (van Meer et al., 2008).

Finally, Membrane Contact Sites (MCS) which are defined as areas of close proximity between membranes of two organelles. MCS with the ER have been reported for almost every other organelle. Indeed, these purpose-built platforms allow the transport of distinct classes of lipids from the ER to other organelles using non-vesicular transport. This transfer is mediated by lipid transfer proteins (LTPs), which thanks to MCS can easily reach the lipid molecules to be transferred between organelles (D'Angelo et al., 2008). Lipid exchange is not a one-sided relationship. Even though this exchange is necessary for the biogenesis of mitochondrial membranes, it is also necessary for general lipid synthesis. For example, the enzyme Psd1 (phosphatidylserine decarboxylase 1), which is necessary for the decarboxylation of PS and PE, resides in mitochondria. This intimately links the ER and mitochondria as the substrate of this reaction must leave the ER and the product needs to go back to the ER from mitochondria (Daum, 1985). Only then will it be distributed to the remaining cellular organelles. One of the most important cellular structures mediating this exchange is the ERMES complex.

In a screen aimed at discovering bridges connecting these 2 organelles using artificial tethers in yeast *S. cerevisiae*, Kornmann and colleagues made an incredible discovery (Kornmann, 2009). In this screen, they identified Mdm12 which is a peripheral MOM protein (Berger et al., 1997). Mdm12 is embedded in a complex containing two other mitochondrial proteins Mdm10 and Mdm34. A fourth protein called Mmm1 (mitochondrial morphology maintenance 1) was long thought to be inserted in the OMM. However, it was finally established that Mmm1 is actually an integral ER protein (Kornmann et al., 2009). This gave birth to the ERMES complex for ER–mitochondria encounter structures with all four proteins making a stable complex at the interface of the ER and the mitochondria (Boldogh et al., 2003; Kornmann et al., 2009).

The four components of ERMES have strong a functional relationship which was shown by genome clustering analyses (Kornmann et al., 2009). In addition, the GTPase Gem1 and Psd1 were part of this cluster which means that the ERMES complex is tightly linked to ER-Mitochondria lipid exchange. Mdm12, Mdm34 and Mmm1 all contain SMP domains(Lee and Hong, 2006; Kopec et al., 2010). Homology searches detected a remote resemblance between SMP domains and a class of lipid-binding proteins TULIPs (Kopec et al., 2010). This family of lipid-binding proteins is characterized by its tubular shape and is called TULIP (tubular lipid-binding). The similarity between SMP and TULIP allows to suggest a predictive model where

SMPs directly mediate lipid exchange between ER and Mitochondrial membranes at MCS (Kopec et al., 2010). Mmm1 and Mdm12 have also been shown to bind phospholipids in vitro, and the structure of the Mmm1 and Mdm12 complex indicates that the proteins come together to form an extended, continuous hydrophobic channel that likely facilitates phospholipid transport (Jeong et al., 2017).

To summarize, the ER which is the principal supplier of bulk lipids to other organelles exhibits an extensive network of contact sites with both secretory (e.g. plasma membrane or *trans*-Golgi) and non-secretory organelles (e.g. mitochondria via the ERMES complex or lipid droplets) to facilitate control over lipid transport and metabolism in response to varying cellular demands (Lev, 2010; Levine, 2004). Taking this into consideration, it is not surprising that the ER is exceptionally sensitive to perturbations in its unique lipid composition and biophysical properties. For instance, an imbalance between saturated and unsaturated phospholipids directly affects the ER and induce a stress response called the UPR that can trigger cell death (Diakogiannaki et al., 2008; Deguil et al., 2011). This is why ER membranes use sensory machineries to maintain membrane fluidity and biophysical properties (Covino et al., 2016), also pairing the synthesis of proteins and lipids to the cell's membrane biogenesis needs (Loewen et al., 2004; Halbleib et al., 2017).

5) Eukaryotic membrane properties Sensors

Membrane homeostatic mechanisms differ between in the early secretory pathway (ER) compared to the late secretory pathway (PM). The latter is thought to control the activity of lipid biosynthetic enzymes directly or via transcriptional programs that adjust lipid metabolic networks (Halbleib et al., 2017; Loewen et al., 2004; O'Hara et al., 2006; Cornell, 2016). In contrast, sense-and-respond systems in the late secretory pathway are more likely to control lipid remodeling processes by fast non-vesicular lipid transport at membrane contact sites(Mesmin et al., 2017, 2013; Bian et al., 2018; Drin, 2014). It is proposed that membrane property sensors can be categorized into 3 distinct classes, based on their molecular mechanisms. Class I senses at membrane surfaces, class II senses properties within the membrane, class III senses membrane properties across the lipid bilayer.

5.1) Class I- Sensing at membrane surfaces

The presence of small G-proteins (e.g. Rabs) and rare signaling lipids (e.g. phosphoinositides) are crucial to the identity of organellar membranes, of course in combination with bulk membrane properties. For example, in the early secretory pathway poor lipid packing results in

abundant hydrophobic "voids" in the water membrane interface. In contrast, in the late secretory pathway there is a high surface charge (Fairn et al., 2011; Yeung et al., 2008; Bigay and Antonny, 2012) due to the enrichment of anionic lipids (mostly PS) in the cytosolic leaflet of these membranes (Chung et al., 2015; Pomorski and Menon, 2006). For these reasons, membrane homeostasis necessitates mechanisms that can sense the presence of such features at membrane surfaces such as the amphiphatic lipid packing sensor (ALPS) motifs of proteins involved in the early secretory pathway (Drin and Antonny, 2010).

5.2) Class III- Sensing across the bilayer

Diverse perturbations of the ER membrane lipid composition, including the accumulation of saturated membrane lipids (Surma et al., 2013; Deguil et al., 2011) activate the **U**nfolded **P**rotein **R**esponse (UPR)(Walter and Ron, 2011b). The UPR is a large-scale transcriptional program (more than 5% of all genes) that controls cellular secretory capacity and protein homeostasis. When activated, the UPR broadly lowers the rate of protein translation but upregulates machinery involved in lipid biosynthesis, ER protein folding, and secretion (Walter and Ron, 2011a). The most conserved transducer of the this response Ire1 has been recently shown to sense membrane perturbations (Volmer and Ron, 2015)by locally compressing the ER membrane (Halbleib et al., 2017). Thus, the oligomeric state and resulting activity of Ire1 is sensitive to membrane material properties, irrespective of the presence of unfolded proteins.

5.3) Class II- Sensing within the membrane

A separate class of proteins senses the membrane properties within the hydrophobic core of the bilayer. Lipid saturation is a key determinant of membrane phase behavior and bulk viscosity. Dedicated machineries in bacteria, cyanobacteria, and fungi modulate lipid acyl chain saturation (Ernst et al., 2016). In yeast, two transcription factors Mga2 and Spt23 responsible for sensing the lipid packing density in the core of the ER membrane (Ballweg and Ernst, 2017). Their sensory mechanism relies on their highly dynamic transmembrane helices (TMHs) and a bulky tryptophan sensor residue conserved in Mga2 and Spt23 (Covino et al., 2016). The TMHs rotate against each other according to the interplay of the sensor residue with the lipid environment. In a membrane with high saturated acyl chains where lipid packing density is high, the Tryptophan is forced to 'hide' into the dimer interface stabilizing a productive rotational orientation allowing for downstream transcription factor activation. On the other hand, when unsaturated lipid content is high, the membrane is less packed, the Tryptophan

swings out into the lipid core (Covino et al., 2016)and Mga2 is stabilized in a non-productive orientation. Given the high sequence similarity of Mga2 and Spt23 in the sensory TMH region (86% sequence identity), it is likely that the activation of Spt23 is regulated via a similar mechanism. So by sensing lipid packing in the hydrophobic core, Mga2 and Spt23 use the ER membrane as a platform for signal integration (Ernst et al., 2016). The main (but not the only) target for the transcription factors Spt23 and Mga2 is the fatty acid desaturase gene *OLE1*. Both mammals and yeasts maintain membrane fluidity by generating CoA-activated, unsaturated fatty acids (UFAs) as lipid building blocks using a Δ9-desaturase: the stearyl-CoA desaturase 1 (SCD-1) in mammals, and OLE1 in *S. cerevisiae*.

6) Controlling membrane fluidity: The OLE pathway

The genome of *S. cerevisiae* encodes only a single and essential FA desaturase called Ole1. This enzyme introduces a Δ9 double bond in activated Fatty Acids such as stearic acid (saturated 18:0) turning it into oleic acid (unsaturated 18:1). The level of Ole1 is tightly controlled by several inter-dependent mechanisms (Surma et al., 2013; Martin et al., 2007). Loss of *OLE1* expression is lethal within few cell divisions and severe morphological changes of cellular organelles can be observed (Zhang et al., 1999). The expression of *OLE1* is controlled by two transcription factors embedded in the ER-membrane *via* a C-terminal TMH: Mga2 and Spt23 (Martin et al., 2007). To activate *OLE1* transcription, these transcription factors are released from the ER-membrane *via* a pathway referred to as the OLE pathway. The membrane-bound precursors of about 120 kDa (also called p120) are recognized by Rsp5, and become ubiquitylated and proteolytically processed by the proteasome. This proteolytic cleavage releases an active transcription factor of about 90 kDa (also called p90) that enters the nucleus and induces the expression of *OLE1* (Hoppe et al., 2000) (**Fig 9)**.

OLE1 is not the only target of the transcription factors Mga2 and Spt23. Highly expressed genes involved in ribosome biogenesis, glycolysis, and lipid metabolism are controlled by these transcription factors (Auld and Silver, 2006). Mga2 has been implicated in the hypoxic response, adaptation to oxidative stress, and zinc homeostasis (Kelley and Ideker, 2009; Jiang et al., 2001). Deletion of both *MGA2* and *SPT23* causes synthetic lethality that is reversed by UFA supplementation (Zhang et al., 1999). Thus, despite the broad spectrum of target genes, *OLE1* appears as the most critical target of Mga2 and Spt23 regulation. The activation of Mga2 and Spt23 is controlled by the membrane lipid environment and can be suppressed when the growth medium is supplemented with UFAs (Hoppe et al., 2000; Covino et al., 2016).

Nonetheless, it is still not entirely clear whether the proteolytic cleavage of Spt23 and Mga2 occurs spontaneously or whether it requires ubiquitylation and the recruitment of the AAA-ATPase Cdc48 and its cofactors.

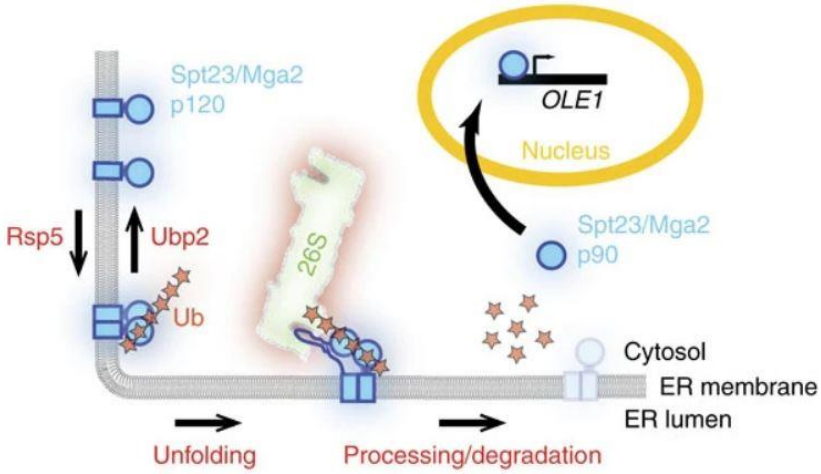

Fig9: Schematic description of the *OLE*-pathway. In this pathway two transcription factors embedded in the ER-membrane, Spt23 and Mga2 which homodimerize when the saturation of lipids acyl chains increases. These membrane-bound precursors (p120 forms) are recognized and ubiquitinated by Rsp5, which promotes their proteasomal endo-proteolysis releasing soluble N-terminal fragments (p90 forms) that function as transcription factors that enters the nucleus and induces the expression of the Δ9-fatty acid desaturase Ole1. Ubiquitin molecules are indicated by red stars. Adapted from: (Cavellini et al., 2017).

The highly conserved AAA-ATPase Cdc48/p97 has been implicated in diverse cellular pathways which we have discussed in earlier sections such as MAD and ERAD (Wolf and Stolz, 2012; Xu et al., 2011). Cdc48 associates with a large number of cofactors to be active. The most famous ones are the heterodimeric Ufd1/Npl4 cofactors which bind ubiquitin-chains and function in several ubiquitin-proteasome dependent pathways including the OLE and the ERAD pathways. Another family of cofactors is characterized by a UBX domain that binds to the N-terminal region of Cdc48 (Neuber et al., 2005; Wang and Lee, 2012; Schuberth and Buchberger, 2008; Kolawa et al., 2013). The Ubx family has seven members in *S. cerevisiae*, and each of these recruits Cdc48 to different cellular locations. Ubx2 for example acts as membrane anchor for Cdc48 in the ER and uses its UBA domain to bind and recruit ubiquitylated substrates to Cdc48 in the ERAD and OLE pathways (Neuber et al., 2005; Surma et al., 2013) but also at MOMs in the mito-TAD pathway (Mårtensson et al., 2019).

However, we still do not know exactly how Cdc48 could contribute to the activation of Mga2 and Spt23. It is possible that the proteolytic processing of Spt23 and Mga2 is completely independent of Cdc48. In this scenario the AAA-ATPase acts only after processing as a segregase to release the processed p90 form from its unprocessed and membrane-embedded interaction partner (Rape et al., 2001; Shcherbik and Haines, 2007). The necessary pulling-force would be provided by ATP-hydrolysis of the AAA-ATPase. The second possibility is that Cdc48 and its cofactors is to facilitate a rapid proteolysis of the C-terminal portion of p120 (Hitchcock et al., 2001; Raasi and Wolf, 2007; Kolawa et al., 2013). This would be reminiscent of its role in the ERAD pathway (Vembar and Brodsky, 2008). Supporting evidence is that interference with the Cdc48/Ufd1/Npl4 complex at the ER-membrane leads to an accumulation of ubiquitylated and unprocessed forms of Spt23 and Mga2 suggesting a retardation of processing (Hitchcock et al., 2001; Rape et al., 2001; Kolawa et al., 2013; Surma et al., 2013). Based on our current knowledge both of these models are still valid. On the other hand, there is no doubt when it comes to the essential role of Rsp5 in the activation of the OLE pathway. In fact, both Mga2 and Spt23 contain a conserved binding motif (LPKY) for binding Rsp5 and their ubiquitylation is dependent on Rsp5 (Shcherbik et al., 2004).

In this regard, the DUB Ubp2 was originally identified as an antagonist of Rsp5 (Kee et al., 2005, 2006) but also recently linked to the SCF-Ubiquitin ligase Mdm30 (Cavellini et al., 2017). Mdm30 plays a central role in the regulation of Fzo1 levels, a protein which is crucial for fusion of outer mitochondrial membranes (Hermann et al., 1998; Rapaport et al., 1998).

This is not surprising as the bulk physicochemical properties of biological membranes broadly regulate protein structure and function, in turn providing a new perspective to mitochondrial dynamics and organelle interactions.

IV- Mitochondrial Dynamics: Mechanisms and Regulation

1) SNAREs v/s DRPs

Membrane fusion is the process whereby two separate lipid bilayers merge to become one. Fusion is essential for the communication between cells and between different intracellular compartments (Jahn and Scheller, 2006; Chernomordik and Kozlov, 2005). There are two types of fusion: homotypic (when similar compartments fuse i.e. mitochondria – mitochondria fusion) and heterotypic fusion (when dissimilar compartments fuse i.e. vesicle exocytosis).

Almost all fusion processes go through hemi-fusion (Chernomordik and Kozlov, 2003), an intermediate stage in which only the closest monolayers are fused before the complete bilayer merging. Membrane fusion intermediates are regulated by cellular proteins that act upon membrane-membrane proximity by bending or remodeling membranes, or by regulating the lipid or protein composition of the respective bilayers (Martens and McMahon, 2008)

However, before membrane fusion can occur several obstacles have to be overcome. Spontaneous membrane fusion in living organisms is opposed by repulsive forces between the approaching bilayers. These forces result from electrostatic repulsion of equally charged membrane surfaces and from hydration repulsion. Moreover, the lateral tension of the bilayer interface has to be overcome (Kozlovsky et al., 2002). For these reasons, membrane fusion events generally require molecules that will tether and dock membranes thus bringing them closer together. This will locally disturb the lipid bilayers (for example, by the induction of extreme membrane curvature) in order to reduce the energy barriers for fusion. The driving force for membrane fusion can come from many sources (i.e. from the energy that is derived from protein-lipid interactions or from protein–protein interactions - and ultimately these reactions will be stimulated by ATP). Directionality might be achieved by the folding of the fusion protein (Martens and McMahon, 2008). Many molecules that are involved in fusion have been identified but the most famous family are the SNARES.

The SNARE protein superfamily includes more than 60 members in both mammalian and yeast cells and are required for each step of the exocytic and endocytic trafficking pathways (Jahn and Scheller, 2006). They have an evolutionarily conserved coiled-coil stretch containing 60–70 amino acids termed as SNARE motif (Kloepper et al., 2007; Fasshauer et al., 1998). Each SNARE motif contributes one helix to this four-helix bundle and the helices are all aligned in parallel in a structure called SNARE complex (Sutton et al., 1998; Antonin et al., 2002). The folding of this bundle is thought to drive the fusion reaction. SNARE complex assembly, disassembly and function are regulated by SNARE-associated factors. SNARE complexes are disassembled by NSF or Sec18p, which are AAA-family ATPase chaperones, along with SNAP or Sec17p which are important to free SNAREs for the second rounds of fusion (Söllner et al., 1993).

Unlike the vast majority of membrane fusion events in the cell which are performed by SNAREs, fusion of mitochondria and of the ER depends on another class of proteins called the **D**ynamin-**R**elated **P**roteins (DRPs) (Hoppins et al., 2009; Hu et al., 2011).

2) Mitochondrial Fusion: a Mitofusin affair

Dynamin-related proteins are mechanochemical GTPases that self-assemble to orchestrate a wide array of cellular processes such as mitochondrial and peroxisomal fission (Drp1 mammals /Dnm1 yeast), mitochondrial fusion (Mfn1/2 mammals and Fzo1 yeast), vacuolar dynamics (Vps1), interferon-induced viral restriction (Mx), plant cell cytokinesis and membrane fission (*Arabidopsis* DRPs) and membrane binding and tethering in bacteria (bacterial dynamin-like proteins BDLPs) (Jimah and Hinshaw, 2019). They provide the mechanical forces necessary for membrane remodeling (Praefcke and McMahon, 2004; Gasper et al., 2009). In this thesis we will only focus on the DRPs that are involved in the remodeling of mitochondrial membranes.

2.1) Mitofusin Characteristics and Topology

When we talk about mitochondrial dynamics we refer to the events of fission and fusion of mitochondrial inner and outer membranes (Westermann, 2010). An equilibrium between the two processes gives mitochondria their tubular shape. These dynamics are crucial for life since they allow mitochondrial morphology adapting to the energy needs of the cell (Schrepfer and Scorrano, 2016) as well as the maintenance of the redox potential, which is the main role of mitochondria (Willems et al., 2015). The DRPs involved in mitochondrial fusion are called Mitofusins and they are conserved in yeast, worms, flies, mice and humans throughout evolution (**Table 3**).

Function	Protein		Domains	Organism	Localization
OM Fusion	DRPs (mitofusins)	Mfn1/2	GTPase domain, HR1, 2 TM, HR2	Mammals	Outer mitochondrial membrane (OMM)
		Marf	GTPase domain, HR1, 2 TM, HR2	*D. Melanogaster*	
		Fzo1	GTPase domain, HR1, 2 TM, HR2		
		Fzo1-1	HRN, GTPase domain, HR1, 2 TM, HR2	*C. elegans*	
		Fzo1	HRN, GTPase domain, HR1, 2 TM, HR2	*S. cerevisiae*	
	accessory	MIB	Zinc finger	Mammals	Cytoplasm
		Bax	3 BH domains, 1 TM		
		Mdm30	F-Box domain	*S. cerevisiae*	
		MitoPLD	1 TM	Mammals	OMM
		Zucchini	1 TM	*D. melanogaster*	
OM+IM fusion		Ugo1	3 TM	*S. cerevisiae*	OMM
IM Fusion	DRPs	OPA1	MTS, 1 TM, HR, GTPase, Middle domain, GED	Mammals	Inner mitochondrial membrane
		Opa1	MTS, 1 TM, HR, GTPase, Middle domain, GED	*D. melanogaster*	
		Eat-3	MTS, 1 TM, HR, GTPase, Middle domain, GED	*C. elegans*	
		Mgm1	MTS, 1 TM, HR, GTPase, Middle domain, GED	*S. cerevisiae*	
	Accessory	YME1L	MTS, 1 TM, ATPase, Protease	Mammals	
		Rhomboid-7	MTS, 7 TM	*D. melanogaster*	
		Pcp1	MTS, 7 TM	*S. cerevisiae*	

Table 3: Domain structures of mitochondrial fusion proteins and their accessory proteins. TM (Trans-membrane domain), HR (Heptad repeat domain), MTS (Mitochondrial targeting sequence), GED (GTPase effector domain). Adapted from (Escobar-Henriques and Joaquim, 2019).

Their sequence is characterized by an N-terminal GTPase domain, and two C-terminal Heptad Repeat domains (HR1 and HR2) that surround the transmembrane (TM) regions. In yeast, an additional HR domain (HRN) is located N-terminal of the GTPase domain (**Fig 10**). The integrity of all of these domains is essential for mitofusin function in mitochondrial fusion (Honda et al., 2005; Cohen et al., 2011b; Koshiba et al., 2004; Eura et al., 2003; Griffin and Chan, 2006; Hermann et al., 1998). It is established Fzo1 is has two distinct TM domains that allow insertion of the protein in mitochondrial outer membranes and the exposure of both the HR1 and HR2 domains into cytoplasm (**Fig10**) (Fritz et al., 2003). Early observations indicated that mitofusins from vertebrates displayed a similar topology (Santel and Fuller, 2001; Rojo et al., 2002). Quite recently, this concept was challenged by bioinformatic phylogenetic analyses showing that fungal Fzo1 proteins exhibit two predicted transmembrane domains, whereas metazoan mitofusins contain only a single transmembrane domain (Mattie et al., 2018). This study shows that MFN1 and MFN2 expose their HR2 to the intermembrane space (IMS) and their HR1 to the cytoplasm. Nonetheless, there are studies showing that HR1 and HR2 form intra- and intermolecular coiled-coil interactions (Koshiba et al., 2004; Huang et al., 2011; Franco et al., 2016; Qi et al., 2016; Cao et al., 2017). In addition, we know that C-terminal tagging of MFN2 could force the exposure of HR2 in the cytoplasm and that this N_{out}–C_{out} topology was competent to rescue mitochondrial fusion partially but significantly in MFN2 knockout cells. Consequently, we could imagine that the two topologies are not mutually exclusive, mitofusins from metazoans can adopt both N_{out}-C_{in} or N_{out}-C_{out} topologies. This co-existence may serve different functions such as the coordination between outer and inner membrane fusion. Regardless of their topology, all mitofusins serve a primary function: docking and fusion of mitochondria.

2.2) Mitochondrial docking and fusion mechanisms

To this day, two possible mechanisms for mitochondrial outer membrane docking are still standing: The first one relies on the HR2 domain of mitofusins. In line with this, the isolated HR2 domain of MFN1 was shown to mediate liposome docking *in vitro* (Daste et al., 2018), and soluble HR1 fragments of MFN2 competing with intramolecular HR1/HR2 interaction (Rojo et al., 2002; Huang et al., 2011; Honda et al., 2005) were hypothesized to expose HR2, allowing the development of a docking-competent MFN2 conformation (Franco et al., 2016). The second model relies on Atlastins which are able to dimerize in the presence of GTP, changing from a closed to open conformation upon GTP hydrolysis leading to a tighter Atlastin dimer (Byrnes et al., 2013; McNew et al., 2013). Recently, the structures of truncated forms of

Mfn1 and Mfn2 were resolved (Cao et al., 2017; Li et al., 2019). These structures were found to have a GDP.AlF_4^- bound state which is in an open conformation (Yan et al., 2018), that transitions to the closed state when bound to GDP.BeF_3^- (Cao et al., 2017; Yan et al., 2018). These findings suggest a model where mitofusins form a homotypic membrane-bridging complex upon GTP binding which brings membranes in close apposition through a GTP-dependent conformational change (Yan et al., 2018) (**Fig 10**).

Despite the presence of truncated Mfn1 and Mfn2 crystal structures (Mini-Mfn1 and Mini-Mfn2) (Cao et al., 2017; Li et al., 2019), the exact nature of the conformational transition of mitofusins leading to mitochondrial docking will require the structural characterization of the membrane-proximal region of the proteins. However, some clues can be found in the structural analogy between Mitofusins and BDLP1, the Bacterial Dynamin-Like Protein 1. The structure of mini-MFN1 is in fact identical to that of the GTPase and neck regions of BDLP1. Secondary structure prediction of MFN1 and computational modeling of full-length Fzo1 using BDLP1 as a template suggest that Mitofusins would share a trunk similar to the trunk region of BDLP1 (Qi et al., 2016; De Vecchis et al., 2017). Thus, it is suspected that mitofusins could mediate membrane approach through a GTP hydrolysis-dependent scissor-like mechanism or by folding back on itself (Yan et al., 2018) (**Fig 10**).

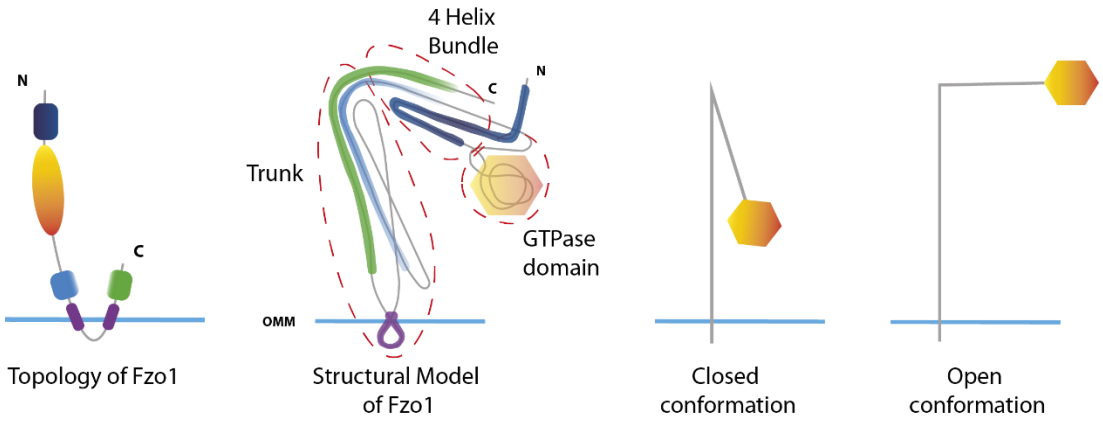

Fig10: From left to right: Topology of Fzo1 on the mitochondrial outer membrane; Structural model of Fzo1 as described in De Vecchis et al; The colors indicate the positions of the HRN, HR1, HR2, TMs and GTPase domains. The four-helix bundle and the trunk of Fzo1 formed in the model are highlighted; Schemes of closed and opened conformations of Fzo1 based on the structural model. GTP hydrolysis pushes the GTPase domain to induce displacement of the four-helix bundle relative to the trunk to yield the opened conformation of Fzo1. In turn, Mdm30 binds the opened (but not the closed) conformation of Fzo1. The GTPase domain is

represented in orange, HRN in dark blue, HR1 and HR2 in light blue and green respectively and finally TM domains in purple. Adapted from: (Alsayyah et al., 2020).

In 2016, the Cohen lab in collaboration with the lab of Dr. Werner Kühlbrandt (Max Planck Institute of Biophysics, Germany) visualized the junction between attached mitochondria isolated from *Saccharomyces cerevisiae* and observed complexes that mediate this attachment. By combining *in vitro* mitochondrial fusion assays with electron cryo-tomography (cryo-ET) they were able to establish a model of mitochondrial outer membrane tethering, docking and fusion in successive steps (Brandt et al., 2016).

Outer membranes of two attached mitochondria are initially tethered by Fzo1-containing globular protein repeats **(Fig 11.A**, Tethering stage). Successive cycles of GTP hydrolysis by mitofusins then allow the fusion process to evolve toward a mitochondrial docking step (**Fig11.A**, Docking stage). Docked intermediates are characterized by a docking ring of protein densities that surrounds areas where outer membranes are separated by less than 3 nm. The fusion of bilayers is then initiated by further GTP hydrolysis in the path of the docking ring where the outer membrane curvature is presumably most pronounced (**Fig 11.A**, Local membrane fusion stage). This set of observations suggests that the formation of Fzo1 oligomers of increasing sizes through successive cycles of GTP binding and hydrolysis progressively brings outer membranes closer from each other and culminates in formation of the docking ring complex which allows fusion at one critical point of membrane curvature (Brandt et al., 2016).

The model proposes that Fzo1 dimerizes in *cis* (on the same membrane) and the resulting *cis*-dimers then engage in *trans*-oligomerization (from opposing membranes) to mediate mitochondrial attachment (Anton et al., 2011). Structural data on mitofusins and other dynamins allowed Fzo1 *cis*-dimers and *trans*-oligomers to be modelled (De Vecchis et al., 2019). It was thereby suggested that the docking ring could form with *cis*-dimers interacting through their GTPase domain (**Fig 11.B**) and *trans* oligomers assembling through the available trunks of the dimers (**Fig 11.B**). GTP-hydrolysis within these oligomers would trigger Fzo1 "sliding" along its trunk thus bringing opposing outer membranes closer from each other. Additional cycles of *cis*-dimerization and *trans*-oligomerization around this first site would result in formation and expansion of the docking ring at the periphery of the increasing contact area (**Fig 11.B**).

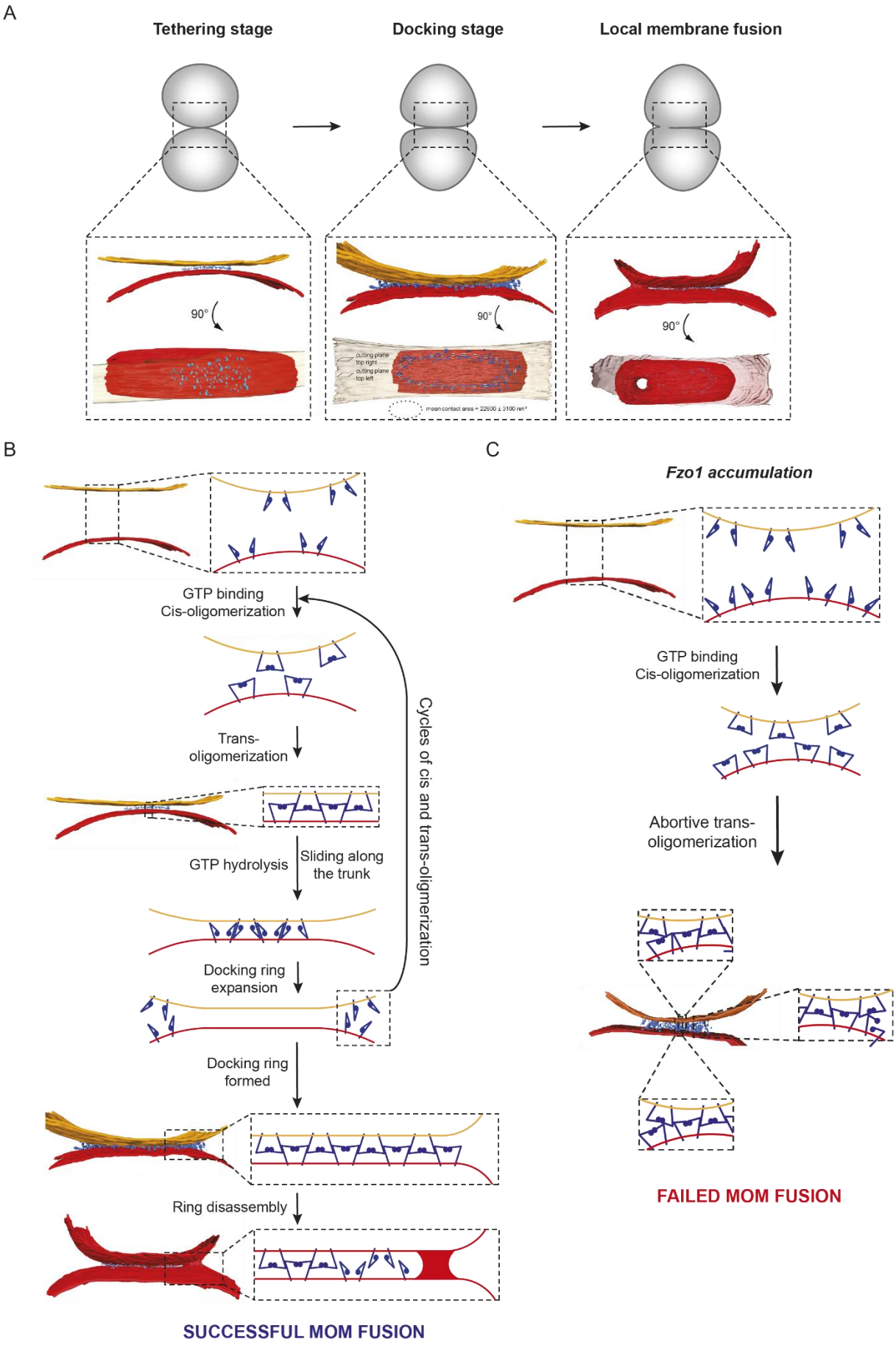
A
Tethering stage
Docking stage
Local membrane fusion
90°
90°
90°
B
GTP binding
Cis-oligomerization
Trans-
oligomerization
GTP hydrolysis
Sliding along
the trunk
Docking ring
expansion
Docking ring
formed
Ring disassembly
Cycles of cis and trans-oligmerization
SUCCESSFUL MOM FUSION
C
Fzo1 accumulation
GTP binding
Cis-oligomerization
Abortive trans-
oligomerization
FAILED MOM FUSION

Fig11: Mechanistic model of outer membrane fusion. **(A)** Schematic representation of *in vitro* mitochondrial attachment and fusion as seen by cryo-ET. 3D renderings of attached outer membranes (in red and yellow) at distinct stages of the fusion process are shown. Protein densities are depicted in blue (Brandt et al., 2016) **(B)** Cis-dimerization of Fzo1 and ubiquitination by Mdm30. Fzo1 is depicted as the 3D model described in (De Vecchis et al., 2017). Its conformational switch and cis dimerization is depicted as in (Brandner et al., 2019). Cis-dimerization of Fzo1 after GTP binding promotes membrane tethering through the formation of Fzo1 trans-oligomers as described in (Brandner et al., 2019). GTP hydrolysis would bring membranes closer together followed by the dissociation of Fzo1 molecules that would redistribute at the edge of this region of close apposition. Successive cycles of GTP binding and hydrolysis would reach high levels in the extension of the surface of apposition surrounded by the docking ring composed of a macromolecular Fzo1 trans-oligomer. Ultimately this would induce fusion where membrane curvature is most pronounced concomitant with dissociation of the docking ring. **(C)** When Fzo1 overexpressed/accumulated, Fzo1 cis-dimers would be stabilized which would disturb the regulated assembly of trans-oligomers causing abortive complexes that inhibit formation of the docking ring and outer membrane fusion fails (brandt et al). Adapted from: (Alsayyah et al., 2020).

In this system, Fzo1 *cis*-dimers that did not engage in *trans*-oligomerization at the initial site of tethering may instead nucleate additional sites of anchoring that would perturb the proper assembly of the docking ring and result in abortive fusion (**Fig 11.C**). Consistent with this possibility, overexpression of Fzo1 increases mitochondrial tethering but abrogates formation of the docking ring and inhibits outer membrane fusion (Brandt et al., 2016).

For these reasons, the clearance of free Fzo1 dimers is crucial as it would favor productive mitochondrial docking and ultimate fusion of outer membranes and this is where the Ubiquitin Proteasome System comes along.

2.3) Regulation of Mitochondrial Outer Membrane fusion by the UPS

It all started from a genome wide screen for genes that are important for **M**itochondrial **D**istribution and **M**orphology (MDM) from the Westermann group (Dimmer et al., 2002). In this very nice paper they identified a gene that causes highly fragmented or aggregated mitochondria: *MDM30*. At the time, we knew that M*DM30* encodes a protein of unknown function which contains an F-box motif involved in targeting of proteins to ubiquitin-dependent proteolysis (Patton et al., 1998). Other studies identified a possible interaction between Mdm30,

Cdc53 and Skp1, two core components of the SCF (Skp1-cullin-F-box) complexes that target proteins for ubiquitin-dependent degradation (Uetz et al., 2000; Skowyra et al., 1997). As ubiquitination was considered crucial for mitochondrial inheritance (Fisk and Yaffe, 1999), they proposed Mdm30 to be a new actor in this process.

Following works by the Langer group linked Mdm30 to Fzo1, showing that the mitofusin accumulates in the absence of Mdm30. Subsequently confirming that Fzo1 is a substrate of the F-Box protein (Escobar-Henriques et al., 2006). Despite the fact that proteins with F-Box domains were known to act as substrate recognition elements for SCF-ubiquitin ligases (Willems et al., 2004; Cardozo and Pagano, 2004; Petroski and Deshaies, 2005), it was proposed that the UPS was not involved in the degradation of the mitofusin (Escobar-Henriques et al., 2006). Two years later, it was clearly demonstrated that Fzo1 was indeed ubiquitinated by Mdm30 and degraded by the proteasome (Cohen et al., 2008). Finally, an agreement was reached on the UPS-mediated degradation of Fzo1 by Mdm30 and its subsequent degradation by the proteasome (Fritz et al., 2003; Cohen et al., 2008; Anton et al., 2011; Cohen et al., 2011b). It is this accumulation of Fzo1 that causes the aggregated mitochondrial morphology seen in *mdm30*Δ cells (Fritz et al., 2003; Escobar-Henriques et al., 2006; Cohen et al., 2008). However, the ubiquitination of Fzo1 by Mdm30 and its subsequent degradation is not constitutive but depends on a key domain of the mitofusin: the GTPase domain (Cohen et al., 2011b).

As it is the case for all DRPs, the sequence of Fzo1 of contains a GTPase domain (**Fig 12** upper part). By inserting point mutations in different domains of the protein, we gained an enormous amount of functional information on the role of each domain in the activity of the mitofusin.

- The V327T mutation was shown to decrease the turnover of Fzo1 by Mdm30 (Amiott et al., 2009). This mutation is analogous to the I213T mutation in the GTPase domain of MFN2 which is responsible for the Charcot Marie Tooth type 2A phenotype, a severe neurodegenerative disease in humans.
- The K200A, S201N, T221S and D195A mutations were found to induce total abolishment of the Mdm30-mediated ubiquitination and degradation of Fzo1 (Anton et al., 2011; Cohen et al., 2011b). These mutations completely lose the ability to bind Mdm30 which explains their stabilization.

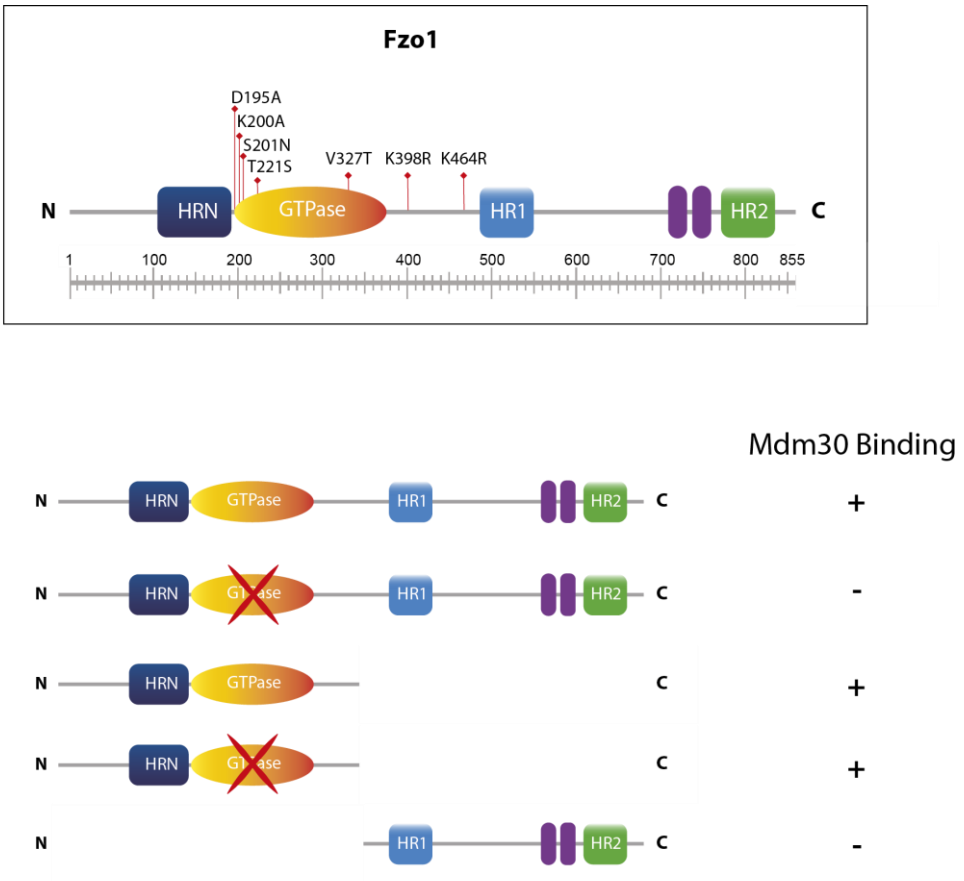

Fig12: Domain organization of the yeast mitofusin Fzo1 and its binding to Mdm30.
Upper part: Fzo1 includes 2 transmembrane domains (purple) that allow exposure of its N- and C-terminals to the cytoplasm. The GTPase domain (yellow-orange) and Heptad Repeat regions HRN, HR1 (blue) and HR2 (green) are indicated. All point mutations mentioned in the main text are also indicated. The scale at the bottom indicates the precise location of each domain. Lower Part: Capacity of Mdm30 to bind distinct truncated/mutated versions of Fzo1. When the GTPase domain is mutated (red cross), Mdm30 does not bind full-length but does bind the N-terminal half of Fzo1 as shown in (Cohen 2011). This suggests a conformational switch where the GTPase domain promotes displacement of the C-terminal half which allows access of Mdm30 to the N-terminal half of Fzo1. Adapted from: (Alsayyah et al., 2020).

Mdm30 was further demonstrated to bind the N-terminal half of Fzo1 whether or not the S201N mutation was introduced in the GTPase domain of this N-terminal truncated portion (Cohen et al., 2011b). In contrast, Mdm30 did not bind the HR1-HR2 containing C-terminal half of Fzo1 (**Fig12** lower part). This set of observations pointed to a model in which the binding site of Mdm30 in the N-terminal half of full length Fzo1 is hindered by the C-terminal half. The activity of the GTPase domain would then induce a conformational switch of Fzo1 that would

allow the recruitment of Mdm30 (**Fig 10**). This is how a relatively "big" complexes like the SCF-Mdm30 ligase and the proteasome are able to access Fzo1 oligomers at mitochondrial junctions. Thanks to these bioinformatical and structural analyses that are available today, we now have the answers to many questions that we could not explain roughly ten years ago when the studies on Mdm30 and its relationship with Fzo1 were published.

E3 ligases target lysines of substrates and in the case of Fzo1, two distinct lysines K464 and K398 are target to Mdm30-dependant ubiquitination (**Fig12-**upper part). They are also proposed to be regulated by two distinct ubiquitin proteases, Ubp2 and Ubp12 (Anton et al., 2013). It was first suggested that Ubp2 antagonizes the Ubiquitination of Fzo1 by an unknown E3 ligase for quality control purposes while Ubp12 antagonizes Mdm30 to promote mitochondrial fusion (Anton et al., 2013). The study concludes that the Lysine 464 is essential for Fzo1 ubiquitination (ub priming) whereas the Lysine 398 was not essential but still required (ub transfer) (Anton et al., 2013). Nonetheless, the structural importance of these lysines not investigated. The lysine 464 was found later on to be involved in a disulfide salt bridge with D335 within the Fzo1 whole peptide which is important for the mitofusins' function (De Vecchis et al., 2017). In conclusion, the K646R mutation does not abolish Fzo1 function because of a ubiquitination defect but rather because of structural fault (De Vecchis et al., 2017). As for the distinctive roles of Ubp2 and Upb12, the inactivation of Ubp2 led to a very fast degradation of Fzo1 and a highly fragmented mitochondrial morphology with decreased respiration (Anton et al., 2013). On the other hand, Upb12 inactivation had no effect on mitochondrial morphology and respiration and the mutation of the DUB's catalytic site had no effect on the ubiquitination pattern of Fzo1 (Anton et al., 2013). Taken altogether, these results weakly support the proposed function of Ubp12 as an antagonist for Mdm30-mediated regulation of Fzo1.

In 2017, Ubp2 was established to be the bona-fide antagonist of Mdm30-dependant ubiquitination of Fzo1 (Cavellini et al., 2017). Ubp2 thus contributes in diminishing the Mdm30-dependant degradation of Fzo1 making it a key factor in the regulation of Fzo1 levels and MOM fusion but also antagonizes Rsp5 which directly controls cellular fatty acid desaturation levels (Kee et al., 2005, 2006).

2.4) Crosstalk between FA desaturation and MOM fusion

The first clue for the study came from the observation that not only Fzo1, but also Ubp2 are targets for Mdm30-dependent ubiquitination and degradation by the proteasome (Cavellini et al., 2017). So in the absence of Mdm30, both Fzo1 and Ubp2 are thus stabilized (**Fig13)**. Notably, the natural stabilization of Ubp2 was found contributing to the defects in respiration and mitochondrial fusion seen in cells lacking Mdm30 (Cavellini et al., 2017). As Ubp2 is antagonizes Rsp5 (Kee et al., 2005), Ubp2 stabilization in *mdm30*Δ cells was shown to antagonize the OLE1 pathway thereby resulting in decreased synthesis of Ole1 (Cavellini et al., 2017). This work thus revealed that lack of Mdm30 not only induces stabilization of Fzo1 and Ubp2 but also decreased desaturation of fatty acids.

Importantly, mitochondrial fusion defects in *mdm30*Δ or *ubp2*Δ cells, in which Fzo1 is either stabilized or rapidly degraded, were rescued by increased or decreased desaturation of fatty acids, respectively (Cavellini et al., 2017). In particular, addition of oleate in wild type cells induced a natural increase of Fzo1. This natural increase of Fzo1 maintained efficient mitochondrial fusion upon high desaturation of fatty acids but was also shown to depend on both Mdm30 and Ubp2 (Cavellini et al., 2017). These observations indicate that the Mdm30-mediated degradation of Fzo1 is not constitutive but tightly controlled by Ubp2, according to the activation status of the Ole1 pathway (**Fig13**). More precisely, Mdm30-mediated degradation of Fzo1 becomes essential for mitochondrial fusion upon low desaturation of fatty acids, but dispensable upon high expression of Ole1 (**Fig13**).

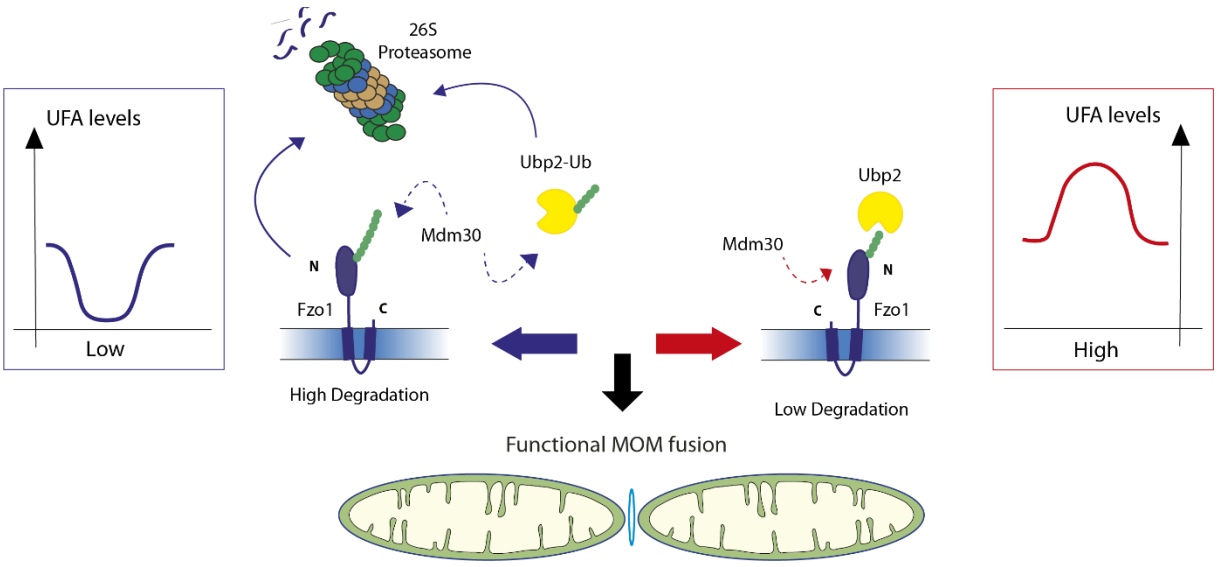

Fig13: Mitochondrial fusion is regulated by a balance between Fzo1 degradation and the desaturation of fatty acids. When the desaturation of fatty acids is low (low UFA), mitochondrial fusion is efficient if the degradation of Fzo1 is high. For this purpose, Ubp2 is

ubiquitinated by Mdm30, which induces its degradation by the proteasome. Mdm30-mediated ubiquitination of Fzo1 is not antagonized which allows extension of ubiquitin chains and efficient proteasomal degradation of the mitofusin. When the desaturation of fatty acids is high (high UFA), mitochondrial fusion is efficient if the level of Fzo1 is also high. For this purpose, the ubiquitination of Fzo1 by Mdm30 is antagonized by Ubp2 which limits the extension of ubiquitin chains and decreases the degradation of the mitofusin. At the bottom, efficient mitochondrial outer membrane (MOM) fusion is symbolized by formation of the Docking ring. Adapted from: (Alsayyah et al., 2020).

While the precise purpose of this balance remains to be investigated, it is possible to speculate on its function. In this regard, the desaturation status of fatty acids is established to be intimately linked to the representation of phospholipids in the cell (Surma et al., 2013). For instance, low desaturation of fatty acids induces a drastic increase in cellular amounts of phosphatidic acid (PA) whereas the overall amount of phosphatidyl choline or phosphatidyl serine decreases (Surma et al., 2013). Intriguingly, derivates of PA have been shown to participate in mitofusin-dependent membrane fusion in mammalian systems (Choi et al., 2006; Ohba et al., 2013). In this context, PA may facilitate outer membrane fusion after formation of a smaller Mitochondrial Docking ring Complex (MDC) thus requiring increased degradation of Fzo1 upon low fatty acids desaturation. Conversely, higher fatty acids desaturation resulting in decreased synthesis of fusogenic lipids would impose stabilization of Fzo1. These higher levels of mitofusin would then allow assembly of an MDC of a size appropriate to trigger fusion of outer membranes (**Fig13**).

2.5) Mitochondrial fusion accessory proteins

Successful MOM fusion is only a pre-requisite to Inner Mitochondrial Membrane (IMM) fusion while coordination between the 2 processes is essential.

In yeast, the coordination function is covered by the protein Ugo1 meaning “fusion” in Japanese (Sesaki and Jensen, 2001; Hoppins et al., 2009). Ugo1 is a modified carrier protein containing 3 transmembrane domains which dimerize forming a complex of 6 TMs typical of carrier proteins (Hoppins et al., 2009; Coonrod et al., 2007). However, a transporter function has not yet been assigned to Ugo1. Ugo1 null cells show a drastic reduction in the number of cristae and cristae junctions (Harner et al., 2011). Due to its physical interaction with both Fzo1 (MOM fusion) and Mgm1 (IMM fusion), Ugo1 was proposed to coordinate the 2 processes which occur simultaneously in vivo (Wong et al., 2003; Sesaki and Jensen, 2004; Hoppins and Nunnari,

2009). Ugo1 interacts directly with Fzo1, independently of Mgm1, via its cytosolic N-terminal domain. Furthermore, it also interacts with Mgm1, independently of Fzo1, via its C-terminal and IMS domain (Sesaki and Jensen, 2004; Wong et al., 2003). In vitro fusion assays also revealed that indeed Ugo1 is required for fusion of both mitochondrial membranes (Hoppins et al., 2009). Ugo1 might function as an adaptor between IM and OM DRPs in early stages of MOM fusion among other functions. Indeed, *Ugo1^{ts}* mutants have been useful for proposing a role for Ugo1 following tethering of either mitochondrial membrane (Hoppins et al., 2009). Thus, Ugo1 could be required for mixing of the lipid membranes, the last step required for membrane fusion. In mammals, a homolog of Ugo1 has been discovered and it interacts with both MFN2 (MOM fusion) and OPA1 (IMM fusion) (Janer et al., 2016). However, knockdown of SLC25A46 was shown to increase mitochondrial fusion (Abrams et al., 2015), which leads us to think that the role for Ugo1 in mitochondrial fusion is not conserved from yeast to metazoans.

Just like the mitochondrial membrane fusion process depends on mitofusins, that is also the case of mitochondrial membrane fission which also depends on Dynamin-related proteins.

3) DRPs and Mitochondrial Fission

Dynamin superfamily members are versatile but the "classical" dynamins are typically involved in membrane scission events in vesicle budding pathways. For example, the *D. melanogaster* protein shibire, the first well-characterized dynamin family member, pinches off newly formed endocytic vesicles from the plasma membrane to release them into the cytosol. Classical dynamins assemble into higher oligomeric structures that form rings and spirals around membranes. These spirals are thought to sever the enclosed membranes following GTP hydrolysis through the mechano-enzymatic activity of dynamin (Praefcke and McMahon, 2004). Dynamin-related proteins have similar roles in the division of membrane-bound organelles, including endosomes, peroxisomes and mitochondria.

3.1) The Mitochondrial Fission Machinery

The master regulator of mitochondrial division in most Eukaryotic organisms is a DRP called Dnm1 (yeast) or Dynamin-Related Protein 1 (DRP1-in mammals). They are soluble proteins containing an N-Terminal GTPase, a middle domain and a C-Terminal GTPase effector domain that is involved in self-assembly. Dnm1 was initially discovered by screening yeast mutants with defective mitochondrial morphology (Otsuga et al., 1998; Bleazard et al., 1999). The re-

localization of Dnm1p from the cytosol to mitochondria is a key step in mitochondrial fission. As one can expect, cells lacking DRP1/Dnm1 exhibits hyperfused mitochondria due to the lack of fission (Otsuga et al., 1998). Mitochondrial Fission is best understood in yeast where recruitment of Dnm1 from the cytosol and assembly in punctate structures on the mitochondrial surface depends on two partner proteins, mitochondrial fission 1 (Fis1) and mitochondrial division protein 1 (Mdv1) (Mozdy et al., 2000; Tieu and Nunnari, 2000). Fis1 is anchored in the MOM via the C-terminal tail and the N-terminal domain is facing the cytosol (Mozdy et al., 2000), providing an interface for interaction with the adaptor protein Mdv1 (Zhang and Chan, 2007). Both Mdv1 and Caf4 are soluble cytosolic proteins acting as molecular adaptors between Dnm1 and Fis1 (Tieu et al., 2002; Griffin et al., 2005).

3.2) Mitochondrial fission mechanisms

First, Fis1 recruits Mdv1 from the cytosol. Membrane-associated Mdv1 then nucleates the assembly of Dnm1–GTP oligomers on the mitochondrial surface. Supported by *in vitro* studies using purified proteins, Mdv1 prefers the GTP-bound form of Dnm1 for binding and stimulates its self-assembly. Therefore, Mdv1 functions as a nucleator for Dnm1 polymerization on mitochondria by inducing or stabilizing favorable Dnm1 conformations (Lackner et al., 2009). Dnm1–GTP oligomers proceed to create spirals that are eventually wrapped around the organelle. Finally, Dnm1 spirals "pinch" the mitochondrial membranes following GTP hydrolysis in a manner that is probably similar to the action of classical dynamins in vesicular budding pathways, resulting in mitochondrial scission (Tieu and Nunnari, 2000; Ingerman et al., 2005; Legesse-Miller et al., 2003; Griffin et al., 2005). Despite Caf4 being dispensable for fission in the presence of Mdv1, it maintains residual fission activity in mutants lacking Mdv1 (Griffin et al., 2005). In *fis1*Δ cells, mitochondria show an elongated and net-like morphology, and most of Dnm1p stays in the cytosol (Mozdy et al., 2000).

The regulation of mitochondrial fission in mammalian cells is way more complicated than in yeast. The dynamin-related protein 1 (Drp1) is the ortholog of Dnm1 (yeast) (Pitts et al., 1999). Structural analysis demonstrates that Drp1 exists in multiple oligomeric states in cells but the minimal functional assembly subunit is a dimer (Macdonald et al., 2014). Like its yeast counterpart, Drp1 is primarily present in the cytosol, but can be recruited via any of its mitochondrial receptors: Fis1, Mff, MIEF1/MiD51, and MIEF2/MiD49. Once at the mitochondrial surface, it is assembled into higher-order complexes that wrap around the mitochondrial surface triggering mitochondrial fission through its GTPase activity (Otera et al.,

2013) (**Fig 14**). Thus, Drp1 and its four mitochondrial receptors constitute the core components of the mitochondrial fission machinery in mammals.

There is a strong evolutionary conservation between Drp1 and Dnm1 but their interacting factors, i.e. Mdv1 and Caf4 (yeast) vs. Mff and MIEFs (mammals) are quite evolutionarily divergent. The yeast Mdv1 and Caf4 proteins have no mammalian homologs, whereas counterparts of mammalian Mff and MIEFs have not yet been identified in yeast (Zhao et al., 2013a). Mammalian Fis1 is no longer an essential mitochondrial receptor responsible for recruitment of the cytosolic Drp1 to the mitochondrial surface unlike yeast Fis1. It is "replaced" by 3 mitochondrial proteins: Mff, MIEF1, and MIEF2 which have been identified as major receptors for translocation of Drp1 to mitochondria in mammals (Gandre-Babbe and van der Bliek, 2008; Otera et al., 2010; Zhao et al., 2011; Palmer et al., 2011). Regardless the model, Drp1 recruitment to mitochondria remains THE critical step for the mitochondrial fission process, but the mechanisms behind this process are still unclear.

3.3) Regulation of Mitochondrial fission by the ER and the actin cytoskeleton

Mitochondrial fission does not occur randomly along the mitochondrial network, it occurs almost exclusively at sites in contact with the ER (Friedman et al., 2011). Indeed, contacts between the ER and mitochondria are not only involved in mitochondrial fusion, but also in mitochondrial division. ER tubules have been observed to wrap around and squeeze the mitochondrial tubule reducing its diameter before Drp1 is recruited thus marking the prospective sites of mitochondrial division (Friedman et al., 2011). Dnm1 and Drp1 oligomerize into helices that are much smaller than the diameter of mitochondria (Dnm1 helices have reported mean diameters of 109 nm in yeast and 129 nm in vitro), so ER tubules need to physically constrict mitochondria to a diameter that is adapted to the size of Dnm1 and Drp1 helices to facilitate their assembly and for fission to be successful (Pitts et al., 1999; Labrousse et al., 1999; Legesse-Miller et al., 2003; Ingerman et al., 2005; Mears et al., 2011) **(Fig 14).**
The mitochondrial fission factor Mff was found to localize localizes in a Drp1-independent manner to mitochondrial constrictions at sites of ER (Friedman et al., 2011). MIEF1 and MIEF2, are also observed at mitochondria-ER contact sites, and co-localized with other fission proteins, such as Drp1 and Mff. However MIEFs are not the essential factors to determine ER-mitochondria constriction sites (Elgass et al., 2015) as they require the presence of Drp1 to form foci, whereas Mff can form foci in cells lacking Drp1 (Richter et al., 2014).

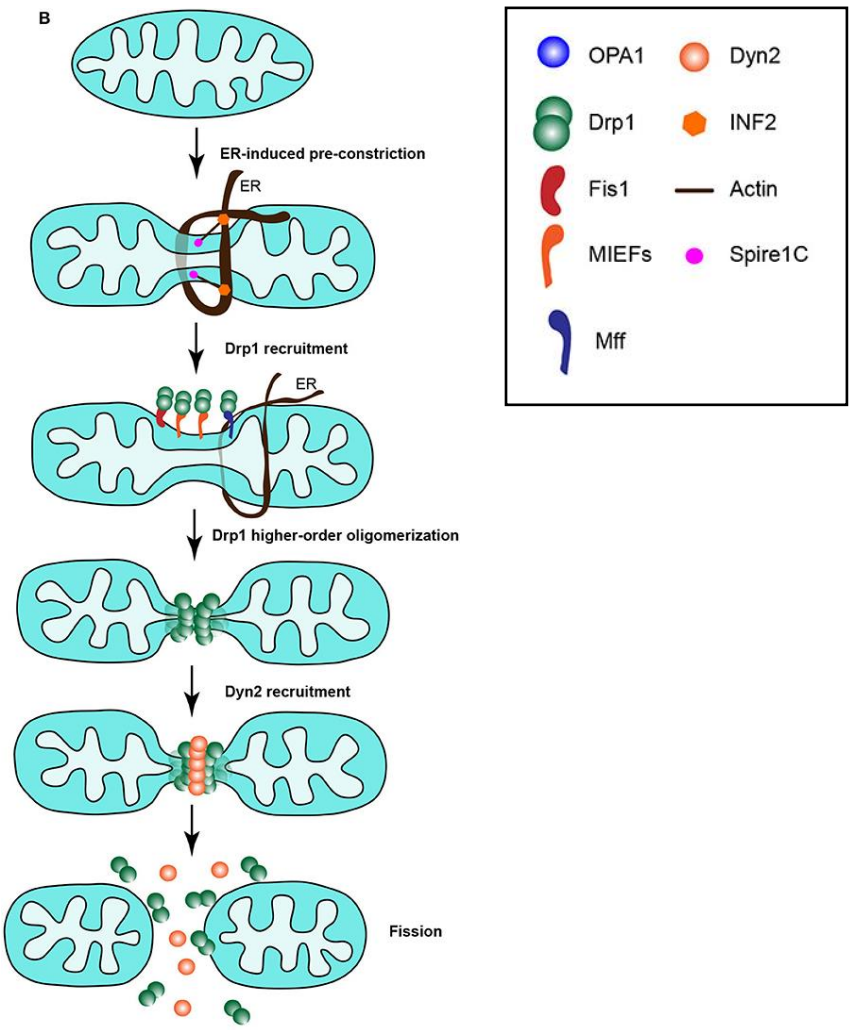

Fig14: Drp1-dependent mitochondrial fission machinery in mammalian cells. In the first step, mitochondria need to be constricted by the ER to a diameter that is adapted to the size of the Drp1 ring. This process also involves actin filaments associated with mitochondria and the ER via Spire1C and INF2, respectively. In turn, Drp1 is recruited by its receptors to mitochondria and assembles to form higher-order oligomers around the mitochondrial tubule. Finally, mitochondria are further constricted by Drp1 oligomerization, and Dyn2 is instantly recruited to finalize the scission of mitochondria through subsequent GTP hydrolysis. Adapted from: (Yu et al., 2020).

In 2017, a very nice study by the Kornmann lab revealed a novel sensing property of Mff (Helle et al., 2017). In fact, the protein has an affinity for mitochondrial tubules of smaller diameter which would lead us to think that physical constriction by the ER causes Mff accumulation, subsequent Drp1 recruitment. This study suggests that Mff acts not only as a sensor but also as an inducer of constrictions. As the protein rapidly accumulates at constricted sites but at high concentrations, it induces and stabilizes constrictions.

Several other DRP1 adapters exist in the cell, hinting at a diversity of determinants for DRP1 recruitment. In this context, MFF might not be the only force sensor on the mitochondrial surface. Similarly, mechanical force by the ER is not the only trigger for mitochondrial fission, the actin cytoskeleton is also involved in regulating mitochondrial fission (Moore and Holzbaur, 2018; Tilokani et al., 2018). An ER-localized actin regulator, INF2 (inverted formin 2) induces actin filaments to drive the initial mitochondrial constriction and then promotes Drp1 recruitment to ER-mitochondria constriction sites (Korobova et al., 2013). Furthermore, attachment of mitochondria to the cell cortex through Num1 (nuclear migration 1) is known to be important for mitochondrial division. From a mechanical standpoint, these anchors are extremely important as we know that membrane scission by classical dynamins is facilitated by the generation of tension on the membrane (Roux et al., 2006).
So just like pulling on a thread at both ends before cutting, it is conceivable that mitochondrial cortex anchors together with cytoskeleton-dependent forces generate tension on mitochondrial membranes to promote mitochondrial fission (Hammermeister et al., 2010).

To conclude, the maintenance of organelle shape and integrity seems to be yet another aspect to be added to the long list of membrane contact site functions. Therefore, it is no surprise that the huge extent to which organelles contact one another is becoming increasingly evident. Nowadays, hardcore cutting-edge imaging techniques allow the visualization of multiple organelles simultaneously over time with increased spatial and temporal resolution. In this Super-Resolution imaging era, inter-organelle contacts will have more and more secrets for us to decipher.

V- Inter-organelle contact sites: ZOOM-ing on Mitochondria

From a historical standpoint, examples of interactions between two distinct organelles were published in the late 1950s (Copeland and Dalton, 1959). But no physiological role was attributed to them, which made it hard to envision MCS as a general and functionally relevant phenomenon. The dogma at the time was that the physical organization of the cytosol was only mediated by anchoring and movement on cytoskeletal elements. Moreover, it was believed that the transfer of small hydrophobic molecules between two organelles was catalyzed by freely diffusing cytosolic proteins, and that soluble metabolites and second messengers travelled long distances (Dennis and Kennedy, 1972). These views played a role in turning away the spotlight from the importance of membrane tethering between two organelles. However, over the last

years a revolution has been happening the field inter-organelle interactions and their role in maintaining cellular homeostasis as publications on the subject are sky-rocketing.
Recent works in the field clearly show that most organelles make functionally relevant contacts with each other. These tether-mediated contact impact on the behavior or function of one or both organelles. As one can imagine, listing all organelle contact sites will take months so we will only focus on the contact sites between mitochondria and other organelles in this chapter. But first, some definitions in the area of contact sites could be useful.

1) What makes a contact site?

Contact sites as the name suggests are areas of close apposition between two independent membranes. Just like membrane fusion, they can homotypic (between identical organelles) or heterotypic (between two different organelles or two different membrane types).
The majority of contact sites studied until now all involved the ER and this is no surprise considering how this organelle is involved in many of the crucial functions of the remaining cellular organelles. In this thesis we will only focus on membrane-membrane contacts.

1.1) Features of Contact sites

A contact site is defined as a tethered proximity between two (bi- or mono-layer) membrane-bound organelles. Despite the mention of "proximity", distance cannot be the sole parameter and juxta-positioning of organelles is not sufficient to be considered a contact site regardless of distance. What is needed to define a contact site is the presence of tethering forces that are the result of interactions between proteins or proteins and lipids. "Docking" is used to describe contacts between fusion intermediates which contributes to distinguish the two topics. Finally, the study of these contacts cannot be fully appreciated and considered useful if they didn't have fulfill a specific function. The most obvious example are ER membrane contact sites and the multiple functions that they fulfill (lipid transfer etc…), several of which are detailed in previous sections. Until now, the most common functions that have been suggested are:

- Molecular Transport (bi-directional) of molecules such as various ions, Ca^{2+}, lipids, amino acids, and metals (Lahiri et al., 2015; Burgoyne et al., 2015; Tatsuta et al., 2014).
- The transmission of signaling information or force cues important for remodeling activities such as organelle biogenesis, dynamics and inheritance (Friedman et al., 2011; Hamasaki et al., 2013; Knoblach and Rachubinski, 2015; Raiborg et al., 2015; Phillips and Voeltz, 2016; Lewis et al., 2016; Hariri et al., 2018).

- The positioning of enzymes such as the phosphatidylinositol phosphate phosphatase Sac1 and the protein tyrosine phosphatase 1B to regulate their activity (Eden et al., 2010; Stefan et al., 2011; Dickson et al., 2016).

Since all contacts must have a function, this requires them to be regulated to not negatively impact cell function. In addition, the duration of a contact is flexible and depends on its function. Just like dynamic transient contacts exist (Kiss and run) others are maintained over long periods of time. Regardless of the duration of the contact, four major types of proteins have been found to be present at the contact sites.

1.2) The four types of proteins found at contact sites

- **Structural proteins:** It is quite obvious that structural proteins make great tethers for holding two organelles together and good spacers that keep membranes at a defined distance without initiating fusion. One example of active spacing is performed by extended-synaptogamins involved in ER–PM contacts in mammals (Giordano et al., 2013). Unlike spacers which are not very well described until now, tethers are way more popular and their numbers do not stop increasing. Tethers are usually directly anchored to one of the two membranes through a TM domain, and they interact with proteins and/or lipids on the partner membrane through a second domain (ORP5/8) (Chung et al., 2015). They can also interact with each other forming homotypic interactions as it is the case of the mammalian mitofusin Mfn2 (de Brito and Scorrano, 2008). Tethers found at contact sites are not restricted to their tethering function, they usually have another function at the membrane where they are found. Usually, multiple tethering pairs are found at the contact site, with variations depending on cellular conditions. This makes studying tethers even more complicated as eliminating one pair of tethers will not necessarily eliminate a contact. Even contact sites that for years were considered to be held by a single tethering pair, such as the NVJ, have new tethering proteins assigned to them such as the tether Mdm1 (Henne et al., 2015). This is why abolishing contact sites has proven impossible until now, like trying to fill holes in a honeycomb with some contact sites requiring the deletion of six different proteins (i.e. the ER–PM contact: Δ*ist2,* Δ*tcb1/2/3,* Δ*scs2*, and Δ*scs22*) to see a dramatic yet incomplete reduction (Manford et al., 2012).
- **Functional proteins:** Contact sites are enriched with proteins that facilitate the function of the contact site. Like ion channels and pumps, lipid transfer proteins, or metabolite channels/transporters, all of which play a role in the exchange of substrates. The best example are the three proteins that have lipid transfer domains are:

Mdm12, Mmm1 and Mdm34 (which are part of the ERMES complex) and PDZD8 (ERMES structural/functional ortholog) that performs a similar role in mammals (Hirabayashi et al., 2017).

- **Sorter/recruitment proteins:** Sorting proteins determine the lipidome and the proteome at the contact site. They are the equivalent of bouncers at the door of the club: accepting or rejecting people - or proteins- at the contact site. They can either bind directly to proteins or indirectly by altering lipids (to define curvature and charge) or the proteins themselves (such as adding post-translational modifications). For example, mitochondria–ER contact sites are thought to have a unique lipid composition relative to each membrane (Sano et al., 2009).
- **Regulator proteins:** Last but not least, regulator proteins are thought to regulate the proteins at the contact site itself. Like p53 changing the redox state of $Ca2^{+}$ handling proteins, thus altering ER–mitochondria tethering (Giorgi et al., 2015).

In total, these classes of proteins help clarify and put some order in the ever-growing list of membrane tethers. We cannot ignore that many proteins fit in more than one category and that many variable combinations can mediate membrane contact sites.

Now that we have reviewed the basics on tethering and contact sites, it's time to zoom in on Mitochondria and the contacts it makes with the remaining cellular organelles.

2) Mitochondrial contacts: how many is too many?

One of mitochondria's fiercest competitors in term of number of contact sites with other organelles is the ER. The relationship between the two organelles dates back to the 1950's, and it's functional aspects started to be investigated in the 90's (Copeland and Dalton, 1959; Vance, 1990; Rizzuto et al., 1998). But mitochondria don't exclusively make contacts with the ER. In reality, mitochondria make contacts with vacuoles (lysosomes), peroxisomes, lipid droplets, endosomes, the Golgi, the plasma membrane (PM), and melanosomes. These contacts are often mediated by multiple, distinct tethering complexes. Some tethering complexes share overlapping functional purposes, while others are more "original" in their roles. In addition, the molecular mechanisms and the dynamics/duration of these contacts can vary dramatically.

Mitochondrial contacts have functional, architectural, and dynamic differences which differentially impact many features of mitochondrial behavior and function. In the following sections, we will detail these functions and the contact sites that intimately affect them.

A more exhaustive list of all tethers between subcellular organelles including mitochondria both in yeast and mammals can also be found in (**Table 4**).

Model	Contact site	Protein	Description	Reference
S. cerevisiae	ER-PM	Scs2	ER receptor for numerous proteins containing a FFAT motif, principal tether in ER-PM contact sites	Murphy and Levine, 2016
		Scs22	Scs2 homolog	
		Ist2	integral ER protein, binds PM via a polybasic region	Manford et al., 2012
		Tcb1/2/3	SMP-domain-containing auxiliary tethers	Toulmay and Prinz, 2011; Manford et al., 2012
		Osh2/3	LTPs, structurally equipped for tethering	Levine and Munro, 2001
		Lam1/2/3/4	LTPs, structurally equipped for tethering	Gatta et al., 2015
	ER-mitochondria	Mmm1, Mdm10/12/34	ER-mitochondria encounter structure (ERMES), Mmm1, Mdm12, and Mdm34 contain SMP domain	Kornmann et al., 2009
		Gem1	Mitochondrial GTPase, ERMES interactor	Kornmann et al., 2011 ; Stroud et al., 2011
		Emc1/2/3/4/5/6	ER membrane complex (EMC), interacts with Tom5	Lahiri et al., 2014
		Tom5	TOM complex subunit, interacts with EMC	
		Tom70/71	TOM complex subunits, interact with Lam6	Elbaz-Alon et al., 2015 ; Murley et al., 2015
		Lam5/6	LTPs, structurally equipped for tethering; Lam6 is an auxiliary tether and interacts with Tom70/71	Gatta et al., 2015 ; Elbaz-Alon et al., 2015 ; Murley et al., 2015
	Nucleus-vacuole	Nvj1, Vac8	nucleus-vacuole junction (NVJ) principal tether pair	Pan et al., 2000
		Osh1	LTP, structurally equipped for tethering	Levine and Munro, 2001
		Tsc13	ER protein required for fatty acid elongation	Kohlwein et al., 2001
		Nvj2	contains SMP domain, structurally equipped for tethering	Toulmay and Prinz, 2011
		Lam5/6	LTPs, structurally equipped for tethering; Lam6 interacts with Vac8	Elbaz-Alon et al., 2015 ; Gatta et al., 2015 ; Murley et al., 2015
		Mdm1	auxiliary NVJ tether, contains TMD and PX domain	Henne et al., 2015
		Nvj3	NVJ component, interacts with Mdm1	
		Vps13	vacuolar protein localizing to NVJ and vCLAMP	Lang et al., 2015b
	Mitochondria-cortex	Num1	binds PM via PH domain and mitochondria via CC domain, required for mitochondrial retention in mother cell	Klecker et al., 2013 ; Lackner et al., 2013
		Mdm36	Num1 partner protein	

		Mmr1	required for mitochondrial transmission to bud, may be required for anchoring at the bud cortex	Swayne et al., 2011
		Mfb1	required for retention of a high-functioning mitochondrial population in mother cells	Pernice et al., 2016
	Mitochondria -vacuole	Vps39	component of the vacuole and mitochondria patch (vCLAMP)	Elbaz-Alon et al., 2014 ; Honscher et al., 2014
		Ypt7	vacuolar Rab GTPase, vCLAMP component	
		Vps13	vacuolar protein localizing to vCLAMP and NVJ	Lang et al., 2015b
		Mcp1	Functional effector of Vps13	John Peter et al. 2017
	ER-peroxisome	Pex3, Inp1	ER-peroxisome tether proteins with a role in peroxisome inheritance	Munck et al., 2009; Knoblach et al., 2013
	Peroxisome-PM	Pex3, Inp1	Anchoring peroxisomes to the mother cell	Hulmes E. et al 2020
	Mitochondria -Peroxisome	Pex34	Transfer of β-oxidation byproducts from peroxisomes to mitochondria	Shai et al 2018
		Fzo1	?	
	ER-LD-Vacuole	Mdm1	Associates with LD through hydrophobic N-ter, binds FAs through PXA domain.	Hariri et al. 2019
Metazoans	ER-PM	VAPs	ER receptors for numerous proteins containing FFAT motif	Murphy and Levine, 2016
		STIM1, Orai	PM Ca^{2+} channel Orai binds to ER integral STIM1 at low luminal Ca^{2+}	Liou et al., 2007
		E-Syt1/2/3	SMP-domain-containing tethers; E-Syt1 is a Ca^{2+}-dependent dynamic tether	Giordano et al., 2013
		Junctophilin1/2/3/4	ER residents, bind PM via MORN domains	Takeshima et al., 2015
		DHPR, RyR	PM and ER Ca^{2+} channels, interact and function in a concerted way	Rebbeck et al., 2011
		ORP5, ORP8	LTPs, dynamic tethers, contain TM and PH domain	Chung et al., 2015 ; Ghai, R., Du, X., Wang, H. *et al.*2017
	ER-mitochondria	MFN1/2	mitochondrial fusion GTPase; an ER MFN2 pool mediates tethering by interacting with mitochondrial MFN1/2	de Brito and Scorrano, 2008
		IP3R, VDAC, Grp75	ER Ca^{2+} release channel IP3R and mitochondrial metabolite channel VDAC are connected, Grp75 may be involved	Szabadkai et al., 2006
		Fis1, BAP31	mitochondrial Fis1 and ER BAP31 interact for transmission of apoptotic signals	Iwasawa et al., 2011

		PTPIP51, VAP	PTPIP51 is a mitochondrial LTP structurally equipped for tethering via VAP binding	De Vos et al., 2012
	ER-endosome	VAPs	ER receptors for numerous proteins containing FFAT motif	Murphy and Levine, 2016
		StARD3, StARD3NL	integral endosomal proteins, interact with ER protein VAP	Alpy et al., 2013
		ORP1L, ORP5	LTPs active at the ER-endosome interface	Rocha et al., 2009 ; Du et al., 2011
		PTP1B, EGFR, Annexin A1	components mediating interplay between ER and multivesicular bodies	Eden et al., 2010 ; Eden et al., 2016
		Protrudin, Rab7	ER protrudin interacts with Rab7 and phosphatidylinositol-3-phosphate on late endosomes	Raiborg et al., 2015
	ER-Golgi	VAPs	ER receptors for numerous proteins containing FFAT motifs	Murphy and Levine, 2016
		OSBP	LTP, dynamic phosphatidylinositol-4-phosphate dependent tether, contains FFAT motif and PH domain	Mesmin et al., 2013
		CERT	LTP, putative dynamic tether	Peretti et al., 2008
		FAPP2	LTP, structurally equipped for tethering	D'Angelo et al., 2007
		Nir2	phosphatidylinositol transfer protein	Peretti et al., 2008
	Lysosome-peroxisome	Synaptotagmin-7	mediates lysosome-peroxisome tethering; cholesterol transfer	Chu et al., 2015
	ER-LD	DGAT2, FATP1	lipid droplet resident DGAT2 and ER resident FATP1 interact and coordinate lipid droplet biogenesis	Xu et al., 2012
	Mitochondria-LD	Perilipin-5	lipid droplet scaffold protein involved in interaction with mitochondria	Wang et al., 2011
	Mitochondria-Lysosome	TBC1D15	regulates lysosomal transport, fusion and maturation in addition to mitochondrial dynamics	Wong Y. et al 2017
	LD-ER-Mitochondria	MIGA2	Binds LD through its amphiphatic helix at the C-ter. Contains FFAT motif that interacts with VAPA and B	Freyre et al. 2019

Table 4: Proteins involved in contact sites in both yeast (*S. cerevisiae*) and Metazoans. ER (Endoplasmic Reticulum); LD (Lipid Droplet); PM (Plasma membrane); FFAT (phenylalanine in an acidic tract); SMP (synaptogamin-like mitochondrial lipid-binding protein); LTP (lipid transfer protein); PH (pleckstrin homology); TM (transmembrane domain); CC (coiled-coil). Adapted from (Eisenberg-Bord et al., 2016).

3) Mitochondrial contacts in distribution and inheritance

Mitochondria do not simply float around the cell. In yeast, the MECA complex (mitochondria–ER–cortex anchor) tethers mitochondria to the PM and cortical ER, bringing these three cellular membranes into close proximity (Lackner et al., 2013). The main protein component of MECA called Num1. This protein which assembles into clusters at the cell cortex directly interacts with the mitochondrial membrane and PM (Ping et al., 2016; Tang et al., 2012). Num1 forms one of the most stable contacts between mitochondria and the cell cortex maintained for extended periods of time (Kraft and Lackner, 2017). Num1 is characterized by a C-terminal pleckstrin homology (PH) domain which binds to phospholipids of the plasma membrane (Yu et al., 2004; Tang et al., 2009), while its N-terminal coiled-coil (CC) domain interacts with Mdm36 and mitochondria (Lackner et al., 2013; Ping et al., 2016). Recently, it was shown that the Num1 CC domain interacts directly with cardiolipin-containing phospholipid membranes, which are characteristic of mitochondria (Ping et al., 2016). Thus, Num1 can be considered as a unique tether with two lipid binding domains having different specificities.
In addition, the tethering activity of Num1 is required for proper mitochondrial distribution and inheritance during budding yeast mitosis (Cerveny et al., 2007; Klecker et al., 2013; Lackner et al., 2013). Thus, Num1-mediated mitochondria–PM contacts affect the spatial distribution of mitochondria within cells in addition to the localization and the timing of dynein anchoring directly affecting spindle orientation.

Mitochondria harbor their own mitochondrial DNA which needs to be passed from mother to daughter cell. Contacts between the ER and mitochondria at sites of mitochondrial divisions are spatially linked to complexes of mitochondrial DNA (mtDNA) and associated proteins called nucleoids. The link between ER-associated mitochondrial division and the maintenance and distribution of nucleoids was first identified in yeast (Murley et al., 2013) and later on described in mammalian cells (Lewis et al., 2016). The association of these two processes is thought to serve as a mechanism of distribution, ensuring that newly-replicated mtDNA is efficiently distributed to daughter cells (Murley et al., 2013; Lewis et al., 2016). The identity of factors that physically and functionally coordinate these 2 processes are still unknown.

4) Mitochondrial contacts in Metabolism and cellular homeostasis

vCLAMP (for vacuole–mitochondria patch) tethers mitochondria to the vacuole in yeast. The formation of vCLAMP is integrated with cellular metabolism and is decreased in respiration conditions (Elbaz-Alon et al., 2014; Hönscher et al., 2014). One of the core components of

vCLAMP is the HOPS (homotypic fusion and vacuole-sorting complex) tethering complex subunit Vps39. Functional studies on vCLAMP were complicated by the functions of the protein outside the context of the contact site making it difficult to discern whether the phenotypes observed in the absence of the protein are due to loss of the contact site or simply the canonical function of the protein. This was eventually overcome by the identification of Vps39 separation-of-function mutants, which are defective for vCLAMP formation but not for HOPS complex function (Bröcker et al., 2012; González Montoro et al., 2018). The vCLAMP-specific functions of Vps39 impact on specific cellular stress response pathways and survival during starvation; however, the underlying functional basis for these processes remain to be determined.

Lam6 (also known as Ltc1) localizes to vacuole-mitochondria as well as to ER–mitochondria and ER–vacuole contacts (Elbaz-Alon et al., 2015; Murley et al., 2015). Lam6 belongs to a StART/VASt domain family of sterol-transporting proteins and has been shown to transport sterols *in vitro* (Murley et al., 2015; Gatta et al., 2015). Lam6 is suggested to be involved in the regulation of membrane lipid composition perhaps by regulating of sterols on mitochondria (Elbaz-Alon et al., 2015; Murley et al., 2015). Although the function of Lam6 at ER–mitochondria contact sites remains unclear, Lam6 is implicated at ER–vacuole contacts to create sterol-enriched vacuole membrane domains. These domains regulate TORC1 signaling, which controls cell growth and metabolism, by spatially segregating TORC1 regulators through the spacing specificity of sterols (Murley et al., 2017).
In addition, organelle-specific receptors for Lam6 are involved in many aspects of organelle biogenesis and function. Lam6 is recruited to mitochondria by Tom70/71 which are mitochondrial preprotein import receptors and to the vacuole by Vac8 which has functions in vacuole transport, autophagy and nucleus–vacuole junction formation (Murley et al., 2015; Tang et al., 2006). If and how Lam6 affects the canonical functions of its organelle receptors and integrates these crucial functions with contact site formation and function are still open questions.

ER–mitochondria contacts are also intimately tied to cellular homeostasis via their impact on autophagy as clearing out dysfunctional components is crucial for cellular wellbeing. Mitophagosomes in yeast and autophagosomes in metazoans have been shown to form at ER–mitochondria contacts. These contacts are suggested to be the source of phospholipids required for the formation of the autophagosome (section **I-2.5**). Disrupting ER–mitochondria contacts by using ERMES mutants (yeast) or by depleting Mfn2 (mammals) decreases the formation of

autophagic vesicles (Hailey et al., 2010; Hamasaki et al., 2013; Böckler and Westermann, 2014). Nonetheless, we must keep in mind that the effects of ER–mitochondria contacts on autophagy vary depending on the autophagic stimulus (Gomez-Suaga et al., 2017). Thus, an important but difficult challenge will be to differentiate the direct and indirect contributions of distinct mitochondrial contacts to the mechanisms and the regulation of various autophagic pathways depending on the stimulus received and the cargo to be cleared.

5) Mitochondrial contacts and Mitochondrial dynamics

As mentioned in a previous section (**IV-3.3**) the ER is present at the vast majority of mitochondrial division events both in yeast and mammalian cells (Friedman et al., 2011). The ER–mitochondria encounter structure (ERMES) mediates contact between mitochondria and the ER at sites of mitochondrial division in yeast (Kornmann et al., 2009; Murley et al., 2013). ER contacts at future division sites thought to induce the initial constriction of mitochondria preceding the recruitment of the dynamin-related proteins that continue the constriction until scission of the mitochondrial membranes by Dnm1/Drp1 and Dyn2 (Friedman et al., 2011; Lee et al., 2016) (section **IV-3** for more detail). Actin polymerization has also been proposed to facilitate mitochondrial division in many ways. First by providing a force-generating system to drive the initial constriction of mitochondria through the direct recruitment of Drp1 to the site of contact. Secondly, by enhancing ER– mitochondria contacts and consequently ER-to-mitochondria calcium transfer leading to constriction of the mitochondrial inner membrane (Korobova et al., 2013; Ji et al., 2017; Chakrabarti et al., 2017). Thus, ER-mitochondria contacts have a considerable impact on the structure of both the outer and inner mitochondrial membranes.

Recently, mitochondria–lysosome contacts have been spatially linked to sites of mitochondrial division (Wong et al., 2018). Indeed, Lysosomal GTP-bound RAB7 was shown to be involved in the formation and the stabilization of mitochondria–lysosome contacts. These contacts are subsequently destabilized by TBC1D15, a RAB7 GAP (GTPase-activating protein) that is recruited to mitochondria by the MOM protein Fis1. Interestingly, the ER and Drp1 are present at sites of lysosome-marked mitochondrial division, raising the question of how contact between mitochondria and multiple organelles at sites of division are regulated and integrated without things getting too “crowded”.

The connection between mitochondria–ER contacts and mitochondrial dynamics is not exclusive to mitochondrial membrane fission. In a recent study using grazing incidence

structured illumination microscopy (GI-SIM) Guo et al examine the ER and mitochondrial dynamics with increased spatial and temporal resolution compared to standard SIM techniques. Amazing videos were obtained showing that the ER is also present at over half of the mitochondrial fusion events observed (Guo et al., 2018). More interestingly, by comparing duration of fusion events they discovered that fusion events not associated with the ER lasted longer (from initial contact to completion of fusion) in comparison to fusion events associated with the ER. Although the molecular basis and functional contributions of ER–mitochondria contact at sites of fusion remain to be determined, it is clear that ER– mitochondria contacts are intimately connected to the division and fusion dynamics of the mitochondrial network.

6) Mitochondrial contacts and molecular transport

Perhaps one of the most widespread functions of inter-organelle contact sites is molecular transport. Contacts between mitochondria and other organelles have been shown to promote exchange of various substrates such as Ca2+, lipid, and various metabolites.

Ca2+ transfer between the ER and Mitochondria through Mitochondria-ER contacts has been described for some time now (Rizzuto et al., 1998). Since then, Ca2+ transfer between the two organelles was shown to be directly implicated in various mitochondrial and cellular functions such as bioenergetics, metabolism, dynamics as well as cell death and autophagy.
The transfer of iron, was also associated with mitochondria contacts. In fact, iron transfer between mitochondria and endosomes happens through Kiss-and-run contacts between the two organelles (Sheftel et al., 2007; Das et al., 2016). The duration of this contact is thought to be regulated by the iron present inside the endosome suggesting that the cargo of the endosome regulates the contact.

Lipids also make their way from one organelle to the other for reasons we have previously described in the latter paraphs (**III-4**). The role of mitochondria mediated inter-organelle contacts for lipid transport was also detailed, especially with the ER. Many of the proteins that mediate mitochondria-organelle contacts contain lipid-binding and lipid-transport domains. As mentioned in previous sections Mmm1, Mdm12, and Mdm34 proteins in the ERMES complex contain a synaptotagmin-like mitochondrial lipid-binding protein (SMP) domains (Kornmann et al., 2009; Kopec et al., 2010; Lee and Hong, 2006). Cells that lack ERMES exhibit defects in phospholipid transport between the ER and mitochondria (Kornmann et al., 2009). The SMP domain protein PDZ8 has been recently suggested to be a possible paralog of the ERMES component Mmm1 in Metazoans (Hirabayashi et al., 2017; Wideman et al., 2018). PDZD8

mediates ER–mitochondria contacts which are proposed to facilitate Ca2+ transfer but a potential role in lipid transfer is yet to be proven. Similarly, another complex called EMC for ER-membrane protein complex (Lahiri et al., 2014) is also proposed to be involved in phospholipid transfer between the ER and mitochondria. The EMC complex is composed of 6 proteins (Emc1–6), it was first established to be implicated in ER protein folding (Jonikas et al., 2009) and it interacts with the MOM protein Tom5. Cells lacking the EMC exhibit reduced ER–mitochondria tethering and decreased transfer of phospholipids from the ER to mitochondria (Lahiri et al., 2014).

The vacuolar protein Vps13 (Vacuolar protein-sorting 13) has been suggested to have similar functions to ERMES both in yeast and mammal (John Peter et al., 2017; Park et al., 2016; Lang et al., 2015; Kumar et al., 2018). In yeast, Vps13 is involved in many inter-organelle contacts including Vacuole-Mitochondria contacts while it's Metazoan homolog VPS13A, localizes to ER-Mitochondria contacts. Vps13 showed phospholipid-transfer and lipid-binding activities *in vitro* and based on the crystal structure of the N-Terminal of the protein (*Chaetomium thermophilum*), it is likely that the protein has a hydrophobic cavity large enough to fit several lipid molecules at the same time thus mirroring ERMES functions (Kumar et al., 2018). In addition, Vps13 seems to be required in the absence of ERMES (Lang et al., 2015; John Peter et al., 2017).

Contacts between the ER and mitochondria are not the only MCS implicated in molecular transport. Quite recently, new studies using proximity detection methods based on split fluorophores, gave us insight on Mitochondria-Peroxisome contacts. Two novel tethers between these organelles have been identified: Pex34 which is a peroxisomal protein, and the yeast mitofusin Fzo1 (Shai et al., 2018). The exact mechanism by which Pex34 mediates these contacts is yet to be revealed but its purpose is to facilitate the transfer of Beta-oxidation byproducts such as citrate from peroxisomes to mitochondria (Shai et al., 2018) (**Fig15**).

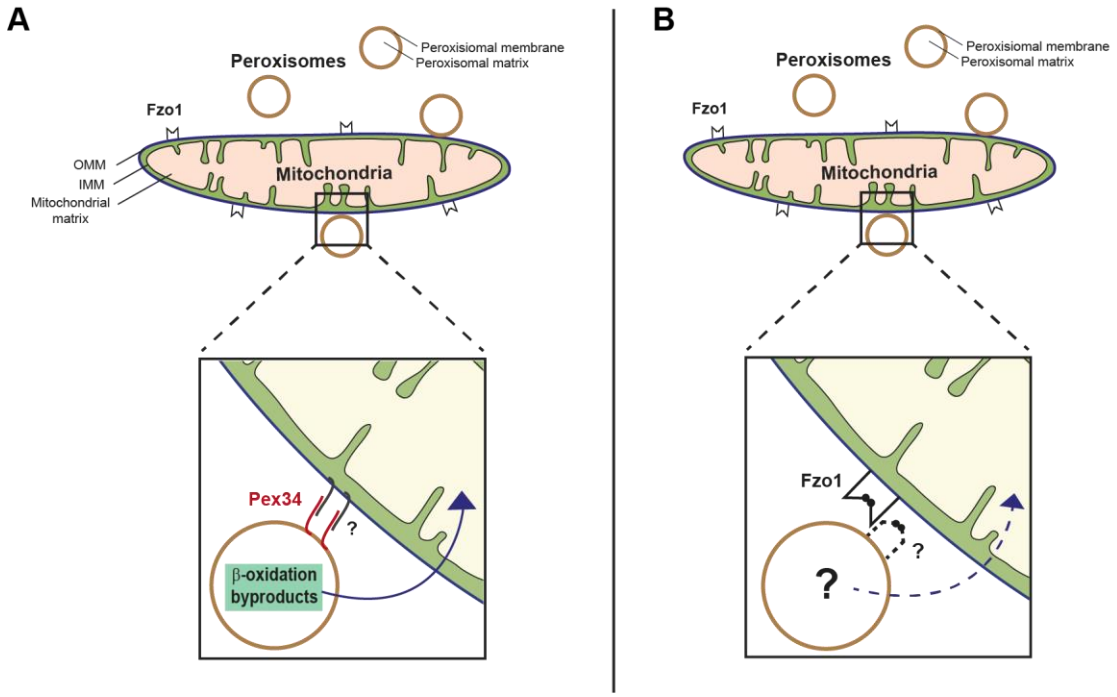

Fig15: Fzo1 and Pex34-mediated contacts between Mitochondria and Peroxisomes. **(A)** Pex34-mediated contacts between peroxisomes and mitochondria. These contacts are supposed to facilitate transport of beta-oxidation byproducts from peroxisomes to mitochondria. The interacting partner of Pex34 on the mitochondrial side is yet to be determined. **(B)** Fzo1-mediated contacts between peroxisomes and mitochondria. Fzo1 is located on mitochondrial outer membranes and it's interacting partner on peroxisomes is yet to be determined. The function of these Fzo1-mediated contacts between the two organelles is still unknown (dashed arrow). All the proteins that are still unknown are indicated by a '?'.

As for the mitofusin Fzo1, it was thought to be exclusively localized on MOMs until now, but it's actual presence on peroxisomal membranes is needs to be proven. This would not be the first time that a mitofusin localizes to another organelle to mediate attachment as Fzo1's mammalian homolog Mfn2 also localizes to ER membranes (de Brito and Scorrano, 2008). The overexpression of Fzo1 was found to promote Peroxisome-Mitochondria contacts but its interaction partner remains to be identified. Knowing that Fzo1 is a DRP which oligomerizes with Fzo1 on adjacent mitochondrial membranes, it is highly probable that a part of Peroxisome-Mitochondria contacts are Fzo1-Fzo1 mediated. Interestingly, Fzo1-Fzo1 tethering between mitochondrial membranes drives homotypic fusion between the two membranes could be possible. Taking this into consideration, one can imagine that Fzo1 mediated heterotypic fusion between mitochondrial and peroxisomal membranes. Although this has never been documented before, a study from the Mcbride lab presents an argument in favor of this theory

showing that newly born peroxisomes are a hybrid of mitochondrial and ER-derived pre-peroxisomes in mammals (Sugiura et al., 2017).

These findings further re-enforce the bond between mitochondria and peroxisomes which are already tightly linked through various metabolic pathways that are indispensable for maintaining cellular homeostasis. Indeed, Substrates are delivered *to* and *from* the peroxisome by dedicated transport machineries, and evidence suggests that dynamic organelle contacts play an important role in the regulation of metabolite transfer and other peroxisomal functions (Schrader et al., 2015; Shai et al., 2016).

VI- Peroxisomes

Peroxisomes house many metabolic pathways that are involved in various aspects of lipid metabolism. This includes enzymes involved in the degradative oxidation; the formation of bile acids and cholesterol; the catabolism of purines, polyamines, and amino acids; glyoxylate metabolism; and the detoxification of reactive oxygen species such as hydrogen peroxide, superoxide anions, and epoxides. It is thus no surprise that peroxisome biogenesis disorders are linked to severe neurological diseases, cancer, diabetes and even early death in humans (Espeel et al., 1995; Singh, 1997; Wangler et al., 2018). Nonetheless, their metabolic importance depends on the functional interplay that they have with other organelles, especially mitochondria. Indeed, only mitochondria can oxidize fatty acids all the way to obtain CO_2 and water while peroxisomes only shorten the fatty acid chain, but produce Acetyl-coA which is important for mitochondrial and cellular functions (e.g. TCA cycle).
Thus, it is clear that both organelles need to work together to maintain metabolic homeostasis. Peroxisomes are present in all eukaryotes except the *Archaezoa* (Cavalier-Smith, 1987a; b). It was first proposed that peroxisomes may have evolved endo-symbiotically but this vision has changed in favor of *de novo* biogenesis from invaginations of regions of other organelles that contained enzymes (De Duve and Baudhuin, 1966; Hoepfner et al., 2005)

1) Peroxisome Structure and Biogenesis

Peroxisomes are typically spheroid ranging from 0.1–1 μm in diameter and are enclosed by a single lipid bilayer. They are densely filled with enzymes for their varied metabolic roles (Lazarow and Fujiki, 1985; Smith and Aitchison, 2013). Peroxisomes do not synthetize their own proteins which another common point they have with mitochondria, proteins are imported and incorporated into peroxisomes post-translationally. Mammalian peroxisomes share a similar lipid composition with the ER, rich in phosphatidylcholine (PC) and phosphatidyl-

ethanolamine (PE), and no cardiolipin (Fujiki et al., 1982; Hardeman et al., 1990), however peroxisomes do not synthetize any lipids. A typical human cell has 100 to 1000 peroxisomes distributed throughout its cytoplasm but their number and size can change dramatically in response to stimuli or stressors (Jean Beltran et al., 2018). In the yeast *Pichia pastoris*, methanol dramatically increases the size of peroxisomes until they dominate the cytosolic volume (Gould et al., 1992). On the other hand, introduction of FAs such as oleate in the media increases the numbers of peroxisomes (Gould et al., 1992; Yan et al., 2008).

In order to modulate organelle number, the cell needs to control biogenic and degradative processes such as *de novo* synthesis, fission of existing organelles; homotypic fusion or heterotypic fusion, maturation, organelle retention or segregation during cell division and last but not least autophagy (Nunnari and Walter, 1996; Warren and Wickner, 1996; Marshall, 2016). To increase peroxisome numbers, the cell can make simple photocopies or template replications of the ones that already exist (Lazarow and Fujiki, 1985; Motley and Hettema, 2007; Menendez-Benito et al., 2013). This happens when a single peroxisome becomes elongated and its membrane and matrix constituents are distributed to the two or more "daughter" peroxisomes. However, before replication the peroxisome grows in size by importing new proteins and expanding its membrane by fusing with PPV's (Pre-Peroxisomal Vesicles) (Titorenko Vladimir I. and Rachubinski Richard A., 1998; Titorenko et al., 2000; Hoepfner et al., 2005; Titorenko and Mullen, 2006). PPV morphologies are diverse and asymmetrical (Titorenko et al., 2000) but can be divided into at least 2 populations all of which bud from the ER during *de novo* peroxisome biogenesis. Evidence suggests that there are additional subtypes (Knoops et al., 2014; Wróblewska et al., 2017). Their ER origin was determined in the dimorphic yeast *Yarrowia lipolytica* due to the presence of N-linked core-glycosylated peroxins Pex2 and Pex16 (Titorenko Vladimir I. and Rachubinski Richard A., 1998; Titorenko et al., 2000). In *Saccharomyces cerevisiae*, the proteins Pex13 and Pex14 travel in vesicles from the ER to peroxisomes (van der Zand et al., 2012). These morphological differences between PPV populations are due to an asymmetric distribution of membrane protein and lipid constituents within the PPV that partition to these different membrane regions. It is proposed that this segregation prevents premature assembly of peroxisomal components in the ER (van der Zand et al., 2012).

Similarly to the formation of COPII vesicles on the ER, cytosolic factors are recruited to the ER membrane surface and ATP hydrolysis is needed for vesicle formation (Lam et al., 2010). In turn, ESCRT-III was suggested to function directly in the scission of PPVs during PPV

biogenesis (Mast et al., 2018). It is thought that peroxisomes fuse with PPV's but mature peroxisomes do not fuse with each other (Motley and Hettema, 2007; Motley et al., 2008). Nonetheless, the protein composition of peroxisomes is intriguing as they are composed both of old and new membrane proteins (Motley and Hettema, 2007; Menendez-Benito et al., 2013). This constitutes an additional argument in favor of the template replication of peroxisomes to increase their numbers.

Peroxisomes can also arise *de novo* from the endoplasmic reticulum (ER) via a maturation process **(Fig 16)**. So why not make peroxisomes from scratch all the time?

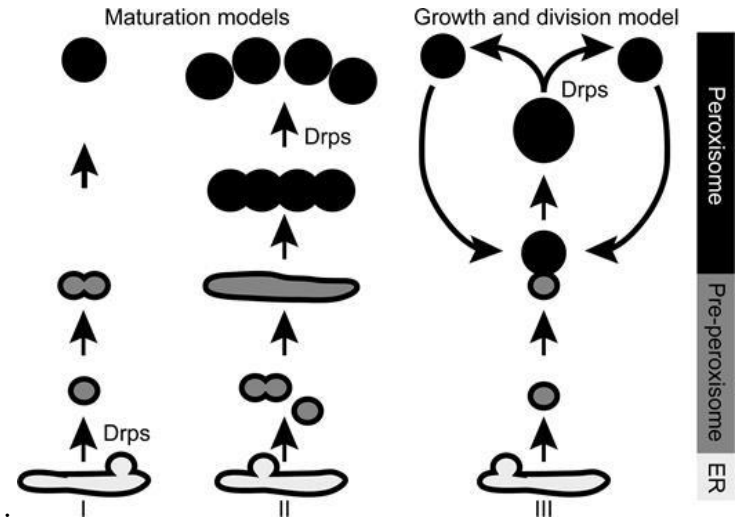

Fig16: Peroxisome biogenesis and proliferation models**.**
Model I and II illustrate de novo biogenesis of peroxisomes from the ER. A process that was later found to be too energy consuming and efficient for the cell. In these models ER-derived membrane structures (MDVs) mature into peroxisomes that import matrix proteins (in black). The role of Drps has been suggested to be either at the ER membrane (model I) or at a later stage in the maturation pathway (model II). Model III illustrates peroxisomes multiplying by fission of existing peroxisomes (black) and the ER provides lipids and some membrane proteins through MDVs (gray) that fuse with the existing peroxisomes. Drps have been proposed to be required for the fission of peroxisomes. Adapted from: (Motley and Hettema, 2007).

In a very nice paper by Motley and Hettema, they show that the ER furnishes some peroxisome membrane components by releasing PPVs **(Fig 16)**. However, yeast cells only used ER budding to produce new peroxisomes by letting them mature when they had none of their own. The process of de novo peroxisome biogenesis from PPV precursors is long (taking ~4 h in yeast) and energetically unfavorable (Hoepfner et al., 2005; Motley and Hettema, 2007). *De novo*

biogenesis has also been visualized in yeast cells deficient in peroxisome inheritance (Chang et al., 2009; Munck et al., 2009). Consequently, yeast cells increase their numbers of peroxisomes principally by growth and division of existing peroxisomes (Motley and Hettema, 2007).

2) The Peroxisomal fission machinery

Peroxisomes can form by growth and division (fission) from pre-existing ones (Lazarow and Fujiki, 1985; Schrader and Fahimi, 2006a). The first step of division is the elongation of the peroxisomal membrane via the conserved peroxisomal membrane Pex11. Pex11 family proteins are associated with the peroxisomal membrane, but exhibit different topologies in various organisms. Mammalian Pex11 proteins are integral membrane proteins with the N- and C-terminal exposed to the cytosol (Schrader et al., 2012). From the Pex11 family, Pex11β is the most commonly expressed in mammalian cells. It remodels and elongates peroxisomal membranes in the initial phase of peroxisomal fission (Delille et al., 2010; Schrader et al., 2012; Yoshida et al., 2015). This remarkable biophysical property of Pex11β depends on its ability to interact with membrane lipids through the amphipathic helices in its N-terminal domain (Opaliński et al., 2011) and intrinsic interaction to form homo-dimeric/oligomeric complexes (Bonekamp et al., 2012; Bonekamp and Schrader, 2012; Itoyama et al., 2012; Yoshida et al., 2015). Although Pex11β has no intrinsic membrane scission activity, it is crucial to assemble key components of the peroxisomal division machinery.

A number of adaptor proteins can recruit Drp1 to the peroxisomal membrane in mammalian cells. Those include the C-tail anchored membrane proteins Fis1 and Mff, which are also found on mitochondria (Gandre-Babbe and van der Bliek, 2008; Koch et al., 2005). As Mff is only found in metazoans, yeast and plants use additional, organism-specific adaptor proteins to recruit Dnm1/DRP (i.e. Mdv1 and Caf4 in yeast (**IV-3**) , PMD1 (Peroxisomal and Mitochondrial Division Factor 1) and Fis1B in plants (Lingard et al., 2008; Pan and Hu, 2011)). These receptors are essential to recruit the GTPase Drp1 to the peroxisomal membrane (Praefcke and McMahon, 2004; Williams and Kim, 2014) which is the main mediator of both peroxisomal and mitochondrial fission in mammals (Schrader and Yoon, 2007). The membrane receptor proteins Mff and Fis1, were reported to interact with Pex11β (Itoyama et al., 2012; Kobayashi et al., 2007; Koch and Brocard, 2012). Pex11p also functions as a **G**TPase **A**ctivating **P**rotein for Dnm1p/DRP1 at the peroxisomal membrane. Following elongation, a final constriction of the membrane is necessary before final membrane separation. As the Drp1 ring has a restricted diameter and cannot encircle a whole organelle, just like mitochondria similar observations have been made for peroxisomes (Koch et al., 2004). After constriction,

Drp1 assembles into ring-like complexes which encircle the constricted organelles (Koch et al., 2003; Smirnova et al., 2001). In turn, GTP hydrolysis drives membrane constriction by inducing conformational change like a "power-stroke" (Bui and Shaw, 2013). GTPase or oligomerization-deficient mutants or reducing levels of Drp1 result in highly elongated, segmented peroxisomes (and mitochondria), which still maintain constriction sites but cannot divide (Koch et al., 2004; Waterham et al., 2007). On the other hand, over-expression of Drp1 has no impact on peroxisome number (Li and Gould, 2003).

Despite these species-specific differences, peroxisomes and mitochondria share the key components of a common DRP-based fission machinery, which appears to be a common evolutionary strategy conserved in mammals, fungi and plants (Schrader and Fahimi, 2006a; Delille et al., 2010).

3) Peroxins and peroxisomal protein import mechanisms

3.1) Peroxisomal Membrane Protein (PMP) import

Peroxisomes have no DNA, so all peroxisomal matrix proteins are encoded in the nucleus, synthesized on free ribosomes and imported post-translationally (Platta and Erdmann, 2007). A family of genes is known to be responsible for the life cycle of the peroxisome: the PEX genes (Distel et al., 1996). To date, 37 peroxins have been characterized. They are typically either peroxisomal membrane proteins or cytosolic chaperones, although a few are also residents of the ER (Farré et al., 2019). Indeed, the ER serves as source material for peroxisomal membranes and as a site for Peroxisomal Membrane Protein (PMP) insertion and maturation before they arrive to their final destination. Peroxins have a myriad of molecular functions (Hettema et al., 2014; Costello and Schrader, 2018; Jansen and van der Klei, 2019).

We have previously discussed the importance of Pex11 in peroxisomal division, but another peroxin is also famous for its implication in the life cycle of a peroxisome: Pex3.

Pex3 is present in every organism where the presence of peroxisomes has been experimentally validated (Schlüter et al., 2006; Gabaldón et al., 2006; Mast et al., 2012). Cells lacking Pex3 are devoid of any vestige of peroxisomes (Hettema et al., 2000; Shimozawa et al., 2000; Hoepfner et al., 2005). Pex3 seems to play a central role in processes of PMP synthesis in the ER (Schmidt et al., 2012) to the formation of PPVs (Mast et al., 2016, 2018), the stability of the peroxisome importomer (Baerends et al., 2000; Hettema et al., 2000; Wróblewska et al., 2017), peroxisome motility and inheritance (Chang et al., 2009; Munck et al., 2009),

peroxisome–ER tethering (Knoblach et al., 2013), peroxisome-vacuole tethering (Wu et al., 2019), and peroxisome turnover (Motley et al., 2012).

Pex3 has a single TM alpha helix near the N-terminus that is anchored in the lipid bilayer (Höhfeld et al., 1991). The portion of Pex3 found on the lumenal side of the lipid bilayer contains a track of conserved basic amino acids that are important for its correct targeting to the ER (Baerends et al., 2000; Fakieh et al., 2013). If these residues are mutated Pex3 is targeted to mitochondria (Fakieh et al., 2013).The cytosolic part of Pex3 which makes up most of the length of the protein is made up by a helical bundle (Sato et al., 2010; Schmidt et al., 2010). At the steady state, Pex3 is at peroxisomes and is usually used in experiments as a peroxisomal marker (Hettema et al., 2000; Hoepfner et al., 2005). Overexpression of Pex3 results in its accumulation at the ER in yeast (Hoepfner et al., 2005; Breker et al., 2013), while it accumulates both at the ER and mitochondria in mammalian cells (Schmidt et al., 2012; Aranovich et al., 2014; Sugiura et al., 2017). In mammalian cells, the overexpression of Pex3 can also stimulate peroxisome turnover followed by the formation of new peroxisomes (Sugiura et al., 2017). This is why Pex3 is considered as a marker for peroxisomes and their sites of biogenesis. Deletion of *PEX3* negatively affects the stability of peroxisomal membrane proteins causing their degradation leading to the collapse of the peroxisomal compartment (Ghaedi et al., 2000).

Pex3 does not act alone, it's the critical receptor and partner of Pex19. Together, these proteins chaperone most PMPs for their insertion into the peroxisomal membrane (Fang et al., 2004; Matsuzaki and Fujiki, 2008). Pex19 surveils the cytosol for newly synthesized PMPs and binds to a hydrophobic membrane peroxisomal targeting sequence (mPTS) located near the transmembrane domain of most PMPs (Sacksteder et al., 2000; Jones et al., 2004). PMPs have one or more targeting sequences (mPTSs) that direct them to the peroxisomal membrane with the correct topology. Although a dozen or so mPTSs have been defined in several yeast and mammalian PMPs, they have no simple consensus sequence. However, most of these PMPs bind Pex19. Pex3 and Pex19 lack any capacity to form a channel in the membrane so it is tricky to imagine how these two proteins can function as a translocon. The sequential two-step amphipathic recruitment of Pex19 and the hydrophobic nature of the portion of Pex3 directly opposed to the lipid bilayer have been proposed to work together to overcome the energy barrier inherent in properly inserting a membrane protein (Chen et al., 2014a). So, it is conceivable that Pex3 and Pex19 could function as a membrane protein insertase for membrane proteins at the peroxisomal membrane (Liu et al., 2016) or at the ER. Indeed, studies suggest that the PMPs

undergo anterograde transport via the ER to peroxisomes. Many peroxins (i.e. Pex3, Pex16, and Pex30) are transported in this fashion. It has been postulated that these PMPs concentrate on the ER and then migrate to peroxisome via ER-derived vesicles that then fuse with membranes of PPVs to allow growth.

3.2) Peroxisomal matrix protein import

Unlike other protein import mechanisms, peroxisomal matrix protein import can accommodate fully folded proteins across the peroxisomal membrane and the assembly of the importomer happens in response to a targeting signal. This import can be divided into four steps: First, the soluble receptors bind their cargo proteins in the cytosol and guide them to a docking site at the peroxisomal membrane. In turn, the receptor–cargo complex shuttles to the luminal site of the peroxisomal membrane. Finally, the complex is disassembled in order to release the cargo and the receptor is returned to the cytosol for an addition round of import.

There are two types of peroxisomal targeting signals (PTSs) to the peroxisomal matrix.
-The most common is the tripeptide PTS1: **S-K-L** (or serine-lysine-leucine) or its conserved variants usually present at the C-terminal (Gould et al., 1989; Brocard and Hartig, 2006).
-The other one is PTS2: (R/K) (L/V/I)) x_5(H/Q) (L/A). usually at N-terminal or internal (Swinkels et al., 1991).
-A few proteins such as the acyl-CoA oxidase in *S. cerevisiae* either have no canonical PTS sequence or have one that is dispensable, suggesting that there may be other sequences yet undefined that allow them to be targeted to the peroxisomal lumen (Eckert and Erdmann, 2003).

Matrix proteins synthesized in the cytosol are bound by cytosolic receptors such as the peroxin Pex5 for proteins ending with PTS1 (Stanley et al., 2006), and Pex7 for PTS2 harboring proteins (Marzioch et al., 1994). These receptor-cargo complexes move to the peroxisome membrane where they dock with protein subcomplexes mainly composed of peroxins that are at the membrane. The docking complex of the peroxisomal import machinery for incoming receptor–cargo complexes is composed of three peroxins: Pex13, Pex14 and Pex17 (Eckert and Erdmann, 2003). The function of Pex17 is unknown. As for Pex13 and Pex14, they interact with one another and they both bind Pex5 (Williams et al., 2005; Kerssen et al., 2006) and Pex14 is believed to make the first contact of the PTS-receptors upon cargo translocation across the peroxisomal membrane. However, the composition of the translocon and the mechanism of translocation are not yet well characterized. It is proposed that components of the docking complex themselves might constitute part of the translocon (Eckert and Erdmann, 2003).

Interestingly, Pex5 changes its membrane topology during the protein import cascade. At the beginning, it is soluble in the cytosol but at the peroxisomal membrane it behaves like an integral membrane protein (Gouveia et al., 2000). Finally, Pex5 reaches the luminal side of the peroxisomal membrane (Dammai and Subramani, 2001) but we still do not know whether the whole receptor–cargo complex or just a part of Pex5 reaches the peroxisomal lumen during translocation (Kunau, 2001). Similarly, Pex7 has been demonstrated to behave like a cycling receptor (Nair et al., 2004) and it is likely that its co-receptor Pex20 also enters the peroxisome (Léon et al., 2006).

Once the cargo reaches the peroxisomal lumen it needs to be released, but this mechanism is not yet understood. In this context, the peroxin Pex8 is suggested to function in disassembling the receptor–cargo complexes or in targeting of Pex8 to the peroxisomes as it contains both the PTS1 and PTS2-sequence (Rayapuram and Subramani, 2006). Nonetheless, the best understood function of Pex8 is that it bridges the docking complex with the peroxisomal really interesting new gene (RING)-finger complex. This complex is composed of the RING-motif containing peroxins Pex2, Pex10 and Pex12 (Agne et al., 2003). The association of these two complexes is called the "importomer" (Agne et al., 2003). Following cargo release, the receptors and coreceptors need to be recycled for additional rounds of import (Dammai and Subramani, 2001; Nair et al., 2004; Léon et al., 2006).

Shortly after, the peroxisomal AAA-ATPases Pex1 and Pex6 were identified as the motor-proteins of Pex5 export (Miyata and Fujiki, 2005; Platta et al., 2005). Their functions are not redundant and rely on the membrane anchors Pex15 and Pex26 in yeast and mammals respectively. ATP binding and hydrolysis is thought to trigger conformational changes generating driving force that allows the receptor to be pulled out of the membrane. Although Pex5 and the AAA-ATPases form a complex at the peroxisomal membrane (Miyata and Fujiki, 2005; Platta et al., 2005; Rosenkranz et al., 2006), no direct interaction of the PTS-receptors with either Pex1 or Pex6 has yet been reported which suggests the implication of a third yet to be determined factor.

To conclude, these dynamic membrane and matrix protein import machineries that we just described are critical for peroxisomes to be able to fulfill their metabolic roles in the cell. Indeed, peroxisomes harbor numerous metabolic reactions such as beta oxidation and the "peroxidative" reaction to name a few, all of which cannot proceed without the correct peroxisomal localization of the respective enzymes needed for the reactions to take place.

4) Peroxisome Metabolism: from ROS to Fatty Acids

4.1) ROS/RNS metabolism

It was the first role discovered for peroxisomes back in 1996 (De Duve and Baudhuin, 1966), which also accounts for the name given to the organelle as it harbors various oxidases that produce H_2O_2 but also in scavenging hydrogen peroxide. Some of the most important enzymes contained by peroxisomes which generate H_2O_2 are (Schrader and Fahimi, 2006b; Fransen et al., 2012; del Río and López-Huertas, 2016):

-Glucose oxidase in yeast

-Glycolate oxidase, xanthine oxidase, nitric oxide synthase in plants

-Urate oxidase, aspartate oxidase, pipecolic acid oxidase, hydroxy-acid oxidase, polyamine oxidase, xanthine oxidase, nitric oxide synthase, in mammals

-Acyl-CoA oxidases in yeast, mammals and plants.

Peroxisomes also produce reactive nitrogen species (RNS) and reactive sulfur species (RSS). S-nitrosoglutathione (GSNO) is produced in the peroxisomes, when nitric oxide (NO) reacts with reduced glutathione (GSH) in the presence of O_2 (del Río, 2011).

Hydrogen Peroxide is not only produced in peroxisomes, the organelles are also scavengers of cellular accumulated ROS. Indeed, peroxisomes harbor anti-oxidant systems such as catalase (CAT), superoxide dismutase (SOD) and glutathione S-transferase (GST) *etc*. which regulate steady-state levels of ROS and thus avoid toxicity and preserving cell viably (Petriv and Rachubinski, 2004; Aksam et al., 2009; Fransen et al., 2012). These systems that control ROS levels are crucial due to the duality in the functions of oxidants.

'ROS' or Reactive oxygen species englobe an array of derivatives of molecular oxygen that occur as a normal attribute of aerobic life. Two molecules under this umbrella are hydrogen peroxide (H_2O_2) and the superoxide anion radical ($O_2^{\cdot -}$). They are key redox signaling agents that are produced by enzymes and/or by aerobic respiration (Veal et al., 2007).

At low physiological levels hydrogen peroxide acts signaling agent which contributes to metabolic regulation and stress responses supporting cellular adaptation to changes in environment and stress conditions (Goldberg et al., 2009; Mesquita et al., 2010; Ristow and Schmeisser, 2011). Several other reactive species are involved in redox signaling such as nitric oxide (NO), hydrogen sulfide and oxidized lipids. Conversely, elevated levels of ROS cause oxidative stress. Indeed, H_2O_2 is toxic at high concentration leading to programmed cell death (Madeo et al., 1999), generating hydroxyl radicals in the presence of redox-active transition metals (Koppenol, 2001) and causes damage to all classes of macromolecules, thereby

impairing their function. For these reasons, H_2O_2 levels (or ROS levels in general) need to be tightly regulated by the activity of H_2O_2 metabolizing enzymes.

4.2) β-oxidation of fatty acids

Aside from ROS metabolism, beta-oxidation of fatty acids is another hallmark function of peroxisomes conserved in all organisms (Lazarow and De Duve, 1976). Fatty acids and their derivatives are essential building blocks for the structural integrity of the cell but also for its metabolical functions. β-oxidation is the major breakdown pathway for fatty acid esters. In mammals, this takes place in peroxisomes but also in mitochondria while this process is exclusively peroxisomal in both yeast and plants (Poirier et al., 2006). The simplicity of the β-oxidation process confined to a single organelle in yeast cells is the reason behind using *Cerevisiae* as a model organism for studying the degradation of fatty acids.
Although yeast can synthesize *de novo* all the fatty acids that it requires (Daum et al., 1998), its ability to take up fatty acids from the environment is vital when alternative nutrients are not available. This constitutes a way to import molecules instead of using energy for biosynthesis.

The first step in the β-oxidation pathway is the activation of fatty acids. In *S. cerevisiae*, VLCFAs (very long chain fatty acids) are activated in the cytosol by acyl CoA synthetases Faa1 and Faa4, then transported into peroxisomes via Pxa1-Pxa2 and Fat1. While activation of MLCFAs (medium and long chain fatty acids) by Faa2 occurs in peroxisomes (Black and DiRusso, 2007; Færgeman et al., 2001, 1997; Hettema et al., 1996; Hiltunen et al., 2003).
The *FAA1* and *FAA4* genes encode acyl-CoA synthetases required for activation of imported exogenous fatty acids. Deletion of both genes restricts import and activation of FAs (Færgeman et al., 2001). In mammals, fatty acyl-CoAs are transported into peroxisomes through the ABCD1 transporter after being activated in the cytosol (Jean Demarquoy and Borgne, 2015).
After activation, the following step is dehydrogenation, then hydration, followed by another dehydrogenation step and finally thiolytic cleavage producing free acetyl-CoA and an acyl-CoA shortened by two carbon atoms (**Fig 17**). The enzymes involved in these reactions are acyl-CoA oxidase, hydratase, dehydrogenase and thiolase respectively. An overview of all the enzymes required for β-oxidation can be found in **Table 5**.

Gene	Enzyme	Localization	pathway	Reference
ANT1	ATP transporter	peroxisomal membrane	β-oxidation	(Palmieri et al., 2001)
PXA1 (*SSH2, PAL1*)	Peroxisomal ABC transporter	peroxisomal membrane		(Shani et al., 1995)
PXA2 (*PAT1*)	Peroxisomal ABC transporter	peroxisomal membrane		(Shani and Valle, 1996)
FAA1	long-chain fatty acyl-CoA ligase	multiple sub-cellular locations		(Duronio et al., 1992) (Johnson et al., 1994)
FAA2 (FAM1)	medium-chain fatty acyl-CoA ligase	peroxisomal matrix		(Johnson et al., 1994)
FAA3	long-chain fatty acyl-CoA ligase	?		(Johnson et al., 1994)
FAA4	long-chain fatty acyl-CoA ligase	cytosol		(Johnson et al., 1994)
FAT1	very long-chain fatty acyl-CoA ligase	multiple sub-cellular locations		(Færgeman et al., 1997)
DCI1 (*EHD2, ECI2*)	$\Delta^{3,5}$-$\Delta^{2,4}$-dienoyl CoA isomerase	peroxisomal matrix		(Gurvitz et al., 1999)
ECI1 (*EHD1*)	Δ^{3}-Δ^{2}-enoyl-CoA isomerase	peroxisomal matrix		(Gurvitz et al., 1998)
SPS19 (*SPX19*)	2,4-dienoyl-CoA reductase	peroxisomal matrix		(Gurvitz et al., 1997)
POT1 (*FOX3, POX3*)	β-ketoacyl-CoA thiolase	peroxisomal matrix		(Erdmann, 1994)
FOX2 (*POX2*)	(3*R*)-hydroxyacyl-CoA dehydrogenase, 2-enoyl-CoA hydratase 2	peroxisomal matrix		(Hiltunen et al., 1992)
POX1 (*FOX1*)	acyl-CoA oxidase	peroxisomal matrix		(Dmochowska et al., 1990)
ACO1	aconitate hydratase	cytosol	Glyoxylate Cycle	(Gangloff et al., 1990)
CIT2	peroxisomal citrate synthase	peroxisomal matrix		(Kim et al., 1986)
ICL1	isocitrate lyase	cytosol		(Fernández et al., 1992)
MLS1	Malate synthase	cytosol, peroxisomal matrix		(Kunze et al., 2002)
MDH2	NAD malate dehydrogenase	cytosol, peroxisomal matrix		(Minard and McAlister-Henn, 1991)
MDH3	NAD malate dehydrogenase	peroxisomal matrix		(Steffan and McAlister-Henn, 1992)
CAT2	carnitine *O*-acetyltransferase	peroxisomal matrix	Carnitine shuttle	(Elgersma et al., 1995)
ACB1	acyl-CoA binding protein	?	?	(Schjerling et al., 1996)

Table 5: Enzymes of the peroxisomal metabolic pathways and their respective localizations. '?' indicate unknowns.

The promoter sequences of the genes involved in FA oxidation harbor a positive cis-acting element that mediates the induction of these genes by fatty acids in the medium. This element is called an oleate response element (ORE) and consists of an inverted repeat containing conserved CGG triplets that are spaced by 14–19 nucleotides (CGG-N14/N19-CCG). The proliferation of peroxisomes and the induction of the beta-oxidation machinery is required for yeast to be able to grow on FA containing media (such as oleate) (Schrader et al., 2016). Compared to yeast, mammalian peroxisomes are more versatile as they are capable of metabolizing not only straight-chain acyl-CoAs but also 2-methyl branched acyl-CoAs, by having multiple acyl-CoA oxidases (Hiltunen et al., 2003). Yeast can utilize both saturated long chain fatty acids (such as palmitic acid) as well as unsaturated fatty acids (such as oleic acid and linoleic acid) as substrates for β-oxidation (van Roermund et al., 2003). The only difference is that for the oxidation of unsaturated fatty acids, *S. cerevisiae* requires auxiliary enzymes like Dci1, Eci1 and Sps19 (Hiltunen et al., 2003) (**Table 5**). Following several rounds of complete lipid breakdown by beta-oxidation, peroxisomal acetyl-coA or propionyl-coA (for odd numbered FAs) is produced.

Acetyl-coA is involved in different metabolic pathways such as *de novo* biogenesis of FAs and sterols, biosynthesis of flavonoids and carotenoids among others, synthesis of metabolites while growing on C_2 carbon sources such as acetate and finally for energy production in the tricarboxylic acid (TCA) cycle. In light of its importance, it is no surprise that Acetyl-coA is not exclusively produced in peroxisomes. In fact, yeast acetyl-CoA metabolism takes place in at least four subcellular compartments: nucleus, mitochondria, cytosol and peroxisomes. Depending on the supply of substrate to the cell, various mechanisms may lead to the formation and utilization of acetyl-CoA. With sugars (such as Glucose) as carbon source, direct formation of acetyl-CoA from pyruvate catalyzed by the pyruvate dehydrogenase complex (PDH) in the mitochondria. In turn this serves as fuel for the TCA cycle. On the other hand, acetyl-CoA generated via direct activation of acetate in an ATP-dependent reaction by an acetyl-CoA synthetase (ACS) in the cytosol is the only source for fatty acid and sterol biosynthesis (Pronk et al., 1996). During growth on oleate, acetyl-CoA is the end product of β-oxidation of straight chain fatty acids, which in yeast exclusively takes place in the peroxisomes (Kunau et al., 1995). Nonetheless, membrane organelles including peroxisomal membranes are not permeable to acetyl-CoA (van Roermund et al., 1995).

Indeed, *in vitro* experiments allowed us to gain insights on peroxisomal membrane permeability (Antonenkov et al., 2009). Studies show that peroxisomal membranes are open to small

metabolites and closed to cofactors and other 'bulky' molecules. The β-oxidation of fatty acids in peroxisomes is accompanied by the reduction of NAD^+ and the formation of acetyl/acyl-CoA while others require oxidation of NADPH (Wanders and Waterham, 2006). These compounds (e.g. NADH, $NADP^+$ and acetyl/acyl-CoA esters) are considered 'bulky' solutes unable to permeate peroxisomal membranes fast enough. A combination of shuttle and channel systems allow the transfer of "bulky" metabolites.

This is notably the case of the metabolite acetyl-coA which must be either synthesized in each subcellular compartment where it is required or be imported using specific transport mechanisms. Until now, two transport mechanisms have been identified (Kunau et al., 1995). The first one is the carnitine/acetyl-carnitine shuttle in which the acetyl-CoA produced in the peroxisomes or the cytosol is conjugated to carnitine by the carnitine acetyl transferase Cat2, which is localized to both peroxisomes and mitochondria (Elgersma et al., 1995) (**Fig 17**). After transport to mitochondria, the mitochondrial form catalyzes the opposite reaction, thereby supplying acetyl-CoA units to the TCA cycle. This system depends on exogenous carnitine supply since carnitine cannot be synthetized *de novo* in *Cerevisiae* (van Roermund et al., 1999). The other transport mechanism consists of synthetizing C_4 dicarboxylic acids from acetyl-CoA via the Glyoxylate shunt. This system is especially used when cells use non-fermentable sources such as ethanol, acetate or glycerol.

4.3) The Glyoxylate cycle

The glyoxylate cycle is actually a shortened TCA cycle (Kornberg and Madsen, 1958) that enables cells to use fatty acids or C_2-units as sole carbon source. There are common enzymes between the Glyoxylate and the TCA cycle, notably malate dehydrogenase (MDH), citrate synthase (CIT) and aconitase (ACO). However instead of having 2 decarboxylation steps, two unique enzymes of the glyoxylate cycle isocitrate lyase (ICL) and malate synthase (MLS) convert isocitrate and acetyl-CoA into succinate and malate (**Table 5**). The cleavage of isocitrate bypasses the decarboxylation reactions splitting the C_6-unit into succinate and glyoxylate (giving its name to the pathway) which in turn is condensed by malate synthase with acetyl-CoA generating free CoA-SH and malate. In order to continue the cycle, malate is reused by malate dehydrogenase with succinate being released as a net product (**Fig 17**). Finally, succinate is used by mitochondria to boost the TCA cycle or to be used as a precursor of amino acid synthesis or carbohydrate biosynthesis. It is also worth noting that a part of the citrate produced by the glyoxylate cycle is also transported to mitochondria (**Fig 17**).

Unlike what was believed for a long time, not all glyoxylate cycle enzymes are peroxisomal as it is the case in bacteria. Glyoxylate cycle enzymes actually have a more complicated subcellular distribution, making it the typical metabolic pathway in which substrates/enzymes move back and forth across membranes **(Fig 17)**. In *S. cerevisiae*, AcoI, Icl1 are cytosolic. The citrate synthase Cit2 is exclusively peroxisomal and it has a C-ter -SKL (PTS1). Recently, Mdh2 was also recently shown to localize to the peroxisomal matrix (Gabay-Maskit et al., 2020) in addition its cytosolic activity (Minard and McAlister-Henn, 1991). The localization of malate synthase Mls1 which is essential for cell growth on non-fermentable carbon sources (Hartig et al., 1992) was a bit trickier to assess. Mls1 has a C-terminal SKL sequence but it's not exclusively peroxisomal. A study by Kunze and colleagues revealed that the enzyme only enters peroxisomes in cells supplied with oleic acid, the protein remains cytosolic in cells grown on ethanol (Kunze et al., 2002). The reason for the advantage of a peroxisomal Mls1 to cells grown on oleic acid is still unknown. This configuration means that citrate, glyoxylate, malate and oxaloacetate have to be transported across the peroxisomal membrane which is impermeable to "bulky" substrates but organic acids (mainly dissociated thus negatively charged) are able to cross. The cytosolic localization of isocitrate lyase in yeast omits the necessity to export succinate from peroxisomes, but requires the import of glyoxylate instead of isocitrate. As for citrate, it's export may also serve a different purpose other than fueling the glyoxylate cycle. Indeed, C_2-unit transfer to mitochondria is beneficial for energy production in the TCA cycle. Physical proximity between peroxisomes and mitochondria might contribute to facilitate this transfer.

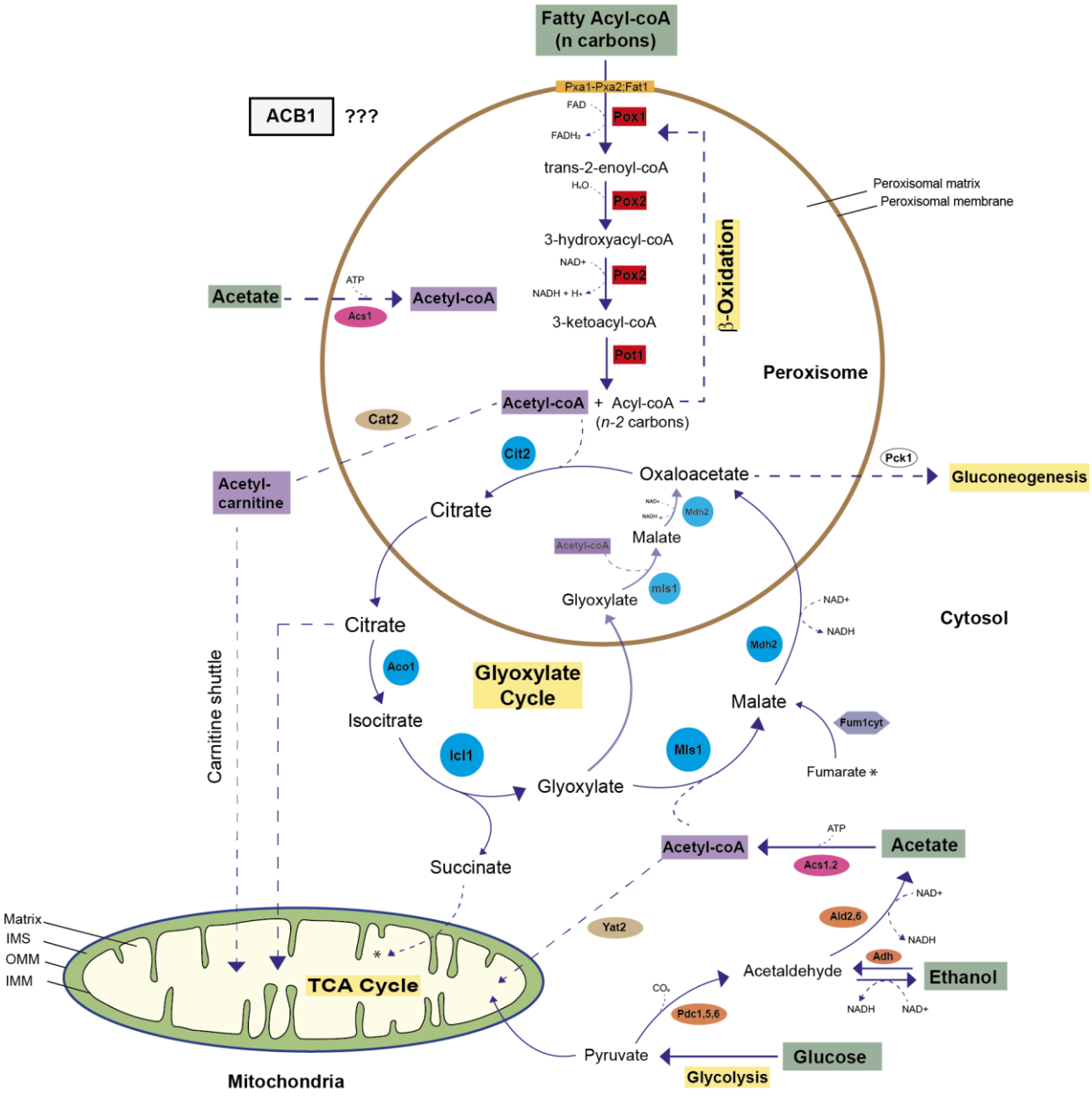

Fig17: Schematic representation of the metabolism pathways at peroxisomes and their connection to mitochondria. Metabolic cycles are highlighted in yellow (TCA, Beta-oxidation, Glyoxylate cycle…). The essential enzymes of beta-oxidation are highlighted in red. The main enzymes of the Glyoxylate cycle are in blue circles. Carbon sources are highlighted in green.

5) Regulation of peroxisomal functions by inter-organelle contacts

Membrane contacts directly impact peroxisome inheritance. This is because peroxisome anchoring ensures that the mother cell retains peroxisomes in budding yeast. The tether that connects peroxisomes to the cortical ER in yeast is made up of two proteins, Inp1 and the peroxisome biogenic protein Pex3. This interaction between Pex3 proteins in *trans* bridged by the peripheral peroxisomal Inp1 plays a part in peroxisome anchoring (Knoblach et al., 2013).

In fact, Inp1 contains at least two binding sites for Pex3 and acts as a molecular hinge that bridges endoplasmic reticular Pex3 and peroxisomal Pex3 into an ER–peroxisome tethering complex (Knoblach et al., 2013). Cells without Inp1 only have mobile peroxisomes that are eventually driven to the bud by Inp2/Myo2-dependent transport. On the other hand, Inp1 overexpression fixes all peroxisomes at cortical positions in the mother cell and fails to transfer any peroxisomes to the bud (Fagarasanu et al., 2005). Quite recently, Inp1 was identified as a plasma membrane–peroxisome tether. Mediating peroxisome retention via an N-terminal domain that binds $PI(4,5)P_2$ and a C-terminal Pex3-binding domain, forming a bridge between the peroxisomal membrane and the plasma membrane (Hulmes et al., 2020).

In addition to regulating membrane inheritance, inter-organelle contacts also regulate peroxisome biogenesis. Contacts between the mammalian peroxisomes and the ER are stabilized by the peroxisomal protein ABCD5 and the ER-localized VAP (for **V**AMP-**a**ssociated **p**rotein) (Costello et al., 2017; Hua et al., 2017). As peroxisomal membranes need to expand during peroxisomal growth, transfer of phospholipids from the ER via ER-Peroxisome contacts directly regulates this expansion and ultimately peroxisomal growth (Costello et al., 2017).

Lipid transfer also occurs via contacts between peroxisomes and Lipid droplets (LDs).
First the peroxisomal protein ABCD1 interacts with the membrane bound AAA-ATPase M1-Spastin found on Lipid droplets forming a tethering complex (Chang et al., 2019). In turn, Spastin recruits the ESCRT-III proteins IST1 and CHMP1B to the lipid droplets. As ESCRT proteins have the capacity to shape membranes, this is thought to facilitate FA trafficking (Chang et al., 2019). This contact site helps facilitate fatty acid transfer from the lipid droplet to the peroxisome and reduces the levels of peroxidated lipids in LDs.

Lipids are not the only substrate which is more easily exchanged by making contact sites between peroxisomes and the remaining cellular organelles. Indeed, specific machineries mediating tethering between peroxisomes and other organelles are also involved in metabolic reactions such as β-oxidation of fatty acids. In yeast, the overexpression of the tether Pex34 increased CO_2 production arising from fatty acid β-oxidation occurring in the peroxisome. The inhibition of citrate production abolished the effects seen by overexpression of Pex34 which suggests that Pex34-mediated contacts are responsible of facilitating the transfer of β-oxidation intermediates between Peroxisomes and Mitochondria while the role of Fzo1-mediated contacts is still unknown (Shai et al., 2018) (**Fig15**).

Part 2: Results

I- Tackling the extra-mitochondrial Fzo1

1) Fzo1 accumulates in the cytosol of *mdm30*Δ cells

When I first started my master's internship in the lab, the paper of N. Shai and colleagues was not yet published. The data we had in the lab suggested that an extra-mitochondrial pool of Fzo1 was present in the cell but we did not know where it was located exactly (**Fig 18**).
I was set out to decipher this novel localization of the yeast mitofusin Fzo1 during my PhD.

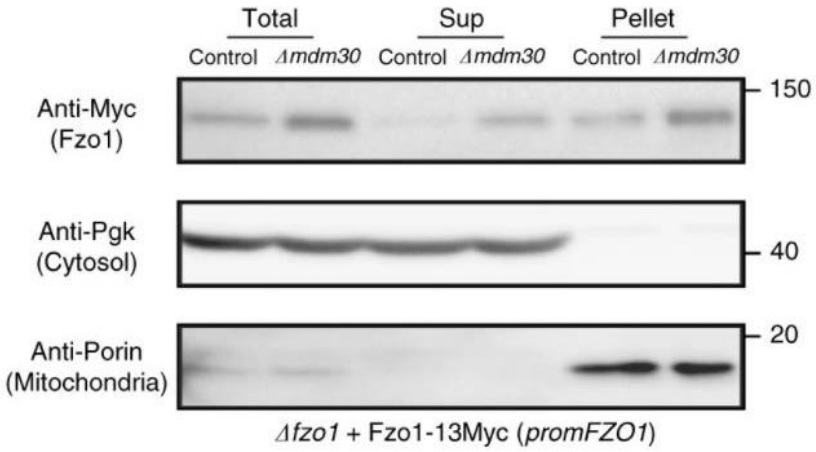

Fig18: Sub-cellular fractionation assay from WT and *mdm30*Δ cells. The unique copy of Fzo1 expressed is tagged with 13Myc epitopes (Fzo1-13Myc). Total lysates were subjected to subcellular fractionation yielding a cytosolic fraction (Sup) and a mitochondria-enriched (Pellet) fraction. All the fractions analyzed by immunoblotting with anti-Myc (Fzo1), anti-Pgk (cytosolic marker) and anti-Porin (mitochondrial marker) antibodies. Fzo1 is detected in a non-mitochondrial fraction more readily visible by deleting *MDM30* where Fzo1 levels are stabilized (Shai et al., 2018).

The deletion of *MDM30* abolishes the UPS-dependent degradation of Fzo1 (Cohen et al., 2011a), stabilizing the levels of the protein (Total). As expected, the levels Fzo1 increase on mitochondrial outer membranes (Pellet). Nonetheless, the presence of Fzo1 in the cytosol which is devoid of mitochondria suggests that this Fzo1 is present on another organelle. As Fzo1 is a DRP with 2 TM domains (**Fig12**), we suspected that it's more likely to be localized on a membrane rather than being free in the cytosol.

In order to determine this localization, I tried using sub-cellular fractionation assays coupled to sucrose gradients. Using this approach, we would separate mitochondria from the remaining membranes in WT and *mdm30*Δ cells then check where Fzo1 localizes along the gradients. The first step of the experiment was to separate the membranes from the cytosol using the same protocol used before (**Fig18**). Then the membrane fraction (containing mitochondria but also other organelles) was placed on a sucrose gradient composed of layers with different sucrose concentrations. This would allow to purify mitochondria according to the density of its membrane. The concentrations of the sucrose cushions ranged between 60% and 15%. The concentrated membrane fraction was gently placed on the top of the gradient (above the 15% fraction) and after centrifugation mitochondria were found at the junction between the 60 and the 42% sucrose layers. Mitochondria were clearly visible after centrifugation as a light white ring. Two types of gradients were used to try this purification: continuous and discontinuous gradients. Continuous gradients allow a gentler separation of membranes while discontinuous gradients exert more mechanical force. Eventually we decided to pick the discontinuous protocol to get a clearer and more efficient separation of mitochondria from the other organelles. After centrifugation, I extracted each layer in order from top to bottom and treated it with TCA before Immuno-blotting.

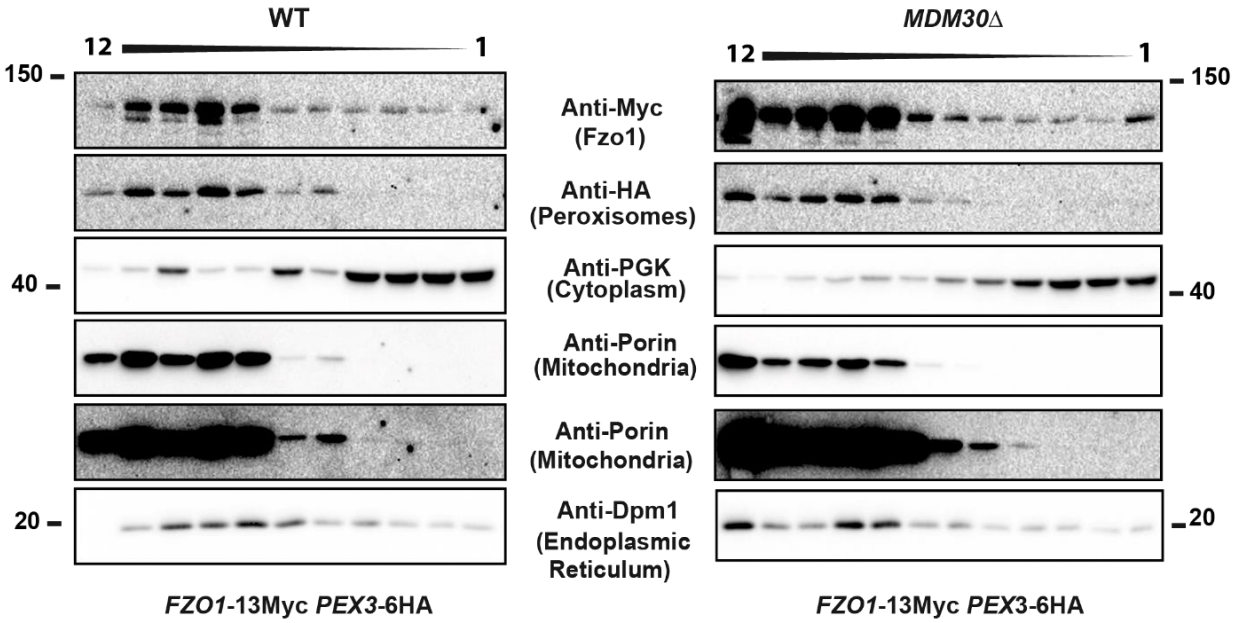

Fig19: Sucrose gradients of Pellets from WT and *mdm30*Δ cells. Total lysates were subjected to subcellular fractionation yielding a cytosolic fraction (Sup) and a mitochondria-enriched (Pellet) fraction. The Pellet fraction was loaded onto a sucrose gradient to isolate mitochondria. Lane 1 represents the top fraction of the gradient and lane 12 represents the bottom fraction.

Fzo1 is tagged with 13Myc epitopes at the genome (*FZO1*-13Myc) and the peroxin Pex3 is tagged with 6 HA epitopes at the genome (*PEX3*-6HA). All the fractions were analyzed by immunoblotting with anti-Myc (Fzo1), anti-Pgk (cytosolic marker), Anti-HA (peroxisomes), anti-Porin (mitochondrial marker) and anti-Dpm1 (ER marker) antibodies. MW in kDa are shown on the right.

By comparing the two gradients, we can clearly see that mitochondria are present in the same fractions in the two gradients (from lane 5 to lane 12) which shows that the separation is identical between the two strains. The lanes with the strongest Fzo1 signal (Fzo1 peak) coincide with the lanes where we have the strongest mitochondrial signal (Porin peak) in both gradients (lanes 6 to 12). This is not surprising since Fzo1's main localization is on mitochondrial outer membranes. However, we see an additional peak of Fzo1 in the *mdm30*Δ gradient which is not present in the WT. This peak of Fzo1 is located from lane 1 to lane 3 on the *mdm30*Δ gradient where there is no mitochondrial signal. Using antibodies against markers from different sub-cellular organelles, we saw that this Fzo1 signal coincided with the PGK1 signal (cytosol) and Dpm1 (ER). These observations allowed us to narrow out this extra-mitochondrial localization of Fzo1 to two possible localizations: either on ER membranes or in light cytosolic organelles (peroxisomes, endosomes …).

Nonetheless, the mitochondrial fraction in the gradient was also not perfectly pure, in addition to an ER contamination we also had a strong peroxisomal contamination. It is likely that most peroxisomes in the pellet fraction are attached to mitochondria which explains why they sedimented in the same fraction and for these reasons we didn't see any detectable peroxisomal signal in the remaining parts of the gradient (**Fig 19**).

Eventually, this approach did not allow us to identify the extra-mitochondrial localization of Fzo1 but it gave us hints on the possible localizations of the protein narrowing the list to ER membranes or light cytosolic organelles such as peroxisomes. Interestingly, around the same time the study by Shai and colleagues showing that Fzo1 is a tether between peroxisomes and mitochondria was published (Shai et al., 2018). In this study, they show that Fzo1 overexpression leads to an increase in Peroxisome-Mitochondria contacts (PerMit contacts to simplify). Although this study establishes Fzo1 as a tether between the two organelles, it suggests but doesn't provide actual proof of Fzo1's peroxisomal localization.

2) Fzo1 naturally localizes to peroxisomal membranes

Logically, this study put us on the trail of peroxisomes so we aimed to prove that the extra-mitochondrial Fzo1 is located on peroxisomal membranes. This time we tried a more direct approach using immuno-precipitation assays of native peroxisomes (i.e. in the absence of detergent) from the cytosolic fractions of WT and *mdm30*Δ cells.

First, we used the peroxisomal protein Pex3 tagged with 6-HA epitopes to pull-down native peroxisomes and we detected Fzo1 by immuno-blotting (**Fig 1C, D**-Alsayyah *et al*.). In the second approach we relied on a different readout, this time using fluorescence microscopy. Like the first experiment, we used the same peroxisomal protein Pex3 tagged with the red fluorescent protein mCherry and Fzo1 was tagged with GFP at the genome. We immuno-precipitated peroxisomes in native conditions thanks to RFP-trap coated magnetic beads that capture red fluorescent proteins. Finally, we observed these beads by fluorescent microscopy which allowed us to quantify the number of beads where we observed a red fluorescent signal coinciding with a green signal indicating the presence of Fzo1 on peroxisomes (**Fig1E, F** - Alsayyah *et al*.). More importantly, this approach revealed that Fzo1 naturally localizes to peroxisomal membranes, and not just accumulates at peroxisomal membranes in *mdm30*Δ cells.

This physiological localization of Fzo1 on peroxisomal membranes was quite intriguing. We speculated that it could simply be due to a rerouting or a Quality Control mechanism that gets rid of misfolded or excess Fzo1 on mitochondria thus transferring it to peroxisomal membranes. In this context, Msp1 is a conserved AAA-ATPase in budding yeast that resides on the outer surfaces of two compartments within cells: mitochondria and peroxisomes (Chen et al., 2014a; Okreglak and Walter, 2014). Msp1 is a quality control protein that prevents accumulation of mistargeted tail-anchored (TA) proteins (Chen et al., 2014b; Weir et al., 2017). If Fzo1's peroxisomal localization is due to mistargeting, it would be gone when Msp1 is inactivated. To test this, we performed the classical sub-cellular fractionation assay in WT, *mdm30*Δ, *msp1*Δ and the *mdm30*Δ *msp1*Δ double mutant and we looked at Fzo1 pools in the different fractions (**Fig20**). *MSP1* deletion of did not affect the peroxisomal localization of Fzo1 which remains visible in the cytosolic fraction of *mdm30*Δ cells.

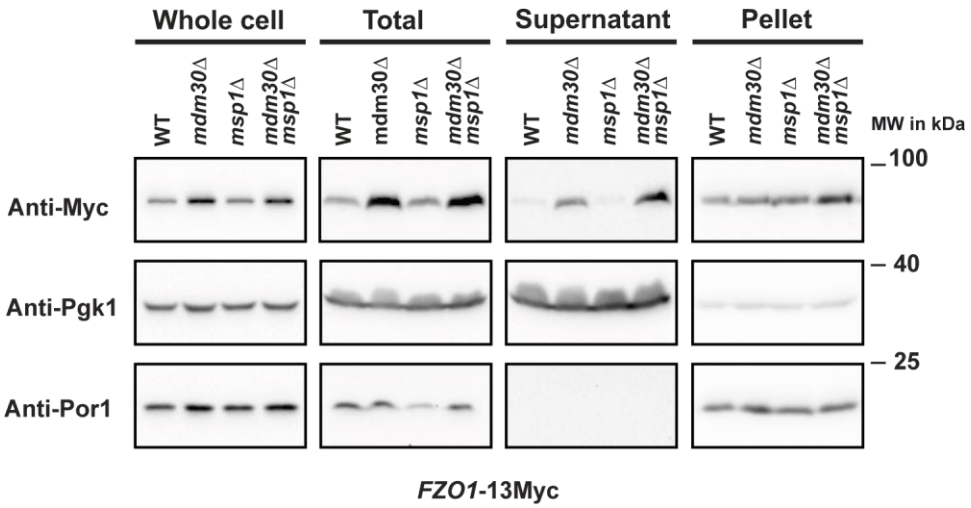

Fig20: Sub-cellular fractionation assay from WT, *mdm30*Δ, *msp1*Δ and *mdm30*Δ *msp1*Δ cells. Fzo1 is tagged with 13Myc epitopes at the genome (Fzo1-13Myc). Total lysates were subjected to subcellular fractionation yielding a cytosolic fraction (Sup) and a mitochondria-enriched (Pellet) fraction. All the fractions were analyzed by immunoblotting with anti-Myc (Fzo1), anti-Pgk1 (cytosolic marker) and anti-Por1 (mitochondrial marker) antibodies. Fzo1 is detected in non-mitochondrial fractions even after *MSP1* deletion.

Taken altogether, these results imply that Fzo1 naturally localizes to peroxisomal membranes. The peroxisomal Fzo1 contributes to PerMit contacts by interacting with the mitochondrial pool of Fzo1 thanks to its oligomerization capacity. By abolishing this oligomerization property using the Fzo1-S201N GTPase domain mutant, we inhibited Fzo1-mediated PerMit contacts and quantified their contribution to the totality of PerMit contacts occurring in the cell (**Fig2C, D** -Alsayyah *et al*.). The following step consisted in understanding how Fzo1-mediated PerMit contacts were regulated in WT cells.

II- Regulation of Fzo1 levels by modulating cellular FA desaturation

Fzo1 is required for mitochondrial outer membrane fusion to take place. However, a dedicated regulation of Fzo1 levels is crucial for this process to be successful. As we have seen in the earlier sections, the yeast mitofusin is regulated by an intricate balance between UPS-mediated turnover and cellular fatty acid desaturation levels (Cavellini et al., 2017). Indeed, when cellular FA desaturation is high, Fzo1 levels are stabilized. Conversely, when FA desaturation is low, Fzo1 turnover increases. In line with these findings, we reasoned peroxisomal Fzo1 levels and in turn Fzo1-mediated PerMit contacts might be modulated by cellular fatty acid desaturation.

1) Modulating FA desaturation by adding Fatty Acids to the media

Playing with FA desaturation is very tricky as Ole1 is the unique yeast Δ9-fatty acid desaturase that converts saturated FAs to unsaturated FAs according to the cell's needs. It is thus no surprise that the regulation of this gene is extremely sensitive and robust at the same time. When culture media is supplemented with saturated FAs such as palmitic acid, the cell adapts to this decrease in saturation consequently increasing turnover of Fzo1. Conversely, when the media is supplemented with unsaturated FAs such as oleic acid, cells naturally adapt and stabilize Fzo1 levels. So, we decided to use this approach in order to simulate natural variations in FA desaturation which would directly affect Fzo1 levels by growing the cells in media supplemented with palmitic or oleic acid.

We tested various concentrations of FAs ranging from 0.1% to 0.5%. In addition, Fzo1 is not a very abundant protein and it's not very well detected by our polyclonal antibody. This is why we used 2 sets of strains to check Fzo1 levels: one in which *FZO1* was placed under the control of an Adh promoter (for better detection) and a WT strain in which *FZO1* is under the control of its endogenous promoter. We also introduced *MDM30* deletions to see if the effect of FAs on Fzo1 levels is abolished (**Fig21-A**). After protein extraction and detection by immunoblotting, no clear-cut changes in Fzo1 levels were visible between the treated and the non-treated cells and almost no difference between the two different FA treatments (**Fig21-A**). This kind of experiment was very difficult to do as fatty acids are not soluble in liquid media, especially palmitic acid. Thus, media supplemented with fatty acids were quite cloudy making growing cells and monitoring their OD (optical density) very difficult. After many attempts, we dropped this particular approach as it was not rendering reproducible results (**Fig21-A**). Moreover, we suspected that long incubation times allowed cells to adapt their lipidome which dampened the effect we were seeking to see on Fzo1 levels so we needed to test another approach.

2) Modulating FA desaturation by adding an extra-copy of Mga2

As mentioned previously, *OLE1* transcription is driven by the soluble factors Mga2 and spt23 after their processing (from p120 to p90 fragments). These soluble N-terminal fragments migrate to the nucleus and induce *OLE1* transcription. Based on this, we constructed a plasmid expressing Mga2 in its p90 form which we introduced in WT and *mdm30*Δ cells. This extra-copy of Mga2 should increase *OLE1* expression and in turn Fzo1 levels (**Fig21-B**). As expected, Fzo1 levels increased in the presence of the extra-copy of Mga2 (+Mga2) in comparison with

the empty vector (v.v) (**Fig21-B**). Nonetheless, even with the addition of the extra-copy of Mga2 we faced the same reproducibility problems as *OLE1* was still under the regulation of its endogenous promoter.

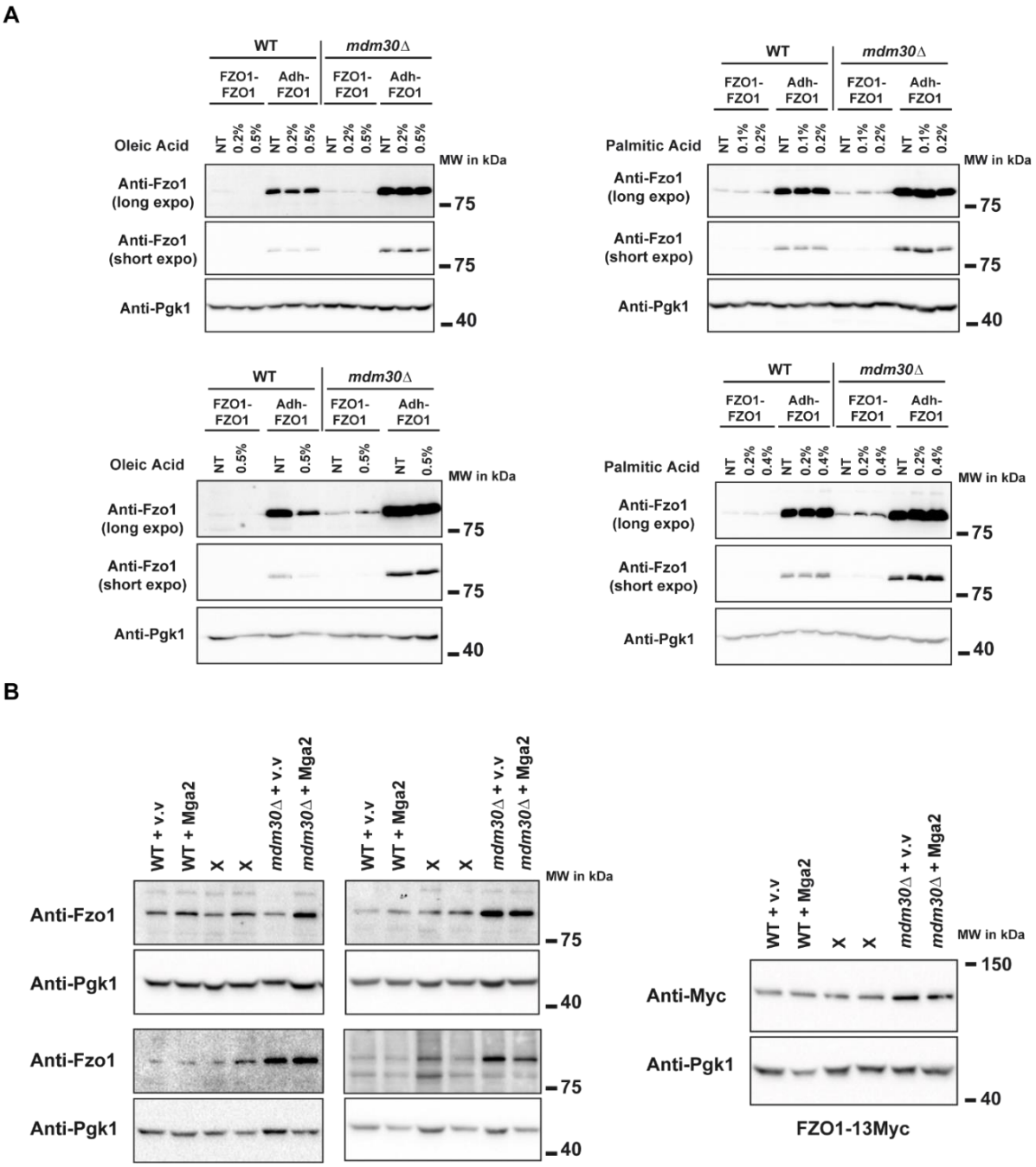

Fig21: Two approaches to modulate cellular FA desaturation. **(A)** Total protein extracts from WT and *mdm30*Δ cells. Strains were grown in different concentrations of Oleic acid (0.2%, 0.5%) or Palmitic Acid (0.1%, 0.2%, 0.4%) or not treated (NT) overnight. **(B)** Total protein extracts from WT and *mdm30*Δ cells transformed either with an empty vector (+v.v) or with an

extra-copy of Mga2 (+Mga2). Extracts were analyzed by anti-Fzo1 and anti-Pgk1 (A and B) and anti-Myc (B) immuno-blotting. MW in kDa are shown on the right.

3) Modulating FA desaturation by controlling the *OLE1* promoter

Ultimately, we were resolved to use the most robust and clean way to control the expression of a gene which is to directly change its promoter. Thus, we decided to clone the *OLE1* gene into different plasmids each one expressing *OLE1* under the control of different promoters.
As *OLE1* is an essential gene its deletion would be lethal; which is why we needed to use a shuffling strategy in order to keep the strains alive. Shuffle strains are quite useful in this situation because a plasmid with a URA selection covers the deletion of a certain gene temporarily until we decide to get rid of it. Through a curation step using 5'FOA, we can get rid of the URA plasmid because it renders uracil metabolism toxic to the cell which ejects the plasmid. Here, a URA plasmid expressing Ole1 covers the genomic *OLE1* deletion so that the cells don't die until it is replaced by the final *OLE1* plasmids that we would have chosen with a TRP selection.

First, I constructed several Ole1 plasmids with URA selection so that we can get rid of them later using 5'FOA (**Fig22**). The cloned *OLE1* gene was tagged with 9-Myc epitopes to follow its expression levels later on by immuno-botting. Each plasmid harbored a different promoter upstream of the *OLE1* gene because we had no idea what effect they would have on the cell and to assess their expression levels (**Fig22**). I tested 4 different promoters, the one with the weakest expression level is Cyc1, then Met25 followed by Adh and finally the Tef promoter with the strongest expression. After transformation with these plasmids, I was able to delete *OLE1* at the genome so that the only copy of *OLE1* expressed in the cell originates from the shuffle plasmid. In order to double check the *OLE1* deletion, I replicated the strains carrying the URA shuffle plasmid twice on 5'FOA forcing the cell to make a difficult choice and eject the plasmid thus causing lethality due to Ole1 loss. Finally, I did the same steps to construct untagged Ole1 plasmids with a TRP selection that would definitely replace the URA shuffle plasmids in *ole1*Δ cells (**Fig S2A** -Alsayyah *et al*.).

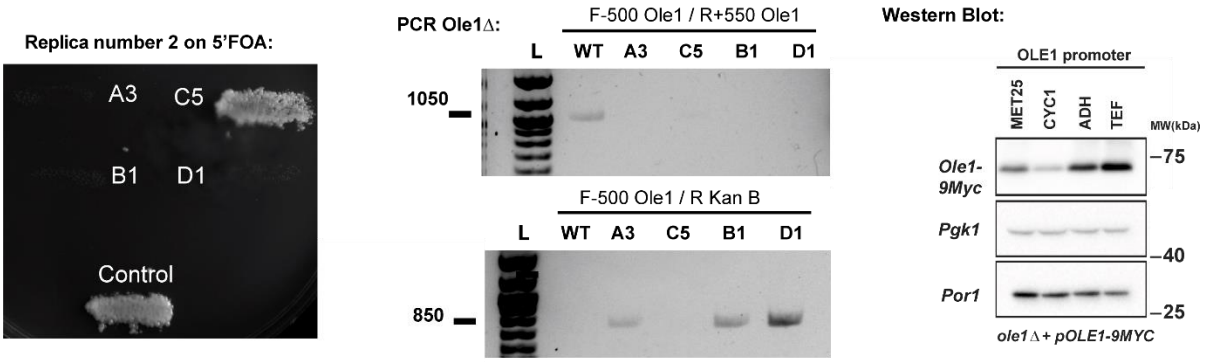

Fig22: Ole1 shuffle strains construction steps. After 2 replicas on 5'FOA media, *OLE1* null cells are totally dead while the control and false deletants grow normally. This is the case of the strain C5 for example which is negative by PCR (F-500 Ole1/R+550 Ole1) for genomic *OLE1* but is unaffected after loss of the URA shuffle plasmid covering for *OLE1* deletion.
I built four Ole1 shuffle plasmids expressing *OLE1* under the control of different promoters. Ole1 is tagged with 9-myc epitopes. Total protein extracts were analyzed by anti-Myc, anti-Pgk1 and anti-Por1 immuno-blotting. MW in kDa are shown on the right.

Once the system we needed to control Ole1 levels was ready, we used it to simulate different desaturation levels consequently modulating Fzo1 levels. Thanks to this tool, we showed that levels of Fzo1 increased upon Ole1 overexpression (TEF condition) and Fzo1 levels decreased in low Ole1 expression (CYC condition) (**Fig3A**-Alsayyah *et al.*) which consolidates previous studies (Cavellini et al., 2017). Moreover, we saw that PerMit contacts increase with high FA desaturation when Fzo1 levels are stabilized (thus mirroring *mdm30*Δ cells) and decrease when FA desaturation is low and Fzo1 turnover is high (**Fig 3D, E**-Alsayyah *et al.*). PerMit contacts thus not only increase with the status of desaturation of FAs but also following the level of Fzo1. Most importantly, the deletion of *MDM30* completely inactivates the whole system (**Fig3F**-Alsayyah *et al.*). *In fine*, we propose a model in which Fzo1-mediated PerMit contacts are regulated by FA desaturation and Mdm30-mediated degradation of Fzo1.

III- The rescue of respiration in *mdm30*Δ cells by an extra-copy of Fzo1

In parallel to investigating the peroxisomal localization of Fzo1, I was also trying to decipher another important result obtained by the team before my arrival to the lab (**Fig23**).

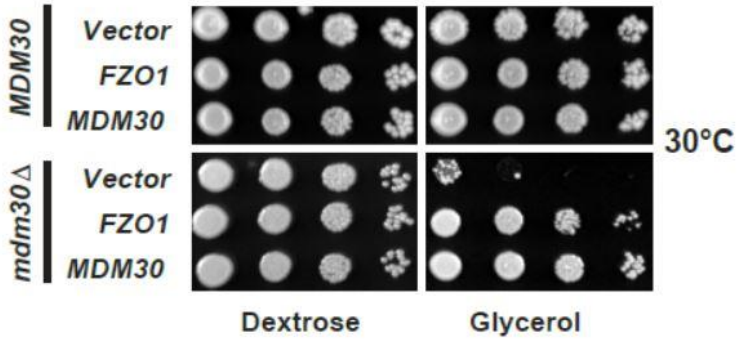

Fig23: Fzo1 rescues the respiratory growth of *mdm30*Δ cells. Dextrose and glycerol spot assays at 30 °C of *MDM30* shuffling strains transformed with an extra-copy of Fzo1 (*FZO1*), a plasmid expressing MDM30 (*MDM30*) or an empty vector (Vector). In the top panels, strains are covered by (*MDM30*) and in the bottom panels strains are cured from the *MDM30* shuffle plasmid (*mdm30*Δ).

In order to assess *S. cerevisiae* respiratory growth, yeast cells are usually grown on media supplemented with glycerol as sole carbon source. Unlike dextrose which can be used for fermentative growth, glycerol is a non-fermentable carbon source that forces yeast to rely on mitochondrial respiration to grow. Mitochondrial respiration requires functional mitochondrial fusion. Consistent with this, the absence of Mdm30 induces decreased respiratory growth on glycerol (Fritz et al., 2003; Cohen et al., 2008) (**Fig 23**, lower panel – vector). This is because Fzo1 levels need to be tightly regulated by Mdm30 for functional mitochondrial fusion to take place (Escobar-Henriques et al., 2006; Cohen et al., 2008, 2011a).
Surprisingly, we saw that adding an extra-copy of FZO1 restores growth on glycerol media for *mdm30*Δ cells (**Fig 23**, lower panel – FZO1). In addition, this rescue requires a functional copy of Fzo1 as the S201N mutation abolishes this rescue (**Fig4B** -Alsayyah *et al*).

This result is counter-intuitive as the stabilization of Fzo1 levels contributes to the mitochondrial fusion deficiency so how is adding more Fzo1 restoring respiratory growth?

1) A primary screen to decipher the function of the extra-copy of Fzo1

In order to understand this rescue, we used the power of genetics and launched an unbiased high-throughput genetic screen for inhibitors of this rescue in collaboration with Maya Schuldiner from the Weizmann Institute of Science.
In this screen we looked for genes that would abolish the rescue by the extra-copy of FZO1. However, the SGA yeast deletion library uses yeast with a BY genetic background, while we

use the W303 background. So first we needed to make sure that our rescue phenotype is reproducible in the BY background before we could launch the screen.

I started by deleting *MDM30* in the alpha SGA ready strain (yMS721) which will be used to mate with the library for the screen, then I transformed these deletants with a plasmid expressing an extra-copy of *FZO1* or an empty vector (**Fig24**). We already know that the respiratory growth defect is only detected at 37°C on glycerol media (Fritz et al., 2003) in the BY background, so we expected the rescue at the same temperature.

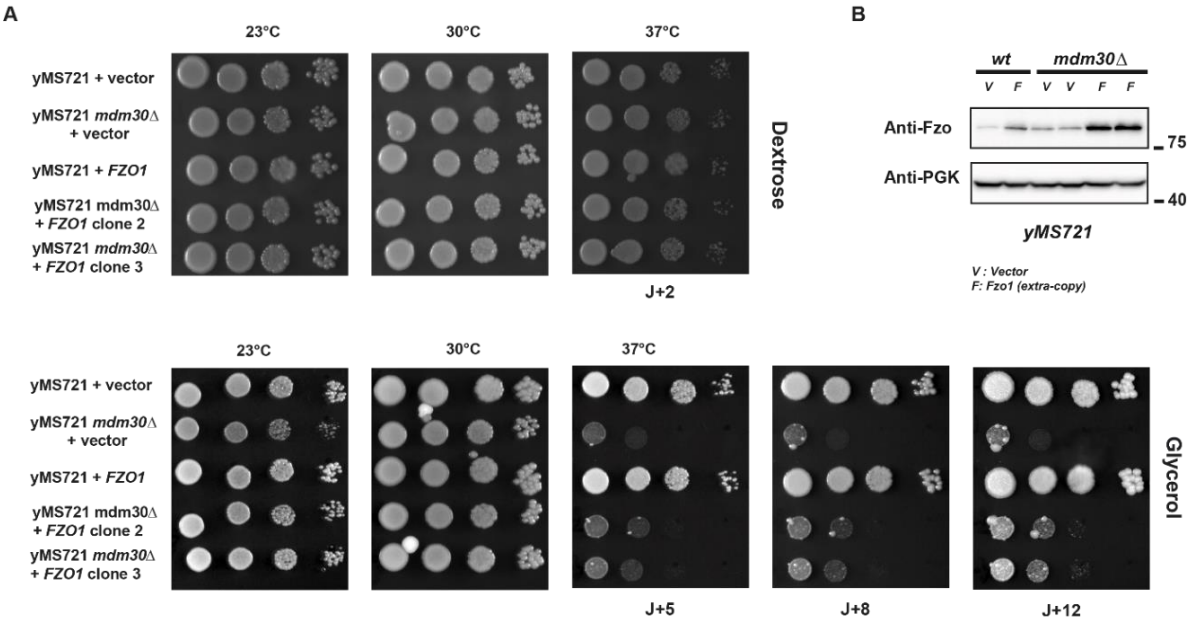

Fig24: Fzo1 rescues the respiratory growth of *mdm30*Δ cells in the BY background at 37°C. **(A)** Dextrose and glycerol spot assays of WT (yMS721) and *mdm30*Δ (yMS721 *mdm30*Δ) strains at 23, 30 and 37°C. Each strain is transformed with an empty vector (Vector) or a plasmid expressing an extra-copy of Fzo1 (*FZO1*). **(B)** Total protein extracts from WT (yMS721) and *mdm30*Δ (yMS721 *mdm30*Δ) strains transformed with an empty vector (V) or an extra-copy of Fzo1 (F). Extracts were analyzed by anti-Fzo1 and anti-Pgk1 immuno-blotting. MW in kDa are shown on the right.

Spot assays using the SGA ready strain (yMS721) confirmed that *mdm30*Δ cells in this background exhibit a growth defect at 37°C (**Fig24**). Consistent with this, the rescue by the extra-copy of Fzo1 was also visible at the same temperature (**Fig 24**). Now that we had determined the right temperature for the screen, I sent the strains to our collaborators to do the screen. In the screen we crossed two different strains with the KO library: *mdm30*Δ + *FZO1* and as a control the corresponding wild type WT + *FZO1*. We chose the WT + *FZO1* as a

control because we noticed in preliminary tests that the *mdm30*Δ + Vector strain exhibited smaller colony size and high variability.

In fine, the hits we were looking for were genes that would not affect WT cells, but would clearly abolish growth in *mdm30*Δ + *FZO1*. In other words, we were looking for genes that wouldn't affect respiration in normal conditions but become necessary in *mdm30*Δ+*FZO1* cells thus guiding us to the pathway behind this rescue. The zygotes obtained after mating with the library were sporulated and, after selection, the resulting haploids containing both the extra Fzo1 plasmid as well as the deletion of *MDM30* and the deletion of the library were grown on glycerol 1536 plate format for 7 days at 37°C (**Fig25**).

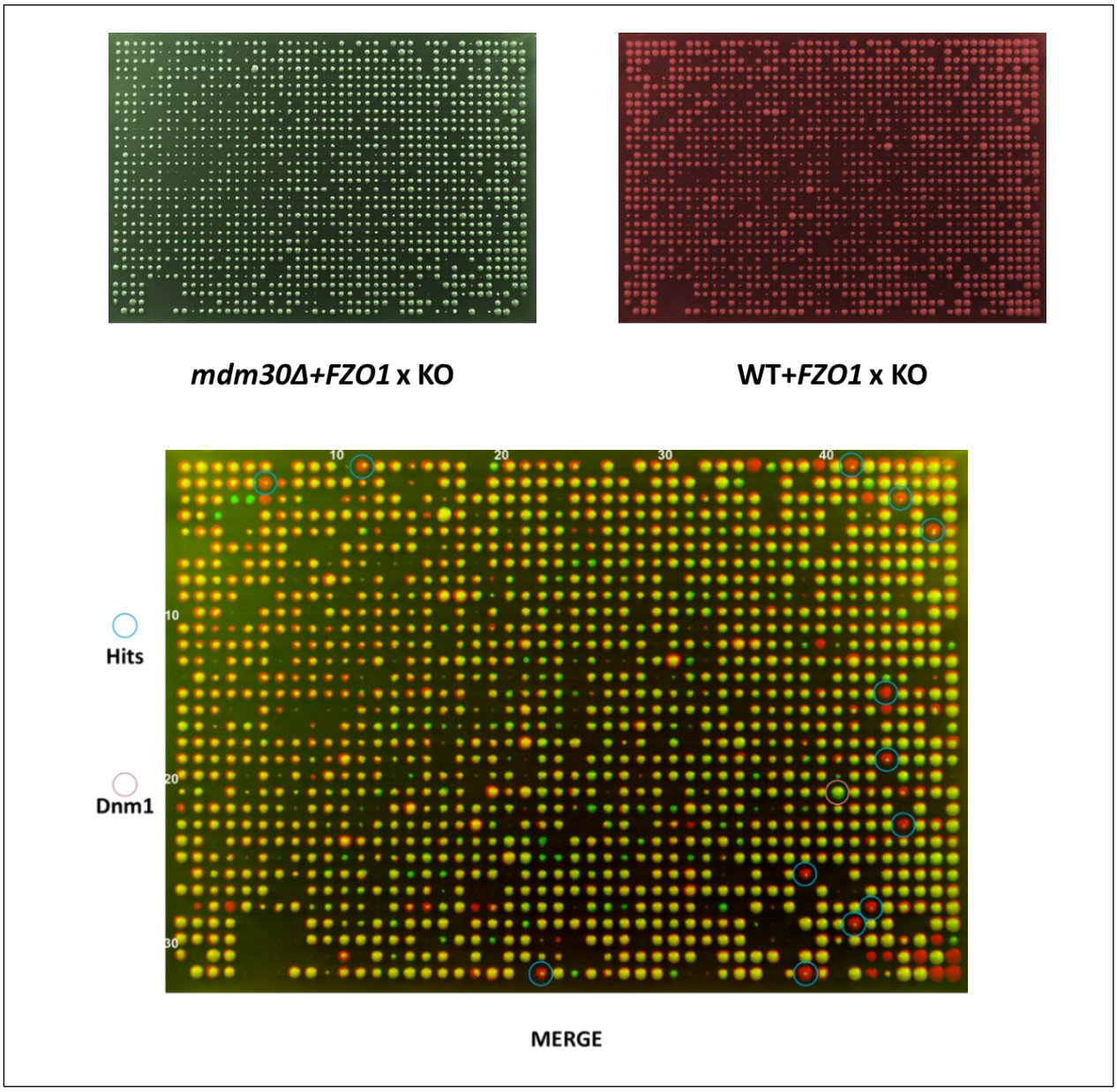

Fig25: High-Throughput SGA screen results on glycerol. 1536 format plates of *mdm30*Δ + *FZO1* and WT + *FZO1* resulting from the crossing with the KO library, sporulation and selection of haploids. To analyze the results, WT plates were colored in red and *mdm30*Δ plates were colored in green. After superposition of the two images (Merge), true hits were indicated by a blue circle. The deletion of Dnm1is indicated by a brown circle.

Hits can be spotted as red dots (they represent unaffected WT cells) with reduced yellow coloration (they represent *mdm30*Δ cells barely growing) indicating a deletion that affects *mdm30*Δ cells specifically (Fig 25). In the case of Dnm1 which is the DRP responsible for mitochondrial membrane fission, the green dot (*mdm30*Δ strain) is unaffected while the yellow dot is very small (WT strain). This effect of Dnm1 deletion consolidates the specificity of the screen because abolishing mitochondrial fission counters the fusion deficiency thus restoring growth of *mdm30*Δ cells on glycerol. However, deletion of Dnm1 in WT cells disrupts this balance causing growth inhibition in WT conditions.

In total, 111 hits were obtained (Table 6a and 6b-Annexe).

Category	**Number of hits**	**Total %**
Miscellaneous	12	10,8
Mitochondria	18	16,2
ER	18	16,2
Unknown	11	9,9
Transcription	7	6,3
Vacuole	4	3,6
Autophagy	4	3,6
Amino acid	4	3,6
Translation-Ribosome	11	9,9
Peroxisome	2	1,8
Replication	6	5,4
UPS	7	6,3
Cell cycle	5	4,5
Actin	2	1,8
Total	111	100%

Table 6a: Summarized list of the genetic screen results (from Table 6b-**Annexe**) divided into 14 groups.

Among these hits, 2 major groups representing two different organelles stood out with 16.2% of the total hits obtained: Mitochondria and the ER. The fact that mitochondrial hits represent a big portion of the hits obtained is not surprising. The haploids are *MDM30* null cells which directly affects mitochondrial function, so adding another deletion (this time from the KO library) that also targets mitochondrial function likely causes an additive effect increasing lethality. The second major group of hits was related to the ER.
Now that we had our list of potential hits in the BY genetic background, we needed to conduct a secondary screen in our genetic background (W303) to confirm them.

2) A secondary screen to verify the hits of the High-Throughput screen

In this secondary screen, the deletions identified in the primary screen were introduced in the *mdm30*Δ shuffle strain. The resulting strains were transformed with the *FZO1* extra-copy plasmid or by an empty vector before curation of the *MDM30* shuffle plasmid on 5-FOA' media. The URA shuffle plasmid is important in this case because expressing Mdm30 covers the *MDM30* deletion so that the cells don't lose their mitochondrial DNA. A consequent curation step using 5'FOA allows us to get rid of the *MDM30* URA plasmid because it will no longer be useful. The resulting *MDM30* negative and *MDM30* positive strains were processed for spot assays on dextrose and glycerol media at 23, 30 and 37°C.

Of course, we could not test all 111 hits as it would have taken a very long time so we carefully made a list of 13 potential hits that we tested by spot assays (**Fig26**).

As the ER was one of the major groups represented by the screen, we chose 6 hits from this group to test in the W303 genetic background: ERV29 (Protein localized to COPII-coated vesicles), CUE1 and 2 (Coupling of Ubiquitin conjugation to ER degradation, involved in ERAD pathway and mRNA decay), LAC1 (Ceramide synthase component), YET1 (ER TM protein) and ECT1 (enzyme involved in PE biosynthesis).
Since we obtained only 2 peroxisomal hits in the whole screen, we decided to test both genes in the spot assays: ACB1 (Acyl-CoA-binding protein) and MLS1 (malate synthase).
Finally, we chose genes to represent the remaining groups: ATP12 (ATP synthase factor), TCD2 (tRNA dehydratase), PRB1 (Vacuolar proteinase B), APD1 (Actin patches) and ATG9 (Autophagy).

To cut the story short, only 2 out of the 13 hits tested turned out to be true hits (**Fig 26-B**). The remaining genes had no effect at all on the rescue by the extra-copy of Fzo1 on glycerol (**Fig 26-A**).

Among these false hits, the deletion of ATP12 erased the rescue by the extra-copy in *mdm30*Δ cells. However, the deletion of this gene also abolished growth in WT cells because it directly affects the assembly of the F1F0 ATP synthase (**Fig 26-A**). This means that the effect we saw on the rescue is not specific and originates from a dominant respiratory defect.

The 2 "true hits" MLS1 and ACB1 completely shifted our attention from the ER as they are both directly related to peroxisomal metabolism, which put us on the trail of two metabolical pathways related to peroxisomes: Beta-oxidation of FAs and the Glyoxylate cycle. Interestingly, the extra-copy of Fzo1 also rescues the growth of *mdm30*Δ cells on Oleate media which further links the rescue to Fatty acids and peroxisomes (**Fig S2D**- Alsayyah et al).

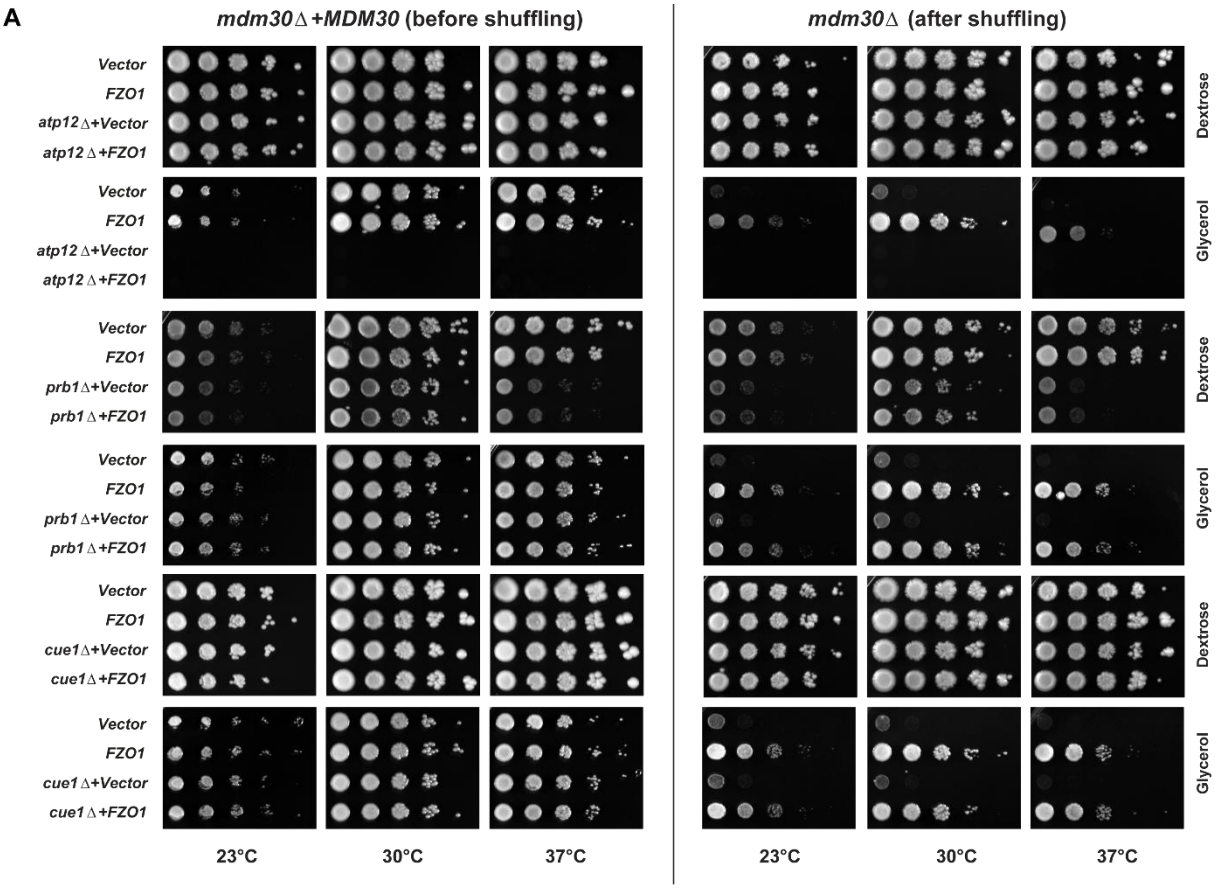

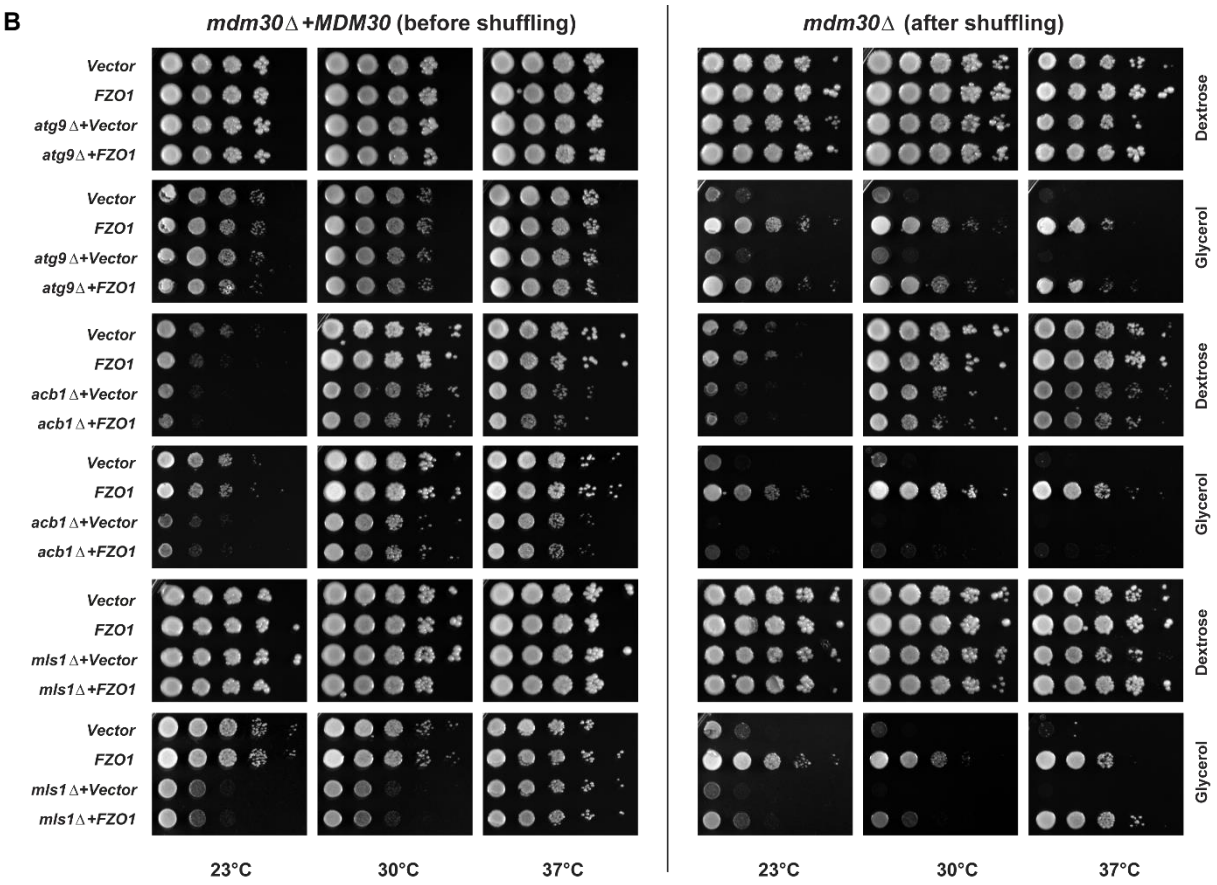

Fig26: Verification 13 potential hits in the W303 genetic background. Spot assays on dextrose and glycerol media of *MDM30* shuffling strains at 23, 30 and 37°C. Each strain is transformed with an empty vector (Vector) or a plasmid expressing an extra-copy of Fzo1 (*FZO1*).

It was intriguing that no genes coding for enzymes of the beta-oxidation pathway were obtained as hits in the screen. This could be explained by the redundancy of the enzymes and the numerous alternative pathways that a substrate can take when one enzyme is "missing". However, having *ACB1* as a hit clearly indicates that fatty acid metabolism is implicated.

IV- Physiological role of Fzo1-mediated PerMit contacts

Despite the many false hits, we know that peroxisomal functions related to the glyoxylate cycle and Fatty acid metabolism are necessary for the rescue by the extra-copy of Fzo1 (**Fig26**). In parallel, we know that Fzo1 accumulates on peroxisomal membranes according to cellular FA desaturation levels (**Fig3B, C** -Alsayyah *et al*).

Taken altogether, these results prompted us to make the link between the two observations as the extra-mitochondrial copy of Fzo1 most probably localizes to peroxisomal membranes. This

makes the rescue by the extra-copy of Fzo1 a powerful readout to understand the function of Fzo1-mediated PerMit contacts. Consequently, we examined the effect of the deletion of the two true hits from the screen *MLS1* and *ACB1* on PerMit contacts in different *OLE1* expression levels (**Fig S3A, B**-Alsayyah *et al*).
Using Structured Illumination Microscopy (SIM), we saw no change in PerMit contacts upon deletion of *MLS1* or *ACB1* regardless of the levels of Ole1 (**Fig S3A, B**-Alsayyah *et al*). However, deletion of these two genes strongly affected mitochondrial morphology depending on FA desaturation levels (**Fig5A** -Alsayyah *et al*).

This effect on mitochondrial networks was the most drastic in low *OLE1* expression (CYC prom) and seemed to dampen with increasing *OLE1* expression (**Fig5A**- Alsayyah *et al*). Since mitochondrial morphologies are an equation of both Fission and Fusion of mitochondria, we needed further observations to identify which one of these two processes was affected in *mls1*Δ and *acb1*Δ cells. Using time-lapse acquisitions by SIM, we observed and quantified mitochondrial fusion and fission events (**5B, C-** Alsayyah *et al*) which revealed that the morphologies observed previously were mainly caused by mitochondrial fusion defects that are more pronounced in low FA desaturation (where we have less PerMit contacts) compared to TEF conditions where PerMit contacts were more abundant. We concluded that PerMit contacts somehow protect mitochondrial fusion against the absence of *ACB1* and *MLS1*.

The functions of the acyl-coA transporter Acb1 are not yet fully understood. On the other hand, Mls1 is an established enzyme of the glyoxylate cycle (**Fig27**). It is either localized in peroxisomes or in the cytosol depending on the carbon source utilized for growth (Kunze et al., 2002) and its main function is generating Malate from Glyoxylate. Mls1 succeeds the cytosolic enzyme Icl1 (Isocitrate Lyase) in the glyoxylate cycle (**Fig27**). Naturally, deletion of *MLS1* induces the accumulation of glyoxylate and succinate generated by Icl1 (**Fig27**). This accumulation seemed more detrimental to mitochondrial fusion in low PerMit contacts (Cyc-*OLE1*) conditions compared to high PerMit contacts (TEF-*OLE1*) (**Fig5A** -Alsayyah *et al*).

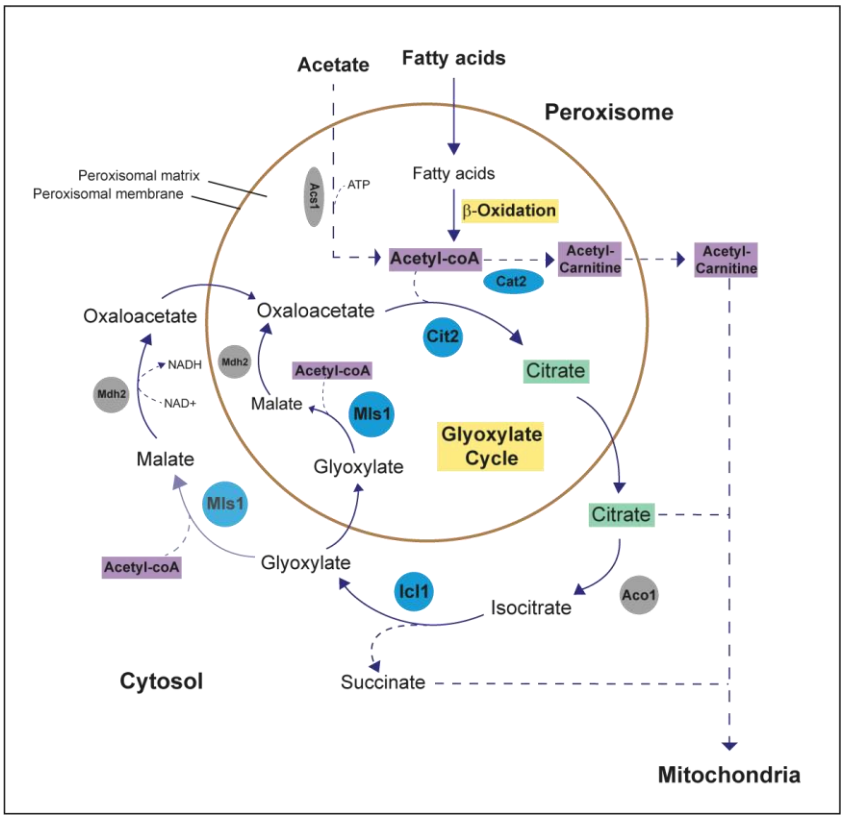

Fig27: The Glyoxylate cycle in *S. cerevisiae*. beta-oxidation and the glyoxylate cycle are the two pathways involved in peroxisomal FA catabolism and are highlighted in yellow. Citrate (highlighted in green) generated by Cit2, Acetyl-CoA (highlighted in purple) in the form of Acetyl-Carnitine generated by Cat2 and Succinate generated by Icl1, can all transit to mitochondria. The enzymes highlighted in blue are all of interest in this study.

We hypothesized that increased PerMit contacts would somehow protect mitochondrial fusion from the accumulation of Icl1 byproducts (i.e. Succinate and Glyoxylate). This prompted us to test the effects of *ICL1* deletion on the *OLE1* shuffle strains and *mls1*Δ cells (**Fig. 6B, C**-Alsayyah *et al*). Interestingly, we found that inactivation of Icl1 had no effect on the rescue by the extra-copy or mitochondrial morphologies no latter the expression level of *OLE1* (**Fig. 6B, C** -Alsayyah *et al*). However, the absence of Icl1 completely abolished the effects we saw in *mls1*Δ cells both in spot assays and on mitochondrial morphologies as if PerMit contacts bypass the requirement for Icl1 and maintain mitochondrial fusion. As we have seen in earlier sections, one of the primary roles of inter-organelle contacts is molecular transport. This is why we suspected that Citrate (the by-product just upstream of Icl1) or Acetyl-coA (through the carnitine shuttle) transport could be involved in this "protection" of mitochondrial fusion that is seen when PerMit contacts are more abundant due to the increase in proximity between the two organelles. Conversely, fewer Fzo1-mediated PerMit contact sites would allow Icl1 to

process the isocitrate generated from early steps of the glyoxylate cycle (**Fig27**), resulting in accumulation of Glyoxylate and Succinate, thus blocking stimulation of mitochondrial fusion. Deletion of *CIT2* and *CAT2* revealed that *CAT2* had no effect on mitochondrial morphology, unlike CIT2 which de-stabilized the level of tubular mitochondrial morphologies even in High *OLE1* expression when PerMit contacts are numerous in the cell (**Fig. 6D**-Alsayyah *et al*). Thus, we propose that lack of citrate synthesis blocks the capacity of Fzo1-mediated PerMit contacts to maintain tubular morphology.

To conclude, these results allowed us to prove that Fzo1 naturally localizes on peroxisomal membranes to promote contacts between peroxisomes and mitochondria. This peroxisomal localization of Fzo1 is actually regulated by Mdm30-mediated degradation of Fzo1 and by cellular FA desaturation. Ultimately, we find that Fzo1 accumulates on peroxisomes when FA desaturation increases in order to stimulate mitochondrial fusion thus maintaining tubular mitochondrial morphology. Our results indicate that the synthesis of peroxisomal Citrate is required for the maintenance of tubular mitochondria through Fzo1-mediated PerMit contacts which facilitate transfer of this by-product to mitochondria (**Fig7**-Alsayyah *et al*).

V- Submitted Manuscript: Alsayyah *et al* 2021.

Full Title: Mitofusin-mediated contacts between mitochondria and peroxisomes regulate mitochondrial fusion

Short Title: **The physiology of Fzo1-mediated PerMit contacts**

Authors: Cynthia Alsayyah[1], Manish K. Singh[1,2], Laetitia Cavellini[1], Nadav Shai[3], Maya Schuldiner[3], Einat Zalckvar[3], Naïma Belgareh-Touzé[1], Christophe Zimmer[2] & Mickael M. Cohen[1*].

Affiliations:

[1] Laboratoire de Biologie Moléculaire et Cellulaire des Eucaryotes, Sorbonne Université, CNRS, UMR8226, Institut de Biologie Physico-Chimique, 75005 Paris, France.

[2] Imaging and Modeling Unit, Pasteur Institute, UMR 3691 CNRS, 75015, Paris, France.

[3] Department of Molecular Genetics, Weizmann Institute of Science, Rehovot, 7610001, Israel.

*Correspondence to: cohen@ibpc.fr

ABSTRACT

Mitofusins are large GTPases triggering fusion of mitochondrial outer membranes. Similarly to human Mfn2, which also tethers Mitochondria to the Endoplasmic Reticulum, the yeast mitofusin Fzo1 stimulates contacts between Peroxisomes and Mitochondria when overexpressed. Yet, the physiological significance and function of these “PerMit” contacts remain unknown. Here, we demonstrate that Fzo1 naturally localizes to peroxisomes and promotes PerMit contacts in physiological conditions. These contacts are regulated through co-modulation of Fzo1 levels by the Ubiquitin-Proteasome System and by the desaturation of fatty acids (FA). Contacts reach a minimum or maximum under low or high FA desaturation, respectively. High throughput genetic screening combined with high resolution fluorescence microscopy reveal that the function of Fzo1-mediated PerMit contacts consists in maintaining efficient mitochondrial fusion upon high FA desaturation. Our data suggest that synthesis of peroxisomal citrate is required for this function. These findings unravel a mechanism by which inter-organelle contacts safeguard efficient mitochondrial fusion.

INTRODUCTION

In vivo, mitochondria assemble as a tubular reticulum in physical contact with endomembrane systems such as the endoplasmic reticulum (ER), the vacuolar/lysosomal compartment, the plasma membrane and the peroxisomes (Lackner, 2019). The morphology of the mitochondrial reticulum is maintained by an equilibrium between fragmentation and fusion of its tubules. Mitochondrial fission as well as fusion of mitochondrial outer and inner membranes are all mediated by large GTPases of the Dynamin-Related Proteins (DRPs) super-family (Ramachandran, 2018). Mitofusins, a sub-class of DRPs integral to mitochondrial outer membranes, auto-oligomerize in *cis* (on the same membrane) and in *trans* (from opposite membranes) in GTPase domain-dependent manner to trigger the tethering and the homotypic fusion of outer membranes (Cohen and Tareste, 2018). This process is mediated by two distinct mitofusins (Mfn1 and Mfn2) in mammalian cells and a single one (Fzo1) in the yeast *Saccharomyces cerevisiae* (from here on simply yeast) (Detmer and Chan, 2007; Eura et al., 2003; Legros et al., 2002; Santel et al., 2003). Notably, Mfn2 also localizes to ER membranes from where it can interact with mitochondrial Mfn1 and Mfn2, thereby promoting tethering between the ER and mitochondria (de Brito and Scorrano, 2008). Mfn2 was also found to mediate mitochondrial tethering with other organelles such as melanosomes (Daniele et al., 2014). Most intriguingly, the yeast mitofusin was more recently proposed to mediate contacts between peroxisomes and mitochondria (Shai et al., 2018), calling for further investigation.

Fzo1-dependent fusion of outer membranes is co-regulated by the ubiquitin proteasome system and by the desaturation of fatty acids (FAs) (Alsayyah et al., 2020; Cavellini et al., 2017). The ubiquitin ligase Mdm30 promotes ubiquitination of Fzo1 during mitochondrial tethering and its subsequent degradation by the proteasome (Anton et al., 2011; Cohen et al., 2011, 2008). Conversely, the ubiquitin protease Ubp2 antagonizes the Mdm30-mediated ubiquitination of Fzo1 and slows down the degradation of the mitofusin (Anton et al., 2013; Cavellini et al., 2017). We have previously shown that Mdm30 also controls the stability of Ubp2 which connects the degradation of Fzo1 with the desaturation of FAs (Cavellini et al., 2017).

FAs are the precursors of the phospholipids that compose all endomembranes bilayers. Their status of desaturation, *i.e.* the formation of double bounds between carbons of their acyl chains, profoundly impacts the cellular composition in phospholipids (Ernst et al., 2016; Surma et al., 2013). In yeast this desaturation is triggered by the Δ9-fatty acid desaturase Ole1. When the overall desaturation within cellular membranes decreases, Rsp5 ubiquitin ligase activates the transcription factors of the *OLE1* gene (Hoppe et al., 2000; Rape et al., 2001; Zhang et al., 1999, 1997). Likewise, excess desaturation within acyl chains of FAs and phospholipids blocks the capacity of Rsp5 to activate

the synthesis of Ole1 (Bossie and Martin, 1989; Hoppe et al., 2000; Rape et al., 2001; Stukey et al., 1989).

Notably, Ubp2 not only antagonizes the Mdm30-mediated ubiquitination of Fzo1 but is also the main antagonist of Rsp5 (Kee et al., 2006, 2005) , which connects Fzo1 regulation with the OLE1 pathway. Upon downregulation of the OLE1 pathway and low FA desaturation, Mdm30 promotes degradation of Ubp2 leading to un-antagonized and increased Mdm30 mediated turnover of Fzo1 (Cavellini et al., 2017). Similarly, when FA desaturation is high, Ubp2 is stabilized and limits the extension of ubiquitin chains that Mdm30 conjugates to the mitofusin, resulting in stabilization of Fzo1 (Cavellini et al., 2017). Mitochondrial fusion remains efficient when Fzo1 and desaturation of FAs are both low or when they are both high (Cavellini et al., 2017).

While the balance between Fzo1 degradation and FA desaturation is essential for efficient mitochondrial fusion, the mechanism by which desaturation of FAs impacts mitochondrial fusion remains obscure. In this regard, the evidence that overexpression of Fzo1 or its stabilization in the absence of Mdm30 promotes physical contacts between mitochondria and peroxisomes (Shai et al., 2018) offers interesting perspectives. An obvious link between FAs, peroxisomes and mitochondria in yeast is beta-oxidation where FAs enter peroxisomes to be catabolized into acetyl-CoA (Hiltunen et al., 2003). Depending on the availability of carbon sources, acetyl-CoA can then either transit to mitochondria to feed the TCA cycle or be rerouted between the cytosol and peroxisomes to feed the glyoxylate cycle (Chen et al., 2012). However, whether increased contacts between peroxisomes and mitochondria triggered by Fzo1 overexpression could employ these pathways is unknown (Shai et al., 2018). Similarly, increased levels of Fzo1 may promote localization of the mitofusin to peroxisomal membranes but the detection of Fzo1 on peroxisomes requires to be confirmed. Most notably, the physiological significance, regulation and function of Fzo1-mediated PerMit contacts remains unexplored. Transfer of material from peroxisomes to mitochondria can be expected, but the nature of this material, the conditions under which its transfer occurs, and the purpose of this transfer remain to be discovered. Here, we addressed and obtained compelling answers to most if not all of these questions.

RESULTS

Fzo1 naturally localizes to peroxisomes.

We have previously found that strong overexpression of Fzo1 in *WT* cells or its natural stabilization in *mdm30Δ* cells favor contacts between mitochondria and peroxisomes (Shai et al., 2018). In particular, we accumulated evidence that increased levels of the yeast mitofusin may induce an extra-mitochondrial localization of Fzo1 to peroxisomes (Shai et al., 2018). We aimed at confirming this possibility but also asked whether such peroxisomal function of Fzo1 could have physiological implications in WT cells.

As expected, peroxisomes labelled with Pex3-mCherry and mitochondria labelled with both Fzo1-GFP (Green Fluorescent Protein) and mito-BFP (Blue Fluorescent Protein) showed a 10% increase in mutual proximity in *mdm30Δ* as compared to *WT* whole cells (Fig. 1a). In mitochondrial enriched fractions, the total of peroxisomes in mitochondrial proximity increased whereas the amounts of peroxisomes in mitochondrial non-proximity decreased (Fig. 1b). This is because the supernatant and cytosol were discarded during preparation of the membrane fraction. Yet, the analysis of PerMit contacts *in vitro* confirmed the *in vivo* results seen in *WT* and *mdm30Δ* cells, thus ruling out the contribution of the cytoskeleton and the confinement of intra-cellular organelles but confirming *bona-fide* contacts between mitochondria and peroxisomes *in vivo*.

Fzo1 accumulates in the cytosolic fraction of *mdm30Δ* cells that is devoid of mitochondria (Shai et al., 2018). This extra-mitochondrial localization of the mitofusin correlates with the increased PerMit contacts seen in the absence of Mdm30 (Fig. 1a and 1b) which suggests that Fzo1 could localize to peroxisomes. We thus designed a protocol to address this possibility. *WT* and *mdm30Δ* cells where *FZO1* and *PEX3* are respectively labeled with 13-Myc and 6-HA epitopes at their genomic loci, were subject to fractionation assays to separate the cytosolic supernatants from the membrane pellets (Fig. 1c). As expected, the supernatants were positive for cytosolic PGK but negative for the mitochondrial Porin (Fig. 1d; Total, Pellet, Sup fractions). Consistent with previous findings (Shai et al., 2018), we also detected a significant signal of Fzo1-13Myc in the supernatant of *mdm30Δ* cells and to a lesser extent but more surprisingly in the supernatant of WT cells (Fig. 1d; Sup fraction). As for Pex3-6HA, the peroxisomal protein was detected in both the membrane and cytosol fractions (Fig. 1d; compare Sup and Pellet fractions). We reasoned that immunoprecipitation of cytosolic Pex3-6HA in the absence of detergent could pool-down native peroxisomes that are not bound to membranes but that could be probed for the presence of Fzo1-13Myc (Fig. 1c). This led to detection of a significant amount of Fzo1-13Myc on presumably native peroxisomes from *mdm30Δ* cells but also from *WT* cells with a decreased level of mitofusin (Fig. 1d; IP-, IP+).

It was important to confirm this observation with a distinct readout. We thus repeated the same protocol of native peroxisome immunoprecipitation but with cells where mitochondria are labelled with mito-BFP and in which either *PEX3* or *FZO1* or both *PEX3* and *FZO1* are genomically labelled with mCherry and GFP, respectively. Following incubation with these cell's supernatants, Mock and Red Fluorescent Protein (RFP)-trap coated beads were analyzed by fluorescence microscopy (Fig.S1a). RFP-traps have an established capacity to bind mCherry specifically. Consistent with this, the vast majority of beads coated with RFP traps were decorated with a specific mCherry signal upon incubation with Pex3-mCherry supernatants (Fig. 1e, S1b and 1f). These mCherry positive beads were negative for BFP labelling (Fig. 1e), confirming that IPed peroxisomes are not bound to mitochondria. However, among RFP-beads incubated with Pex3-mCherry/Fzo1-GFP/mito-BFP supernatants, 25% were positive for GFP labelling when the supernatant came from WT cells and this GFP staining reached 45% when the supernatant came from *mdm30Δ* cells (Fig. 1e and 1f). Importantly, these specific GFP signals were totally washed away upon incubation of the beads with detergent-containing buffers (Fig. S1c). These results not only confirm that Fzo1 localizes to peroxisomes in *mdm30Δ* cells but also indicate that the mitofusin is also present on peroxisomes from *WT* cells.

Fzo1 is a natural PerMit tether in WT cells.

The peroxisomal localization of the yeast mitofusin in WT cells suggests that Fzo1 could tether mitochondria to peroxisomes in physiological conditions. Abolishing the membrane tethering capacity of Fzo1 may thereby decrease PerMit contacts as compared to WT cells. In this regard, mutations in the GTPase domain not only block oligomerization properties of the mitofusin but also inhibit its binding to Mdm30 (Anton et al., 2011; Brandt et al., 2016; Cohen et al., 2011). Similarly to the WT version of Fzo1 in *mdm30Δ* cells, the GTPase mutant Fzo1 S201N is thus stabilized even in the presence of Mdm30 (Anton et al., 2011; Cohen et al., 2011). Consistent with this, we observed that the level of extra-mitochondrial Fzo1 S201N is increased as compared to WT Fzo1 in cytosolic supernatants obtained from fractionation of *MDM30* positive cells (Fig. 2a). Moreover, immunoprecipitation of native peroxisomes from cytosolic fractions confirmed that the amount of Fzo1 at peroxisomes also increases upon mutation of the GTPase domain (Fig. 2b). This led to analyze PerMit contacts in *WT* as compared to *FZO1 S201N* whole cells labelled with Pex3-mCherry and Fzo1-GFP (Fig. 2c). Strikingly, mutation of the GTPase domain decreased contacts by about 12% which was confirmed in mitochondrial enriched fractions with a decrease of about 7% (Fig. 2d). These results indicate that when Fzo1 is not functional, its capacity to mediate PerMit contacts is affected. Fzo1 is involved in 7

to 12 % of all PerMit contacts in WT cells confirming the yeast mitofusin as a natural tether between peroxisomes and mitochondria.

Similar to mitochondrial tethering, Fzo1-mediated PerMit contacts require the integrity of the mitofusin GTPase domain. This strongly suggests that peroxisomal Fzo1 may connect with mitochondrial Fzo1 to trigger PerMit tethering. We reasoned that this could be tested by evaluating the capacity of peroxisomes from *mdm30Δ* cells with increased amounts of WT Fzo1 to bind mitochondria purified from either *WT* or *FZO1 S201N* cells. We therefore incubated RFP traps in native conditions with the cytosolic fraction of *mdm30Δ* cells in which mitochondria are labelled with mito-GFP and where Pex3 is either unlabeled or tagged with mCherry (Fig. 2e, Panel I). As expected, RFP-trap beads were decorated with mCherry after incubation with PEX3-mCherry supernatants exclusively (Fig. S1d). Most importantly, GFP signals were not detected on the beads (Fig. S1d) which further confirms that peroxisomes purified from cytosolic fractions are not bound to mitochondria (Fig. 1e). We thus subsequently incubated mCherry-positive and negative RFP traps with mitochondrial enriched fractions from *WT* and *FZO1 S201N* cells labelled with mito-GFP that were prepared extemporaneously (Fig. 2e, Panels II and III). Notably, all PerMit tethers that are distinct from Fzo1 may already saturate their respective mitochondrial acceptor sites in these mitochondrial enriched fractions, which should leave mitochondrial Fzo1 as the only available PerMit tether in these *ex-vivo* PerMit contact assays. After washing steps, fluorescence microscopy analysis allowed detecting GFP signals in all batches of beads, including Pex3-mCherry positive (Fig. 2e, Bottom) and negative (Fig. S1e) beads. Upon incubation with *WT FZO1* mitochondria, 67 % of the GFP staining was found on mCherry positive beads and the remaining 33% on mCherry negative beads (Fig. 2f). In the presence of *FZO1 S201N* mitochondria, this ratio was inverted with the majority of GFP staining accumulating on the negative control (Fig. 2f; 54% on mCherry negative beads Vs 46% on mCherry positive beads). These results indicate that the PerMit tethering mediated through WT peroxisomal Fzo1 is abolished upon mutation of the GTPase domain on mitochondrial Fzo1 but also confirm that all PerMit contacts that are formed *ex-vivo* are mediated by Fzo1. Peroxisomal Fzo1 thus interacts with mitochondrial Fzo1 to promote PerMit tethering.

Fzo1-mediated PerMit contacts are regulated by FA desaturation.

Our data indicate that, in WT cells, a small pool of Fzo1 naturally localizes to peroxisomes to interact with the larger pool of Fzo1 located on mitochondria. Stabilization of Fzo1 in the absence of Mdm30 not only increases the amount of the mitofusin on peroxisomes but also induces increased PerMit contacts. We asked whether such increase in Fzo1-mediated PerMit contacts could occur in a

more physiological fashion. In this regard, we have previously demonstrated that increased desaturation of FAs induces a natural stabilization of Fzo1 by slowing down its Mdm30-dependent degradation (Cavellini et al., 2017). In this context, increased unsaturated fatty acids (UFAs) should stabilize the mitofusin which may induce accumulation of extra-mitochondrial Fzo1. However, the addition of extra-cellular UFAs induce complex feedback loops on Ole1, the only fatty acid desaturase in yeast, which results in decreased production of endogenous UFAs (Bossie and Martin, 1989; Hoppe et al., 2000; Surma et al., 2013). Addition of exogenous UFAs is therefore not optimal to maintain constant degrees of unsaturation. We thus designed *OLE1* shuffle strains in which the desaturase Ole1 is expressed under the control of distinct promoters of low (*CYC* or *MET* promoters) to strong (*ADH* or *TEF* promoters) forces (Fig. S2a, b and c). High expression of Ole1 from the *TEF* promoter induced accumulation of endogenous Fzo1 whereas low expression of Ole1 from the *CYC* promoter resulted in decreased levels of the mitofusin as compared to the WT control with the *OLE1* promoter (Fig. 3a). These results are consistent with our previous findings demonstrating that high or low desaturation of fatty acids result in stabilization or degradation of Fzo1, respectively (Cavellini et al., 2017).

We employed this system to assess the cytosolic localization of Fzo1 according to the level of expression of Ole1. Fractionation assays with *WT*, *OLE1 CYC*, *OLE1 TEF* and *mdm30Δ* cells, all genomically tagged with *FZO1-13MYC*, revealed that high Ole1 expression from the *TEF* promoter induces an extra-mitochondrial accumulation of Fzo1-13Myc in the cytosolic supernatant (Fig. 3b). Anti-Myc IPs of supernatants confirmed this increased presence of Fzo1-13Myc in the cytosolic fraction of cells overexpressing Ole1 (Fig. 3c). This led to evaluate PerMit contacts in *OLE1*, *CYC-OLE1* and *TEF-OLE1* cells (Fig. 3d). Consistent with the increased level of Fzo1 upon Ole1 overexpression, PerMit contacts increased by 10% in *TEF-OLE1* as compared to *OLE1* cells (Fig. 3e). Moreover, lower level of Fzo1 in *CYC-OLE1* cells correlated with a 10% decrease in PerMit contacts as compared to the *OLE1* control (Fig. 3e). PerMit contacts thus not only increase with the status of desaturation of FAs but also with the level of Fzo1. Importantly, inactivation of *MDM30* abolished these effects and increased PerMit contacts regardless of the expression level of *OLE1* (Fig. 3f). Taken together, these observations indicate that Fzo1-mediated PerMit contacts are naturally regulated by FA desaturation and Mdm30-mediated degradation of Fzo1.

Fzo1 rescues the respiratory growth of *mdm30Δ* cells.

We have previously shown that mitochondrial fusion can be significantly rescued in the absence of Mdm30 (Cavellini et al., 2017). This rescue requires increased desaturation of FAs but also increased expression of Fzo1 through addition of a plasmid encoding for an extra-copy of *FZO1*

(Cavellini et al., 2017). The requirement for this extra-*FZO1* copy is rather counter intuitive as stabilization of Fzo1 in the absence of Mdm30 is partly causal in mitochondrial fusion deficiency (Cohen et al., 2008; Fritz et al., 2003). Consistent with this, the absence of Mdm30 induces decreased respiratory growth on media supplemented with glycerol as the only source of carbon (Cohen et al., 2008; Fritz et al., 2003). Yet, we serendipitously observed that the *FZO1* plasmid alone induces a significant rescue of this phenotype at 30°C (Fig.4a). This unexpected rescue requires a functional copy of Fzo1 as the *S201N* mutation inhibited the effect of extra Fzo1 (Fig.4b). We also observed that the extra copy rescues the otherwise abolished growth of mdm30 null cells on Oleate media (Fig.S2d), suggesting that the extra copy may improve peroxisomal function. We thus launched an unbiased genetic screen to seek for genes that participate in the improved respiratory growth of *mdm30Δ* cells by the extra-*FZO1*.

An extra copy of *FZO1* on either a *WT* or *mdm30Δ* background were integrated into a collection of strains representing deletions in the majority of all yeast non-essential proteins (Fig. 4c). *MDM30* and *mdm30Δ* haploid strains carrying the extra copy of *FZO1* and an additional single mutation were grown for 7 days on glycerol media (that does not allow growth in the absence of a functional respiratory capacity) and positive hits were defined as candidates that maintained growth in the presence but not in the absence of *MDM30* (see Materials and Methods). This primary screen provided several hits that were subsequently verified in a secondary screen where deletion candidates were reintroduced in *MDM30* shuffle cells, in the presence or in the absence of the extra-copy of *FZO1*. After *MDM30* curing on 5-FOA (see materials and methods), a true hit was expected to induce a strong inhibition of the respiratory rescue of *mdm30Δ* cells by extra-*FZO1* but have more limited effects on *MDM30* positive cells. Besides numerous false positive hits (Fig. S2e), this secondary screen yielded only two genes, *ACB1* and *MLS1*, that fulfilled the conditions required for a true positive candidate (Fig. 4d, 4e and S2f). *ACB1* encodes a fatty-acyl-CoA binding protein that is involved in the biosynthesis of long-chain fatty acids (Schjerling et al., 1996). Most importantly, Mls1 is the malate synthase enzyme involved in the peroxisomal glyoxylate cycle (Hartig et al., 1992). Inactivation of either *ACB1* or *MLS1* does weakly affect growth of *MDM30* positive or negative cells on either dextrose or glycerol media but nearly abolishes the respiratory rescue of *mdm30Δ* cells by the extra copy of Fzo1 at 30 or 23°C, respectively (Fig. 4d and 4e).

Acb1 and Mls1 regulate mitochondrial dynamics.

The above observations above resulting from an unbiased genetic screen point again to fatty acids with *ACB1* and peroxisomes with *MLS1*. A seductive possibility is that the natural localization of

Fzo1 to peroxisomes and its role in mediating contacts with mitochondria involves FAs and the glyoxylate cycle to serve a specific function. In this context, we aimed at analyzing *MLS1* and *ACB1* in the prism of Fzo1-mediated functions. Upon expression of *OLE1* from the *CYC*, *TEF* or from its own promoter, inactivation of either *MLS1* or *ACB1* did not affect the amount of PerMit contacts (Fig. S3a and S3b). Nonetheless, significant changes in mitochondrial morphology were observed in *MLS1* and *ACB1* negative as compared to *WT* cells, depending on the expression level of *OLE1* (Fig. 5a; *CYC*, *OLE1*, *TEF*). During low expression of *OLE1* from the *CYC* promoter (Fig. 5a; *CYC*), absence of either *MLS1* or *ACB1* induced a drastic decrease in the amount of cells with tubular mitochondria (75% in *WT* vs 15% in mutant cells). Upon expression of *OLE1* from its own promoter (Fig. 5a; *OLE1*), this decrease in tubular mitochondria persisted but to a lesser extent (75% in *WT* vs 40% in mutant cells). Interestingly, overexpression of *OLE1* from the *TEF* promoter (Fig. 5a; *TEF*) affected mitochondrial morphology with only 40% of WT cells with tubular networks. Yet, the deletion of either *MLS1* or *ACB1* did no longer induce any decrease in tubular mitochondria (40% in *WT* vs 40% in mutant cells). These results not only reveal an involvement of *ACB1* and *MLS1* in mitochondrial dynamics but also indicate that as FA desaturation and Fzo1-mediated PerMit contacts increase, the specific impact of *ACB1* and *MLS1* deletion on mitochondrial networks decreases.

To substantiate and confirm these observations, it was essential deciphering whether these changes in mitochondrial morphology are caused by variations in mitochondrial fusion, mitochondrial fission or other processes. Reminiscent of the peroxisomes biogenesis process in mammalian cells (Sugiura et al., 2017), one could not exclude that trans-interaction between peroxisomal and mitochondrial Fzo1 could trigger transient fusion between peroxisomal and mitochondrial outer membranes. We reasoned that if such fusion events would occur, the peroxisomal marker, RFP-SKL, which is located in the peroxisomal lumen should diffuse, even subtly, into the mitochondrial network labeled with OM45-GFP, which is located on the outer membrane. *OLE1*, *CYC-OLE1* and *TEF-OLE1* cells genomically labeled with *OM45-GFP* and *RFP-SKL* were thus processed for time-lapse acquisitions by Structured Illumination Microscopy (SIM). This approach allowed clear visualization of the dynamics of PerMit contacts (Fig. S3c). It also provided a mean to observe homotypic interactions between peroxisomes (Fig. S3d), on one hand, and mitochondria (Fig. 5b and 5c), on the other hand. While peroxisomes could remain in contact with the mitochondrial network for periods as long as 70 seconds, the transfer of RFP-SKL into the mitochondrial network as predicted to occur upon fusion between peroxisomal and mitochondrial membranes was never detected (Fig. S3c). Similarly, we observed peroxisomal separation (Fig. S3d), likely corresponding to peroxisomal fission events (Koch et al., 2003; Lazarow and Fujiki, 1985; Schrader and Fahimi, 2006), but the potential merging of individual peroxisomes was not captured. These results do not favor the hypothesis that peroxisomal Fzo1

triggers the heterotypic fusion between peroxisomes and mitochondria or the homotypic fusion between peroxisomes. We next focused our analysis on the quantification of mitochondrial fusion and fission events (Fig. 5b and 5c). Consistent with our mitochondrial morphology data, we observed an appropriate equilibrium between fusion and fission events in *CYC-OLE1* and *OLE1* cells (Fig. 5b and 5c; *WT CYC* and *WT OLE1*). In *TEF-OLE1* cells, fusion slightly decreased (Fig. 5c; *WT TEF*) whereas fission slightly increased (Fig. 5b; *WT TEF*) which is in agreement with the partial loss of tubular mitochondria when *OLE1* is overexpressed (Fig. 5a; *TEF*). We then pursued this analysis in the same set of cells that we inactivated for *ACB1*.

After inactivation of *ACB1*, fission events decreased only very slightly (about 1 to 2%) as compared to all *ACB1* positive conditions (Fig. 5b) and kept the same pattern as in *ACB1* positive cells with equivalent fragmentation in *CYC-OLE1* and *OLE1* cells and a faint increase in *TEF-OLE1* (about 2% as compared to *CYC* and *OLE1*). Upon low expression of *OLE1* and decreased PerMit contacts, the fusion events diminished significantly from 8% in *ACB1* positive cells to 3% in the absence of *ACB1* (Fig. 5c; *CYC*). Decrease in fusion events was also observed in *OLE1* cells (Fig. 5c; *OLE1*) but to a more limited extent (about 2%) as compared to *CYC-OLE1* (about 5%). In contrast, inactivation of *ACB1* did not affect mitochondrial fusion in the *TEF-OLE1* condition where *OLE1* is overexpressed and the Fzo1-mediated PerMit contacts are the highest (Fig. 5c; *TEF*). These results indicate that the effects of *ACB1* inactivation on mitochondrial morphology in *CYC-OLE1* and *OLE1* cells (Fig. 5a) are mainly caused by respectively strong and weak deficiencies in mitochondrial fusion (Fig. 5c). Most importantly, they indicate that *TEF-OLE1* cells are protected against mitochondrial fusion defects (Fig. 5c). Consequently, as FA desaturation and Fzo1-mediated PerMit contacts increase, they protect mitochondrial fusion against inactivation of *ACB1*, which also likely explains the effects on mitochondrial morphology seen upon inactivation of *MLS1* (Fig. 5a).

Synthesis of peroxisomal citrate regulates mitochondrial dynamics.

Acb1 is thought to transport newly synthesized acyl-CoA esters to acyl-CoA-consuming processes (Rasmussen et al., 1994; Schjerling et al., 1996). While such transport may occur through peroxisomes, this remains to be demonstrated for Acb1 which makes the impact of *ACB1* inactivation on mitochondrial fusion hazardous to interpret. Conversely, Mls1 is an established enzyme of the glyoxylate cycle (Fig. 6a). It is either localized in peroxisomes or in the cytosol depending on the carbon source utilized for growth (Kunze et al., 2002). In either case, the precise function of Mls1 consists in generating Malate from Glyoxylate that is itself generated by Icl1, the Isocitrate Lyase strictly localized in the cytosol (Fig. 6a). In this context, inactivation of *MLS1* should induce accumulation of Glyoxylate

and Succinate, both generated by Icl1, which would be detrimental for mitochondrial fusion in low FA desaturation and decreased Fzo1-mediated PerMit contacts. In contrast, high FA desaturation and increased Fzo1-mediated PerMit contacts would somehow protect mitochondrial fusion against accumulation of Icl1 byproducts. This led us testing the effect that *ICL1* inactivation could induce on the phenotypes seen in *mls1Δ* cells (Fig. 6b and 6c). As opposed to the inactivation of *MLS1*, the absence of *ICL1* did not affect the glycerol growth rescue of *MDM30* null cells by the extra copy of Fzo1 (Fig. 6b). Most notably, inactivation of *ICL1* induced a striking reversion of the effect resulting from *MLS1* deletion at both 23 and 30°C (Fig. 6b and S4a). Consistent with this finding, mitochondrial morphology in *icl1Δ* cells at 23°C was indiscernible from the morphology of mitochondrial networks in *WT* cells but also when *ICL1* was co-inactivated with *MLS1* (*mls1Δ icl1Δ* cells) in *CYC-OLE1*, in *OLE1* or in *TEF-OLE1* conditions (Fig. 6c). Interestingly, co-inactivation of *MLS1* and *ICL1* even improved the tubular morphology of *TEF-OLE1* cells at 30°C (Fig. S4b). These key observations indicate that the absence of Icl1 abolishes the effects of *MLS1* inactivation in low FA desaturation. This implies that decreased mitochondrial fusion in *CYC-OLE1* and *OLE1 mls1Δ* cells as compared to *TEF-OLE1 mls1Δ* cells is not a consequence of decreased FA desaturation but is rather linked to the decrease in Fzo1-mediated PerMit contacts. Icl1 is thus causal in the mitochondrial dynamics deficiency seen in the absence of *MLS1* when Fzo1-mediated PerMit contacts decrease. However, increased Fzo1-mediated PerMit contacts seen in the *TEF-OLE1* condition would somehow bypass Icl1 and maintain tubular mitochondrial morphology because of efficient mitochondrial fusion.

An intriguing possibility could be that peroxisomes in contact with mitochondria could favor the mitochondrial transfer of early byproducts from the Glyoxylate cycle upstream of Icl1. In the early steps of the Glyoxylate cycle (Kunze et al., 2006), the peroxisomal enzyme *CIT2* generates Citrate from Acetyl-CoA and Oxalo-acetate (Fig. 6a). Citrate is then transported to the cytosol where it is converted into Isocitrate that is subsequently used by Icl1 to generate Glyoxylate and Succinate (Fig. 6a). Importantly, Citrate can also be redirected to mitochondria, similarly to peroxisomal Acetyl-CoA that can exit peroxisomes in the form of Acetyl-Carnitine generated by the peroxisomal enzyme *CAT2* (Fig. 6a). In this context, increased PerMit contacts would transfer Citrate or Acetyl-Carnitine to mitochondria before Icl1 can be reached, which would stimulate mitochondrial fusion. On the other hand, decreased PerMit contacts would allow Icl1 to process the isocitrate generated from early steps of the glyoxylate cycle, resulting in accumulation of Glyoxylate and Succinate, thus blocking stimulation of mitochondrial fusion. We reasoned that if Fzo1-mediated PerMit contacts allow the transfer of Citrate or Acetyl-CoA to mitochondria, the inactivation of *CIT2* or *CAT2* should impact mitochondrial morphology in *CYC-OLE1* and *OLE1* but also in the more robust *TEF-OLE1* condition. While inactivation of *CAT2* had no effect at all as compared to WT cells, the absence of *CIT2* induced a decrease in tubular

mitochondria in *CYC-OLE1* and *OLE1* cells and most remarkably in the *TEF-OLE1* condition (Fig. 6d). This indicates that specifically blocking the peroxisomal synthesis of Citrate affects the capacity of Fzo1-mediated PerMit contacts to maintain tubular morphology.

Our observation thus demonstrate that Fzo1 naturally localizes to peroxisomes to promote their contacts with mitochondria. This peroxisomal localization of Fzo1 is regulated by Mdm30 and FA desaturation. We find that Fzo1 accumulates on peroxisomes when FA desaturation increases to stimulate and maintain tubular mitochondrial morphology and efficient mitochondrial fusion. Our results indicate that the synthesis of peroxisomal Citrate is required for the maintenance of tubular mitochondria by Fzo1-mediated PerMit contacts (Fig. 7).

DISCUSSION

Much as vesicular transport, the last decade has seen physical membrane contacts between organelles emerging as a key process ensuring efficient communication across cellular compartments (Prinz et al., 2020). It is now established that the ER, mitochondria, the lysosomal/vacuolar compartment, peroxisomes or the plasma membrane are entirely insulated from each other but have the ability to exchange material through physical associations between their respective lipid bilayers (Eisenberg-Bord et al., 2016; Gatta and Levine, 2017). The list of factors mediating these contacts does not cease growing, often shedding new light on the function of specific protein complexes or lipids (Gatta and Levine, 2017; Kornmann et al., 2009; Lahiri et al., 2015; Prinz et al., 2020). Likewise, many molecular components that transit between organelles through their respective contact sites have been identified. However, the means by which contact sites increase or decrease and for which purposes, remains more elusive.

These considerations are well illustrated by the recent discovery of Fzo1 as a potential PerMit tether (Shai et al., 2018). In addition to its well established role in triggering tethering and fusion of mitochondrial outer membranes, overexpression of the mitofusin was shown to stimulate attachment of peroxisomes to mitochondria (Shai et al., 2018). Furthermore, the data provided in this study were highly suggestive of Fzo1 localization to peroxisomes when mitofusin levels were increased. While a link with Mdm30-mediated degradation of Fzo1 was highlighted (Shai et al., 2018)**,** the physiological significance of these observations remained to be addressed.

Since peroxisomes are an essential hub for fatty acids metabolism, the potential role of Fzo1 as a PerMit tether echoed our initial discovery that mitochondrial fusion is governed by a balance between Fzo1 degradation and FA desaturation (Cavellini et al., 2017). However, beside a common involvement of Mdm30, the possibility that the two pathways could be intricately tied required further

investigation. Moreover numerous fundamental questions remained. How does FA desaturation regulate mitochondrial fusion? Does Fzo1 mediate PerMit contacts in physiological conditions and if so, how is this regulated? Last but not least, what purpose could be served by Fzo1-mediated PerMit contacts?

In the current study, we provide conclusive answers to most, if not all of, these questions. We demonstrate that Fzo1 naturally localizes to peroxisomes (Fig. 1) and contributes to about 10% of overall PerMit Contacts in WT cells (Fig. 2). The amount of Fzo1 localized at peroxisomes and its propensity to mediate contacts with mitochondria is conditioned by degradation or stabilization of the mitofusin and this rate of Mdm30-mediated turnover of Fzo1 is governed by the status of FA desaturation (Fig. 3). Our results indicate that peroxisomal Fzo1 interacts with mitochondrial Fzo1 to tether peroxisomes to mitochondria (Fig. 2f). These Fzo1-mediated PerMit contacts do not promote heterotypic fusion between mitochondria and peroxisomes (Fig. S3c) and peroxisomal Fzo1 does not promote homotypic fusion between peroxisomes (Fig. S3d). However, Fzo1-mediated PerMit contacts are essential to maintain efficient mitochondrial fusion as FA desaturation increases (Fig. 5c). Our data indicate that this stimulation of mitochondrial fusion requires the synthesis of peroxisomal Citrate but not the peroxisomal export of Acetyl-coA (Fig. 6d). Each of these findings will now be discussed separately.

The impact of Mdm30 and FA desaturation on Fzo1-mediated PerMit contacts.

Similar to its preferred localization at mitochondria, our data infer that the localization of Fzo1 at peroxisomes is natural (Fig. 1 and 2). The amount of Fzo1 at peroxisomes is regulated by Mdm30 and the status of FA desaturation (Fig. 3). We have shown previously that upon high FA desaturation, the ubiquitin protease Ubp2 trims the ubiquitin chains added by Mdm30 on Fzo1, which results in stabilization of the mitofusin (Cavellini et al., 2017). Conversely, Mdm30 promotes ubiquitination and degradation of Ubp2 upon low FA desaturation, which results in un-antagonized and increased Mdm30-mediated turnover of Fzo1 (Cavellini et al., 2017). This mechanism explains the impact of FA desaturation on Fzo1-mediated PerMit contacts as this regulation is abolished upon inactivation of *MDM30* (Fig. 3e and 3f).

Fzo1-mediated PerMit contacts and mitochondrial fusion stimulation as FA desaturation increases.

Our findings indicate that Fzo1-mediated PerMit contacts are required to maintain efficient mitochondrial fusion as FA desaturation increases. Consistent with this, we observe that low desaturation does not impact mitochondrial dynamics as opposed to high desaturation, which induces a small increase in mitochondrial fission and an equivalent decrease in mitochondrial fusion (Fig. 5b and 5c). This slight imbalance between fusion and fission results in a significant decrease in tubular

mitochondria (Fig. 5a). This impact of high FA desaturation on mitochondrial dynamics might be linked to remodeling of the phospholipidome (Surma et al., 2013), which will require further investigation in future studies. Nonetheless, this effect also easily explains the requirement for Fzo1-mediated PerMit contacts to maintain efficient mitochondrial fusion as FA desaturation increases.

Mechanism of mitochondrial fusion stimulation by Fzo1-mediated PerMit contacts.

The mechanism stimulating mitochondrial fusion likely involves a transfer of material from peroxisomes to mitochondria. We show that inactivating *CAT2* and thus inhibiting peroxisomal exit and mitochondrial import of Acetyl-coA does not impact mitochondrial dynamics (Fig. 6d). However inhibiting the synthesis of peroxisomal Citrate does induce a specific decrease in tubular mitochondria in low but also in high FA desaturation conditions (Fig. 6d). This effect upon high FA desaturation is particularly relevant as this is the condition where Fzo1-mediated PerMit contacts are the highest and in which mitochondrial dynamics is protected against inactivation of *MLS1* or *ACB1* (Fig. 3e and Fig.5). This implies that synthesis of peroxisomal Citrate in proximity to mitochondria is required to maintain normal mitochondrial dynamics and efficient mitochondrial fusion. Consistent with this, peroxisomal Citrate transits to mitochondria through specific transporters (Klingenberg, 1972; Robinson et al., 1971). Once transported to mitochondria, Citrate can feed the oxidative TCA cycle which, in turn, is known to stimulate the mitochondrial membrane potential (Jazwinski, 2014). Notably, the mitochondrial membrane potential is an essential component of mitochondrial fusion (Legros et al., 2002; Meeusen et al., 2004; Song et al., 2007). In this context, the mitochondrial transfer of Citrate by Fzo1-mediated PerMit contacts could stimulate mitochondrial fusion by maintaining an efficient mitochondrial membrane potential that would otherwise be affected by high FA desaturation. Among other non-mutually exclusive possibilities this effect on membrane potential is the easiest and most likely explanation to interpret the impact that Fzo1-mediated PerMit contacts and Citrate could exert on mitochondrial fusion upon high FA desaturation (Fig. 7b).

Mitochondrial fusion inhibition under low FA desaturation and inactivation of *MLS1*.

While Fzo1-mediated PerMit contacts are the rarest and may not even occur under low FA desaturation, other PerMit contacts mediated by distinct factors may be able to allow the mitochondrial transport of peroxisomal Citrate (Fig. 7a), as was demonstrated previously for PerMit contacts mediated by Pex34 (Shai et al., 2018). Yet, inactivation of *MLS1* induced very strong perturbations of mitochondrial dynamics in this condition (Fig. 5a). This observation raises the possibility that the transfer of material between peroxisomes and mitochondria is affected. In this regard, Icl1 produces Glyoxylate and Succinate from Isocitrate. Glyoxylate is used by Mls1 to generate Malate while Succinate can be transported to mitochondria (Kunze et al., 2006). Upon inactivation of

MLS1, accumulation of Succinate into mitochondria may compete with the transport of Citrate, which would result in mitochondrial fusion inhibition (Fig. 7a). In line with this possibility, inactivation of *ICL1* and abrogation of Succinate synthesis totally corrected the mitochondrial morphology defects induced by the absence of Mls1 (Fig. 6c).

The role of Acb1 in the regulation of Fzo1-mediated PerMit contacts.

Our data demonstrate that inactivation of *ACB1* induces the same effects as those observed with inactivation of *MLS1*, indicating that the proteins encoded by both genes are involved in the same pathway (Fig. 4 and 5). While we do provide conclusive interpretations of the effects linked to *MLS1* inactivation (Fig. 6b and 6c), we can only speculate about the role of Acb1 at this stage. Acb1 is established to bind activated acyl chains, *i.e.* acyl chains conjugated with Coenzyme A, with very high affinity (Rasmussen et al., 1994; Rosendal et al., 1993). In this context, Acb1 has been proposed to transport activated acyl chains to acyl-CoA consuming processes (Rasmussen et al., 1994; Schjerling et al., 1996). Among these processes, a role in transport of FAs into peroxisomes would be consistent with a function in peroxisomal Citrate synthesis through β-oxidation. This would explain the drop in mitochondrial fusion we observed in *acb1Δ* cells upon low desaturation and in the absence of Fzo1-mediated PerMit contacts (Fig. 5d). Conversely, increased PerMit contacts seen upon high desaturation would compensate the decreased synthesis of Citrate by facilitating its transfer to mitochondria (Fig. 7b). Further investigation will be required to clarify this potential role of Acb1 in transport of FAs into peroxisomes. Yet, the established capacity of Acb1 to bind acyl chains, already suggests that β-oxidation of FAs is likely a main source of peroxisomal Acetyl-coA for Citrate synthesis and stimulation of mitochondrial fusion by Fzo1-mediated PerMit contacts.

Mitochondrial contacts with other organelles: a conserved function between Fzo1 and Mfn2?

Fzo1 localizes to peroxisomes (Fig. 1) and has an apparent capacity to interact with mitochondrial Fzo1 (Fig. 2), which results in contacts between peroxisomes and mitochondria. This feature is strikingly reminiscent of the localization of the human mitofusin Mfn2 to ER membranes (de Brito and Scorrano, 2008). Its interaction with mitochondrial Mfn1 and Mfn2 promotes contacts between ER and mitochondrial membranes (de Brito and Scorrano, 2008). These Mfn2-dependent ER-Mito contacts have been attributed several functions (Csordás et al., 2018; Moltedo et al., 2019). However, as far as we know, their role in stimulation of mitochondrial fusion has not been investigated. Yet, mitochondrial fusion has been found to be significantly more rapid at sites of contact with the ER (12,5 sec with contact *vs* 21,9 sec without contact, on average) (Guo et al., 2018). The finding that Fzo1-mediated PerMit contacts regulate mitochondrial fusion may thus open novel perspectives

regarding the function of ER-mito contacts mediated by Mfn2 and in the physiopathology of the Charcot Marie Tooth type II A disease caused by Mfn2 mutations (Züchner et al., 2004).

MATERIAL AND METHODS

Yeast strains and growth conditions

The *S. cerevisiae* strains and plasmids used in this study are listed in Supplementary Table 1 and 2 respectively. Standard methods were used for growth, transformation and genetic manipulation of *S. cerevisiae*. Complete media or Minimal synthetic media [Difco yeast nitrogen base (Voigt Global Distribution Inc, Lawrence, KS), and drop out solution] were supplemented with the following carbon sources: 2% dextrose (SD; YPD for complete media), 2% glycerol (SG; YPG for complete media) or 0,2% Oleic Acid (YPO) (previously dissolved in pure ethanol) supplemented with 1% Tergitol (Lockshon et al., 2007; Sherman, 2002). In the indicated strains (see Supplementary Table 1), *FZO1*, *PEX3, OM45, OLE1* and other genes were chromosomally deleted or C-terminally tagged using conventional homologous recombination approaches (Gueldener et al., 2002; Longtine et al., 1998).

Generation of *FZO1*, *MDM30* and *OLE1* shuffle strains

FZO1 and *MDM30* null cells lose their mitochondrial DNA because of decreased mitochondrial fusion efficiency (Fritz et al., 2003). A plasmid-shuffle strategy was thus employed to ensure a reliable genetic analysis of *mdm30Δ* and *fzo1Δ* cells as described in (Cavellini et al., 2017). Unlike *FZO1* and *MDM30*, the *OLE1* gene is essential in *S. cerevisiae* (Zhang et al., 1999). Consequently, wild type W303 cells were transformed with *pRS416-OLE1-9MYC* (*OLE1* shuffle plasmid) prior to the chromosomal deletion of *OLE1* to generate *OLE1* shuffle strains and keep the cells alive. *OLE1* inactivation was verified by replica-plating *OLE1* shuffle strains on 5'-fluoroorotic acid (5-FOA) plates in the absence of an additional plasmid expressing *OLE1*. Loss of the uracil *OLE1* shuffle plasmid resulted in 100% lethality which confirmed absence of *OLE1*.

To yield strains used in this study, *FZO1*, *MDM30* and *OLE1* shuffle strains were then transformed with plasmids under selection of interest listed in Supplementary Table 2. Ten colonies were systematically isolated on SD selective media lacking uracil and replica-plated on corresponding SG and 5-FOA plates. Strains grown on 5-FOA plates and cured from shuffling plasmids were in turn replica-plated on SD and SG selective plates containing uracil. The glycerol growth phenotypes of strains covered by or cured from the shuffling plasmids were reproducibly observed in 100% of clones tested after 1 to 3 days of growth at 30 °C. Representative colonies were used in subsequent experiments.

Protein extracts and Immunoblotting

1OD of cells (1mL) grown in SD media were collected during the growth exponential phase (OD_{600}=0.5–1) and total protein extracts were prepared using the NaOH/trichloroacetic acid lysis method (Volland et al., 1994). Briefly, lysis was performed with 100 µL of 1M NaOH on ice for 10 minutes before protein precipitation with 100 µL of TCA (50%) on ice for 30 minutes. Proteins were then pelleted and

resuspended in Sample Buffer (13.33 mM Tris-HCL (pH 6.8),1.6 mM EDTA, 1.6% SDS, 40 mM DTT, 8% Glycerol, 0.016% Bromophenol Blue, 333 mM Tris-Base) and solubilized at 70°C for 10 minutes. Proteins were separated on SDS–PAGE (8% or 10% Acrylamide) and transferred onto nitrocellulose membranes (Amersham Hybond-ECL; GE Healthcare). The primary antibodies used for immunoblotting were: monoclonal anti-Pgk1 (1/20,000, AbCam, ab113687), monoclonal anti-HA (1/1,000, 12CA5, Invitrogen, 71-5500), monoclonal anti-Por1 (1/1,000, AbCam, ab110326), monoclonal anti-Myc (1/1,000, 9E10, Invitrogen, R950-25), polyclonal anti-Fzo1 (1/1,000, generated by Covalab). Primary antibodies were detected by secondary anti-mouse or anti-rabbit antibodies conjugated to horseradish peroxidase (HRP, 1/5,000, Sigma-Aldrich, 12-348 and A5278), followed by incubation with the Clarity Western ECL Substrate (Bio-Rad). Immunoblotting images were acquired with a Gel Doc XR+ (Bio-Rad) before treatment and quantification with the Image Lab 6.0 software (Bio-Rad). The cytosolic protein PGK1 was used as a loading control to normalize loading of other proteins relative to the WT conditions. Data reported are the mean and s.e.m (error bars) of three independent experiments.

Cellular fractionation assay

Cells were grown overnight in SD media to exponential phase (OD_{600} = 0.5–1) and 500 ODs were collected by centrifugation at 1500×g for 5 minutes before getting resuspended in 0.1 M Tris-HCl pH=9.4 - 50 mM β-mercapto-ethanol (1 ml per 20 ODs of cells) and incubated for 1 h at 30°C to begin cell wall lysis (Gregg et al., 2009; Meisinger et al., 2000). Following centrifugation, cells were washed with 1.2M sorbitol and resuspended in 1.2M sorbitol (1 ml per 50 ODs) supplemented with Zymolyase (Zymo Research; Orange, CA) (10 µl per 50 ODs) to initiate cell wall digestion and generate spheroplasts. After a 1h30 incubation at 30°C, spheroplasts were collected at 1500g and washed with 1.2M sorbitol to finally be resuspended in ice-cold Homogenization Buffer [10 mM Tris-HCl (pH 7.4), 0.6 M sorbitol, 1 mM EDTA, 0.2% (w/v) BSA + protease inhibitor pills (Protease Inhibitor Cocktail; Sigma-Aldrich) and 1 mM Pefabloc (Sigma-Aldrich)]. Spheroplasts were disrupted by douncing on ice (100 times with a medium size glass dounce of 15mL) and the resulting homogenate cleared by centrifugation at 3000×*g* for 5 minutes. The cleared homogenate (Total fraction) was then subjected to centrifugation at 10,170×*g* for 10 min, yielding a soluble fraction in the supernatant (Sup) and a mitochondrial enriched membrane fraction (Pellet). The soluble fraction was subsequently subjected to an additional centrifugation at 10,170×g for 5 minutes to clear the supernatant from any residual mitochondrial contamination. Aliquots of each fraction were collected and treated with TCA as described above prior to immunoblotting.

Structured Illumination Microscopy (SIM)

Strains were grown in dextrose medium at 30°C to mid-log phase and 1mL of culture was centrifuged at 1500g for 3 minutes in a 1.5 mL Eppendorf tube. After resuspension of cell pellets into 50µL of YPD media, 5 µL of cell suspension was loaded on 25 mm coverslip (#CG15XH, THORLABS) and placed in a magnetic chamber (#CM-B25-1, Quorum Technologies). Yeast cells were immobilized using a YPD pad placed over the cell suspension, which helps to spread the cells homogenously into a single layer suitable for imaging. Super-Resolution (SR) images of yeast cells were acquired using a Structured Illumination Microscopy (SIM) Zeiss LSM 780 Elyra microscope (Carl Zeiss, Germany) controlled by the Zen software. The microscope was equipped with an oil immersion 100x Plan-Apochromat objective with a 1.46 numerical aperture and an additional 1.6x lens. For detection, an EMCCD Andor Ixon 887 1K camera was used. One SR-SIM image was reconstructed from nine images acquired from three different phases and three different angles. Acquisition parameters were adapted to optimize the signal to noise ratio according to yeast strains. SIM images were processed with ZEN software and then channel alignment was performed using 100 nm TetraSpeck fluorescent beads (Cat#T7279, Invitrogen) embedded in the same conditions as the sample. SIM images were analyzed and quantified using ImageJ (National Institute of Health) open-source software.

In vitro imaging of PerMit contacts

Cells in which Fzo1 and/or Pex3 are genomically tagged with GFP or mCherry at their C-terminus were grown to exponential phase and subjected to cellular fractionation assays (see above). The isolated mitochondrial fractions were fixed with 2 Volumes of 8% formaldehyde in PBS 1X for at least 20 minutes at room temperature then stained with 1X MitoLite blue FX490 (AAT-Bioquest) for 30 minutes at 4°C to increase mitochondrial staining in blue. Cover slips were coated beforehand by incubation for 5 minutes in 100µl poly-D-Lysine at 0.1% (w/v in water). After removal of excess poly-D-Lysine by suction, coated coverslips were left to dry for 90 minutes. Following washing of the coverslips twice with PBS 1X, 100µl of the final mitochondrial suspension was placed on the slips for 5 minutes then washed again with PBS to remove excess membranes. Imaging of PerMit contacts in the mitochondria enriched fractions was achieved by conventional fluorescence microscopy. Contacts between peroxisomes and mitochondria were determined by the proximity of the red signal (Pex3-mCherry) with the green (Fzo1-GFP) and blue signal (mitolite and mito-BFP) which indicated a likely attachment between the 2 organelles. Data reported are the mean and s.e.m (error bars) of three independent experiments.

Native immunoprecipitation of peroxisomes

Cells grown to exponential phase were subject to fractionation as described above. Aliquots of Total, Pellet and Supernatants (pre-IP lysate) fractions were diluted and heated in sample buffer for subsequent immunoblotting. The remaining supernatant was collected after the two centrifugations

at 10,170×*g* while the membrane pellet enriched in mitochondria was discarded. The supernatant was then diluted two-fold in homogenization buffer supplemented with protease inhibitor but without any detergent agent before being split in half. Each supernatant half was incubated overnight on spinning wheel (12 rpm) at 4 °C with protein G-Sepharose beads (rec-Protein G-Sepharose 4B Conjugate, Invitrogen) in the absence (IP-) or in the presence (IP+) of anti-HA antibodies (12CA5, Invitrogen, 71-5500). The next day, the beads were washed with detergent-free homogenization buffer and heated in sample buffer before resolution by SDS–PAGE and analysis by immunoblotting as described above and with indicated antibodies.

RFP-Trap peroxisome Immunoprecipitation assay

In this assay, strains in which Fzo1 and/or Pex3 are C-terminally tagged at the genome with GFP and mCherry fluorophores respectively were employed (*MCY1667*, *MCY1580*, *MCY1675*, *MCY1673*, *MCY1551*, *MCY1677*). 200 to 250 ODs of cells grown at exponential phase were first subjected to fractionation as described above. The resulting supernatant was diluted two-fold (25 OD/mL) in homogenization buffer supplemented with protease inhibitors but without detergent and processed for native IP of peroxisomes. The diluted supernatant split in two halves was incubated overnight with (IP+) RFP-Trap Magnetic Agarose beads (rtma, ChromoTek) or with (IP-) binding control magnetic Agarose beads (bmab, ChromoTek) at a concentration of 1 µl of beads/5 OD cells. The next day, the beads were collected using a magnetic rack (GE Magrack 6) and washed three times for 5 minutes each with homogenization buffer (with or without 0.6% TritonX100 as indicated) on spinning wheel at 4°C. The beads were subsequently fixed with 3.7% formaldehyde for at least 20 minutes at room temperature, followed by imaging in fluorescence mounting medium (Dako).

Peroxisome/Mitochondria proximity mixing assays

Peroxisome immunoprecipitation using RFP Traps (see above) was the first step of the mixing assays. Peroxisomes from *mdm30Δ* strains in which Pex3 is either un-tagged (*MCY1842*) or C-terminally tagged at the genome with a mCherry epitope (*MCY1551*), were pulled down using RFP-Trap magnetic beads. The next day, after washing with homogenization buffer, the beads were incubated with purified mt-GFP tagged mitochondria that were prepared the same day. Mitochondria labelled with mt-GFP were purified from cells which express either a WT copy of *FZO1* (*MCY1889*) or the GTPase domain mutant (*S201N*) of Fzo1 (*MCY1891*). These cells grown at exponential phase were subjected to fractionation as described above, yet, in this case, the supernatant was discarded and the membrane pellet enriched in mitochondria was resuspended in homogenization buffer (1OD/µL). The mitochondrial pellet was then split in two halves that were further diluted two-fold in homogenization buffer before incubation with each set of beads overnight at 4°C on spinning wheel (12rpm). On the following day and after 3

consecutive washing cycles with homogenization buffer on spinning wheel for 5 minutes, the beads were imaged by conventional fluorescence microscopy.

Spot assays

Cultures grown overnight in SD medium were pelleted, resuspended at OD_{600}=1, and serially diluted (1:10) five times in water. Three microliters of the dilutions were spotted on Dextrose, Glycerol, Oleic Acid plates (with the appropriate amino acid selection) and grown for 2 to 4 days (Dextrose) or 3 to 6 days (Glycerol and Oleic Acid) at 23, 30 or 37 °C.

High-Throughput Genetic Screen

The rescue of *mdm30Δ* cells by the extra copy of *FZO1* prompted us to perform a genetic screen to search for gene deletions that could abolish this rescue. This screen was carried through Synthetic Genetic Array (SGA) techniques (Cohen and Schuldiner, 2011) using the *Mat alpha SGA* ready strain *yMS721* and a *Mat a G418* selection yeast deletion library (Giaever et al., 2002) that are built in the *BY* genetic yeast background. In this background, the respiratory growth defect of *mdm30Δ* cells is only detected at 37°C on glycerol media (Fritz et al., 2003). After confirming the rescue by the *FZO1* extra copy is also seen in this background and at this temperature, *yMS721* was transformed by the extra *FZO1* copy plasmid (MC250) to yield the *MCY1513* strain (Supplementary Table 1). *MDM30* was subsequently deleted in *MCY1513* to generate the *MCY1528* strain. *WT* (*MCY1513*) and *mdm30Δ* (*MCY1528*) strains were mated with the *Mat a* yeast deletion library (Giaever et al., 2002), the zygotes obtained after mating were sporulated and, after selection, the resulting haploid strains containing both the extra fzo1 plasmid as well as the deletion of *MDM30* and the deletion of the library were grown on glycerol 1536 plate format for 7 days at 37°C. To manipulate libraries in 1536-colony high-density format, a RoToR bench top colony arrayer (Singer Instruments) was used. In this primary screen, the positive hits were defined as candidates that present a growth defect in the *mdm30Δ* context but that are unaffected in the *WT* control. Taking advantage of the identical disposition of deletion mutants on *WT* and *mdm30Δ* plates, the screening of the hits was performed using a colorization approach. Briefly, *WT* colonies were colored in red while *mdm30Δ* colonies were colored in green. Superimposition of *WT* red plates over *mdm30Δ* green plates resulted in a vast majority of yellow colonies. The potential hits corresponded to red colonies with significantly reduced yellow coloration reflecting a growth defect of *mdm30Δ* as compared to *WT*. This approach yielded a dozen of potential hits that were subsequently verified in a secondary screen carried out in the *W303* background.

In this secondary screen deletions identified in the primary screen were introduced in the *mdm30Δ* shuffle strain MCY970. The resulting strains were transformed with the *FZO1* extra copy plasmid (*MC250*) or by an empty vector (*MC219*) before curation of the *MDM30* shuffle plasmid on 5-FOA

media. The resulting *MDM30* negative and *MDM30* positive strains were processed for spot assays on Dextrose, Glycerol and Oleate media at 23, 30 and 37°C. This secondary screen yielded only two high confidence hits. Inactivation of *ACB1* or *MLS1* induced significant inhibition of the respiratory rescue of *mdm30Δ* cells by the extra-copy of *FZO1* but had more limited effects on *MDM30* positive cells.

Widefield Fluorescence Microscopy

Samples were prepared as described in the section of mitochondrial network morphology unless stated otherwise. Fluorescence microscopy was carried out with a Zeiss Axio Observer.Z1 microscope (Carl Zeiss S.A.S.) with a × 63 oil immersion objective equipped with the following filter sets: FITC (Filter set 10-Alexa 489, Excitation BP 450/490, Beam Splitter FT 510, Emission BP 515-565) for GFP, HC(Filter set F36-508 Chroma, Excitation BP 562-40, Beam Splitter HC-BS 593, Emission BP 641/75) for RFP, DAPI (Excitation BP 365-12, Beam Splitter FT 395, Emission LP 397-∞) for BFP.Cell contours were visualized with Nomarski optics. Images were acquired with an ORCA-R2 charge-coupled device camera (Hamamatsu). Images were treated and analyzed with ZEN 3.1 (Blue edition) and ImageJ (National Institute of Health).

Mitochondrial network morphology

Mitochondrial morphology was scored in cells genomically expressing OM45-GFP or mt-GFP as indicated. Strains were grown in dextrose medium at 30°C (unless indicated otherwise) to mid-log phase and fixed with 3.7% formaldehyde for at least 20 minutes at room temperature. Morphology phenotypes were assessed in at least 100 cells. Data reported are the mean and s.e.m (error bars) from three independent experiments.

Time lapse fluorescence imaging and quantification of fusion and fission events

Strains were grown in dextrose medium at 30°C to mid-log phase, and samples were prepared as described above in the SIM section of the methods. Time-lapse images were acquired for 3 to 5 min duration for a 5-10 sec time interval depending on the experiments.

Fusion events represent 2 independent mitochondrial tubules forming contacts and consequently fusing outer membranes forming a single mitochondrial tubule. As for fission events, they represent a single mitochondrial tubule which is progressively constricted and detaches leading to 2 independent mitochondrial tubules. Fusion and fission events were analyzed during the full lapse of the video and normalized to the total number of cells in video. Multiple videos were analyzed giving a total of at least 100 cells and data reported are the mean and s.e.m (error bars) of three independent experiments.

ACKNOWLEDGMENTS

Research in the Cohen laboratory is supported by the Agence Nationale de la Recherche (ANR) grants, labex DYNAMO (ANR-11-LABX-0011-DYNAMO), MOMIT (ANR-17-CE13-0026-01) and MITOFUSION (ANR-19-CE11-0018). C.A. was supported by a three-year doctoral grant from the PSL Idex Program (ANR-10-IDEX-0001-02 PSL) and by a fourth-year doctoral grant from the Fondation pour la Recherche Médicale (FRM-FDT202012010377). C.Z. also acknowledges funding by ANR (ANR-17-CE13-0026-01) and by Institut Pasteur. We gratefully acknowledge the Imagopole—Citech of Institut Pasteur (Paris, France) as well as the France–BioImaging infrastructure network supported by the French National Research Agency (ANR-10–INSB–04; Investments for the Future) for the use of the Zeiss LSM 780 Elyra PS1 microscope. MS is an incumbent of the Dr. Gilbert Omenn and Martha Darling Professorial Chair in Molecular Genetics. Work in the Schuldiner lab was supported by a ERC CoG Peroxisystem (646604). The authors declare no competing financial interests.

AUTHOR CONTRIBUTIONS

C.A. performed all the experiments under the supervision of M.M.C and N.B.T. L.C. and N.B.T. generated strains and plasmids. M.K.S. and C.Z. performed the Structured Illumination Microscopy acquisitions. N.S., E.Z. and M.S. performed the high throughput genetic screen. M.M.C. and C.A. conceived the project and wrote the manuscript with contributions of all the authors.

REFERENCES

Alsayyah C, Ozturk O, Cavellini L, Belgareh-Touzé N, Cohen MM. 2020. The regulation of mitochondrial homeostasis by the ubiquitin proteasome system. *Biochim Biophys Acta Bioenerg* **1861**:148302. doi:10.1016/j.bbabio.2020.148302

Anton F, Dittmar G, Langer T, Escobar-Henriques M. 2013. Two deubiquitylases act on mitofusin and regulate mitochondrial fusion along independent pathways. *Mol Cell* **49**:487–98. doi:10.1016/j.molcel.2012.12.003

Anton F, Fres JM, Schauss A, Pinson B, Praefcke GJ, Langer T, Escobar-Henriques M. 2011. Ugo1 and Mdm30 act sequentially during Fzo1-mediated mitochondrial outer membrane fusion. *J Cell Sci* **124**:1126–35. doi:10.1242/jcs.073080

Bossie MA, Martin CE. 1989. Nutritional regulation of yeast delta-9 fatty acid desaturase activity. *J Bacteriol* **171**:6409–6413. doi:10.1128/jb.171.12.6409-6413.1989

Brandt T, Cavellini L, Kuhlbrandt W, Cohen MM. 2016. A mitofusin-dependent docking ring complex triggers mitochondrial fusion in vitro. *Elife* **5**. doi:10.7554/eLife.14618

Cavellini L, Meurisse J, Findinier J, Erpapazoglou Z, Belgareh-Touze N, Weissman AM, Cohen MM. 2017. An ubiquitin-dependent balance between mitofusin turnover and fatty acids desaturation regulates mitochondrial fusion. *Nat Commun* **8**:15832. doi:10.1038/ncomms15832

Chen Y, Siewers V, Nielsen J. 2012. Profiling of cytosolic and peroxisomal acetyl-CoA metabolism in Saccharomyces cerevisiae. *PLoS One* **7**:e42475. doi:10.1371/journal.pone.0042475

Cohen MM, Amiott EA, Day AR, Leboucher GP, Pryce EN, Glickman MH, McCaffery JM, Shaw JM, Weissman AM. 2011. Sequential requirements for the GTPase domain of the mitofusin Fzo1 and the ubiquitin ligase SCFMdm30 in mitochondrial outer membrane fusion. *J Cell Sci* **124**:1403–10. doi:10.1242/jcs.079293

Cohen MM, Tareste D. 2018. Recent insights into the structure and function of Mitofusins in mitochondrial fusion. *F1000Res* **7**. doi:10.12688/f1000research.16629.1

Cohen MMJ, Leboucher GP, Livnat-Levanon N, Glickman MH, Weissman AM. 2008. Ubiquitin-proteasome-dependent degradation of a mitofusin, a critical regulator of mitochondrial fusion. *Mol Biol Cell* **19**:2457–2464. doi:10.1091/mbc.e08-02-0227

Cohen Y, Schuldiner M. 2011. Advanced methods for high-throughput microscopy screening of genetically modified yeast libraries. *Methods Mol Biol* **781**:127–159. doi:10.1007/978-1-61779-276-2_8

Csordás G, Weaver D, Hajnóczky G. 2018. Endoplasmic Reticulum-Mitochondrial Contactology: Structure and Signaling Functions. *Trends Cell Biol* **28**:523–540. doi:10.1016/j.tcb.2018.02.009

Daniele T, Hurbain I, Vago R, Casari G, Raposo G, Tacchetti C, Schiaffino MV. 2014. Mitochondria and melanosomes establish physical contacts modulated by Mfn2 and involved in organelle biogenesis. *Curr Biol* **24**:393–403. doi:10.1016/j.cub.2014.01.007

de Brito OM, Scorrano L. 2008. Mitofusin 2 tethers endoplasmic reticulum to mitochondria. *Nature* **456**:605–610. doi:10.1038/nature07534

Detmer SA, Chan DC. 2007. Complementation between mouse Mfn1 and Mfn2 protects mitochondrial fusion defects caused by CMT2A disease mutations. *J Cell Biol* **176**:405–414. doi:10.1083/jcb.200611080

Eisenberg-Bord M, Shai N, Schuldiner M, Bohnert M. 2016. A Tether Is a Tether Is a Tether: Tethering at Membrane Contact Sites. *Dev Cell* **39**:395–409. doi:10.1016/j.devcel.2016.10.022

Ernst R, Ejsing CS, Antonny B. 2016. Homeoviscous Adaptation and the Regulation of Membrane Lipids. *J Mol Biol* **428**:4776–4791. doi:10.1016/j.jmb.2016.08.013

Eura Y, Ishihara N, Yokota S, Mihara K. 2003. Two mitofusin proteins, mammalian homologues of FZO, with distinct functions are both required for mitochondrial fusion. *J Biochem* **134**:333–344. doi:10.1093/jb/mvg150

Fritz S, Weinbach N, Westermann B. 2003. Mdm30 is an F-box protein required for maintenance of fusion-competent mitochondria in yeast. *Mol Biol Cell* **14**:2303–2313. doi:10.1091/mbc.e02-12-0831

Gatta AT, Levine TP. 2017. Piecing Together the Patchwork of Contact Sites. *Trends Cell Biol* **27**:214–229. doi:10.1016/j.tcb.2016.08.010

Giaever G, Chu AM, Ni L, Connelly C, Riles L, Véronneau S, Dow S, Lucau-Danila A, Anderson K, André B, Arkin AP, Astromoff A, El-Bakkoury M, Bangham R, Benito R, Brachat S, Campanaro S, Curtiss M, Davis K, Deutschbauer A, Entian K-D, Flaherty P, Foury F, Garfinkel DJ, Gerstein M, Gotte D, Güldener U, Hegemann JH, Hempel S, Herman Z, Jaramillo DF, Kelly DE, Kelly SL, Kötter P, LaBonte D, Lamb DC, Lan N, Liang H, Liao H, Liu L, Luo C, Lussier M, Mao R, Menard P, Ooi SL, Revuelta JL, Roberts CJ, Rose M, Ross-Macdonald P, Scherens B, Schimmack G, Shafer B, Shoemaker DD, Sookhai-Mahadeo S, Storms RK, Strathern JN, Valle G, Voet M, Volckaert G, Wang C, Ward TR, Wilhelmy J, Winzeler EA, Yang Y, Yen G, Youngman E, Yu K, Bussey H, Boeke JD, Snyder M, Philippsen P, Davis RW, Johnston M. 2002. Functional profiling of the Saccharomyces cerevisiae genome. *Nature* **418**:387–391. doi:10.1038/nature00935

Gregg C, Kyryakov P, Titorenko VI. 2009. Purification of mitochondria from yeast cells. *J Vis Exp*. doi:10.3791/1417

Gueldener U, Heinisch J, Koehler GJ, Voss D, Hegemann JH. 2002. A second set of loxP marker cassettes for Cre-mediated multiple gene knockouts in budding yeast. *Nucleic Acids Res* **30**:e23. doi:10.1093/nar/30.6.e23

Guo Y, Li Di, Zhang S, Yang Y, Liu J-J, Wang X, Liu C, Milkie DE, Moore RP, Tulu US, Kiehart DP, Hu J, Lippincott-Schwartz J, Betzig E, Li Dong. 2018. Visualizing Intracellular Organelle and Cytoskeletal Interactions at Nanoscale Resolution on Millisecond Timescales. *Cell* **175**:1430-1442.e17. doi:10.1016/j.cell.2018.09.057

Hartig A, Simon MM, Schuster T, Daugherty JR, Yoo HS, Cooper TG. 1992. Differentially regulated malate synthase genes participate in carbon and nitrogen metabolism of S. cerevisiae. *Nucleic Acids Res* **20**:5677–5686. doi:10.1093/nar/20.21.5677

Hiltunen JK, Mursula AM, Rottensteiner H, Wierenga RK, Kastaniotis AJ, Gurvitz A. 2003. The biochemistry of peroxisomal beta-oxidation in the yeast Saccharomyces cerevisiae. *FEMS Microbiol Rev* **27**:35–64. doi:10.1016/S0168-6445(03)00017-2

Hoppe T, Matuschewski K, Rape M, Schlenker S, Ulrich HD, Jentsch S. 2000. Activation of a membrane-bound transcription factor by regulated ubiquitin/proteasome-dependent processing. *Cell* **102**:577–586. doi:10.1016/s0092-8674(00)00080-5

Jazwinski SM. 2014. The retrograde response: a conserved compensatory reaction to damage from within and from without. *Prog Mol Biol Transl Sci* **127**:133–154. doi:10.1016/B978-0-12-394625-6.00005-2

Kee Y, Lyon N, Huibregtse JM. 2005. The Rsp5 ubiquitin ligase is coupled to and antagonized by the Ubp2 deubiquitinating enzyme. *EMBO J* **24**:2414–2424. doi:10.1038/sj.emboj.7600710

Kee Y, Muñoz W, Lyon N, Huibregtse JM. 2006. The deubiquitinating enzyme Ubp2 modulates Rsp5-dependent Lys63-linked polyubiquitin conjugates in Saccharomyces cerevisiae. *J Biol Chem* **281**:36724–36731. doi:10.1074/jbc.M608756200

Klingenberg M. 1972. Kinetic study of the tricarboxylate carrier in rat liver mitochondria. *Eur J Biochem* **26**:587–594. doi:10.1111/j.1432-1033.1972.tb01801.x

Koch A, Thiemann M, Grabenbauer M, Yoon Y, McNiven MA, Schrader M. 2003. Dynamin-like protein 1 is involved in peroxisomal fission. *J Biol Chem* **278**:8597–8605. doi:10.1074/jbc.M211761200

Kornmann B, Currie E, Collins SR, Schuldiner M, Nunnari J, Weissman JS, Walter P. 2009. An ER-mitochondria tethering complex revealed by a synthetic biology screen. *Science* **325**:477–481. doi:10.1126/science.1175088

Kunze M, Kragler F, Binder M, Hartig A, Gurvitz A. 2002. Targeting of malate synthase 1 to the peroxisomes of Saccharomyces cerevisiae cells depends on growth on oleic acid medium. *Eur J Biochem* **269**:915–922. doi:10.1046/j.0014-2956.2001.02727.x

Kunze M, Pracharoenwattana I, Smith SM, Hartig A. 2006. A central role for the peroxisomal membrane in glyoxylate cycle function. *Biochim Biophys Acta* **1763**:1441–1452. doi:10.1016/j.bbamcr.2006.09.009

Lackner LL. 2019. The Expanding and Unexpected Functions of Mitochondria Contact Sites. *Trends Cell Biol* **29**:580–590. doi:10.1016/j.tcb.2019.02.009

Lahiri S, Toulmay A, Prinz WA. 2015. Membrane contact sites, gateways for lipid homeostasis. *Curr Opin Cell Biol* **33**:82–87. doi:10.1016/j.ceb.2014.12.004

Lazarow PB, Fujiki Y. 1985. Biogenesis of peroxisomes. *Annu Rev Cell Biol* **1**:489–530. doi:10.1146/annurev.cb.01.110185.002421

Legros F, Lombès A, Frachon P, Rojo M. 2002. Mitochondrial fusion in human cells is efficient, requires the inner membrane potential, and is mediated by mitofusins. *Mol Biol Cell* **13**:4343–4354. doi:10.1091/mbc.e02-06-0330

Lockshon D, Surface LE, Kerr EO, Kaeberlein M, Kennedy BK. 2007. The Sensitivity of Yeast Mutants to Oleic Acid Implicates the Peroxisome and Other Processes in Membrane Function. *Genetics* **175**:77–91. doi:10.1534/genetics.106.064428

Longtine MS, McKenzie A, Demarini DJ, Shah NG, Wach A, Brachat A, Philippsen P, Pringle JR. 1998. Additional modules for versatile and economical PCR-based gene deletion and modification in Saccharomyces cerevisiae. *Yeast* **14**:953–961. doi:10.1002/(SICI)1097-0061(199807)14:10<953::AID-YEA293>3.0.CO;2-U

Meeusen S, McCaffery JM, Nunnari J. 2004. Mitochondrial fusion intermediates revealed in vitro. *Science* **305**:1747–1752. doi:10.1126/science.1100612

Meisinger C, Sommer T, Pfanner N. 2000. Purification of Saccharomcyes cerevisiae mitochondria devoid of microsomal and cytosolic contaminations. *Anal Biochem* **287**:339–342. doi:10.1006/abio.2000.4868

Moltedo O, Remondelli P, Amodio G. 2019. The Mitochondria-Endoplasmic Reticulum Contacts and Their Critical Role in Aging and Age-Associated Diseases. *Front Cell Dev Biol* **7**:172. doi:10.3389/fcell.2019.00172

Prinz WA, Toulmay A, Balla T. 2020. The functional universe of membrane contact sites. *Nat Rev Mol Cell Biol* **21**:7–24. doi:10.1038/s41580-019-0180-9

Ramachandran R. 2018. Mitochondrial dynamics: The dynamin superfamily and execution by collusion. *Semin Cell Dev Biol* **76**:201–212. doi:10.1016/j.semcdb.2017.07.039

Rape M, Hoppe T, Gorr I, Kalocay M, Richly H, Jentsch S. 2001. Mobilization of processed, membrane-tethered SPT23 transcription factor by CDC48(UFD1/NPL4), a ubiquitin-selective chaperone. *Cell* **107**:667–677. doi:10.1016/s0092-8674(01)00595-5

Rasmussen JT, Faergeman NJ, Kristiansen K, Knudsen J. 1994. Acyl-CoA-binding protein (ACBP) can mediate intermembrane acyl-CoA transport and donate acyl-CoA for beta-oxidation and glycerolipid synthesis. *Biochem J* **299 (Pt 1)**:165–170. doi:10.1042/bj2990165

Robinson BH, Williams GR, Halperin ML, Leznoff CC. 1971. Factors affecting the kinetics and equilibrium of exchange reactions of the citrate-transporting system of rat liver mitochondria. *J Biol Chem* **246**:5280–5286.

Rosendal J, Ertbjerg P, Knudsen J. 1993. Characterization of ligand binding to acyl-CoA-binding protein. *Biochem J* **290 (Pt 2)**:321–326. doi:10.1042/bj2900321

Santel A, Frank S, Gaume B, Herrler M, Youle RJ, Fuller MT. 2003. Mitofusin-1 protein is a generally expressed mediator of mitochondrial fusion in mammalian cells. *J Cell Sci* **116**:2763–2774. doi:10.1242/jcs.00479

Schjerling CK, Hummel R, Hansen JK, Borsting C, Mikkelsen JM, Kristiansen K, Knudsen J. 1996. Disruption of the gene encoding the acyl-CoA-binding protein (ACB1) perturbs acyl-CoA metabolism in Saccharomyces cerevisiae. *J Biol Chem* **271**:22514–22521. doi:10.1074/jbc.271.37.22514

Schrader M, Fahimi HD. 2006. Growth and division of peroxisomes. *Int Rev Cytol* **255**:237–290. doi:10.1016/S0074-7696(06)55005-3

Shai N, Yifrach E, van Roermund CWT, Cohen N, Bibi C, IJlst L, Cavellini L, Meurisse J, Schuster R, Zada L, Mari MC, Reggiori FM, Hughes AL, Escobar-Henriques M, Cohen MM, Waterham HR, Wanders RJA, Schuldiner M, Zalckvar E. 2018. Systematic mapping of contact sites reveals tethers and a function for the peroxisome-mitochondria contact. *Nat Commun* **9**:1761. doi:10.1038/s41467-018-03957-8

Sherman F. 2002. Getting started with yeast. *Methods Enzymol* **350**:3–41. doi:10.1016/s0076-6879(02)50954-x

Song Z, Chen H, Fiket M, Alexander C, Chan DC. 2007. OPA1 processing controls mitochondrial fusion and is regulated by mRNA splicing, membrane potential, and Yme1L. *J Cell Biol* **178**:749–755. doi:10.1083/jcb.200704110

Stukey JE, McDonough VM, Martin CE. 1989. Isolation and characterization of OLE1, a gene affecting fatty acid desaturation from Saccharomyces cerevisiae. *J Biol Chem* **264**:16537–16544.

Sugiura A, Mattie S, Prudent J, McBride HM. 2017. Newly born peroxisomes are a hybrid of mitochondrial and ER-derived pre-peroxisomes. *Nature* **542**:251–254. doi:10.1038/nature21375

Surma MA, Klose C, Peng D, Shales M, Mrejen C, Stefanko A, Braberg H, Gordon DE, Vorkel D, Ejsing CS, Farese R Jr, Simons K, Krogan NJ, Ernst R. 2013. A lipid E-MAP identifies Ubx2 as a critical regulator of lipid saturation and lipid bilayer stress. *Mol Cell* **51**:519–30. doi:10.1016/j.molcel.2013.06.014

Volland C, Urban-Grimal D, Géraud G, Haguenauer-Tsapis R. 1994. Endocytosis and degradation of the yeast uracil permease under adverse conditions. *J Biol Chem* **269**:9833–9841.

Zhang S, Burkett TJ, Yamashita I, Garfinkel DJ. 1997. Genetic redundancy between SPT23 and MGA2: regulators of Ty-induced mutations and Ty1 transcription in Saccharomyces cerevisiae. *Mol Cell Biol* **17**:4718–4729. doi:10.1128/MCB.17.8.4718

Zhang S, Skalsky Y, Garfinkel DJ. 1999. MGA2 or SPT23 is required for transcription of the delta9 fatty acid desaturase gene, OLE1, and nuclear membrane integrity in Saccharomyces cerevisiae. *Genetics* **151**:473–483.

Züchner S, Mersiyanova IV, Muglia M, Bissar-Tadmouri N, Rochelle J, Dadali EL, Zappia M, Nelis E, Patitucci A, Senderek J, Parman Y, Evgrafov O, Jonghe PD, Takahashi Y, Tsuji S, Pericak-Vance MA, Quattrone A, Battaloglu E, Polyakov AV, Timmerman V, Schröder JM, Vance JM, Battologlu E. 2004. Mutations in the mitochondrial GTPase mitofusin 2 cause Charcot-Marie-Tooth neuropathy type 2A. *Nat Genet* **36**:449–451. doi:10.1038/ng1341

FIGURE LEGENDS

Figure 1: Fzo1 naturally localizes to peroxisomes. **(a and b)** Imaging of Whole Cells by Structured Illumination Microscopy (SIM) or their corresponding Mitochondrial Enriched Fractions (MEFs) by conventional fluorescence microscopy. *WT* and *mdm30Δ* cells were genomically labelled with indicated fluorescent proteins (*MCY1675* and *MCY1677* cured from the *MDM30* shuffle plasmid). MEFs were additionally stained with mitolite blue to increase mitochondrial staining. Scale bars for Whole Cells (delimited in white) or MEFs correspond to 1 or 5 μm, respectively. Graphs on the right depict the percentage of proximity and non-proximity of peroxisomes (mCherry signals) to mitochondria (GFP/BFP signals) in *WT* (blue bars) and *mdm30Δ* (red bars) Whole Cells (Left) or MEFs (Right). Error bars represent the s.e.m (standard error of the mean) from three independent experiments. ***P<0.005 (one-way analysis of variance (ANOVA))**. (c and d)** Native Immuno-Precipitation of peroxisomes from *WT* and *mdm30Δ* cells genomically labelled for *PEX3-6HA* and *FZO1-13MYC* (*MCY1488 and MCY1490*). Right scheme: Cells were processed for fractionation assays to yield whole cell (Total), cytosol (Sup) and membrane (Pellet) fractions. Cytosol fractions were then split in two halves and incubated O.N. with anti-HA coated (IP+) or uncoated (IP-) beads in the absence of detergent to pull-down Pex3-6HA native peroxisomes specifically. Left western blots (WB): After washing, all fractions (Total, Pellet, Sup, IP+ and IP-) were processed for western blotting with anti-Myc, anti-HA, anti-PGK and anti-Porin. Short and long exposures of anti-Myc and anti-Porin WB are shown. Molecular Weights in kDa are indicated on the right. Asterisk (*) corresponds to BSA contained in the distinct fractions. **(e and f)** Same experiment as in (c and d) but with *WT* and *mdm30Δ* cells genomically labelled for *PEX3-mCherry*, *FZO1-GFP* and *mt-BFP* (*MCY1667, MCY1591, MCY1675 and MCY1673, MCY1597, MCY1677* cured from the *MDM30* shuffle plasmid), mock (-) or RFP (+) Trap beads and analysis of beads with DIC or fluorescence microscopy of GFP, RFP or BFP (see also Fig. S1a). Scale bars for RFP Trap beads in (e) correspond to 10 μm. The corresponding mock control is shown in Fig. S1b. The graph in (f) depicts the percentage of beads with RFP (red), GFP (green) or BFP (blue) fluorescence. Error bars represent the s.e.m from three independent experiments.

Figure 2: Fzo1 is a natural PerMit tether in WT cells. **(a)** *WT* and *FZO1-S201N* cells labelled for *PEX3-6HA,* and *FZO1-13MYC* (*MCY1779 and MCY1780*) were processed for fractionation assays to yield whole cell (Total), cytosol (Sup) and membrane (Pellet) fractions that were analyzed by western blotting with anti-Myc, anti-HA, anti-PGK and anti-Porin. Short and long exposures of anti-Myc and anti-Porin WB are shown. Molecular Weights in kDa are indicated on the right. **(b)** Native IP of peroxisomes from the cytosolic fraction of *WT* and *FZO1-S201N* cells labelled for *mt-BFP* and *FZO1-*

GFP only or for both *PEX3-mCherry* and *FZO1-GFP* (*MCY1802, MCY1803, MCY1804, MCY1805*) with mock (-) or RFP (+) Trap beads. After analysis by fluorescence microscopy, the graph depicts the percentage of beads with mCherry (red) or GFP (green) fluorescence. Error bars represent the s.e.m from three independent experiments. **(c and d)** Fluorescence microscopy of Whole Cells or their corresponding Mitochondrial Enriched Fractions (MEFs). Percentage of proximity and non-proximity of peroxisomes (mCherry signals) to mitochondria (GFP/BFP signals) in (c) *WT* (blue bars) and *FZO1-S201N* (red bars) whole cells labelled for both *PEX3-mCherry* and *FZO1-GFP* (*MCY1771* and *MCY1772*) or (d) their corresponding Mitochondria Enriched Fractions. Error bars represent the s.e.m from three independent experiments. * P=0.05, ** P<0.05 (one-way analysis of variance (ANOVA)). **(e)** *Ex-vivo* PerMit contact assays. Cytosolic fractions of *mdm30Δ* mito-*GFP* cells either genomically labelled or unlabeled for *PEX3-mCherry* (*MCY1842* and *MCY1847* cured from the *MDM30* shuffle plasmid) were incubated with RFP Trap beads overnight and verified by fluorescence microscopy (see Fig. S1d) after washing (Panel I). In parallel, diluted membrane fractions from *WT FZO1* or *FZO1-S201N* cells genomically labelled with *mito-GFP* (*MCY1843* transformed with *pRS314-FZO1* (*MC250*) or *pRS314-FZO1-S201N* (*MC544*)) were prepared (Panel II) and incubated overnight with mCherry positive or negative beads from Panel I (Panel III). After washing, mCherry positive or negative beads (see Fig. S1e) were analyzed by DIC and fluorescence microscopy (Panel IV). **(f)** Analysis of *Ex-vivo* PerMit contact assays. The graph depicts the percentage of mCherry positive (green) or negative beads (grey) with GFP signal upon incubation with *WT FZO1* or *FZO1-S201N* mitochondria. Error bars represent the s.e.m from three independent experiments. *** P<0.005 (one-way analysis of variance (ANOVA)).

Figure 3: Fzo1-mediated PerMit contacts are regulated by FA desaturation. **(a)** Whole cell extracts of *ole1Δ* strains shuffled with *OLE1*, *CYC* or *TEF pOLE1* plasmids (*MCY1861, MCY1863, MCY1865*) were processed for western blotting with anti-Fzo1, anti-PGK and anti-Porin. Molecular Weights in kDa are indicated on the right. The Fzo1/PGK1 ratio in each condition was then quantified relative to the *OLE1* promoter condition. Error bars represent the s.e.m from three independent experiments. ** P<0.05 (one-way analysis of variance (ANOVA)). **(b and c)** *WT*, *mdm30Δ* and *ole1Δ* cells shuffled with *CYC* or *TEF pOLE1* plasmids, genomically labelled for *FZO1-13MYC* (*MCY1488, MCY1490* and *MCY1785* transformed with *pRS414-CYC-OLE1* (*MC540*) or *pRS414-TEF-OLE1* (*MC541*)) were processed for fractionation assays to yield Total (whole cell), Sup (cytosol) and Pellet (membrane) fractions (b). Cytosol fractions were subsequently processed for denaturating IPs with anti-Myc or a mock beads (c). All fractions and IPs were analyzed by western blotting with anti-Myc, anti-PGK and anti-Porin. Molecular Weights in kDa are indicated on the right of the blots. **(d)** *ole1Δ* strains genomically labelled for *PEX3-mCherry* and *mito-GFP* were shuffled with *OLE1*, *CYC* or *TEF pOLE1* plasmids (*MCY1861,*

MCY1863, MCY1865) and processed for whole cells imaging by SIM. Scale bars for Whole Cells (delimited in white) correspond to 1 μm. **(e)** The graph depicts the percentage of proximity and non-proximity peroxisomes (mCherry signals) to mitochondria (GFP signals) in *CYC-OLE1* (yellow bars) *OLE1* (blue bars) and *TEF-OLE1* (red bars) cells from (d). Error bars represent the s.e.m from three independent experiments. ***P*<0.05 (one-way analysis of variance (ANOVA)). NS, not significant. **(f)** Same as (e) but in cells inactivated for *MDM30* (*MCY1959* transformed with *pRS414-CYC-OLE1* (*MC540*) or *pRS414-TEF-OLE1* (*MC541*) or *pRS414-OLE1-OLE1* (*MC543*)).

Figure 4: Fzo1 rescues the respiratory growth of *mdm30Δ* cells. **(a)** Dextrose and glycerol spot assays at 30 °C of *MDM30* shuffling strains (*MCY971*) transformed with *pRS314-FZO1* (*MC250*), *pRS314-MDM30* (*MC344*) or an empty vector (*MC219*) and covered by (*MDM30*) or cured from (*mdm30Δ*) the *MDM30* shuffle plasmid. **(b)** Top: Domain organization of Fzo1 (residues 1 to 855 from the N- to the C-terminal extremity) with the GTPase domain (Dark blue), the Heptad Repeats HRN (Light blue), HR1 and HR2 (Orange), the Trans-membrane domains (Yellow) and the S201N mutation (Red arrow). Bottom: Same as (a) but with *MDM30* shuffling strains (*MCY970*) transformed with *pRS314-FZO1* (*MC250*), *pRS314-FZO1 S201N* (*MC544*) or an empty vector (*MC219*). **(c)** High throughput screen for deletion candidates that abolish the respiratory rescue of *mdm30Δ* cells by Fzo1. *WT* (*MCY1513*) and *mdm30Δ* (*MCY1528*) cells transformed with *pRS416-FZO1* (*MC322*) were crossed with the deletion library SGA::G418 and resulting diploid cells were sporulated. Following appropriate selection (see Materials and Methods), single (*MDM30 xxxΔ*) and double deletion (*mdm30Δ xxxΔ*) haploid cells were grown for 7 days on glycerol media. Candidates of interest were characterized as deletions that decreased growth of the double mutant as compared to the single mutant. **(d and e)** Confirmed candidates after the secondary screen. Dextrose and glycerol spot assays at 30 °C (d) and 23°C (e) of *MDM30* (*MCY970*), *MDM30 acb1Δ* (*MCY1612*) and *MDM30 mls1Δ* (*MCY1649*) shuffling strains transformed with *pRS314-FZO1* (*MC250*) or an empty vector (*MC219*) and covered by (*mdm30Δ + MDM30*) or cured from (*mdm30Δ*) the *MDM30* shuffle plasmid.

Figure 5: Acb1 and Mls1 regulate mitochondrial fusion. **(a)** Top: examples of cells genomically labelled for *OM45-GFP* (*MCY1899*) with tubular (blue) or non-tubular (red) mitochondrial networks; Scale bar, 5 μM. Bottom: Percentage of cells with tubular (blue) or non-tubular (red) mitochondria from *OLE1* (*WT*), *OLE1 acb1Δ* (*acb1Δ*) and *OLE1 mls1Δ* (*mls1Δ*) shuffling strains genomically labelled for *OM45-GFP* and *RFP-SKL* and shuffled with *OLE1*, *CYC* or *TEF pOLE1* plasmids (*MCY1899*, *MCY1980*, *MCY1987*). Error bars represent the s.e.m from three independent experiments. ***P*<0.05, ****P*<0.005 (one-way

analysis of variance (ANOVA)). NS, not significant. More than 100 cells were analyzed per sample. **(b and c)** Left images: Examples of time lapse acquisitions with 10 second intervals of mitochondrial fission (b) and fusion (c) events (indicated by white arrows) by SIM with cells genomically labelled for *OM45-GFP* (*MCY1936*); Scale bars, 5 µM (Left fields) or 1 µM (Right zooms). Right graphs: Percentage of fission (b) and fusion (c) events par cell in *WT* (grey columns) and *acb1Δ* (black columns) strains from (a). Error bars represent the s.e.m from three independent experiments. ***P*<0.05 (one-way analysis of variance (ANOVA)). NS, not significant.

Figure 6: Synthesis of peroxisomal citrate regulates mitochondrial dynamics. **(a)** The Glyoxylate cycle in S. cerevisiae. See main text. All enzymes inactivated in this study are in blue. B-oxidation and the glyoxylate cycle are the two pathways involved in peroxisomal FA catabolism and are highlighted in yellow. Citrate (highlighted in green) generated by Cit2, Acetyl-CoA (highlighted in purple) in the form of Acetyl-Carnitine generated by Cat2 and Succinate generated by Icl1, can all transit to mitochondria. **(b)** Dextrose and glycerol spot assays at 23 °C of *MDM30 mls1Δ* (*MCY1649)*, *MDM30 icl1Δ* (*MCY1909*) and *MDM30 mls1Δ icl1Δ* (*MCY1911*) shuffling strains transformed with *pRS314-FZO1* (*MC250*) or an empty vector (*MC219*) and covered by (*mdm30Δ + MDM30*) or cured from (*mdm30Δ*) the *MDM30* shuffle plasmid. **(c)** Top: examples of cells genomically labelled for *mito-GFP* (*MCY1835*) with tubular (blue) or non-tubular (red) mitochondrial networks; Scale bar, 5 µM. Bottom: Percentage of cells with tubular (blue) or non-tubular (red) mitochondria at 23°C from *OLE1* (*WT*), *OLE1 mls1Δ* (*mls1Δ*), *OLE1 icl1Δ* (*icl1Δ*) and *OLE1 mls1Δ icl1Δ* (*mls1Δ icl1Δ*) shuffling strains genomically labelled for *mito-GFP* and shuffled with *OLE1*, *CYC* or *TEF pOLE1* plasmids (*MCY1835*, *MCY1989*, *MCY2002*, *MCY2003*). Error bars represent the s.e.m. from three independent experiments. ***P*<0.05, ****P*<0.005 (one-way analysis of variance (ANOVA)). NS, not significant. More than 100 cells were analyzed per sample. **(d)** Same as (c) but at 30°C and with *OLE1* (*WT*), *OLE1 cit2Δ* (*cit2Δ*) and *OLE1 cat2Δ* (*cat2Δ*) shuffling strains genomically labelled for *mito-GFP* and shuffled with *OLE1*, *CYC* or *TEF pOLE1* plasmids (*MCY1835, MCY2023, MCY2032*).

Figure 7: Model of mitochondrial fusion regulation by Fzo1-mediated PerMit contacts. **(a)** Upon low FA desaturation, Fzo1 undergoes increased Mdm30-mediated degradation which limits its accumulation on peroxisomes and precludes formation of Fzo1-mediated PerMit contacts. Other PerMit contacts mediated by distinct factors either identified (Pex34, for instance) or yet to be identified, would promote the transfer of Citrate generated by Cit2 to the mitochondrial network thus feeding the TCA cycle and, among other effects, maintaining the mitochondrial membrane potential

required for productive mitochondrial fusion. On the other hand, Citrate generated by free peroxisomes would enter the Glyoxylate cycle thereby generating succinate that can transit to mitochondria. Inactivation of *MLS1*, would result in accumulation of Glyoxylate and Succinate, resulting in mitochondrial fusion inhibition. **(b)** Upon high FA desaturation, Mdm30-mediated degradation of Fzo1 decreases which promotes accumulation of the mitofusin on peroxisomes and favors the formation of Fzo1-mediated PerMit contacts. This would result in increased transfer of Citrate into mitochondria thereby stimulating the mitochondrial membrane potential and counteracting the negative impact that desaturation of FA and phospho-lipids may have on mitochondrial fusion. As opposed to low FA desaturation, inactivation of *MLS1* under high FA desaturation does not have any effect on mitochondrial fusion as compared to WT cells because of the protection provided by the increase in Fzo1-mediated PerMit contacts.

SUPPLEMENTAL MATERIAL

Figure S1: (a) Native Immuno-Precipitation of peroxisomes from *WT* and *mdm30Δ* cells genomically labelled for *PEX3-mCherry*, *FZO1-GFP* and *mt-BFP* (*MCY1667, MCY1591, MCY1675 and MCY1673, MCY1597, MCY1677* cured from the *MDM30* shuffle plasmid). Cells were processed for fractionation assays to yield whole cell (Total), cytosol (Sup) and membrane (Pellet) fractions. Cytosol fractions were then split in two halves and incubated O.N. with mock (-) or RFP (+) Trap beads in the absence of detergent to pull-down Pex3-mCherry native peroxisomes specifically. After washing, beads were analyzed with DIC or fluorescence microscopy for detection of Fzo1 (GFP), Pex3 (RFP) and mitochondria (BFP). **(b)** DIC and fluorescence microscopy analysis of mock beads after washing (see also Fig. 1e for RFP Trap beads). Scale bars correspond to 10 μm. Note that GFP, RFP or BFP signals are not detected, indicating that peroxisomes (Pex3-mCherry), mitochondria (mt-BFP) or Fzo1-GFP do not bind non-specifically to the beads. **(c)** Same experiment as in Fig. S1a but washing of RFP Trap beads was performed either in the absence (NT) or in the presence (T) of Triton detergent. The graph shows the percentage of beads with BFP (blue), mCherry (red) or GFP (green) signal in each condition. Note that Fzo1-GFP is detected in the NT condition, in the absence of BFP signal and thus in the absence of mitochondria, but that this Fzo1-GFP is lost in the presence of detergent. This confirms that the mitofusin is embedded in peroxisomes from *WT* and *mdm30Δ* cells. **(d)** Ex-vivo PerMit contact assays (Panel I). DIC and Fluorescence microscopy analysis of RFP Trap beads after overnight incubation with the cytosolic fractions of *mdm30Δ mito-GFP* cells either genomically labelled or unlabeled for *PEX3-mCherry* (*MCY1842* and *MCY1847* cured from the *MDM30* shuffle plasmid). Note the negative signal for GFP, confirming that mitochondria are absent from cytosolic fractions and do not pull-down with peroxisomes. **(e)** *Ex-vivo* PerMit contact assays (Panel III). DIC and Fluorescence microscopy analysis of untagged peroxisomes RFP Trap beads from S1d (bottom row) after overnight incubation with the

membrane fractions of *WT FZO1* and *FZO1 S201N* cells genomically labelled for *mito-GFP* (*MCY1843* transformed with *pRS314-FZO1* (*MC250*) or *pRS314-FZO1-S201N* (*MC544*)). Note the positive signal for GFP that reflects the non-specific binding of mitochondria to RFP Traps and that is quantified in Fig. 2f (grey portions of the bars).

Figure S2: (a, b and c) Preparation and characterization of *OLE1* shuffle strains. **(a)** *ole1Δ* cells covered by a *pOLE1-9MYC* shuffle plasmid with *URA3* selection were transformed with an empty vector or with *pOLE1* plasmids under control of *OLE1*, *CYC* or *TEF* promoters with *TRP1* selection. Resulting double transformants were patched on Synthetic Dextrose media without Uracil and Tryptophan (SD -U-T) and replica-plated on Synthetic Glycerol media without Uracil and Tryptophan (SG -U-T) or on 5-FOA media without Tryptophan (5-FOA -TRP) to initiate curation of the *pOLE1-9MYC* shuffle plasmid with *URA3* selection. Note that after a second replicate on 5-FOA media without Tryptophan, the growth of the empty vector strain was abolished as expected since *OLE1* is essential for viability. **(b)** Whole cell extracts of *ole1Δ* strains shuffled with *MET25*, *CYC*, *ADH* or *TEF pOLE1-9MYC* plasmids (*MCY1798*, *MCY1797*, *MCY1796*, *MCY1795*) were processed for western blotting with anti-Myc, anti-PGK and anti-Porin. Molecular Weights in kDa are indicated on the right. Note that the stronger the promoter (*TEF* > *ADH* > *MET25* > *CYC*), the highest the expression of Ole1-9Myc. **(c)** Dextrose, Glycerol and Oleate spot assays at 23, 30 and 37 °C of *ole1Δ* strains (*MCY1781*) shuffled with *OLE1*, *CYC* or *TEF pOLE1* plasmids (*MC540*, *MC541*, *MC543*). Besides on Dextrose at 23°C, the relative growth of *OLE1*, *CYC-OLE1* or *TEF-OLE1* cells is not significantly different. **(d)** Dextrose, Glycerol and Oleate spot assays at 30 °C of *ole1Δ mdm30Δ* strains (*MCY1959*) transformed with *pRS314-FZO1* (*MC250*) or an empty vector (*MC219*) and shuffled with *OLE1*, *CYC* or *TEF pOLE1* plasmids *(MC540*, *MC541*, *MC543*). Note that the extra copy of *FZO1* not only rescues the growth of *mdm30Δ* cells on glycerol but also on Oleate, suggesting a stimulation of peroxisomal function. **(e)** Examples of false positive hits of the primary screen that were characterized in the secondary screen. Dextrose and glycerol spot assays at 30 °C of *MDM30* (*MCY970*), *MDM30 atp12Δ* (*MCY1616*) and *MDM30 erv29Δ* (*MCY1610*) shuffling strains transformed with *pRS314-FZO1* (*MC250*) or an empty vector (*MC219*) and covered by (*mdm30Δ + MDM30*) or cured from (*mdm30Δ*) the *MDM30* shuffle plasmid. Absence of *ATP12* (a factor required for assembly of the ATP synthase) abolishes the respiratory rescue of *mdm30Δ* cells by *FZO1* but also blocks the respiratory growth of *MDM30* positive cells. Absence of *ERV29* (a factor involved in COPII vesicles formation) does not affect the respiratory rescue of *mdm30Δ* cells by *FZO1*. **(f)** Confirmed candidates after the secondary screen. Dextrose, Glycerol and Oleate spot assays at 23, 30 and 37 °C of *MDM30* (*MCY970*), *MDM30 acb1Δ* (*MCY1612*) and *MDM30 mls1Δ* (*MCY1649*) shuffling strains transformed with *pRS314-FZO1* (*MC250*) or an empty vector (*MC219*) and covered by (*mdm30Δ + MDM30*) or cured from (*mdm30Δ*) the *MDM30* shuffle plasmid. Note that the absence of *ACB1* affects

the respiratory rescue of *mdm30Δ* cells by *FZO1* at higher temperatures (30 and 37°C) whereas the absence of *MLS1* does so at lower temperatures (23 and 30°C). Interestingly, the absence of *ACB1* also affects the growth rescue of *mdm30Δ* cells by *FZO1* on Oleate at 23 and 30°C. As expected, absence of *MLS1* abolishes the growth of all cells on Oleate media.

Figure S3: (a and b) PerMit contacts in *acb1Δ* and *mls1Δ* cells. *ole1Δ* strains inactivated for *ACB1* (a, *acb1Δ*) or *MLS1* (b, *mls1Δ*) genomically labelled for *OM45-GFP* and *RFP-SKL* were shuffled with *OLE1*, *CYC* or *TEF pOLE1* plasmids (*MCY1980*, *MCY1987*) and processed for whole cells imaging by SIM (a) or confocal microscopy (b). The graph depicts the percentage of proximity and non-proximity of peroxisomes (RFP signals) to mitochondria (GFP signals) in *CYC-OLE1* (yellow bars) *OLE1* (blue bars) and *TEF-OLE1* (red bars) cells. Error bars represent the s.e.m from three independent experiments. ***P*<0.05, ****P*<0.005 (one-way analysis of variance (ANOVA)). Note that inactivation of either *ACB1* or *MLS1* does not modify the amount of PerMit contact in *CYC-OLE1*, *OLE1* or *TEF-OLE1* conditions as compared to *WT* cells (see Fig. 3e). **(c)** Example of time lapse acquisitions with 10 seconds intervals of a peroxisome in contact with mitochondria (indicated by white arrows) by SIM fluorescence microscopy with cells genomically labelled for *OM45-GFP* and *RFP-SKL* (*MCY1935*); Scale bars, 5 µM (Left fields) or 1 µM (Right zooms). Note that for this period as long as 70 seconds, the contact does not induce any detectable transfer of RFP in mitochondria which does not support heterotypic fusion between peroxisomes and mitochondria. **(d)** Example of time lapse acquisitions with 30 seconds intervals of a peroxisomes undergoing separation (indicated by white arrows) by SIM fluorescence microscopy with cells genomically labelled for *PEX3-mCherry* and *Fzo1-GFP* (*MCY1675*); Scale bars, 5 µM (Left fields) or 1 µM (Right zooms). Note that such separation that likely corresponds to peroxisomal division was recurrently observed as opposed to association between peroxisomes that would be expected for peroxisomal fusion that was never observed.

Figure S4: (a) Dextrose, Glycerol and Oleate spot assays at 23, 30 and 37 °C of *MDM30* (*MCY970*), *MDM30 mls1Δ* (*MCY1649*), *MDM30 icl1Δ* (*MCY1909*) and *MDM30 mls1Δ icl1Δ* (*MCY1911*) shuffling strains transformed with *pRS314-FZO1* (*MC250*) or an empty vector (*MC219*) and covered by (*mdm30Δ + MDM30*) or cured from (*mdm30Δ*) the *MDM30* shuffle plasmid. Compare the growth of *mls1Δ* and *mls1Δ icl1Δ* cells on glycerol media and note that the respiratory growth rescue of *mdm30Δ* cells by the extra-copy of *FZO1* is lost at 23 and 30°C in the absence of *MLS1* but is totally recovered upon deletion of *ICL1*. **(b)** Percentage of cells with tubular (blue) or non-tubular (red) mitochondria at 30°C from *OLE1* (*WT*), *OLE1 mls1Δ* (*mls1Δ*), *OLE1 icl1Δ* (*icl1Δ*) and *OLE1 mls1Δ icl1Δ* (*mls1Δ icl1Δ*) shuffling strains genomically labelled for *mito-GFP* and shuffled with *OLE1*, *CYC* or *TEF pOLE1* plasmids (*MCY1835*, *MCY1989*, *MCY2002*, *MCY2003*). Error bars represent the s.e.m from three independent experiments. ***P*<0.05 (one-way analysis of variance (ANOVA)). NS, not significant. More than 100

cells were analyzed per sample. Note that the inactivation of *ICL1* in *mls1⊿* cells not only restores the tubular morphology in the absence of *MLS1* in the *CYC-OLE1* condition but also significantly improves the morphology of the mitochondrial network in the *TEF-OLE1* condition.

Table S1: Table of *S. cerevisiae* strains used in this study.

Table S2: Table of plasmids used in this study.

Video 1: Mitochondrial fission event (see Fig 5b). Fission event analyzed by time-lapse Structured Illumination Microscopy (SIM) in *OM45-GFP* labelled cells. Total duration 1 minute with one acquisition every 10 seconds**.** Scale bar 1 µM. Playback speed 1 frame per second.

Video 2: Mitochondrial fusion event (see Fig 5c). Fusion event analyzed by time-lapse SIM in *OM45-GFP* labelled cells. Total duration 1 minute with one acquisition every 10 seconds**.** Scale bar 1 µM. Playback speed 1 frame per second.

Video 3: PerMit contact behavior (see Fig S3c). Strains with of mitochondrial outer membranes (*OM45-GFP*) and peroxisomal matrix (*RFP-SKL*) labelling were analyzed by time-lapse SIM. Peroxisomal attachment over a total duration of 70 seconds with one acquisition every 10 seconds**.** Scale bar 1 µM. Playback speed 1 frame per second.

Video 4: Peroxisomal fission event (see fig S3d). Strains with peroxisomal membranes labelling (*PEX3-mcherry*) were analyzed by time-lapse SIM. Peroxisomal dissociation event with total duration of 3,5 minutes and one acquisition every 30 seconds**.** Scale bar 1 µM. Playback speed 1 frame per second.

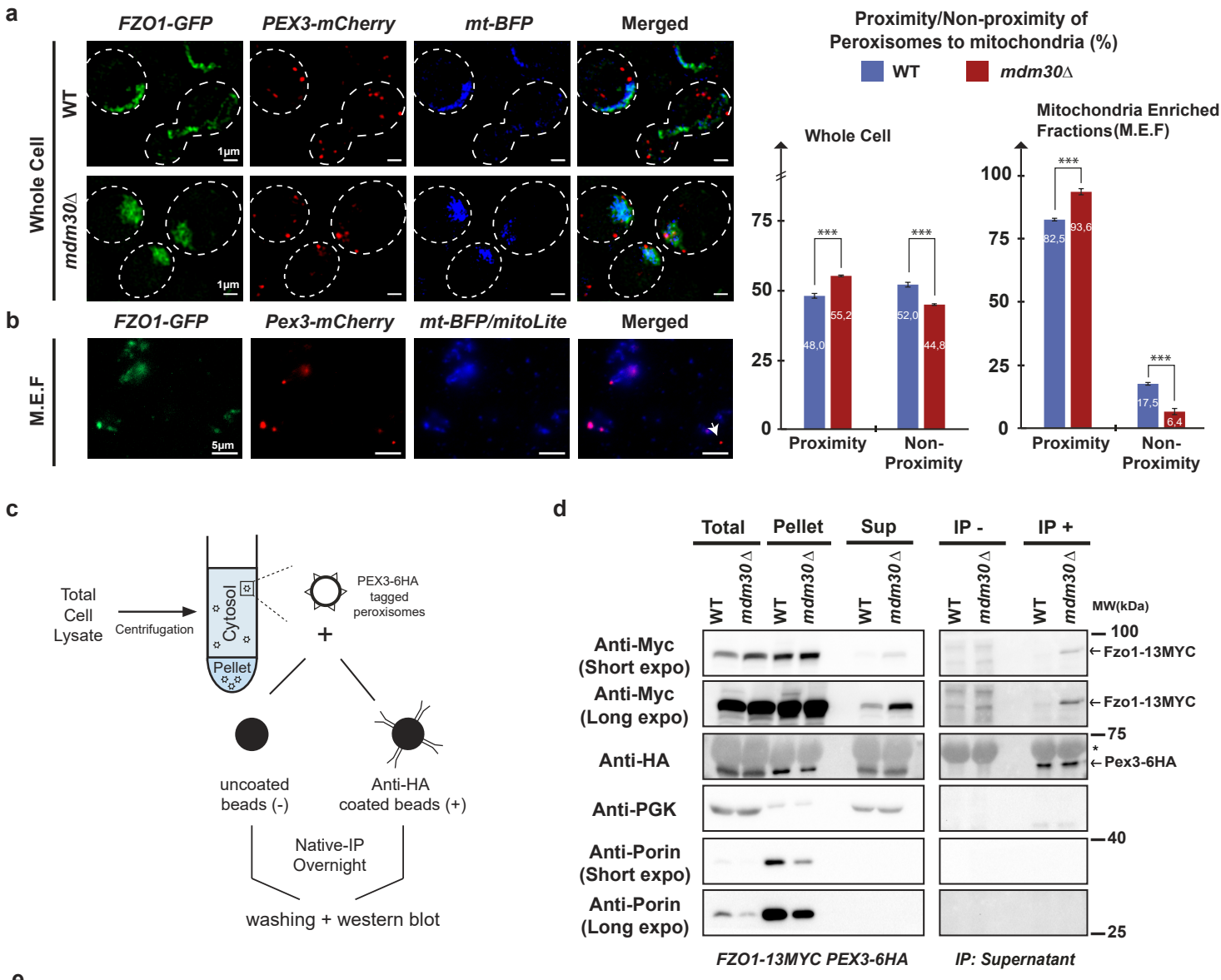
a
FZO1-GFP
PEX3-mCherry
mt-BFP
Merged
Whole Cell
WT
mdm30Δ
1µm
b
FZO1-GFP
Pex3-mCherry
mt-BFP/mitoLite
Merged
M.E.F
5µm
Proximity/Non-proximity of Peroxisomes to mitochondria (%)
WT
mdm30Δ
Whole Cell
Mitochondria Enriched Fractions(M.E.F)
***
48,0
55,2
52,0
44,8
82,5
93,6
17,5
6,4
Proximity
Non-Proximity
c
Total Cell Lysate
Centrifugation
Cytosol
Pellet
PEX3-6HA tagged peroxisomes
uncoated beads (-)
Anti-HA coated beads (+)
Native-IP Overnight
washing + western blot
d
Total
Pellet
Sup
IP -
IP +
WT
mdm30Δ
MW(kDa)
Anti-Myc (Short expo)
Anti-Myc (Long expo)
Anti-HA
Anti-PGK
Anti-Porin (Short expo)
Anti-Porin (Long expo)
100
Fzo1-13MYC
75
Pex3-6HA
40
25
FZO1-13MYC PEX3-6HA
IP: Supernatant
e
RFP Trap beads (+)
mdm30Δ FZO1-GFP
mdm30Δ PEX3-mCherry mt-BFP
mdm30Δ FZO1-GFP PEX3-mCherry mt-BFP
(A)
(B)
(C)
GFP
RFP
BFP
DIC
10µm
f
% of fluorescent beads
mock (-) / RFP (+) beads
100
75
50
25
0
27,5
44,4
A
B
C
WT
mdm30Δ

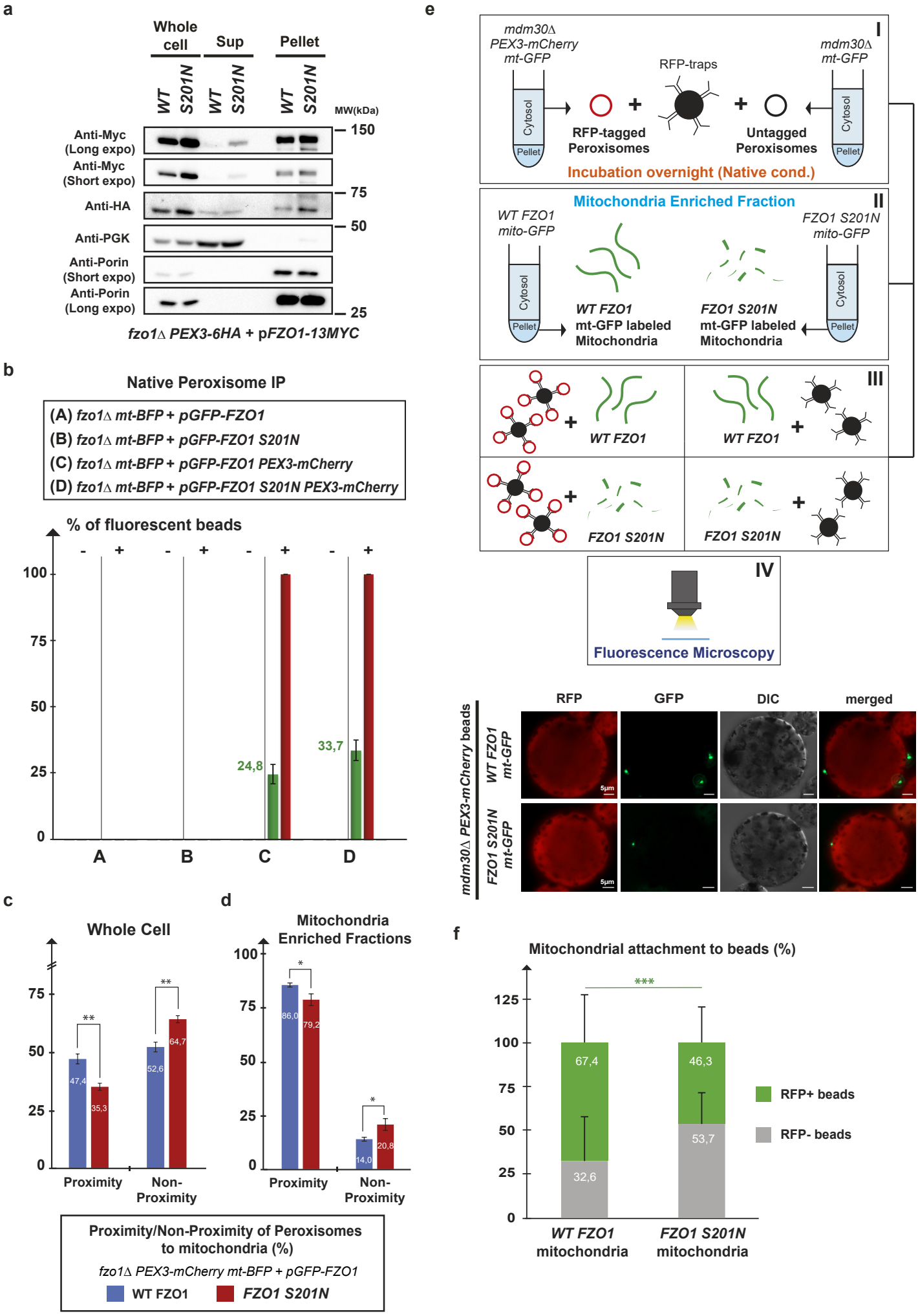
a
Whole cell
Sup
Pellet
WT
S201N
MW(kDa)
Anti-Myc (Long expo)
Anti-Myc (Short expo)
Anti-HA
Anti-PGK
Anti-Porin (Short expo)
Anti-Porin (Long expo)
150
75
50
25
fzo1Δ PEX3-6HA + pFZO1-13MYC
b
Native Peroxisome IP
(A) fzo1Δ mt-BFP + pGFP-FZO1
(B) fzo1Δ mt-BFP + pGFP-FZO1 S201N
(C) fzo1Δ mt-BFP + pGFP-FZO1 PEX3-mCherry
(D) fzo1Δ mt-BFP + pGFP-FZO1 S201N PEX3-mCherry
% of fluorescent beads
24,8
33,7
A
B
C
D
c
Whole Cell
47,4
35,3
52,6
64,7
Proximity
Non-Proximity
d
Mitochondria Enriched Fractions
86,0
79,2
14,0
20,8
Proximity
Non-Proximity
Proximity/Non-Proximity of Peroxisomes to mitochondria (%)
fzo1Δ PEX3-mCherry mt-BFP + pGFP-FZO1
WT FZO1
FZO1 S201N
e
mdm30Δ PEX3-mCherry mt-GFP
mdm30Δ mt-GFP
RFP-traps
RFP-tagged Peroxisomes
Untagged Peroxisomes
Cytosol
Pellet
Incubation overnight (Native cond.)
Mitochondria Enriched Fraction
WT FZO1 mito-GFP
FZO1 S201N mito-GFP
WT FZO1 mt-GFP labeled Mitochondria
FZO1 S201N mt-GFP labeled Mitochondria
WT FZO1
FZO1 S201N
Fluorescence Microscopy
RFP
GFP
DIC
merged
mdm30Δ PEX3-mCherry beads
WT FZO1 mt-GFP
FZO1 S201N mt-GFP
5μm
f
Mitochondrial attachment to beads (%)
***
67,4
32,6
46,3
53,7
RFP+ beads
RFP- beads
WT FZO1 mitochondria
FZO1 S201N mitochondria

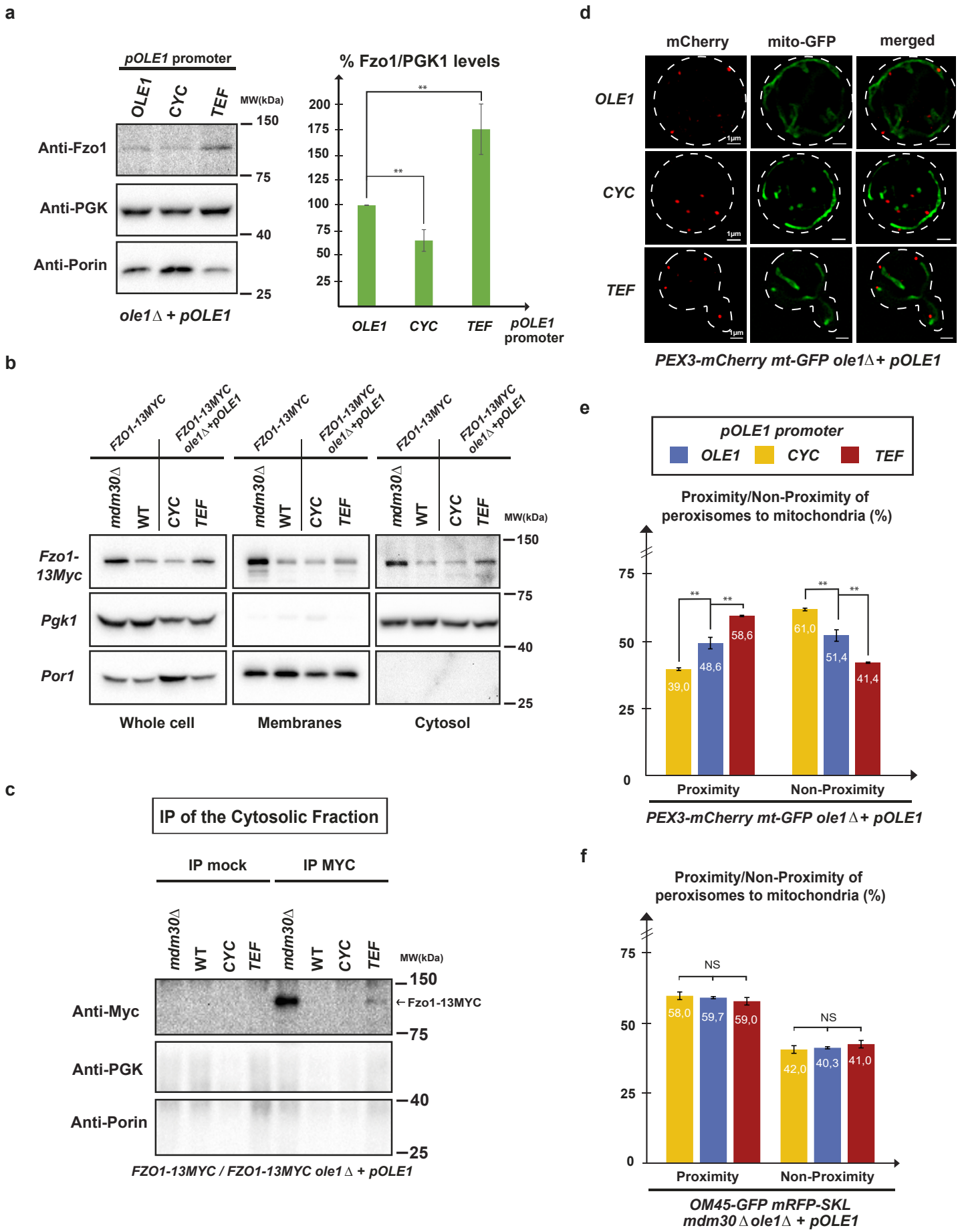
a
pOLE1 promoter
OLE1
CYC
TEF
MW(kDa)
150
75
40
25
Anti-Fzo1
Anti-PGK
Anti-Porin
ole1Δ + pOLE1
% Fzo1/PGK1 levels
200
175
150
125
100
75
50
25
**
**
OLE1
CYC
TEF
pOLE1 promoter
b
FZO1-13MYC
FZO1-13MYC ole1Δ+pOLE1
mdm30Δ
WT
CYC
TEF
MW(kDa)
150
75
40
25
Fzo1-13Myc
Pgk1
Por1
Whole cell
Membranes
Cytosol
c
IP of the Cytosolic Fraction
IP mock
IP MYC
mdm30Δ
WT
CYC
TEF
MW(kDa)
150
←Fzo1-13MYC
75
40
25
Anti-Myc
Anti-PGK
Anti-Porin
FZO1-13MYC / FZO1-13MYC ole1Δ + pOLE1
d
mCherry
mito-GFP
merged
OLE1
CYC
TEF
1μm
PEX3-mCherry mt-GFP ole1Δ+ pOLE1
e
pOLE1 promoter
OLE1
CYC
TEF
Proximity/Non-Proximity of peroxisomes to mitochondria (%)
75
50
25
0
**
**
**
**
39,0
48,6
58,6
61,0
51,4
41,4
Proximity
Non-Proximity
PEX3-mCherry mt-GFP ole1Δ+ pOLE1
f
Proximity/Non-Proximity of peroxisomes to mitochondria (%)
75
50
25
0
NS
NS
58,0
59,7
59,0
42,0
40,3
41,0
Proximity
Non-Proximity
OM45-GFP mRFP-SKL
mdm30Δole1Δ + pOLE1

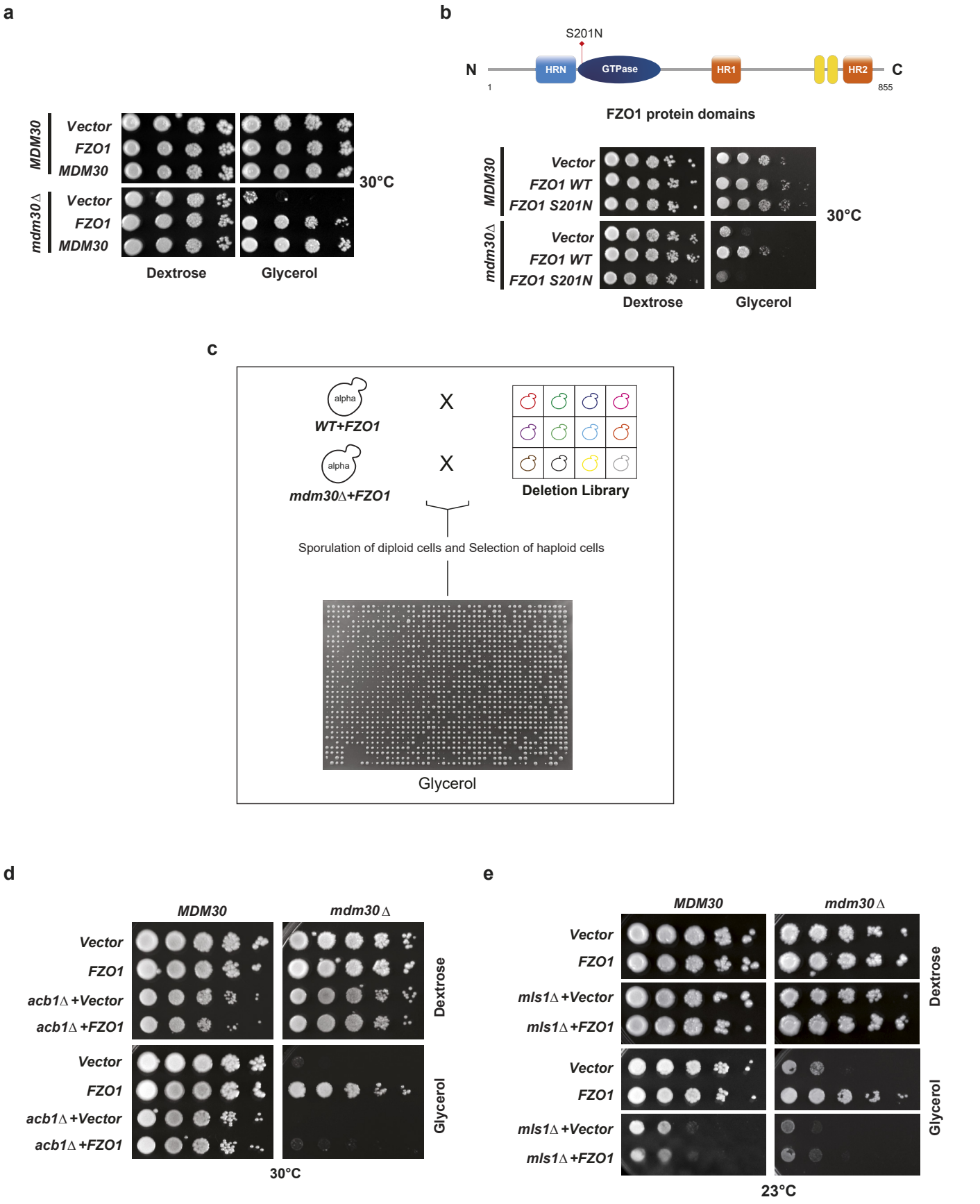
a
MDM30
Vector
FZO1
MDM30
mdm30Δ
Vector
FZO1
MDM30
30°C
Dextrose
Glycerol
b
S201N
N
HRN
GTPase
HR1
HR2
C
1
855
FZO1 protein domains
MDM30
Vector
FZO1 WT
FZO1 S201N
mdm30Δ
Vector
FZO1 WT
FZO1 S201N
30°C
Dextrose
Glycerol
c
alpha
WT+FZO1
X
alpha
mdm30Δ+FZO1
X
Deletion Library
Sporulation of diploid cells and Selection of haploid cells
Glycerol
d
MDM30
mdm30Δ
Vector
FZO1
acb1Δ+Vector
acb1Δ+FZO1
Dextrose
Vector
FZO1
acb1Δ+Vector
acb1Δ+FZO1
Glycerol
30°C
e
MDM30
mdm30Δ
Vector
FZO1
mls1Δ+Vector
mls1Δ+FZO1
Dextrose
Vector
FZO1
mls1Δ+Vector
mls1Δ+FZO1
Glycerol
23°C

a

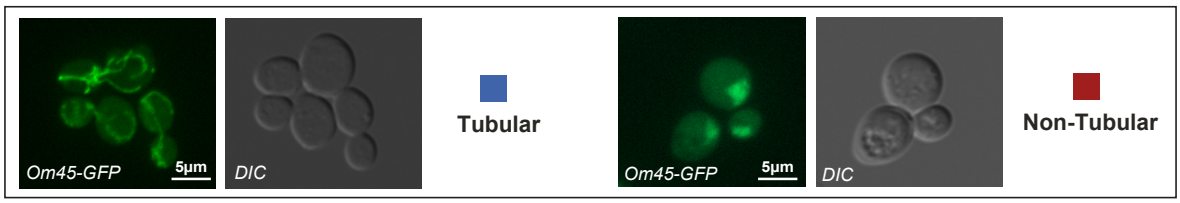
Om45-GFP
5µm
DIC
Tubular
Om45-GFP
5µm
DIC
Non-Tubular

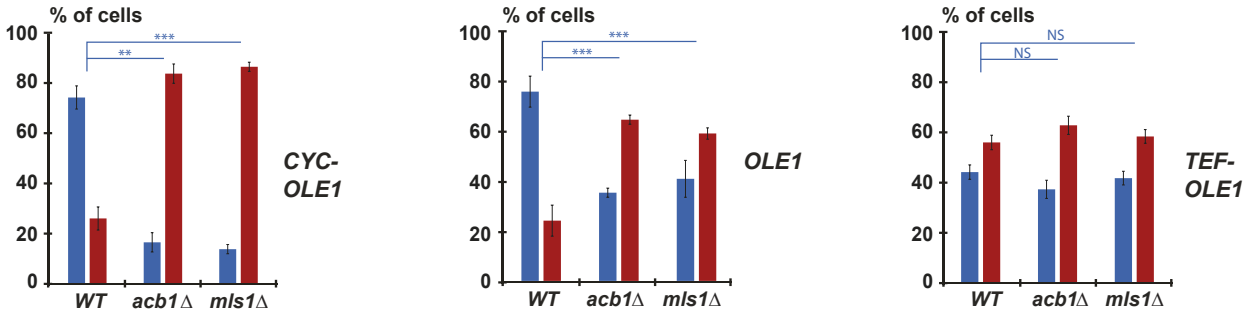
% of cells
100
80
60
40
20
0
***
**
WT
acb1Δ
mls1Δ
CYC-OLE1
% of cells
***
***
OLE1
% of cells
NS
NS
TEF-OLE1

b

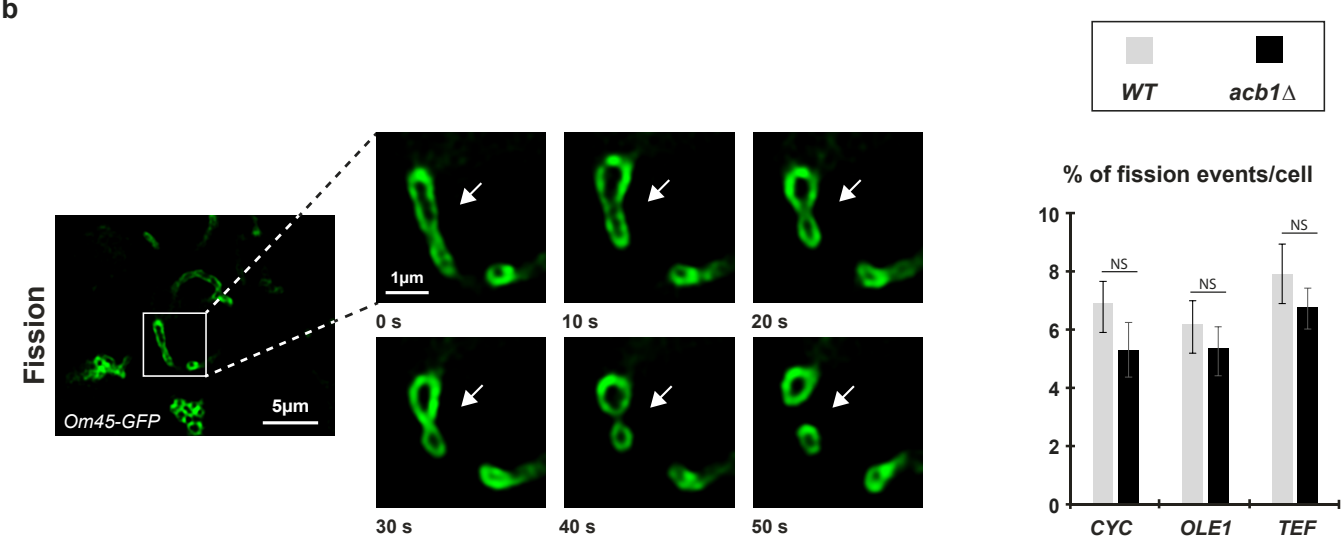
WT
acb1Δ
Fission
Om45-GFP
5µm
1µm
0 s
10 s
20 s
30 s
40 s
50 s
% of fission events/cell
10
8
6
4
2
0
NS
NS
NS
CYC
OLE1
TEF
OM45-GFP mRFP-SKL
ole1Δ + pOLE1

c

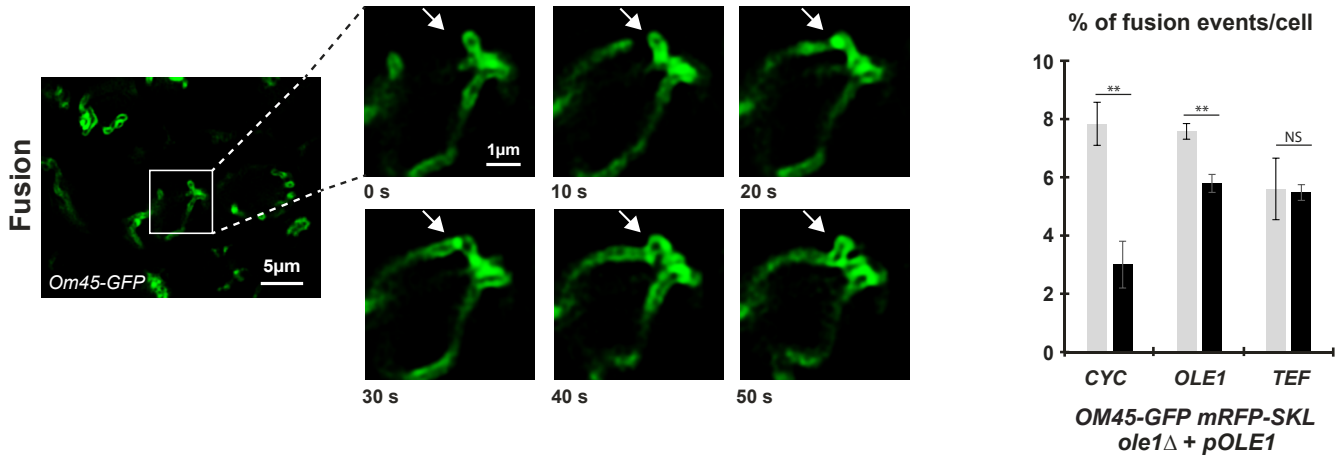
Fusion
Om45-GFP
5µm
1µm
0 s
10 s
20 s
30 s
40 s
50 s
% of fusion events/cell
10
8
6
4
2
0
**
**
NS
CYC
OLE1
TEF
OM45-GFP mRFP-SKL
ole1Δ + pOLE1

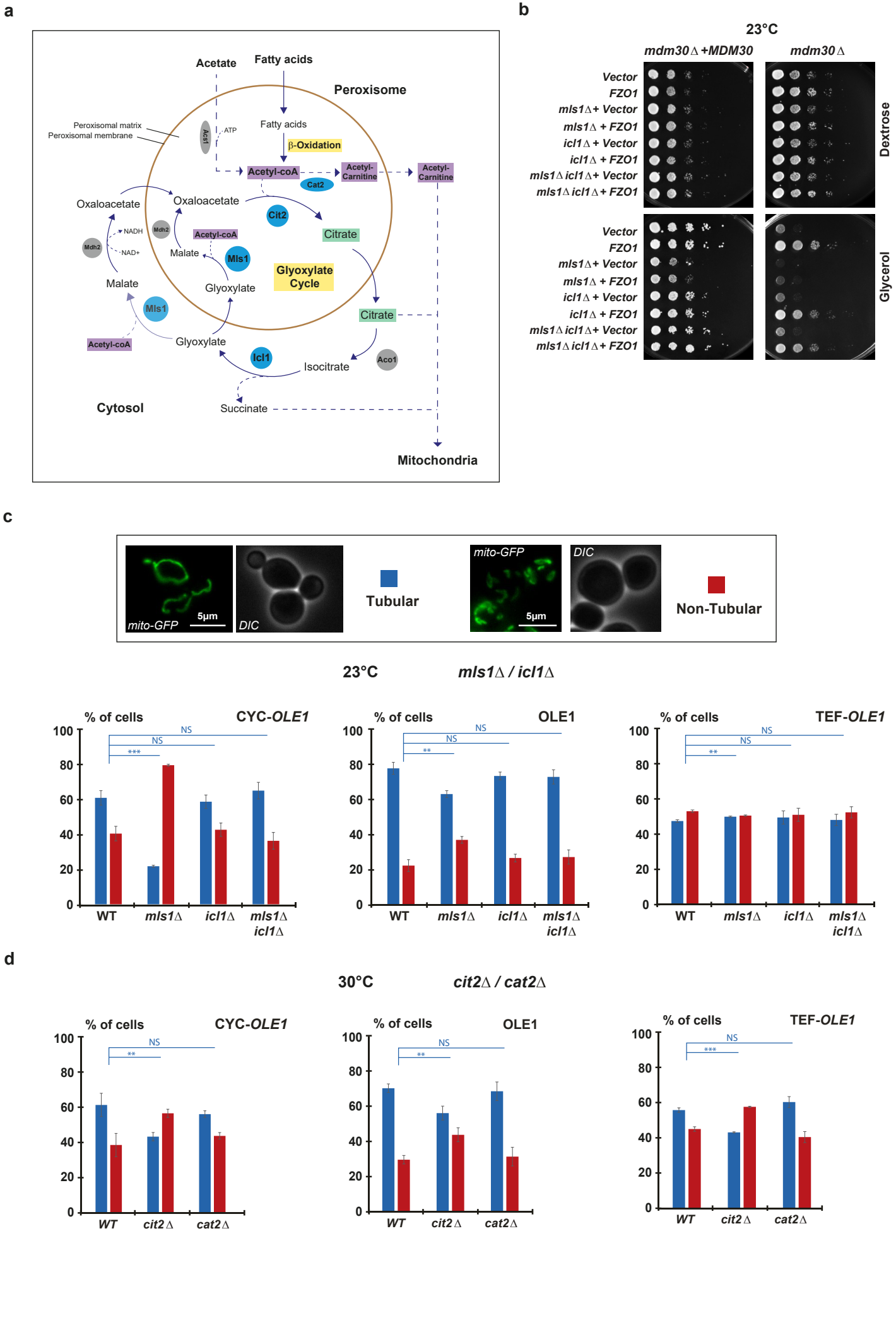
a
Acetate
Fatty acids
Peroxisome
Peroxisomal matrix
Peroxisomal membrane
Acs1
ATP
Fatty acids
β-Oxidation
Acetyl-coA
Cat2
Acetyl-Carnitine
Acetyl-Carnitine
Oxaloacetate
Oxaloacetate
Cit2
Mdh2
NADH
NAD+
Mdh2
Acetyl-coA
Citrate
Malate
Mls1
Glyoxylate Cycle
Malate
Glyoxylate
Mls1
Citrate
Acetyl-coA
Glyoxylate
Icl1
Isocitrate
Aco1
Cytosol
Succinate
Mitochondria
b
23°C
mdm30Δ +MDM30
mdm30Δ
Vector
FZO1
mls1Δ+ Vector
mls1Δ + FZO1
icl1Δ + Vector
icl1Δ + FZO1
mls1Δ icl1Δ+ Vector
mls1Δ icl1Δ+ FZO1
Dextrose
Glycerol
c
mito-GFP
5µm
DIC
Tubular
mito-GFP
DIC
5µm
Non-Tubular
23°C
mls1Δ / icl1Δ
% of cells
CYC-OLE1
NS
NS
***
100
80
60
40
20
0
WT
mls1Δ
icl1Δ
mls1Δ icl1Δ
% of cells
OLE1
NS
NS
**
WT
mls1Δ
icl1Δ
mls1Δ icl1Δ
% of cells
TEF-OLE1
NS
NS
**
WT
mls1Δ
icl1Δ
mls1Δ icl1Δ
d
30°C
cit2Δ / cat2Δ
% of cells
CYC-OLE1
NS
**
WT
cit2Δ
cat2Δ
% of cells
OLE1
NS
**
WT
cit2Δ
cat2Δ
% of cells
TEF-OLE1
NS
***
WT
cit2Δ
cat2Δ

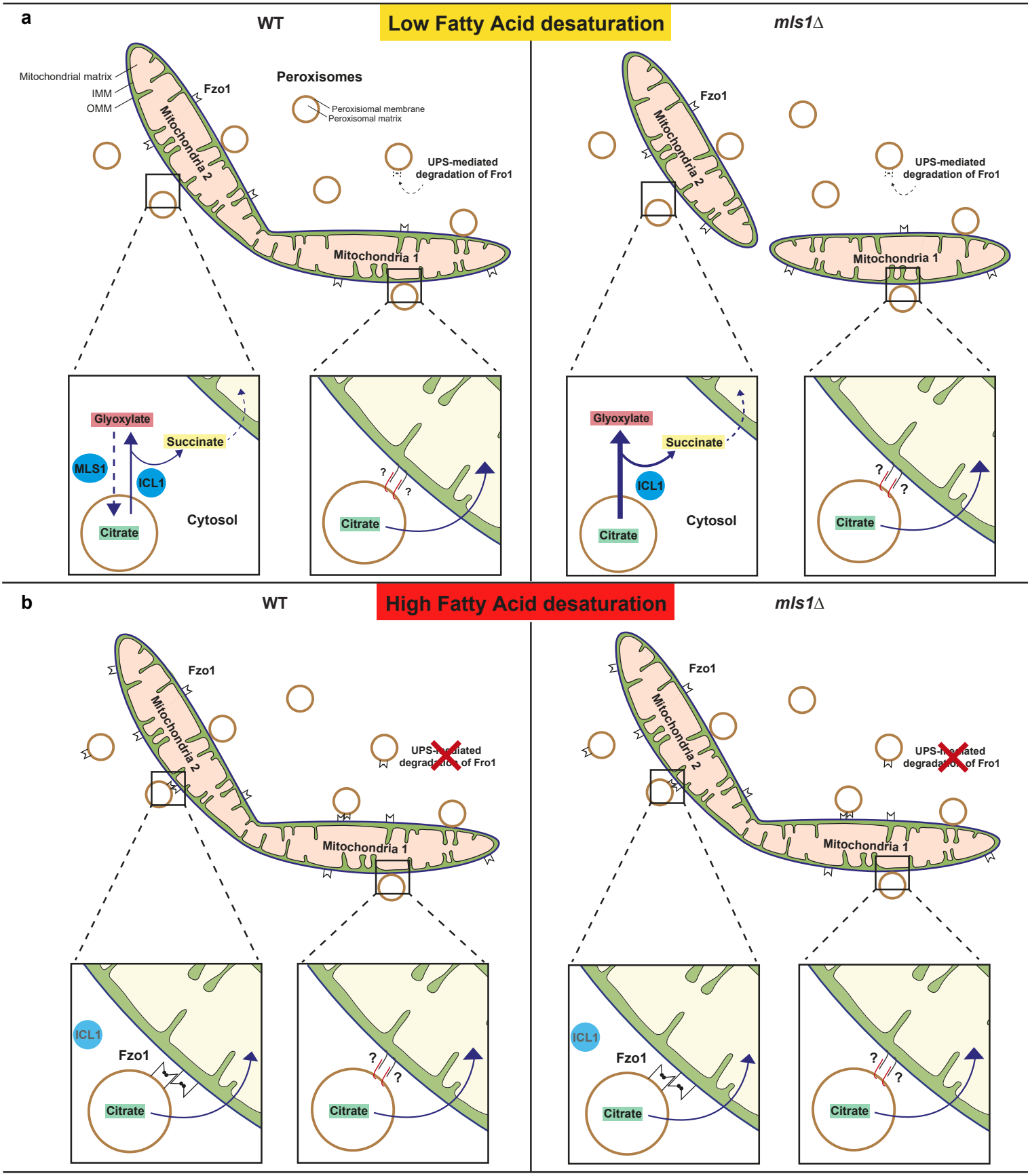
a
WT
Low Fatty Acid desaturation
mls1Δ
Mitochondrial matrix
IMM
OMM
Fzo1
Peroxisomes
Peroxisomal membrane
Peroxisomal matrix
Mitochondria 2
Mitochondria 1
UPS-mediated degradation of Fro1
Glyoxylate
Succinate
MLS1
ICL1
Citrate
Cytosol
?
b
WT
High Fatty Acid desaturation
mls1Δ
Fzo1
Mitochondria 2
Mitochondria 1
ICL1
Citrate
?

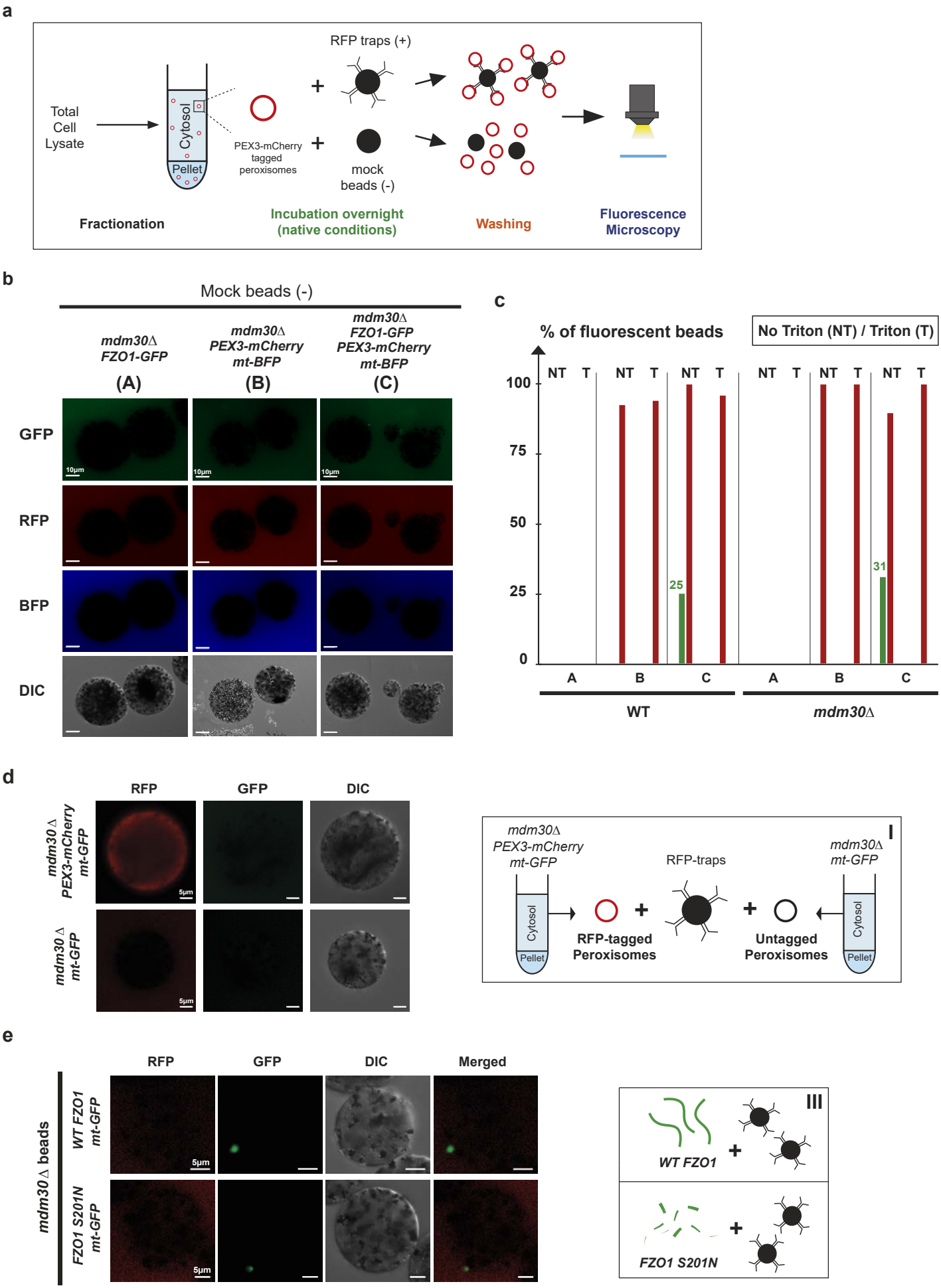
a
RFP traps (+)
Total Cell Lysate
Cytosol
Pellet
PEX3-mCherry tagged peroxisomes
mock beads (-)
Fractionation
Incubation overnight (native conditions)
Washing
Fluorescence Microscopy
b
Mock beads (-)
mdm30Δ FZO1-GFP
mdm30Δ PEX3-mCherry mt-BFP
mdm30Δ FZO1-GFP PEX3-mCherry mt-BFP
(A)
(B)
(C)
GFP
RFP
BFP
DIC
10µm
c
% of fluorescent beads
No Triton (NT) / Triton (T)
NT T
100
75
50
25
0
25
31
A
B
C
WT
mdm30Δ
d
RFP
GFP
DIC
mdm30Δ PEX3-mCherry mt-GFP
mdm30Δ mt-GFP
5µm
mdm30Δ PEX3-mCherry mt-GFP
RFP-traps
mdm30Δ mt-GFP
I
Cytosol
Pellet
RFP-tagged Peroxisomes
Untagged Peroxisomes
e
RFP
GFP
DIC
Merged
mdm30Δ beads
WT FZO1 mt-GFP
FZO1 S201N mt-GFP
5µm
III
WT FZO1
FZO1 S201N

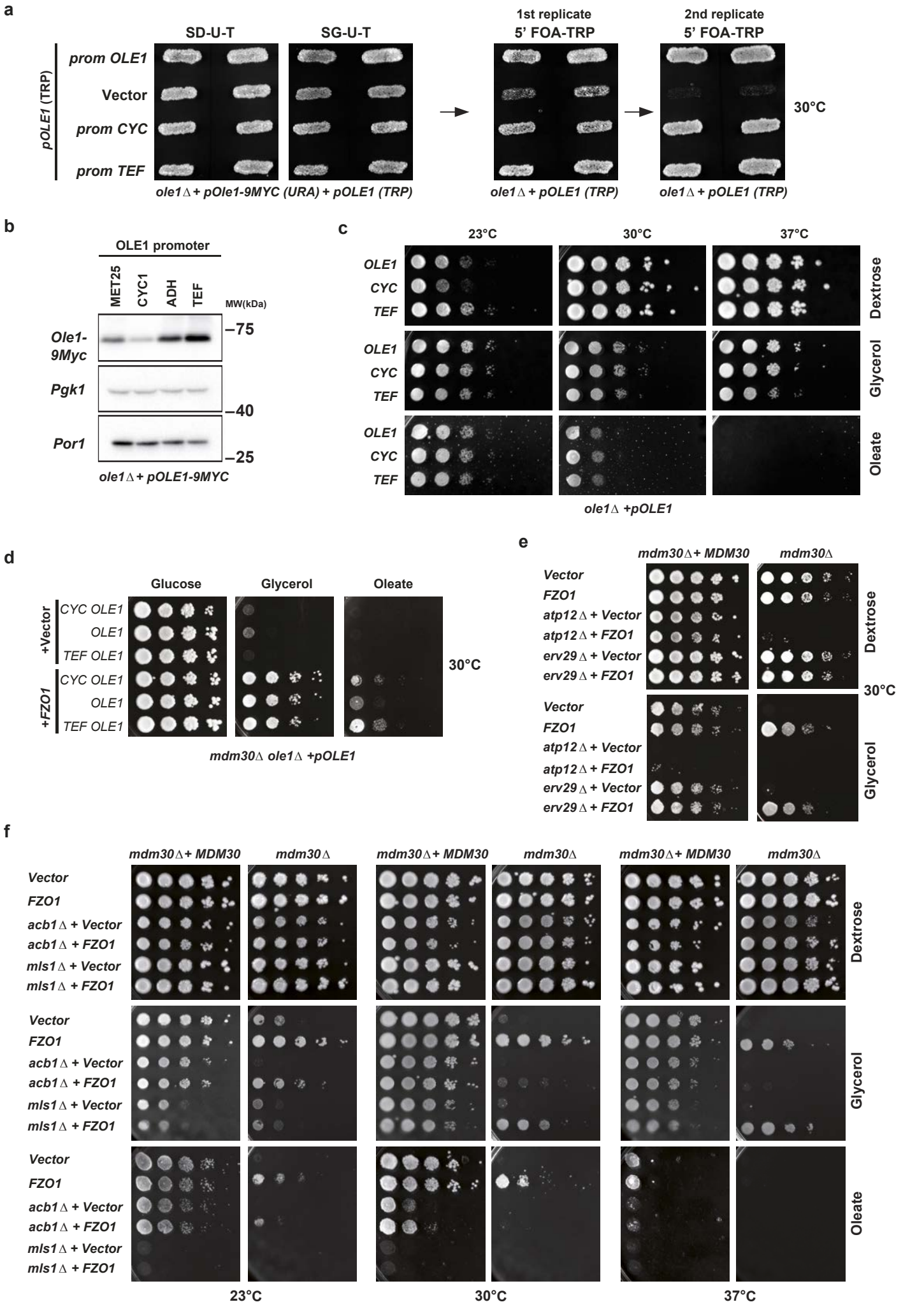
a
SD-U-T
SG-U-T
1st replicate
5' FOA-TRP
2nd replicate
5' FOA-TRP
pOLE1 (TRP)
prom OLE1
Vector
prom CYC
prom TEF
30°C
ole1Δ + pOle1-9MYC (URA) + pOLE1 (TRP)
ole1Δ + pOLE1 (TRP)
ole1Δ + pOLE1 (TRP)
b
OLE1 promoter
MET25
CYC1
ADH
TEF
MW(kDa)
Ole1-9Myc
Pgk1
Por1
75
40
25
ole1Δ + pOLE1-9MYC
c
23°C
30°C
37°C
OLE1
CYC
TEF
Dextrose
Glycerol
Oleate
ole1Δ +pOLE1
d
Glucose
Glycerol
Oleate
+Vector
+FZO1
CYC OLE1
OLE1
TEF OLE1
30°C
mdm30Δ ole1Δ +pOLE1
e
mdm30Δ+ MDM30
mdm30Δ
Vector
FZO1
atp12Δ + Vector
atp12Δ + FZO1
erv29Δ + Vector
erv29Δ + FZO1
Dextrose
30°C
Glycerol
f
mdm30Δ+ MDM30
mdm30Δ
Vector
FZO1
acb1Δ + Vector
acb1Δ + FZO1
mls1Δ + Vector
mls1Δ + FZO1
Dextrose
Glycerol
Oleate
23°C
30°C
37°C

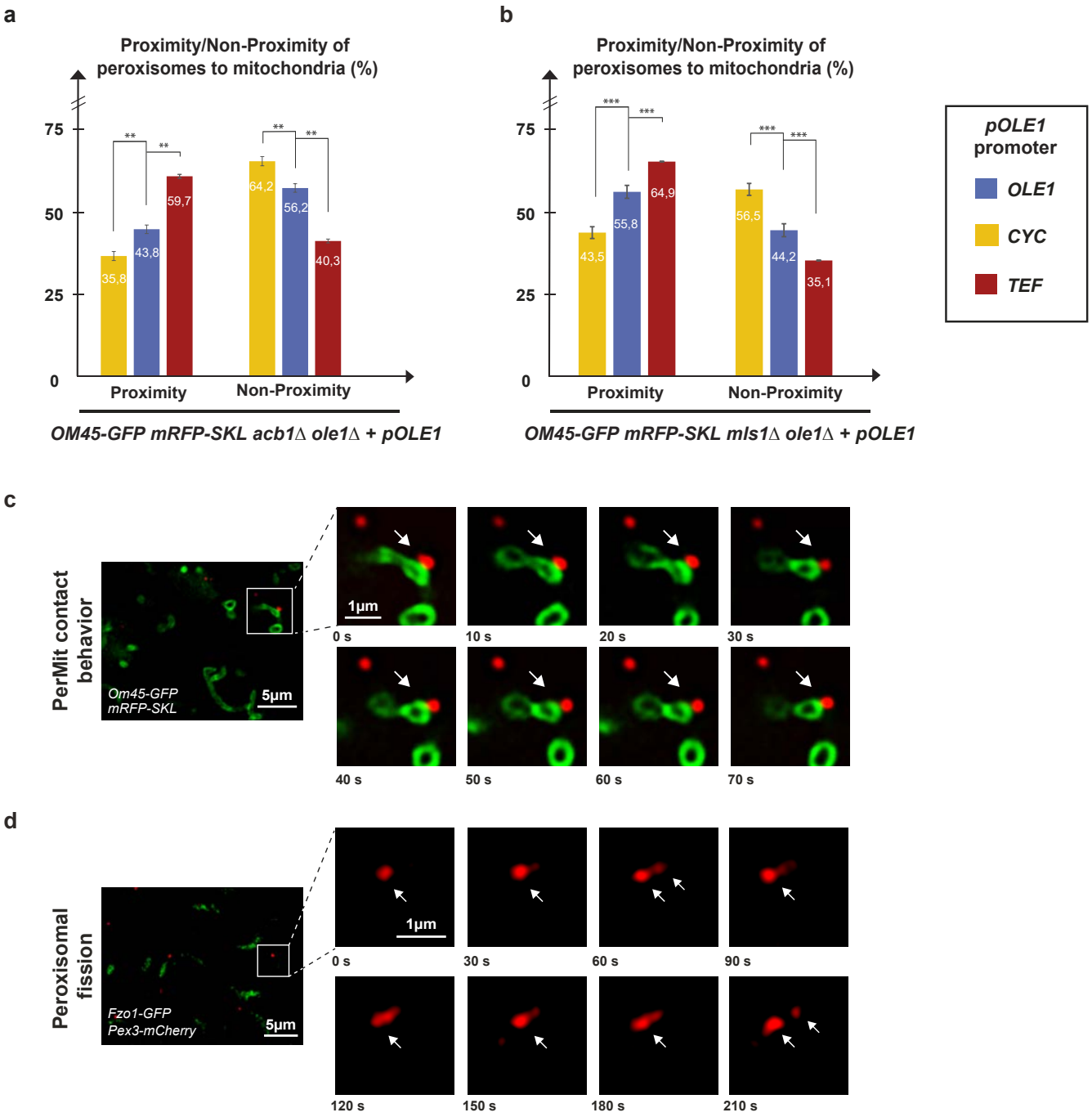
a
Proximity/Non-Proximity of peroxisomes to mitochondria (%)
75
50
25
0
35,8
43,8
59,7
64,2
56,2
40,3
**
**
**
**
Proximity
Non-Proximity
OM45-GFP mRFP-SKL acb1Δ ole1Δ + pOLE1
b
Proximity/Non-Proximity of peroxisomes to mitochondria (%)
75
50
25
0
43,5
55,8
64,9
56,5
44,2
35,1
***
***
***
***
Proximity
Non-Proximity
OM45-GFP mRFP-SKL mls1Δ ole1Δ + pOLE1
pOLE1 promoter
OLE1
CYC
TEF
c
PerMit contact behavior
Om45-GFP
mRFP-SKL
5µm
1µm
0 s
10 s
20 s
30 s
40 s
50 s
60 s
70 s
d
Peroxisomal fission
Fzo1-GFP
Pex3-mCherry
5µm
1µm
0 s
30 s
60 s
90 s
120 s
150 s
180 s
210 s

a

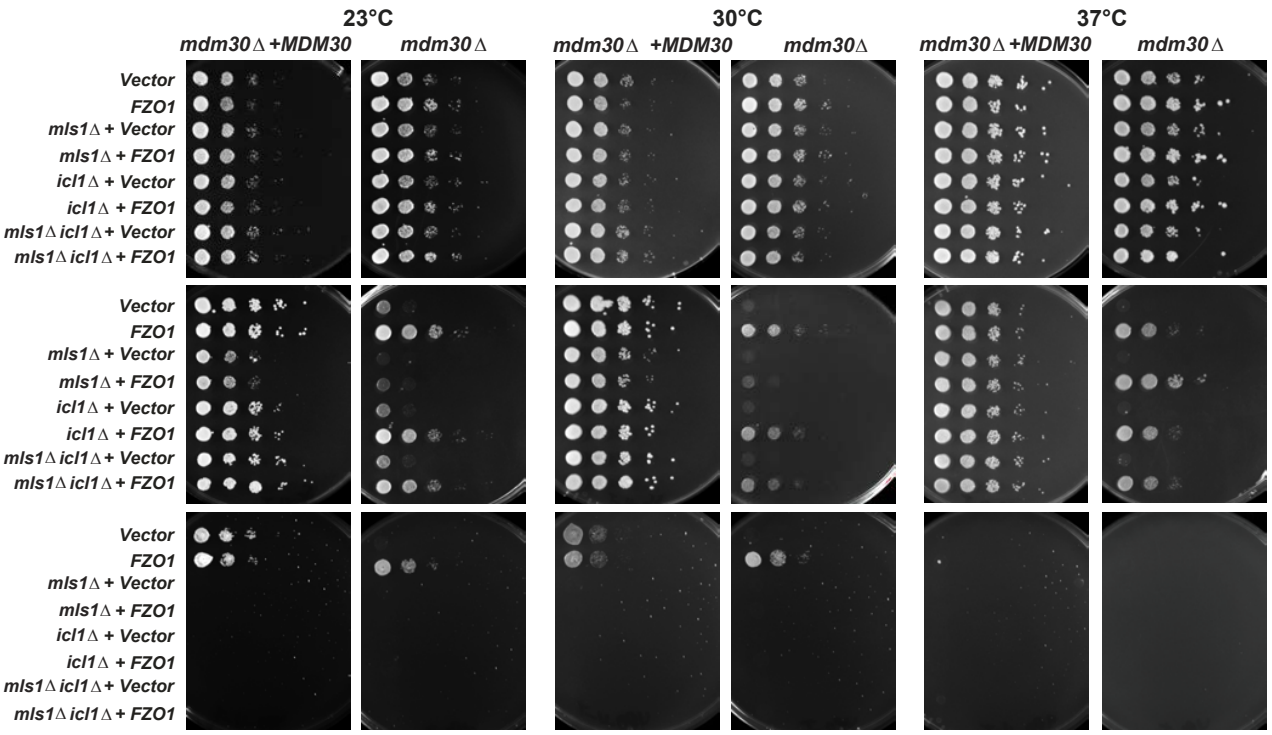
23°C
30°C
37°C
mdm30Δ +MDM30
mdm30Δ
Vector
FZO1
mls1Δ + Vector
mls1Δ + FZO1
icl1Δ + Vector
icl1Δ + FZO1
mls1Δ icl1Δ + Vector
mls1Δ icl1Δ + FZO1
Dextrose
Glycerol
Oleate

b

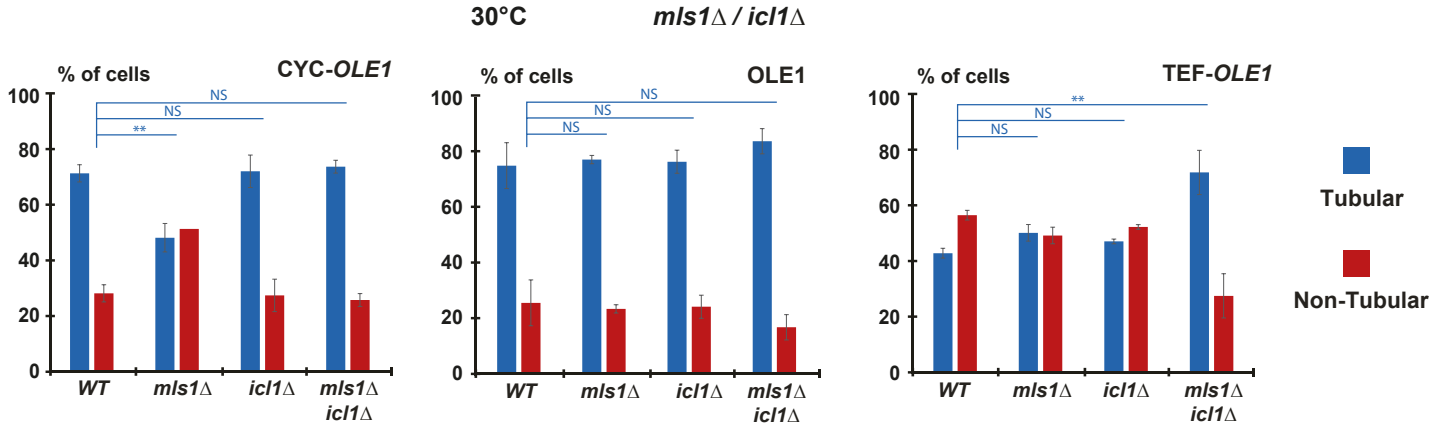
30°C
mls1Δ / icl1Δ
% of cells
CYC-OLE1
OLE1
TEF-OLE1
NS
**
WT
mls1Δ
icl1Δ
mls1Δ icl1Δ
Tubular
Non-Tubular

Part 3: Discussion and Perspectives

The field of physical inter-organelle contacts has been booming for the last decade and many labs are trying to "ride the wave". The contacts between organelles are emerging as a key process ensuring efficient communication across cellular compartments (Prinz et al., 2020). In a shared and common compartment like the cell which -if you really think about it- is quite crowded, organelles have a very high likelihood of coming together. It is thus no surprise that cellular organelles such as the ER, mitochondria, the lysosomal/vacuolar compartment, peroxisomes or the plasma membrane are not just avoiding each other like we do in Parisian metro stations, but actually communicate with through physical associations between their respective lipid bilayers (Eisenberg-Bord et al., 2016; Gatta and Levine, 2017). Thanks to the many techniques that are being developed to study these contacts, the list of factors which we now call "tethers" keeps on growing and growing consequently revealing unprecedented functions of specific protein complexes or lipids (Gatta and Levine, 2017; Prinz et al., 2020; Kornmann et al., 2009; Lahiri et al., 2015).

Aside from its role in tethering and fusion of mitochondrial outer membranes, Fzo1 has been shown to mediate Peroxisome-Mitochondria (PerMit) contacts when overexpressed (Shai et al., 2018). Even though the physiological relevance of these observations was still unclear, the regulation of Fzo1's localization seemed to involve the UPS-mediated turnover of the protein (Shai et al., 2018). Two (not so) separate roads brought us to the involvement of fatty acids in these contacts: the first one is that peroxisomes are known to be essential hubs of fatty acid metabolism. The second one originated from the initial discovery that mitochondrial fusion is governed by a balance between Fzo1 degradation and FA desaturation (Cavellini et al., 2017).

These two studies provided the biggest pieces of the puzzle for our story which began with numerous fundamental questions: What is the physiological relevance of Fzo1's peroxisomal localization? How does FA desaturation regulate mitochondrial fusion? Does Fzo1 mediate PerMit contacts in physiological conditions and if so, how is this regulated? Last but not least, what purpose could be served by Fzo1-mediated PerMit contacts? The road to provide answers for these questions was not straight and even.

I- Targeting and stabilization of Fzo1 at peroxisomal membranes

The first big challenge was proving the peroxisomal localization of Fzo1 (Fig1- Alsayyah *et al.*) which led to the discovery that Fzo1 localizes to peroxisomal membranes in WT cells. This novel physiological localization raises the question on the targeting mechanisms of Fzo1 to distinct membranes. In reality, Fzo1 is proposed to use similar hydrophobic residues near it's TM as MFN for proper localization and function (Huang et al., 2017). It is not excluded that an unidentified peroxisomal targeting sequence is present in the sequence of Fzo1. An observation that supports this possibility is the interaction of Fzo1 with the peroxisomal targeting protein Pex19 and the insertase Pex14 which was demonstrated by co-Immunoprecipitation assays (Shai et al., 2018) as Pex19 binds the hydrophobic mPTS located near the TM domain of most peroxisomal membrane proteins (Sacksteder et al., 2000; Jones et al., 2004). Thus, these interactions most likely facilitate the targeting and insertion of Fzo1 in peroxisomal membranes, in turn providing possible insight on the targeting and stabilization of Fzo1 to MOM membranes.

Interestingly, Fzo1 tightly interacts with the outer membrane component Ugo1 which is essential for outer and inner mitochondrial membrane fusion (Sesaki and Jensen, 2001, 2004; Hoppins et al., 2009). Ugo1 binds both Fzo1 (MOM) and Mgm1 (MIM), bridging the interactions between the two fusion proteins which coordinates their respective fusion events in addition to driving the crucial lipid-mixing step during mitochondrial fusion (Sesaki and Jensen, 2001, 2004; Hoppins et al., 2009). In comparison to the interaction between Fzo1 and Pex19 and Pex14, we can speculate that Ugo1-Fzo1 interactions may not only be required to coordinate Fzo1's functions at mitochondria (i.e. fusion) but also contributes to the targeting and the stabilization of Fzo1 to MOMs. This hypothesis could be soon put to the test through the production of an Fzo1 recombinant protein. If Ugo1 contributes to the targeting and the stabilization of Fzo1 to membranes, the production of Fzo1 in bacteria would be more efficient when Fzo1 is expressed in parallel to Ugo1 vs the expression of Fzo1 alone.

II- Fzo1 regulation at peroxisomal membranes

Fzo1 mediates mitochondrial outer membrane fusion at mitochondria. The first step of this process is tethering the 2 adjacent mitochondrial membranes in a close proximity for subsequent fusion of MOMs. At peroxisomal membranes, Fzo1 tethers peroxisomes to mitochondria via Fzo1-Fzo1 mediated interactions (Fig 2- Alsayyah et al). The GTPase domain of Fzo1 plays an

important role in PerMit contacts (similarly to mitochondrial membranes) as it directly affects the oligomerization properties of the mitofusin. In our study, we found that Fzo1-mediated contacts contribute to approx. 10% of the total contacts between the Peroxisomes and Mitochondria in WT cells (Fig 2-Alsayyah et al).

As Fzo1 is responsible for the homotypic fusion of mitochondrial membranes, the idea that it could also mediate heterotypic fusion between peroxisomes and mitochondria cannot be ignored. An attractive idea on paper but is it really beneficial for the cell?
Fusing peroxisomes to mitochondria is no simple task. It would require to overcome the energy barrier in order to deform both peroxisomal and mitochondrial membranes and induce mixing. This seems hazardous considering the difference in properties and lipid composition between the two membranes and the energetic cost compared to simple tethering. In line with this, our SIM time lapse acquisitions did not provide any data that support the heterotypic fusion hypothesis, neither between peroxisomes and mitochondria nor between two peroxisomes (Fig S3-Alsayyah et al). The regulation of PerMit contacts which are faster and less energy consuming seems to be a far more efficient strategy to use for substrate transfer.

In this context, we find that the amount of Fzo1 localized at peroxisomes thus its propensity to mediate contacts with mitochondria is conditioned by degradation or stabilization of the mitofusin by the SCF-ubiquitin ligase Mdm30. This rate of Mdm30-mediated turnover of Fzo1 is in turn governed by the status of FA desaturation in the cell (Fig. 3- Alsayyah et al).
Upon high FA desaturation, the ubiquitin protease Ubp2 trims the ubiquitin chains added by Mdm30 on Fzo1, which results in stabilization of the mitofusin (Cavellini et al., 2017). Conversely, Mdm30 promotes ubiquitination and degradation of Ubp2 upon low FA desaturation, which results in un-antagonized and increased Mdm30-mediated turnover of Fzo1 (Cavellini et al., 2017). This mechanism explains the impact of FA desaturation on Fzo1-mediated PerMit contacts, which are modulated according to cellular desaturation levels. This regulation is completely abolished upon the inactivation of *MDM30* (Fig3- Alsayyah *et al*). Nonetheless, we still do not know if any cofactors (i.e. Cdc48), Dubs (i.e. Ubp3) or other ligases are potentially implicated in the regulation of the peroxisomal Fzo1.

III- PerMit contacts protect functional mitochondrial fusion

Furthermore, contacts between peroxisomes and mitochondria do not happen randomly at mitochondrial membranes. In fact, PerMit contacts were found to be localized near areas of the

mitochondrial matrix where the PDH complex is enriched (Cohen et al., 2014). This primary observation already sheds the light on the possible involvement of beta-oxidation by-products in PerMit contacts and their function. In line with this, Pex34-mediated PerMit contacts were found to promote acetyl-coA and citrate transfer from peroxisomes to mitochondria in turn boosting mitochondrial respiration (Shai et al., 2018). Unlike in Pex34 overexpression conditions, the CO_2 measurements in conditions of Fzo1 overexpression were inconclusive, so the purpose of Fzo1-mediated contacts remained unknown. To clarify this mystery, we used a genetic readout in which we added an extra-copy of Fzo1 to *mdm30*Δ cells that rescued respiratory growth on glycerol media (Fig 4-Alsayyah et al). This readout shows that an increase in Fzo1 levels and in turn PerMit contacts has beneficial effect on mitochondrial respiration, in line with previous observations showing that adding an extra-copy of Fzo1 also rescues mitochondrial fusion in *mdm30*Δ cells (Cavellini et al., 2017). Two genes which abolish this rescue were identified: *ACB1* and *MLS1*, both directly related to peroxisomes and fatty acids (Fig 4-Alsayyah et al).

As Fzo1-mediated PerMit contacts are not constitutive and vary according to FA desaturation, we found that Fzo1-mediated PerMit contacts are required to maintain efficient mitochondrial fusion as FA desaturation increases (Fig5- Alsayyah et al). Consistent with this, we observe that low desaturation does not impact mitochondrial dynamics as opposed to high desaturation where we see a decrease in mitochondrial fusion (Fig5-Alsayyah et al). By abolishing *ACB1* and *MLS1*, mitochondrial fusion levels plummeted in low FA desaturation while mitochondrial fusion was unaffected in high FA desaturation. Of course we do not exclude that under low FA desaturation, other PerMit contacts mediated by distinct factors should be able to favor the mitochondrial transport of by-products such as peroxisomal Citrate as was demonstrated previously for PerMit contacts mediated by Pex34 (Shai et al., 2018). Nonetheless, the strong perturbations of mitochondrial dynamics upon inactivation of *MLS1* and *ACB1* in low FA conditions raises the possibility that the transfer of some by-products between peroxisomes and mitochondria may blocked. The fact that mitochondrial fusion remained unchanged in the same context upon high FA desaturation, clearly indicates that Fzo1-mediated PerMit counteract these defects (Fig. 5-Alsayyah et al).

IV- Citrate transfer stimulates mitochondrial fusion through PerMit contacts

To decipher the mechanism stimulating mitochondrial fusion, we looked closely at the transfer of by-products from peroxisomes to mitochondria. In the absence of malate synthase (Mls1),

we block malate synthesis and the enzyme upstream of Mls1, Isocitrate Lyase (Icl1) keeps producing glyoxylate and succinate (Fig 6-Alsayyah et al). This glyoxylate being produced cannot be re-used or integrated in the TCA cycle, while succinate will be transferred to mitochondria thus competing with citrate transport. This increase in Succinate transfer to mitochondria seems to be deleterious for mitochondrial fusion. In line with this, the deletion of *ICL1* completely rescued the defect we saw in *mls1*Δ cells (Fig 6-Alsayyah et al). By inactivating Icl1, we stop excess Succinate synthesis which appears to be beneficial for mitochondrial fusion.

As for the second hit Acb1, we know that it's a transporter which binds to activated acyl chains (i.e. acyl chains conjugated with Coenzyme A) with very high affinity (Rosendal et al., 1993; Rasmussen et al., 1994). In this context, Acb1 has been proposed to transport activated acyl chains to acyl-CoA consuming processes (Schjerling et al., 1996; Rasmussen et al., 1994). This established capacity of Acb1 to bind acyl chains, suggests that beta-oxidation of FAs could likely be a main source of peroxisomal Acetyl-coA for peroxisomal citrate synthesis. However, further investigation will be required to clarify this potential role of Acb1 in transport of FAs into peroxisomes. Nonetheless, if Acb1 transports activated fatty acids into peroxisomes for peroxisomal citrate synthesis, this would clearly explain the drop in mitochondrial fusion we observe in the absence of Fzo1-mediated PerMit contacts upon low FA desaturation. Conversely, increased PerMit contacts seen upon high desaturation would compensate the decreased synthesis of Citrate by facilitating its transfer to mitochondria.

As our data clearly point at a pivotal role for citrate in the maintenance of functional mitochondrial fusion, we needed to excluded the involvement of acetyl-coA. In turn, we tested this by inactivating *CAT2* (which conjugates carnitine to acetyl-coA allowing it to shuttle from peroxisome to mitochondria) thus inhibiting peroxisomal exit and mitochondrial import of Acetyl-coA which did not impact mitochondrial dynamics (Fig6- Alsayyah *et al*).
On the other hand, we show that inhibiting the synthesis of peroxisomal Citrate does induce a specific decrease in tubular mitochondria in low but also in high FA desaturation conditions (Fig6- Alsayyah *et al*). This effect upon high FA desaturation is particularly relevant as this is the condition where Fzo1-mediated PerMit contacts are the highest and in which mitochondrial dynamics were protected against inactivation of *MLS1* or *ACB1* (Fig3,5-Alsayyah *et al*). This implies that synthesis of peroxisomal Citrate in proximity to mitochondria is required to maintain efficient mitochondrial fusion in specific conditions.

Consistent with this, peroxisomal Citrate transits to mitochondria through specific transporters (Klingenberg, 1972; Robinson et al., 1971). Abolishing Citrate transfer by deleting genes such as *CTP1* which codes for a mitochondrial citrate transporter could further consolidate our theory. Once transported to mitochondria, Citrate can feed the oxidative TCA cycle which, in turn, is known to stimulate the mitochondrial membrane potential (Jazwinski, 2014). Notably, the mitochondrial membrane potential is an essential component of mitochondrial fusion (Legros et al., 2002; Meeusen et al., 2004; Song et al., 2007). In this context, the mitochondrial transfer of Citrate by Fzo1-mediated PerMit contacts could stimulate mitochondrial fusion by maintaining an efficient mitochondrial membrane potential.

An additional hit obtained from the screen that we have not tested further consolidates our hypothesis. The gene *SDH5* which codes for Succinate Dehydrogenase 5, is highly conserved protein among eukaryotes and resides in the mitochondrial matrix (Hao et al., 2009). Sdh5's main activity relies in its interaction with one of the catalytic subunits of the SDH (Succinate dehydrogenase) complex also known as Mitochondrial Complex II. To cut the story short, Sdh5 binds to Sdh1 and promotes its flavinylation (i.e. the incorporation of the flavin adenine dinucleotide or FAD cofactor) which is necessary for succinate dehydrogenase (SDH) complex assembly and activity (Enyenihi and Saunders, 2003; Deutschbauer et al., 2002; Kim et al., 2012; Hao et al., 2009). The SDH complex is responsible for the oxidation of succinate to fumarate coupled with the reduction of ubiquinone to ubiquinol. These reactions feed both the TCA cycle and the electron transport chain. In other words, in the absence of Sdh5, the SDH complex is blocked and cannot oxidize succinate to fumarate consequently blocking its entry to the TCA cycle. It is thus no surprise that we found *SDH5* as a potential hit for the inhibition of the rescue by the extra-copy of Fzo1 as its function goes hand in hand with our previous observations. Inhibiting SDH5, and in turn the contribution of succinate to the TCA cycle and the electron transport chain would counter the beneficial effect of the peroxisomal citrate transfer to mitochondria.

Taken altogether, these observations suggest that a balance between peroxisomal Citrate and Succinate entry into mitochondria needs to be maintained for efficient mitochondrial fusion to take place. This would be achieved by tethering the two organelles through PerMit contacts that would facilitate the transfer of selective by-products into mitochondria. These contacts mediated by Fzo1 (but also other tethers) would be modulated in response to different cellular conditions such as changes in FA desaturation.

V- Mitochondrial fusion v/s lipidome remodeling

This study reveals the impact of extreme changes in FA desaturation on processes like mitochondrial fusion. Increasing unsaturated fatty acids by overexpressing *OLE1* or adding unsaturated FAs to the media probably causes an extended remodeling of the cellular phospho-lipidome (Surma et al., 2013). This would directly affect mitochondrial membranes (among other membranes) changing their lipid composition thus altering their respective properties (Ernst et al., 2016).

Membrane properties like fluidity or curvature are essential parameters when it comes to membrane dynamics and when these properties are altered, it may render mitochondrial outer membranes more or less "fusogenic" meaning that they are more or less able to fuse. Unsaturated fatty acids for example have kinked shapes and form fluid bilayers. Conversely, saturated lipids form non-fluid gel phases (Ernst et al., 2016). Consequently, the proteins that are responsible of driving mitochondrial fusion such as Fzo1 need to be simultaneously regulated to "handle" these membranes. We can speculate that the stabilization of Fzo1 may thus be required for fusion of outer membranes that are now more fluid and less 'fusogenic' upon increased desaturation of fatty acids. These higher levels of mitofusin would then allow assembly of a Mitochondrial Docking ring Complex (MDC) of an appropriate size to trigger fusion of outer membranes (Fig11). This stabilization also increases Fzo1-mediated PerMit contacts facilitating citrate transfer to the mitochondrial matrix to stimulate mitochondrial fusion. Conversely, when saturated FA levels are high and bilayers are tightly packed, a higher Fzo1-turnover by Mdm30 is required. Lower levels of Fzo1 would ensure the formation of a perhaps smaller MDC which is sufficient for successful mitochondrial membrane and PerMit contacts would be scarce. Excess Fzo1 levels in these conditions are thought to block the formation of the MDC resulting in abortive fusion (Brandt et al., 2016; Cavellini et al., 2017).

Fully understanding these processes will first require a dissection of the potential impact of FA saturation on the phospholipid composition of mitochondrial membranes. This can be achieved by purification assays of mitochondria followed by lipidomic analyses of their respective membranes. These analyses will allow us to track the changes in composition of membranes and in turn their physical properties giving us a basis for a more in-depth understanding of the organization of mitofusins at the mitochondrial surface. And yet, this is only the tip of the iceberg.

VI- Inter-organelle contacts: a defensive shield for mitochondrial dynamics?

Fzo1 is not be the only protein impacted by such changes in membrane properties due to lipidome remodeling. Changes in lipid metabolism can directly affect sorting of tail-anchored proteins (Krumpe et al., 2012), but also the regulation of voltage- and ligand- gated ion channels (Antollini and Barrantes, 2016). It has been documented that high concentrations of unsaturated fatty acids lead to an elevation of cytosolic Ca^{2+} in pancreatic cells (Chang et al., 2015). In addition, dysfunction in fatty acid metabolism is implicated in disease conditions, such as cardiovascular disease, several neurological diseases like Parkinson's disease, Alzheimer's disease (Virmani et al., 2015; Maulik et al., 2019).

Looking back at our results, we can expect that in high fatty acid desaturation conditions, voltage gated ion channels and calcium channels could be directly affected.
This could be due to changes in membrane permeability and integrity, in turn causing perturbations in mitochondrial membrane potential and diminishing the capacity of mitochondria to fuse. Fzo1-mediated PerMit contacts in this condition could help re-establish this balance by driving the TCA cycle and boosting mitochondrial potential.
These observations are reminiscent of the functions of Mfn2 on ER membranes (de Brito and Scorrano, 2008). The human mitofusin localizes at MOMs and at ER membranes mediating interactions between the two organelles. This interaction is essential for mitochondrial energy metabolism and Ca^{2+} transfer among other functions (Rowland and Voeltz, 2012; Csordás et al., 2018; Moltedo et al., 2019). Nonetheless, no substantial proof of a direct contribution of Mfn2-mediated contacts between the ER and Mitochondria to mitochondrial fusion. However, it has been documented that the ER is present more than previously expected at MOM fusion sites. In addition, videos of fusion events also show that fusion events lasted longer in the absence than in the presence of the ER (Guo et al., 2018). The idea that potential metabolite transfer in the presence of ER contacts at mitochondrial fusion sites could be stimulating the fusion process is yet to be investigated.

In the future, it would not only be interesting to dig further into the potential changes of entire proteomes of organellar membranes (such as the outer mitochondrial membrane or peroxisomal membranes) in response to changes in the cellular lipidome. But also, to decipher how different organellar membranes sense-and-respond to environmental cues and stresses to maintain their individual properties and functions.

Part 4: Materials and Methods

1) Yeast strains and Growth conditions

The *S. cerevisiae* strains and plasmids used in this study are listed in Supplementary Table 1 and 2 respectively. Standard methods were used for growth, transformation and genetic manipulation of *S. cerevisiae*. Complete media or Minimal synthetic media [Difco yeast nitrogen base (Voigt Global Distribution Inc, Lawrence, KS), and drop out solution] were supplemented with the following carbon sources: 2% dextrose (SD; YPD for complete media), 2% glycerol (SG; YPG for complete media) or 0,2% Oleic Acid (YPO) (previously dissolved in pure ethanol) supplemented with 1% Tergitol (Sherman, 2002; Lockshon et al., 2007). Where indicated media were supplemented with 0.1, 0.2 or 0.5% saturated/unsaturated fatty acids (previously dissolved in pure ethanol) and 1% Tergitol with equivalent non-treated samples were supplemented with 1% Tergitol only.

2) Generation of MDM30 and OLE1 shuffle strains

MDM30 null cells lose their mitochondrial DNA because of decreased mitochondrial fusion efficiency (Fritz et al., 2003). A plasmid-shuffle strategy was thus employed to ensure a reliable genetic analysis of *mdm30Δ* and *fzo1Δ* cells as described in (Cavellini et al., 2017). Unlike *MDM30*, the *OLE1* gene is essential in *S. cerevisiae* (Stukey et al., 1989).Consequently, wild type W303 cells were transformed with *pRS416-OLE1-9MYC* (*OLE1* shuffle plasmid) prior to the chromosomal deletion of *OLE1* to generate *OLE1* shuffle strains and keep the cells alive. *OLE1* inactivation was verified by replica-plating *OLE1* shuffle strains on 5′-fluoroorotic acid (5′-FOA) plates in the absence of an additional plasmid expressing OLE1. Loss of the uracil *OLE1* shuffle plasmid resulted in 100% lethality which confirmed absence of *OLE1*.
To yield strains used in this study, *MDM30* and *OLE1* shuffle strains were then transformed with plasmids under selection of interest listed in Supplementary Table 2. Ten colonies were systematically isolated on SD selective media lacking uracil and replica-plated on corresponding SG and 5′-FOA plates. Strains grown on 5′-FOA plates and cured from shuffling plasmids were in turn replica-plated on SD and SG selective plates containing uracil. The glycerol growth phenotypes of strains covered by or cured from the shuffling plasmids were reproducibly observed in 100% of clones tested after 1 to 3 days of growth at 30 °C. Representative colonies were used in subsequent experiments.

3) Protein extracts and Immunoblotting

1OD of cells (1mL) grown in SD media were collected during the growth exponential phase (OD_{600}=0.5–1) and total protein extracts were prepared using the NaOH/trichloroacetic acid lysis method (Volland et al., 1994). Briefly, lysis was performed with 100 µL of 1M NaOH on ice for 10 minutes before protein precipitation with 100 µL of TCA (50%) on ice for 30 minutes. Proteins were then pelleted and resuspended in Sample Buffer (13.33 mM Tris-HCL (pH 6.8),1.6 mM EDTA, 1.6% SDS, 40 mM DTT, 8% Glycerol, 0.016% Bromophenol Blue, 333 mM Tris-Base) and solubilized at 70°C for 10 minutes. Proteins were separated on SDS–PAGE (8% or 10% Acrylamide) and transferred onto nitrocellulose membranes (Amersham Hybond-ECL; GE Healthcare). The primary antibodies used for immunoblotting were: monoclonal anti-Pgk1 (1/20,000, AbCam, ab113687), monoclonal anti-HA (1/1,000, 12CA5, Invitrogen, 71-5500), monoclonal anti-Por1 (1/1,000, AbCam, ab110326), monoclonal anti-Myc (1/1,000, 9E10, Invitrogen, R950-25), polyclonal anti-Fzo1 (1/1,000, generated by Covalab). Primary antibodies were detected by secondary anti-mouse or anti-rabbit antibodies conjugated to horseradish peroxidase (HRP, 1/5,000, Sigma-Aldrich, 12-348 and A5278), followed by incubation with the Immun-Star Western C Kit (Bio-Rad). Immunoblotting images were acquired with a Gel Doc XR+ (Bio-Rad) before treatment and quantification with the Image Lab 6.0 software (Bio-Rad). The cytosolic protein PGK1 was used as a loading control to normalize loading of other proteins relative to the WT conditions.

4) Cellular fractionation assay

Cells were grown overnight in SD media to exponential phase (OD_{600} = 0.5–1) and 500 ODs were collected by centrifugation at 1500×g for 5 minutes before getting resuspended in 0.1 M Tris-HCl pH=9.4 - 50 mM β-mercapto-ethanol (1 ml per 20 ODs of cells) and incubated for 1 h at 30°C to begin cell wall lysis (Meisinger et al., 2000; Gregg et al., 2009). Following centrifugation, cells were washed with 1.2M sorbitol and resuspended in 1.2M sorbitol (1 ml per 50 ODs) supplemented with Zymolyase (Zymo Research; Orange, CA) (10 µl per 50 ODs) to initiate cell wall digestion and generate spheroplasts. After a 1h30 incubation at 30°C, spheroplasts were collected at 1500g and washed with 1.2M sorbitol to finally be resuspended in ice-cold Homogenization Buffer [10 mM Tris-HCl (pH 7.4), 0.6 M sorbitol, 1 mM EDTA, 0.2% (w/v) BSA + protease inhibitor pills (Protease Inhibitor Cocktail; Sigma-Aldrich) and 1 mM Pefabloc (Sigma-Aldrich)]. Spheroplasts were disrupted by douncing on ice (100 times with a medium size glass dounce of 15mL) and the resulting homogenate cleared by centrifugation at 3000×*g* for 5 minutes. The cleared homogenate (Total fraction) was then subjected to centrifugation at 10,170×*g* for 10 min, yielding a soluble fraction in the supernatant

(Sup) and a mitochondrial enriched membrane fraction (Pellet). The soluble fraction was subsequently subjected to an additional centrifugation at 10,170×g for 5 minutes to clear the supernatant from any residual mitochondrial contamination. The mitochondrial pellet was then loaded on a sucrose gradient (Meisinger et al., 2006). Sucrose step gradients were prepared: 1,5mL 60% sucrose/EM (w/v) at the bottom of the centrifuge tube, following 4mL 32%, 1,5 mL 23% and 1,5mL 15% sucrose/EM (w/v). The homogenate was loaded on top of the gradient and centrifuged at 134,000g for 1h at 2 °C. Mitochondria were finally recovered at the 60/32% junction using a pipette. Aliquots of each fraction were collected and treated with TCA as described above prior to immunoblotting.

5) Spot Assays

Cultures grown overnight in SD medium were pelleted, resuspended at OD_{600}=1, and serially diluted (1:10) five times in water. Three microliters of the dilutions were spotted on Dextrose, Glycerol, Oleic Acid plates (with the appropriate amino acid selection) and grown for 2 to 4 days (Dextrose) or 3 to 6 days (Glycerol and Oleic Acid) at 23, 30 or 37 °C.

6) High-Throughput Genetic Screen

The screen was carried through Synthetic Genetic Array (SGA) techniques (Cohen and Schuldiner, 2011) using the *Mat alpha SGA* ready strain *yMS721* and a *Mat a G418* selection yeast deletion library (Giaever et al., 2002) that are built in the *BY* genetic yeast background. In this background, the respiratory growth defect of *mdm30Δ* cells is only detected at 37°C on glycerol media (Fritz et al., 2003). *WT* and *mdm30Δ* strains were mated with the *Mat a* yeast deletion library (Giaever et al., 2002) and the resulting zygotes were grown on glycerol 1536 plate format for 7 days at 37°C. To manipulate libraries in 1536-colony high-density format, a RoToR bench top colony arrayer (Singer Instruments) was used. In this primary screen, the positive hits were defined as candidates that present a growth defect in the *mdm30Δ* context but that are unaffected in the *WT* control. Taking advantage of the identical disposition of deletion mutants on *WT* and *mdm30Δ* plates, the screening of the hits was performed using a colorization approach. Briefly, *WT* colonies were colored in red while *mdm30Δ* colonies were colored in green. Superimposition of *WT* red plates over *mdm30Δ* green plates resulted in a vast majority of yellow colonies. The potential hits corresponded to red colonies with significantly reduced yellow coloration reflecting a growth defect of *mdm30Δ* as compared to *WT*.

Yeast strains and plasmids used in this study can be found in the Supplementary Tables 1 and 2 respectively (Annexe).

Part 5: Bibliography

Abrams, A.J., R.B. Hufnagel, A. Rebelo, C. Zanna, N. Patel, M.A. Gonzalez, I.J. Campeanu, L.B. Griffin, S. Groenewald, A.V. Strickland, F. Tao, F. Speziani, L. Abreu, R. Schüle, L. Caporali, C. La Morgia, A. Maresca, R. Liguori, R. Lodi, Z.M. Ahmed, K.L. Sund, X. Wang, L.A. Krueger, Y. Peng, C.E. Prada, C.A. Prows, K. Bove, E.K. Schorry, A. Antonellis, H.H. Zimmerman, O.A. Abdul-Rahman, Y. Yang, S.M. Downes, J. Prince, F. Fontanesi, A. Barrientos, A.H. Nemeth, V. Carelli, T. Huang, S. Zuchner, and J.E. Dallman. 2015. Mutations in the UGO1-like protein SLC25A46 cause an optic atrophy spectrum disorder. *Nat Genet*. 47:926–932. doi:10.1038/ng.3354.

Agne, B., N.M. Meindl, K. Niederhoff, H. Einwächter, P. Rehling, A. Sickmann, H.E. Meyer, W. Girzalsky, and W.-H. Kunau. 2003. Pex8p: An Intraperoxisomal Organizer of the Peroxisomal Import Machinery. *Molecular Cell*. 11:635–646. doi:10.1016/S1097-2765(03)00062-5.

Aksam, E.B., B. de Vries, I.J. van der Klei, and J.A.K.W. Kiel. 2009. Preserving organelle vitality: peroxisomal quality control mechanisms in yeast. *FEMS Yeast Research*. 9:808–820. doi:10.1111/j.1567-1364.2009.00534.x.

Alsayyah, C., O. Ozturk, L. Cavellini, N. Belgareh-Touzé, and M.M. Cohen. 2020. The regulation of mitochondrial homeostasis by the ubiquitin proteasome system. *Biochimica et Biophysica Acta (BBA) - Bioenergetics*. 1861:148302. doi:10.1016/j.bbabio.2020.148302.

Amiott, E.A., M.M. Cohen, Y. Saint-Georges, A.M. Weissman, and J.M. Shaw. 2009. A mutation associated with CMT2A neuropathy causes defects in Fzo1 GTP hydrolysis, ubiquitylation, and protein turnover. *Mol Biol Cell*. 20:5026–35. doi:10.1091/mbc.E09-07-0622.

Antollini, S.S., and F.J. Barrantes. 2016. Fatty Acid Regulation of Voltage- and Ligand-Gated Ion Channel Function. *Front Physiol*. 7:573. doi:10.3389/fphys.2016.00573.

Anton, F., G. Dittmar, T. Langer, and M. Escobar-Henriques. 2013. Two deubiquitylases act on mitofusin and regulate mitochondrial fusion along independent pathways. *Mol Cell*. 49:487–98. doi:10.1016/j.molcel.2012.12.003.

Anton, F., J.M. Fres, A. Schauss, B. Pinson, G.J. Praefcke, T. Langer, and M. Escobar-Henriques. 2011. Ugo1 and Mdm30 act sequentially during Fzo1-mediated mitochondrial outer membrane fusion. *J Cell Sci*. 124:1126–35. doi:10.1242/jcs.073080.

Antonenkov, V.D., S. Mindthoff, S. Grunau, R. Erdmann, and J.K. Hiltunen. 2009. An involvement of yeast peroxisomal channels in transmembrane transfer of glyoxylate cycle intermediates. *The International Journal of Biochemistry & Cell Biology*. 41:2546–2554. doi:10.1016/j.biocel.2009.08.014.

Antonin, W., D. Fasshauer, S. Becker, R. Jahn, and T.R. Schneider. 2002. Crystal structure of the endosomal SNARE complex reveals common structural principles of all SNAREs. *Nat Struct Mol Biol*. 9:107–111. doi:10.1038/nsb746.

Aoki, Y., T. Kanki, Y. Hirota, Y. Kurihara, T. Saigusa, T. Uchiumi, and D. Kang. 2011. Phosphorylation of Serine 114 on Atg32 mediates mitophagy. *MBoC*. 22:3206–3217. doi:10.1091/mbc.e11-02-0145.

Apaja, P.M., H. Xu, and G.L. Lukacs. 2010. Quality control for unfolded proteins at the plasma membrane. *Journal of Cell Biology*. 191:553–570. doi:10.1083/jcb.201006012.

Aranovich, A., R. Hua, A.D. Rutenberg, and P.K. Kim. 2014. PEX16 contributes to peroxisome maintenance by constantly trafficking PEX3 via the ER. *J Cell Sci*. 127:3675–3686. doi:10.1242/jcs.146282.

Ashery, U., N. Bielopolski, A. Lavi, B. Barak, L. Michaeli, Y. Ben-Simon, A. Sheinin, D. Bar-On, Z. Shapira, and I. Gottfried. 2014. Chapter Two - The Molecular Mechanisms Underlying Synaptic Transmission: A View of the Presynaptic Terminal. *In* The Synapse. V. Pickel and M. Segal, editors. Academic Press, Boston. 21–109.

Auld, K.L., and P.A. Silver. 2006. Transcriptional Regulation by the Proteasome as a Mechanism for Cellular Protein. *Cell Cycle*. 5:1503–1505. doi:10.4161/cc.5.14.2979.

Babst, M. 2014. Quality control at the plasma membrane: One mechanism does not fit all. *Journal of Cell Biology*. 205:11–20. doi:10.1083/jcb.201310113.

Baerends, R.J., K.N. Faber, A.M. Kram, J.A. Kiel, I.J. van der Klei, and M. Veenhuis. 2000. A stretch of positively charged amino acids at the N terminus of Hansenula polymorpha Pex3p is involved in incorporation of the protein into the peroxisomal membrane. *J Biol Chem*. 275:9986–9995. doi:10.1074/jbc.275.14.9986.

Ballweg, S., and R. Ernst. 2017. Control of membrane fluidity: the OLE pathway in focus. *Biological Chemistry*. 398:215–228. doi:10.1515/hsz-2016-0277.

Bard, J.A.M., E.A. Goodall, E.R. Greene, E. Jonsson, K.C. Dong, and A. Martin. 2018. Structure and Function of the 26S Proteasome. *Annu. Rev. Biochem.* 87:697–724. doi:10.1146/annurev-biochem-062917-011931.

Bays, N.W., R.G. Gardner, L.P. Seelig, C.A. Joazeiro, and R.Y. Hampton. 2001. Hrd1p/Der3p is a membrane-anchored ubiquitin ligase required for ER-associated degradation. *Nat Cell Biol*. 3:24–29. doi:10.1038/35050524.

Belgareh-Touzé, N., L. Cavellini, and M.M. Cohen. 2017. Ubiquitination of ERMES components by the E3 ligase Rsp5 is involved in mitophagy. *Autophagy*. 13:114–132. doi:10.1080/15548627.2016.1252889.

Belgareh-Touzé, N., S. Léon, Z. Erpapazoglou, M. Stawiecka-Mirota, D. Urban-Grimal, and R. Haguenauer-Tsapis. 2008. Versatile role of the yeast ubiquitin ligase Rsp5p in intracellular trafficking. *Biochemical Society Transactions*. 36:791–796. doi:10.1042/BST0360791.

Berger, K.H., L.F. Sogo, and M.P. Yaffe. 1997. Mdm12p, a Component Required for Mitochondrial Inheritance That Is Conserved between Budding and Fission Yeast. *Journal of Cell Biology*. 136:545–553. doi:10.1083/jcb.136.3.545.

Bian, X., Y. Saheki, and P. De Camilli. 2018. Ca2+ releases E-Syt1 autoinhibition to couple ER-plasma membrane tethering with lipid transport. *The EMBO Journal*. 37:219–234. doi:10.15252/embj.201797359.

Bigay, J., and B. Antonny. 2012. Curvature, Lipid Packing, and Electrostatics of Membrane Organelles: Defining Cellular Territories in Determining Specificity. *Developmental Cell*. 23:886–895. doi:10.1016/j.devcel.2012.10.009.

Black, P.N., and C.C. DiRusso. 2007. Yeast acyl-CoA synthetases at the crossroads of fatty acid metabolism and regulation. *Biochimica et Biophysica Acta (BBA) - Molecular and Cell Biology of Lipids*. 1771:286–298. doi:10.1016/j.bbalip.2006.05.003.

Bleazard, W., J.M. McCaffery, E.J. King, S. Bale, A. Mozdy, Q. Tieu, J. Nunnari, and J.M. Shaw. 1999. The dynamin-related GTPase Dnm1 regulates mitochondrial fission in yeast. *Nat Cell Biol*. 1:298–304. doi:10.1038/13014.

Böckler, S., and B. Westermann. 2014. Mitochondrial ER Contacts Are Crucial for Mitophagy in Yeast. *Developmental Cell*. 28:450–458. doi:10.1016/j.devcel.2014.01.012.

Bodnar, N.O., and T.A. Rapoport. 2017. Molecular Mechanism of Substrate Processing by the Cdc48 ATPase Complex. *Cell*. 169:722-735.e9. doi:10.1016/j.cell.2017.04.020.

Boldogh, I.R., D.W. Nowakowski, H.-C. Yang, H. Chung, S. Karmon, P. Royes, and L.A. Pon. 2003. A Protein Complex Containing Mdm10p, Mdm12p, and Mmm1p Links Mitochondrial Membranes and DNA to the Cytoskeleton-based Segregation Machinery. *MBoC*. 14:4618–4627. doi:10.1091/mbc.e03-04-0225.

Bonekamp, N.A., P. Sampaio, F.V. de Abreu, G.H. Lüers, and M. Schrader. 2012. Transient Complex Interactions of Mammalian Peroxisomes Without Exchange of Matrix or Membrane Marker Proteins. *Traffic*. 13:960–978. doi:10.1111/j.1600-0854.2012.01356.x.

Bonekamp, N.A., and M. Schrader. 2012. Transient complex peroxisomal interactions. *Communicative & Integrative Biology*. 5:534–537. doi:10.4161/cib.21508.

Bordallo, J., R.K. Plemper, A. Finger, and D.H. Wolf. 1998. Der3p/Hrd1p Is Required for Endoplasmic Reticulum-associated Degradation of Misfolded Lumenal and Integral Membrane Proteins. *MBoC*. 9:209–222. doi:10.1091/mbc.9.1.209.

Brandman, O., and R.S. Hegde. 2016. Ribosome-associated protein quality control. *Nat Struct Mol Biol*. 23:7–15. doi:10.1038/nsmb.3147.

Brandner, A., D. De Vecchis, M. Baaden, M.M. Cohen, and A. Taly. 2019. Physics-based oligomeric models of the yeast mitofusin Fzo1 at the molecular scale in the context of membrane docking. *Mitochondrion*. 49:234–244. doi:10.1016/j.mito.2019.06.010.

Brandt, T., L. Cavellini, W. Kuhlbrandt, and M.M. Cohen. 2016. A mitofusin-dependent docking ring complex triggers mitochondrial fusion in vitro. *Elife*. 5. doi:10.7554/eLife.14618.

Braun, R.J., and B. Westermann. 2017. With the Help of MOM: Mitochondrial Contributions to Cellular Quality Control. *Trends in Cell Biology*. 27:441–452. doi:10.1016/j.tcb.2017.02.007.

Breker, M., M. Gymrek, and M. Schuldiner. 2013. A novel single-cell screening platform reveals proteome plasticity during yeast stress responses. *J Cell Biol*. 200:839–850. doi:10.1083/jcb.201301120.

Breslow, D.K., S.R. Collins, B. Bodenmiller, R. Aebersold, K. Simons, A. Shevchenko, C.S. Ejsing, and J.S. Weissman. 2010. Orm family proteins mediate sphingolipid homeostasis. *Nature*. 463:1048–1053. doi:10.1038/nature08787.

van den Brink-van der Laan, E., J. Antoinette Killian, and B. de Kruijff. 2004. Nonbilayer lipids affect peripheral and integral membrane proteins via changes in the lateral pressure profile. *Biochimica et Biophysica Acta (BBA) - Biomembranes*. 1666:275–288. doi:10.1016/j.bbamem.2004.06.010.

de Brito, O.M., and L. Scorrano. 2008. Mitofusin 2 tethers endoplasmic reticulum to mitochondria. *Nature*. 456:605–10. doi:10.1038/nature07534.

Brocard, C., and A. Hartig. 2006. Peroxisome targeting signal 1: Is it really a simple tripeptide? *Biochimica et Biophysica Acta (BBA) - Molecular Cell Research*. 1763:1565–1573. doi:10.1016/j.bbamcr.2006.08.022.

Bröcker, C., A. Kuhlee, C. Gatsogiannis, H.J. kleine Balderhaar, C. Hönscher, S. Engelbrecht-Vandré, C. Ungermann, and S. Raunser. 2012. Molecular architecture of the multisubunit homotypic fusion and vacuole protein sorting (HOPS) tethering complex. *PNAS*. 109:1991–1996.

Brown, D.A., and E. London. 1998. Structure and Origin of Ordered Lipid Domains in Biological Membranes. *Journal of Membrane Biology*. 164:103–114. doi:10.1007/s002329900397.

Bruderer, R.M., C. Brasseur, and H.H. Meyer. 2004. The AAA ATPase p97/VCP Interacts with Its Alternative Co-factors, Ufd1-Npl4 and p47, through a Common Bipartite Binding Mechanism*. *Journal of Biological Chemistry*. 279:49609–49616. doi:10.1074/jbc.M408695200.

Brügger, B., R. Sandhoff, S. Wegehingel, K. Gorgas, J. Malsam, J.B. Helms, W.-D. Lehmann, W. Nickel, and F.T. Wieland. 2000. Evidence for Segregation of Sphingomyelin and Cholesterol during Formation of Copi-Coated Vesicles. *Journal of Cell Biology*. 151:507–518. doi:10.1083/jcb.151.3.507.

Bui, H.T., and J.M. Shaw. 2013. Dynamin Assembly Strategies and Adaptor Proteins in Mitochondrial Fission. *Current Biology*. 23:R891–R899. doi:10.1016/j.cub.2013.08.040.

Burcoglu, J., L. Zhao, and C. Enenkel. 2015. Nuclear Import of Yeast Proteasomes. *Cells*. 4:387–405. doi:10.3390/cells4030387.

Burgoyne, T., S. Patel, and E.R. Eden. 2015. Calcium signaling at ER membrane contact sites. *Biochimica et Biophysica Acta (BBA) - Molecular Cell Research*. 1853:2012–2017. doi:10.1016/j.bbamcr.2015.01.022.

Byrnes, L.J., A. Singh, K. Szeto, N.M. Benvin, J.P. O'Donnell, W.R. Zipfel, and H. Sondermann. 2013. Structural basis for conformational switching and GTP loading of the large G protein atlastin. *EMBO J*. 32:369–384. doi:10.1038/emboj.2012.353.

Cao, Y.-L., S. Meng, Y. Chen, J.-X. Feng, D.-D. Gu, B. Yu, Y.-J. Li, J.-Y. Yang, S. Liao, D.C. Chan, and S. Gao. 2017. MFN1 structures reveal nucleotide-triggered dimerization critical for mitochondrial fusion. *Nature*. 542:372–376. doi:10.1038/nature21077.

Cardozo, T., and M. Pagano. 2004. The SCF ubiquitin ligase: insights into a molecular machine. *Nat Rev Mol Cell Biol*. 5:739–751. doi:10.1038/nrm1471.

Carvalho, P., V. Goder, and T.A. Rapoport. 2006. Distinct Ubiquitin-Ligase Complexes Define Convergent Pathways for the Degradation of ER Proteins. *Cell*. 126:361–373. doi:10.1016/j.cell.2006.05.043.

Casanovas, A., R.R. Sprenger, K. Tarasov, D.E. Ruckerbauer, H.K. Hannibal-Bach, J. Zanghellini, O.N. Jensen, and C.S. Ejsing. 2015. Quantitative Analysis of Proteome and Lipidome Dynamics Reveals Functional Regulation of Global Lipid Metabolism. *Chemistry & Biology*. 22:412–425. doi:10.1016/j.chembiol.2015.02.007.

Cavalier-Smith, T. 1987a. The Origin of Eukaryote and Archaebacterial Cells. *Annals of the New York Academy of Sciences*. 503:17–54. doi:10.1111/j.1749-6632.1987.tb40596.x.

Cavalier-Smith, T. 1987b. The Simultaneous Symbiotic Origin of Mitochondria, Chloroplasts, and Microbodies. *Annals of the New York Academy of Sciences*. 503:55–71. doi:10.1111/j.1749-6632.1987.tb40597.x.

Cavellini, L., J. Meurisse, J. Findinier, Z. Erpapazoglou, N. Belgareh-Touzé, A.M. Weissman, and M.M. Cohen. 2017. An ubiquitin-dependent balance between mitofusin turnover and fatty acids desaturation regulates mitochondrial fusion. *Nature Communications*. 8:15832. doi:10.1038/ncomms15832.

Cerveny, K.L., S.L. Studer, R.E. Jensen, and H. Sesaki. 2007. Yeast Mitochondrial Division and Distribution Require the Cortical Num1 Protein. *Developmental Cell*. 12:363–375. doi:10.1016/j.devcel.2007.01.017.

Chakrabarti, R., W.-K. Ji, R.V. Stan, J. de Juan Sanz, T.A. Ryan, and H.N. Higgs. 2017. INF2-mediated actin polymerization at the ER stimulates mitochondrial calcium uptake, inner membrane constriction, and division. *Journal of Cell Biology*. 217:251–268. doi:10.1083/jcb.201709111.

Chan, N.C., A.M. Salazar, A.H. Pham, M.J. Sweredoski, N.J. Kolawa, R.L.J. Graham, S. Hess, and D.C. Chan. 2011. Broad activation of the ubiquitin–proteasome system by Parkin is critical for mitophagy. *Human Molecular Genetics*. 20:1726–1737. doi:10.1093/hmg/ddr048.

Chang, C.-L., A.V. Weigel, M.S. Ioannou, H.A. Pasolli, C.S. Xu, D.R. Peale, G. Shtengel, M. Freeman, H.F. Hess, C. Blackstone, and J. Lippincott-Schwartz. 2019. Spastin tethers lipid droplets to peroxisomes and directs fatty acid trafficking through ESCRT-III. *Journal of Cell Biology*. 218:2583–2599. doi:10.1083/jcb.201902061.

Chang, J., F.D. Mast, A. Fagarasanu, D.A. Rachubinski, G.A. Eitzen, J.B. Dacks, and R.A. Rachubinski. 2009. Pex3 peroxisome biogenesis proteins function in peroxisome inheritance as class V myosin receptors. *J Cell Biol*. 187:233–246. doi:10.1083/jcb.200902117.

Chang, Y.-T., M.-C. Chang, C.-C. Tung, S.-C. Wei, and J.-M. Wong. 2015. Distinctive roles of unsaturated and saturated fatty acids in hyperlipidemic pancreatitis. *World J Gastroenterol*. 21:9534–9543. doi:10.3748/wjg.v21.i32.9534.

Chen, Y., and G.W. Dorn. 2013. PINK1-Phosphorylated Mitofusin 2 Is a Parkin Receptor for Culling Damaged Mitochondria. *Science*. 340:471–475. doi:10.1126/science.1231031.

Chen, Y., L. Pieuchot, R.A. Loh, J. Yang, T.M.A. Kari, J.Y. Wong, and G. Jedd. 2014a. Hydrophobic handoff for direct delivery of peroxisome tail-anchored proteins. *Nat Commun*. 5:5790. doi:10.1038/ncomms6790.

Chen, Y.-C., G.K.E. Umanah, N. Dephoure, S.A. Andrabi, S.P. Gygi, T.M. Dawson, V.L. Dawson, and J. Rutter. 2014b. Msp1/ATAD1 maintains mitochondrial function by facilitating the degradation of mislocalized tail-anchored proteins. *The EMBO Journal*. 33:1548–1564. doi:10.15252/embj.201487943.

Chernomordik, L.V., and M.M. Kozlov. 2003. Protein-Lipid Interplay in Fusion and Fission of Biological Membranes. *Annu. Rev. Biochem.* 72:175–207. doi:10.1146/annurev.biochem.72.121801.161504.

Chernomordik, L.V., and M.M. Kozlov. 2005. Membrane Hemifusion: Crossing a Chasm in Two Leaps. *Cell*. 123:375–382. doi:10.1016/j.cell.2005.10.015.

Choi, S.Y., P. Huang, G.M. Jenkins, D.C. Chan, J. Schiller, and M.A. Frohman. 2006. A common lipid links Mfn-mediated mitochondrial fusion and SNARE-regulated exocytosis. *Nat Cell Biol*. 8:1255–62.

Christianson, J.C., J.A. Olzmann, T.A. Shaler, M.E. Sowa, E.J. Bennett, C.M. Richter, R.E. Tyler, E.J. Greenblatt, J. Wade Harper, and R.R. Kopito. 2012. Defining human ERAD networks through an integrative mapping strategy. *Nat Cell Biol*. 14:93–105. doi:10.1038/ncb2383.

Chung, J., F. Torta, K. Masai, L. Lucast, H. Czapla, L.B. Tanner, P. Narayanaswamy, M.R. Wenk, F. Nakatsu, and P.D. Camilli. 2015. PI4P/phosphatidylserine countertransport at ORP5- and ORP8-mediated ER–plasma membrane contacts. *Science*. 349:428–432. doi:10.1126/science.aab1370.

Clague, M.J., C. Heride, and S. Urbé. 2015. The demographics of the ubiquitin system. *Trends in Cell Biology*. 25:417–426. doi:10.1016/j.tcb.2015.03.002.

Cohen, M.M., E.A. Amiott, A.R. Day, G.P. Leboucher, E.N. Pryce, M.H. Glickman, J.M. McCaffery, J.M. Shaw, and A.M. Weissman. 2011a. Sequential requirements for the GTPase domain of the mitofusin Fzo1 and the ubiquitin ligase SCFMdm30 in mitochondrial outer membrane fusion. *J Cell Sci*. 124:1403–10. doi:10.1242/jcs.079293.

Cohen, M.M., E.A. Amiott, A.R. Day, G.P. Leboucher, E.N. Pryce, M.H. Glickman, J.M. McCaffery, J.M. Shaw, and A.M. Weissman. 2011b. Sequential requirements for the GTPase domain of the

mitofusin Fzo1 and the ubiquitin ligase SCFMdm30 in mitochondrial outer membrane fusion. *Journal of Cell Science*. 124:1403–1410. doi:10.1242/jcs.079293.

Cohen, M.M.J., G.P. Leboucher, N. Livnat-Levanon, M.H. Glickman, and A.M. Weissman. 2008. Ubiquitin-proteasome-dependent degradation of a mitofusin, a critical regulator of mitochondrial fusion. *Mol Biol Cell*. 19:2457–2464. doi:10.1091/mbc.E08-02-0227.

Cohen, Y., Y.A. Klug, L. Dimitrov, Z. Erez, S.G. Chuartzman, D. Elinger, I. Yofe, K. Soliman, J. Gärtner, S. Thoms, R. Schekman, Y. Elbaz-Alon, E. Zalckvar, and M. Schuldiner. 2014. Peroxisomes are juxtaposed to strategic sites on mitochondria. *Mol. BioSyst.* 10:1742–1748. doi:10.1039/C4MB00001C.

Cohen, Y., and M. Schuldiner. 2011. Advanced methods for high-throughput microscopy screening of genetically modified yeast libraries. *Methods Mol Biol*. 781:127–159. doi:10.1007/978-1-61779-276-2_8.

Coonrod, E.M., M.A. Karren, and J.M. Shaw. 2007. Ugo1p Is a Multipass Transmembrane Protein with a Single Carrier Domain Required for Mitochondrial Fusion. *Traffic*. 8:500–511. doi:10.1111/j.1600-0854.2007.00550.x.

Copeland, D.E., and A.J. Dalton. 1959. An Association between Mitochondria and the Endoplasmic Reticulum in Cells of the Pseudobranch Gland of a Teleost. *The Journal of Biophysical and Biochemical Cytology*. 5:393–396. doi:10.1083/jcb.5.3.393.

Cornell, R.B. 2016. Membrane lipid compositional sensing by the inducible amphipathic helix of CCT. *Biochimica et Biophysica Acta (BBA) - Molecular and Cell Biology of Lipids*. 1861:847–861. doi:10.1016/j.bbalip.2015.12.022.

Costello, J.L., I.G. Castro, C. Hacker, T.A. Schrader, J. Metz, D. Zeuschner, A.S. Azadi, L.F. Godinho, V. Costina, P. Findeisen, A. Manner, M. Islinger, and M. Schrader. 2017. ACBD5 and VAPB mediate membrane associations between peroxisomes and the ER. *Journal of Cell Biology*. 216:331–342. doi:10.1083/jcb.201607055.

Costello, J.L., and M. Schrader. 2018. Unloosing the Gordian knot of peroxisome formation. *Curr Opin Cell Biol*. 50:50–56. doi:10.1016/j.ceb.2018.02.002.

Covino, R., S. Ballweg, C. Stordeur, J.B. Michaelis, K. Puth, F. Wernig, A. Bahrami, A.M. Ernst, G. Hummer, and R. Ernst. 2016. A Eukaryotic Sensor for Membrane Lipid Saturation. *Mol Cell*. 63:49–59.

Csordás, G., D. Weaver, and G. Hajnóczky. 2018. Endoplasmic Reticulum-Mitochondrial Contactology: Structure and Signaling Functions. *Trends Cell Biol*. 28:523–540. doi:10.1016/j.tcb.2018.02.009.

Dammai, V., and S. Subramani. 2001. The Human Peroxisomal Targeting Signal Receptor, Pex5p, Is Translocated into the Peroxisomal Matrix and Recycled to the Cytosol. *Cell*. 105:187–196. doi:10.1016/S0092-8674(01)00310-5.

D'Angelo, G., M. Vicinanza, and M.A. De Matteis. 2008. Lipid-transfer proteins in biosynthetic pathways. *Current Opinion in Cell Biology*. 20:360–370. doi:10.1016/j.ceb.2008.03.013.

Das, A., S. Nag, A.B. Mason, and M.M. Barroso. 2016. Endosome–mitochondria interactions are modulated by iron release from transferrin. *Journal of Cell Biology*. 214:831–845. doi:10.1083/jcb.201602069.

Daste, F., C. Sauvanet, A. Bavdek, J. Baye, F. Pierre, R. Le Borgne, C. David, M. Rojo, P. Fuchs, and D. Tareste. 2018. The heptad repeat domain 1 of Mitofusin has membrane destabilization function in mitochondrial fusion. *EMBO reports*. 19:e43637. doi:10.15252/embr.201643637.

Daum, G. 1985. Lipids of mitochondria. *Biochimica et Biophysica Acta (BBA) - Reviews on Biomembranes*. 822:1–42. doi:10.1016/0304-4157(85)90002-4.

Daum, G., N.D. Lees, M. Bard, and R. Dickson. 1998. Biochemistry, cell biology and molecular biology of lipids of Saccharomyces cerevisiae. *Yeast*. 14:1471–1510. doi:10.1002/(SICI)1097-0061(199812)14:16<1471::AID-YEA353>3.0.CO;2-Y.

De Duve, C., and P. Baudhuin. 1966. Peroxisomes (microbodies and related particles). *Physiol Rev*. 46:323–357. doi:10.1152/physrev.1966.46.2.323.

De Vecchis, D., A. Brandner, M. Baaden, M.M. Cohen, and A. Taly. 2019. A Molecular Perspective on Mitochondrial Membrane Fusion: From the Key Players to Oligomerization and Tethering of Mitofusin. *The Journal of Membrane Biology*. 252:293–306. doi:10.1007/s00232-019-00089-y.

De Vecchis, D., L. Cavellini, M. Baaden, J. Hénin, M.M. Cohen, and A. Taly. 2017. A membrane-inserted structural model of the yeast mitofusin Fzo1. *Sci Rep*. 7:10217. doi:10.1038/s41598-017-10687-2.

Deguil, J., L. Pineau, E.C.R. Snyder, S. Dupont, L. Beney, A. Gil, G. Frapper, and T. Ferreira. 2011. Modulation of Lipid-Induced ER Stress by Fatty Acid Shape. *Traffic*. 12:349–362. doi:10.1111/j.1600-0854.2010.01150.x.

Delille, H.K., B. Agricola, S.C. Guimaraes, H. Borta, G.H. Lüers, M. Fransen, and M. Schrader. 2010. Pex11pβ-mediated growth and division of mammalian peroxisomes follows a maturation pathway. *Journal of Cell Science*. 123:2750–2762. doi:10.1242/jcs.062109.

Dennis, E.A., and E.P. Kennedy. 1972. Intracellular sites of lipid synthesis and the biogenesis of mitochondria. *Journal of Lipid Research*. 13:263–267. doi:10.1016/S0022-2275(20)39421-9.

Deutschbauer, A.M., R.M. Williams, A.M. Chu, and R.W. Davis. 2002. Parallel phenotypic analysis of sporulation and postgermination growth in Saccharomyces cerevisiae. *Proc Natl Acad Sci U S A*. 99:15530–15535. doi:10.1073/pnas.202604399.

Di Paolo, G., and P. De Camilli. 2006. Phosphoinositides in cell regulation and membrane dynamics. *Nature*. 443:651–657. doi:10.1038/nature05185.

Diakogiannaki, E., H.J. Welters, and N.G. Morgan. 2008. Differential regulation of the endoplasmic reticulum stress response in pancreatic β-cells exposed to long-chain saturated and monounsaturated fatty acids. *Journal of Endocrinology*. 197:553–563. doi:10.1677/JOE-08-0041.

Dickson, E.J., J.B. Jensen, O. Vivas, M. Kruse, A.E. Traynor-Kaplan, and B. Hille. 2016. Dynamic formation of ER–PM junctions presents a lipid phosphatase to regulate phosphoinositides. *Journal of Cell Biology*. 213:33–48. doi:10.1083/jcb.201508106.

Dimmer, K.S., S. Fritz, F. Fuchs, M. Messerschmitt, N. Weinbach, W. Neupert, and B. Westermann. 2002. Genetic Basis of Mitochondrial Function and Morphology inSaccharomyces cerevisiae. *MBoC*. 13:847–853. doi:10.1091/mbc.01-12-0588.

Distel, B., R. Erdmann, S.J. Gould, G. Blobel, D.I. Crane, J.M. Cregg, G. Dodt, Y. Fujiki, J.M. Goodman, W.W. Just, J.A. Kiel, W.H. Kunau, P.B. Lazarow, G.P. Mannaerts, H.W. Moser, T. Osumi, R.A. Rachubinski, A. Roscher, S. Subramani, H.F. Tabak, T. Tsukamoto, D. Valle, I. van der Klei, P.P. van Veldhoven, and M. Veenhuis. 1996. A unified nomenclature for peroxisome biogenesis factors. *Journal of Cell Biology*. 135:1–3. doi:10.1083/jcb.135.1.1.

Drin, G. 2014. Topological Regulation of Lipid Balance in Cells. *Annu. Rev. Biochem.* 83:51–77. doi:10.1146/annurev-biochem-060713-035307.

Drin, G., and B. Antonny. 2010. Amphipathic helices and membrane curvature. *FEBS Letters*. 584:1840–1847. doi:10.1016/j.febslet.2009.10.022.

Eckert, J.H., and R. Erdmann. 2003. Peroxisome biogenesis. *In* Reviews of Physiology, Biochemistry and Pharmacology. Springer, Berlin, Heidelberg. 75–121.

Eden, E.R., I.J. White, A. Tsapara, and C.E. Futter. 2010. Membrane contacts between endosomes and ER provide sites for PTP1B–epidermal growth factor receptor interaction. *Nat Cell Biol*. 12:267–272. doi:10.1038/ncb2026.

Eisenberg-Bord, M., N. Shai, M. Schuldiner, and M. Bohnert. 2016. A Tether Is a Tether Is a Tether: Tethering at Membrane Contact Sites. *Dev Cell*. 39:395–409. doi:10.1016/j.devcel.2016.10.022.

Elbaz-Alon, Y., M. Eisenberg-Bord, V. Shinder, S.B. Stiller, E. Shimoni, N. Wiedemann, T. Geiger, and M. Schuldiner. 2015. Lam6 Regulates the Extent of Contacts between Organelles. *Cell Reports*. 12:7–14. doi:10.1016/j.celrep.2015.06.022.

Elbaz-Alon, Y., E. Rosenfeld-Gur, V. Shinder, A.H. Futerman, T. Geiger, and M. Schuldiner. 2014. A Dynamic Interface between Vacuoles and Mitochondria in Yeast. *Developmental Cell*. 30:95–102. doi:10.1016/j.devcel.2014.06.007.

Elgass, K.D., E.A. Smith, M.A. LeGros, C.A. Larabell, and M.T. Ryan. 2015. Analysis of ER–mitochondria contacts using correlative fluorescence microscopy and soft X-ray tomography of mammalian cells. *Journal of Cell Science*. 128:2795–2804. doi:10.1242/jcs.169136.

Elgersma, Y., C.W. van Roermund, R.J. Wanders, and H.F. Tabak. 1995. Peroxisomal and mitochondrial carnitine acetyltransferases of Saccharomyces cerevisiae are encoded by a single gene. *EMBO J*. 14:3472–3479.

Enyenihi, A.H., and W.S. Saunders. 2003. Large-scale functional genomic analysis of sporulation and meiosis in Saccharomyces cerevisiae. *Genetics*. 163:47–54.

Ernst, R., S. Ballweg, and I. Levental. 2018. Cellular mechanisms of physicochemical membrane homeostasis. *Current Opinion in Cell Biology*. 53:44–51. doi:10.1016/j.ceb.2018.04.013.

Ernst, R., C.S. Ejsing, and B. Antonny. 2016. Homeoviscous Adaptation and the Regulation of Membrane Lipids. *Journal of Molecular Biology*. 428:4776–4791. doi:10.1016/j.jmb.2016.08.013.

Escobar-Henriques, M., B. Westermann, and T. Langer. 2006. Regulation of mitochondrial fusion by the F-box protein Mdm30 involves proteasome-independent turnover of Fzo1. *J Cell Biol*. 173:645–50. doi:10.1083/jcb.200512079.

Espeel, M., H. Mandel, F. Poggi, J.A. Smeitink, R.J. Wanders, I. Kerckaert, R.B. Schutgens, J.M. Saudubray, B.T. Poll-The, and F. Roels. 1995. Peroxisome mosaicism in the livers of peroxisomal deficiency patients. *Hepatology*. 22:497–504.

Eura, Y., N. Ishihara, S. Yokota, and K. Mihara. 2003. Two Mitofusin Proteins, Mammalian Homologues of FZO, with Distinct Functions Are Both Required for Mitochondrial Fusion. *The Journal of Biochemistry*. 134:333–344. doi:10.1093/jb/mvg150.

Eura, Y., H. Yanamoto, Y. Arai, T. Okuda, T. Miyata, and K. Kokame. 2012. Derlin-1 Deficiency Is Embryonic Lethal, Derlin-3 Deficiency Appears Normal, and Herp Deficiency Is Intolerant to Glucose Load and Ischemia in Mice. *PLOS ONE*. 7:e34298. doi:10.1371/journal.pone.0034298.

Færgeman, N.J., P.N. Black, X.D. Zhao, J. Knudsen, and C.C. DiRusso. 2001. The Acyl-CoA Synthetases Encoded within FAA1 andFAA4 in Saccharomyces cerevisiaeFunction as Components of the Fatty Acid Transport System Linking Import, Activation, and Intracellular Utilization *. *Journal of Biological Chemistry*. 276:37051–37059. doi:10.1074/jbc.M100884200.

Færgeman, N.J., C.C. DiRusso, A. Elberger, J. Knudsen, and P.N. Black. 1997. Disruption of the Saccharomyces cerevisiae Homologue to the Murine Fatty Acid Transport Protein Impairs Uptake and Growth on Long-chain Fatty Acids*. *Journal of Biological Chemistry*. 272:8531–8538. doi:10.1074/jbc.272.13.8531.

Fagarasanu, M., A. Fagarasanu, Y.Y.C. Tam, J.D. Aitchison, and R.A. Rachubinski. 2005. Inp1p is a peroxisomal membrane protein required for peroxisome inheritance in Saccharomyces cerevisiae. *Journal of Cell Biology*. 169:765–775. doi:10.1083/jcb.200503083.

Fairn, G.D., N.L. Schieber, N. Ariotti, S. Murphy, L. Kuerschner, R.I. Webb, S. Grinstein, and R.G. Parton. 2011. High-resolution mapping reveals topologically distinct cellular pools of phosphatidylserine. *Journal of Cell Biology*. 194:257–275. doi:10.1083/jcb.201012028.

Fakieh, M.H., P.J.M. Drake, J. Lacey, J.M. Munck, A.M. Motley, and E.H. Hettema. 2013. Intra-ER sorting of the peroxisomal membrane protein Pex3 relies on its luminal domain. *Biol Open*. 2:829–837. doi:10.1242/bio.20134788.

Fang, Y., J.C. Morrell, J.M. Jones, and S.J. Gould. 2004. PEX3 functions as a PEX19 docking factor in the import of class I peroxisomal membrane proteins. *J Cell Biol*. 164:863–875. doi:10.1083/jcb.200311131.

Farré, J.-C., S.S. Mahalingam, M. Proietto, and S. Subramani. 2019. Peroxisome biogenesis, membrane contact sites, and quality control. *EMBO Rep*. 20:e46864. doi:10.15252/embr.201846864.

Fasshauer, D., R.B. Sutton, A.T. Brunger, and R. Jahn. 1998. Conserved structural features of the synaptic fusion complex: SNARE proteins reclassified as Q- and R-SNAREs. *PNAS*. 95:15781–15786.

Fisk, H.A., and M.P. Yaffe. 1999. A role for ubiquitination in mitochondrial inheritance in Saccharomyces cerevisiae. *J Cell Biol*. 145:1199–208.

Foot, N., T. Henshall, and S. Kumar. 2017. Ubiquitination and the Regulation of Membrane Proteins. *Physiol Rev*. 97:253–281. doi:10.1152/physrev.00012.2016.

Foresti, O., A. Ruggiano, H.K. Hannibal-Bach, C.S. Ejsing, and P. Carvalho. 2013. Sterol homeostasis requires regulated degradation of squalene monooxygenase by the ubiquitin ligase Doa10/Teb4. *eLife*. 2:e00953. doi:10.7554/eLife.00953.

Francisco, L.M., P.T. Sage, and A.H. Sharpe. 2010. The PD-1 pathway in tolerance and autoimmunity. *Immunological Reviews*. 236:219–242. doi:10.1111/j.1600-065X.2010.00923.x.

Franco, A., R.N. Kitsis, J.A. Fleischer, E. Gavathiotis, O.S. Kornfeld, G. Gong, N. Biris, A. Benz, N. Qvit, S.K. Donnelly, Y. Chen, S. Mennerick, L. Hodgson, D. Mochly-Rosen, and G.W. Dorn. 2016. Correcting mitochondrial fusion by manipulating mitofusin conformations. *Nature*. 540:74–79. doi:10.1038/nature20156.

Fransen, M., M. Nordgren, B. Wang, and O. Apanasets. 2012. Role of peroxisomes in ROS/RNS-metabolism: Implications for human disease. *Biochimica et Biophysica Acta (BBA) - Molecular Basis of Disease*. 1822:1363–1373. doi:10.1016/j.bbadis.2011.12.001.

Friedman, J.R., L.L. Lackner, M. West, J.R. DiBenedetto, J. Nunnari, and G.K. Voeltz. 2011. ER Tubules Mark Sites of Mitochondrial Division. *Science*. 334:358–362. doi:10.1126/science.1207385.

Fritz, S., N. Weinbach, and B. Westermann. 2003. Mdm30 is an F-box protein required for maintenance of fusion-competent mitochondria in yeast. *Mol Biol Cell*. 14:2303–13. doi:10.1091/mbc.E02-12-0831.

Fujiki, Y., S. Fowler, H. Shio, A.L. Hubbard, and P.B. Lazarow. 1982. Polypeptide and phospholipid composition of the membrane of rat liver peroxisomes: comparison with endoplasmic reticulum and mitochondrial membranes. *Journal of Cell Biology*. 93:103–110. doi:10.1083/jcb.93.1.103.

Gabaldón, T., B. Snel, F. van Zimmeren, W. Hemrika, H. Tabak, and M.A. Huynen. 2006. Origin and evolution of the peroxisomal proteome. *Biol Direct*. 1:8. doi:10.1186/1745-6150-1-8.

Gabay-Maskit, S., L.D. Cruz-Zaragoza, N. Shai, M. Eisenstein, C. Bibi, N. Cohen, T. Hansen, E. Yifrach, N. Harpaz, R. Belostotsky, W. Schliebs, M. Schuldiner, R. Erdmann, and E. Zalckvar. 2020. A piggybacking mechanism enables peroxisomal localization of the glyoxylate cycle enzyme Mdh2 in yeast. *Journal of Cell Science*. 133. doi:10.1242/jcs.244376.

Gandre-Babbe, S., and A.M. van der Bliek. 2008. The Novel Tail-anchored Membrane Protein Mff Controls Mitochondrial and Peroxisomal Fission in Mammalian Cells. *MBoC*. 19:2402–2412. doi:10.1091/mbc.e07-12-1287.

Gasper, R., S. Meyer, K. Gotthardt, M. Sirajuddin, and A. Wittinghofer. 2009. It takes two to tango: regulation of G proteins by dimerization. *Nat Rev Mol Cell Biol*. 10:423–429. doi:10.1038/nrm2689.

Gatta, A.T., and T.P. Levine. 2017. Piecing Together the Patchwork of Contact Sites. *Trends Cell Biol*. 27:214–229. doi:10.1016/j.tcb.2016.08.010.

Gatta, A.T., L.H. Wong, Y.Y. Sere, D.M. Calderón-Noreña, S. Cockcroft, A.K. Menon, and T.P. Levine. 2015. A new family of StART domain proteins at membrane contact sites has a role in ER-PM sterol transport. *eLife*. 4:e07253. doi:10.7554/eLife.07253.

Gegg, M.E., J.M. Cooper, K.-Y. Chau, M. Rojo, A.H.V. Schapira, and J.-W. Taanman. 2010. Mitofusin 1 and mitofusin 2 are ubiquitinated in a PINK1/parkin-dependent manner upon induction of mitophagy. *Human Molecular Genetics*. 19:4861–4870. doi:10.1093/hmg/ddq419.

Ghaedi, K., M. Honsho, N. Shimozawa, Y. Suzuki, N. Kondo, and Y. Fujiki. 2000. PEX3 is the causal gene responsible for peroxisome membrane assembly-defective Zellweger syndrome of complementation group G. *Am J Hum Genet*. 67:976–981. doi:10.1086/303086.

Giaever, G., A.M. Chu, L. Ni, C. Connelly, L. Riles, S. Véronneau, S. Dow, A. Lucau-Danila, K. Anderson, B. André, A.P. Arkin, A. Astromoff, M. El-Bakkoury, R. Bangham, R. Benito, S. Brachat, S. Campanaro, M. Curtiss, K. Davis, A. Deutschbauer, K.-D. Entian, P. Flaherty, F. Foury, D.J. Garfinkel, M. Gerstein, D. Gotte, U. Güldener, J.H. Hegemann, S. Hempel, Z. Herman, D.F. Jaramillo, D.E. Kelly, S.L. Kelly, P. Kötter, D. LaBonte, D.C. Lamb, N. Lan, H. Liang, H. Liao, L. Liu, C. Luo, M. Lussier, R. Mao, P. Menard, S.L. Ooi, J.L. Revuelta, C.J. Roberts, M. Rose, P. Ross-Macdonald, B. Scherens, G. Schimmack, B. Shafer, D.D. Shoemaker, S. Sookhai-Mahadeo, R.K. Storms, J.N. Strathern, G. Valle, M. Voet, G. Volckaert, C. Wang, T.R. Ward, J. Wilhelmy, E.A. Winzeler, Y. Yang, G. Yen, E. Youngman, K. Yu, H. Bussey, J.D. Boeke, M. Snyder, P. Philippsen, R.W. Davis, and M. Johnston. 2002. Functional profiling of the Saccharomyces cerevisiae genome. *Nature*. 418:387–391. doi:10.1038/nature00935.

Giordano, F., Y. Saheki, O. Idevall-Hagren, S.F. Colombo, M. Pirruccello, I. Milosevic, E.O. Gracheva, S.N. Bagriantsev, N. Borgese, and P. De Camilli. 2013. PI(4,5)P2-Dependent and Ca2+-Regulated ER-PM Interactions Mediated by the Extended Synaptotagmins. *Cell*. 153:1494–1509. doi:10.1016/j.cell.2013.05.026.

Giorgi, C., M. Bonora, G. Sorrentino, S. Missiroli, F. Poletti, J.M. Suski, F. Galindo Ramirez, R. Rizzuto, F. Di Virgilio, E. Zito, P.P. Pandolfi, M.R. Wieckowski, F. Mammano, G. Del Sal, and P.

Pinton. 2015. p53 at the endoplasmic reticulum regulates apoptosis in a Ca2 -dependent manner. *PNAS*. 112:1779–1784.

Goldberg, A.A., S.D. Bourque, P. Kyryakov, C. Gregg, T. Boukh-Viner, A. Beach, M.T. Burstein, G. Machkalyan, V. Richard, S. Rampersad, D. Cyr, S. Milijevic, and V.I. Titorenko. 2009. Effect of calorie restriction on the metabolic history of chronologically aging yeast. *Experimental Gerontology*. 44:555–571. doi:10.1016/j.exger.2009.06.001.

Goldstein, J.L., R.A. DeBose-Boyd, and M.S. Brown. 2006. Protein Sensors for Membrane Sterols. *Cell*. 124:35–46. doi:10.1016/j.cell.2005.12.022.

Gomez-Suaga, P., S. Paillusson, R. Stoica, W. Noble, D.P. Hanger, and C.C.J. Miller. 2017. The ER-Mitochondria Tethering Complex VAPB-PTPIP51 Regulates Autophagy. *Current Biology*. 27:371–385. doi:10.1016/j.cub.2016.12.038.

González Montoro, A., K. Auffarth, C. Hönscher, M. Bohnert, T. Becker, B. Warscheid, F. Reggiori, M. van der Laan, F. Fröhlich, and C. Ungermann. 2018. Vps39 Interacts with Tom40 to Establish One of Two Functionally Distinct Vacuole-Mitochondria Contact Sites. *Developmental Cell*. 45:621-636.e7. doi:10.1016/j.devcel.2018.05.011.

Gould, S.J., G.A. Keller, N. Hosken, J. Wilkinson, and S. Subramani. 1989. A conserved tripeptide sorts proteins to peroxisomes. *Journal of Cell Biology*. 108:1657–1664. doi:10.1083/jcb.108.5.1657.

Gould, S.J., D. McCollum, A.P. Spong, J.A. Heyman, and S. Subramani. 1992. Development of the yeast Pichia pastoris as a model organism for a genetic and molecular analysis of peroxisome assembly. *Yeast*. 8:613–628. doi:10.1002/yea.320080805.

Gouveia, A.M.M., C. Reguenga, M.E.M. Oliveira, C. Sá-Miranda, and J.E. Azevedo. 2000. Characterization of Peroxisomal Pex5p from Rat Liver: Pex5p IN THE Pex5p-Pex14p MEMBRANE COMPLEX IS A TRANSMEMBRANE PROTEIN*. *Journal of Biological Chemistry*. 275:32444–32451. doi:10.1074/jbc.M004366200.

Gregg, C., P. Kyryakov, and V.I. Titorenko. 2009. Purification of mitochondria from yeast cells. *J Vis Exp*. doi:10.3791/1417.

Griffin, E.E., and D.C. Chan. 2006. Domain interactions within Fzo1 oligomers are essential for mitochondrial fusion. *J Biol Chem*. 281:16599–606. doi:10.1074/jbc.M601847200.

Griffin, E.E., J. Graumann, and D.C. Chan. 2005. The WD40 protein Caf4p is a component of the mitochondrial fission machinery and recruits Dnm1p to mitochondria. *Journal of Cell Biology*. 170:237–248. doi:10.1083/jcb.200503148.

Groll, M., L. Ditzel, J. Löwe, D. Stock, M. Bochtler, H.D. Bartunik, and R. Huber. 1997. Structure of 20S proteasome from yeast at 2.4Å resolution. *Nature*. 386:463–471. doi:10.1038/386463a0.

Groll, M., W. Heinemeyer, S. Jäger, T. Ullrich, M. Bochtler, D.H. Wolf, and R. Huber. 1999. The catalytic sites of 20S proteasomes and their role in subunit maturation: A mutational and crystallographic study. *PNAS*. 96:10976–10983.

Guo, Y., D. Li, S. Zhang, Y. Yang, J.-J. Liu, X. Wang, C. Liu, D.E. Milkie, R.P. Moore, U.S. Tulu, D.P. Kiehart, J. Hu, J. Lippincott-Schwartz, E. Betzig, and D. Li. 2018. Visualizing Intracellular Organelle and Cytoskeletal Interactions at Nanoscale Resolution on Millisecond Timescales. *Cell*. 175:1430-1442.e17. doi:10.1016/j.cell.2018.09.057.

Haglund, K., and I. Dikic. 2012. The role of ubiquitylation in receptor endocytosis and endosomal sorting. *Journal of Cell Science*. 125:265–275. doi:10.1242/jcs.091280.

Hailey, D.W., A.S. Rambold, P. Satpute-Krishnan, K. Mitra, R. Sougrat, P.K. Kim, and J. Lippincott-Schwartz. 2010. Mitochondria Supply Membranes for Autophagosome Biogenesis during Starvation. *Cell*. 141:656–667. doi:10.1016/j.cell.2010.04.009.

Halbleib, K., K. Pesek, R. Covino, H.F. Hofbauer, D. Wunnicke, I. Hänelt, G. Hummer, and R. Ernst. 2017. Activation of the Unfolded Protein Response by Lipid Bilayer Stress. *Molecular Cell*. 67:673-684.e8. doi:10.1016/j.molcel.2017.06.012.

Hamasaki, M., N. Furuta, A. Matsuda, A. Nezu, A. Yamamoto, N. Fujita, H. Oomori, T. Noda, T. Haraguchi, Y. Hiraoka, A. Amano, and T. Yoshimori. 2013. Autophagosomes form at ER–mitochondria contact sites. *Nature*. 495:389–393. doi:10.1038/nature11910.

Hammermeister, M., K. Schödel, and B. Westermann. 2010. Mdm36 Is a Mitochondrial Fission-promoting Protein in Saccharomyces cerevisiae. *MBoC*. 21:2443–2452. doi:10.1091/mbc.e10-02-0096.

Hao, H.-X., O. Khalimonchuk, M. Schraders, N. Dephoure, J.-P. Bayley, H. Kunst, P. Devilee, C.W.R.J. Cremers, J.D. Schiffman, B.G. Bentz, S.P. Gygi, D.R. Winge, H. Kremer, and J. Rutter. 2009. SDH5, a Gene Required for Flavination of Succinate Dehydrogenase, Is Mutated in Paraganglioma. *Science*. 325:1139–1142. doi:10.1126/science.1175689.

Harayama, T., and H. Riezman. 2018. Understanding the diversity of membrane lipid composition. *Nat Rev Mol Cell Biol*. 19:281–296. doi:10.1038/nrm.2017.138.

Hardeman, D., C. Versantvoort, J.M. van den Brink, and H. van den Bosch. 1990. Studies on peroxisomal membranes. *Biochim Biophys Acta*. 1027:149–154. doi:10.1016/0005-2736(90)90078-3.

Hariri, H., S. Rogers, R. Ugrankar, Y.L. Liu, J.R. Feathers, and W.M. Henne. 2018. Lipid droplet biogenesis is spatially coordinated at ER–vacuole contacts under nutritional stress. *EMBO reports*. 19:57–72. doi:10.15252/embr.201744815.

Harner, M., C. Körner, D. Walther, D. Mokranjac, J. Kaesmacher, U. Welsch, J. Griffith, M. Mann, F. Reggiori, and W. Neupert. 2011. The mitochondrial contact site complex, a determinant of mitochondrial architecture. *The EMBO Journal*. 30:4356–4370. doi:10.1038/emboj.2011.379.

Hartig, A., M.M. Simon, T. Schuster, J.R. Daugherty, H.S. Yoo, and T.G. Cooper. 1992. Differentially regulated malate synthase genes participate in carbon and nitrogen metabolism of S.cerevisiae. *Nucleic Acids Research*. 20:5677–5686. doi:10.1093/nar/20.21.5677.

Hartl, F.U., and M. Hayer-Hartl. 2009. Converging concepts of protein folding in vitro and in vivo. *Nat Struct Mol Biol*. 16:574–581. doi:10.1038/nsmb.1591.

Hein, C., J.-Y. Springael, C. Volland, R. Haguenauer-Tsapis, and B. André. 1995. NPI1, an essential yeast gene involved in induced degradation of Gap1 and Fur4 permeases, encodes the Rsp5 ubiquitin—protein ligase. *Molecular Microbiology*. 18:77–87. doi:10.1111/j.1365-2958.1995.mmi_18010077.x.

Helle, S.C.J., Q. Feng, M.J. Aebersold, L. Hirt, R.R. Grüter, A. Vahid, A. Sirianni, S. Mostowy, J.G. Snedeker, A. Šarić, T. Idema, T. Zambelli, and B. Kornmann. 2017. Mechanical force induces mitochondrial fission. *eLife*. 6:e30292. doi:10.7554/eLife.30292.

Henne, W.M., L. Zhu, Z. Balogi, C. Stefan, J.A. Pleiss, and S.D. Emr. 2015. Mdm1/Snx13 is a novel ER–endolysosomal interorganelle tethering protein. *Journal of Cell Biology*. 210:541–551. doi:10.1083/jcb.201503088.

Henry, S.A., S.D. Kohlwein, and G.M. Carman. 2012. Metabolism and Regulation of Glycerolipids in the Yeast Saccharomyces cerevisiae. *Genetics*. 190:317–349. doi:10.1534/genetics.111.130286.

Hermann, G.J., J.W. Thatcher, J.P. Mills, K.G. Hales, M.T. Fuller, J. Nunnari, and J.M. Shaw. 1998. Mitochondrial Fusion in Yeast Requires the Transmembrane GTPase Fzo1p. *J Cell Biol*. 143:359–73.

Hershko, A., and A. Ciechanover. 1998. The ubiquitin system. *Annu. Rev. Biochem.* 67:425–479. doi:10.1146/annurev.biochem.67.1.425.

Hettema, E.H., R. Erdmann, I. van der Klei, and M. Veenhuis. 2014. Evolving models for peroxisome biogenesis. *Curr Opin Cell Biol*. 29:25–30. doi:10.1016/j.ceb.2014.02.002.

Hettema, E.H., W. Girzalsky, M. van Den Berg, R. Erdmann, and B. Distel. 2000. Saccharomyces cerevisiae pex3p and pex19p are required for proper localization and stability of peroxisomal membrane proteins. *EMBO J*. 19:223–233. doi:10.1093/emboj/19.2.223.

Hettema, E.H., C.W. van Roermund, B. Distel, M. van den Berg, C. Vilela, C. Rodrigues-Pousada, R.J. Wanders, and H.F. Tabak. 1996. The ABC transporter proteins Pat1 and Pat2 are required for import of long-chain fatty acids into peroxisomes of Saccharomyces cerevisiae. *The EMBO Journal*. 15:3813–3822. doi:10.1002/j.1460-2075.1996.tb00755.x.

Hiller, M., A. Finger, M. Schweiger, and D. Wolf. 1996. ER Degradation of a Misfolded Luminal Protein by the Cytosolic Ubiquitin-Proteasome Pathway. *Science (New York, N.Y.)*. 273:1725–8. doi:10.1126/science.273.5282.1725.

Hiltunen, J.K., A.M. Mursula, H. Rottensteiner, R.K. Wierenga, A.J. Kastaniotis, and A. Gurvitz. 2003. The biochemistry of peroxisomal β-oxidation in the yeast *Saccharomyces cerevisiae*. *FEMS Microbiol Rev*. 27:35–64. doi:10.1016/S0168-6445(03)00017-2.

Hirabayashi, Y., S.-K. Kwon, H. Paek, W.M. Pernice, M.A. Paul, J. Lee, P. Erfani, A. Raczkowski, D.S. Petrey, L.A. Pon, and F. Polleux. 2017. ER-mitochondria tethering by PDZD8 regulates Ca2+ dynamics in mammalian neurons. *Science*. 358:623–630. doi:10.1126/science.aan6009.

Hitchcock, A.L., H. Krebber, S. Frietze, A. Lin, M. Latterich, and P.A. Silver. 2001. The Conserved Npl4 Protein Complex Mediates Proteasome-dependent Membrane-bound Transcription Factor Activation. *MBoC*. 12:3226–3241. doi:10.1091/mbc.12.10.3226.

Hoepfner, D., D. Schildknegt, I. Braakman, P. Philippsen, and H.F. Tabak. 2005. Contribution of the endoplasmic reticulum to peroxisome formation. *Cell*. 122:85–95. doi:10.1016/j.cell.2005.04.025.

Höhfeld, J., M. Veenhuis, and W.H. Kunau. 1991. PAS3, a Saccharomyces cerevisiae gene encoding a peroxisomal integral membrane protein essential for peroxisome biogenesis. *J Cell Biol*. 114:1167–1178. doi:10.1083/jcb.114.6.1167.

Holthuis, J.C.M., and T.P. Levine. 2005. Lipid traffic: floppy drives and a superhighway. *Nat Rev Mol Cell Biol*. 6:209–220. doi:10.1038/nrm1591.

Holthuis, J.C.M., and A.K. Menon. 2014. Lipid landscapes and pipelines in membrane homeostasis. *Nature*. 510:48–57. doi:10.1038/nature13474.

Honda, S., T. Aihara, M. Hontani, K. Okubo, and S. Hirose. 2005. Mutational analysis of action of mitochondrial fusion factor mitofusin-2. *Journal of Cell Science*. 118:3153–3161. doi:10.1242/jcs.02449.

Hönscher, C., M. Mari, K. Auffarth, M. Bohnert, J. Griffith, W. Geerts, M. van der Laan, M. Cabrera, F. Reggiori, and C. Ungermann. 2014. Cellular Metabolism Regulates Contact Sites between Vacuoles and Mitochondria. *Developmental Cell*. 30:86–94. doi:10.1016/j.devcel.2014.06.006.

Hoppe, T., K. Matuschewski, M. Rape, S. Schlenker, H.D. Ulrich, and S. Jentsch. 2000. Activation of a membrane-bound transcription factor by regulated ubiquitin/proteasome-dependent processing. *Cell*. 102:577–86.

Hoppins, S., J. Horner, C. Song, J.M. McCaffery, and J. Nunnari. 2009. Mitochondrial outer and inner membrane fusion requires a modified carrier protein. *J Cell Biol*. 184:569–81. doi:10.1083/jcb.200809099.

Hoppins, S., and J. Nunnari. 2009. The molecular mechanism of mitochondrial fusion. *Biochimica et Biophysica Acta (BBA) - Molecular Cell Research*. 1793:20–26. doi:10.1016/j.bbamcr.2008.07.005.

Hovsepian, J., V. Albanèse, M. Becuwe, V. Ivashov, D. Teis, and S. Léon. 2018. The yeast arrestin-related protein Bul1 is a novel actor of glucose-induced endocytosis. *MBoC*. 29:1012–1020. doi:10.1091/mbc.E17-07-0466.

Hovsepian, J., Q. Defenouillère, V. Albanèse, L. Váchová, C. Garcia, Z. Palková, and S. Léon. 2017. Multilevel regulation of an α-arrestin by glucose depletion controls hexose transporter endocytosis. *Journal of Cell Biology*. 216:1811–1831. doi:10.1083/jcb.201610094.

Hu, J., W.A. Prinz, and T.A. Rapoport. 2011. Weaving the Web of ER Tubules. *Cell*. 147:1226–1231. doi:10.1016/j.cell.2011.11.022.

Hua, R., D. Cheng, É. Coyaud, S. Freeman, E. Di Pietro, Y. Wang, A. Vissa, C.M. Yip, G.D. Fairn, N. Braverman, J.H. Brumell, W.S. Trimble, B. Raught, and P.K. Kim. 2017. VAPs and ACBD5 tether peroxisomes to the ER for peroxisome maintenance and lipid homeostasis. *Journal of Cell Biology*. 216:367–377. doi:10.1083/jcb.201608128.

Huang, P., C.A. Galloway, and Y. Yoon. 2011. Control of Mitochondrial Morphology Through Differential Interactions of Mitochondrial Fusion and Fission Proteins. *PLOS ONE*. 6:e20655. doi:10.1371/journal.pone.0020655.

Huang, X., X. Zhou, X. Hu, A.S. Joshi, X. Guo, Y. Zhu, Q. Chen, W.A. Prinz, and J. Hu. 2017. Sequences flanking the transmembrane segments facilitate mitochondrial localization and membrane fusion by mitofusin. *Proc Natl Acad Sci USA*. 114:E9863–E9872. doi:10.1073/pnas.1708782114.

Hulmes, G.E., J.D. Hutchinson, N. Dahan, J.M. Nuttall, E.G. Allwood, K.R. Ayscough, and E.H. Hettema. 2020. The Pex3–Inp1 complex tethers yeast peroxisomes to the plasma membrane. *Journal of Cell Biology*. 219:e201906021. doi:10.1083/jcb.201906021.

Hurley, J.H. 2010. The ESCRT complexes. *Critical Reviews in Biochemistry and Molecular Biology*. 45:463–487. doi:10.3109/10409238.2010.502516.

Infante, R.E., and A. Radhakrishnan. 2017. Continuous transport of a small fraction of plasma membrane cholesterol to endoplasmic reticulum regulates total cellular cholesterol. *eLife*. 6:e25466. doi:10.7554/eLife.25466.

Ingerman, E., E.M. Perkins, M. Marino, J.A. Mears, J.M. McCaffery, J.E. Hinshaw, and J. Nunnari. 2005. Dnm1 forms spirals that are structurally tailored to fit mitochondria. *Journal of Cell Biology*. 170:1021–1027. doi:10.1083/jcb.200506078.

Itoyama, A., M. Honsho, Y. Abe, A. Moser, Y. Yoshida, and Y. Fujiki. 2012. Docosahexaenoic acid mediates peroxisomal elongation, a prerequisite for peroxisome division. *Journal of Cell Science*. 125:589–602. doi:10.1242/jcs.087452.

Izawa, T., S.-H. Park, L. Zhao, F.U. Hartl, and W. Neupert. 2017. Cytosolic Protein Vms1 Links Ribosome Quality Control to Mitochondrial and Cellular Homeostasis. *Cell*. 171:890-903.e18. doi:10.1016/j.cell.2017.10.002.

Jahn, R., and R.H. Scheller. 2006. SNAREs — engines for membrane fusion. *Nat Rev Mol Cell Biol*. 7:631–643. doi:10.1038/nrm2002.

Janer, A., J. Prudent, V. Paupe, S. Fahiminiya, J. Majewski, N. Sgarioto, C. Des Rosiers, A. Forest, Z.-Y. Lin, A.-C. Gingras, G. Mitchell, H.M. McBride, and E.A. Shoubridge. 2016. SLC25A46 is required for mitochondrial lipid homeostasis and cristae maintenance and is responsible for Leigh syndrome. *EMBO Molecular Medicine*. 8:1019–1038. doi:10.15252/emmm.201506159.

Janmey, P.A., and P.K.J. Kinnunen. 2006. Biophysical properties of lipids and dynamic membranes. *Trends in Cell Biology*. 16:538–546. doi:10.1016/j.tcb.2006.08.009.

Jansen, R.L.M., and I.J. van der Klei. 2019. The peroxisome biogenesis factors Pex3 and Pex19: multitasking proteins with disputed functions. *FEBS Lett*. 593:457–474. doi:10.1002/1873-3468.13340.

Jazwinski, S.M. 2014. The retrograde response: a conserved compensatory reaction to damage from within and from without. *Prog Mol Biol Transl Sci*. 127:133–154. doi:10.1016/B978-0-12-394625-6.00005-2.

Jean Beltran, P.M., K.C. Cook, Y. Hashimoto, C. Galitzine, L.A. Murray, O. Vitek, and I.M. Cristea. 2018. Infection-Induced Peroxisome Biogenesis Is a Metabolic Strategy for Herpesvirus Replication. *Cell Host Microbe*. 24:526-541.e7. doi:10.1016/j.chom.2018.09.002.

Jean Demarquoy, F., and oise L. Borgne. 2015. Crosstalk between mitochondria and peroxisomes. *World Journal of Biological Chemistry*. 6:301–309. doi:10.4331/wjbc.v6.i4.301.

Jensen, J.P., P.W. Bates, M. Yang, R.D. Vierstra, and A.M. Weissman. 1995. Identification of a Family of Closely Related Human Ubiquitin Conjugating Enzymes (∗). *Journal of Biological Chemistry*. 270:30408–30414. doi:10.1074/jbc.270.51.30408.

Jeong, H., J. Park, Y. Jun, and C. Lee. 2017. Crystal structures of Mmm1 and Mdm12–Mmm1 reveal mechanistic insight into phospholipid trafficking at ER-mitochondria contact sites. *PNAS*. 114:E9502–E9511.

Ji, W.-K., R. Chakrabarti, X. Fan, L. Schoenfeld, S. Strack, and H.N. Higgs. 2017. Receptor-mediated Drp1 oligomerization on endoplasmic reticulum. *Journal of Cell Biology*. 216:4123–4139. doi:10.1083/jcb.201610057.

Jiang, Y., M.J. Vasconcelles, S. Wretzel, A. Light, C.E. Martin, and M.A. Goldberg. 2001. MGA2 Is Involved in the Low-Oxygen Response Element-Dependent Hypoxic Induction of Genes inSaccharomyces cerevisiae. *Molecular and Cellular Biology*. 21:6161–6169. doi:10.1128/MCB.21.18.6161-6169.2001.

Jimah, J.R., and J.E. Hinshaw. 2019. Structural Insights into the Mechanism of Dynamin Superfamily Proteins. *Trends in Cell Biology*. 29:257–273. doi:10.1016/j.tcb.2018.11.003.

John Peter, A.T., B. Herrmann, D. Antunes, D. Rapaport, K.S. Dimmer, and B. Kornmann. 2017. Vps13-Mcp1 interact at vacuole–mitochondria interfaces and bypass ER–mitochondria contact sites. *Journal of Cell Biology*. 216:3219–3229. doi:10.1083/jcb.201610055.

Jones, J.M., J.C. Morrell, and S.J. Gould. 2004. PEX19 is a predominantly cytosolic chaperone and import receptor for class 1 peroxisomal membrane proteins. *J Cell Biol*. 164:57–67. doi:10.1083/jcb.200304111.

Jonikas, M.C., S.R. Collins, V. Denic, E. Oh, E.M. Quan, V. Schmid, J. Weibezahn, B. Schwappach, P. Walter, J.S. Weissman, and M. Schuldiner. 2009. Comprehensive Characterization of Genes Required for Protein Folding in the Endoplasmic Reticulum. *Science*. 323:1693–1697. doi:10.1126/science.1167983.

Kane, L.A., M. Lazarou, A.I. Fogel, Y. Li, K. Yamano, S.A. Sarraf, S. Banerjee, and R.J. Youle. 2014. PINK1 phosphorylates ubiquitin to activate Parkin E3 ubiquitin ligase activity. *Journal of Cell Biology*. 205:143–153. doi:10.1083/jcb.201402104.

Kazlauskaite, A., C. Kondapalli, R. Gourlay, D.G. Campbell, M.S. Ritorto, K. Hofmann, D.R. Alessi, A. Knebel, M. Trost, and M.M.K. Muqit. 2014. Parkin is activated by PINK1-dependent phosphorylation of ubiquitin at Ser65. *Biochemical Journal*. 460:127–141. doi:10.1042/BJ20140334.

Kee, Y., N. Lyon, and J.M. Huibregtse. 2005. The Rsp5 ubiquitin ligase is coupled to and antagonized by the Ubp2 deubiquitinating enzyme. *Embo J*. 24:2414–24.

Kee, Y., W. Munoz, N. Lyon, and J.M. Huibregtse. 2006. The deubiquitinating enzyme Ubp2 modulates Rsp5-dependent Lys63-linked polyubiquitin conjugates in Saccharomyces cerevisiae. *J Biol Chem*. 281:36724–31.

Kelley, R., and T. Ideker. 2009. Genome-Wide Fitness and Expression Profiling Implicate Mga2 in Adaptation to Hydrogen Peroxide. *PLOS Genetics*. 5:e1000488. doi:10.1371/journal.pgen.1000488.

Kerssen, D., E. Hambruch, W. Klaas, H.W. Platta, B. de Kruijff, R. Erdmann, W.-H. Kunau, and W. Schliebs. 2006. Membrane Association of the Cycling Peroxisome Import Receptor Pex5p*. *Journal of Biological Chemistry*. 281:27003–27015. doi:10.1074/jbc.M509257200.

Kikkert, M., R. Doolman, M. Dai, R. Avner, G. Hassink, S. van Voorden, S. Thanedar, J. Roitelman, V. Chau, and E. Wiertz. 2004. Human HRD1 Is an E3 Ubiquitin Ligase Involved in Degradation of Proteins from the Endoplasmic Reticulum *. *Journal of Biological Chemistry*. 279:3525–3534. doi:10.1074/jbc.M307453200.

Kim, H.J., M.-Y. Jeong, U. Na, and D.R. Winge. 2012. Flavinylation and assembly of succinate dehydrogenase are dependent on the C-terminal tail of the flavoprotein subunit. *J Biol Chem*. 287:40670–40679. doi:10.1074/jbc.M112.405704.

Klecker, T., D. Scholz, J. Förtsch, and B. Westermann. 2013. The yeast cell cortical protein Num1 integrates mitochondrial dynamics into cellular architecture. *Journal of Cell Science*. 126:2924–2930. doi:10.1242/jcs.126045.

Klemm, R.W., C.S. Ejsing, M.A. Surma, H.-J. Kaiser, M.J. Gerl, J.L. Sampaio, Q. de Robillard, C. Ferguson, T.J. Proszynski, A. Shevchenko, and K. Simons. 2009. Segregation of sphingolipids and sterols during formation of secretory vesicles at the trans-Golgi network. *Journal of Cell Biology*. 185:601–612. doi:10.1083/jcb.200901145.

Klingenberg, M. 1972. Kinetic study of the tricarboxylate carrier in rat liver mitochondria. *Eur J Biochem*. 26:587–594. doi:10.1111/j.1432-1033.1972.tb01801.x.

Kloepper, T.H., C.N. Kienle, and D. Fasshauer. 2007. An Elaborate Classification of SNARE Proteins Sheds Light on the Conservation of the Eukaryotic Endomembrane System. *MBoC*. 18:3463–3471. doi:10.1091/mbc.e07-03-0193.

Knoblach, B., and R.A. Rachubinski. 2015. Transport and Retention Mechanisms Govern Lipid Droplet Inheritance in Saccharomyces cerevisiae. *Traffic*. 16:298–309. doi:10.1111/tra.12247.

Knoblach, B., X. Sun, N. Coquelle, A. Fagarasanu, R.L. Poirier, and R.A. Rachubinski. 2013. An ER-peroxisome tether exerts peroxisome population control in yeast. *The EMBO Journal*. 32:2439–2453. doi:10.1038/emboj.2013.170.

Knoops, K., S. Manivannan, M.N. Cepińska, A.M. Krikken, A.M. Kram, M. Veenhuis, and I.J. van der Klei. 2014. Preperoxisomal vesicles can form in the absence of Pex3. *Journal of Cell Biology*. 204:659–668. doi:10.1083/jcb.201310148.

Kobayashi, S., A. Tanaka, and Y. Fujiki. 2007. Fis1, DLP1, and Pex11p coordinately regulate peroxisome morphogenesis. *Experimental Cell Research*. 313:1675–1686. doi:10.1016/j.yexcr.2007.02.028.

Kobayashi, T., and A.K. Menon. 2018. Transbilayer lipid asymmetry. *Current Biology*. 28:R386–R391. doi:10.1016/j.cub.2018.01.007.

Koch, A., G. Schneider, G.H. Lüers, and M. Schrader. 2004. Peroxisome elongation and constriction but not fission can occur independently of dynamin-like protein 1. *Journal of Cell Science*. 117:3995–4006. doi:10.1242/jcs.01268.

Koch, A., M. Thiemann, M. Grabenbauer, Y. Yoon, M.A. McNiven, and M. Schrader. 2003. Dynamin-like Protein 1 Is Involved in Peroxisomal Fission*. *Journal of Biological Chemistry*. 278:8597–8605. doi:10.1074/jbc.M211761200.

Koch, A., Y. Yoon, N.A. Bonekamp, M.A. McNiven, and M. Schrader. 2005. A Role for Fis1 in Both Mitochondrial and Peroxisomal Fission in Mammalian Cells. *MBoC*. 16:5077–5086. doi:10.1091/mbc.e05-02-0159.

Koch, J., and C. Brocard. 2012. PEX11 proteins attract Mff and human Fis1 to coordinate peroxisomal fission. *Journal of Cell Science*. 125:3813–3826. doi:10.1242/jcs.102178.

Kolawa, N., M.J. Sweredoski, R.L.J. Graham, R. Oania, S. Hess, and R.J. Deshaies. 2013. Perturbations to the Ubiquitin Conjugate Proteome in Yeast Δubx Mutants Identify Ubx2 as a Regulator of Membrane Lipid Composition. *Mol Cell Proteomics*. 12:2791–2803. doi:10.1074/mcp.M113.030163.

Komander, D., and M. Rape. 2012. The Ubiquitin Code. *Annu. Rev. Biochem.* 81:203–229. doi:10.1146/annurev-biochem-060310-170328.

Kopec, K.O., V. Alva, and A.N. Lupas. 2010. Homology of SMP domains to the TULIP superfamily of lipid-binding proteins provides a structural basis for lipid exchange between ER and mitochondria. *Bioinformatics*. 26:1927–1931. doi:10.1093/bioinformatics/btq326.

Koppenol, W.H. 2001. The Haber-Weiss cycle – 70 years later. *Redox Report*. 6:229–234. doi:10.1179/135100001101536373.

Kornberg, H.L., and N.B. Madsen. 1958. The metabolism of C2 compounds in micro-organisms. 3. Synthesis of malate from acetate via the glyoxylate cycle*. *Biochemical Journal*. 68:549–557. doi:10.1042/bj0680549.

Kornmann, B., E. Currie, S.R. Collins, M. Schuldiner, J. Nunnari, J.S. Weissman, and P. Walter. 2009. An ER-Mitochondria Tethering Complex Revealed by a Synthetic Biology Screen. *Science*. 325:477–481. doi:10.1126/science.1175088.

Korobova, F., V. Ramabhadran, and H.N. Higgs. 2013. An Actin-Dependent Step in Mitochondrial Fission Mediated by the ER-Associated Formin INF2. *Science*. 339:464–467. doi:10.1126/science.1228360.

Koshiba, T., S.A. Detmer, J.T. Kaiser, H. Chen, J.M. McCaffery, and D.C. Chan. 2004. Structural Basis of Mitochondrial Tethering by Mitofusin Complexes. *Science*. 305:858–862. doi:10.1126/science.1099793.

Koyano, F., K. Okatsu, H. Kosako, Y. Tamura, E. Go, M. Kimura, Y. Kimura, H. Tsuchiya, H. Yoshihara, T. Hirokawa, T. Endo, E.A. Fon, J.-F. Trempe, Y. Saeki, K. Tanaka, and N. Matsuda. 2014. Ubiquitin is phosphorylated by PINK1 to activate parkin. *Nature*. 510:162–166. doi:10.1038/nature13392.

Koynova, R., and M. Caffrey. 1998. Phases and phase transitions of the phosphatidylcholines. *Biochimica et Biophysica Acta (BBA) - Reviews on Biomembranes*. 1376:91–145. doi:10.1016/S0304-4157(98)00006-9.

Kozlovsky, Y., L.V. Chernomordik, and M.M. Kozlov. 2002. Lipid Intermediates in Membrane Fusion: Formation, Structure, and Decay of Hemifusion Diaphragm. *Biophysical Journal*. 83:2634–2651. doi:10.1016/S0006-3495(02)75274-0.

Kraft, L.M., and L.L. Lackner. 2017. Mitochondria-driven assembly of a cortical anchor for mitochondria and dynein. *Journal of Cell Biology*. 216:3061–3071. doi:10.1083/jcb.201702022.

Krumpe, K., I. Frumkin, Y. Herzig, N. Rimon, C. Özbalci, B. Brügger, D. Rapaport, and M. Schuldiner. 2012. Ergosterol content specifies targeting of tail-anchored proteins to mitochondrial outer membranes. *MBoC*. 23:3927–3935. doi:10.1091/mbc.e11-12-0994.

Kumar, N., M. Leonzino, W. Hancock-Cerutti, F.A. Horenkamp, P. Li, J.A. Lees, H. Wheeler, K.M. Reinisch, and P. De Camilli. 2018. VPS13A and VPS13C are lipid transport proteins differentially localized at ER contact sites. *Journal of Cell Biology*. 217:3625–3639. doi:10.1083/jcb.201807019.

Kunau, W.-H. 2001. Peroxisomes: The extended shuttle to the peroxisome matrix. *Current Biology*. 11:R659–R662. doi:10.1016/S0960-9822(01)00386-4.

Kunau, W.-H., V. Dommes, and H. Schulz. 1995. β-Oxidation of fatty acids in mitochondria, peroxisomes, and bacteria: A century of continued progress. *Progress in Lipid Research*. 34:267–342. doi:10.1016/0163-7827(95)00011-9.

Kunze, M., F. Kragler, M. Binder, A. Hartig, and A. Gurvitz. 2002. Targeting of malate synthase 1 to the peroxisomes of *Saccharomyces cerevisiae* cells depends on growth on oleic acid medium: Subcellular localization of yeast Mls1p. *European Journal of Biochemistry*. 269:915–922. doi:10.1046/j.0014-2956.2001.02727.x.

Kwon, Y.T., and A. Ciechanover. 2017. The Ubiquitin Code in the Ubiquitin-Proteasome System and Autophagy. *Trends in Biochemical Sciences*. 42:873–886. doi:10.1016/j.tibs.2017.09.002.

Labrousse, A.M., M.D. Zappaterra, D.A. Rube, and A.M. van der Bliek. 1999. C. elegans Dynamin-Related Protein DRP-1 Controls Severing of the Mitochondrial Outer Membrane. *Molecular Cell*. 4:815–826. doi:10.1016/S1097-2765(00)80391-3.

Lackner, L.L. 2019. The Expanding and Unexpected Functions of Mitochondria Contact Sites. *Trends Cell Biol*. 29:580–590. doi:10.1016/j.tcb.2019.02.009.

Lackner, L.L., J.S. Horner, and J. Nunnari. 2009. Mechanistic Analysis of a Dynamin Effector. *Science*. 325:874–877. doi:10.1126/science.1176921.

Lackner, L.L., H. Ping, M. Graef, A. Murley, and J. Nunnari. 2013. Endoplasmic reticulum-associated mitochondria–cortex tether functions in the distribution and inheritance of mitochondria. *PNAS*. 110:E458–E467.

Lahiri, S., J.T. Chao, S. Tavassoli, A.K.O. Wong, V. Choudhary, B.P. Young, C.J.R. Loewen, and W.A. Prinz. 2014. A Conserved Endoplasmic Reticulum Membrane Protein Complex (EMC) Facilitates Phospholipid Transfer from the ER to Mitochondria. *PLOS Biology*. 12:e1001969. doi:10.1371/journal.pbio.1001969.

Lahiri, S., A. Toulmay, and W.A. Prinz. 2015. Membrane contact sites, gateways for lipid homeostasis. *Current Opinion in Cell Biology*. 33:82–87. doi:10.1016/j.ceb.2014.12.004.

Lam, S.K., N. Yoda, and R. Schekman. 2010. A vesicle carrier that mediates peroxisome protein traffic from the endoplasmic reticulum. *Proc Natl Acad Sci U S A*. 107:21523–21528. doi:10.1073/pnas.1013397107.

Lang, A.B., A.T.J. Peter, P. Walter, and B. Kornmann. 2015. ER–mitochondrial junctions can be bypassed by dominant mutations in the endosomal protein Vps13. *Journal of Cell Biology*. 210:883–890. doi:10.1083/jcb.201502105.

Lange, Y., and T.L. Steck. 2016. Active membrane cholesterol as a physiological effector. *Chemistry and Physics of Lipids*. 199:74–93. doi:10.1016/j.chemphyslip.2016.02.003.

Lazarow, P.B., and C. De Duve. 1976. A fatty acyl-CoA oxidizing system in rat liver peroxisomes; enhancement by clofibrate, a hypolipidemic drug. *PNAS*. 73:2043–2046.

Lazarow, P.B., and Y. Fujiki. 1985. Biogenesis of Peroxisomes. *Annu. Rev. Cell. Biol.* 1:489–530. doi:10.1146/annurev.cb.01.110185.002421.

Lee, I., and W. Hong. 2006. Diverse membrane-associated proteins contain a novel SMP domain. *The FASEB Journal*. 20:202–206. doi:10.1096/fj.05-4581hyp.

Lee, J.E., L.M. Westrate, H. Wu, C. Page, and G.K. Voeltz. 2016. Multiple dynamin family members collaborate to drive mitochondrial division. *Nature*. 540:139–143. doi:10.1038/nature20555.

Legesse-Miller, A., R.H. Massol, and T. Kirchhausen. 2003. Constriction and Dnm1p Recruitment Are Distinct Processes in Mitochondrial Fission. *MBoC*. 14:1953–1963. doi:10.1091/mbc.e02-10-0657.

Legros, F., A. Lombès, P. Frachon, and M. Rojo. 2002. Mitochondrial fusion in human cells is efficient, requires the inner membrane potential, and is mediated by mitofusins. *Mol Biol Cell*. 13:4343–4354. doi:10.1091/mbc.e02-06-0330.

Léon, S., Z. Erpapazoglou, and R. Haguenauer-Tsapis. 2008. Ear1p and Ssh4p Are New Adaptors of the Ubiquitin Ligase Rsp5p for Cargo Ubiquitylation and Sorting at Multivesicular Bodies. *MBoC*. 19:2379–2388. doi:10.1091/mbc.e08-01-0068.

Léon, S., and R. Haguenauer-Tsapis. 2009. Ubiquitin ligase adaptors: Regulators of ubiquitylation and endocytosis of plasma membrane proteins. *Experimental Cell Research*. 315:1574–1583. doi:10.1016/j.yexcr.2008.11.014.

Léon, S., L. Zhang, W.H. McDonald, J. Yates III, J.M. Cregg, and S. Subramani. 2006. Dynamics of the peroxisomal import cycle of PpPex20p: Ubiquitin-dependent localization and regulation. *Journal of Cell Biology*. 172:67–78. doi:10.1083/jcb.200508096.

Lev, S. 2010. Non-vesicular lipid transport by lipid-transfer proteins and beyond. *Nat Rev Mol Cell Biol*. 11:739–750. doi:10.1038/nrm2971.

Levental, K.R., J.H. Lorent, X. Lin, A.D. Skinkle, M.A. Surma, E.A. Stockenbojer, A.A. Gorfe, and I. Levental. 2016. Polyunsaturated Lipids Regulate Membrane Domain Stability by Tuning Membrane Order. *Biophysical Journal*. 110:1800–1810. doi:10.1016/j.bpj.2016.03.012.

Levental, K.R., E. Malmberg, J.L. Symons, Y.-Y. Fan, R.S. Chapkin, R. Ernst, and I. Levental. 2020. Lipidomic and biophysical homeostasis of mammalian membranes counteracts dietary lipid perturbations to maintain cellular fitness. *Nat Commun*. 11:1339. doi:10.1038/s41467-020-15203-1.

Levine, T. 2004. Short-range intracellular trafficking of small molecules across endoplasmic reticulum junctions. *Trends in Cell Biology*. 14:483–490. doi:10.1016/j.tcb.2004.07.017.

Lewis, S.C., L.F. Uchiyama, and J. Nunnari. 2016. ER-mitochondria contacts couple mtDNA synthesis with mitochondrial division in human cells. *Science*. 353. doi:10.1126/science.aaf5549.

Li, X., and S.J. Gould. 2003. The Dynamin-like GTPase DLP1 Is Essential for Peroxisome Division and Is Recruited to Peroxisomes in Part by PEX11*. *Journal of Biological Chemistry*. 278:17012–17020. doi:10.1074/jbc.M212031200.

Li, Y.-J., Y.-L. Cao, J.-X. Feng, Y. Qi, S. Meng, J.-F. Yang, Y.-T. Zhong, S. Kang, X. Chen, L. Lan, L. Luo, B. Yu, S. Chen, D.C. Chan, J. Hu, and S. Gao. 2019. Structural insights of human mitofusin-2 into mitochondrial fusion and CMT2A onset. *Nat Commun*. 10:4914. doi:10.1038/s41467-019-12912-0.

Lingard, M.J., S.K. Gidda, S. Bingham, S.J. Rothstein, R.T. Mullen, and R.N. Trelease. 2008. Arabidopsis PEROXIN11c-e, FISSION1b, and DYNAMIN-RELATED PROTEIN3A Cooperate in Cell Cycle–Associated Replication of Peroxisomes. *The Plant Cell*. 20:1567–1585. doi:10.1105/tpc.107.057679.

Lippincott-Schwartz, J., J.S. Bonifacino, L.C. Yuan, and R.D. Klausner. 1988. Degradation from the endoplasmic reticulum: Disposing of newly synthesized proteins. *Cell*. 54:209–220. doi:10.1016/0092-8674(88)90553-3.

Liu, Y., Y. Yagita, and Y. Fujiki. 2016. Assembly of Peroxisomal Membrane Proteins via the Direct Pex19p-Pex3p Pathway. *Traffic*. 17:433–455. doi:10.1111/tra.12376.

Liu, Z., Z. Gong, W.-X. Jiang, J. Yang, W.-K. Zhu, D.-C. Guo, W.-P. Zhang, M.-L. Liu, and C. Tang. 2015. Lys63-linked ubiquitin chain adopts multiple conformational states for specific target recognition. *eLife*. 4:e05767. doi:10.7554/eLife.05767.

Lockshon, D., L.E. Surface, E.O. Kerr, M. Kaeberlein, and B.K. Kennedy. 2007. The Sensitivity of Yeast Mutants to Oleic Acid Implicates the Peroxisome and Other Processes in Membrane Function. *Genetics*. 175:77–91. doi:10.1534/genetics.106.064428.

Loewen, C.J.R., M.L. Gaspar, S.A. Jesch, C. Delon, N.T. Ktistakis, S.A. Henry, and T.P. Levine. 2004. Phospholipid Metabolism Regulated by a Transcription Factor Sensing Phosphatidic Acid. *Science*. 304:1644–1647. doi:10.1126/science.1096083.

Macdonald, P.J., N. Stepanyants, N. Mehrotra, J.A. Mears, X. Qi, H. Sesaki, and R. Ramachandran. 2014. A dimeric equilibrium intermediate nucleates Drp1 reassembly on mitochondrial membranes for fission. *MBoC*. 25:1905–1915. doi:10.1091/mbc.e14-02-0728.

MacGurn, J.A. 2014. Garbage on, garbage off: new insights into plasma membrane protein quality control. *Current Opinion in Cell Biology*. 29:92–98. doi:10.1016/j.ceb.2014.05.001.

Madeo, F., E. Fröhlich, M. Ligr, M. Grey, S.J. Sigrist, D.H. Wolf, and K.-U. Fröhlich. 1999. Oxygen Stress: A Regulator of Apoptosis in Yeast. *Journal of Cell Biology*. 145:757–767. doi:10.1083/jcb.145.4.757.

Manford, A.G., C.J. Stefan, H.L. Yuan, J.A. MacGurn, and S.D. Emr. 2012. ER-to-Plasma Membrane Tethering Proteins Regulate Cell Signaling and ER Morphology. *Developmental Cell*. 23:1129–1140. doi:10.1016/j.devcel.2012.11.004.

Marsh, D. 2008. Protein modulation of lipids, and vice-versa, in membranes. *Biochimica et Biophysica Acta (BBA) - Biomembranes*. 1778:1545–1575. doi:10.1016/j.bbamem.2008.01.015.

Marshall, R.S., F. McLoughlin, and R.D. Vierstra. 2016. Autophagic Turnover of Inactive 26S Proteasomes in Yeast Is Directed by the Ubiquitin Receptor Cue5 and the Hsp42 Chaperone. *Cell Reports*. 16:1717–1732. doi:10.1016/j.celrep.2016.07.015.

Marshall, R.S., and R.D. Vierstra. 2019. Dynamic Regulation of the 26S Proteasome: From Synthesis to Degradation. *Front. Mol. Biosci.* 6. doi:10.3389/fmolb.2019.00040.

Marshall, W.F. 2016. Cell Geometry: How Cells Count and Measure Size. *Annu. Rev. Biophys.* 45:49–64. doi:10.1146/annurev-biophys-062215-010905.

Martens, S., and H.T. McMahon. 2008. Mechanisms of membrane fusion: disparate players and common principles. *Nat Rev Mol Cell Biol*. 9:543–556. doi:10.1038/nrm2417.

Mårtensson, C.U., C. Priesnitz, J. Song, L. Ellenrieder, K.N. Doan, F. Boos, A. Floerchinger, N. Zufall, S. Oeljeklaus, B. Warscheid, and T. Becker. 2019. Mitochondrial protein translocation-associated degradation. *Nature*. 569:679–683. doi:10.1038/s41586-019-1227-y.

Martin, C.E., C.-S. Oh, and Y. Jiang. 2007. Regulation of long chain unsaturated fatty acid synthesis in yeast. *Biochimica et Biophysica Acta (BBA) - Molecular and Cell Biology of Lipids*. 1771:271–285. doi:10.1016/j.bbalip.2006.06.010.

Marzioch, M., R. Erdmann, M. Veenhuis, and W. h. Kunau. 1994. PAS7 encodes a novel yeast member of the WD-40 protein family essential for import of 3-oxoacyl-CoA thiolase, a PTS2-containing protein, into peroxisomes. *The EMBO Journal*. 13:4908–4918. doi:10.1002/j.1460-2075.1994.tb06818.x.

Mast, F.D., T. Herricks, K.M. Strehler, L.R. Miller, R.A. Saleem, R.A. Rachubinski, and J.D. Aitchison. 2018. ESCRT-III is required for scissioning new peroxisomes from the endoplasmic reticulum. *Journal of Cell Biology*. 217:2087–2102. doi:10.1083/jcb.201706044.

Mast, F.D., A. Jamakhandi, R.A. Saleem, D.J. Dilworth, R.S. Rogers, R.A. Rachubinski, and J.D. Aitchison. 2016. Peroxins Pex30 and Pex29 Dynamically Associate with Reticulons to Regulate Peroxisome Biogenesis from the Endoplasmic Reticulum. *J Biol Chem*. 291:15408–15427. doi:10.1074/jbc.M116.728154.

Mast, F.D., R.A. Rachubinski, and J.B. Dacks. 2012. Emergent complexity in Myosin V-based organelle inheritance. *Mol Biol Evol*. 29:975–984. doi:10.1093/molbev/msr264.

Matsuda, N., S. Sato, K. Shiba, K. Okatsu, K. Saisho, C.A. Gautier, Y. Sou, S. Saiki, S. Kawajiri, F. Sato, M. Kimura, M. Komatsu, N. Hattori, and K. Tanaka. 2010. PINK1 stabilized by mitochondrial depolarization recruits Parkin to damaged mitochondria and activates latent Parkin for mitophagy. *Journal of Cell Biology*. 189:211–221. doi:10.1083/jcb.200910140.

Matsuzaki, T., and Y. Fujiki. 2008. The peroxisomal membrane protein import receptor Pex3p is directly transported to peroxisomes by a novel Pex19p- and Pex16p-dependent pathway. *J Cell Biol*. 183:1275–1286. doi:10.1083/jcb.200806062.

Mattie, S., J. Riemer, J.G. Wideman, and H.M. McBride. 2018. A new mitofusin topology places the redox-regulated C terminus in the mitochondrial intermembrane space. *Journal of Cell Biology*. 217:507–515. doi:10.1083/jcb.201611194.

Maulik, M., S. Mitra, A.M. Basmayor, B. Lu, B.E. Taylor, and A. Bult-Ito. 2019. Genetic Silencing of Fatty Acid Desaturases Modulates α-Synuclein Toxicity and Neuronal Loss in Parkinson-Like Models of C. elegans. *Front. Aging Neurosci.* 11. doi:10.3389/fnagi.2019.00207.

McLelland, G.-L., V. Soubannier, C.X. Chen, H.M. McBride, and E.A. Fon. 2014. Parkin and PINK1 function in a vesicular trafficking pathway regulating mitochondrial quality control. *The EMBO Journal*. 33:282–295. doi:10.1002/embj.201385902.

McNew, J.A., H. Sondermann, T. Lee, M. Stern, and F. Brandizzi. 2013. GTP-Dependent Membrane Fusion. *Annu. Rev. Cell Dev. Biol.* 29:529–550. doi:10.1146/annurev-cellbio-101512-122328.

Mears, J.A., L.L. Lackner, S. Fang, E. Ingerman, J. Nunnari, and J.E. Hinshaw. 2011. Conformational changes in Dnm1 support a contractile mechanism for mitochondrial fission. *Nat Struct Mol Biol*. 18:20–6. doi:10.1038/nsmb.1949.

van Meer, G., D.R. Voelker, and G.W. Feigenson. 2008. Membrane lipids: where they are and how they behave. *Nat Rev Mol Cell Biol*. 9:112–124. doi:10.1038/nrm2330.

Meeusen, S., J.M. McCaffery, and J. Nunnari. 2004. Mitochondrial fusion intermediates revealed in vitro. *Science*. 305:1747–1752. doi:10.1126/science.1100612.

Meisinger, C., N. Pfanner, and K.N. Truscott. 2006. Isolation of yeast mitochondria. *Methods Mol Biol*. 313:33–39. doi:10.1385/1-59259-958-3:033.

Meisinger, C., T. Sommer, and N. Pfanner. 2000. Purification of Saccharomcyes cerevisiae mitochondria devoid of microsomal and cytosolic contaminations. *Anal Biochem*. 287:339–342. doi:10.1006/abio.2000.4868.

Menendez-Benito, V., S.J. van Deventer, V. Jimenez-Garcia, M. Roy-Luzarraga, F. van Leeuwen, and J. Neefjes. 2013. Spatiotemporal analysis of organelle and macromolecular complex inheritance. *Proc Natl Acad Sci U S A*. 110:175–180. doi:10.1073/pnas.1207424110.

Mesmin, B., J. Bigay, J. Moser von Filseck, S. Lacas-Gervais, G. Drin, and B. Antonny. 2013. A Four-Step Cycle Driven by PI(4)P Hydrolysis Directs Sterol/PI(4)P Exchange by the ER-Golgi Tether OSBP. *Cell*. 155:830–843. doi:10.1016/j.cell.2013.09.056.

Mesmin, B., J. Bigay, J. Polidori, D. Jamecna, S. Lacas-Gervais, and B. Antonny. 2017. Sterol transfer, PI4P consumption, and control of membrane lipid order by endogenous OSBP. *The EMBO Journal*. 36:3156–3174. doi:10.15252/embj.201796687.

Mesquita, A., M. Weinberger, A. Silva, B. Sampaio-Marques, B. Almeida, C. Leão, V. Costa, F. Rodrigues, W.C. Burhans, and P. Ludovico. 2010. Caloric restriction or catalase inactivation extends yeast chronological lifespan by inducing H2O2 and superoxide dismutase activity. *PNAS*. 107:15123–15128.

Meyer, H.H., J.G. Shorter, J. Seemann, D. Pappin, and G. Warren. 2000. A complex of mammalian Ufd1 and Npl4 links the AAA-ATPase, p97, to ubiquitin and nuclear transport pathways. *The EMBO Journal*. 19:2181–2192. doi:10.1093/emboj/19.10.2181.

Minard, K.I., and L. McAlister-Henn. 1991. Isolation, nucleotide sequence analysis, and disruption of the MDH2 gene from Saccharomyces cerevisiae: evidence for three isozymes of yeast malate dehydrogenase. *Mol Cell Biol*. 11:370–380. doi:10.1128/mcb.11.1.370-380.1991.

Miyata, N., and Y. Fujiki. 2005. Shuttling Mechanism of Peroxisome Targeting Signal Type 1 Receptor Pex5: ATP-Independent Import and ATP-Dependent Export. *Molecular and Cellular Biology*. 25:10822–10832. doi:10.1128/MCB.25.24.10822-10832.2005.

Moltedo, O., P. Remondelli, and G. Amodio. 2019. The Mitochondria-Endoplasmic Reticulum Contacts and Their Critical Role in Aging and Age-Associated Diseases. *Front Cell Dev Biol*. 7:172. doi:10.3389/fcell.2019.00172.

Moore, A.S., and E.L. Holzbaur. 2018. Mitochondrial-cytoskeletal interactions: dynamic associations that facilitate network function and remodeling. *Current Opinion in Physiology*. 3:94–100. doi:10.1016/j.cophys.2018.03.003.

Moravcevic, K., C.L. Oxley, and M.A. Lemmon. 2012. Conditional Peripheral Membrane Proteins: Facing up to Limited Specificity. *Structure*. 20:15–27. doi:10.1016/j.str.2011.11.012.

Motley, A.M., and E.H. Hettema. 2007. Yeast peroxisomes multiply by growth and division. *Journal of Cell Biology*. 178:399–410. doi:10.1083/jcb.200702167.

Motley, A.M., J.M. Nuttall, and E.H. Hettema. 2012. Pex3-anchored Atg36 tags peroxisomes for degradation in Saccharomyces cerevisiae. *EMBO J*. 31:2852–2868. doi:10.1038/emboj.2012.151.

Motley, A.M., G.P. Ward, and E.H. Hettema. 2008. Dnm1p-dependent peroxisome fission requires Caf4p, Mdv1p and Fis1p. *Journal of Cell Science*. 121:1633–1640. doi:10.1242/jcs.026344.

Mozdy, A.D., J.M. McCaffery, and J.M. Shaw. 2000. Dnm1p Gtpase-Mediated Mitochondrial Fission Is a Multi-Step Process Requiring the Novel Integral Membrane Component Fis1p. *Journal of Cell Biology*. 151:367–380. doi:10.1083/jcb.151.2.367.

Munck, J.M., A.M. Motley, J.M. Nuttall, and E.H. Hettema. 2009. A dual function for Pex3p in peroxisome formation and inheritance. *J Cell Biol*. 187:463–471. doi:10.1083/jcb.200906161.

Murley, A., L.L. Lackner, C. Osman, M. West, G.K. Voeltz, P. Walter, and J. Nunnari. 2013. ER-associated mitochondrial division links the distribution of mitochondria and mitochondrial DNA in yeast. *eLife*. 2:e00422. doi:10.7554/eLife.00422.

Murley, A., R.D. Sarsam, A. Toulmay, J. Yamada, W.A. Prinz, and J. Nunnari. 2015. Ltc1 is an ER-localized sterol transporter and a component of ER–mitochondria and ER–vacuole contacts. *Journal of Cell Biology*. 209:539–548. doi:10.1083/jcb.201502033.

Murley, A., J. Yamada, B.J. Niles, A. Toulmay, W.A. Prinz, T. Powers, and J. Nunnari. 2017. Sterol transporters at membrane contact sites regulate TORC1 and TORC2 signaling. *Journal of Cell Biology*. 216:2679–2689. doi:10.1083/jcb.201610032.

Nadav, E., A. Shmueli, H. Barr, H. Gonen, A. Ciechanover, and Y. Reiss. 2003. A novel mammalian endoplasmic reticulum ubiquitin ligase homologous to the yeast Hrd1. *Biochemical and Biophysical Research Communications*. 303:91–97. doi:10.1016/S0006-291X(03)00279-1.

Nair, D.M., P.E. Purdue, and P.B. Lazarow. 2004. Pex7p translocates in and out of peroxisomes in Saccharomyces cerevisiae. *Journal of Cell Biology*. 167:599–604. doi:10.1083/jcb.200407119.

Narendra, D., A. Tanaka, D.-F. Suen, and R.J. Youle. 2008. Parkin is recruited selectively to impaired mitochondria and promotes their autophagy. *Journal of Cell Biology*. 183:795–803. doi:10.1083/jcb.200809125.

Neuber, O., E. Jarosch, C. Volkwein, J. Walter, and T. Sommer. 2005. Ubx2 links the Cdc48 complex to ER-associated protein degradation. *Nat Cell Biol*. 7:993–998. doi:10.1038/ncb1298.

Neupert, W. 2015. A Perspective on Transport of Proteins into Mitochondria: A Myriad of Open Questions. *Journal of Molecular Biology*. 427:1135–1158. doi:10.1016/j.jmb.2015.02.001.

Nguyen, T.N., B.S. Padman, and M. Lazarou. 2016. Deciphering the Molecular Signals of PINK1/Parkin Mitophagy. *Trends in Cell Biology*. 26:733–744. doi:10.1016/j.tcb.2016.05.008.

Nunnari, J., and P. Walter. 1996. Regulation of Organelle Biogenesis. *Cell*. 84:389–394. doi:10.1016/S0092-8674(00)81283-0.

O'Hara, L., G.-S. Han, S. Peak-Chew, N. Grimsey, G.M. Carman, and S. Siniossoglou. 2006. Control of Phospholipid Synthesis by Phosphorylation of the Yeast Lipin Pah1p/Smp2p Mg2+-dependent Phosphatidate Phosphatase*. *Journal of Biological Chemistry*. 281:34537–34548. doi:10.1074/jbc.M606654200.

Ohba, Y., T. Sakuragi, E. Kage-Nakadai, N.H. Tomioka, N. Kono, R. Imae, A. Inoue, J. Aoki, N. Ishihara, T. Inoue, S. Mitani, and H. Arai. 2013. Mitochondria-type GPAT is required for mitochondrial fusion. *The EMBO Journal*. 32:1265–1279. doi:10.1038/emboj.2013.77.

Ohtake, F., and H. Tsuchiya. 2017. The emerging complexity of ubiquitin architecture. *The Journal of Biochemistry*. 161:125–133. doi:10.1093/jb/mvw088.

Okamoto, K., N. Kondo-Okamoto, and Y. Ohsumi. 2009. Mitochondria-Anchored Receptor Atg32 Mediates Degradation of Mitochondria via Selective Autophagy. *Developmental Cell*. 17:87–97. doi:10.1016/j.devcel.2009.06.013.

Okatsu, K., M. Kimura, T. Oka, K. Tanaka, and N. Matsuda. 2015. Unconventional PINK1 localization to the outer membrane of depolarized mitochondria drives Parkin recruitment. *Journal of Cell Science*. 128:964–978. doi:10.1242/jcs.161000.

Okatsu, K., T. Oka, M. Iguchi, K. Imamura, H. Kosako, N. Tani, M. Kimura, E. Go, F. Koyano, M. Funayama, K. Shiba-Fukushima, S. Sato, H. Shimizu, Y. Fukunaga, H. Taniguchi, M. Komatsu, N. Hattori, K. Mihara, K. Tanaka, and N. Matsuda. 2012. PINK1 autophosphorylation upon membrane potential dissipation is essential for Parkin recruitment to damaged mitochondria. *Nat Commun*. 3:1016. doi:10.1038/ncomms2016.

Okatsu, K., M. Uno, F. Koyano, E. Go, M. Kimura, T. Oka, K. Tanaka, and N. Matsuda. 2013. A Dimeric PINK1-containing Complex on Depolarized Mitochondria Stimulates Parkin Recruitment*. *Journal of Biological Chemistry*. 288:36372–36384. doi:10.1074/jbc.M113.509653.

Okiyoneda, T., P.M. Apaja, and G.L. Lukacs. 2011. Protein quality control at the plasma membrane. *Current Opinion in Cell Biology*. 23:483–491. doi:10.1016/j.ceb.2011.04.012.

Okiyoneda, T., G. Veit, R. Sakai, M. Aki, T. Fujihara, M. Higashi, S. Susuki-Miyata, M. Miyata, N. Fukuda, A. Yoshida, H. Xu, P.M. Apaja, and G.L. Lukacs. 2018. Chaperone-Independent Peripheral Quality Control of CFTR by RFFL E3 Ligase. *Developmental Cell*. 44:694-708.e7. doi:10.1016/j.devcel.2018.02.001.

Okreglak, V., and P. Walter. 2014. The conserved AAA-ATPase Msp1 confers organelle specificity to tail-anchored proteins. *Proc Natl Acad Sci U S A*. 111:8019–8024. doi:10.1073/pnas.1405755111.

Opaliński, Ł., J.A.K.W. Kiel, C. Williams, M. Veenhuis, and I.J. van der Klei. 2011. Membrane curvature during peroxisome fission requires Pex11. *The EMBO Journal*. 30:5–16. doi:10.1038/emboj.2010.299.

Ordureau, A., S.A. Sarraf, D.M. Duda, J.-M. Heo, M.P. Jedrychowski, V.O. Sviderskiy, J.L. Olszewski, J.T. Koerber, T. Xie, S.A. Beausoleil, J.A. Wells, S.P. Gygi, B.A. Schulman, and J.W. Harper. 2014. Quantitative Proteomics Reveal a Feedforward Mechanism for Mitochondrial PARKIN Translocation and Ubiquitin Chain Synthesis. *Molecular Cell*. 56:360–375. doi:10.1016/j.molcel.2014.09.007.

Otera, H., N. Ishihara, and K. Mihara. 2013. New insights into the function and regulation of mitochondrial fission. *Biochimica et Biophysica Acta (BBA) - Molecular Cell Research*. 1833:1256–1268. doi:10.1016/j.bbamcr.2013.02.002.

Otera, H., C. Wang, M.M. Cleland, K. Setoguchi, S. Yokota, R.J. Youle, and K. Mihara. 2010. Mff is an essential factor for mitochondrial recruitment of Drp1 during mitochondrial fission in mammalian cells. *Journal of Cell Biology*. 191:1141–1158. doi:10.1083/jcb.201007152.

Otsuga, D., B.R. Keegan, E. Brisch, J.W. Thatcher, G.J. Hermann, W. Bleazard, and J.M. Shaw. 1998. The Dynamin-related GTPase, Dnm1p, Controls Mitochondrial Morphology in Yeast. *Journal of Cell Biology*. 143:333–349. doi:10.1083/jcb.143.2.333.

Palikaras, K., E. Lionaki, and N. Tavernarakis. 2018. Mechanisms of mitophagy in cellular homeostasis, physiology and pathology. *Nat Cell Biol*. 20:1013–1022. doi:10.1038/s41556-018-0176-2.

Palmer, C.S., L.D. Osellame, D. Laine, O.S. Koutsopoulos, A.E. Frazier, and M.T. Ryan. 2011. MiD49 and MiD51, new components of the mitochondrial fission machinery. *EMBO reports*. 12:565–573. doi:10.1038/embor.2011.54.

Pan, R., and J. Hu. 2011. The conserved fission complex on peroxisomes and mitochondria. *Plant Signaling & Behavior*. 6:870–872. doi:10.4161/psb.6.6.15241.

Park, J.-S., M.K. Thorsness, R. Policastro, L.L. McGoldrick, N.M. Hollingsworth, P.E. Thorsness, and A.M. Neiman. 2016. Yeast Vps13 promotes mitochondrial function and is localized at membrane contact sites. *MBoC*. 27:2435–2449. doi:10.1091/mbc.E16-02-0112.

Patton, E.E., A.R. Willems, and M. Tyers. 1998. Combinatorial control in ubiquitin-dependent proteolysis: don't Skp the F-box hypothesis. *Trends in Genetics*. 14:236–243. doi:10.1016/S0168-9525(98)01473-5.

Petriv, O.I., and R.A. Rachubinski. 2004. Lack of Peroxisomal Catalase Causes a Progeric Phenotype in Caenorhabditis elegans*. *Journal of Biological Chemistry*. 279:19996–20001. doi:10.1074/jbc.M400207200.

Petroski, M.D., and R.J. Deshaies. 2005. Function and regulation of cullin–RING ubiquitin ligases. *Nat Rev Mol Cell Biol*. 6:9–20. doi:10.1038/nrm1547.

Phillips, M.J., and G.K. Voeltz. 2016. Structure and function of ER membrane contact sites with other organelles. *Nat Rev Mol Cell Biol*. 17:69–82. doi:10.1038/nrm.2015.8.

Pichler, H., B. Gaigg, C. Hrastnik, G. Achleitner, S.D. Kohlwein, G. Zellnig, A. Perktold, and G. Daum. 2001. A subfraction of the yeast endoplasmic reticulum associates with the plasma membrane and has a high capacity to synthesize lipids. *European Journal of Biochemistry*. 268:2351–2361. doi:10.1046/j.1432-1327.2001.02116.x.

Ping, H.A., L.M. Kraft, W. Chen, A.E. Nilles, and L.L. Lackner. 2016. Num1 anchors mitochondria to the plasma membrane via two domains with different lipid binding specificities. *Journal of Cell Biology*. 213:513–524. doi:10.1083/jcb.201511021.

Piper, R.C., I. Dikic, and G.L. Lukacs. 2014. Ubiquitin-Dependent Sorting in Endocytosis. *Cold Spring Harb Perspect Biol*. 6:a016808. doi:10.1101/cshperspect.a016808.

Pitts, K. r., Y. Yoon, E. w. Krueger, and M. a. McNiven. 1999. The Dynamin-like Protein DLP1 Is Essential for Normal Distribution and Morphology of the Endoplasmic Reticulum and Mitochondria in Mammalian Cells. *MBoC*. 10:4403–4417. doi:10.1091/mbc.10.12.4403.

Platta, H.W., and R. Erdmann. 2007. The peroxisomal protein import machinery. *FEBS Letters*. 581:2811–2819. doi:10.1016/j.febslet.2007.04.001.

Platta, H.W., S. Grunau, K. Rosenkranz, W. Girzalsky, and R. Erdmann. 2005. Functional role of the AAA peroxins in dislocation of the cycling PTS1 receptor back to the cytosol. *Nat Cell Biol*. 7:817–822. doi:10.1038/ncb1281.

Poirier, Y., V.D. Antonenkov, T. Glumoff, and J.K. Hiltunen. 2006. Peroxisomal β-oxidation—A metabolic pathway with multiple functions. *Biochimica et Biophysica Acta (BBA) - Molecular Cell Research*. 1763:1413–1426. doi:10.1016/j.bbamcr.2006.08.034.

Pomorski, T., and A.K. Menon. 2006. Lipid flippases and their biological functions. *Cell. Mol. Life Sci.* 63:2908–2921. doi:10.1007/s00018-006-6167-7.

Praefcke, G.J.K., and H.T. McMahon. 2004. The dynamin superfamily: universal membrane tubulation and fission molecules? *Nat Rev Mol Cell Biol*. 5:133–147. doi:10.1038/nrm1313.

Prinz, W.A., A. Toulmay, and T. Balla. 2020. The functional universe of membrane contact sites. *Nat Rev Mol Cell Biol*. 21:7–24. doi:10.1038/s41580-019-0180-9.

Pronk, J.T., H.Y. Steensma, and J.P.V. Dijken. 1996. Pyruvate Metabolism in Saccharomyces cerevisiae. *Yeast*. 12:1607–1633. doi:10.1002/(SICI)1097-0061(199612)12:16<1607::AID-YEA70>3.0.CO;2-4.

Puca, L., and C. Brou. 2014. α-Arrestins – new players in Notch and GPCR signaling pathways in mammals. *Journal of Cell Science*. 127:1359–1367. doi:10.1242/jcs.142539.

Qi, Y., L. Yan, C. Yu, X. Guo, X. Zhou, X. Hu, X. Huang, Z. Rao, Z. Lou, and J. Hu. 2016. Structures of human mitofusin 1 provide insight into mitochondrial tethering. *J Cell Biol*. 215:621–629. doi:10.1083/jcb.201609019.

Raasi, S., and D.H. Wolf. 2007. Ubiquitin receptors and ERAD: A network of pathways to the proteasome. *Seminars in Cell & Developmental Biology*. 18:780–791. doi:10.1016/j.semcdb.2007.09.008.

Raiborg, C., E.M. Wenzel, N.M. Pedersen, H. Olsvik, K.O. Schink, S.W. Schultz, M. Vietri, V. Nisi, C. Bucci, A. Brech, T. Johansen, and H. Stenmark. 2015. Repeated ER–endosome contacts promote endosome translocation and neurite outgrowth. *Nature*. 520:234–238. doi:10.1038/nature14359.

Rapaport, D., M. Brunner, W. Neupert, and B. Westermann. 1998. Fzo1p is a mitochondrial outer membrane protein essential for the biogenesis of functional mitochondria in Saccharomyces cerevisiae. *J Biol Chem*. 273:20150–5.

Rape, M., T. Hoppe, I. Gorr, M. Kalocay, H. Richly, and S. Jentsch. 2001. Mobilization of processed, membrane-tethered SPT23 transcription factor by CDC48(UFD1/NPL4), a ubiquitin-selective chaperone. *Cell*. 107:667–77.

Rapoport, T.A. 2007. Protein translocation across the eukaryotic endoplasmic reticulum and bacterial plasma membranes. *Nature*. 450:663–669. doi:10.1038/nature06384.

Rasmussen, J.T., N.J. Faergeman, K. Kristiansen, and J. Knudsen. 1994. Acyl-CoA-binding protein (ACBP) can mediate intermembrane acyl-CoA transport and donate acyl-CoA for beta-oxidation and glycerolipid synthesis. *Biochem J*. 299 (Pt 1):165–170. doi:10.1042/bj2990165.

Rayapuram, N., and S. Subramani. 2006. The importomer—A peroxisomal membrane complex involved in protein translocation into the peroxisome matrix. *Biochimica et Biophysica Acta (BBA) - Molecular Cell Research*. 1763:1613–1619. doi:10.1016/j.bbamcr.2006.08.035.

Richter, V., C.S. Palmer, L.D. Osellame, A.P. Singh, K. Elgass, D.A. Stroud, H. Sesaki, M. Kvansakul, and M.T. Ryan. 2014. Structural and functional analysis of MiD51, a dynamin receptor required for mitochondrial fission. *Journal of Cell Biology*. 204:477–486. doi:10.1083/jcb.201311014.

del Río, L.A. 2011. Peroxisomes as a cellular source of reactive nitrogen species signal molecules. *Archives of Biochemistry and Biophysics*. 506:1–11. doi:10.1016/j.abb.2010.10.022.

del Río, L.A., and E. López-Huertas. 2016. ROS Generation in Peroxisomes and its Role in Cell Signaling. *Plant and Cell Physiology*. 57:1364–1376. doi:10.1093/pcp/pcw076.

Ristow, M., and S. Schmeisser. 2011. Extending life span by increasing oxidative stress. *Free Radical Biology and Medicine*. 51:327–336. doi:10.1016/j.freeradbiomed.2011.05.010.

Rizzuto, R., P. Pinton, W. Carrington, F.S. Fay, K.E. Fogarty, L.M. Lifshitz, R.A. Tuft, and T. Pozzan. 1998. Close Contacts with the Endoplasmic Reticulum as Determinants of Mitochondrial Ca2+ Responses. *Science*. 280:1763–1766. doi:10.1126/science.280.5370.1763.

Robinson, B.H., G.R. Williams, M.L. Halperin, and C.C. Leznoff. 1971. Factors affecting the kinetics and equilibrium of exchange reactions of the citrate-transporting system of rat liver mitochondria. *J Biol Chem*. 246:5280–5286.

van Roermund, C. w., Y. Elgersma, N. Singh, R. j. Wanders, and H. f. Tabak. 1995. The membrane of peroxisomes in Saccharomyces cerevisiae is impermeable to NAD(H) and acetyl-CoA under in vivo conditions. *The EMBO Journal*. 14:3480–3486. doi:10.1002/j.1460-2075.1995.tb07354.x.

van Roermund, C.W.T., E.H. Hettema, M. van den Berg, H.F. Tabak, and R.J.A. Wanders. 1999. Molecular characterization of carnitine-dependent transport of acetyl-CoA from peroxisomes to mitochondria in Saccharomyces cerevisiae and identification of a plasma membrane carnitine transporter, Agp2p. *The EMBO Journal*. 18:5843–5852. doi:10.1093/emboj/18.21.5843.

van Roermund, C.W.T., H.R. Waterham, L. Ijlst, and R.J.A. Wanders. 2003. Fatty acid metabolism in Saccharomyces cerevisiae. *Cellular and Molecular Life Sciences (CMLS)*. 60:1838–1851. doi:10.1007/s00018-003-3076-x.

Rojo, M., F. Legros, D. Chateau, and A. Lombès. 2002. Membrane topology and mitochondrial targeting of mitofusins, ubiquitous mammalian homologs of the transmembrane GTPase Fzo. *J Cell Sci*. 115:1663–1674.

Rose, C.M., M. Isasa, A. Ordureau, M.A. Prado, S.A. Beausoleil, M.P. Jedrychowski, D.J. Finley, J.W. Harper, and S.P. Gygi. 2016. Highly Multiplexed Quantitative Mass Spectrometry Analysis of Ubiquitylomes. *Cell Systems*. 3:395-403.e4. doi:10.1016/j.cels.2016.08.009.

Rosendal, J., P. Ertbjerg, and J. Knudsen. 1993. Characterization of ligand binding to acyl-CoA-binding protein. *Biochem J*. 290 (Pt 2):321–326. doi:10.1042/bj2900321.

Rosenkranz, K., I. Birschmann, S. Grunau, W. Girzalsky, W.-H. Kunau, and R. Erdmann. 2006. Functional association of the AAA complex and the peroxisomal importomer. *The FEBS Journal*. 273:3804–3815. doi:10.1111/j.1742-4658.2006.05388.x.

Roux, A., K. Uyhazi, A. Frost, and P. De Camilli. 2006. GTP-dependent twisting of dynamin implicates constriction and tension in membrane fission. *Nature*. 441:528–531. doi:10.1038/nature04718.

Rowland, A.A., and G.K. Voeltz. 2012. Endoplasmic reticulum–mitochondria contacts: function of the junction. *Nat Rev Mol Cell Biol*. 13:607–615. doi:10.1038/nrm3440.

Ruggiano, A., O. Foresti, and P. Carvalho. 2014. ER-associated degradation: Protein quality control and beyond. *Journal of Cell Biology*. 204:869–879. doi:10.1083/jcb.201312042.

Rusiñol, A.E., Z. Cui, M.H. Chen, and J.E. Vance. 1994. A unique mitochondria-associated membrane fraction from rat liver has a high capacity for lipid synthesis and contains pre-Golgi secretory proteins including nascent lipoproteins. *Journal of Biological Chemistry*. 269:27494–27502. doi:10.1016/S0021-9258(18)47012-3.

Russell, S.J., K.A. Steger, and S.A. Johnston. 1999. Subcellular Localization, Stoichiometry, and Protein Levels of 26 S Proteasome Subunits in Yeast *. *Journal of Biological Chemistry*. 274:21943–21952. doi:10.1074/jbc.274.31.21943.

Sacksteder, K.A., J.M. Jones, S.T. South, X. Li, Y. Liu, and S.J. Gould. 2000. PEX19 binds multiple peroxisomal membrane proteins, is predominantly cytoplasmic, and is required for peroxisome membrane synthesis. *J Cell Biol*. 148:931–944. doi:10.1083/jcb.148.5.931.

Sano, R., I. Annunziata, A. Patterson, S. Moshiach, E. Gomero, J. Opferman, M. Forte, and A. d'Azzo. 2009. GM1-Ganglioside Accumulation at the Mitochondria-Associated ER Membranes Links ER Stress to Ca2+-Dependent Mitochondrial Apoptosis. *Molecular Cell*. 36:500–511. doi:10.1016/j.molcel.2009.10.021.

Santel, A., and M.T. Fuller. 2001. Control of mitochondrial morphology by a human mitofusin. *J Cell Sci*. 114:867–874.

Sardana, R., L. Zhu, and S.D. Emr. 2018. Rsp5 Ubiquitin ligase–mediated quality control system clears membrane proteins mistargeted to the vacuole membrane. *Journal of Cell Biology*. 218:234–250. doi:10.1083/jcb.201806094.

Sarraf, S.A., M. Raman, V. Guarani-Pereira, M.E. Sowa, E.L. Huttlin, S.P. Gygi, and J.W. Harper. 2013. Landscape of the PARKIN-dependent ubiquitylome in response to mitochondrial depolarization. *Nature*. 496:372–376. doi:10.1038/nature12043.

Sato, Y., H. Shibata, T. Nakatsu, H. Nakano, Y. Kashiwayama, T. Imanaka, and H. Kato. 2010. Structural basis for docking of peroxisomal membrane protein carrier Pex19p onto its receptor Pex3p. *EMBO J*. 29:4083–4093. doi:10.1038/emboj.2010.293.

Schjerling, C.K., R. Hummel, J.K. Hansen, C. Borsting, J.M. Mikkelsen, K. Kristiansen, and J. Knudsen. 1996. Disruption of the gene encoding the acyl-CoA-binding protein (ACB1) perturbs acyl-CoA metabolism in Saccharomyces cerevisiae. *J Biol Chem*. 271:22514–22521. doi:10.1074/jbc.271.37.22514.

Schlüter, A., S. Fourcade, R. Ripp, J.L. Mandel, O. Poch, and A. Pujol. 2006. The evolutionary origin of peroxisomes: an ER-peroxisome connection. *Mol Biol Evol*. 23:838–845. doi:10.1093/molbev/msj103.

Schmidt, F., D. Dietrich, R. Eylenstein, Y. Groemping, T. Stehle, and G. Dodt. 2012. The role of conserved PEX3 regions in PEX19-binding and peroxisome biogenesis. *Traffic*. 13:1244–1260. doi:10.1111/j.1600-0854.2012.01380.x.

Schmidt, F., N. Treiber, G. Zocher, S. Bjelic, M.O. Steinmetz, H. Kalbacher, T. Stehle, and G. Dodt. 2010. Insights into peroxisome function from the structure of PEX3 in complex with a soluble fragment of PEX19. *J Biol Chem*. 285:25410–25417. doi:10.1074/jbc.M110.138503.

Schrader, M., N.A. Bonekamp, and M. Islinger. 2012. Fission and proliferation of peroxisomes. *Biochimica et Biophysica Acta (BBA) - Molecular Basis of Disease*. 1822:1343–1357. doi:10.1016/j.bbadis.2011.12.014.

Schrader, M., J. Costello, L.F. Godinho, and M. Islinger. 2015. Peroxisome-mitochondria interplay and disease. *Journal of Inherited Metabolic Disease*. 38:681–702. doi:10.1007/s10545-015-9819-7.

Schrader, M., J.L. Costello, L.F. Godinho, A.S. Azadi, and M. Islinger. 2016. Proliferation and fission of peroxisomes — An update. *Biochimica et Biophysica Acta (BBA) - Molecular Cell Research*. 1863:971–983. doi:10.1016/j.bbamcr.2015.09.024.

Schrader, M., and H.D. Fahimi. 2006a. Growth and Division of Peroxisomes. *In* International Review of Cytology. K.W. Jeon, editor. Academic Press. 237–290.

Schrader, M., and H.D. Fahimi. 2006b. Peroxisomes and oxidative stress. *Biochimica et Biophysica Acta (BBA) - Molecular Cell Research*. 1763:1755–1766. doi:10.1016/j.bbamcr.2006.09.006.

Schrader, M., and Y. Yoon. 2007. Mitochondria and peroxisomes: Are the 'Big Brother' and the 'Little Sister' closer than assumed? *BioEssays*. 29:1105–1114. doi:10.1002/bies.20659.

Schrepfer, E., and L. Scorrano. 2016. Mitofusins, from Mitochondria to Metabolism. *Molecular Cell*. 61:683–694. doi:10.1016/j.molcel.2016.02.022.

Schuberth, C., and A. Buchberger. 2008. UBX domain proteins: major regulators of the AAA ATPase Cdc48/p97. *Cell Mol Life Sci*. 65:2360–71. doi:10.1007/s00018-008-8072-8.

Sesaki, H., and R.E. Jensen. 2001. UGO1 Encodes an Outer Membrane Protein Required for Mitochondrial Fusion. *Journal of Cell Biology*. 152:1123–1134. doi:10.1083/jcb.152.6.1123.

Sesaki, H., and R.E. Jensen. 2004. Ugo1p Links the Fzo1p and Mgm1p GTPases for Mitochondrial Fusion *. *Journal of Biological Chemistry*. 279:28298–28303. doi:10.1074/jbc.M401363200.

Sezgin, E., I. Levental, S. Mayor, and C. Eggeling. 2017. The mystery of membrane organization: composition, regulation and roles of lipid rafts. *Nat Rev Mol Cell Biol*. 18:361–374. doi:10.1038/nrm.2017.16.

Shai, N., M. Schuldiner, and E. Zalckvar. 2016. No peroxisome is an island - Peroxisome contact sites. *Biochim Biophys Acta*. 1863:1061–1069. doi:10.1016/j.bbamcr.2015.09.016.

Shai, N., E. Yifrach, C.W.T. van Roermund, N. Cohen, C. Bibi, L. IJlst, L. Cavellini, J. Meurisse, R. Schuster, L. Zada, M.C. Mari, F.M. Reggiori, A.L. Hughes, M. Escobar-Henriques, M.M. Cohen, H.R. Waterham, R.J.A. Wanders, M. Schuldiner, and E. Zalckvar. 2018. Systematic mapping of contact sites reveals tethers and a function for the peroxisome-mitochondria contact. *Nat Commun*. 9:1761. doi:10.1038/s41467-018-03957-8.

Sharpe, H.J., T.J. Stevens, and S. Munro. 2010. A Comprehensive Comparison of Transmembrane Domains Reveals Organelle-Specific Properties. *Cell*. 142:158–169. doi:10.1016/j.cell.2010.05.037.

Shcherbik, N., and D.S. Haines. 2007. Cdc48p(Npl4p/Ufd1p) binds and segregates membrane-anchored/tethered complexes via a polyubiquitin signal present on the anchors. *Mol Cell*. 25:385–97.

Shcherbik, N., Y. Kee, N. Lyon, J.M. Huibregtse, and D.S. Haines. 2004. A Single PXY Motif Located within the Carboxyl Terminus of Spt23p and Mga2p Mediates a Physical and Functional Interaction with Ubiquitin Ligase Rsp5p *. *Journal of Biological Chemistry*. 279:53892–53898. doi:10.1074/jbc.M410325200.

Sheftel, A.D., A.-S. Zhang, C. Brown, O.S. Shirihai, and P. Ponka. 2007. Direct interorganellar transfer of iron from endosome to mitochondrion. *Blood*. 110:125–132. doi:10.1182/blood-2007-01-068148.

Shenoy, S.K., and R.J. Lefkowitz. 2011. β-arrestin-mediated receptor trafficking and signal transduction. *Trends in Pharmacological Sciences*. 32:521–533. doi:10.1016/j.tips.2011.05.002.

Sherman, F. 2002. Getting started with yeast. *Methods Enzymol*. 350:3–41. doi:10.1016/s0076-6879(02)50954-x.

Shevchenko, A., and K. Simons. 2010. Lipidomics: coming to grips with lipid diversity. *Nat Rev Mol Cell Biol*. 11:593–598. doi:10.1038/nrm2934.

Shimozawa, N., Y. Suzuki, Z. Zhang, A. Imamura, K. Ghaedi, Y. Fujiki, and N. Kondo. 2000. Identification of PEX3 as the gene mutated in a Zellweger syndrome patient lacking peroxisomal remnant structures. *Hum Mol Genet*. 9:1995–1999. doi:10.1093/hmg/9.13.1995.

Simons, M., and G. Raposo. 2009. Exosomes – vesicular carriers for intercellular communication. *Current Opinion in Cell Biology*. 21:575–581. doi:10.1016/j.ceb.2009.03.007.

Singh, I. 1997. Biochemistry of peroxisomes in health and disease. *Mol Cell Biochem*. 167:1–29. doi:10.1023/A:1006883229684.

Skowyra, D., K.L. Craig, M. Tyers, S.J. Elledge, and J.W. Harper. 1997. F-Box Proteins Are Receptors that Recruit Phosphorylated Substrates to the SCF Ubiquitin-Ligase Complex. *Cell*. 91:209–219. doi:10.1016/S0092-8674(00)80403-1.

Smirnova, E., L. Griparic, D.-L. Shurland, and A.M. van der Bliek. 2001. Dynamin-related Protein Drp1 Is Required for Mitochondrial Division in Mammalian Cells. *MBoC*. 12:2245–2256. doi:10.1091/mbc.12.8.2245.

Smith, J.J., and J.D. Aitchison. 2013. Peroxisomes take shape. *Nat Rev Mol Cell Biol*. 14:803–817. doi:10.1038/nrm3700.

Söllner, T., M.K. Bennett, S.W. Whiteheart, R.H. Scheller, and J.E. Rothman. 1993. A protein assembly-disassembly pathway in vitro that may correspond to sequential steps of synaptic vesicle docking, activation, and fusion. *Cell*. 75:409–418. doi:10.1016/0092-8674(93)90376-2.

Sommer, T., and S. Jentsch. 1993. A protein translocation defect linked to ubiquitin conjugation at the endoplasmic reticulum. *Nature*. 365:176–179. doi:10.1038/365176a0.

Song, Z., H. Chen, M. Fiket, C. Alexander, and D.C. Chan. 2007. OPA1 processing controls mitochondrial fusion and is regulated by mRNA splicing, membrane potential, and Yme1L. *J Cell Biol*. 178:749–755. doi:10.1083/jcb.200704110.

Soubannier, V., G.-L. McLelland, R. Zunino, E. Braschi, P. Rippstein, E.A. Fon, and H.M. McBride. 2012. A Vesicular Transport Pathway Shuttles Cargo from Mitochondria to Lysosomes. *Current Biology*. 22:135–141. doi:10.1016/j.cub.2011.11.057.

Spence, J., S. Sadis, A.L. Haas, and D. Finley. 1995. A ubiquitin mutant with specific defects in DNA repair and multiubiquitination. *Molecular and Cellular Biology*. 15:1265–1273. doi:10.1128/MCB.15.3.1265.

Spratt, D.E., R. Julio Martinez-Torres, Y.J. Noh, P. Mercier, N. Manczyk, K.R. Barber, J.D. Aguirre, L. Burchell, A. Purkiss, H. Walden, and G.S. Shaw. 2013. A molecular explanation for the recessive nature of parkin -linked Parkinson's disease. *Nat Commun*. 4:1983. doi:10.1038/ncomms2983.

Stanley, W.A., F.V. Filipp, P. Kursula, N. Schüller, R. Erdmann, W. Schliebs, M. Sattler, and M. Wilmanns. 2006. Recognition of a Functional Peroxisome Type 1 Target by the Dynamic Import Receptor Pex5p. *Molecular Cell*. 24:653–663. doi:10.1016/j.molcel.2006.10.024.

Stefan, C.J., A.G. Manford, D. Baird, J. Yamada-Hanff, Y. Mao, and S.D. Emr. 2011. Osh Proteins Regulate Phosphoinositide Metabolism at ER-Plasma Membrane Contact Sites. *Cell*. 144:389–401. doi:10.1016/j.cell.2010.12.034.

Stewart, M.D., T. Ritterhoff, R.E. Klevit, and P.S. Brzovic. 2016. E2 enzymes: more than just middle men. *Cell Res*. 26:423–440. doi:10.1038/cr.2016.35.

Stukey, J.E., V.M. McDonough, and C.E. Martin. 1989. Isolation and characterization of OLE1, a gene affecting fatty acid desaturation from Saccharomyces cerevisiae. *J Biol Chem*. 264:16537–16544.

Sugiura, A., S. Mattie, J. Prudent, and H.M. McBride. 2017. Newly born peroxisomes are a hybrid of mitochondrial and ER-derived pre-peroxisomes. *Nature*. 542:251–254. doi:10.1038/nature21375.

Sugiura, A., G.-L. McLelland, E.A. Fon, and H.M. McBride. 2014. A new pathway for mitochondrial quality control: mitochondrial-derived vesicles. *The EMBO Journal*. 33:2142–2156. doi:10.15252/embj.201488104.

Surma, M.A., C. Klose, D. Peng, M. Shales, C. Mrejen, A. Stefanko, H. Braberg, D.E. Gordon, D. Vorkel, C.S. Ejsing, R. Farese, K. Simons, N.J. Krogan, and R. Ernst. 2013. A Lipid E-MAP Identifies

Ubx2 as a Critical Regulator of Lipid Saturation and Lipid Bilayer Stress. *Molecular Cell*. 51:519–530. doi:10.1016/j.molcel.2013.06.014.

Sutton, R.B., D. Fasshauer, R. Jahn, and A.T. Brunger. 1998. Crystal structure of a SNARE complex involved in synaptic exocytosis at 2.4 Å resolution. *Nature*. 395:347–353. doi:10.1038/26412.

Swanson, R., M. Locher, and M. Hochstrasser. 2001. A conserved ubiquitin ligase of the nuclear envelope/endoplasmic reticulum that functions in both ER-associated and Matα2 repressor degradation. *Genes Dev.* 15:2660–2674. doi:10.1101/gad.933301.

Swatek, K.N., and D. Komander. 2016. Ubiquitin modifications. *Cell Res*. 26:399–422. doi:10.1038/cr.2016.39.

Swinkels, B. w., S. j. Gould, A. g. Bodnar, R. a. Rachubinski, and S. Subramani. 1991. A novel, cleavable peroxisomal targeting signal at the amino-terminus of the rat 3-ketoacyl-CoA thiolase. *The EMBO Journal*. 10:3255–3262. doi:10.1002/j.1460-2075.1991.tb04889.x.

Tanaka, A., M.M. Cleland, S. Xu, D.P. Narendra, D.-F. Suen, M. Karbowski, and R.J. Youle. 2010a. Proteasome and p97 mediate mitophagy and degradation of mitofusins induced by Parkin. *Journal of Cell Biology*. 191:1367–1380. doi:10.1083/jcb.201007013.

Tanaka, A., M.M. Cleland, S. Xu, D.P. Narendra, D.-F. Suen, M. Karbowski, and R.J. Youle. 2010b. Proteasome and p97 mediate mitophagy and degradation of mitofusins induced by Parkin. *Journal of Cell Biology*. 191:1367–1380. doi:10.1083/jcb.201007013.

Tang, F., Y. Peng, J.J. Nau, E.J. Kauffman, and L.S. Weisman. 2006. Vac8p, an Armadillo Repeat Protein, Coordinates Vacuole Inheritance With Multiple Vacuolar Processes. *Traffic*. 7:1368–1377. doi:10.1111/j.1600-0854.2006.00458.x.

Tang, R., W.Y. Langdon, and J. Zhang. 2019. Regulation of immune responses by E3 ubiquitin ligase Cbl-b. *Cellular Immunology*. 340:103878. doi:10.1016/j.cellimm.2018.11.002.

Tang, X., B.St. Germain, and W.-L. Lee. 2012. A novel patch assembly domain in Num1 mediates dynein anchoring at the cortex during spindle positioning. *Journal of Cell Biology*. 196:743–756. doi:10.1083/jcb.201112017.

Tang, X., J.J. Punch, and W.-L. Lee. 2009. A CAAX motif can compensate for the PH domain of Num1 for cortical dynein attachment. *Cell Cycle*. 8:3182–3190. doi:10.4161/cc.8.19.9731.

Tatsuta, T., M. Scharwey, and T. Langer. 2014. Mitochondrial lipid trafficking. *Trends in Cell Biology*. 24:44–52. doi:10.1016/j.tcb.2013.07.011.

Taxis, C., R. Hitt, S.-H. Park, P.M. Deak, Z. Kostova, and D.H. Wolf. 2003. Use of Modular Substrates Demonstrates Mechanistic Diversity and Reveals Differences in Chaperone Requirement of ERAD *. *Journal of Biological Chemistry*. 278:35903–35913. doi:10.1074/jbc.M301080200.

Tieu, Q., and J. Nunnari. 2000. Mdv1p Is a Wd Repeat Protein That Interacts with the Dynamin-Related Gtpase, Dnm1p, to Trigger Mitochondrial Division. *Journal of Cell Biology*. 151:353–366. doi:10.1083/jcb.151.2.353.

Tieu, Q., V. Okreglak, K. Naylor, and J. Nunnari. 2002. The WD repeat protein, Mdv1p, functions as a molecular adaptor by interacting with Dnm1p and Fis1p during mitochondrial fission. *Journal of Cell Biology*. 158:445–452. doi:10.1083/jcb.200205031.

Tilokani, L., S. Nagashima, V. Paupe, and J. Prudent. 2018. Mitochondrial dynamics: overview of molecular mechanisms. *Essays in Biochemistry*. 62:341–360. doi:10.1042/EBC20170104.

Titorenko, V.I., H. Chan, and R.A. Rachubinski. 2000. Fusion of Small Peroxisomal Vesicles in Vitro Reconstructs an Early Step in the in Vivo Multistep Peroxisome Assembly Pathway of Yarrowia lipolytica. *Journal of Cell Biology*. 148:29–44. doi:10.1083/jcb.148.1.29.

Titorenko, V.I., and R.T. Mullen. 2006. Peroxisome biogenesis: the peroxisomal endomembrane system and the role of the ER. *Journal of Cell Biology*. 174:11–17. doi:10.1083/jcb.200604036.

Titorenko Vladimir I. and Rachubinski Richard A. 1998. Mutants of the Yeast Yarrowia lipolyticaDefective in Protein Exit from the Endoplasmic Reticulum Are Also Defective in Peroxisome Biogenesis. *Molecular and Cellular Biology*. 18:2789–2803. doi:10.1128/MCB.18.5.2789.

Trempe, J.-F., V. Sauvé, K. Grenier, M. Seirafi, M.Y. Tang, M. Ménade, S. Al-Abdul-Wahid, J. Krett, K. Wong, G. Kozlov, B. Nagar, E.A. Fon, and K. Gehring. 2013. Structure of Parkin Reveals Mechanisms for Ubiquitin Ligase Activation. *Science*. 340:1451–1455. doi:10.1126/science.1237908.

Uetz, P., L. Giot, G. Cagney, T.A. Mansfield, R.S. Judson, J.R. Knight, D. Lockshon, V. Narayan, M. Srinivasan, P. Pochart, A. Qureshi-Emili, Y. Li, B. Godwin, D. Conover, T. Kalbfleisch, G. Vijayadamodar, M. Yang, M. Johnston, S. Fields, and J.M. Rothberg. 2000. A comprehensive analysis of protein–protein interactions in Saccharomyces cerevisiae. *Nature*. 403:623–627. doi:10.1038/35001009.

Valm, A.M., S. Cohen, W.R. Legant, J. Melunis, U. Hershberg, E. Wait, A.R. Cohen, M.W. Davidson, E. Betzig, and J. Lippincott-Schwartz. 2017. Applying systems-level spectral imaging and analysis to reveal the organelle interactome. *Nature*. 546:162–167. doi:10.1038/nature22369.

Vance, J.E. 1990. Phospholipid synthesis in a membrane fraction associated with mitochondria. *Journal of Biological Chemistry*. 265:7248–7256. doi:10.1016/S0021-9258(19)39106-9.

van der Zand, A., J. Gent, I. Braakman, and H.F. Tabak. 2012. Biochemically Distinct Vesicles from the Endoplasmic Reticulum Fuse to Form Peroxisomes. *Cell*. 149:397–409. doi:10.1016/j.cell.2012.01.054.

Vashist, S., and D.T.W. Ng. 2004. Misfolded proteins are sorted by a sequential checkpoint mechanism of ER quality control. *Journal of Cell Biology*. 165:41–52. doi:10.1083/jcb.200309132.

Veal, E.A., A.M. Day, and B.A. Morgan. 2007. Hydrogen Peroxide Sensing and Signaling. *Molecular Cell*. 26:1–14. doi:10.1016/j.molcel.2007.03.016.

Vembar, S.S., and J.L. Brodsky. 2008. One step at a time: endoplasmic reticulum-associated degradation. *Nat Rev Mol Cell Biol*. 9:944–957. doi:10.1038/nrm2546.

Virmani, A., L. Pinto, O. Bauermann, S. Zerelli, A. Diedenhofen, Z.K. Binienda, S.F. Ali, and F.R. van der Leij. 2015. The Carnitine Palmitoyl Transferase (CPT) System and Possible Relevance for Neuropsychiatric and Neurological Conditions. *Mol Neurobiol*. 52:826–836. doi:10.1007/s12035-015-9238-7.

Volland, C., D. Urban-Grimal, G. Géraud, and R. Haguenauer-Tsapis. 1994. Endocytosis and degradation of the yeast uracil permease under adverse conditions. *J Biol Chem*. 269:9833–9841.

Volmer, R., and D. Ron. 2015. Lipid-dependent regulation of the unfolded protein response. *Current Opinion in Cell Biology*. 33:67–73. doi:10.1016/j.ceb.2014.12.002.

Walter, P., and D. Ron. 2011a. The Unfolded Protein Response: From Stress Pathway to Homeostatic Regulation. *Science*. 334:1081–1086. doi:10.1126/science.1209038.

Walter, P., and D. Ron. 2011b. The Unfolded Protein Response: From Stress Pathway to Homeostatic Regulation. *Science*. 334:1081–1086. doi:10.1126/science.1209038.

Wanders, R.J.A., and H.R. Waterham. 2006. Biochemistry of Mammalian Peroxisomes Revisited. *Annu. Rev. Biochem.* 75:295–332. doi:10.1146/annurev.biochem.74.082803.133329.

Wang, C.-W., and S.-C. Lee. 2012. The ubiquitin-like (UBX)-domain-containing protein Ubx2/Ubxd8 regulates lipid droplet homeostasis. *Journal of Cell Science*. 125:2930–2939. doi:10.1242/jcs.100230.

Wang, D., F. Zheng, S. Holmberg, and G.B. Kohlhaw. 1999. Yeast Transcriptional Regulator Leu3p: SELF-MASKING, SPECIFICITY OF MASKING, AND EVIDENCE FOR REGULATION BY THE INTRACELLULAR LEVEL OF Leu3p *. *Journal of Biological Chemistry*. 274:19017–19024. doi:10.1074/jbc.274.27.19017.

Wang, Y., D. Argiles-Castillo, E.I. Kane, A. Zhou, and D.E. Spratt. 2020. HECT E3 ubiquitin ligases – emerging insights into their biological roles and disease relevance. *Journal of Cell Science*. 133:jcs228072. doi:10.1242/jcs.228072.

Wangler, M.F., L. Hubert, T.R. Donti, M.J. Ventura, M.J. Miller, N. Braverman, K. Gawron, M. Bose, A.B. Moser, R.O. Jones, W.B. Rizzo, V.R. Sutton, Q. Sun, A.D. Kennedy, and S.H. Elsea. 2018. A metabolomic map of Zellweger spectrum disorders reveals novel disease biomarkers. *Genet Med*. 20:1274–1283. doi:10.1038/gim.2017.262.

Ward, C.L., S. Omura, and R.R. Kopito. 1995. Degradation of CFTR by the ubiquitin-proteasome pathway. *Cell*. 83:121–127. doi:10.1016/0092-8674(95)90240-6.

Warren, G., and W. Wickner. 1996. Organelle Inheritance. *Cell*. 84:395–400. doi:10.1016/S0092-8674(00)81284-2.

Waterham, H.R., J. Koster, C.W.T. van Roermund, P.A.W. Mooyer, R.J.A. Wanders, and J.V. Leonard. 2007. A Lethal Defect of Mitochondrial and Peroxisomal Fission. *New England Journal of Medicine*. 356:1736–1741. doi:10.1056/NEJMoa064436.

Wauer, T., and D. Komander. 2013. Structure of the human Parkin ligase domain in an autoinhibited state. *The EMBO Journal*. 32:2099–2112. doi:10.1038/emboj.2013.125.

Weir, N.R., R.A. Kamber, J.S. Martenson, and V. Denic. 2017. The AAA protein Msp1 mediates clearance of excess tail-anchored proteins from the peroxisomal membrane. *eLife*. 6:e28507. doi:10.7554/eLife.28507.

Wen, X., and D.J. Klionsky. 2016. An overview of macroautophagy in yeast. *Journal of Molecular Biology*. 428:1681–1699. doi:10.1016/j.jmb.2016.02.021.

Westermann, B. 2010. Mitochondrial fusion and fission in cell life and death. *Nat Rev Mol Cell Biol*. 11:872–884. doi:10.1038/nrm3013.

Wideman, J.G., D.L. Balacco, T. Fieblinger, and T.A. Richards. 2018. PDZD8 is not the 'functional ortholog' of Mmm1, it is a paralog. *F1000Res*. 7:1088. doi:10.12688/f1000research.15523.1.

Wiertz, E.J.H.J., D. Tortorella, M. Bogyo, J. Yu, W. Mothes, T.R. Jones, T.A. Rapoport, and H.L. Ploegh. 1996. Sec6l-mediated transfer of a membrane protein from the endoplasmic reticulum to the proteasome for destruction. *Nature*. 384:432–438. doi:10.1038/384432a0.

Willems, A.R., M. Schwab, and M. Tyers. 2004. A hitchhiker's guide to the cullin ubiquitin ligases: SCF and its kin. *Biochimica et Biophysica Acta (BBA) - Molecular Cell Research*. 1695:133–170. doi:10.1016/j.bbamcr.2004.09.027.

Willems, P.H.G.M., R. Rossignol, C.E.J. Dieteren, M.P. Murphy, and W.J.H. Koopman. 2015. Redox Homeostasis and Mitochondrial Dynamics. *Cell Metabolism*. 22:207–218. doi:10.1016/j.cmet.2015.06.006.

Williams, C., M. van den Berg, and B. Distel. 2005. Saccharomyces cerevisiae Pex14p contains two independent Pex5p binding sites, which are both essential for PTS1 protein import. *FEBS Letters*. 579:3416–3420. doi:10.1016/j.febslet.2005.05.011.

Williams, M., and K. Kim. 2014. From membranes to organelles: Emerging roles for dynamin-like proteins in diverse cellular processes. *European Journal of Cell Biology*. 93:267–277. doi:10.1016/j.ejcb.2014.05.002.

Wolf, D.H., and A. Stolz. 2012. The Cdc48 machine in endoplasmic reticulum associated protein degradation. *Biochim Biophys Acta*. 1823:117–24. doi:10.1016/j.bbamcr.2011.09.002.

Wong, E.D., J.A. Wagner, S.V. Scott, V. Okreglak, T.J. Holewinske, A. Cassidy-Stone, and J. Nunnari. 2003. The intramitochondrial dynamin-related GTPase, Mgm1p, is a component of a protein complex that mediates mitochondrial fusion. *Journal of Cell Biology*. 160:303–311. doi:10.1083/jcb.200209015.

Wong, Y.C., D. Ysselstein, and D. Krainc. 2018. Mitochondria–lysosome contacts regulate mitochondrial fission via RAB7 GTP hydrolysis. *Nature*. 554:382–386. doi:10.1038/nature25486.

Wróblewska, J.P., L.D. Cruz-Zaragoza, W. Yuan, A. Schummer, S.G. Chuartzman, R. de Boer, S. Oeljeklaus, M. Schuldiner, E. Zalckvar, B. Warscheid, R. Erdmann, and I.J. van der Klei. 2017. Saccharomyces cerevisiae cells lacking Pex3 contain membrane vesicles that harbor a subset of peroxisomal membrane proteins. *Biochimica et Biophysica Acta (BBA) - Molecular Cell Research*. 1864:1656–1667. doi:10.1016/j.bbamcr.2017.05.021.

Wu, H., R. de Boer, A.M. Krikken, A. Akşit, W. Yuan, and I.J. van der Klei. 2019. Peroxisome development in yeast is associated with the formation of Pex3-dependent peroxisome-vacuole contact sites. *Biochim Biophys Acta Mol Cell Res*. 1866:349–359. doi:10.1016/j.bbamcr.2018.08.021.

Wu, X., L. Li, and H. Jiang. 2016. Doa1 targets ubiquitinated substrates for mitochondria-associated degradation. *Journal of Cell Biology*. 213:49–63. doi:10.1083/jcb.201510098.

Xia, D., W.K. Tang, and Y. Ye. 2016. Structure and function of the AAA+ ATPase p97/Cdc48p. *Gene*. 583:64–77. doi:10.1016/j.gene.2016.02.042.

Xu, S., G. Peng, Y. Wang, S. Fang, and M. Karbowski. 2011. The AAA-ATPase p97 is essential for outer mitochondrial membrane protein turnover. *MBoC*. 22:291–300. doi:10.1091/mbc.e10-09-0748.

Yagishita, N., K. Ohneda, T. Amano, S. Yamasaki, A. Sugiura, K. Tsuchimochi, H. Shin, K. Kawahara, O. Ohneda, T. Ohta, S. Tanaka, M. Yamamoto, I. Maruyama, K. Nishioka, A. Fukamizu, and T. Nakajima. 2005. Essential Role of Synoviolin in Embryogenesis *. *Journal of Biological Chemistry*. 280:7909–7916. doi:10.1074/jbc.M410863200.

Yan, L., Y. Qi, X. Huang, C. Yu, L. Lan, X. Guo, Z. Rao, J. Hu, and Z. Lou. 2018. Structural basis for GTP hydrolysis and conformational change of MFN1 in mediating membrane fusion. *Nat Struct Mol Biol*. 25:233–243. doi:10.1038/s41594-018-0034-8.

Yan, M., D.A. Rachubinski, S. Joshi, R.A. Rachubinski, and S. Subramani. 2008. Dysferlin domain-containing proteins, Pex30p and Pex31p, localized to two compartments, control the number and size of oleate-induced peroxisomes in Pichia pastoris. *Mol Biol Cell*. 19:885–898. doi:10.1091/mbc.e07-10-1042.

Yau, R., and M. Rape. 2016. The increasing complexity of the ubiquitin code. *Nat Cell Biol*. 18:579–586. doi:10.1038/ncb3358.

Ye, Y., H.H. Meyer, and T.A. Rapoport. 2001. The AAA ATPase Cdc48/p97 and its partners transport proteins from the ER into the cytosol. *Nature*. 414:652–656. doi:10.1038/414652a.

Yeung, T., G.E. Gilbert, J. Shi, J. Silvius, A. Kapus, and S. Grinstein. 2008. Membrane Phosphatidylserine Regulates Surface Charge and Protein Localization. *Science*. 319:210–213. doi:10.1126/science.1152066.

Yoshida, Y., H. Niwa, M. Honsho, A. Itoyama, and Y. Fujiki. 2015. Pex11mediates peroxisomal proliferation by promoting deformation of the lipid membrane. *Biology Open*. 4:710–721. doi:10.1242/bio.201410801.

Yu, J.W., J.M. Mendrola, A. Audhya, S. Singh, D. Keleti, D.B. DeWald, D. Murray, S.D. Emr, and M.A. Lemmon. 2004. Genome-Wide Analysis of Membrane Targeting by S. cerevisiae Pleckstrin Homology Domains. *Molecular Cell*. 13:677–688. doi:10.1016/S1097-2765(04)00083-8.

Yu, R., U. Lendahl, M. Nistér, and J. Zhao. 2020. Regulation of Mammalian Mitochondrial Dynamics: Opportunities and Challenges. *Front. Endocrinol.* 11:374. doi:10.3389/fendo.2020.00374.

Zhang, S., Y. Skalsky, and D.J. Garfinkel. 1999. MGA2 or SPT23 Is Required for Transcription of the Δ9 Fatty Acid Desaturase Gene, OLE1, and Nuclear Membrane Integrity in Saccharomyces cerevisiae. *Genetics*. 151:473–483. doi:10.1093/genetics/151.2.473.

Zhang, Y., and D.C. Chan. 2007. Structural basis for recruitment of mitochondrial fission complexes by Fis1. *PNAS*. 104:18526–18530.

Zhao, J., U. Lendahl, and M. Nistér. 2013a. Regulation of mitochondrial dynamics: convergences and divergences between yeast and vertebrates. *Cell. Mol. Life Sci.* 70:951–976. doi:10.1007/s00018-012-1066-6.

Zhao, J., T. Liu, S. Jin, X. Wang, M. Qu, P. Uhlén, N. Tomilin, O. Shupliakov, U. Lendahl, and M. Nistér. 2011. Human MIEF1 recruits Drp1 to mitochondrial outer membranes and promotes mitochondrial fusion rather than fission. *The EMBO Journal*. 30:2762–2778. doi:10.1038/emboj.2011.198.

Zhao, Y., J.A. MacGurn, M. Liu, and S. Emr. 2013b. The ART-Rsp5 ubiquitin ligase network comprises a plasma membrane quality control system that protects yeast cells from proteotoxic stress. *eLife*. 2:e00459. doi:10.7554/eLife.00459.

Zheng, N., and N. Shabek. 2017. Ubiquitin Ligases: Structure, Function, and Regulation. *Annu. Rev. Biochem.* 86:129–157. doi:10.1146/annurev-biochem-060815-014922.

Annexes

Plate ID	Gene	Protein	Localization + Function
01_01_12	YNL273W	TOF1	Replication pausing complex
01_01_42	YMR262W	unknown	
01_02_06	YEL068C	unknown	ER-vacuole
01_03_45	YML086C	ALO1	Mitochondria (D-Arabinono-1,4-lactone oxidase)
01_05_47	YLR011W	LOT6	Nucleus-cytosol (FMN-dependent NAD(P)H:quinone reductase)
01_15_44	YOL071W	SDH5	Mitochondria (Succinate DeHydrogenase)
01_19_44	YPL273W	SAM4	Nucleus-cytosol (S-Adenosyl-Methionine metabolism)
01_23_45	YMR009W	ADI1	Nucleus-cytosol (Acireductone dioxygenease involved in methionine salvage pathway)
01_26_39	YBR267W	REI1	Cytosol (Cytoplasmic pre-60S factor)
01_28_43	YEL052W	AFG1	Mitochondria (ATPase that may act as a chaperone for cytochrome c oxidase subunits
01_29_42	YNL278W	CAF120	Part of the CCR4-NOT transcriptional regulatory complex
01_32_23	YEL060C	PRB1	Vacuolar proteinase B with H3 N-terminal endopeptidase activity
01_32_39	YEL064C	AVT2	ER (Amino acid Vacuolar Transport)
02_01_11	YKL065C	YET1	ER (unknown)
02_01_12	YLR356W	ATG33	Mitochondrial mitophagy-specific protein
02_01_23	YKL068W	NUP100	NPC
02_01_25	YLR165C	PUS5	Mitochondria (Pseudo-uridine synthase)
02_02_06	YNL176C	TDA7	Vacuole (Cell cycle-regulated gene of unknown function)
02_02_12	YDR262W	Unknown	Vacuole (unknown)
02_02_15	YPR170C	Unknown	
02_03_11	YOR140W	SFL1	Transcriptional repressor and activator (autophagy?)
02_03_12	YGL202W	ARO8	Cytosol (Aromatic aminotransferase I)
02_03_33	YGR034W	RPL26B	Cytosol (Ribosomal 60S subunit protein L26B)
02_03_45	YGR037C	ACB1	Acyl-CoA-binding protein; transports newly synthesized acyl-CoA esters from fatty acid synthetase (Fas1p-Fas2p) to acyl-CoA-consuming processes
02_04_16	YGR284C	ERV29	ER (Protein localized to COPII-coated vesicles)
02_04_19	YGL034C	Unknown	
02_04_43	YGL042C	Unknown	
02_05_47	YKL090W	CUE2	Unknown (has two CUE domains that bind ubiquitin)

02_06_21	YPL046C	ELC1	Elongin C, forms a complex with Cul3p
02_06_35	YPR198W	SGE1	ER-plasma membrane (multidrug transporter)
02_07_43	YOR173W	DCS2	Cytosol (m (7) GpppX pyrophosphatase regulator)
02_09_42	YJL180C	ATP12	Mitochondria (Assembly factor for F1 sector of mitochondrial F1F0 ATP synthase)
02_11_03	YOR177C	MPC54	Component of the meiotic outer plaque
02_11_04	YGL228W	SHE10	ER (involved in outer spore wall assembly)
02_14_47	YER144C	UBP5	concentrates at the bud neck
02_16_42	YFL032W	Unknown	
02_16_47	YGL096W	TOS8	Homeodomain-containing protein and putative transcription factor
02_17_03	YKL123W	Unknown	
02_19_14	YDR185C	UPS3	Mitochondrial protein of unknown function; similar to Ups1p and Ups2p
02_19_44	YGR007W	ECT1	Catalyzes the second step of phosphatidylethanolamine biosynthesis
02_20_19	YNL237W	YTP1	Probable type-III integral membrane protein of unknown function; has regions of similarity to mitochondrial electron transport proteins
02_21_01	YKL008C	LAC1	ER (Ceramide synthase component)
02_21_45	YKL027W	TCD2	Mitochondria (tRNA threonyl-carbamoyl-adenosine dehydratase)
02_22_01	YPR120C	CLB5	B-type cyclin involved in DNA replication during S phase
02_23_45	YOR108W	LEU9	Mitochondria (Leucine biosynthesis)
02_26_39	YGR232W	NAS6	Conserved 19S regulatory particle assembly-chaperone
02_29_42	YLR351C	NIT3	Mitochondria
02_32_10	YGR259C	Unknown	
02_32_27	YNL191W	DUG3	Deficient in Utilization of Glutathione
02_32_44	YOL092W	YPQ1	Putative vacuolar membrane transporter for cationic amino acids
03_03_10	YDR028C	REG1	Regulatory subunit of type 1 protein phosphatase Glc7
03_03_33	YPR045C	THP3	Protein that may have a role in transcription elongation
03_05_48	YJR145C	RPS4A	Protein component of the small (40S) ribosomal subunit
03_07_36	YJR062C	NTA1	N-Terminal Amidase (N-end rule)
03_08_26	YBR151W	APD1	Required for normal localization of actin patches
03_08_44	YDR457W	TOM1	E3 ubiquitin ligase of the hect-domain class
03_12_45	YIL162W	SUC2	sucrose hydrolyzing enzyme
03_12_48	YDR476C	Unknown	ER
03_14_39	YBR066C	NRG2	Negative Regulator of Glucose-controlled genes

03_19_46	YCR068W	ATG15	Phospholipase
03_19_48	YDL149W	ATG9	Cycles between the phagophore assembly site (PAS)
03_22_47	YNL117W	MLS1	Peroxisome (Malate synthase, enzyme of the glyoxylate cycle)
03_23_30	YCR085W	Unknown	
03_25_42	YJR074W	MOG1	Involved in nuclear protein import
04_13_48	YNL277W	MET2	First step of the methionine biosynthetic pathway
04_26_29	YKL096C-B	Unknown	
05_01_43	YLR163C	MAS1	Beta subunit of the mitochondrial processing protease
05_03_09	YBL073W	Unknown	
05_03_27	YDL148C	NOP14	Nucleolar protein; forms a complex with Noc4p that mediates maturation and nuclear export of 40S ribosomal subunits
05_03_48	YKL033W	TTI1	Chromatin remodeling
05_03_47	YDL164C	CDC9	DNA ligase I found in the nucleus and Mitochondria
05_04_25	YOR110W	TFC7	RNA pol III transcription initiation factor complex (TFIIIC) subunit
05_06_33	YLR291C	GCD7	Beta subunit of the translation initiation factor eIF2B
05_08_41	YOR181W	LAS17	Actin assembly factor
05_09_23	YMR203W	TOM40	Component of the TOM (translocase of outer membrane) complex
05_09_38	YDR531W	CAB1	catalyzes the first committed step in the universal biosynthetic pathway for synthesis of coenzyme A
05_09_43	YNL007C	SIS1	Type II HSP40 co-chaperone that interacts with the HSP70 protein Ssa1p
05_10_39	YNL181W	PBR1	ER (Putative oxidoreductase)
05_10_41	YLR378C	SEC61	Conserved ER protein translocation channel
05_11_42	YJL001W	PRE3	Beta 1 subunit of the 20S proteasome
05_11_43	YDR047W	HEM12	Catalyzes the fifth step in the heme biosynthetic pathway
05_11_46	YJL002C	OST1	Alpha subunit of the oligo-saccharyl-transferase complex of the ER lumen
05_11_47	YDR052C	DBF4	Required for Cdc7p kinase activity and initiation of DNA replication
05_11_48	YKL154W	SRP102	Signal recognition particle (SRP) receptor beta subunit
05_13_45	YGL098W	USE1	Essential SNARE protein localized to the ER
05_13_38	YER025W	GCD11	Gamma subunit of the translation initiation factor eIF2
05_13_39	YNR053C	NOG2	associates with pre-60S ribosomal subunits in the nucleolus and is required for their nuclear export and maturation

05_13_46	YER038C	KRE29	Involved in removal of X-shaped DNA structures that arise between sister chromatids during DNA replication and repair
05_13_47	YOL149W	DCP1	Decapping complex removes the 5' cap structure from mRNAs prior to their degradation
05_14_41	YML025C	YML6	Mitochondrial ribosomal protein of the large subunit
05_14_43	YNL262W	POL2	Catalytic subunit of DNA polymerase (II) epsilon
05_15_43	YDR113C	PDS1	Securin; inhibits anaphase by binding separin Esp1p
05_15_47	YDR118W	APC4	Subunit of the Anaphase-Promoting Complex/Cyclosome (APC/C)
05_15_48	YKR022C	NTR2	ER? involved in spliceosome disassembly
05_16_41	YOR310C	NOP58	Involved in pre-rRNA processing, 18S rRNA synthesis, and snoRNA synthesis
05_19_40	YLL011W	SOF1	Required for biogenesis of 40S (small) ribosomal subunit
05_19_43	YDR182W	CDC1	ER Putative mannose-ethanolamine phosphate phosphodiesterase
05_19_47	YDR187C	Unknown	
05_21_43	YPL252C	YAH1	Ferredoxin of the mitochondrial matrix
05_21_44	YHL015W	RPS20	Protein component of the small (40S) ribosomal subunit
05_21_48	YHR005C	GPA1	Endosome Subunit of the G protein involved in pheromone response
05_22_39	YOL022C	TSR4	required for correct processing of 20S pre-rRNA
05_22_45	YMR113W	FOL3	Involved in folic acid biosynthesis
05_22_47	YOL034W	SMC5	Structural Maintenance of Chromosomes
05_24_45	YPL122C	TFB2	Involved in transcription initiation
05_25_43	YAL041W	CDC24	Required for polarity establishment and maintenance
05_25_46	YGL011C	SCL1	Alpha 1 subunit of the 20S proteasome
05_26_45	YMR218C	TRS130	Endosome-Golgi Component of transport protein particle (TRAPP) complex II
05_27_47	YDR302W	GPI11	ER membrane protein involved in a late step of GPI anchor assembly
05_29_35	YBL030C	PET9	ADP/ATP carrier of the mitochondrial inner membrane
05_30_39	YOR060C	SLD7	Role in chromosomal DNA replication deletion mutant has aberrant mitochondria
05_31_34	YJR072C	NPA3	Role in transport of RNA polymerase II to the nucleus

Table 6b: Exhaustive list of the High-Throughput genetic screen results. Genes and their corresponding proteins are grouped according to their function and localization (known and unknown). Plates from 01 to 04 correspond to the full deletion library and plate 05 corresponds to a damp library with hypo-morphic alleles. A total of 14 groups is listed in Table 6a. All genes were identified from SGD (Saccharomyces Genome Database: yeastgenome.org).

Supplementary Table 1: S. cerevisiae strains used in this study.

Name	Parental strains	Genotype	Occurrence In the study	Reference
W303 WT (MCY553)	W303	*Mata ura3-1 trp1-1 leu2-3,112 his3-11,15 can1-100 RAD5 ADE2*	Used to build FZO1 and MDM30 shuffle strains	Gift from T. Teixeira
W303 WT (MCY554)	W303	*MATα ura3-1 trp1-1 leu2-3,112 his3-11,15 can1-100 RAD5 ADE2*		Gift from T. Teixeira
FZO1-GFP (MCY1667)	W303 (MCY553)	*Mata ura3-1 trp1-1 leu2-3,112 his3-11,15 can1-100 RAD5 ADE2 FZO1-EGFP::KANMX6*	1E, 1F, S1A, S1B, S1C	This study
PEX3-mCherry mt-BFP (MCY 1591)	W303 (MCY553)	*Mata ura3-1 trp1-1 leu2-3,112 his3-11,15 can1-100 RAD5 ADE2 PEX3-mCherry::NAT mt-BFP::LEU2*	1E, 1F, S1A, S1B, S1C	This study
FZO1-GFP PEX3-mCherry mt-BFP (MCY1675)	W303 (MCY553)	*Mata ura3-1 trp1-1 leu2-3,112 his3-11,15 can1-100 RAD5 ADE2 PEX3-mCherry::NAT mt-BFP::LEU2 FZO1-EGFP::KANMX6*	1A,1B,1E,1F, S1A, S1B, S1C, S3D	This study
mdm30Δ FZO1-GFP +pMDM30 (MCY1673)	W303 (MCY970)	*Mata ura3-1 trp1-1 leu2-3,112 his3-11,15 can1-100 RAD5 ADE2 MDM30::LoxP FZO1-EGFP::KANMX6 + PRS316-MDM30*	1E, 1F, S1A, S1B, S1C	This study
mdm30Δ PEX3-mCherry mt-BFP +pMDM30 (MCY 1597)	W303 (MCY970)	*Mata ura3-1 trp1-1 leu2-3,112 his3-11,15 can1-100 RAD5 ADE2 MDM30::KANMX6 PEX3-mCherry::NAT mt-BFP::LEU2 + PRS316-MDM30*	1E, 1F, S1A, S1B, S1C	This study
mdm30Δ FZO1-GFP PEX3-mCherry mt-BFP +pMDM30 (MCY1677)	W303 (MCY970)	*Mata ura3-1 trp1-1 leu2-3,112 his3-11,15 can1-100 RAD5 ADE2 MDM30::LoxP PEX3-mCherry::NAT mt-BFP::LEU2 FZO1-EGFP::KANMX6 + PRS316-MDM30*	1A,1B,1E,1F, S1A, S1B, S1C	This study
FZO1-13MYC PEX3-6HA (MCY1488)	W303 (MCY553)	*Mata ura3-1 trp1-1 leu2-3,112 his3-11,15 can1-100 RAD5 ADE2 FZO1-13MYC::HIS5+ PEX3-6HA::NAT*	1D,3B,3C	This study
mdm30Δ FZO1-13MYC PEX3-6HA (MCY1490)	W303 (MCY971)	*MATα ura3-1 trp1-1 leu2-3,112 his3-11,15 can1-100 RAD5 ADE2 MDM30::KANMX6 FZO1-13MYC::HIS5 PEX3-6HA::NAT*	1D,3B,3C	This study
fzo1Δ + pFZO1 (URA) (MCY572)	W303	*MATα ura3-1 trp1-1 leu2-3,112 his3-11,15 can1-100 RAD5 ADE2 FZO1::LEU2 +PRS416-FZO1*		(Cavellini et al., 2017)
fzo1Δ PEX3-6HA +pFZO1-13MYC (MCY1779)	W303 (MCY572)	*MATα ura3-1 trp1-1 leu2-3,112 his3-11,15 can1-100 RAD5 ADE2 FZO1::LEU2 PEX3-6HA::Nat +PRS414-FZO1-13MYC*	2A	This study
fzo1Δ PEX3-6HA +pFZO1S201N-13MYC (MCY1780)	W303 (MCY572)	*MATα ura3-1 trp1-1 leu2-3,112 his3-11,15 can1-100 RAD5 ADE2 Pex3-6HA::NAT FZO1::LEU2 +PRS414-FZO1S201N-13MYC*	2A	This study

fzo1Δ +pFzo1-URA (MCY1569)	W303	*Mata FZO1::LoxP ura3-1 trp1-1 leu2-3,112 his3-11,15 can1-100 RAD5 ADE2 +PRS416-FZO1*		This study
fzo1Δ PEX3-mCherry mt-BFP + pGFP-Link-FZO1 prom ADH (MCY1802)	W303 (MCY1569)	*Mata FZO1::LoxP ura3-1 trp1-1 leu2-3,112 his3-11,15 can1-100 RAD5 ADE2 PEX3-mCherry::NAT mt-BFP::LEU2 +PRS414-GFP-FZO1*	2B	This study
fzo1Δ PEX3-mCherry mt-BFP +pGFP-Link-FZO1S201N prom ADH (MCY1803)	W303 (MCY1569)	*Mata FZO1::LoxP ura3-1 trp1-1 leu2-3,112 his3-11,15 can1-100 RAD5 ADE2 PEX3-mCherry::NAT mt-BFP::LEU2 +PRS414-GFP-FZO1S201N*	2B	This study
fzo1Δ mt-BFP + pGFP-Link-FZO1 prom ADH (MCY1804)	W303 (MCY1569)	*Mata FZO1::LoxP ura3-1 trp1-1 leu2-3,112 his3-11,15 can1-100 RAD5 ADE2 mt-BFP::LEU2 +PRS414-GFP-FZO1*	2B	This study
fzo1Δ mt-BFP + pGFP-Link-FZO1S201N prom ADH (MCY1805)	W303 (MCY1569)	*Mata FZO1::LoxP ura3-1 trp1-1 leu2-3,112 his3-11,15 can1-100 RAD5 ADE2 mtBFP::LEU2 +PRS414-GFP-FZO1S201N*	2B	This study
fzo1Δ PEX3-mCherry mt-BFP + pGFP-Link-FZO1 (MCY1771)	W303 (MCY1569)	*Mata FZO1::LoxP ura3-1 trp1-1 leu2-3,112 his3-11,15 can1-100 RAD5 ADE2 PEX3-mCherry::NAT mt-BFP::LEU2 +PRS414-GFP-FZO1*	2C,2D	This study
fzo1Δ PEX3-mCherry mt-BFP +pGFP-Link-FZO1S201N (MCY1772)	W303 (MCY1569)	*Mata FZO1::LoxP ura3-1 trp1-1 leu2-3,112 his3-11,15 can1-100 RAD5 ADE2 Pex3-mCherry::NAT mt-BFP::LEU2 + PRS414-GFP-FZO1S201N*	2C,2D	This study
mdm30Δ mt-GFP +pMDM30 (MCY1842)	W303 (MCY970)	*Mata ura3-1 trp1-1 leu2-3,112 his3-11,15 can1-100 RAD5 ADE2 MDM30::KANMX6 mt-GFP::LEU2 + PRS316-MDM30*	2E, S1D, S1E	This study
fzo1Δ mt-GFP +pFZO1 (URA) (MCY1843)	W303 (MCY1569)	*Mata FZO1::LoxP ura3-1 trp1-1 leu2-3,112 his3-11,15 can1-100 RAD5 ADE2 mt-GFP::LEU2 +PRS416-FZO1*	2E, S1E	This study
mdm30Δ PEX3-mCherry mt-GFP +pMDM30 (MCY1847)	W303 (MCY1842)	*Mata ura3-1 trp1-1 leu2-3,112 his3-11,15 can1-100 RAD5 ADE2 MDM30::KANMX6 mt-GFP::LEU2 Pex3-mCherry::NAT + PRS316-MDM30*	2E, S1D	This study
ole1Δ + pOLE1-9MYC (MCY1781)	W303 (MCY553)	*Mata ura3-1 trp1-1 leu2-3,112 his3-11,15 can1-100 RAD5 ADE2 OLE1::KANMX6 + PRS416-CYC-OLE1-9MYC*	S2C	This study
ole1Δ mt-GFP PEX3-mCherry + pOLE1 prom OLE1 (MCY1861)	W303 (MCY1781)	*Mata ura3-1 trp1-1 leu2-3,112 his3-11,15 can1-100 RAD5 ADE2 OLE1::KANMX6 mt-GFP::LEU2 PEX3-mCherry::NAT + PRS414-OLE1-OLE1*	3A,3D,3E	This study
ole1Δ mt-GFP PEX3-mCherry + pOLE1 prom CYC (MCY1863)	W303 (MCY1781)	*Mata ura3-1 trp1-1 leu2-3,112 his3-11,15 can1-100 RAD5 ADE2 OLE1::KANMX6 mt-GFP::LEU2 PEX3-mCherry::NAT + PRS414-CYC-OLE1*	3A,3D,3E	This study

ole1Δ mt-GFP PEX3-mCherry + pOLE1 prom TEF (MCY1865)	W303 (MCY1781)	*Mata ura3-1 trp1-1 leu2-3,112 his3-11,15 can1-100 RAD5 ADE2 OLE1::KANMX6 mt-GFP::LEU2 PEX3-mCherry::NAT + PRS414-TEF-OLE1*	3A,3D,3E	This study
ole1Δ FZO1-13MYC PEX3-6HA + pOLE1-9MYC (MCY1785)	W303 (MCY1488)	*Mata ura3-1 trp1-1 leu2-3,112 his3-11,15 can1-100 RAD5 ADE2 FZO1-13MYC::HIS5 PEX3-6HA::NAT OLE1::KANMX6 + PRS416-ADH OLE1-9MYC*	3B,3C	This study
mdm30Δ ole1Δ OM45-GFP RFP-SKL +pOLE1-9MYC (MCY1959)	W303 (MCY1490)	*MATα ura3-1 trp1-1 can1-100 RAD5 ADE2 OLE1::KAN OM45-EGFP::HIS RFP-SKL::LEU MDM30::NAT + PRSRS416-CYC-OLE1-9MYC*	3F, S2D	This study
mdm30Δ +pMDM30 (MCY970)	W303	*Mata ura3-1 trp1-1 leu2-3,112 his3-11,15 can1-100 MDM30::KANMX6 + PRS316-MDM30*	4B,4D,4E,6B, S2E, S2F, S4A	(Cavellini et al., 2017)
alpha SGA ready strain yMS721 (MCY1510)	BY4741	*MATα his3Δ1 leu2Δ0 met15Δ0ura3Δ0 can1Δ::STE2pr-spHIS5 lyp1Δ::STE3pr-LEU2*		gift from M. Schuldiner
yMS721 +pFZO1 (MCY1513)	BY4741 (MCY1510)	*MATα his3Δ1 leu2Δ0 met15Δ0ura3Δ0 can1Δ::STE2pr-spHIS5 lyp1Δ::STE3pr-LEU2 + PRS416-FZO1*	4C	This study
yMS721 mdm30Δ +pFZO1 (MCY1528)	BY4741 (MCY1510)	*MATα his3Δ1 leu2Δ0 met15Δ0ura3Δ0 can1Δ::STE2pr-spHIS5 lyp1Δ::STE3pr-LEU2 MDM30::NAT + PRS416-FZO1*	4C	This study
mdm30Δ acb1Δ +pMdm30 (MCY1612)	W303 (MCY970)	*Mata ura3-1 trp1-1 leu2-3,112 his3-11,15 can1-100 RAD5 ADE2 MDM30::KANMX6 ACB1::NAT + PRS316-MDM30*	4D, 6B, S2F	This study
mdm30Δ mls1Δ +pMDM30 (MCY1649)	W303 (MCY970)	*Mata ura3-1 trp1-1 leu2-3,112 his3-11,15 can1-100 RAD5 ADE2 MDM30::KANMX6 MLS1::NAT + PRS316-MDM30*	4E,6B, S2F, S4A	This study
ole1Δ OM45-GFP RFP-SKL +pOLE1-9MYC (MCY1899)	W303 (MCY1781)	*Mata ura3-1 trp1-1 leu2-3,112 his3-11,15 can1-100 RAD5 ADE2 OLE1::KANMX6 OM45-EGFP::HIS5 RFP-SKL::LEU2 + PRS416-CYC-OLE1-9MYC*	5A,5B,5C	This study
ole1Δ acb1Δ OM45-GFP RFP-SKL +pOLE1-9MYC (MCY1980)	W303 (MCY1899)	*Mata ura3-1 trp1-1 leu2-3,112 his3-11,15 can1-100 RAD5 ADE2 OLE1::KANMX6 OM45-EGFP::HIS5 RFP-SKL::LEU2 ACB1::NAT +PRS416-CYC-OLE1-9MYC*	5A,5B,5C, S3A	This study
ole1Δ mls1Δ OM45-GFP RFP-SKL +pOLE1-9MYC (MCY1987)	W303 (MCY1899)	*Mata ura3-1 trp1-1 leu2-3,112 his3-11,15 can1-100 RAD5 ADE2 OLE1::KANMX6 OM45-EGFP::HIS5 RFP-SKL::LEU2 MLS1::NAT +PRS416-CYC-OLE1-9MYC*	5A, S3B	This study
mdm30Δ mls1Δ icl1Δ +pMDM30 (MCY1911)	W303 (MCY970)	*Mata ura3-1 trp1-1 leu2-3,112 his3-11,15 can1-100 RAD5 ADE2 MDM30::KANMX6 MLS1::NAT ICL1::HIS5 +PRS316-MDM30*	6B, S4A	This study
ole1Δ mt-GFP +pOLE1-9MYC (MCY1835)	W303 (MCY1781)	*Mata ura3-1 trp1-1 leu2-3,112 his3-11,15 can1-100 RAD5 ADE2 OLE1::KANMX6 mt-GFP::LEU2 + PRS416-CYC-OLE1-9MYC*	6C,6D, S4B	This study
ole1Δ mls1Δ mt-GFP +pOLE1-9MYC (MCY1989)	W303 (MCY1835)	*Mata ura3-1 trp1-1 leu2-3,112 his3-11,15 can1-100 RAD5 ADE2 OLE1::KANMX6 mt-*	6C, S4B	This study

		GFP::LEU2 MLS1::NAT + PRS416-CYC-OLE1-9MYC		
ole1Δ icl1Δ mt-GFP +pOLE1-9MYC (MCY2002)	W303 (MCY1835)	*Mata ura3-1 trp1-1 leu2-3,112 his3-11,15 can1-100 RAD5 ADE2 OLE1::KANMX6 mt-GFP::LEU2 ICL1::NAT + PRS416-CYC-OLE1-9MYC*	6C, S4B	This study
ole1Δ mls1Δ icl1Δ mt-GFP +pOLE1-9MYC (MCY2003)	W303 (MCY1835)	*Mata ura3-1 trp1-1 leu2-3,112 his3-11,15 can1-100 RAD5 ADE2 OLE1::KANMX6 mt-GFP::LEU2 MLS1::NAT ICL1::HIS5 +p416-CYC-OLE1-9MYC*	6C, S4B	This study
mdm30Δ atp12Δ +pMDM30 (MCY1616)	W303 (MCY970)	*Mata ura3-1 trp1-1 leu2-3,112 his3-11,15 can1-100 RAD5 ADE2 MDM30::KANMX6 ATP12::NAT +PRS316-MDM30*	S2E	This study
mdm30Δ erv29Δ +pMDM30 (MCY1610)	W303 (MCY970)	*Mata ura3-1 trp1-1 leu2-3,112 his3-11,15 can1-100 RAD5 ADE2 MDM30::KANMX6 ERV29::NAT +PRS316-MDM30*	S2E	This study
mdm30Δ icl1Δ +pMDM30 (MCY1909)	W303 (MCY970)	*Mata ura3-1 trp1-1 leu2-3,112 his3-11,15 can1-100 RAD5 ADE2 MDM30::KANMX6 ICL1::HIS5 +PRS316-MDM30*	6B, S4A	This study
ole1Δ + pOLE1-9MYC (MCY1783)	W303 (MCY553)	*Mata ura3-1 trp1-1 leu2-3,112 his3-11,15 can1-100 RAD5 ADE2 OLE1::KANMX6 + PRS416-ADH-OLE1-9MYC*	S2A	This study
mdm30Δ +pMDM30 (MCY971)	W303	*MATα ura3-1 trp1-1 leu2-3,112 his3-11,15 can1-100 MDM30::KANMX6 + PRS316-MDM30*	4A	(Cavellini et al., 2017)
ole1Δ FZO1-13MYC PEX3-6HA +pOLE1-9MYC prom CYC (MCY1797)	W303 (MCY1781)	*Mata ura3-1 trp1-1 leu2-3,112 his3-11,15 can1-100 RAD5 ADE2 OLE1::KANMX6 + PRS414-CYC-OLE1-9MYC*	S2B	This study
ole1Δ FZO1-13MYC PEX3-6HA +pOLE1-9MYC prom MET25 (MCY1798)	W303 (MCY1781)	*Mata ura3-1 trp1-1 leu2-3,112 his3-11,15 can1-100 RAD5 ADE2 OLE1::KANMX6 + PRS414-MET25-OLE1-9MYC*	S2B	This study
ole1Δ FZO1-13MYC PEX3-6HA +pOLE1-9MYC prom ADH (MCY1796)	W303 (MCY1781)	*Mata ura3-1 trp1-1 leu2-3,112 his3-11,15 can1-100 RAD5 ADE2 OLE1::KANMX6 + PRS414-ADH-OLE1-9MYC*	S2B	This study
ole1Δ FZO1-13MYC PEX3-6HA +pOLE1-9MYC prom TEF (MCY1795)	W303 (MCY1781)	*Mata ura3-1 trp1-1 leu2-3,112 his3-11,15 can1-100 RAD5 ADE2 OLE1::KANMX6 + PRS414-TEF-OLE1-9MYC*	S2B	This study
ole1Δ cit2Δ mt-GFP +pOLE1-9MYC (MCY2023)	W303 (MCY1835)	*Mata ura3-1 trp1-1 leu2-3,112 his3-11,15 can1-100 RAD5 ADE2 OLE1::KANMX6 CIT2::NAT mt-GFP::LEU2 + PRS416-CYC OLE1-9MYC*	6D	This study

ole1Δ cat2Δ mt-GFP +pOLE1-9MYC (MCY2032)	W303 (MCY1835)	*Mata ura3-1 trp1-1 leu2-3,112 his3-11,15 can1-100 RAD5 ADE2 OLE1::KANMX6 CAT2::HIS5 mt-GFP::LEU2 +PRS416-CYC-OLE1-9MYC*	6D	This study
ole1Δ OM45-GFP RFP-SKL + pOLE1 prom CYC (MCY1936)	W303 (MCY1899)	*Mata ura3-1 trp1-1 leu2-3,112 his3-11,15 can1-100 RAD5 ADE2 OLE1::KANMX6 OM45-EGFP::HIS5 RFP-SKL::LEU2 +p414-CYC-OLE1-9MYC*	5B,5C	This study
ole1Δ OM45-GFP RFP-SKL + pOLE1 prom OLE1 (MCY1935)	W303 (MCY1899)	*Mata ura3-1 trp1-1 leu2-3,112 his3-11,15 can1-100 RAD5 ADE2 OLE1::KANMX6 OM45-EGFP::HIS5 RFP-SKL::LEU2 +p414-CYC-OLE1-9MYC*	S3C	This study

Supplementary Table 2: Plasmids used in this study.

Name	Description	Occurrence in the study	Reference
pRS314 (MC219)	CEN, *TRP1*, Amp	4A,4B,4D, 4E, 6B, S2A, S2D, S2E, S4A	(Sikorski and Hieter, 1989)
pRS416-FZO1 (MC322)	CEN, *FZO1 promoter FZO1*, URA3, Amp	FZO1 shuffling plasmid	(Griffin and Chan, 2006)
pRS314-FZO1 (MC250)	CEN, *FZO1 promoter FZO1 TRP1*, Amp	2E,4A,4B, 4D,4E,6B, S1E, S2D, S2E, S4A	(Cohen et al., 2011)
pRS314-FZO1S201N (MC544)	CEN, *FZO1 promoter FZO1S201N, TRP1*, Amp	2E,4B, S1E	(Cohen et al., 2011)
pRS316-MDM30 (MC331)	CEN, *MDM30 promoter MDM30*, *URA3*, Amp	MDM30 shuffling plasmid	(Cavellini et al., 2017)
pRS414-FZO1-13MYC (MC333)	CEN, *FZO1 promoter FZO1-13MYC*, *TRP1*, Amp	2A	(Cavellini et al., 2017)
pRS414-FZO1-S201N-13MYC (MC389)	CEN, *FZO1 promoter FZO1S201N-13MYC, TRP1*, Amp	2A	this study
pRS414-ADH GFP-link-Fzo1 (MC538)	CEN, *ADH promoter GFP-link-FZO1, TRP1*, Amp	2B	this study
pRS414-ADH GFP-link-FZO1S201N (MC539)	CEN, *ADH promoter GFP-link-FZO1S201N, TRP1*, Amp	2B	this study
pRS414-GFP-Link-FZO1 (MC261)	CEN, *FZO1 promoter GFP-Link-FZO1*, *TRP1*, Amp	2C,2D	this study
pRS414-GFP-Link-FZO1S201N (MC426)	CEN, *FZO1 promoter GFP-Link-FZO1S201N, TRP1*, Amp	2C,2D	this study
pRS416-CYC OLE1-9MYC (MC545)	CEN, *CYC promoter OLE1-9MYC, URA3*, Amp	Ole1 shuffling plasmid	this study
p416-ADH OLE1-9MYC (MC546)	CEN, *ADH promoter OLE1-9MYC, URA3*, Amp	Ole1 shuffling plasmid	this study
pRS414-MET25 OLE1-9MYC (MC536)	CEN, *MET25 promoter Ole1-9MYC, TRP1*, Amp	S2B	this study
pRS414-ADH OLE1-9MYC (MC 534)	CEN, *ADH promoter OLE1-9MYC, TRP1*, Amp	S2B	this study
pRS414-CYC OLE1-9MYC (MC535)	CEN, *CYC promoter OLE1-9MYC, TRP1*, Amp	S2B	this study
pRS414-TEF OLE1-9MYC (MC533)	CEN, *TEF promoter OLE1-9MYC, TRP1*, Amp	S2B	this study
pRS414-CYC OLE1 (MC540)	CEN, *CYC promoter OLE1, TRP1,* Amp	3A,3B,3C,3D,3E,3F,5A,5B,5C, 6C,6D, S2A,S2C, S2D,S3A, S3B,S4B	this study
pRS414-TEF OLE1 (MC541)	CEN, *TEF promoter OLE1, TRP1,* Amp	3A,3B,3C 3D,3E,3F,5A,5B,5C,6C,6D, S2A,S2C,S2D S3A,S3B,S4B	this study

pRS414-OLE1 OLE1 (MC543)	CEN, *OLE1 promoter OLE1, TRP1,* Amp	3A,3D,3E,3F,5A,5B,5C,6C,6D, S2A,S2C, S3A,S3B,S3C,S2D,S4B	this study
YIplac128 mRFP-SKL (MC547)	*FAA2 promoter mRFP-SKL, LEU2/INT*, Amp	Used for construction of *RFP-SKL* tagged strains	this study
YIplac128 mito-BFP (MC460)	*TEF promoter mito-BFP, LEU2/INT*, Amp	Used for construction of *mt-BFP* tagged strains	this study

BBA - Bioenergetics 1861 (2020) 148302

Contents lists available at ScienceDirect

BBA - Bioenergetics

journal homepage: www.elsevier.com/locate/bbabio

The regulation of mitochondrial homeostasis by the ubiquitin proteasome system

Cynthia Alsayyah, Oznur Ozturk, Laetitia Cavellini, Naïma Belgareh-Touzé, Mickael M. Cohen*

Sorbonne Université, CNRS, UMR8226, Institut de Biologie Physico-Chimique, Laboratoire de Biologie Moléculaire et Cellulaire des Eucaryotes, F-75005 Paris, France

ARTICLE INFO

Keywords:
Mitochondria
Ubiquitin
Proteasome
Mitochondrial fusion
Mitophagy
Mitochondrial quality control

ABSTRACT

From mitochondrial quality control pathways to the regulation of specific functions, the Ubiquitin Proteasome System (UPS) could be compared to a Swiss knife without which mitochondria could not maintain its integrity in the cell. Here, we review the mechanisms that the UPS employs to regulate mitochondrial function and efficiency. For this purpose, we depict how Ubiquitin and the Proteasome participate in diverse quality control pathways that safeguard entry into the mitochondrial compartment. A focus is then achieved on the UPS-mediated control of the yeast mitofusin Fzo1 which provides insights into the complex regulation of this particular protein in mitochondrial fusion. We ultimately dissect the mechanisms by which the UPS controls the degradation of mitochondria by autophagy in both mammalian and yeast systems. This organization should offer a useful overview of this abundant but fascinating literature on the crosstalks between mitochondria and the UPS.

1. Introduction

Mitochondria constitute an extended tubular network which is maintained by an equilibrium between ongoing fusion and fission events of their outer and inner membranes [1]. These dynamics are crucial for life since they allow mitochondrial morphology adapting to the energy needs of the cell [2] as well as the maintenance of the redox potential, which is the main role of mitochondria [3]. The mitochondrial network indeed provides the cell with ATP, a form of energy currency generated by oxidative phosphorylation through complexes of the electron transport chain and the ATP synthase lodged in the cristae of the mitochondrial inner membrane [4]. In addition to this oxidative phosphorylation process and a myriad of biochemical pathways [5], mitochondria are involved in ageing and developmental processes [6,7]. Mitochondria are also semi-autonomous organelles as they harbor their own DNA. However, mitochondria rely on nuclear DNA as the 13 mtDNA encoded polypeptides are restricted to subunits of the oxidative phosphorylation system [8]. Nuclear encoded mitochondrial proteins are synthetized as precursors on cytosolic ribosomes before entering mitochondria through the TOM (Translocase of Outer Membrane) and TIM (Translocase of inner membrane) complexes [9]. Consequently, the quality of these imported proteins is tightly regulated in the cytosol to avoid any mitochondrial dysfunction.

The first line of defense to protect mitochondria in all eukaryotes are molecular chaperones, such as HSP70 and HSP90, which usher import-competent unfolded proteins and protect them from non-specific interactions [10–13]. Once they have reached their destination, proteins targeted to mitochondria enter *via* TOM and TIM, the two main channels embedded in both mitochondrial membranes [14]. Chaperones are also present inside mitochondria to ensure proper folding before and after import or acute stress [15–18].

The second line of defense heavily relies on several mitochondrial proteases to sustain mitochondrial homeostasis and prevent accumulation of damaged proteins that could lead to mitochondrial dysfunction [19]. Whether in yeast or humans, all mitochondrial compartments have their specific proteases with the exception of outer membranes for which protein degradation relies almost exclusively on the cytosolic Ubiquitin Proteasome System (UPS) [20].

When all of these coping and defense mechanisms fail to preserve mitochondria and cellular homeostasis is compromised, damaged mitochondria need to be eliminated. Some damaged mitochondrial components can be eliminated by mitochondria-derived vesicles or MDVs in mammals [21]. Nonetheless, a different death sentence awaits whole mitochondria in all kingdoms of life. Impaired mitochondria are first “rejected” and separated from the rest of the mitochondrial network by mitochondrial fission events [22]. These dissociated mitochondria will in turn be cleared by mitophagy, a mechanism of autophagy dedicated to mitochondria that has strong links with the UPS in metazoans but

* Corresponding author.
E-mail address: cohen@ibpc.fr (M.M. Cohen).

https://doi.org/10.1016/j.bbabio.2020.148302
Received 11 June 2020; Received in revised form 5 August 2020; Accepted 24 August 2020
Available online 27 August 2020
0005-2728/

also in yeast.

The objective of this chapter will thus consist in reviewing the mechanisms that the UPS employs to regulate mitochondrial function and efficiency. For this purpose, the review will be organized in three main sections: In the first part, we will depict how Ubiquitin and the Proteasome participate in diverse quality control pathways that safeguard entry into the mitochondrial compartment in both vegetative and stress conditions. In the second part, we will focus on the regulation of the yeast mitofusin Fzo1 by the UPS which will provide a clear example of the complexity that underlies the function of this particular protein in mitochondrial fusion and its intimate crosstalk with Ubiquitin. In the third and final section, we will dissect the mechanisms by which the UPS controls mitophagy in both mammalian and yeast systems. This organization should *in fine* offer a useful overview of these processes and will provide some clarification on this abundant but altogether fascinating literature.

2. The ubiquitin proteasome system and mitochondrial quality control

Ubiquitin is a small polypeptide of 76 amino acids that covalently links to other polypeptides or to itself to form chains that can get disassembled, like "Lego" pieces. This process of ubiquitination involves a multistep enzymatic cascade [23] where, at least, 3 distinct enzymes participate in attaching one or more ubiquitin subunits to lysine residues of a target protein [24,25]. The three types of enzymes driving this reaction include a single ubiquitin activating enzyme E1, several ubiquitin-conjugating enzymes E2s and even more ubiquitin ligase E3s which contribute to the broad substrate specificity of ubiquitination (Fig. 1). Once ubiquitin gets activated by the E1, it is next transferred to the cysteine residue of an E2 through a thioester bond [26]. The E3 then facilitates the transfer of the ubiquitin from the E2 to the lysine residue of the target substrate through an isopeptide linkage (Fig. 1). This transfer occurs directly from the E2 to the substrate with RING (Really Interesting New Gene)-domain E3s. With HECT (Homologous to the E6-AP Carboxyl Terminus) or RBR (Ring Between Ring)-domain E3s, ubiquitin is first conjugated to the catalytic cysteine of the E3 through a thio-ester linkage before conjugation to the lysine of the target substrate [27]. Importantly, Ubiquitin contains 7 lysine residues (K6, 11, 27, 29, 33, 48, 63) and an amino terminus which allows the formation of polymeric ubiquitin chains [28]. A myriad of combinations of ubiquitin linkages are thus possible, many of which leading to distinct outcomes [29,30]. For instance, K63-linked poly-ubiquitin chains can regulate the subcellular localization of target molecules, their affinity to partner proteins and/or their activity [29,31,32]. In contrast, K48-linked ubiquitination leads to the degradation of target substrates by the 26S proteasome, a multi-subunit enzyme complex that breaks down peptide bonds in its proteolytic core [33]. Thus, the Ubiquitin proteasome system (UPS) is a primary cytosolic "predator" of misfolded and damaged proteins.

The most thoroughly studied and best understood protein quality control by the UPS takes place at the ER. In this ER Associated Degradation (ERAD) pathway found in both yeast and mammalian systems, damaged proteins are retro-translocated from the ER and ubiquitinated thereby allowing their extraction from the membrane and their ultimate degradation by the cytosolic proteasome [34]. Mitochondrial Associated Degradation (MAD) is a similar quality control system that takes place at the mitochondrial outer membrane [35] and its main actors are most often conserved throughout evolution. MAD is thought to employ the same machinery as ERAD to extract proteins from the outer membrane and trigger their degradation by the UPS [36]. This machinery relies on the essential AAA-ATPase Cdc48, one of the most abundant cellular proteins, highly conserved in all eukaryotes (p97 in mammals). In yeast, Cdc48 works in concert with several identified co-factors including Ufd1, Npl4, Ubx2 and Doa1 in both ERAD and MAD [36–40] to recognize poly-ubiquitinated substrates, dissociate them from their protein complexes or respective membranes and allow their turnover by the proteasome [41,42].

In vegetative conditions, yeast and mammalian chaperones (such as HSP70 and HSP90) ensure correct folding and escort of proteins on their transit to mitochondria (Fig. 2, Panel I). In *Saccharomyces cerevisiae*, efficient mitochondrial import also relies on the continuous

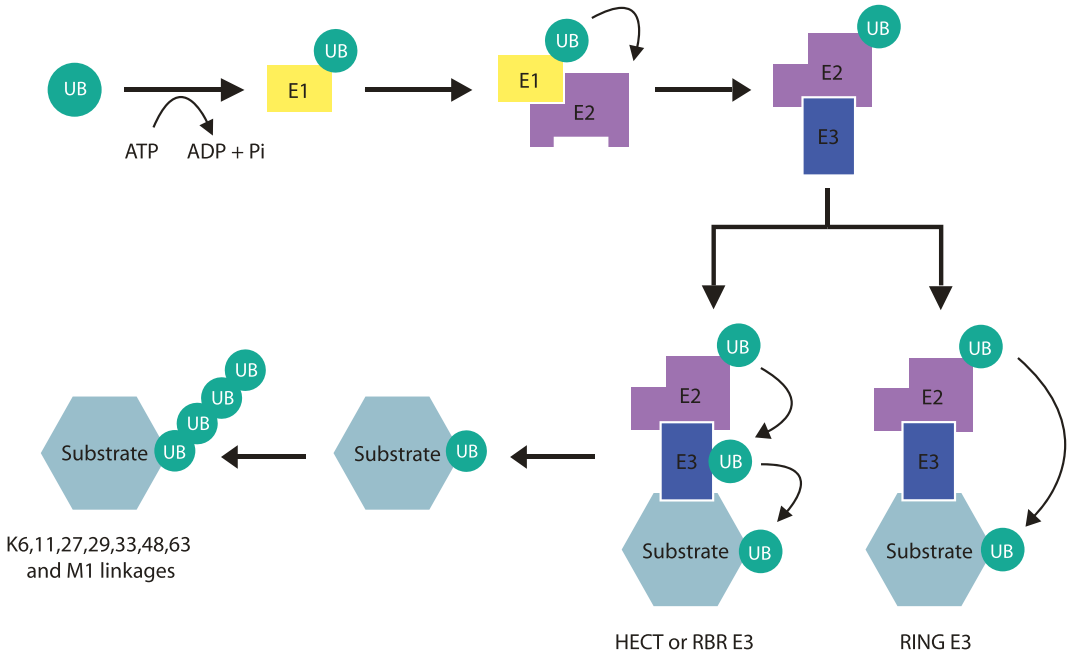

Fig. 1. The Ubiquitination cascade. An ubiquitin activating enzyme E1, promotes a thioester bond between the C-terminus of ubiquitin and the catalytic cysteine of a conjugating enzyme E2. The ubiquitin ligase then links the loaded E2 to a specific substrate. The direct (RING E3s) or sequential (HECT or RBR E3s) transfer of ubiquitin from the E2 to the substrate then induces the formation of an isopeptide bond between the C-terminus of ubiquitin and a target lysine of the substrate. With its seven lysines or its N-terminal methionine, ubiquitin can itself be the target of the ubiquitination cascade. This results in the formation of chains with diverse ubiquitin linkages that can trigger very distinct functions.

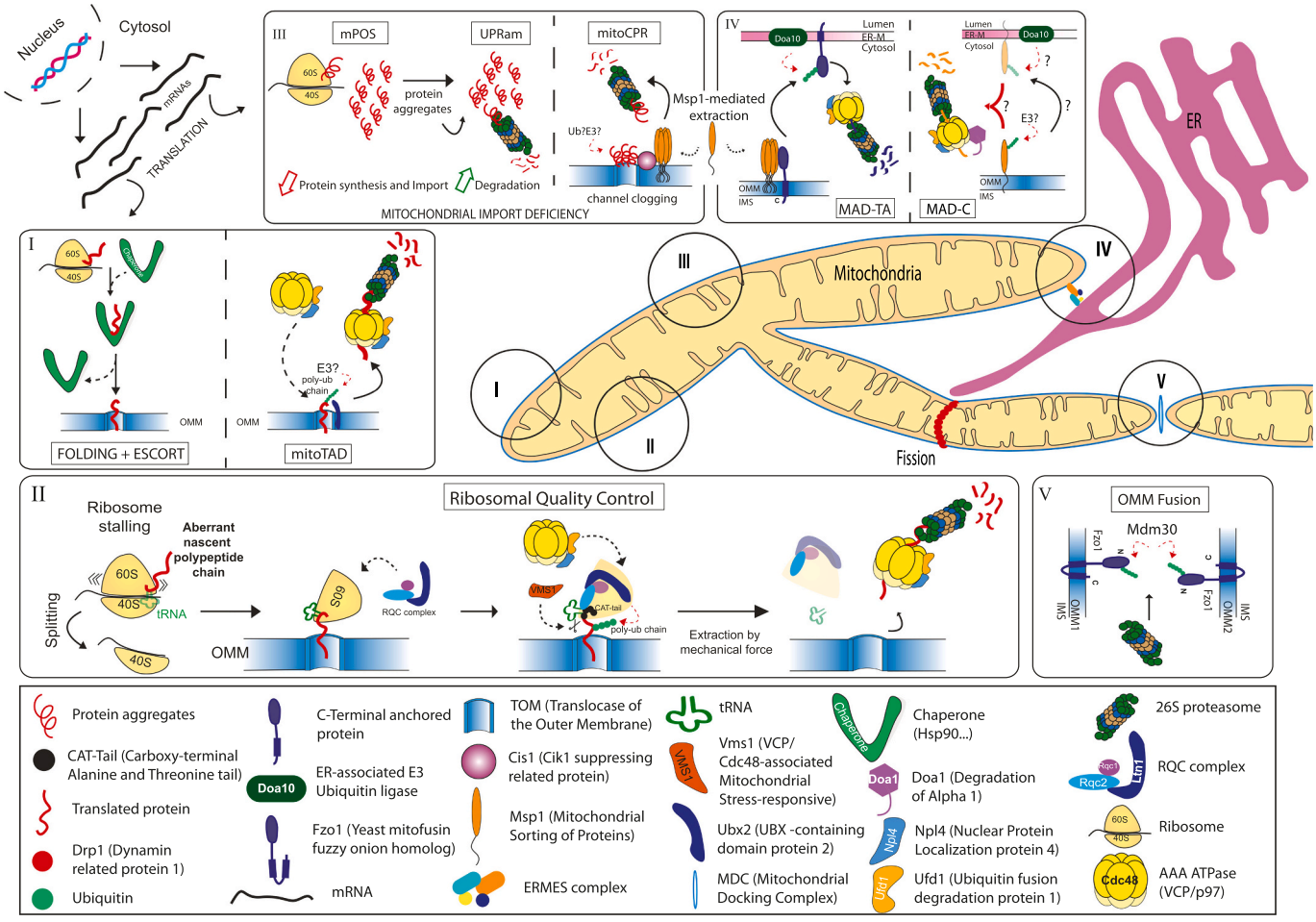

Fig. 2. UPS-mediated degradation at the mitochondrial outer membrane. Mitochondrial morphology is maintained by ongoing events of fusion and fission and intimate contacts with the ER. The UPS, through E3s that are known (Ltn1, Doa10, Mdm30) or yet to be identified, safeguards the transport of proteins inside the organelle but also specific proteins embedded in outer membranes. (I) In the absence of cellular stress, proteins encoded by the nuclear genome are synthesized, folded and escorted to mitochondria. Import through the TOM complex is continuously monitored by the TOM Associated Degradation (mitoTAD) pathway. (II) Upon ribosomal stalling, the Ribosomal Quality Control (RQC) pathway is activated which also prevents clogging of the TOM channel. (III) When the level of stress increases and the mitochondrial import is inhibited, the mitochondrial Precursor Over-accumulation Stress (mPOS) initiates the Unfolded Protein Response Activated by the mis-targeting of proteins (UPRam) which allows clearance of protein aggregates. If clogging of the TOM channel persists, the Mitochondrial Compromised Protein import Response (mitoCPR) is activated. (IV) Two Mitochondrial Associated Degradation (MAD) pathways that may share some common features also target mis-targeted Tail Anchored proteins (MAD-TA) and C-terminally anchored outer membranes proteins (MAD-C). (V) The yeast mitofusin Fzo1 is regulated by the UPS during Outer Mitochondrial Membrane (OMM) fusion.

monitoring of the TOM channel by a specific kind of MAD where the TOM channel constitutively interacts with the Cdc48 adaptor Ubx2 [43]. In this mitochondrial Translocation Associated Degradation (mitoTAD) pathway, proteins that clog the TOM import channel are ubiquitinated and recognized by a mitochondrial pool of Ubx2 which promotes their extraction by the Cdc48-Ufd1-Npl4 complex and their degradation by the proteasome (Fig. 2, Panel I).

Given that the majority of mitochondrial proteins are synthesized by cytosolic ribosomes, it is also important that the translation products remain under surveillance by a Ribosomal Quality Control (RQC) system in order to maintain mitochondrial homeostasis [44,45]. Consistent with this, Cdc48 and its cofactors Npl4 and Ufd1 are also involved in this process (Fig. 2, Panel II). Upon translation stalling, ribosomes split resulting in a 60S subunit, which remains bound to the nascent polypeptide chain [46]. The RQC complex composed of Rqc1, Rqc2, Cdc48 and the Ubiquitin ligase Ltn1 (Listerin in mammals) [47] is then recruited (Fig. 2, Panel II). Rqc2 binds charged t-RNAs that induce the elongation of nascent polypeptide chains with C-terminal Alanine and Threonine residues (CAT-tailing) [48]. This elongation exposes lysine residues of the incomplete chain that is ubiquitinated by the Ltn1 ubiquitin ligase [49,50]. The peptidyl-tRNA hydrolase Vms1 (ANKZF1 in mammals) then triggers the release of the CAT-tailed peptide from the tRNA [51,52] and Rqc1 recruits the Cdc48-Npl4-Ufd1 complex for extraction from the 60S ribosome and subsequent degradation by 26S proteasomes [53]. Notably, the released polypeptides can be successfully ubiquitinated and degraded by the 26S proteasome but they can also form CAT-tail dependent aggregates in the cytosol [54,55]. This RQC system has mainly been investigated in yeast but the conservation of most RQC components in metazoans favors an overall similar quality control in mammalian ribosomes [45].

Upon stress or when mitochondrial protein import is defective in *Saccharomyces cerevisiae*, mitoprotein-induced stress responses are triggered (Fig. 2, Panel III), all coordinated by a transcriptional regulatory pathway [56]. The accumulation of mitochondrial protein aggregates in the cytosol (mPOS, Mitochondrial Precursor Over-accumulation) reduces protein synthesis and import [57]. This accumulation activates the UPRam (Unfolded Protein Response activated by the mis-targeting of proteins) inducing the degradation of the protein aggregates by the 26S proteasome [58]. Ultimately, when the TOM channel is clogged by yeast protein aggregates, the Mitochondrial

Compromised Protein import Response (mitoCPR) is activated [59]. In this process, Cis1 recruits the AAA-ATPase Msp1 (ATAD1 in mammals) to the TOM70 receptor in order to remove non-imported precursor proteins that will subsequently be degraded by the proteasome (Fig. 2, Panel III). While all these processes have been identified in yeast, their conservation in mammals awaits clear analysis. Whether ATAD1 has the same role as Msp1 in mitoCPR is for instance yet to be investigated.

However, ATAD1 in human and mouse seems to have a similar role as yeast Msp1 in the Mitochondrial Associated Degradation of Tail Anchored proteins (MAD-TA). During MAD-TA (Fig. 2, Panel IV), tail anchored proteins that are mis-targeted to mitochondria are recognized by Msp1/ATAD1 which allows their extraction and degradation in the cytosol [60–62]. In *Saccharomyces cerevisiae*, Msp1 is thought to have the capacity to extract and transfer TA-proteins from the outer membrane to the ER at mitochondria-ER contact sites while the ERMES complex, the main ER-mitochondria tether in yeast [63], does not seem required for this function [64,65]. Once embedded in ER membranes TA-proteins are treated as ERAD substrates, which includes ubiquitination by the ERAD E3 Doa10, extraction by the Cdc48-Ufd1-Npl4 complex and degradation by cytosolic proteasomes [64,65]. Whether ATAD1 promotes degradation of TA-proteins by ERAD in mammals remains unknown.

Similar to Npl4, Ufd1 or Ubx2, Doa1 is yet another Cdc48 cofactor previously implicated in yeast ERAD that has been implicated in MAD. In the so called MAD-C pathway (Fig. 2, Panel IV), the Cdc48-Doa1 complex was shown to participate in the proteasomal degradation of diverse substrates such as the yeast mitofusin Fzo1, the ERMES component Mdm34, the import complex protein Tom70 and even the AAA-ATPase Msp1 [40]. Their extraction from the outer membrane and direct degradation by the proteasome has been postulated but, as we will see later in this review, their processing by a MAD-TA like pathway cannot be ruled out (Fig. 2, Panel IV).

All together, we have listed the numerous UPS-dependent quality control and defense mechanisms guarding mitochondrial homeostasis and integrity. The substrates of these mechanisms are diverse, ranging from misfolded to transmembrane proteins located on the mitochondrial surface but also within mitochondria, on the inner membrane and even the cristae [66,214–218]. However, within these potential substrates for UPS-mediated degradation, Mitofusins represent a specific category of mitochondrial proteins that stands out in most pathways described above.

3. Ubiquitination of the yeast mitofusin Fzo1

3.1. UPS-mediated control of Fzo1 by Mdm30

Mitofusins are conserved throughout evolution and belong to the Dynamin family of large GTPases [67–69]. Embedded in mitochondrial outer membranes, their primary role is to mediate anchoring and initiate homotypic fusion of mitochondria (Fig. 2, Panel V). Two mitofusins, MFN1 and MFN2, are expressed in mammals and both are essential for fusion of mitochondrial outer membranes [70–73]. However, while mutation of MFN2 is causal in the Charcot Marie-Tooth Type 2A (CMT2A) disease, similar mutations in MFN1 are not [74–77]. UPS regulation of metazoan mitofusins (MFN1 and MFN2) is fundamental in mitophagy (see Section 3) whereas the sole yeast mitofusin Fzo1 may be a degradation substrate in several of the pathways mentioned Section 1 (see below). Moreover, Mdm30-mediated ubiquitination of Fzo1 is central to the process of mitochondrial fusion (Fig. 2, Panel V).

Benedickt Westermann and colleagues identified the F-box protein Mdm30 as an important regulator of mitochondrial fusion in yeast [78]. In this seminal study, deletion of *MDM30* was demonstrated to inhibit mitochondrial fusion leading to a particular phenotype of mitochondrial aggregation. Moreover, Fzo1 was found to accumulate in the absence of the F-box protein. Mdm30 was subsequently confirmed to promote degradation of Fzo1 [79]. However, while F-box domain proteins were known to act as substrate recognition elements of multisubunit SCF ubiquitin ligases [80–82], it was proposed that the SCF, Ubiquitin, or the proteasome were not involved in the Mdm30-dependent turnover of the yeast mitofusin [79]. Two years later, this interpretation was radically challenged as the SCF and the proteasome were shown to participate in the Mdm30-mediated degradation of Fzo1 and the yeast mitofusin was unequivocally demonstrated to be ubiquinated by the SCFMdm30 ubiquitin ligase [83]. Ultimately, the UPS-dependent control of Fzo1 reached a consensus [84,85]. The straightforward conclusions of this set of studies was that Mdm30 is part of an SCF E3 that promotes ubiquitination of Fzo1 and its subsequent degradation by the proteasome [78,83]. In this context, Fzo1 accumulation would block mitochondrial fusion resulting in the mitochondrial aggregation phenotype seen in *MDM30* null cells [78,79,83].

In 2005, Albert Neutzner and Richard Youle discovered that Fzo1 is subject to proteasomal degradation upon extended treatment with the alpha factor mating pheromone [86]. Mdm30 was excluded from inducing this degradation. Moreover, Mdm30-mediated ubiquitination of Fzo1 is detected in vegetative condition, indicating that this vegetative turnover of Fzo1 is very distinct from that observed upon alpha-factor treatment.

Importantly, the Mdm30-dependent ubiquitination of the yeast mitofusin depends on the integrity of the Fzo1 GTPase domain (Fig. 3A). The V327T mutation in the GTPase domain of Fzo1, which is analogous to the CMT2A I213T mutation in the GTPase domain of MFN2, was shown to decrease the turnover of Fzo1 by Mdm30 [87]. Shortly after, a set of four additional mutations in the GTPase domain of Fzo1 (K200A, S201N, T221S and D195A) was found to induce total abolishment of the Mdm30-mediated ubiquitination and degradation of Fzo1 [84,85]. Notably, full length Fzo1 K200A, S201N and T221S do not bind Mdm30, which explains their stability and lack of ubiquitination [85]. Mdm30 was further demonstrated to bind the N-terminal half of Fzo1 whether or not the S201N mutation was introduced in the GTPase domain of this N-terminal truncated portion [85]. In contrast, Mdm30 did not bind the HR1-HR2 containing C-terminal half of Fzo1 (Fig. 3B). This set of observations pointed to a model in which the binding site of Mdm30 in the N-terminal half of full length Fzo1 is hindered by the C-terminal half. The activity of the GTPase domain would then induce a conformational switch of Fzo1 that would allow the recruitment of Mdm30 (Fig. 3C).

The conformational switch of mitofusins has yet to be experimentally observed but it is currently thought to take place during mitochondrial tethering, in the course of mitofusin auto-oligomerization in *trans* [69,88]. Consistent with this, multiple observations pointed to the requirement of Mdm30-dependent ubiquitination and degradation of Fzo1 during mitochondrial attachment [84,85]. Furthermore, employment of the N-end rule pathway was used to bypass the requirement of Mdm30 in mitochondrial fusion and Fzo1 degradation [85]. This allowed demonstrating that it is the ongoing turnover of Fzo1 that is important to maintain efficient mitochondrial fusion rather than the simple regulation of Fzo1 steady state levels.

3.2. Role of the UPS in mitochondrial fusion

When this set of studies was published, roughly ten years ago, it was difficult to conceive that the multimeric SCFMdm30 ubiquitin ligase and the 3000 kDa 26S proteasome could access Fzo1 oligomers at the junction of anchored mitochondria. Since Fzo1 is essential for fusion of mitochondrial outer membranes [89–91], it was also difficult to understand why the mitofusin needs to be degraded for fusion to proceed. Nonetheless, recent structural observations of the mitofusin-mediated membrane fusion process provide significant novel insights on these issues [69,76,92–96].

Mitochondrial tethering and ultimate fusion of outer membranes have been shown to occur through successive steps [96]. It was shown that outer membranes of two attached mitochondria are initially

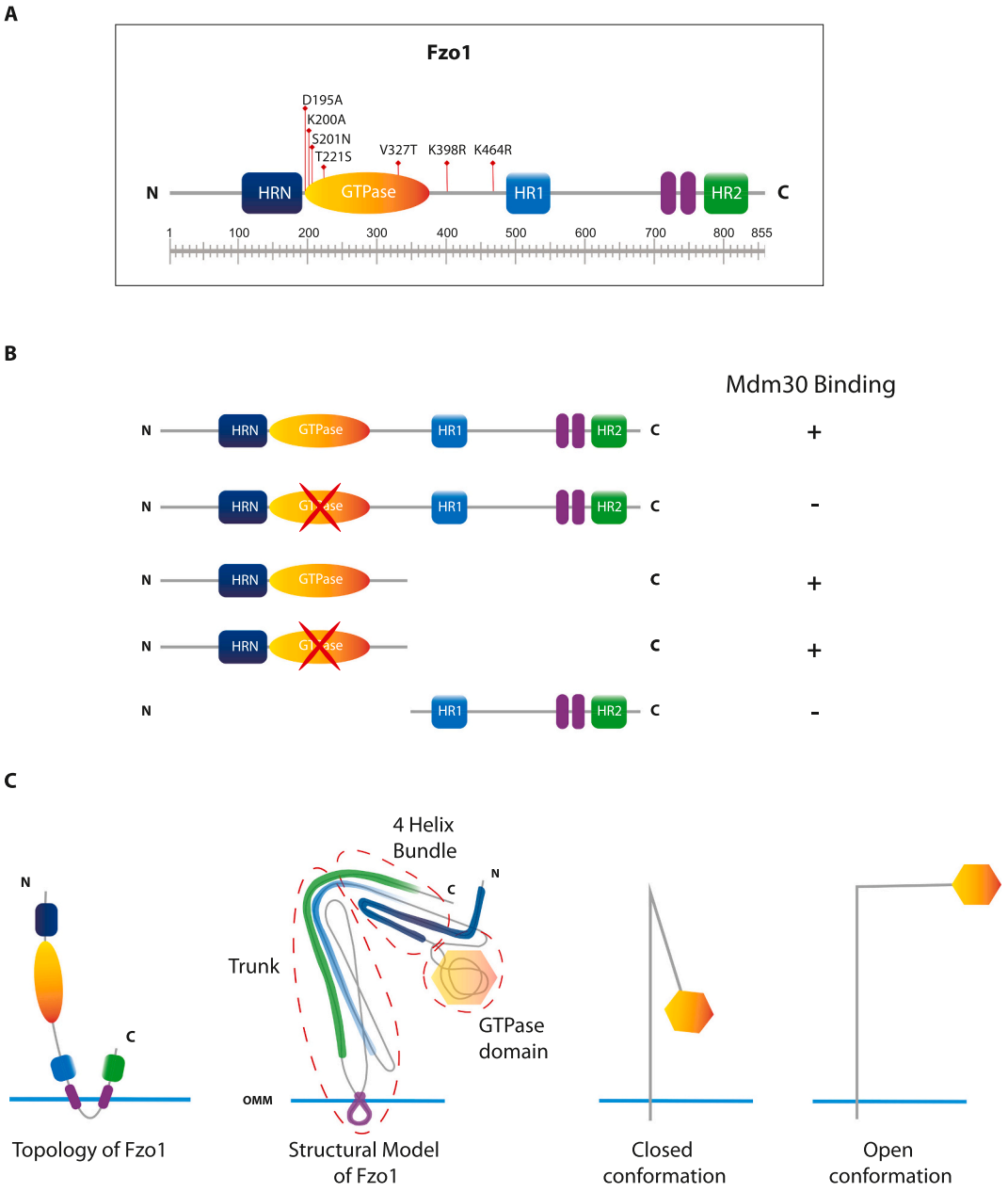

Fig. 3. The yeast mitofusin Fzo1 and its binding to Mdm30. (A) Fzo1 includes a bipartite transmembrane domain (purple) that allows exposure of its N- and C-terminal extremities in the cytoplasm. The GTPase domain (yellow-orange) and Heptad Repeat regions HRN, HR1 (blue) and HR2 (green) are indicated. All point mutations mentioned in the main text are also indicated. The scale at the bottom indicates the precise location of each domain. (B) Capacity of Mdm30 to bind distinct versions of Fzo1. When the GTPase domain is mutated (red cross), Mdm30 does not bind full-length but does bind the N-terminal half of Fzo1 as shown in [85]. This suggests a conformational switch where the GTPase domain promotes displacement of the C-terminal half which allows access of Mdm30 to the N-terminal half of Fzo1. (C) From left to right: Topology of Fzo1 on the mitochondrial outer membrane; Structural model of Fzo1 as described in [94]; The colors indicate the positions of the HRN, HR1, HR2, TMs and GTPase domains. The four-helix bundle and the trunk of Fzo1 formed in the model are highlighted; Schemes of closed and opened conformations of Fzo1 based on the structural model. The GTPase domain would induce displacement of the four-helix bundle relative to the trunk to yield the opened conformation of Fzo1. Mdm30 would bind the opened but not the closed conformation of Fzo1.

tethered by Fzo1-containing globular protein repeats (Fig. 4A, Tethering stage). Successive cycles of GTP hydrolysis by mitofusins then allow the fusion process to evolve toward a mitochondrial docking step (Fig. 4A, Docking stage). Docked intermediates are characterized by a docking ring of protein densities that surrounds areas where outer membranes are separated by less than 3 nm. The fusion of bilayers is then initiated by further GTP hydrolysis in the path of the docking ring where the outer membrane curvature is presumably most pronounced (Fig. 4A, Local membrane fusion stage). This set of observations suggests that the formation of Fzo1 oligomers of increasing sizes through successive cycles of GTP binding and hydrolysis progressively brings outer membranes closer from each other and culminates in formation of the docking ring complex which allows fusion at one critical point of membrane curvature. In this context, the requirement for regulated assembly of Fzo1 oligomers by the UPS during formation of the docking ring becomes amenable to speculation.

Fzo1 is proposed to dimerize in *cis* (on the same membrane) and the resulting *cis*-dimers to engage in *trans*-oligomerization (from opposing membranes) to mediate mitochondrial attachment [84]. Based on several structural insights on mitofusins and other dynamins, Fzo1 *cis*-

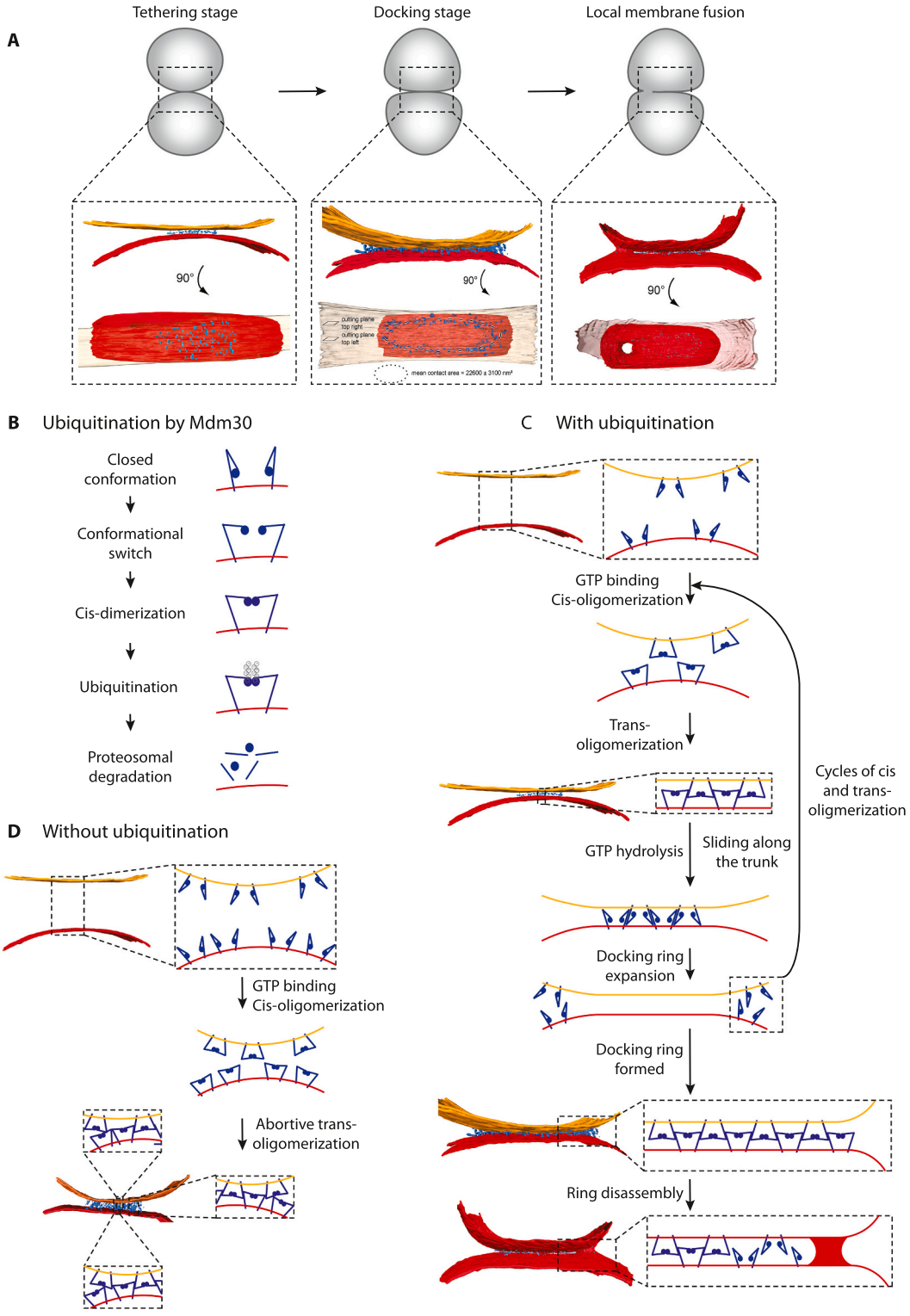

Fig. 4. A mechanistic model of outer membrane fusion and its regulation by the UPS. (A) *In vitro* mitochondrial attachment and fusion as observed by cryo-ET (see main text). 3D renderings of attached outer membranes (in red and yellow) at distinct stages of the fusion process are shown. Protein densities are depicted in blue. These data are from Brandt et al. [96]. (B) Cis-dimerization of Fzo1 and ubiquitination by Mdm30. Fzo1 is depicted as the 3D model described in DeVecchis et al. [94] Its conformational switch and cis dimerization is depicted as in Brandner et al. [97]. Mdm30 would promote ubiquitination and degradation of free cis-dimers in which Fzo1 has undergone its conformational switch. (C) Cis-dimerization of Fzo1 after GTP binding would induce membrane tethering through the formation of Fzo1 trans-oligomers as described in Brandner et al. [97]. GTP hydrolysis within the oligomers would bring membranes closer together followed by the dissociation of Fzo1 molecules that would redistribute at the edge of this region of close apposition. Successive cycles of GTP binding and hydrolysis would culminate in the extension of the surface of apposition surrounded by the docking ring composed of a macromolecular Fzo1 trans-oligomer. The ultimate cycle would induce fusion where membrane curvature is most pronounced concomitant with dissociation of the docking ring. (D) In the absence of Mdm30, Fzo1 cis-dimers would be stabilized which would perturb the regulated assembly of trans-oligomers thereby resulting in abortive complexes that inhibit formation of the docking ring and block outer membrane fusion as upon Fzo1 overexpression in Brandt et al. [96].

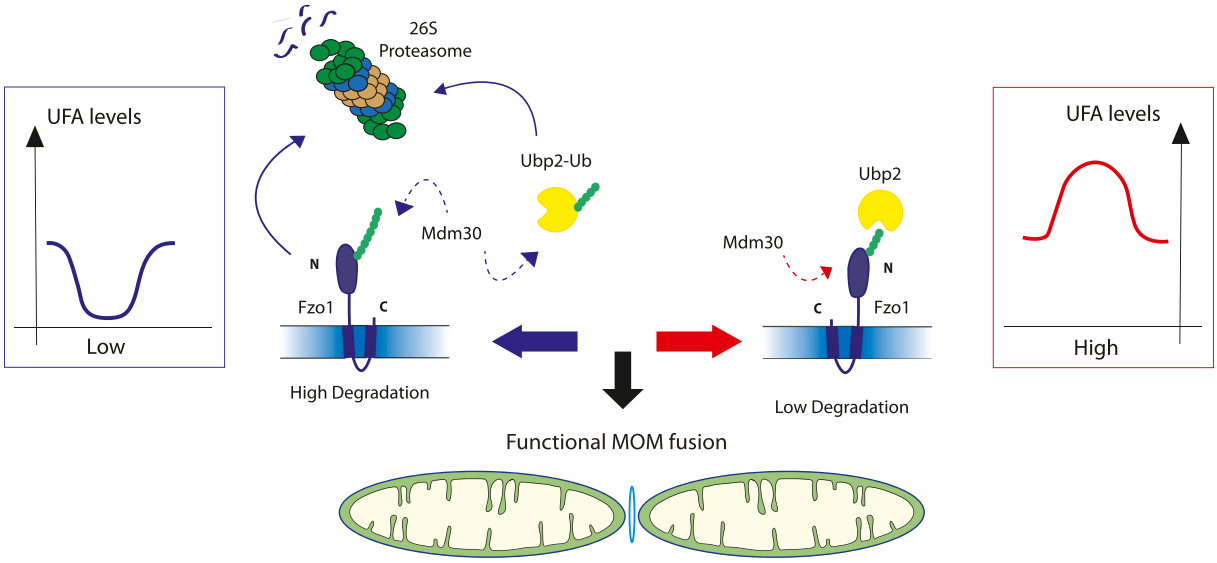

Fig. 5. Mitochondrial fusion is regulated by a balance between Fzo1 degradation and the desaturation of fatty acids. When the desaturation of fatty acids is low (low UFA), mitochondrial fusion is efficient if the degradation of Fzo1 is high. For this purpose, Ubp2 is ubiquitinated by Mdm30, which induces its degradation by the proteasome. Mdm30-mediated ubiquitination of Fzo1 is not antagonized which allows extension of ubiquitin chains and efficient proteasomal degradation of the mitofusin. When the desaturation of fatty acids is high (high UFA), mitochondrial fusion is efficient if the level of Fzo1 is also high. For this purpose, the ubiquitination of Fzo1 by Mdm30 is antagonized by Ubp2 which limits the extension of ubiquitin chains and decreases the degradation of the mitofusin. At the bottom, efficient mitochondrial outer membrane (MOM) fusion is symbolized by formation of the Docking ring.

dimers and *trans*-oligomers were recently modelled [97]. It was thereby suggested that the docking ring could form with cis dimers interacting through their GTPase domain (Fig. 4B and C) and *trans* oligomers assembling through the available trunks of the dimers (Fig. 4C). GTP hydrolysis within these oligomers would induce Fzo1 sliding along its trunk thus bringing opposing outer membranes closer from each other. Additional cycles of *cis*-dimerization and *trans*-oligmerization around this initial site would result in formation and expansion of the docking ring at the periphery of the increasing contact area (Fig. 4C). In this system, Fzo1 *cis*-dimers that did not engage in *trans*-oligomerization at the initial site of tethering may instead nucleate additional sites of anchoring that would perturb the proper assembly of the docking ring and result in abortive fusion (Fig. 4D). Consistent with this possibility, overexpression of Fzo1 increases mitochondrial tethering but abrogates formation of the docking ring and inhibits outer membrane fusion [96]. In this context, free Fzo1 dimers may be targeted for ubiquitination as their respective monomers have operated the conformational switch required for Mdm30 binding [85]. These dimers would subsequently be cleared by proteasomal degradation (Fig. 4B). As outer membranes get closer together and the docking ring assembles, the ongoing Mdm30-mediated proteasomal degradation of free Fzo1 dimers would favor productive mitochondrial docking and ultimate fusion of outer membranes (Fig. 4C).

3.3. Regulation of Mdm30-mediated ubiquitination of Fzo1

3.3.1. Target lysines and ubiquitin proteases

The proposed model of Fzo1 oligomerization and resulting role of Fzo1 degradation in mitochondrial fusion above remains speculative, which warrants additional efforts and discoveries on this topic. In parallel, whether Mdm30-mediated ubiquitination and degradation of Fzo1 is constitutive or whether it is itself regulated needs to be addressed. In this regard, Fzo1 was shown to be ubiquitinated on two distinct lysine residues (K464 and K398, Fig. 3A) and proposed to be regulated by two distinct ubiquitin proteases, Ubp2 and Ubp12 [98]. It was thereby suggested that Ubp2 antagonizes the ubiquitination of Fzo1 promoted by an unknown ubiquitin ligase involved in mitochondrial quality control whereas Ubp12 triggers the Mdm30-mediated ubiquitination on K464 and K398 of Fzo1 to regulate mitochondrial fusion [98].The mutation of K398 and K464 into Arginine (Fig. 3A) led to the interpretation that K464 is essential for Fzo1 ubiquitination whereas K398 is not essential but required for formation of the normal pattern of Mdm30-mediated ubiquitination [98]. Consistent with these assumptions, respiration was strongly decreased by the K398R mutation of Fzo1 but totally abolished by the K464R mutation. This led to propose that Fzo1 ubiquitination is primed on K464 and then transferred on K398 [98]. Yet, the possibility that K464R alters Fzo1 structure and abolishes its function was not evaluated. K464 was later found to be involved in the establishment of a disulfide bridge with D335 within the Fzo1 whole polypeptide [94]. In particular, swap charge mutations between the two residues demonstrated the importance of this K464-D335 bridge for Fzo1 function [94]. These observations thus revealed that the K464R mutation does not abolish Fzo1 function because of ubiquitination inhibition but does so because of Fzo1 structural defects.

Regarding the role of ubiquitin proteases, inactivation of Ubp2 induced very fast degradation of Fzo1 and consequently very low levels of the mitofusin, which was accompanied with a phenotype of high mitochondrial fragmentation and markedly decreased respiration [98]. In contrast, the inactivation of Ubp12 had very weak phenotypes with a slight increase in Fzo1 levels and no effect on mitochondrial fragmentation or respiration. Mutation of the Ubp12 catalytic site had no effect on the ubiquitination pattern of Fzo1 besides a marginal increase in Fzo1 modified species that was proportional to the slight increase of Fzo1 level in the absence of Ubp12 [98]. In face of this weak impact of *UBP12* deletion on Fzo1 ubiquitination and mitochondrial fusion it was thus difficult to understand how Ubp12 could antagonize the Mdm30-dependent regulation of Fzo1. In fact, this function was later found to be carried out by Ubp2 [99]. More precisely, Ubp2 was shown to restrict the length of K48-linked ubiquitin chains added on K398 of Fzo1, thereby slowing down the Mdm30-dependent proteasomal degradation of the mitofusin [99]. These observations established Ubp2 as the bonafide antagonist of Mdm30-dependent ubiquitination on K398 of Fzo1 (Fig. 5).

3.3.2. An unexpected link with the desaturation of fatty acids

The role for Ubp2 capacity to tune Fzo1 turnover required being clarified. A first clue in this regard, came from the unexpected finding that, together with Fzo1, Mdm30 can also target Ubp2 for ubiquitination and degradation by the proteasome [99]. In the absence of Mdm30, both Fzo1 and Ubp2 are thus stabilized (Fig. 5). Notably, the natural stabilization of Ubp2 was found contributing to the defects in respiration and mitochondrial fusion seen in cells lacking Mdm30 [99]. Consistent with this, Ubp2 is an important antagonist of the HECT domain ubiquitin ligase Rsp5 [100] and one main function of Rsp5 is to activate the synthesis of the Δ9-fatty acid desaturase Ole1 in the so called Ole1 pathway [101]. Ubp2 stabilization in *MDM30* null cells was shown to antagonize this pathway thereby resulting in decreased synthesis of Ole1 [99]. This work thus revealed that lack of Mdm30 not only induces stabilization of Fzo1 and Ubp2 but also decreased desaturation of fatty acids.

Importantly, mitochondrial fusion defects in *mdm30* or *ubp2* null cells, in which Fzo1 is either stabilized or rapidly degraded, were rescued by increased or decreased desaturation of fatty acids, respectively [99]. In particular, addition of oleate in wild type cells induced a natural increase of Fzo1. This natural increase of Fzo1 maintained efficient mitochondrial fusion upon high desaturation of fatty acids but was also shown to depend on both Mdm30 and Ubp2 [99]. These observations [99] indicate that the Mdm30-mediated degradation of Fzo1 is not constitutive but tightly controlled by Ubp2, according to the activation status of the Ole1 pathway (Fig. 5). More precisely, Mdm30-mediated degradation of Fzo1 becomes essential for mitochondrial fusion upon low desaturation of fatty acids, but dispensable upon high expression of Ole1 (Fig. 5).

While the precise purpose of this balance remains to be investigated, it is possible to speculate on its function. In this regard, the desaturation status of fatty acids is established to be intimately linked to the representation of phospholipids in the cell [102]. For instance, low desaturation of fatty acids induces a drastic increase in cellular amounts of phosphatidic acid (PA) whereas the overall amount of phosphatidyl choline or phosphatidyl serine decreases [102]. Intriguingly, derivates of PA have been shown to participate in mitofusin-dependent membrane fusion in mammalian systems [103,104]. In this context, PA may facilitate outer membrane fusion after formation of a smaller Mitochondrial Docking ring Complex (MDC) thus requiring increased degradation of Fzo1 upon low fatty acids desaturation. Conversely, higher fatty acids desaturation resulting in decreased synthesis of fusogenic lipids would impose stabilization of Fzo1. These higher levels of mitofusin would then allow assembly of an MDC of a size appropriate to trigger fusion of outer membranes (Fig. 5).

3.4. Alternative pathways of Fzo1 degradation

Numerous other factors have been shown to be implicated in the UPS-mediated degradation of Fzo1. Among those, inactivation of Vms1, Cdc48, Ubx2, Doa1 or Ubp3 have all been shown to impact Fzo1 levels. Whether these factors control the Mdm30-mediated degradation of Fzo1 or whether they control turnover of the mitofusin through other pathways and other ubiquitin ligases has not always been necessarily considered. In particular, it is striking that most if not all of these factors have established roles in quality control mechanisms and especially ER-Associated Degradation (ERAD), which contrasts with the apparent dedicated role of Mdm30-mediated degradation of Fzo1 in the regulation of mitochondrial fusion.

3.4.1. Vms1

Vms1 was identified in 2010 as a factor required for protein quality control at the mitochondria [105]. This factor comprising a ring finger domain, an ankyrin repeat region and a characteristic Vms1-like domain, all conserved in other species, was shown to interact specifically with the AAA-ATPase Cdc48 [105]. While Cdc48 interacts with the heterodimer Npl4-Ufd1 in ERAD, Vms1 was shown to bind Npl4 but not Ufd1 [105]. It was thus proposed that the Cdc48-Npl4-Vms1 complex could ensure a protein quality control function at the mitochondria similar to the function of the Cdc48-Npl4-Ufd1 complex at the ER. Consistent with this, Vms1 and Cdc48 were found to be implicated in Fzo1 degradation [105]. Importantly, this degradation did not depend on Mdm30 and exclusively occurred in stress conditions [105]. In agreement with this observation, Fzo1 turnover in the absence of stress was only marginally affected by the inactivation of Cdc48 or Vms1 [106], which drastically contrasts with the strong stabilization of Fzo1 in the absence of Mdm30. Notably, a more precise function in Ribosome Quality Control (RQC) was later attributed to Vms1 (see Section 1-Fig. 2, Panel II). In 2017, Vms1 was found to bind 60S ribosomes at the mitochondria and shown to participate in CAT-tailing inhibition to prevent import of CAT-tailed polypeptides in mitochondria [45]. Shortly after, Vms1 was characterized as a peptidyl-tRNA hydrolase that promotes release of the nascent chain thus facilitating its subsequent extraction and degradation [51,52]. This set of findings thus suggest that Cdc48 and the RQC pathway (Fig. 2, Panel II) could trigger Fzo1 for proteasomal degradation under stress conditions.

3.4.2. Cdc48

Cdc48 has also been found to inhibit the degradation of Fzo1 in vegetative growth [107]. In this work, specific inactivation of the ATPase was found to induce faster degradation of the mitofusin. This counterintuitive result was explained by the possibility that Cdc48 could promote the degradation of Ubp12 [107]. In this context, Ubp12 would be stabilized upon inactivation of Cdc48, which would induce faster turnover of Fzo1. Yet, lack of Ubp12 did not induce stabilization of Fzo1 upon Cdc48 inactivation [107]. Consequently, the unexpected impact of Cdc48 on Fzo1 in vegetative growth remains to be explained. In this regard, Cdc48 is a key factor in the Ole1 pathway that is essential to activate synthesis of the fatty acid desaturase [101,108]. Inactivation of Cdc48 thus induces decreased desaturation of fatty acids [108]. Taking into consideration that decreased desaturation of fatty acids promotes increased degradation of Fzo1 [99], this would very well explain the decreased level of Fzo1 upon inactivation of Cdc48 (Fig. 5, low UFA).

3.4.3. Ubx2

Another regulator of Fzo1 degradation is Ubx2, the ER-resident cofactor of Cdc48. First identified for its role in ERAD [39,109,110], Ubx2 was also demonstrated to perform a key function in the Ole1 pathway [102]. Consistent with this, lack of Ubx2 was shown to decrease desaturation of fatty acids and to induce remodeling of the cellular phospholipidome [102]. This may explain the intriguing observation that Fzo1 oligomerization properties could be regulated by Ubx2 [111], which may link Ubx2 to the Mdm30-mediated control of Fzo1 [99]. However, in contrast to Cdc48 [107], inactivation of Ubx2 does not increase degradation but induces a weak stabilization of Fzo1 under vegetative growth [112]. Ubx2 interacts with the mitofusin [112], suggesting its direct involvement in Fzo1 turnover. Yet, stabilization of Fzo1 upon inactivation of Ubx2 is not as strong as upon inactivation of Mdm30. In particular, Fzo1 is not stabilized when Ubx2 and Ubp2 are co-inactivated [112], which drastically contrasts with the total inhibition of Fzo1 degradation upon co-inactivation of Mdm30 and Ubp2 [99]. This demonstrates that Ubx2 controls Fzo1 turnover through a pathway that is distinct from Mdm30.

Importantly, a small pool of Ubx2 localizes on outer membranes (Fig. 2, Panel I) to promote the mito-TAD quality control process [43]. Which ubiquitin ligase acts in this pathway remains to be identified (Fig. 2, Panel I). Nonetheless, Vms1 was functionally linked to this mito-TAD pathway [43], suggesting that RQC and Ltn1 could be involved in the ubiquitination of stalled mitochondrial substrates. Alternatively, the ubiquitin ligases Ubr1 and San1 were recently found to participate in a MAD pathway involving Ubx2, Cdc48, Doa1,

Proteasomes as well as the Hsp70 chaperones Sis1 and Ssa1–4 [113]. In this study, Fzo1 was confirmed to be stabilized upon inactivation of Ubx2 but the mitofusin was not affected in the absence of Doa1 nor upon inactivation of the Hsp70 machinery [113]. It remains thus possible but yet to be proven that Ubx2-mediated degradation of Fzo1 involves ubiquitination by Ltn1, Ubr1 or San1.

3.4.4. Doa1

The Cdc48 co-factor Doa1 has recently been involved in MAD but it was also clearly excluded from impacting Fzo1 turnover in vegetative growth [113]. This notably contrasts with previous work showing that Doa1 recruits Cdc48 to promote degradation of the mitofusin in the absence of stress [40]. Here, co-inactivation of Cdc48 and Mdm30 led to additive stabilization of Fzo1 as compared to single impairments of the ATPase or the E3 [40]. This strongly suggests that Cdc48 promotes degradation of Fzo1 through a pathway that is distinct from the Mdm30-mediated turnover of the mitofusin. Yet, the Doa1-Cdc48 complex was also shown to interact with ubiquitinated species of Fzo1 in the presence but not in the absence of Mdm30 [40]. These Fzo1 ubiquitinated species migrated higher than those usually added by Mdm30 [40]. It is thus possible that aggregation of Fzo1 in the absence of Mdm30 (Fig. 4D), precluded pull-down of Fzo1 molecules modified by a ligase distinct from Mdm30. As mentioned earlier for Ubx2, the ubiquitin ligases Ltn1, Ubr1 or San1 could therefore also be involved in this Doa1-Cdc48 pathway (Fig. 2, Panel IV, MAD-C). Nonetheless this interesting study [40] opened yet another possibility involving the AAA ATPase Msp1. Inactivation of both Cdc48 and Doa1 were found to induce strong stabilization of Msp1 [40], which is well established to control the mis-localization of tail-anchored proteins [61,62,114]. In particular, Msp1 has the ability to induce translocation of substrates from mitochondria to the ER [64,65]. The ERAD E3 Doa10 then promotes ubiquitination of the translocated proteins followed by their Cdc48-mediated extraction and ultimate proteasomal degradation (Fig. 2, Panel IV, MAD-TA). Whether Doa1 could promote Fzo1 turnover through this Msp1-Doa10-Cdc48 axis is thus an exciting possibility that should not be excluded (Fig. 2, Panel IV, MAD-C). This possibility also applies to Ubx2-mediated degradation of Fzo1 as the MITO-TAD pathway has been functionally linked to Msp1 [43].

While Doa1 clearly promotes degradation of Fzo1 [40], the controversy on its involvement in vegetative growth [113] has also been nicely resolved [115]. The steady state level of Fzo1 was shown to drastically drop down in old cells but also in young cells treated with concanamycin A, a specific inhibitor of the vacuolar ATPase which mimics age-related modifications on mitochondria [115]. This decrease was shown to be proteasome dependent and inactivation of Doa1 strikingly blocked this specific turnover of Fzo1 in old cells [115]. Taken together, the data presented in this interesting study were rather consistent in proving that Mdm30 and Rsp5 have no involvement in this degradation [115]. It will thus be very interesting to check whether Doa1-mediated degradation of Fzo1 in old cells involves Ltn1, Ubr1, San1 or Doa10 ubiquitin ligases (Fig. 2, Panel IV, MAD-C).

3.4.5. Ubp2, Ubp12 and Ubp3

Altogether, it is without a doubt that the yeast mitofusin Fzo1 could be a natural substrate for distinct mitochondrial quality control pathways. Nonetheless deep uncertainty remains regarding the ubiquitin ligases that could target Fzo1 for degradation in these situations. In parallel, the involvement of Mdm30 in the regulation of mitochondrial fusion is well established. Several factors involved in quality control processes could participate in this specific process. Yet, this might take place through an indirect impact on the Ole1 pathway rather than through a direct action on Fzo1 ubiquitinated species. The ubiquitin protease Ubp2, as both the antagonist of Mdm30-mediated ubiquitination of Fzo1 and a substrate for Mdm30-dependent degradation [99], is also absolutely central in the regulation of mitochondrial fusion (Fig. 5). On the other hand, the other ubiquitin protease, Ubp12, might have a more indirect effect on Fzo1 [98,107]. In this regard, *UBP12* inactivation has been proposed to induce stabilization of Ubp2 [107]. As the antagonist of Mdm30-mediated degradation of Fzo1 [99], this stabilization of Ubp2 (Fig. 5, high UFA) would be consistent with the weak increase in mitofusin levels seen upon *UBP12* inactivation [98]. Nonetheless, how Ubp12 could favor the degradation of Ubp2 remains unclear. Intriguingly, inactivation of a third ubiquitin protease, Ubp3, was recently shown to perturb mitochondrial dynamics [111]. Absence of *UBP3* induced stabilization of both Ubp2 and Ubp12 but had surprisingly no effect on Fzo1 degradation [111]. While these results are difficult to reconcile, one cannot exclude that the three UBPs could be involved in other pathways involved in mitochondrial homeostasis. In fact, this is even likely as Ubp3 and Rsp5, a ligase antagonized by Ubp2 [100], have been implicated in mitophagy, the degradation of mitochondria by autophagy [116,117].

4. Ubiquitination and mitophagy

4.1. The main principles of mitophagy

Mitophagy is a selective form of autophagy that leads to the clearance of unnecessary or damaged mitochondria by the lysosomal/vacuolar compartment. This specific type of mitochondrial degradation occurs through either macromitophagy or micromitophagy depending on how mitochondria or mitochondrial fragments are targeted to the lysosome. During macromitophagy, mitochondria destined to be cleared are recognized by the autophagic machinery and subsequently enveloped by a double membrane structure called the autophagosome. The autophagosome then fuses with the lysosome before its mitochondrial content gets degraded by lysosomal proteases [118]. Micromitophagy is less described and does not involve the formation of an autophagosome. Instead, vesicles that bud from the mitochondria are then targeted to the lysosome [119]. In this section, we will mainly focus on macromitophagy, hereafter referred as mitophagy.

The autophagic machinery relies on Atg8 (LC3 and GABARAP in mammals), an ubiquitin like protein that has the exceptional ability to conjugate itself to lipids through a thioester cascade that involves E1-like, E2-like and E3-like enzymes [120]. This allows Atg8/LC3 to be lipidated to the membrane of the autophagosome where it is exposed. There, Atg8/LC3 can interact with autophagy receptor proteins that contain a specific WXXL sequence called the AIM/LIR (Atg8 Interacting Motif/LC3 Interacting Region) domain [121]. This receptor-mediated mitophagy coexists with ubiquitin-dependent mitophagy where specific adaptor proteins with a ubiquitin binding domain and an AIM/LIR domain connect Atg8/LC3 to ubiquitinated proteins on mitochondrial outer membranes (Figs. 6 and 8).

Atg32 (Autophagy related protein 32), the receptor involved in yeast mitophagy (Fig. 8), is a single spanning transmembrane protein with its N-terminal domain facing the cytosol and harboring the AIM/LIR domain [122,123]. After induction of mitophagy, Atg32 is phosphorylated and interacts with the soluble protein adaptor Atg11 [124]. Atg11 targets the complex to the pre-autophagosomal assembly site where Atg32 can interact with lipidated Atg8 that is anchored to the membrane of the autophagosome [123].

In mammalian cells, several mitophagy receptors with their AIM/LIR motif have been found on mitochondrial outer membranes. These include NIX/BNIP3L (BCL2 interacting protein 3 like) involved in mitophagy during erythrocyte or neuronal differentiation, FUNDC1 (Fun14 domain containing 1) and BNIP3 for hypoxia induced mitophagy, BCL2L13 (Bcl2 Like Protein 13) a proposed functional homolog of Atg32, FKBP8 (FKBP prolyl isomerase 8) or AMBRA1 [125–132]. Even though receptor-mediated mitophagy is distinct from ubiquitin-dependent mitophagy, its regulation by ubiquitin has been clearly demonstrated. Ubiquitination of FUNDC1 by the RING domain ligase MITOL/MARCH5 occurs at the very beginning of hypoxia to induce proteasomal degradation of FUNDC1, resulting in decreased mitophagy

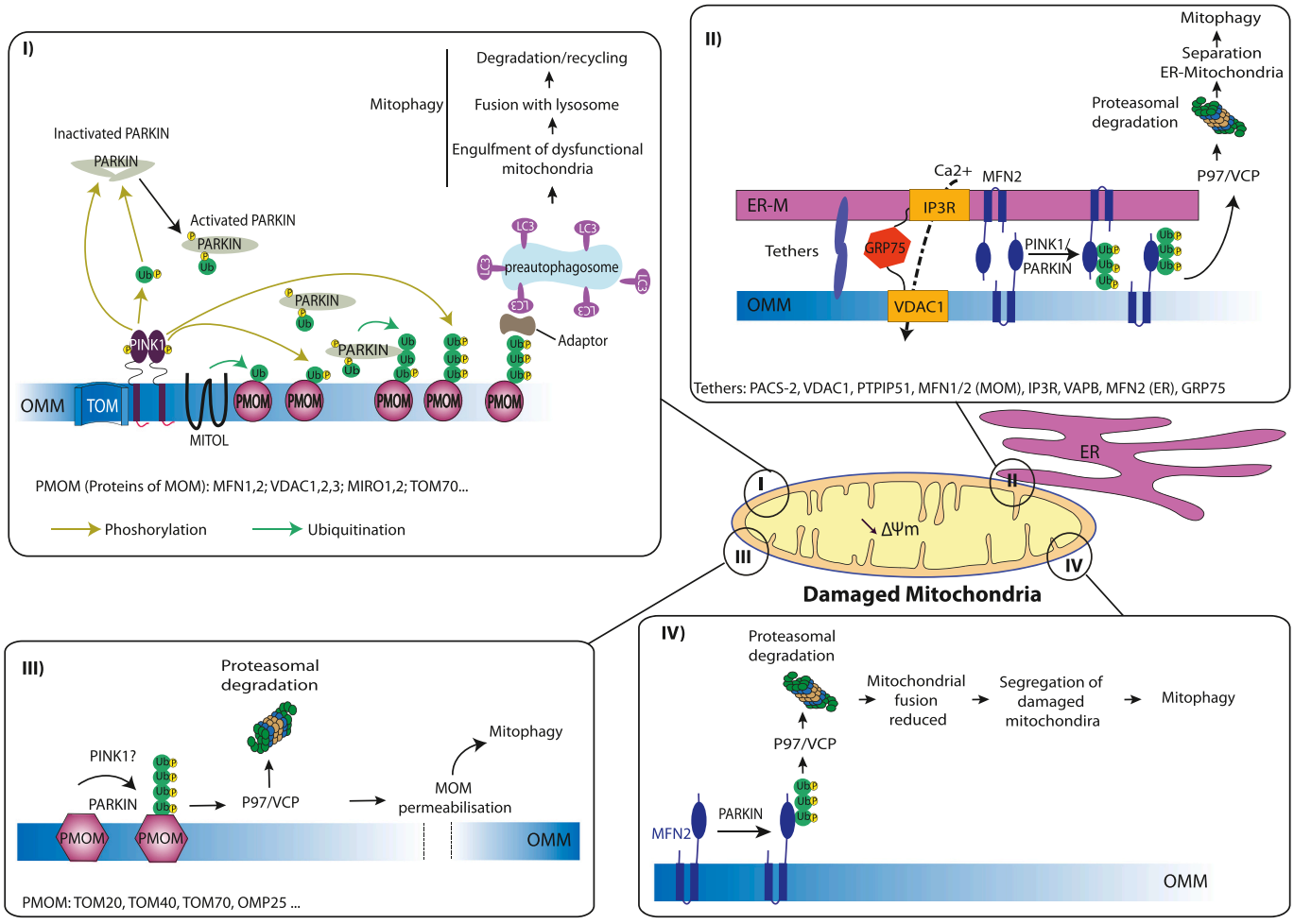

Fig. 6. Ubiquitin-dependent mitophagy in metazoans. (I) In damaged mitochondria that have lost their membrane potential (ΔΨm), the import of PINK1 is blocked which induces its accumulation on the mitochondrial outer membrane. Autophosphorylation, dimerization and association with the TOM complex activate PINK1 which phosphorylates ubiquitin either free or already conjugated to substrates by MITOL. Parkin activation through binding of phospho-ubiquitin and phosphorylation by PINK1 leads to its recruitment to the mitochondria where it associates with phospho-ubiquitinated substrates and induces massive ubiquitination of proteins from the outer membrane. Phospho-ubiquitinated substrates associate with ubiquitin binding adaptors that themselves bind to LC3 on pre-autophagosomal membranes. After full engulfment in the autophagosome that fuses with the lysosome, mitochondria are degraded and their components recycled in the cytosol. (II) This process of mitophagy requires dissociation of mitochondria from the ER that are normally connected by several tethers. One of these tethers, MFN2, is a target of phospho-ubiquitination by PINK1/PARKIN which induces its p97/VCP-mediated extraction from the outer membrane and subsequent degradation by the proteasome, resulting in dissociation of mitochondria from the ER. (III) After mitochondrial damage and in parallel to mitophagy, numerous proteins of the outer membrane (TOM20, TOM40…) are ubiquitinated by PARKIN, extracted by p97/VCP and degraded by the proteasome leading to permeabilization and rupture of the outer membrane. (IV) After loss of ΔΨm, sequential ubiquitination of MFN1 and MFN2 by PARKIN, extraction by p97/VCP and degradation by the proteasome also leads to a decrease in mitochondrial fusion which participates in segregating damaged mitochondria for subsequent degradation by mitophagy.

[133]. This process was proposed to protect the cell at the beginning of hypoxia from improper mitophagy [133]. PHB2 (Prohibitin2) is yet another peculiar mitophagy receptor [134]. Embedded in the mitochondrial inner membrane in a large heterodimeric complex with PHB1, PHB2 becomes accessible to LC3 after rupture of the outer membrane consecutive to ubiquitination and proteasomal degradation of outer membrane proteins. Notably, such regulation of mitophagy by ubiquitin is distinct from ubiquitin-dependent mitophagy which holds a significant importance in metazoan.

A main feature of ubiquitin-dependent mitophagy, is that the modifier, ubiquitin, is itself modified by phosphorylation [135–137]. This phospho-ubiquitination process involves the mitochondrial targeted protein kinase PINK1 (Phosphatase and Tensin homolog (PTEN)-Induced putative Kinase 1) and the ubiquitin ligase PARKIN (Fig. 6, Panel I). Following induction of mitophagy, the two enzymes trigger the phospho-ubiquitination of numerous proteins from the mitochondrial outer membrane. The phospho-ubiquitin tag is then recognized and bound by ubiquitin binding adaptors such as OPTN (optineurin) and NDP52 (nuclear domain 10 protein 52) that are the primary receptors for mitophagy [138] or p62, TAX1BP1 (Tax1 binding protein 1) and NBR1 (neighbor of BRCA1 gene 1) [139]. These adaptor proteins contain an ubiquitin interacting motif and an AIM/LIR motif that connect ubiquitinated proteins from the outer membrane to Atg8-like proteins on the autophagosomal membrane. Damaged mitochondria are then associated to autophagosomes before disposal in the lysosome (Fig. 6, Panel I).

4.2. *The mitochondrial kinase PINK1 and the ubiquitin ligase PARKIN*

Under normal conditions, the serine/threonine kinase PINK1 is targeted to mitochondria and degraded very rapidly (Fig. 7A). After import through the TOM and TIM complexes, the mitochondrial targeting peptide of PINK1 is cleaved by MPP (mitochondrial processing peptidase), before its IMM (Inner Mitochondrial Membrane) spanning domain gets further cleaved by PARL (Presenilin-associated rhomboid-like) [140,141]. This cleavage induces the retrotranslocation of PINK1

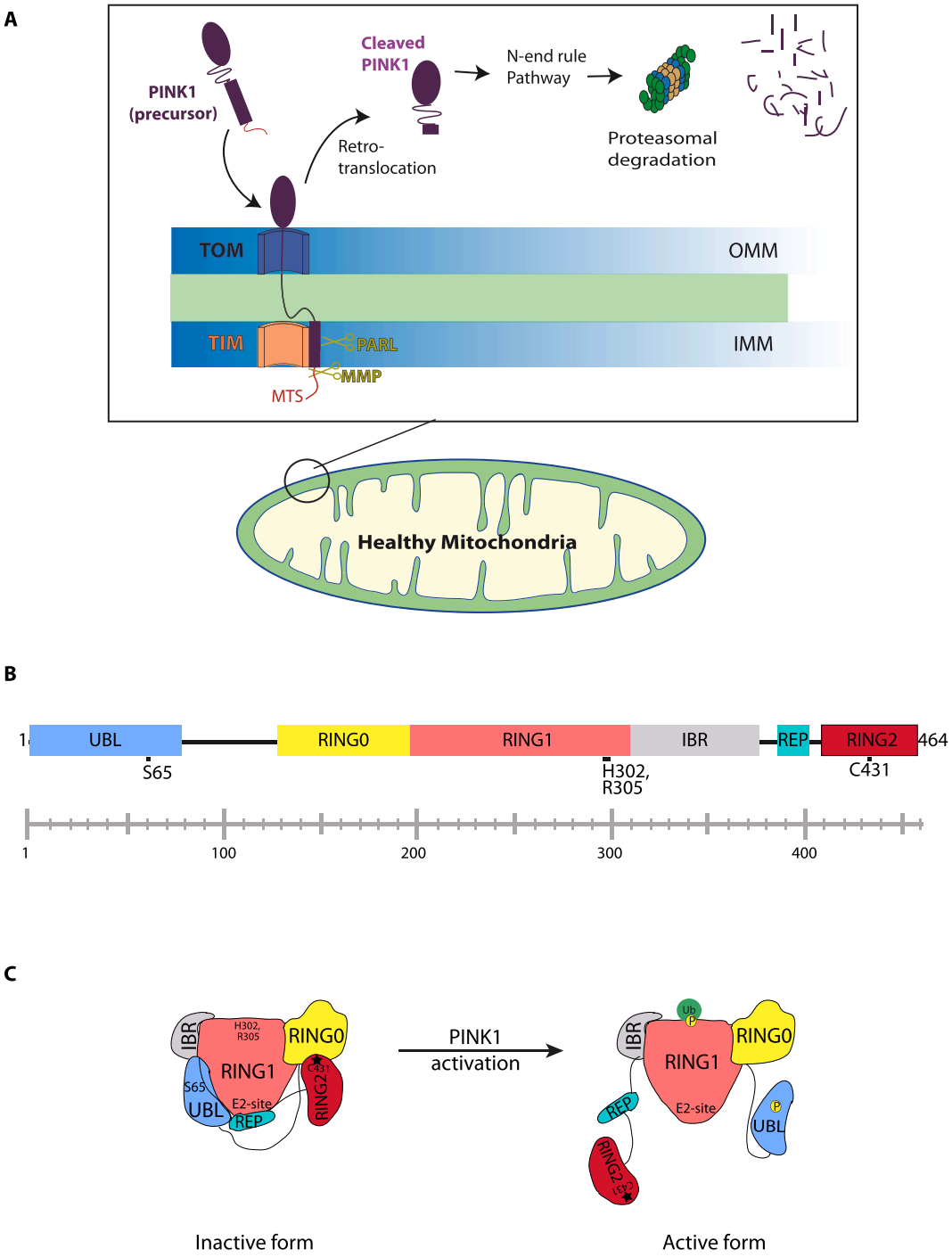

Fig. 7. PINK1 targeting to mitochondria and conformations of the RBR ubiquitin ligase PARKIN. (A) In healthy mitochondria PINK1 levels are low. The kinase is imported into mitochondria and retro-translocated to the cytosol to be degraded by the UPS N-end rule pathway. (B) The distinct domains of PARKIN are indicated. His302 and Arg305 on RING1, Ser65 on the Ubl and Cys431 on RING2 are the main residues implicated in the activation of the E3. The scale bar at the bottom indicates the relative position of each domain. (C) Transition of PARKIN from the inactive to the active state initiates with the binding of phospho-ubiquitin to His302 and Arg305 of RING1. This displaces the Ubl that is phosphorylated on Ser65 by PINK1 which gives robust access to the E2 binding site on RING1. Since RBR ligases function like HECT E3s, ubiquitin from the loaded E2 can be transferred to the catalytic Cys431 of RING2 that became accessible after its dissociation from RING0.

to the cytosol and its subsequent degradation by the UPS through the N-end rule pathway (Fig. 7A). As a result of this turnover, the level of PINK1 is very low on healthy mitochondria with an efficient membrane potential (ΔΨm) [142]. However, upon treatment with mitochondrial uncouplers such as CCCP (Carbonyl Cyanide 3-Chlorophenylhydrazone), the ΔΨm drops down and the import of PINK1 is inhibited. In these depolarized mitochondria, the kinase is trapped on the outer membrane where it forms a dimer in association with the TOM complex (Fig. 6, Panel I). At this stage, PINK1 activates and induces its autophosphorylation [143–145]. A cascade of PINK1-dependent phosphorylation then targets mono and poly-ubiquitin on the conserved Serine 65 residue of ubiquitin but also the ubiquitin ligase PARKIN on its Ubl (Ubiquitin like) domain [135,137]. This induces the transfer of PARKIN from the cytosol to depolarized mitochondria where the E3 ubiquitinates a massive amount of substrates on outer membranes [146–152].

PARKIN, is a RING/HECT hybrid E3 of the RBR family of ubiquitin

ligases (Fig. 7B–C). Its distinct domains include the Ubiquitin-like (Ubl) domain that contains the S65 phosphorylation site for PINK1, a Repressor (REP) domain as well as four Zinc-coordinating RING-like domains, RING0, RING1, IBR (In between Ring), and RING2. RING1 is the binding site for the E2 whereas RING2 contains the catalytic cysteine (Cys431) that binds ubiquitin through a thioester bond before transfer to the substrate (Fig. 7B). PARKIN is located in the cytoplasm in a tightly packed autoinhibited state [153–155]. The Ubl domain is bound to RING1, rendering S65 hardly accessible for phosphorylation by PINK1 whereas the REP domain interacts with RING1, thereby masking the binding site for the E2 (Fig. 7C, Inactive form). In parallel, RING0 obstructs the ubiquitin acceptor cysteine 431 on RING2 [154–157]. Interestingly, PARKIN begins its activation after binding to phospho-ubiquitin which acts as an allosteric modulator. The interaction of the phosphate with His302 and Arg305 on RING1 induces the dissociation of the Ubl domain that becomes accessible for phosphorylation by PINK1 (Fig. 7C, Active form). Subsequent conformational changes promote the release of RING2 from RING0, converting PARKIN to its fully active state before targeting to mitochondria [154,156]. The mechanism of this translocation from the cytosol to mitochondria after loss of $\Delta\Psi m$ has been extensively debated. PINK1 was initially proposed to be the receptor for PARKIN on depolarized mitochondria [150]. The employment of ubiquitin mutants demonstrated nonetheless that poly-phosphorylated ubiquitin is the genuine PARKIN receptor on damaged mitochondria [158,159]. Consistent with this, the activation and mitochondrial recruitment of PARKIN was recently found to be delayed upon inactivation of the RING domain ligase MITOL/MARCH5 [160]. In this context, the primary ubiquitination step would be mediated by MITOL/MARCH5 which is localized at the outer membrane [160]. PINK1-dependent phosphorylation of ubiquitin and PARKIN activation would then trigger the ubiquitination of numerous substrates on outer membranes (Fig. 6, Panel I). As shown previously, the resulting ubiquitin chains are subsequently phosphorylated by PINK1 which enhances the recruitment of PARKIN molecules to mitochondria in a feed-forward amplification process [161].

As opposed to other ubiqutin ligases, PARKIN does not seem to recognize a specific amino acid sequence on its substrates but was proposed to ubiquitinate outer membrane proteins in a non-selective manner [160]. Among these hundreds of PARKIN substrates, including the voltage anion channels VDAC1, 2, 3, the GTPases MIRO1 and 2 or the translocase of the outer membrane TOM70, mitofusins (MFN1 and 2) were the first substrates to be identified approximately a decade ago [162]. In addition to the decoration of outer membrane proteins with phospho-ubiquitin and subsequent autophagosomal recruitment, PARKIN-dependent ubiquitination was shown to induce the proteasomal turnover of numerous proteins of the outer membrane. For instance, proteasome-dependent degradation of factors such as TOM components leads to the rupture and permeabilization of the outer membrane in parallel to mitophagy [163] (Fig. 6, Panel III). MFN1 and 2 were shown to be ubiquitinated by PARKIN and degraded by the proteasome in a p97 dependent manner leading to reduced mitochondrial fusion followed by segregation of defective mitochondria [147] (Fig. 6, Panel IV). More recently, this degradation of mitofusins was linked to the dissociation of mitochondria from the ER before engulfment by the autophagosome [164] (Fig. 6, Panel II).

4.3. Mitochondria-ER contact sites and mitophagy

Contact sites between mitochondria and the ER were first described by electron microscopy in the middle of the 20th century [165]. The later purification of MAM (Mitochondria Associated Membranes), and their biochemical analysis demonstrated their involvement in lipid biosynthesis [166]. Soon after it was proposed that MAM are sites of Ca^{2+} transfer, a process that was subsequently shown to rely on VDAC1 on mitochondria and the Ca^{2+} release channel IP3R on the ER [167,168] (Fig. 6, Panel II). In the last decade, the concept of MERC (Mitochondria ER Contact sites) has emerged as multi-tasking platforms involved in many processes such as lipid transfer, mitochondrial fission or mitophagy [169,170]. A main characteristic of MERC relies on the physical connection of their membranes by protein tethers [171]. On the outer membrane, these tethers include PACS-2, VDAC1, PTPIP51 or the mitofusins MFN1 and MFN2 whereas IP3R, VAPB and MFN2 act on the ER membrane [172]. The landmark discovery that MFN2 also localizes on the ER led to the finding that mitofusins are enriched at MERC and involved in the regulation of these contact sites [173]. Whether MFN2 increases or diminishes the distance between the ER and mitochondria is subject to controversy [173–176]. Nonetheless, its involvement as a regulator of MERC association and function is widely accepted and was shown to be regulated by ubiquitination (Fig. 6, Panel II).

In PARKIN KO cells, the level of MFN2 at MERC increases, the mitochondria-ER distance as well as contact sites are affected and the transfer of Ca^{2+} from the ER to mitochondrial is perturbed [177,178]. This effect is specific of MFN2 since a mutation in its HR1 domain (K416R) blocks its PARKIN-mediated ubiquitination and decreases ER-Mito contacts as well as Ca^{2+} transfer [178]. The separation of mitochondria from the ER is also required for efficient mitophagy [164]. PINK1/PARKIN induce phospho-ubiquitination of MFN2 leading to its extraction from outer membranes by p97 which promotes dissociation of the ER from mitochondria (Fig. 6, Panel II) prior to further phospho-ubiquitination and processing for mitophagy [164]. After CCCP treatment (30–60 min), MFN2 is ubiquitinated rapidly, ahead of other substrates such as TOM20 or MIRO that are modified hours later [164]. This indicates that ubiquitination of MFN2 is an early event in the process of mitophagy.

In addition to PARKIN, MUL1 and MITOL/MARCH5 are two other ligases that regulate MERC through ubiquitination of MFN2. MUL1, also denominated MAPL (Mitochondrial-Anchored Protein Ligase), MULAN (Mitochondrial Ubiquitin Ligase Activator of NF-κB) or GIDE (Growth Inhibition and Death E3 ligase), is a mitochondrial outer membrane anchored protein. Besides its role as an ubiquitin ligase, MUL1 preferentially conjugates the ubiquitin-like protein SUMO (Small Ubiquitin Modifier) to its substrates. One of its targets is the mitochondrial fission Dynamin DRP1. Once sumoylated, DRP1 induces mitochondrial fission and stabilizes MERCs which is a prerequisite for ca^{2+} flux and induction of apoptosis [179,180]. MUL1 also binds and ubiquitinates MFN2 to regulate the function of the mitofusin negatively [181]. This MUL1-dependent ubiquitination of MFN2 regulates mitophagy before PARKIN during mild stress or in parallel to PARKIN during high stress [181,182]. The ubiquitin ligase MITOL promotes K63 polyubiquitination of mitochondrial MFN2 on the lysine 192 localized in the GTPase domain. This ubiquitination does not induce proteasomal degradation or mitophagy but was proposed to stimulate oligomerization of mitochondrial and ER-resident MFN2 thereby improving the formation of MERCs [183]. MITOL may thus have a dual role in promoting MERCs and in initiating PARKIN/PINK1 feed forward process (Fig. 6, Panel I) required for ubiquitin-dependent mitophagy [160].

Notably, other ubiquitin ligases including SMURF1 (SMAD Ubiquitination Regulatory Factor 1), Gp78, HUWE1 or MGNR1 have been involved in mitofusins ubiquitination and mitophagy but their mechanism of action remains to be fully described [184–187]. MFN1 has also been shown to be ubiquitinated by HUWE1 to induce apoptosis [188]. In parallel, several deubiquitination enzymes of the USP (Ubiquitin Specific Protease) family have been implicated in the regulation of MFN2 and Mitophagy. USP8 was shown to antagonize ubiquitination by PARKIN and counteract mitophagy [189] whereas USP15, USP30 and USP35 were found to deubiquitinate MFN2 and other outer membrane proteins initially modified by PARKIN [190–192].

PARKIN which is undoubtedly the main ligase involved in macro-mitophagy has also been implicated in other forms of mitophagy. In piecemeal mitophagy, the accumulation of misfolded protein aggregates in the mitochondrial matrix induces the segregation of

mitochondrial portions, in a DRP1-dependent mechanism, and their degradation by PARKIN/PINK1-dependent mitophagy [22]. PARKIN was also shown to induce the sequestration of mitochondria in early endosomes before fusion with lysosome [193]. In another form of micromitophagy, that also requires PARKIN and PINK1, budding of vesicles from the mitochondrial outer membrane generates mitochondria derived vesicles (MDVs) independent of Drp1. These MDVs subsequently fuse with endosomes before merging with the lysosome [194–196]. In yeast, Mitochondria Derived Compartments (MDCs) have been described in old cells [197]. Their formation requires components of the autophagy and mitochondrial fission machineries. MDCs then carry a specific set of outer and inner membrane proteins that are degraded after transport to the vacuole. No role for ubiquitin has been described in this pathway and whether MDCs correspond to membrane vesicle compartments remains to be confirmed.

4.4. Ubiquitin and mitophagy in yeast

As opposed to mitofusins from metazoans, the yeast mitofusin Fzo1 has never been involved in mitophagy nor in the establishment of ER-Mitochondria contact sites. However, the yeast mitofusin was recently found to participate in the tethering of mitochondria to peroxisomes [198]. This function was deduced from the observation that overexpression of Fzo1 increases PerMit (Peroxisome-Mitochondria) contacts [198]. The functional significance of these PerMit contacts mediated by Fzo1 remains to be elucidated and, while a potential role for ubiquitination has been suggested, the precise mechanism of Fzo1 involvement in PerMit contacts needs to be further investigated.

While Fzo1 is not involved in the establishment of MERCs in yeast, this function is widely accepted to be established by the multi-protein complex ERMES (ER-Mitochondria Encounter Structure) (Fig. 8) which includes Mmm1, an integral membrane protein of the ER, Mdm34 and Mdm10, two integral proteins of the mitochondrial outer membrane as well as the soluble protein Mdm12 [63]. Similar to MERCs in mammalian cells, ERMES-mediated contacts are essential for mitochondrial dynamics or ca^{2+} and phospholipid exchange but have also been implicated in mitophagy [199]. This involvement in mitophagy was first evidenced by the observation that ERMES colocalizes with components of the autophagosome [200]. Since Mdm34, Mmm1 and Mdm12 contain SMP (Synaptotagmin-like Mitochondrial-lipid binding Protein) domains that allow the binding of glycerophospholipids and especially phosphatidylcholine [201–203], this led suggesting a role for ERMES in the transfer of lipids from the ER to the growing autophagosome during mitophagy [200].

Shortly after, the first clue for an involvement of ubiquitin in yeast mitophagy came with the employment of a synthetic quantitative array (SQA) technology [116]. In this form of high throughput screen, an enzymatic reaction was used for the detection of general autophagy and specific mitophagy defects in the yeast knock-out strain collection. Cells were treated with Rapamycin for induction of mitophagy and the deubiquitinating enzyme Ubp3 as well as its cofactor Bre5 [204,205] were identified both as inhibitors of mitophagy and activators of general autophagy. It was confirmed that deletion of either *UBP3* or *BRE5* leads to an increased induction of mitophagy upon treatment with Rapamycin but also upon other mitophagy inducing conditions. In addition, Ubp3 and Bre5 were shown to be recruited to mitochondria after induction of mitophagy, thus suggesting a direct role of the deubiquitination complex on mitochondrial proteins. These results are reminiscent of ubiquitin-mediated mitophagy in metazoans. However, while Ltn1 and Rsp5 are two E3s that were previously known to be counteracted by Ubp3/Bre5 in either ribophagy for Ltn1 or autophagy of misfolded cytosolic proteins for Rsp5 [206], the substrates of the Ubp3/Bre5 complex and the ligase(s) that are involved in yeast mitophagy remained unknown.

Mdm34 and Mdm12 were subsequently found to be subject to ubiquitination by Rsp5 [40,117] (Fig. 8). Both proteins contain L/PPXY (PY) motifs that are recognized by the WW domains of Rsp5 [40,117]. Mutagenesis of the Mdm34 PY motif not only inhibited Rsp5-mediated ubiquitination of both Mdm34 and Mdm12 but was also found to induce defects in mitophagy [117]. Similar to metazoans, yeast mitophagy thus depends on a link between MERCs and ubiquitination (Fig. 8). While ubiquitinated by Rsp5, Mdm34 was highly stable and still detected after 4 h of cycloheximide (CHX) treatment [117]. However, in a distinct genetic background, Mdm34 was rapidly degraded and no longer detected after 30 min of CHX chase [40]. This degradation was dependent on Rsp5, Doa1, Cdc48 and the proteasome. Rsp5-mediated ubiquitination of Mdm34 is thus implicated in both regulation of mitophagy but also in MAD of Mdm34 (Fig. 8). This

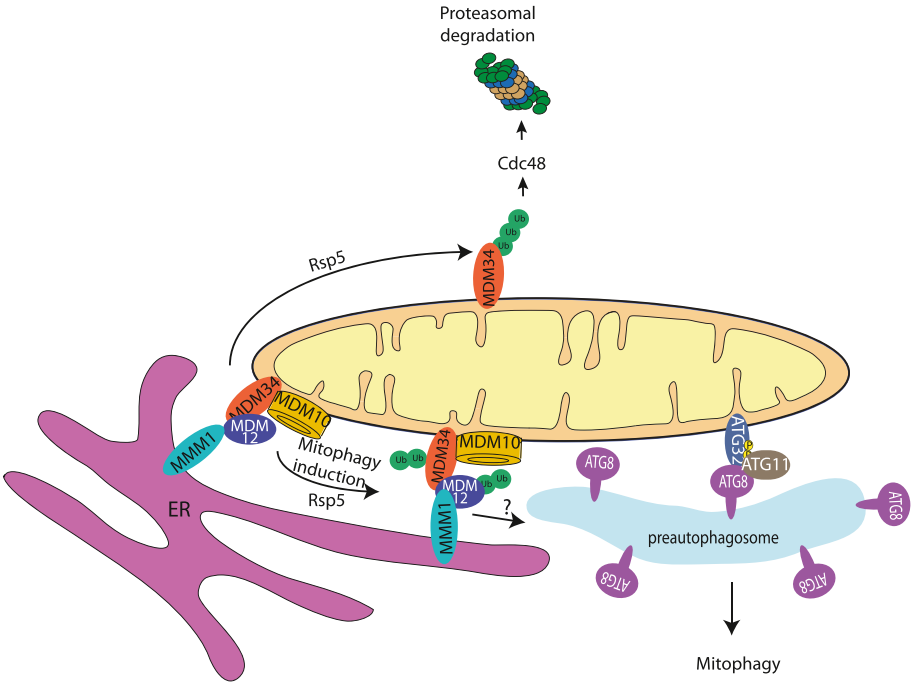

Fig. 8. Mitophagy in yeast. Targeting to the autophagosome begins with phosphorylation of the mitochondrial autophagy receptor Atg32. Phosphorylated Atg32 interacts with the protein adaptor Atg11 and the complex is targeted to the pre-autophagosomal site assembly where Atg32 can interact with Atg8 that is anchored in the membrane of the pre-autophagosome. Yeast mitophagy also involves the contacts between the ER and the mitochondria that are mediated by the ERMES complex composed of Mdm10, Mdm34, Mdm12 and Mmm1. In conditions of mitophagy induction, Mdm34 and Mdm12 are ubiquitinated by Rsp5. While inhibition of this ubiquitination affects mitophagy, its precise function remains to be understood. ERMES has been proposed to provide lipids to the growing autophagosome and ubiquitination could play a role in this phenomenon. Alternatively, Rsp5 could promote the targeting of mitochondria to the autophagosome, similar to PARKIN. In fact, in analogy to PARKIN with metazoan mitofusins, Rsp5-mediated ubiquitination of Mdm34 is not only involved in mitophagy but also promotes its Cdc48-dependent proteasomal degradation.

ability of Rsp5 to favor proteasomal degradation of Mdm34 or to facilitate efficient mitophagy could relate to distinct lysines that are targeted for ubiquitination within Mdm34 or, more likely, to the nature of ubiquitin linkages that are used to modify the ERMES component.

Rsp5 conjugates monoubiquitin and short K63 linked chains on Mdm34 and Mdm12 [117]. This type of ubiqutination is preferred by Rsp5 but is a poor trigger for proteasomal degradation as opposed to K48-linked chains composed of four ubiquitin moieties or more [207]. However, it has been shown that Rsp5 is also able to catalyze the formation of K11, K33 and K48 chains *in vitro* [208]. Moreover, editing of ubiquitin chains through trimming by DUBs and re-extension has been described. For instance, K63 linked chains added on RNA polII by Rsp5 are trimmed by Ubp2 to leave only monoubitin that is further elongated with K48-linked ubiquitin chains by another E3 ligase (elongin/cullin complex) before ultimate targeting to the proteasome [209]. In addition, after heat shock, K63 linked ubiquitin chains added by Rsp5 are not only trimmed by Ubp2 and Ubp3 but the increase in temperature also induces Rsp5 to catalyze K48-ubiquitination on trimmed chains to promote degradation of the substrates by the proteasome [210,211]. It is thus highly conceivable that specific DUBs involved in the editing of ubiquitin chains made by Rsp5 dictate the fate of Mdm34 toward induction of mitophagy or proteasomal degradation. Ubp3 is a very good candidate for this function given its ability to negatively regulate mitophagy and its involvement in the editing of K63 chains made by Rsp5.

Notably, whether Mdm34 is engaged in the formation of the ERMES complex or whether Mdm34 is free of any interaction with ERMES components could also drastically modify the effect of its Rsp5-mediated ubiquitination. In this regard, the ubiquitination of both Mdm34 and Mdm12 upon induction of mitophagy [117] indicates that Rsp5 modifies both proteins while associated in the ERMES complex (Fig. 8). Similar to mammalian mitophagy, this ubiquitination may induce the dissociation of MERCS and facilitate the engulfment of defective mitochondria in autophagosomes. A non-mutual exclusive possibility is that Rsp5-mediated ubiquitination of ERMES could be recognized by yeast autophagy receptors such as CUET proteins that act as ubiquitin-Atg8 adaptors [212]. In this context, ubiquitin-dependent mitophagy in yeast would also share some very strong similarities with metazoans. However, if yeast ubiquitin has been shown to be phosphorylated on Serine 37 and this phosphorylation has been implicated in membrane trafficking [213], the kinase involved in this phosphorylation remains unknown and the involvement of phospho-ubiquitin in yeast autophagy is not established. The role of the UPS in yeast mitophagy thus holds yet to be discovered features (Fig. 8) that will reveal the extent of homology between yeast and mammalian systems.

5. Conclusion

We have seen multiple facets of mitochondrial homeostasis regulation by the UPS. From mitochondrial quality control pathways to the regulation of specific functions, the UPS could be compared as a Swiss knife without which mitochondria could simply not maintain its integrity in the cell. Nonetheless, what is now evident was not so obvious fifteen years ago when mitochondria, despite all its complexity, was already known to be devoid of ubiquitin. It was then conceived that the surface of the organelle could be subject to a UPS-mediated regulation similar to that taking place on the ER membrane. The Mdm30-mediated control of Fzo1, the PARKIN-dependent regulation of mitophagy and, more recently, the successive discovery of diverse MAD pathways, not only confirmed this initial view but also overtook all expectations. The next challenges will now consist in taking a step backward and identify the ligases involved in each MAD pathway as well as their intrinsic relationships. Regarding mitochondrial fusion, it will be informative to investigate its control in mammalian cells as deeply as it has been carried out in yeast over the last twelve years. As for mitophagy, the legacy of all discoveries achieved in metazoans will undoubtedly benefit dissecting the role of the UPS in yeast mitochondrial clearance. The UPS and mitochondria still have a lot of new gifts to offer for the next decade.

Declaration of competing interest

The authors declare that they have no known competing financial interests or personal relationships that could have appeared to influence the work reported in this paper.

Acknowledgments

Research in the Cohen laboratory is supported by the labex Agence Nationale de la Recherche (ANR), France DYNAMO (ANR-11-LABX-0011-DYNAMO), MOMIT (ANR-17-CE13-0026-01) and MITOFUSION (ANR-19-CE11-0018). C.A. was supported by a three-year doctoral grant from the PSL Idex Program (ANR-10-IDEX-0001-02 PSL) and by a fourth-year doctoral grant from the Fondation pour la Recherche Médicale (FRM), France.

Author contributions

CA wrote the introduction and Section 1. MMC wrote Section 2. NBT wrote Section 3. MMC edited the whole manuscript. CA generated Figs. 1, 2, 3 and 5. LC generated Fig. 4. OO generated Figs. 6 and 8. NBT generated Fig. 7 and supervised the design of Figs. 6 and 8. MMC supervised the design of all Figures.

References

[1] B. Westermann, Mitochondrial fusion and fission in cell life and death, Nat. Rev. Mol. Cell Biol. 11 (2010) 872–884.
[2] E. Schrepfer, L. Scorrano, Mitofusins, from mitochondria to metabolism, Mol. Cell 61 (2016) 683–694.
[3] P.H. Willems, R. Rossignol, C.E. Dieteren, M.P. Murphy, W.J. Koopman, Redox homeostasis and mitochondrial dynamics, Cell Metab. 22 (2015) 207–218.
[4] A.M. van der Bliek, M.M. Sedensky, P.G. Morgan, Cell biology of the mitochondrion, Genetics 207 (2017) 843.
[5] J. Nunnari, A. Suomalainen, Mitochondria: in sickness and in health, Cell 148 (2012) 1145–1159.
[6] N. Sun, R.J. Youle, T. Finkel, The mitochondrial basis of aging, Mol. Cell 61 (2016) 654–666.
[7] H. Zhang, K.J. Menzies, J. Auwerx, The role of mitochondria in stem cell fate and aging, Development 145 (2018) dev143420.
[8] J.W. Taanman, The mitochondrial genome: structure, transcription, translation and replication, Biochim. Biophys. Acta 1410 (1999) 103–123.
[9] W. Neupert, A perspective on transport of proteins into mitochondria: a myriad of open questions, J. Mol. Biol. 427 (2015) 1135–1158.
[10] R.J. Deshaies, B.D. Koch, M. Werner-Washburne, E.A. Craig, R. Schekman, A subfamily of stress proteins facilitates translocation of secretory and mitochondrial precursor polypeptides, Nature 332 (1988) 800–805.
[11] J.C. Young, N.J. Hoogenraad, F.U. Hartl, Molecular chaperones Hsp90 and Hsp70 deliver preproteins to the mitochondrial import receptor Tom70, Cell 112 (2003) 41–50.
[12] L. Zanphorlin, T. Lima, M. Wong, T. Balbuena, C. Minetti, D. Remeta, J. Young, L. Barbosa, F. Gozzo, C. Ramos, Heat shock protein 90 kDa (Hsp90) has a second functional interaction site with the mitochondrial import receptor Tom70, J. Biol. Chem. 291 (2016) (jbc.M115.710137).
[13] T. Jores, J. Lawatscheck, V. Beke, M. Franz-Wachtel, K. Yunoki, J.C. Fitzgerald, B. Macek, T. Endo, H. Kalbacher, J. Buchner, D. Rapaport, Cytosolic Hsp70 and Hsp40 chaperones enable the biogenesis of mitochondrial β-barrel proteins, J. Cell Biol. 217 (2018) 3091–3108.
[14] N. Pfanner, B. Warscheid, N. Wiedemann, Mitochondrial proteins: from biogenesis to functional networks, Nat. Rev. Mol. Cell Biol. 20 (2019) 267–284.
[15] Y. Kubo, T. Tsunehiro, S.-i. Nishikawa, M. Nakai, E. Ikeda, A. Toh-e, N. Morishima, T. Shibata, T. Endo, Two distinct mechanisms operate in the reactivation of heat-denatured proteins by the mitochondrial Hsp70/Mdj1p/Yge1p chaperone system11, J. Mol. Biol. 286 (1999) 447–464.
[16] T. Bender, I. Lewrenz, S. Franken, C. Baitzel, W. Voos, Mitochondrial enzymes are protected from stress-induced aggregation by mitochondrial chaperones and the Pim1/LON protease, Mol. Biol. Cell 22 (2011) 541–554.
[17] M.Y. Cheng, F.U. Hartl, J. Martin, R.A. Pollock, F. Kalousek, W. Neupert, E.M. Hallberg, R.L. Hallberg, A.L. Horwich, Mitochondrial heat-shock protein hsp60 is essential for assembly of proteins imported into yeast mitochondria, Nature 337 (1989) 620–625.
[18] D.S. Reading, R.L. Hallberg, A.M. Myers, Characterization of the yeast HSP60 gene coding for a mitochondrial assembly factor, Nature 337 (1989) 655–659.

[19] M.-P. Hamon, A.-L. Bulteau, B. Friguet, Mitochondrial proteases and protein quality control in ageing and longevity, Ageing Res. Rev. 23 (2015) 56–66.
[20] P. Bragoszewski, M. Turek, A. Chacinska, Control of mitochondrial biogenesis and function by the ubiquitin-proteasome system, Open Biol. 7 (2017).
[21] A. Sugiura, G.-L. McLelland, E.A. Fon, H.M. McBride, A new pathway for mitochondrial quality control: mitochondrial-derived vesicles, EMBO J. 33 (2014) 2142–2156.
[22] J.L. Burman, S. Pickles, C. Wang, S. Sekine, J.N.S. Vargas, Z. Zhang, A.M. Youle, C.L. Nezich, X. Wu, J.A. Hammer, R.J. Youle, Mitochondrial fission facilitates the selective mitophagy of protein aggregates, J. Cell Biol. 216 (2017) 3231–3247.
[23] A. Hershko, A. Ciechanover, The ubiquitin system for protein degradation, Annu. Rev. Biochem. 61 (1992) 761–807.
[24] D. Komander, M. Rape, The ubiquitin code, Annu. Rev. Biochem. 81 (2012) 203–229.
[25] M.J. Clague, C. Heride, S. Urbé, The demographics of the ubiquitin system, Trends Cell Biol. 25 (2015) 417–426.
[26] M.D. Stewart, T. Ritterhoff, R.E. Klevit, P.S. Brzovic, E2 enzymes: more than just middle men, Cell Res. 26 (2016) 423–440.
[27] N. Zheng, N. Shabek, Ubiquitin ligases: structure, function, and regulation, Annu. Rev. Biochem. 86 (2017) 129–157.
[28] R. Yau, M. Rape, The increasing complexity of the ubiquitin code, Nat. Cell Biol. 18 (2016) 579–586.
[29] Y.T. Kwon, A. Ciechanover, The ubiquitin code in the ubiquitin-proteasome system and autophagy, Trends Biochem. Sci. 42 (2017) 873–886.
[30] F. Ohtake, H. Tsuchiya, The emerging complexity of ubiquitin architecture, J. Biochem. 161 (2016) 125–133.
[31] J. Spence, S. Sadis, A.L. Haas, D. Finley, A ubiquitin mutant with specific defects in DNA repair and multiubiquitination, Mol. Cell. Biol. 15 (1995) 1265.
[32] Z. Liu, Z. Gong, W.-X. Jiang, J. Yang, W.-K. Zhu, D.-C. Guo, W.-P. Zhang, M.-L. Liu, C. Tang, Lys63-linked ubiquitin chain adopts multiple conformational states for specific target recognition, Elife 4 (2015) e05767.
[33] J.A.M. Bard, E.A. Goodall, E.R. Greene, E. Jonsson, K.C. Dong, A. Martin, Structure and function of the 26S proteasome, Annu. Rev. Biochem. 87 (2018) 697–724.
[34] X. Wu, T.A. Rapoport, Mechanistic insights into ER-associated protein degradation, Curr. Opin. Cell Biol. 53 (2018) 22–28.
[35] R.J. Braun, B. Westermann, With the help of MOM: mitochondrial contributions to cellular quality control, Trends Cell Biol. 27 (2017) 441–452.
[36] Y. Ye, H.H. Meyer, T.A. Rapoport, The AAA ATPase Cdc48/p97 and its partners transport proteins from the ER into the cytosol, Nature 414 (2001) 652–656.
[37] H.H. Meyer, J.G. Shorter, J. Seemann, D. Pappin, G. Warren, A complex of mammalian ufd1 and npl4 links the AAA-ATPase, p97, to ubiquitin and nuclear transport pathways, EMBO J. 19 (2000) 2181–2192.
[38] R.M. Bruderer, C. Brasseur, H.H. Meyer, The AAA ATPase p97/VCP interacts with its alternative co-factors, Ufd1-Npl4 and p47, through a common bipartite binding mechanism, J. Biol. Chem. 279 (2004) 49609–49616.
[39] O. Neuber, E. Jarosch, C. Volkwein, J. Walter, T. Sommer, Ubx2 links the Cdc48 complex to ER-associated protein degradation, Nat. Cell Biol. 7 (2005) 993–998.
[40] X. Wu, L. Li, H. Jiang, Doa1 targets ubiquitinated substrates for mitochondria-associated degradation, J. Cell Biol. 213 (2016) 49–63.
[41] D. Xia, W.K. Tang, Y. Ye, Structure and function of the AAA+ ATPase p97/Cdc48p, Gene 583 (2016) 64–77.
[42] N.O. Bodnar, T.A. Rapoport, Molecular mechanism of substrate processing by the Cdc48 ATPase complex, Cell 169 (e729) (2017) 722–735.
[43] C.U. Martensson, C. Priesnitz, J. Song, L. Ellenrieder, K.N. Doan, F. Boos, A. Floerchinger, N. Zufall, S. Oeljeklaus, B. Warscheid, T. Becker, Mitochondrial protein translocation-associated degradation, Nature 569 (2019) 679–683.
[44] O. Brandman, R.S. Hegde, Ribosome-associated protein quality control, Nat. Struct. Mol. Biol. 23 (2016) 7–15.
[45] T. Izawa, S.-H. Park, L. Zhao, F.U. Hartl, W. Neupert, Cytosolic protein Vms1 links ribosome quality control to mitochondrial and cellular homeostasis, Cell 171 (e818) (2017) 890–903.
[46] C.J. Shoemaker, D.E. Eyler, R. Green, Dom34:Hbs1 promotes subunit dissociation and peptidyl-tRNA drop-off to initiate no-go decay, Science (New York, N.Y.) 330 (2010) 369–372.
[47] O. Brandman, J. Stewart-Ornstein, D. Wong, A. Larson, C.C. Williams, G.-W. Li, S. Zhou, D. King, P.S. Shen, J. Weibezahn, J.G. Dunn, S. Rouskin, T. Inada, A. Frost, J.S. Weissman, A ribosome-bound quality control complex triggers degradation of nascent peptides and signals translation stress, Cell 151 (2012) 1042–1054.
[48] P.S. Shen, J. Park, Y. Qin, X. Li, K. Parsawar, M.H. Larson, J. Cox, Y. Cheng, A.M. Lambowitz, J.S. Weissman, O. Brandman, A. Frost, Protein synthesis. Rqc2p and 60S ribosomal subunits mediate mRNA-independent elongation of nascent chains, Science (New York, N.Y.) 347 (2015) 75–78.
[49] M.H. Bengtson, C.A.P. Joazeiro, Role of a ribosome-associated E3 ubiquitin ligase in protein quality control, Nature 467 (2010) 470–473.
[50] K.K. Kostova, K.L. Hickey, B.A. Osuna, J.A. Hussmann, A. Frost, D.E. Weinberg, J.S. Weissman, CAT-tailing as a fail-safe mechanism for efficient degradation of stalled nascent polypeptides, Science 357 (2017) 414–417.
[51] O. Zurita Rendón, E.K. Fredrickson, C.J. Howard, J. Van Vranken, S. Fogarty, N.D. Tolley, R. Kalia, B.A. Osuna, P.S. Shen, C.P. Hill, A. Frost, J. Rutter, Vms1p is a release factor for the ribosome-associated quality control complex, Nat. Commun. 9 (2018) 2197.
[52] R. Verma, K.M. Reichermeier, A.M. Burroughs, R.S. Oania, J.M. Reitsma, L. Aravind, R.J. Deshaies, Vms1 and ANKZF1 peptidyl-tRNA hydrolases release nascent chains from stalled ribosomes, Nature 557 (2018) 446–451.
[53] Q. Defenouillère, Y. Yao, J. Mouaikel, A. Namane, A. Galopier, L. Decourty, A. Doyen, C. Malabat, C. Saveanu, A. Jacquier, M. Fromont-Racine, Cdc48-associated complex bound to 60S particles is required for the clearance of aberrant translation products, Proc. Natl. Acad. Sci. 110 (2013) 5046–5051.
[54] Y.-J. Choe, S.-H. Park, T. Hassemer, R. Körner, L. Vincenz-Donnelly, M. Hayer-Hartl, F.U. Hartl, Failure of RQC machinery causes protein aggregation and proteotoxic stress, Nature 531 (2016) 191–195.
[55] R. Yonashiro, E.B. Tahara, M.H. Bengtson, M. Khokhrina, H. Lorenz, K.-C. Chen, Y. Kigoshi-Tansho, J.N. Savas, J.R. Yates, S.A. Kay, E.A. Craig, A. Mogk, B. Bukau, C.A.P. Joazeiro, The Rqc2/Tae2 subunit of the ribosome-associated quality control (RQC) complex marks ribosome-stalled nascent polypeptide chains for aggregation, Elife 5 (2016) e11794.
[56] F. Boos, L. Krämer, C. Groh, F. Jung, P. Haberkant, F. Stein, F. Wollweber, A. Gackstatter, E. Z√∂ller, M. van der Laan, M.M. Savitski, V. Benes, J.M. Herrmann, Mitochondrial protein-induced stress triggers a global adaptive transcriptional programme, Nat Cell Biol 21 (2019) 442–451.
[57] X. Wang, X.J. Chen, A cytosolic network suppressing mitochondria-mediated proteostatic stress and cell death, Nature 524 (2015) 481–484.
[58] L. Wrobel, U. Topf, P. Bragoszewski, S. Wiese, M.E. Sztolsztener, S. Oeljeklaus, A. Varabyova, M. Lirski, P. Chroscicki, S. Mroczek, E. Januszewicz, A. Dziembowski, M. Koblowska, B. Warscheid, A. Chacinska, Mistargeted mitochondrial proteins activate a proteostatic response in the cytosol, Nature 524 (2015) 485–488.
[59] H. Weidberg, A. Amon, MitoCPR- a surveillance pathway that protects mitochondria in response to protein import stress, Science 360 (2018) eaan4146.
[60] Ł. Opaliński, T. Becker, N. Pfanner, Clearing tail-anchored proteins from mitochondria, Proc. Natl. Acad. Sci. U. S. A. 111 (2014) 7888–7889.
[61] Y.-C. Chen, G.K.E. Umanah, N. Dephoure, S.A. Andrabi, S.P. Gygi, T.M. Dawson, V.L. Dawson, J. Rutter, Msp1/ATAD1 maintains mitochondrial function by facilitating the degradation of mislocalized tail-anchored proteins, EMBO J. 33 (2014) 1548–1564.
[62] V. Okreglak, P. Walter, The conserved AAA-ATPase Msp1 confers organelle specificity to tail-anchored proteins, Proc. Natl. Acad. Sci. U. S. A. 111 (2014) 8019–8024.
[63] B. Kornmann, E. Currie, S.R. Collins, M. Schuldiner, J. Nunnari, J.S. Weissman, P. Walter, An ER-mitochondria tethering complex revealed by a synthetic biology screen, Science 325 (2009) 477–481.
[64] V. Dederer, A. Khmelinskii, A.G. Huhn, V. Okreglak, M. Knop, M.K. Lemberg, Cooperation of mitochondrial and ER factors in quality control of tail-anchored proteins, Elife (2019) 8.
[65] S. Matsumoto, K. Nakatsukasa, C. Kakuta, Y. Tamura, M. Esaki, T. Endo, Msp1 clears mistargeted proteins by facilitating their transfer from mitochondria to the ER, Mol. Cell 76 (2019) 191–205 (e110).
[66] P.C. Liao, D.M.A. Wolken, E. Serrano, P. Srivastava, L.A. Pon, Mitochondria-associated degradation pathway (MAD) function beyond the outer membrane, Cell Rep. 32 (2020) 107902.
[67] R. Ramachandran, Mitochondrial dynamics: the dynamin superfamily and execution by collusion, Sem. Cell Dev. Biol. 76 (2018) 201–212.
[68] S. Mattie, J. Riemer, J.G. Wideman, H.M. McBride, A new mitofusin topology places the redox-regulated C terminus in the mitochondrial intermembrane space, J. Cell Biol. 217 (2018) 507–515.
[69] M.M. Cohen, D. Tareste, Recent insights into the structure and function of Mitofusins in mitochondrial fusion, F1000Research (2018) 7.
[70] M. Rojo, F. Legros, D. Chateau, A. Lombes, Membrane topology and mitochondrial targeting of mitofusins, ubiquitous mammalian homologs of the transmembrane GTPase Fzo, J. Cell Sci. 115 (2002) 1663–1674.
[71] H. Chen, S.A. Detmer, A.J. Ewald, E.E. Griffin, S.E. Fraser, D.C. Chan, Mitofusins Mfn1 and Mfn2 coordinately regulate mitochondrial fusion and are essential for embryonic development, J. Cell Biol. 160 (2003) 189–200.
[72] A. Santel, S. Frank, B. Gaume, M. Herrler, R.J. Youle, M.T. Fuller, Mitofusin-1 protein is a generally expressed mediator of mitochondrial fusion in mammalian cells, J. Cell Sci. 116 (2003) 2763–2774.
[73] Y. Eura, N. Ishihara, S. Yokota, K. Mihara, Two mitofusin proteins, mammalian homologues of FZO, with distinct functions are both required for mitochondrial fusion, J. Biochem. 134 (2003) 333–344.
[74] S. Zuchner, I.V. Mersiyanova, M. Muglia, N. Bissar-Tadmouri, J. Rochelle, E.L. Dadali, M. Zappia, E. Nelis, A. Patitucci, J. Senderek, Y. Parman, O. Evgrafov, P.D. Jonghe, Y. Takahashi, S. Tsuji, M.A. Pericak-Vance, A. Quattrone, E. Battaloglu, A.V. Polyakov, V. Timmerman, J.M. Schroder, J.M. Vance, Mutations in the mitochondrial GTPase mitofusin 2 cause Charcot-Marie-tooth neuropathy type 2A, Nat. Genet. 36 (2004) 449–451.
[75] S.A. Detmer, D.C. Chan, Complementation between mouse Mfn1 and Mfn2 protects mitochondrial fusion defects caused by CMT2A disease mutations, J. Cell Biol. 176 (2007) 405–414.
[76] Y.-J. Li, Y.-L. Cao, J.-X. Feng, Y. Qi, S. Meng, J.-F. Yang, Y.-T. Zhong, S. Kang, X. Chen, L. Lan, L. Luo, B. Yu, S. Chen, D.C. Chan, J. Hu, S. Gao, Structural insights of human mitofusin-2 into mitochondrial fusion and CMT2A onset, Nat. Commun. 10 (2019) 4914.
[77] S.R. Sloat, B.N. Whitley, E.A. Engelhart, S. Hoppins, Identification of a mitofusin specificity region that confers unique activities to Mfn1 and Mfn2, Mol. Biol. Cell 30 (2019) 2309–2319.
[78] S. Fritz, N. Weinbach, B. Westermann, Mdm30 is an F-box protein required for maintenance of fusion-competent mitochondria in yeast, Mol. Biol. Cell 14 (2003) 2303–2313.
[79] M. Escobar-Henriques, B. Westermann, T. Langer, Regulation of mitochondrial fusion by the F-box protein Mdm30 involves proteasome-independent turnover of Fzo1, J. Cell Biol. 173 (2006) 645–650.

[80] T. Cardozo, M. Pagano, The SCF ubiquitin ligase: insights into a molecular machine, Nat. Rev. Mol. Cell Biol. 5 (2004) 739–751.
[81] A.R. Willems, M. Schwab, M. Tyers, A hitchhiker's guide to the cullin ubiquitin ligases: SCF and its kin, Biochim. Biophys. Acta 1695 (2004) 133–170.
[82] M.D. Petroski, R.J. Deshaies, Function and regulation of cullin-RING ubiquitin ligases, Nat. Rev. Mol. Cell Biol. 6 (2005) 9–20.
[83] M.M.J. Cohen, G.P. Leboucher, N. Livnat-Levanon, M.H. Glickman, A.M. Weissman, Ubiquitin-proteasome-dependent degradation of a mitofusin, a critical regulator of mitochondrial fusion, Mol. Biol. Cell 19 (2008) 2457–2464.
[84] F. Anton, J.M. Fres, A. Schauss, B. Pinson, G.J. Praefcke, T. Langer, M. Escobar-Henriques, Ugo1 and Mdm30 act sequentially during Fzo1-mediated mitochondrial outer membrane fusion, J. Cell Sci. 124 (2011) 1126–1135.
[85] M.M. Cohen, E.A. Amiott, A.R. Day, G.P. Leboucher, E.N. Pryce, M.H. Glickman, J.M. McCaffery, J.M. Shaw, A.M. Weissman, Sequential requirements for the GTPase domain of the mitofusin Fzo1 and the ubiquitin ligase SCFMdm30 in mitochondrial outer membrane fusion, J. Cell Sci. 124 (2011) 1403–1410.
[86] A. Neutzner, R.J. Youle, Instability of the mitofusin Fzo1 regulates mitochondrial morphology during the mating response of the yeast Saccharomyces cerevisiae, J. Biol. Chem. 280 (2005) 18598–18603.
[87] E.A. Amiott, M.M. Cohen, Y. Saint-Georges, A.M. Weissman, J.M. Shaw, A mutation associated with CMT2A neuropathy causes defects in Fzo1 GTP hydrolysis, ubiquitylation, and protein turnover, Mol. Biol. Cell 20 (2009) 5026–5035.
[88] T. Koshiba, S.A. Detmer, J.T. Kaiser, H. Chen, J.M. McCaffery, D.C. Chan, Structural basis of mitochondrial tethering by mitofusin complexes, Science (New York, N.Y.) 305 (2004) 858–862.
[89] G.J. Hermann, J.W. Thatcher, J.P. Mills, K.G. Hales, M.T. Fuller, J. Nunnari, J.M. Shaw, Mitochondrial fusion in yeast requires the transmembrane GTPase Fzo1p, J. Cell Biol. 143 (1998) 359–373.
[90] D. Rapaport, M. Brunner, W. Neupert, B. Westermann, Fzo1p is a mitochondrial outer membrane protein essential for the biogenesis of functional mitochondria in *Saccharomyces cerevisiae*, J. Biol. Chem. 273 (1998) 20150–20155.
[91] S. Meeusen, J.M. McCaffery, J. Nunnari, Mitochondrial fusion intermediates revealed in vitro, Science (New York, N.Y.) 305 (2004) 1747–1752.
[92] Y. Qi, L. Yan, C. Yu, X. Guo, X. Zhou, X. Hu, X. Huang, Z. Rao, Z. Lou, J. Hu, Structures of human mitofusin 1 provide insight into mitochondrial tethering, J. Cell Biol. 215 (2016) 621–629.
[93] Y.-L. Cao, S. Meng, Y. Chen, J.-X. Feng, D.-D. Gu, B. Yu, Y.-J. Li, J.-Y. Yang, S. Liao, D.C. Chan, S. Gao, MFN1 structures reveal nucleotide-triggered dimerization critical for mitochondrial fusion, Nature 542 (2017) 372–376.
[94] D. De Vecchis, L. Cavellini, M. Baaden, J. Henin, M.M. Cohen, A. Taly, A membrane-inserted structural model of the yeast mitofusin Fzo1, Sci. Rep. 7 (2017) 10217.
[95] L. Yan, Y. Qi, X. Huang, C. Yu, L. Lan, X. Guo, Z. Rao, J. Hu, Z. Lou, Structural basis for GTP hydrolysis and conformational change of MFN1 in mediating membrane fusion, Nat. Struct. Mol. Biol. 25 (2018) 233–243.
[96] T. Brandt, L. Cavellini, W. Kuhlbrandt, M.M. Cohen, A mitofusin-dependent docking ring complex triggers mitochondrial fusion in vitro, Elife 5 (2016) 36634.
[97] A. Brandner, D. De Vecchis, M. Baaden, M.M. Cohen, A. Taly, Physics-based oligomeric models of the yeast mitofusin Fzo1 at the molecular scale in the context of membrane docking, Mitochondrion 49 (2019) 234–244.
[98] F. Anton, G. Dittmar, T. Langer, M. Escobar-Henriques, Two deubiquitylases act on mitofusin and regulate mitochondrial fusion along independent pathways, Mol. Cell 49 (2013) 487–498.
[99] L. Cavellini, J. Meurisse, J. Findinier, Z. Erpapazoglou, N. Belgareh-Touzé, A.M. Weissman, M.M. Cohen, An ubiquitin-dependent balance between mitofusin turnover and fatty acids desaturation regulates mitochondrial fusion, Nat. Commun. 8 (2017) 15832.
[100] Y. Kee, N. Lyon, J.M. Huibregtse, The Rsp5 ubiquitin ligase is coupled to and antagonized by the Ubp2 deubiquitinating enzyme, EMBO J. 24 (2005) 2414–2424.
[101] T. Hoppe, K. Matuschewski, M. Rape, S. Schlenker, H.D. Ulrich, S. Jentsch, Activation of a membrane-bound transcription factor by regulated ubiquitin/proteasome-dependent processing, Cell 102 (2000) 577–586.
[102] M.A. Surma, C. Klose, D. Peng, M. Shales, C. Mrejen, A. Stefanko, H. Braberg, D.E. Gordon, D. Vorkel, C.S. Ejsing, R. Farese Jr., K. Simons, N.J. Krogan, R. Ernst, A lipid E-MAP identifies Ubx2 as a critical regulator of lipid saturation and lipid bilayer stress, Mol. Cell 51 (2013) 519–530.
[103] S.Y. Choi, P. Huang, G.M. Jenkins, D.C. Chan, J. Schiller, M.A. Frohman, A common lipid links Mfn-mediated mitochondrial fusion and SNARE-regulated exocytosis, Nat. Cell Biol. 8 (2006) 1255–1262.
[104] Y. Ohba, T. Sakuragi, E. Kage-Nakadai, N.H. Tomioka, N. Kono, R. Imae, A. Inoue, J. Aoki, N. Ishihara, T. Inoue, S. Mitani, H. Arai, Mitochondria-type GPAT is required for mitochondrial fusion, EMBO J. 32 (2013) 1265–1279.
[105] J.-M. Heo, N. Livnat-Levanon, E.B. Taylor, K.T. Jones, N. Dephoure, J. Ring, J. Xie, J.L. Brodsky, F. Madeo, S.P. Gygi, K. Ashrafi, M.H. Glickman, J. Rutter, A stress-responsive system for mitochondrial protein degradation, Mol. Cell 40 (2010) 465–480.
[106] M. Esaki, T. Ogura, Cdc48p/p97-mediated regulation of mitochondrial morphology is Vms1p-independent, J. Struct. Biol. 179 (2012) 112–120.
[107] T. Simoes, R. Schuster, F. den Brave, M. Escobar-Henriques, Cdc48 regulates a deubiquitylase cascade critical for mitochondrial fusion, Elife 8 (2018) 30015.
[108] M. Rape, T. Hoppe, I. Gorr, M. Kalocay, H. Richly, S. Jentsch, Mobilization of processed, membrane-tethered SPT23 transcription factor by CDC48(UFD1/NPL4), a ubiquitin-selective chaperone, Cell 107 (2001) 667–677.
[109] R. Hartmann-Petersen, M. Wallace, K. Hofmann, G. Koch, A.H. Johnsen, K.B. Hendil, C. Gordon, The Ubx2 and Ubx3 cofactors direct Cdc48 activity to proteolytic and nonproteolytic ubiquitin-dependent processes, Curr. Biol. 14 (2004) 824–828.
[110] C. Schuberth, A. Buchberger, Membrane-bound Ubx2 recruits Cdc48 to ubiquitin ligases and their substrates to ensure efficient ER-associated protein degradation, Nat. Cell Biol. 7 (2005) 999–1006.
[111] A. Chowdhury, T. Ogura, M. Esaki, Two Cdc48 cofactors Ubp3 and Ubx2 regulate mitochondrial morphology and protein turnover, J. Biochem. 164 (2018) 349–358.
[112] S. Nahar, A. Chowdhury, T. Ogura, M. Esaki, A AAA ATPase Cdc48 with a cofactor Ubx2 facilitates ubiquitylation of a mitochondrial fusion-promoting factor Fzo1 for proteasomal degradation, J. Biochem. 167 (2020) 279–286.
[113] M.B. Metzger, J.L. Scales, M.F. Dunklebarger, J. Loncarek, A.M. Weissman, A protein quality control pathway at the mitochondrial outer membrane, Elife (2020) 9.
[114] M.L. Wohlever, A. Mateja, P.T. McGilvray, K.J. Day, R.J. Keenan, Msp1 Is a membrane protein dislocase for tail-anchored proteins, Mol. Cell 67 (e196) (2017) 194–202.
[115] J.M. Goodrum, A.R. Lever, T.K. Coody, D.E. Gottschling, A.L. Hughes, Rsp5 and Mdm30 reshape the mitochondrial network in response to age-induced vacuole stress, Mol. Biol. Cell 30 (2019) 2141–2154.
[116] M. Müller, P. Kötter, C. Behrendt, E. Walter, C.Q. Scheckhuber, K.-D. Entian, A.S. Reichert, Synthetic quantitative array technology identifies the Ubp3-Bre5 deubiquitinase complex as a negative regulator of mitophagy, Cell Rep. 10 (2015) 1215–1225.
[117] N. Belgareh-Touzé, L. Cavellini, M.M. Cohen, Ubiquitination of ERMES components by the E3 ligase Rsp5 is involved in mitophagy, Autophagy 13 (2017) 114–132.
[118] K. Palikaras, E. Lionaki, N. Tavernarakis, Mechanisms of mitophagy in cellular homeostasis, physiology and pathology, Nat. Cell Biol. 20 (2018) 1013–1022.
[119] J.J. Lemasters, Variants of mitochondrial autophagy_ types 1 and 2 mitophagy and micromitophagy (type 3), Redox Biol. 2 (2014) 749–754.
[120] X. Wen, D.J. Klionsky, An overview of macroautophagy in yeast, J. Mol. Biol. 428 (2016) 1681–1699.
[121] T. Johansen, T. Lamark, Selective autophagy: ATG8 family proteins, LIR motifs and cargo receptors, J. Mol. Biol. 432 (2020) 80–103.
[122] T. Kanki, K. Wang, Y. Cao, M. Baba, K.D. J, Atg32 is a mitochondrial protein that confers selectivity during mitophagy, Dev. Cell 17 (2009) 98–109.
[123] K. Okamoto, N. Kondo-Okamoto, Y. Ohsumi, Mitochondria-anchored receptor Atg32 mediates degradation of mitochondria via selective autophagy, Dev. Cell 17 (2009) 87–97.
[124] Y. Aoki, T. Kanki, Y. Hirota, Y. Kurihara, T. Saigusa, T. Uchiumi, D. Kang, Phosphorylation of serine 114 on Atg32 mediates mitophagy, Mol. Biol. Cell 22 (2011) 3206–3217.
[125] Z. Bhujabal, Å.B. Birgisdottir, E. Sjøttem, H.B. Brenne, A. Øvervatn, S. Habisov, V. Kirkin, T. Lamark, T. Johansen, FKBP8 recruits LC3A to mediate Parkin-independent mitophagy, EMBO Rep. 18 (2017) 947–961.
[126] L. Esteban-Martínez, E. Sierra Filardi, R.S. McGreal, M. Salazar-Roa, G. Mariño, E. Seco, S. Durand, D. Enot, O. Graña, M. Malumbres, A. Cvekl, A.M. Cuervo, G. Kroemer, P. Boya, Programmed mitophagy is essential for the glycolytic switch during cell differentiation, EMBO J. 36 (2017) 1688–1706.
[127] T. Murakawa, O. Yamaguchi, A. Hashimoto, S. Hikoso, T. Takeda, T. Oka, H. Yasui, H. Ueda, Y. Akazawa, H. Nakayama, M. Taneike, T. Misaka, S. Omiya, A.M. Shah, A. Yamamoto, K. Nishida, Y. Ohsumi, K. Okamoto, Y. Sakata, K. Otsu, Bcl-2-like protein 13 is a mammalian Atg32 homologue that mediates mitophagy and mitochondrial fragmentation, Nat. Commun., 6 (2015) 1514.
[128] K. Otsu, T. Murakawa, O. Yamaguchi, BCL2L13 is a mammalian homolog of the yeast mitophagy receptor Atg32, Autophagy 11 (2015) 1932–1933.
[129] F. Strappazzon, F. Nazio, M. Corrado, V. Cianfanelli, A. Romagnoli, G.M. Fimia, S. Campello, R. Nardacci, M. Piacentini, M. Campanella, F. Cecconi, AMBRA1 is able to induce mitophagy via LC3 binding, regardless of PARKIN and p62/SQSTM1, Cell Death Differ. 22 (2015) 419–432.
[130] L. Liu, D. Feng, G. Chen, M. Chen, Q. Zheng, P. Song, Q. Ma, C. Zhu, R. Wang, W. Qi, L. Huang, P. Xue, B. Li, X. Wang, H. Jin, J. Wang, F. Yang, P. Liu, Y. Zhu, S. Sui, Q. Chen, Mitochondrial outer-membrane protein FUNDC1 mediates hypoxia-induced mitophagy in mammalian cells, Nature 14 (2012) 177–185.
[131] H. Sandoval, P. Thiagarajan, S.K. Dasgupta, A. Schumacher, J.T. Prchal, M. Chen, J. Wang, Essential role for Nix in autophagic maturation of erythroid cells, Nature 454 (2008) 232–235.
[132] R.L. Schweers, J. Zhang, M.S. Randall, M.R. Loyd, W. Li, F.C. Dorsey, M. Kundu, J.T. Opferman, J.L. Cleveland, J.L. Miller, P.A. Ney, NIX is required for programmed mitochondrial clearance during reticulocyte maturation, Proc. Natl. Acad. Sci. U. S. A. 104 (2007) 19500–19505.
[133] Z. Chen, L. Liu, Q. Cheng, Y. Li, H. Wu, W. Zhang, Y. Wang, S.A. Sehgal, S. Siraj, X. Wang, J. Wang, Y. Zhu, Q. Chen, Mitochondrial E3 ligase MARCH5 regulates FUNDC1 to fine-tune hypoxic mitophagy, EMBO Rep. 18 (2017) 495–509.
[134] Y. Wei, W.-C. Chiang, R. Sumpter, P. Mishra, B. Levine, Prohibitin 2 is an inner mitochondrial membrane mitophagy receptor, Cell 168 (e210) (2017) 224–238.
[135] L.A. Kane, M. Lazarou, A.I. Fogel, Y. Li, K. Yamano, S.A. Sarraf, S. Banerjee, R.J. Youle, PINK1 phosphorylates ubiquitin to activate Parkin E3 ubiquitin ligase activity, J. Cell Biol. 205 (2014) 143–153.
[136] A. Kazlauskaite, C. Kondapalli, R. Gourlay, D.G. Campbell, M.S. Ritorto, K. Hofmann, D.R. Alessi, A. Knebel, M. Trost, M.M.K. Muqit, Parkin is activated by PINK1-dependent phosphorylation of ubiquitin at Ser65, Biochem. J. 460 (2014) 127–141.
[137] F. Koyano, K. Okatsu, H. Kosako, Y. Tamura, E. Go, M. Kimura, Y. Kimura, H. Tsuchiya, H. Yoshihara, T. Hirokawa, T. Endo, E.A. Fon, J.-F.ß. Trempe,

Y. Saeki, K. Tanaka, N. Matsuda, Ubiquitin is phosphorylated by PINK1 to activate parkin, Nature 510 (2014) 162–166.
[138] M. Lazarou, D.A. Sliter, L.A. Kane, S.A. Sarraf, C. Wang, J.L. Burman, D.P. Sideris, A.I. Fogel, R.J. Youle, The ubiquitin kinase PINK1 recruits autophagy receptors to induce mitophagy, Nature 524 (2015) 309–314.
[139] T.N. Nguyen, B.S. Padman, M. Lazarou, Deciphering the molecular signals of PINK1/Parkin mitophagy, Trends Cell Biol. 26 (2016) 733–744.
[140] M. Lazarou, S.M. Jin, L.A. Kane, R.J. Youle, Role of PINK1 binding to the TOM complex and alternate intracellular membranes in recruitment and activation of the E3 ligase Parkin, Dev. Cell 22 (2012) 320–333.
[141] A.W. Greene, K. Grenier, M.A. Aguileta, S. Muise, R. Farazifard, M.E. Haque, H.M. Mcbride, D.S. Park, E.A. Fon, Mitochondrial processing peptidase regulates PINK1 processing, import and Parkin recruitment, EMBO Rep. 13 (2012) 378–385.
[142] S. Sekine, R.J. Youle, PINK1 import regulation; a fine system to convey mitochondrial stress to the cytosol, BMC Biol. 16 (2018) 2.
[143] K. Okatsu, T. Oka, M. Iguchi, K. Imamura, H. Kosako, N. Tani, M. Kimura, E. Go, F. Koyano, M. Funayama, K. Shiba-Fukushima, S. Sato, H. Shimizu, Y. Fukunaga, H. Taniguchi, M. Komatsu, N. Hattori, K. Mihara, K. Tanaka, N. Matsuda, PINK1 autophosphorylation upon membrane potential dissipation is essential for Parkin recruitment to damaged mitochondria, Nat. Commun. 3 (2012) 1016.
[144] K. Okatsu, M. Uno, F. Koyano, E. Go, M. Kimura, T. Oka, K. Tanaka, N. Matsuda, A dimeric PINK1-containing complex on depolarized mitochondria stimulates Parkin recruitment, J. Biol. Chem. 288 (2013) 36372–36384.
[145] K. Okatsu, M. Kimura, T. Oka, K. Tanaka, N. Matsuda, Unconventional PINK1 localization to the outer membrane of depolarized mitochondria drives Parkin recruitment, J. Cell Sci. 128 (2015) 964–978.
[146] D. Narendra, A. Tanaka, D.F. Suen, R.J. Youle, Parkin is recruited selectively to impaired mitochondria and promotes their autophagy, J. Cell Biol. 183 (2008) 795–803.
[147] A. Tanaka, M.M. Cleland, S. Xu, D.P. Narendra, D.-F. Suen, M. Karbowski, R.J. Youle, Proteasome and p97 mediate mitophagy and degradation of mitofusins induced by Parkin, J. Cell Biol. 191 (2010) 1367–1380.
[148] N. Matsuda, S. Sato, K. Shiba, K. Okatsu, K. Saisho, C.A. Gautier, Y.-s. Sou, S. Saiki, S. Kawajiri, F. Sato, M. Kimura, M. Komatsu, N. Hattori, K. Tanaka, PINK1 stabilized by mitochondrial depolarization recruits Parkin to damaged mitochondria and activates latent Parkin for mitophagy, J. Cell Biol. 189 (2010) 211–221.
[149] N.C. Chan, A.M. Salazar, A.H. Pham, M.J. Sweredoski, N.J. Kolawa, R.L.J. Graham, S. Hess, D.C. Chan, Broad activation of the ubiquitin-proteasome system by Parkin is critical for mitophagy, Hum. Mol. Genet. 20 (2011) 1726–1737.
[150] Y. Chen, G.W. Dorn, PINK1-phosphorylated mitofusin 2 is a Parkin receptor for culling damaged mitochondria, Science 340 (2013) 471–475.
[151] S.A. Sarraf, M. Raman, V. Guarani-Pereira, M.E. Sowa, E.L. Huttlin, S.P. Gygi, J.W. Harper, Landscape of the PARKIN-dependent ubiquitylome in response to mitochondrial depolarization, Nature 496 (2013) 372–376.
[152] C.M. Rose, M. Isasa, A. Ordureau, M.A. Prado, S.A. Beausoleil, M.P. Jedrychowski, D.J. Finley, J.W. Harper, S.P. Gygi, Highly multiplexed quantitative mass spectrometry analysis of ubiquitylomes, Cell Syst. 3 (e394) (2016) 395–403.
[153] D.E. Spratt, R.J. Martinez-Torres, Y.J. Noh, P. Mercier, N. Manczyk, K.R. Barber, J.D. Aguirre, L. Burchell, A. Purkiss, H. Walden, G.S. Shaw, A molecular explanation for the recessive nature of parkin-linked Parkinson's disease, Nat. Commun. 4 (2013) 1983.
[154] J.-F. Trempe, V. Sauvé, K. Grenier, M. Seirafi, M.Y. Tang, M. Ménade, S. Al-Abdul-Wahid, J. Krett, K. Wong, G. Kozlov, B. Nagar, E.A. Fon, K. Gehring, Structure of parkin reveals mechanisms for ubiquitin ligase activation, Science 340 (2013) 1451–1455.
[155] T. Wauer, D. Komander, Structure of the human Parkin ligase domain in an autoinhibited state, EMBO J. 32 (2013) 2099–2112.
[156] B.E. Riley, J.C. Lougheed, K. Callaway, M. Velasquez, E. Brecht, L. Nguyen, T. Shaler, D. Walker, Y. Yang, K. Regnstrom, L. Diep, Z. Zhang, S. Chiou, M. Bova, D.R. Artis, N. Yao, J. Baker, T. Yednock, J.A. Johnston, Structure and function of Parkin E3 ubiquitin ligase reveals aspects of RING and HECT ligases, Nat. Commun. 4 (2013) 1982.
[157] V. Sauvé, A. Lilov, M. Seirafi, M. Vranas, S. Rasool, G. Kozlov, T. Sprules, J. Wang, J.-F. Trempe, K. Gehring, A Ubl/ubiquitin switch in the activation of Parkin, EMBO J. 34 (2015) 2492–2505.
[158] K. Shiba-Fukushima, T. Arano, G. Matsumoto, T. Inoshita, S. Yoshida, Y. Ishihama, K.-Y. Ryu, N. Nukina, N. Hattori, Y. Imai, Phosphorylation of mitochondrial polyubiquitin by PINK1 promotes Parkin mitochondrial tethering, PLoS Genet. 10 (2014) e1004861.
[159] K. Okatsu, F. Koyano, M. Kimura, H. Kosako, Y. Saeki, K. Tanaka, N. Matsuda, Phosphorylated ubiquitin chain is the genuine Parkin receptor, J. Cell Biol. 209 (2015) 111–128.
[160] F. Koyano, K. Yamano, H. Kosako, K. Tanaka, N. Matsuda, Parkin recruitment to impaired mitochondria for nonselective ubiquitylation is facilitated by MITOL, J. Biol. Chem. 294 (2019) 10300–10314.
[161] A. Ordureau, S.A. Sarraf, D.M. Duda, J.-M. Heo, M.P. Jedrychowski, V.O. Sviderskiy, J.L. Olszewski, J.T. Koerber, T. Xie, S.A. Beausoleil, J.A. Wells, S.P. Gygi, B.A. Schulman, J.W. Harper, Quantitative proteomics reveal a feedforward mechanism for mitochondrial PARKIN translocation and ubiquitin chain synthesis, Mol. Cell 56 (2014) 360–375.
[162] M.E. Gegg, J.M. Cooper, K.-Y. Chau, M. Rojo, A.H.V. Schapira, J.-W. Taanman, Mitofusin 1 and mitofusin 2 are ubiquitinated in a PINK1/parkin-dependent manner upon induction of mitophagy, Hum. Mol. Genet. 19 (2010) 4861–4870.
[163] S.R. Yoshii, C. Kishi, N. Ishihara, N. Mizushima, Parkin mediates proteasome-dependent protein degradation and rupture of the outer mitochondrial membrane, J. Biol. Chem. 286 (2011) 19630–19640.
[164] G.-L. McLelland, T. Goiran, W. Yi, G. Dorval, C.X. Chen, N.D. Lauinger, A.I. Krahn, S. Valimehr, A. Rakovic, I. Rouiller, T.M. Durcan, J.-F. Trempe, E.A. Fon, Mfn2 ubiquitination by PINK1/parkin gates the p97-dependent release of ER from mitochondria to drive mitophagy, Elife 7 (2018) e16038.
[165] W. Bernhard, C. Rouiller, Close topographical relationship between mitochondria and ergastoplasm of liver cells in a definite phase of cellular activity, J. Biophys. Biochem. Cytol. 2 (1956) 73–78.
[166] J.E. Vance, Phospholipid synthesis in a membrane fraction associated with mitochondria, J. Biol. Chem. 265 (1990) 7248–7256.
[167] R. Rizzuto, M. Brini, M. Murgia, T. Pozzan, Microdomains with high Ca2+ close to IP3-sensitive channels that are sensed by neighboring mitochondria, Science 262 (1993) 744–747.
[168] G. Szabadkai, K. Bianchi, P.T. Várnai, D. De Stefani, M.R. Wieckowski, D. Cavagna, A.I. Nagy, T.S. Balla, R. Rizzuto, Chaperone-mediated coupling of endoplasmic reticulum and mitochondrial Ca2+ channels, J. Cell Biol. 175 (2006) 901–911.
[169] M. Giacomello, L. Pellegrini, The coming of age of the mitochondria-ER contact: a matter of thickness, Cell Death Differ. 23 (2016) 1417–1427.
[170] P. Veeresh, H. Kaur, D. Sarmah, L. Mounica, G. Verma, V. Kotian, R. Kesharwani, K. Kalia, A. Borah, X. Wang, K.R. Dave, A.M. Rodriguez, D.R. Yavagal, P. Bhattacharya, Endoplasmic reticulum-mitochondria crosstalk: from junction to function across neurological disorders, Ann. N.Y. Acad. Sci. 1457 (2019) 41–60.
[171] M. Eisenberg-Bord, N. Shai, M. Schuldiner, M. Bohnert, A tether is a tether is a tether: tethering at membrane contact sites, Dev. Cell 39 (2016) 395–409.
[172] Z. Erpapazoglou, F. Mouton-Liger, O. Corti, From dysfunctional endoplasmic reticulum-mitochondria coupling to neurodegeneration, Neurochem. Int. (2017) 1–13.
[173] O.M. de Brito, L. Scorrano, Mitofusin 2 tethers endoplasmic reticulum to mitochondria, Nature 456 (2008) 605–610.
[174] P. Cosson, A. Marchetti, M. Ravazzola, L. Orci, Mitofusin-2 independent juxtaposition of endoplasmic reticulum and mitochondria: an ultrastructural study, PLoS One 7 (2012) e46293.
[175] R. Filadi, E. Greotti, G. Turacchio, A. Luini, T. Pozzan, P. Pizzo, Mitofusin 2 ablation increases endoplasmic reticulum-mitochondria coupling, Proc. Natl. Acad. Sci. U. S. A. 112 (2015) E2174–E2181.
[176] D. Naon, M. Zaninello, M. Giacomello, T. Varanita, F. Grespi, S. Lakshminaranayan, A. Serafini, M. Semenzato, S. Herkenne, M.I. Hernández-Alvarez, A. Zorzano, D. De Stefani, G.W. Dorn, L. Scorrano, Critical reappraisal confirms that Mitofusin 2 is an endoplasmic reticulum-mitochondria tether, Proc. Natl. Acad. Sci. U. S. A. 113 (2016) 11249–11254.
[177] C.A. Gautier, Z. Erpapazoglou, F. Mouton-Liger, M.P. Muriel, F. Cormier, S. Bigou, S. Duffaure, M. Girard, B. Foret, A. Iannielli, V. Broccoli, C. Dalle, D. Bohl, P.P. Michel, J.-C. Corvol, A. Brice, O. Corti, The endoplasmic reticulum-mitochondria interface is perturbed in PARK2 knockout mice and patients with PARK2 mutations, Hum. Mol. Genet. 25 (2016) 2972–2984.
[178] V. Basso, E. Marchesan, C. Peggion, J. Chakraborty, S. von Stockum, M. Giacomello, D. Ottolini, V. Debattisti, F. Caicci, E. Tasca, V. Pegoraro, C. Angelini, A. Antonini, A. Bertoli, M. Brini, E. Ziviani, Regulation of ER-mitochondria contacts by Parkin via Mfn2, Pharmacol. Res. 138 (2018) 43–56.
[179] E. Braschi, R. Zunino, H.M. Mcbride, MAPL is a new mitochondrial SUMO E3 ligase that regulates mitochondrial fission, EMBO Rep. 10 (2009) 748–754.
[180] J. Prudent, R. Zunino, A. Sugiura, S. Mattie, G.C. Shore, H.M. Mcbride, MAPL SUMOylation of Drp1 stabilizes an ER/mitochondrial platform required for cell death, Mol. Cell 59 (2015) 941–955.
[181] J. Yun, R. Puri, H. Yang, M.A. Lizzio, C. Wu, Z.-H. Sheng, M. Guo, MUL1 acts in parallel to the PINK1/parkin pathway in regulating mitofusin and compensates for loss of PINK1/parkin, Elife 3 (2014) e01958.
[182] R. Puri, X.-T. Cheng, M.-Y. Lin, N. Huang, Z.-H. Sheng, Mul1 restrains Parkin-mediated mitophagy in mature neurons by maintaining ER-mitochondrial contacts, Nat. Commun. 10 (2019) 3645.
[183] A. Sugiura, S. Nagashima, T. Tokuyama, T. Amo, Y. Matsuki, S. Ishido, Y. Kudo, H.M. Mcbride, T. Fukuda, N. Matsushita, R. Inatome, S. Yanagi, MITOL regulates endoplasmic reticulum-mitochondria contacts via mitofusin2, Mol. Cell 51 (2013) 20–34.
[184] A. Orvedahl, R. Sumpter, G. Xiao, A. Ng, Z. Zou, Y. Tang, M. Narimatsu, C. Gilpin, Q. Sun, M. Roth, C.V. Forst, J.L. Wrana, Y.E. Zhang, K. Luby-Phelps, R.J. Xavier, Y. Xie, B. Levine, Image-based genome-wide siRNA screen identifies selective autophagy factors, Nature 480 (2011) 113–117.
[185] M. Fu, P. St-Pierre, J. Shankar, P.T.C. Wang, B. Joshi, I.R. Nabi, Regulation of mitophagy by the Gp78 E3 ubiquitin ligase, Mol. Biol. Cell 24 (2013) 1153–1162.
[186] A. Di Rita, A. Peschiaroli, P.D. A'cunzo, D. Strobbe, Z. Hu, J. Gruber, M. Nygaard, M. Lambrughi, G. Melino, E. Papaleo, J. Dengjel, S. El Alaoui, M. Campanella, V. Dötsch, V.V. Rogov, F. Strappazzon, F. Cecconi, HUWE1 E3 ligase promotes PINK1/PARKIN-independent mitophagy by regulating AMBRA1 activation via IKKα, Nat. Commun. 9 (2018) 3755.
[187] R. Mukherjee, O. Chakrabarti, Ubiquitin-mediated regulation of the E3 ligase GP78 by MGRN1 in trans affects mitochondrial homeostasis, J. Cell Sci. 129 (2016) 757–773.
[188] G.P. Leboucher, Y.C. Tsai, M. Yang, K.C. Shaw, M. Zhou, T.D. Veenstra, M.H. Glickman, A.M. Weissman, Stress-induced phosphorylation and proteasomal degradation of mitofusin 2 facilitates mitochondrial fragmentation and apoptosis, Mol. Cell 47 (2012) 547–557.
[189] T.M. Durcan, M.Y. Tang, J.R. Pérusse, E.A. Dashti, M.A. Aguileta, G.-L. McLelland, P. Gros, T.A. Shaler, D. Faubert, B. Coulombe, E.A. Fon, USP8 regulates mitophagy by removing K6-linked ubiquitin conjugates from parkin, EMBO J. 33 (2014) 2473–2491.

[190] B. Bingol, J.S. Tea, L. Phu, M. Reichelt, C.E. Bakalarski, Q. Song, O. Foreman, D.S. Kirkpatrick, M. Sheng, The mitochondrial deubiquitinase USP30 opposes parkin-mediated mitophagy, Nature 510 (2014) 370–375.
[191] T. Cornelissen, D. Haddad, F. Wauters, C. Van Humbeeck, W. Mandemakers, B. Koentjoro, C. Sue, K. Gevaert, B. De Strooper, P. Verstreken, W. Vandenberghe, The deubiquitinase USP15 antagonizes Parkin-mediated mitochondrial ubiquitination and mitophagy, Hum. Mol. Genet. 23 (19) (2014) 5227–5242.
[192] Y. Wang, M. Serricchio, M. Jauregui, R. Shanbhag, T. Stoltz, C.T. Di Paolo, P.K. Kim, G.A. McQuibban, Deubiquitinating enzymes regulate PARK2-mediated mitophagy, Autophagy 11 (2015) 595–606.
[193] B.C. Hammerling, R.H. Najor, M.Q. Cortez, S.E. Shires, L.J. Leon, E.R. Gonzalez, D. Boassa, S. Phan, A. Thor, R.E. Jimenez, H. Li, R.N. Kitsis, G.W. Dorn, J. Sadoshima, M.H. Ellisman, A.B. Gustafsson, A Rab5 endosomal pathway mediates Parkin-dependent mitochondrial clearance, Nat. Commun. 8 (2017) 14050.
[194] V. Soubannier, G.-L. McLelland, R. Zunino, E. Braschi, P. Rippstein, E.A. Fon, H.M. Mcbride, A vesicular transport pathway shuttles cargo from mitochondria to lysosomes, Curr. Biol. 22 (2012) 135–141.
[195] V. Soubannier, P. Rippstein, B.A. Kaufman, E.A. Shoubridge, H.M. Mcbride, Reconstitution of mitochondria derived vesicle formation demonstrates selective enrichment of oxidized cargo, PLoS One 7 (2012) e52830.
[196] G.-L. McLelland, V. Soubannier, C.X. Chen, H.M. Mcbride, E.A. Fon, Parkin and PINK1 function in a vesicular trafficking pathway regulating mitochondrial quality control, EMBO J. 33 (2014) 282–295.
[197] A.L. Hughes, C.E. Hughes, K.A. Henderson, N. Yazvenko, D.E. Gottschling, Selective sorting and destruction of mitochondrial membrane proteins in aged yeast, Elife (2016) 5.
[198] N. Shai, E. Yifrach, C.W.T. van Roermund, N. Cohen, C. Bibi, L. Ijlst, L. Cavellini, J. Meurisse, R. Schuster, L. Zada, M.C. Mari, F.M. Reggiori, A.L. Hughes, M. Escobar-Henriques, M.M. Cohen, H.R. Waterham, R.J.A. Wanders, M. Schuldiner, E. Zalckvar, Systematic mapping of contact sites reveals tethers and a function for the peroxisome-mitochondria contact, Nat. Commun. 9 (2018) 1761.
[199] M.S. Herrera-Cruz, T. Simmen, Of yeast, mice and men: MAMs come in two flavors, Biol. Direct 12 (2017) 3.
[200] S. Böckler, B. Westermann, Mitochondrial ER contacts are crucial for mitophagy in yeast, Dev. Cell 28 (2014) 450–458.
[201] A.P. AhYoung, J. Jiang, J. Zhang, X. Khoi Dang, J.A. Loo, Z.H. Zhou, P.F. Egea, Conserved SMP domains of the ERMES complex bind phospholipids and mediate tether assembly, Proc. Nat. Acad. Sci. U.S.A 112 (2015) E3179–E3188.
[202] K.O. Kopec, V. Alva, A.N. Lupas, Homology of SMP domains to the TULIP superfamily of lipid-binding proteins provides a structural basis for lipid exchange between ER and mitochondria, Bioinformatics 26 (2010) 1927–1931.
[203] C. Petrungaro, B. Kornmann, Lipid exchange at ER-mitochondria contact sites: a puzzle falling into place with quite a few pieces missing, Curr. Opin. Cell Biol. 57 (2019) 71–76.
[204] M. Cohen, F. Stutz, C. Dargemont, Deubiquitination, a new player in Golgi to endoplasmic reticulum retrograde transport, J. Biol. Chem. 278 (2003) 51989–51992.
[205] M. Cohen, F. Stutz, N. Belgareh, R. Haguenauer-Tsapis, C. Dargemont, Ubp3 requires a cofactor, Bre5, to specifically de-ubiquitinate the COPII protein, Sec23, Nat. Cell Biol. 5 (2003) 661–667.
[206] B. Ossareh-Nazari, C.A. Niño, M.H. Bengtson, J.-W. Lee, C.A.P. Joazeiro, C. Dargemont, Ubiquitylation by the Ltn1 E3 ligase protects 60S ribosomes from starvation-induced selective autophagy, J. Cell Biol. 204 (2014) 909–917.
[207] J.S. Thrower, L. Hoffman, M. Rechsteiner, C.M. Pickart, Recognition of the polyubiquitin proteolytic signal, EMBO J. 19 (2000) 94–102.
[208] H.C. Kim, J.M. Huibregtse, Polyubiquitination by HECT E3s and the determinants of chain type specificity, Mol. Cell. Biol. 29 (2009) 3307–3318.
[209] M. Harreman, M. Taschner, S. Sigurdsson, R. Anindya, J. Reid, B. Somesh, S.E. Kong, C.A.S. Banks, R.C. Conaway, J.W. Conaway, J.Q. Svejstrup, Distinct ubiquitin ligases act sequentially for RNA polymerase II polyubiquitylation, Proc. Natl. Acad. Sci. U. S. A. 106 (2009) 20705–20710.
[210] N.N. Fang, G.T. Chan, M. Zhu, S.A. Comyn, A. Persaud, R.J. Deshaies, D. Rotin, J. Gsponer, T. Mayor, Rsp5/Nedd4 is the main ubiquitin ligase that targets cytosolic misfolded proteins following heat stress, Nature 16 (2014) 1227–1237.
[211] N.N. Fang, M. Zhu, A. Rose, K.-P. Wu, T. Mayor, Deubiquitinase activity is required for the proteasomal degradation of misfolded cytosolic proteins upon heat-stress, Nat. Commun. 7 (2016) 1–16.
[212] K. Lu, I. Psakhye, S. Jentsch, Autophagic clearance of polyQ proteins mediated by ubiquitin-Atg8 adaptors of the conserved CUET protein family, Cell 158 (2014) 549–563.
[213] S. Lee, J.M. Tumolo, A.C. Ehlinger, K.K. Jernigan, S.J. Qualls-Histed, P.C. Hsu, W.H. McDonald, W.J. Chazin, J.A. MacGurn, Ubiquitin turnover and endocytic trafficking in yeast are regulated by Ser57 phosphorylation of ubiquitin, Elife 6 (2017).
[214] P. Bragoszewski, et al., The ubiquitin-proteasome system regulates mitochondrial intermembrane space proteins, Mol. Cell Biol. 33 (11) (2013) 2136–2148.
[215] P. Bragoszewski, et al., Retro-translocation of mitochondrial intermembrane space proteins, Proc. Natl. Acad. Sci. U. S. A. 112 (25) (2015) 7713–7718.
[216] J. Lavie, et al., Ubiquitin-dependent degradation of mitochondrial proteins regulates energy metabolism, Cell Rep. 23 (10) (2018) 2852–2863.
[217] G. Lehmann, et al., Ubiquitination of specific mitochondrial matrix proteins, Biochem. Biophys. Res. Commun. 475 (1) (2016) 13–18.
[218] V. Azzu, M.D. Brand, Degradation of an intramitochondrial protein by the cytosolic proteasome, J. Cell Sci. 123 (4) (2010) 578–585.

Résumé

Au cours de la dernière décennie, nous sommes passés de l'image erronée des mitochondries comme étant des organelles rondes isolées à une vision beaucoup plus précise. En effet, les mitochondries avec toutes les autres organelles partagent un appartement commun qu'on appelle la cellule. Comme tout colocataires, ils échangent et communiquent entre eux au quotidien, non seulement pour conserver leurs fonctions propres mais aussi pour atteindre un objectif commun important : le maintien de l'homéostasie cellulaire.

Cette communication peut être indirecte, par le biais du trafic vésiculaire par exemple ou directe par des contacts physiques transitoires entre les différentes organelles. Lorsqu'il s'agit de contacts physiques inter-organites, les mitochondries se classent en tête grâce à leur nature dynamique. En effet, les mitochondries sont des organites très dynamiques dont la morphologie est maintenue par des événements de fusion et de fission de leurs membranes respectives (Westermann, 2010). Le processus de fusion de la membrane externe en particulier n'est pas une tâche simple, et requiert un équilibre complexe entre deux systèmes clés (Cavellini et al., 2017). Le premier est le Système Ubiquitine Protéasome, réputé pour son rôle crucial dans le renouvellement des protéines et des organites, le trafic, la réparation de l'ADN, l'endocytose, les voies de signalisation, la progression du cycle cellulaire etc... (Foot et al., 2017). La deuxième pièce du puzzle est la voie OLE qui est essentielle pour la biosynthèse *de novo* des acides gras insaturés qui constituent les briques lipidiques des membranes biologiques (Ernst et al., 2016). Le « cross-talk » entre ces 2 systèmes est essentiel pour que la fusion de la membrane externe mitochondriale soit réussi (Cavellini et al., 2017).

Grâce à cette dynamique de fusion et fission, les réseaux mitochondriaux s'adaptent rapidement aux besoins énergétiques de la cellule (Schrepfer et Scorrano, 2016), maintiennent le potentiel redox (Willems et al., 2015) et interagissent avec la plupart voir même toutes les organelles cellulaires (Lackner, 2019). Peut-être le plus ancien et le plus célèbre partenaire d'interaction de la mitochondrie identifié est le réticulum endoplasmique, leur relation fonctionnelle a été établie depuis les années 90 (Vance, 1990). Depuis, le domaine est en plein essor grâce à différentes technologies permettant de caractériser les contacts organites et les protéines qui participent à ces interactions. De l'imagerie spectrale (Valm et al., 2017) à la détection de proximité de fluorophores « Split Venus » (Shai et al., 2018), plein de nouvelles découvertes sont désormais possibles.

Récemment, une nouvelle étude a mis les contacts Peroxysome-Mitochondries, qui étaient jusqu'à présent assez obscurs, sous les projecteurs. En utilisant une technique de complémentation de fluorophores Vénus divisés, les chercheurs de l'équipe de Maya Schuldiner (Weizmann Institute of Science) ont identifié deux nouvelles protéines médiant l'ancrage entre les Peroxysomes et les Mitochondries. La première est Pex34, une protéine membranaire des peroxysomes et la deuxième est la mitofusine de levure Fzo1 (Shai et al., 2018).

Cette étude a particulièrement suscité notre intérêt car Fzo1 n'a jamais été suggérée (ou prouvée) d'être localisée sur des membranes autres que celles des mitochondries où elle exerce son rôle principal :'attacher les membranes externes de mitochondries adjacentes afin d'entrainer la fusion homotypique de la membrane externe mitochondriale. La mitofusine est désormais placée au cœur des contacts Peroxysome-Mitochondries mais cette découverte est encore truffée de points d'interrogation auxquels j'ai essayé de trouver des réponses au cours de ma thèse. En caractérisant d'abord les contacts Peroxysome-Mitochondries médiés par Fzo1 et en déchiffrant les mécanismes à l'origine de leur régulation dans des cellules sauvages. Nous avons finalement cherché à comprendre la fonction de ces contacts médiés par Fzo1 dans la cellule.

Pour comprendre les contacts médiés par Fzo1 il faut d'abord s'attarder sur la régulation de la protéine elle-même. En effet la régulation des niveaux de Fzo1 met d'abord en jeu le Système Ubiquitine Protéasome ainsi que la voie OLE.

L'ubiquitine est un petit polypeptide de 76 acides aminés qui se lie de manière covalente à d'autres polypeptides ou à lui-même pour former des chaînes qui peuvent s'assembler et se désassembler comme des morceaux de « Lego ». Ce processus d'ubiquitination implique une cascade enzymatique à plusieurs étapes (Hershko et Ciechanover,1998) où, au moins, 3 enzymes distinctes participent à la fixation d'une ou plusieurs sous-unités d'ubiquitine aux résidus lysine d'une protéine cible (Komander et Rape, 2012 ; Clague et al., 2015). L'ubiquitination est un processus complexe mais réversible, de nombreuses enzymes dé-ubiquitinantes (DUB) sont présentes dans la cellule. La découverte que l'ubiquitine peut également être phosphorylée, acétylée ou SUMOylée a élargi le champ des possibles (Swatek et Komander, 2016 ; Stewart et al., 2016 ; Kwon et Ciechanover, 2017 ; Ohtake et Tsuchiya, 2017 ; Liu et al., 2015). La bible de l'ubiquitine une fois connue sous le nom de « The Ubiquitin code » (Komander et Rape, 2012) est désormais « The expanded Ubiquitin code » (Swatek et Komander, 2016). Une myriade de combinaisons de liaisons ubiquitine sont

possibles, dont beaucoup conduisent à des résultats distincts (Kwon et Ciechanover, 2017 ; Ohtake et Tsuchiya, 2017). Les deux types de chaînes d'ubiquitine prédominantes dans la cellule sont : les chaînes à liaison K48 qui représentent plus de 50 % de toutes les liaisons dans la cellule et les chaînes liées à K63 (Swatek et Komander, 2016). Les chaînes liées à K63 peuvent réguler la localisation subcellulaire de molécules cibles, leur affinité pour les protéines partenaires et/ou leur activité (Liu et al., 2015 ; Kwon et Ciechanover, 2017 ; Spence et al., 1995). En revanche, l'ubiquitination liée à K48 conduit à la dégradation des substrats cibles par le protéasome 26S, un complexe à multi-sous-unités qui brise les liaisons peptidiques dans son noyau protéolytique (Bard et al., 2018). Les protéasomes sont notoirement efficaces en raison de leur dynamique comportement : en se dissociant en sous-particules libres qui font la navette entre le cytoplasme et le noyau en réponse à différents défis de croissance, de développement ou d'environnement (Marshall et al., 2016 ; Russell et al., 1999 ; Marshall et Vierstra, 2019). Pour cela, il n'est pas surprenant que la plupart des protéines soient dégradées par le Système Ubiquitine Protéasome, ce qui en fait le principal « prédateur » cytosolique des protéines mal repliées et endommagées. Grâce à la dégradation des protéines et au contrôle qualité (par exemple : au RE par l'ERAD pour Endoplasmic Reticulum associated degradation ou à la Mitochondrie par le MAD pour Mitochondria Associated Degradation). Ce système joue un rôle très important dans de nombreux processus cellulaires tels que la transduction du signal, la progression du cycle cellulaire, la mort cellulaire, le développement, la mitophagie, l'endocytose, l'homéostasie des membranes et des organelles.

Une des protéines cibles de ce système est Fzo1, la mitofusine de levure qui se trouve à la membrane externe des mitochondries. L'histoire a commencé à partir d'un screen génétique chez la levure cherchant à identifier des gènes importants pour la Distribution et la Morphologie Mitochondriale (MDM) du groupe de Benedikt Westermann (Dimmer et al., 2002). Dans cette étude pionnière, ils ont identifié un gène qui provoque une fragmentation et agrégation des mitochondries : *MDM30*. A l'époque, on savait que *MDM30* code pour une protéine qui contient un motif F-box impliqué dans le ciblage des protéines vers une protéolyse ubiquitine-dépendante (Patton et al., 1998). D'autres études ont identifié une interaction possible entre Mdm30, Cdc53 et Skp1, deux composants essentiels des complexes SCF (Skp1-cullin-F-box) qui ciblent protéines pour la dégradation dépendante de l'ubiquitine (Uetz et al., 2000; Skowyra et al., 1997). Comme l'ubiquitination était considérée comme cruciale pour l'hérédité mitochondriale (Fisk et Yaffe, 1999), ils ont proposé que Mdm30 était

un nouvel acteur dans ce processus. Par la suite, des travaux du groupe Langer ont relié Mdm30 à Fzo1, montrant que la mitofusine s'accumule en l'absence de Mdm30. Confirmant par la suite que Fzo1 est un substrat de la Protéine F-Box (Escobar-Henriques et al., 2006). Malgré le fait que les protéines avec F-Box domaines étaient connus pour agir comme des éléments de reconnaissance de substrat pour les ligases SCF-ubiquitine (Willems et al., 2004 ; Cardozo et Pagano, 2004 ; Petroski et Deshaies, 2005), il a été proposé que le système ubiquitine protéasome n'était pas impliqué dans la dégradation de la mitofusine (Escobar-Henriques et al., 2006). Deux ans plus tard, il a été clairement démontré que le Fzo1 était bien ubiquitiné par Mdm30 et dégradée par le protéasome (Cohen et al., 2008). Enfin, un accord a été atteint sur la dégradation induite par l'ubiquitination de Fzo1 par Mdm30 et sa dégradation ultérieure par le protéasome (Fritz et al., 2003 ; Cohen et al., 2008 ; Anton et al., 2011 ; Cohen et al.,2011). C'est donc cette accumulation de Fzo1 qui provoque la morphologie mitochondriale agrégée observé dans les cellules *mdm30Δ* (Fritz et al., 2003 ; Escobar-Henriques et al., 2006 ; Cohen et al., 2008). Cependant, l'ubiquitination du Fzo1 par la ligase Mdm30 et sa dégradation ultérieure n'est pas constitutive mais dépend de l'intégrité d'un domaine clé de la mitofusine, le domaine GTPase (Cohen et al.,2011). Il a en outre été démontré que Mdm30 se lie à la moitié N-terminale de Fzo1. L'activité du domaine GTPase induirait alors un changement conformationnel de Fzo1 qui permet le recrutement de Mdm30. En 2017, l'enzyme de dé-ubiquitination Ubp2 a été établie comme antagoniste de l'ubiquitination Mdm30-dépendante de Fzo1 (Cavellini et al., 2017). Ubp2 contribue ainsi à diminuer les longues chaines d'ubiquitine et donc la dégradation de Fzo1, ce qui en fait un facteur clé dans la régulation des niveaux de Fzo1 et la fusion de la membrane externe de la mitochondrie. Toutefois, Ubp2 antagonise également la ligase Rsp5 qui contrôle directement le niveau de désaturation des acides gras dans la cellule (Kee et al., 2005, 2006).

Nous arrivons ainsi à la deuxième partie du puzzle : les niveaux de désaturation des acides gras et la voie OLE. La voie OLE, dont Rsp5 est un acteur majeur, est essentielle pour la biosynthèse *de novo* des acides gras insaturés qui constituent les briques lipidiques des membranes biologiques. Le premier indice du « cross-talk » entre la désaturation et la régulation de Fzo1 est venu de l'observation que non seulement Fzo1, mais aussi Ubp2 sont des cibles de Mdm30 (Cavellini et al., 2017). Ainsi, en l'absence de Mdm30, Fzo1 et Ubp2 sont stabilisés. Comme Ubp2 est un antagoniste de Rsp5 (Kee et al., 2005), la stabilisation d'Ubp2 dans les cellules *mdm30Δ* bloque la voie OLE entraînant ainsi une diminution de la synthèse de l'enzyme Ole1 (Cavellini et al.,2017). Cette enzyme est responsable de l'insertion

de doublés dans les chaines acyles des acides gras, les transformant ainsi en acides gras insaturés. Ce travail a ainsi révélé que l'absence de Mdm30 induit non seulement la stabilisation de Fzo1 et Ubp2 mais aussi une diminution de la désaturation des acides gras due à la synthèse continue de l'enzyme Ole1. Par conséquence, les défauts de fusion mitochondriale dans les cellules *mdm30Δ* ou *ubp2Δ* (où Fzo1 est soit stabilisé soit rapidement dégradé) ont été sauvés par une désaturation accrue ou diminuée acides gras respectivement (Cavellini et al., 2017). L'augmentation naturelle de Fzo1 lors d'une désaturation élevée des acides gras et le maintien de son efficacité de médier la fusion mitochondriale démontré que ce processus dépend à la fois Mdm30 et Ubp2 (Cavellini et al., 2017). Ces observations indiquent que la dégradation Mdm30-dependante de Fzo1 n'est pas constitutive mais elle est étroitement contrôlée par Ubp2, cette balance permet de maintenir une fusion mitochondriale fonctionnelle selon l'état de désaturation dans la cellule. Plus précisément, la dégradation de Fzo1 par Mdm30 devient essentielle pour la fusion mitochondriale lors d'une faible désaturation d'acides gras, mais dispensable en cas d'expression élevée d'Ole1 (donc en cas de haute désaturation).

La mitofusine Fzo1, qui jusqu'à présent a été documentée comme étant exclusivement localisée sur la membrane externe de la mitochondrie a été récemment suspectée de se localiser aux peroxysomes. En effet, dans une étude très intéressante, Shai N. et al ont identifié Fzo1 comme une protéine d'ancrage entre les peroxysomes et la mitochondrie. Plus précisément, ils ont observé que la surexpression de Fzo1 favorisait les contacts Peroxysome-Mitochondrie (appelés contacts « PerMit » pour simplifier), mais le partenaire d'interaction de Fzo1 reste à identifier (Shai et al., 2018). De plus, la présence de Fzo1 à la membrane peroxysomale dans des cellules sauvages reste à prouver. Si ce processus est physiologique, il serait aussi intéressant de comprendre comment les contacts Fzo1-dependants entre les peroxysomes et la mitochondrie sont régulés et quel est leur rôle dans la cellule.

Ce n'est pas la première fois qu'une mitofusine se retrouve à la membrane d'une autre organelle que la mitochondrie pour médier l'attachement entre ces deux : l'homologue mammifère de Fzo1, Mfn2 se localise également au RE (de Brito et Scorrano, 2008) médiant ainsi l'attachement entre le RE et la mitochondrie. Sachant que Fzo1 est une dynamine qui oligomérise avec le Fzo1 sur les membranes mitochondriales adjacentes, il est fort probable qu'une partie de des contacts peroxysomes-mitochondries soient médiés par des interactions homotypiques Fzo1-Fzo1. Il serait même possible d'imaginer que la connexion Fzo1-Fzo1 entre les membranes mitochondriales et peroxysomales puisse entraîner une fusion

hétérotypique entre les deux membranes comme c'est le cas pour les membranes externes de la mitochondrie. Bien qu'une fusion entre mitochondrie et peroxysome n'ait jamais été documentée auparavant, une étude du laboratoire de Heidi Mcbride présente un argument en faveur de cette théorie en montrant que les peroxysomes nouvellement nés sont des hybrides de pré-peroxysomes mitochondriaux et aussi dérivés du RE chez les mammifères (Sugiura et al., 2017).

Ces découvertes renforcent encore le lien entre les mitochondries et les peroxysomes qui sont déjà étroitement liés par diverses voies métaboliques indispensables au maintien de l'homéostasie cellulaire. En effet, différents substrats sont livrés depuis le peroxysome vers la mitochondrie par des machineries de transport dédiées, et les preuves suggèrent que les contacts dynamiques entre ces organelles jouent aussi un rôle important dans la régulation de ce transfert des métabolites ainsi que d'autres fonctions peroxysomales (Schrader et al., 2015 ; Shai et al., 2016). Chez la levure, les contacts médiés par Pex34 sont responsables de faciliter le transfert de produits intermédiaires de la β-oxydation entre les peroxysomes et les mitochondries tandis que le rôle des contacts médiés par Fzo1 est toujours un mystère à élucider (Shai et al., 2018).

Durant la première partie de ma thèse je me suis focalisée sur la localisation extra-mitochondriale de Fzo1 pour prouver que Fzo1 est bien situé aux peroxysomes. Les premiers indices de cette localisation venaient du surnageant de cellules *mdm30Δ*, comme la suppression de *MDM30* abolit la dégradation de Fzo1 (Cohen et al.,2011) stabilisant les niveaux de la protéine. Les niveaux de Fzo1 augmentent donc sur les membranes mitochondriales. Néanmoins, la présence de Fzo1 dans le cytosol dépourvu de mitochondries suggère que ce Fzo1 est présent sur une autre organelle (Shai et al., 2018). De plus, Fzo1 est étant une dynamine avec 2 domaines transmembranaires, nous soupçonnons qu'elle est plus susceptible d'être localisée sur une membrane plutôt que d'être libre dans le cytosol. Afin de déterminer cette localisation, plusieurs approches non fructueuses ont étés tentées (fractionnements subcellulaires) avant d'éventuellement prouver la présence de Fzo1 aux peroxysomes grâce à une approche d'immunoprécipitation native de peroxysomes avec des billes magnétiques RFP-Traps. Cette approche ne nous a pas seulement permis de prouver la présence de Fzo1 sur les peroxysomes dans des cellules *mdm30Δ* mais aussi dans des cellules sauvages. Fzo1 se localise donc naturellement aux peroxysomes impliquant par conséquence une régulation bien précise de cette localisation ainsi que des contacts PerMit médiés par cette protéine.

Dans la deuxième partie de ma thèse je me suis focalisée sur la régulation de ses contacts dans la cellule. Fzo1 est nécessaire pour la fusion de la membrane externe de la mitochondrie et donc sa régulation implique une balance entre la dégradation Mdm30-dependante de Fzo1 et les niveaux de désaturation des acides gras de la cellule (Cavellini et al., 2017). En effet, lorsque la désaturation est élevée, les niveaux de Fzo1 sont stabilisés, et inversement lorsque la désaturation est faible, les niveaux de Fzo1 augmentent. Conformément à ces résultats, nous avons raisonné les niveaux de Fzo1 peroxysomaux sont à leur tour soumis à la même régulation et donc les contacts PerMit médiés par Fzo1 pourraient être modulés naturellement par la désaturation des acides gras cellulaires.

Jouer avec la désaturation des acides gras n'est pas une mince affaire, car Ole1 est l'unique désaturase d'acides gras présente dans la levure qui convertit les acides gras saturés en insaturés en fonction des besoins de la cellule. Ce n'est donc pas surprenant que la régulation de ce gène soit à la fois extrêmement sensible et robuste. Pour contrer ce problème, nous avons changé directement le promoteur du gène OLE1. Ainsi, nous avons décidé de cloner le gène OLE1 dans différents plasmides exprimant chacun OLE1 sous le contrôle de différents promoteurs. Une fois le système pour contrôler les niveaux d'Ole1 était prêt, nous l'avons utilisé pour simuler différents niveaux de désaturation modulant par conséquent les niveaux de Fzo1. Grâce à cet outil, nous avons montré que les niveaux de Fzo1 ont augmenté lors de la surexpression d'Ole1 (condition TEF) et les niveaux de Fzo1 ont diminué en faible expression d'Ole1 (condition CYC) ce qui consolide les précédentes études (Cavellini et al., 2017). De plus, nous avons vu que les contacts PerMit augmentent avec une désaturation élevée et lorsque les niveaux de Fzo1 sont stabilisés (reflétant ainsi les cellules *mdm30Δ*) et diminuent lorsque la désaturation est faible et la dégradation de du Fzo1 est élevée. Ces contacts sont donc modulés par le niveau de désaturation en acides gras dans la cellule et les niveaux de Fzo1. La suppression de MDM30 inactive complètement l'ensemble du système de régulation des contacts PerMit Fzo1-dependants.

La troisième et dernière partie de ma thèse était dédiée à déchiffrer la fonction de ces contacts PerMit Fzo1-dependants dans la cellule. Pour cela on disposait dans l'équipe d'un résultat clé. Afin d'évaluer la croissance respiratoire de *S. cerevisiae*, les levures sont généralement cultivées sur un milieu où le glycérol est la seule source de carbone. Contrairement au dextrose qui peut être utilisé pour la fermentation, le glycérol est une source de carbone non fermentable qui oblige la levure à utiliser la respiration pour pousser. La respiration mitochondriale nécessite des mitochondries fonctionnelles et une fusion mitochondriale

efficace. En cohérence avec cela, l'absence de Mdm30 induit une diminution de la croissance respiratoire sur glycérol (Fritz et al., 2003 ; Cohen et al., 2008). Ceci étant dû à l'excès de Fzo1 qui perturbe le processus de fusion (Escobar-Henriques et al., 2006 ; Cohen et al., 2008, 2011). Étonnamment, nous avons vu que l'ajout d'une copie supplémentaire de FZO1 restaure la croissance sur les milieux de glycérol des cellules *mdm30Δ*. De plus, ce sauvetage nécessite une copie fonctionnelle de Fzo1 ce qui indique que c'est un phénomène actif. Ce résultat est extrêmement contre-intuitif car la stabilisation des niveaux de Fzo1 contribue au défaut de fusion mitochondriale, alors pourquoi l'ajout de Fzo1 rétablit-il la croissance respiratoire ? Dans le contexte de notre projet, ce résultat étonnant commence à avoir du sens. On peut imaginer que cette deuxième copie de Fzo1 renforce l'efficacité des contacts PerMit Fzo1-dependants déjà présents dans la cellule et donc contribue à restaurer la respiration mitochondriale et par conséquent la croissance sur glycérol.

Afin de décortiquer ce résultat nous avons utilisé une approche non-biaisée avec crible génétique en collaboration avec l'équipe de Maya Schuldiner (Weizmann Institute of Science). Ce screen avait pour but de trouver des gènes inhibiteurs de la croissance sur glycérol par la 2^{e} copie de Fzo1 sans pour autant affecter la croissance des cellules sauvages comme contrôle. Deux gènes sont ressortis de ce crible : *MLS1* et *ACB1*, tous deux directement liés au métabolisme des peroxysomal et aux acides gras, ce qui nous a vite mis sur la piste de l'implication des peroxysomes dans ce sauvetage de la respiration avec la 2^{e} copie de Fzo1. En parallèle, nous savons que Fzo1 s'accumule aux peroxysomes selon le niveau de désaturation en acide gras de la cellule. Nous avons donc regardé l'effet des délétions des deux gènes obtenus dans le crible *MLS1* et *ACB1* tout d'abord sur les contacts PerMit dans différentes expressions OLE1. En utilisant la microscopie à haute résolution, nous n'avons constaté aucun changement dans les contacts PerMit en l'absence de *MLS1* ou *ACB1* quels que soient le niveau d'Ole1. Cependant, la délétion de ces deux gènes a fortement affecté la morphologie mitochondriale en fonction du niveau de désaturation en acides gras. Cet effet sur les réseaux mitochondriaux était le plus drastique dans la faible expression d'OLE1 (en désaturation basse) et semblait s'atténuer avec l'augmentation de l'expression d'OLE1 (désaturation haute). Afin de déterminer si ces effets sur la morphologie mitochondriale sont dus à un problème dans les processus de fusion ou de fission, nous avons enregistré des vidéos de cellules en microscopie à haute résolution afin de suivre le réseau mitochondrial durant le temps. Nous avons ensuite quantifié le nombre d'évènements de fusion et de fission mitochondriale qui ont révélé que les morphologies aberrantes observées

dans les mutants étaient principalement causées par des défauts de fusion mitochondriale qui sont plus prononcés en basse désaturation d'acides gras où nous avons moins de contacts PerMit par rapport à des conditions de haute désaturation en acides gras où les contacts PerMit sont les plus abondants. Nous avons conclu que les contacts de PerMit protègent en quelque sorte la fusion mitochondriale contre l'absence d'*ACB1* et de *MLS1*.

D'une part, les fonctions du transporteur d'acyl-coA Acb1 ne sont pas encore entièrement comprises. D'autre part, Mls1 est une enzyme établie du cycle du glyoxylate dont la localisation est aussi connue : aux peroxysomes ou dans le cytosol selon la source de carbone utilisée pour la croissance (Kunze et al.,2002) et sa fonction principale est de générer du malate à partir du glyoxylate. Mls1 succède à l'enzyme Icl1 (Isocitrate Lyase) dans le cycle du glyoxylate qui elle est cytosolique. Naturellement, la suppression de MLS1 induit l'accumulation de glyoxylate et de succinate générés par Icl1. Cette accumulation semblait affecter négativement la fusion mitochondriale dans des conditions où les contacts PerMit sont moins nombreux (Cyc-OLE1) par rapport aux contacts PerMit élevés (TEF-OLE1).

Nous avions donc émis l'hypothèse qu'une augmentation des contacts PerMit protégerait en quelque sorte la fusion mitochondriale de l'accumulation des produits intermédiaires de Icl1 (c'est-à-dire le succinate et le glyoxylate). Cela nous a poussé à tester les effets de la délétion *ICL1* sur les souches exprimant les différents niveaux de OLE1 et les cellules *mls1Δ*. A notre grande surprise, nous avons constaté que l'inactivation de Icl1 tout seul n'avait aucun effet sur les morphologies mitochondriales quel que soit le niveau d'expression d'*OLE1*. Cependant, l'absence d'Icl1 a complètement aboli les effets que nous avons vus dans cellules *mls1Δ* sur les morphologies mitochondriales ce qui suggère que les contacts PerMit Fzo1-dependants permettaient de court-circuiter Icl1 et maintenir la fusion mitochondriale. En effet, il se trouve que l'un des principaux rôles des contacts inter-organelles est le transport moléculaire. C'est pourquoi nous avons soupçonné que le citrate (le produit intermédiaire juste en amont de Icl1, produit par l'enzyme Cit2) ou l'Acétyl-CoA (produite par le biais de la navette carnitine) pourrait être impliqué dans cette « protection » de la fusion mitochondriale qui est présente lorsque les contacts PerMit sont plus abondants en raison de l'augmentation de la proximité entre les deux organelles. Inversement, moins de sites de contact PerMit médiés par Fzo1 permettraient à Icl1 de prendre en charge l'isocitrate généré à partir des premières étapes du cycle du glyoxylate résultant à une accumulation de Glyoxylate et de Succinate, bloquant ainsi la stimulation de la fusion mitochondriale.

La suppression de *CIT2* et *CAT2* a révélé que *CAT2* n'avait aucun effet sur la morphologie mitochondriale, contrairement à *CIT2* qui déstabilisait le niveau des morphologies mitochondriales tubulaires même lorsque les contacts PerMit sont nombreux dans la cellule. Ainsi nous proposons que le manque de synthèse de citrate bloque la capacité des contacts PerMit médiés par Fzo1 de maintenir la morphologie tubulaire du réseau mitochondrial.

En conclusion, mes résultats nous ont permis de prouver que Fzo1 se localise naturellement aux peroxysomes pour favoriser les contacts entre les peroxysomes et les mitochondries. Cette localisation peroxysomale de Fzo1 est en fait régulée par la dégradation de Fzo1 par Mdm30 et le niveau de désaturation en acide gras de la cellule. En effet, nous trouvons que Fzo1 s'accumule sur les peroxysomes lorsque la désaturation des acides gras augmente, afin de stimuler la fusion mitochondriale maintenant ainsi le réseau mitochondrial tubulaire normal. Nos résultats indiquent aussi que la synthèse du citrate peroxysomal est requise pour le maintien des mitochondries tubulaires grâce aux contacts PerMit médiés par Fzo1 qui faciliteraient le transfert de ces produits intermédiaires comme le citrate du peroxysome vers les mitochondries.

Pour aller plus loin, le domaine des contacts physiques entre les organelles est en plein essor depuis une dizaine d'années et de nombreux laboratoires essaient de suivre la tendance. Les contacts entre organelles sont maintenant plus que jamais considérés comme des éléments clé assurant une communication efficace dans la cellule (Prinz et al., 2020). Dans un compartiment partagé et commun comme la cellule qui – si on y pense - est assez bondé, les organelles ont une très forte probabilité de se croiser. Il n'est donc pas surprenant qu'elles n'aillent pas s'éviter mais plutôt l'inverse : se rejoindre et communiquer par des associations physiques entre leurs membranes respectives (Eisenberg-Bord et al., 2016 ; Gatta et Levine, 2017). Grace à de nombreuses techniques qui se développent pour étudier ces contacts, la liste des facteurs que nous maintenant appeler « tethers » continue de s'élargir (Gatta et Levine, 2017 ; Prinz et al., 2020 ; Kornmann et al., 2009 ; Lahiri et al., 2015).

La mitofusine de levure Fzo1 s'ajoute à présent à cette liste. Outre son rôle dans l'ancrage et la fusion de la membrane externe des mitochondries, Fzo1 va aussi médier les contacts Peroxysome-Mitochondries (PerMit) lorsqu'elle est surexprimée (Shai et al., 2018). Même si la pertinence physiologique de ces observations n'était pas encore claire, la régulation de la localisation de Fzo1 semble indiquer que la dégradation de cette protéine par le système ubiquitine protéasome était impliquée (Shai et al., 2018). Deux chemins (pas si) séparés nous ont amenés à l'implication des acides gras dans ces contacts : le premier est que les

peroxysomes sont connus pour être un élément essentiel du métabolisme des acide gras. Le second est né de la découverte initiale que la fusion mitochondriale est régie par un équilibre entre la dégradation du Fzo1 et la désaturation des acides gras dans la cellule (Cavellini et al., 2017). Ces deux études ont fourni les plus grandes pièces du puzzle de notre histoire qui a commencé avec nombreuses questions fondamentales auxquelles on a pu répondre dans notre étude.

La découverte de la localisation peroxysomale de Fzo1 dans des cellules sauvages nous amène à s'interroger sur les mécanismes d'adressage de Fzo1 pour une membrane distincte. En réalité, Fzo1 est proposé d'utiliser des résidus hydrophobes similaires près de son domaine transmembranaire pour conduisant sa localisation appropriée (Huang et al., 2017). Il n'est pas exclu qu'une séquence d'adressage peroxysomale non identifiée soit présente dans la séquence de Fzo1. Une remarque qui soutient cette possibilité est l'interaction de Fzo1 avec la protéine d'adressage peroxysomal Pex19 et l'insertase Pex14 qui a été démontrée par des tests de co-immunoprécipitation (Shai et al., 2018) car Pex19 se lie à la séquence d'adressage hydrophobe situé près du domaine transmembranaire de la plupart des protéines membranaires peroxysomales (Sacksteder et al., 2000 ; Jones et al., 2004). Ainsi, ces interactions faciliteraient très probablement l'adressage et l'insertion de Fzo1 dans les membranes peroxysomales.

Fzo1 médie la fusion de la membrane externe des mitochondries en attachant les 2 membranes mitochondriales adjacentes à proximité immédiate pour ensuite médier la fusion des deux. Au niveau des membranes peroxysomales, Fzo1 attache les peroxysomes aux mitochondries via des interactions homotypiques Fzo1-Fzo1. Ceci pourrait amener à imaginer que Fzo1 pourrait également médier la fusion hétérotypique entre les peroxysomes et les mitochondries comme la fusion homotypique des membranes mitochondriales. Une idée très séduisante sur le papier mais est-elle vraiment possible ? La fusion des peroxysomes aux mitochondries n'est pas une tâche simple. Il faudrait surmonter la barrière d'énergie afin de déformer à la fois les deux membranes peroxysomales et mitochondriales et induire le mélange de lipides. Cela semble hasardeux en tenant compte de la différence de propriétés et de composition lipidique entre les deux membranes et le coût énergétique par rapport à un simple ancrage. En effet, les acquisitions de vidéos en microscopie à haute résolution n'ont fourni aucune donnée supportant l'hypothèse de la fusion hétérotypique et d'un mélange de contenus, ni entre peroxysomes et mitochondries ni entre deux peroxysomes.

De plus, les contacts PerMit se sont avérés localisés près des zones de la matrice mitochondriale où le complexe PDH est enrichi (Cohen et al., 2014). Cette observation soutient l'implication possible des produits intermédiaires de la bêta-oxydation dans les contacts PerMit et leur fonction. Dans cette optique, les contacts PerMit médiés par Pex34 ont été suggérés de favoriser le transfert d'Acétyl-CoA et de citrate des peroxysomes aux mitochondries pour stimuler la respiration mitochondriale (Shai et al., 2018). Nos résultats montrent aussi que le transfert de citrate est facilité par les contacts PerMit médiés par Fzo1. Ce citrate peroxysomal alimenterait le cycle oxydatif du TCA et contribuerais au maintien d'un potentiel membranaire mitochondrial efficace (Jazwinski, 2014). Le potentiel de membrane est une composante essentielle de la fusion mitochondriale (Legros et al., 2002 ; Meeusen et al., 2004 ; Song et al., 2007) ce qui expliquerait comment ce transfert de citrate facilité par les contacts physiques entre les peroxysomes et la mitochondrie pourrait stimuler la fusion mitochondriale.

Ces contacts mitofusine-dépendants entre peroxysomes et mitochondries sont comparables aux fonctions de la mitofusine Mfn2 sur les membranes du RE (de Brito et Scorrano, 2008). La mitofusine humaine se localise au niveau de la membrane externe de la mitochondrie et des membranes du RE médiant ainsi les interactions entre ces deux organelles. Cette interaction est essentielle pour le métabolisme et transfert de Ca2+ entre autres (Rowland et Voeltz, 2012 ; Csordás et al., 2018 ; Moltedo et al., 2019). Néanmoins, aucune étude n'a abordé la possibilité d'une contribution potentielle de ces contacts médiés par Mfn2 au maintien de la fusion mitochondriale chez les mammifères. Pourtant, il existe des indices qui pointent vers cela. Il a été documenté que les d'événements de fusion durent plus longtemps dans en l'absence qu'en présence du RE (Guo et al., 2018). La possibilité que des métabolites transférés à la mitochondrie par les contacts avec le RE au niveau des sites de fusion pourraient stimuler ce processus reste ouverte à la spéculation.

RÉSUMÉ

Les mitochondries sont des organelles très dynamiques qui subissent des phénomènes de fission et de fusion constants de leurs membranes extérieures et intérieures. Ces processus sont essentiels pour le maintien des fonctions mitochondriales essentielles telles que la phosphorylation oxydative ou la signalisation du calcium.

D'un point de vue moléculaire, la fusion et la fission mitochondriale dépendent tous les deux des grandes GTPases de la famille des protéines de type dynamine. Les dynamines qui favorisent l'attachement et la fusion des membranes mitochondriales extérieures sont appelés les mitofusines. La mitofusine de la levure Fzo1 est une GTPase transmembranaire située dans la membrane externe de la mitochondrie. Son oligomérisation favorise l'attachement suivi de la fusion de la membrane externe mitochondriale. Fzo1 a été proposé récemment comme une protéine d'attachement potentielle entre les peroxysomes et les mitochondries lorsqu'elle est surexprimée.

Durant ma thèse, j'ai pu prouver que Fzo1 se trouve réellement aux peroxysomes dans des conditions physiologiques et oligomérise avec le Fzo1 mitochondrial créant ainsi des contacts entre les peroxysomes et les mitochondries. Nous avons découvert que ces contacts Fzo1-dépendants sont modulés par les niveaux de désaturation en acide gras et qu'ils permettent le transfert mitochondrial des produits intermédiaires pour stimuler la fusion mitochondriale.

MOTS CLÉS

Mitochondrie, peroxysome, mitofusine, ubiquitine, contacts, fusion membranaire.

ABSTRACT

Mitochondria are highly dynamic organelles that undergo constant fission and fusion of their outer and inner membranes. These processes are critical to maintain essential mitochondrial functions such as oxidative phosphorylation or calcium signaling.

On a molecular basis, mitochondrial fusion and fission both depend on large GTPases of the Dynamin-Related Protein (DRP) family. The DRPs that mediate attachment and fusion of mitochondrial outer membranes are called the Mitofusins. The yeast mitofusin Fzo1 is located in the mitochondrial outer membrane. Its oligomerization promotes mitochondrial tethering followed by mitochondrial outer membrane fusion.

Fzo1 has recently been proposed as a potential tether between peroxisomes and mitochondria when overexpressed. In my thesis, we were able to prove that Fzo1 naturally localizes to peroxisomes and oligomerizes with the mitochondrial Fzo1 thus creating Fzo1-Fzo1 contacts between peroxisomes and mitochondria. We discovered that these Fzo1-mediated contacts allow the mitochondrial transfer of early byproducts of the glyoxylate cycle to stimulate mitochondrial fusion according to cellular fatty acid desaturation levels.

KEYWORDS

Mitochondria, peroxisome, mitofusin, ubiquitin, contacts, membrane fusion.